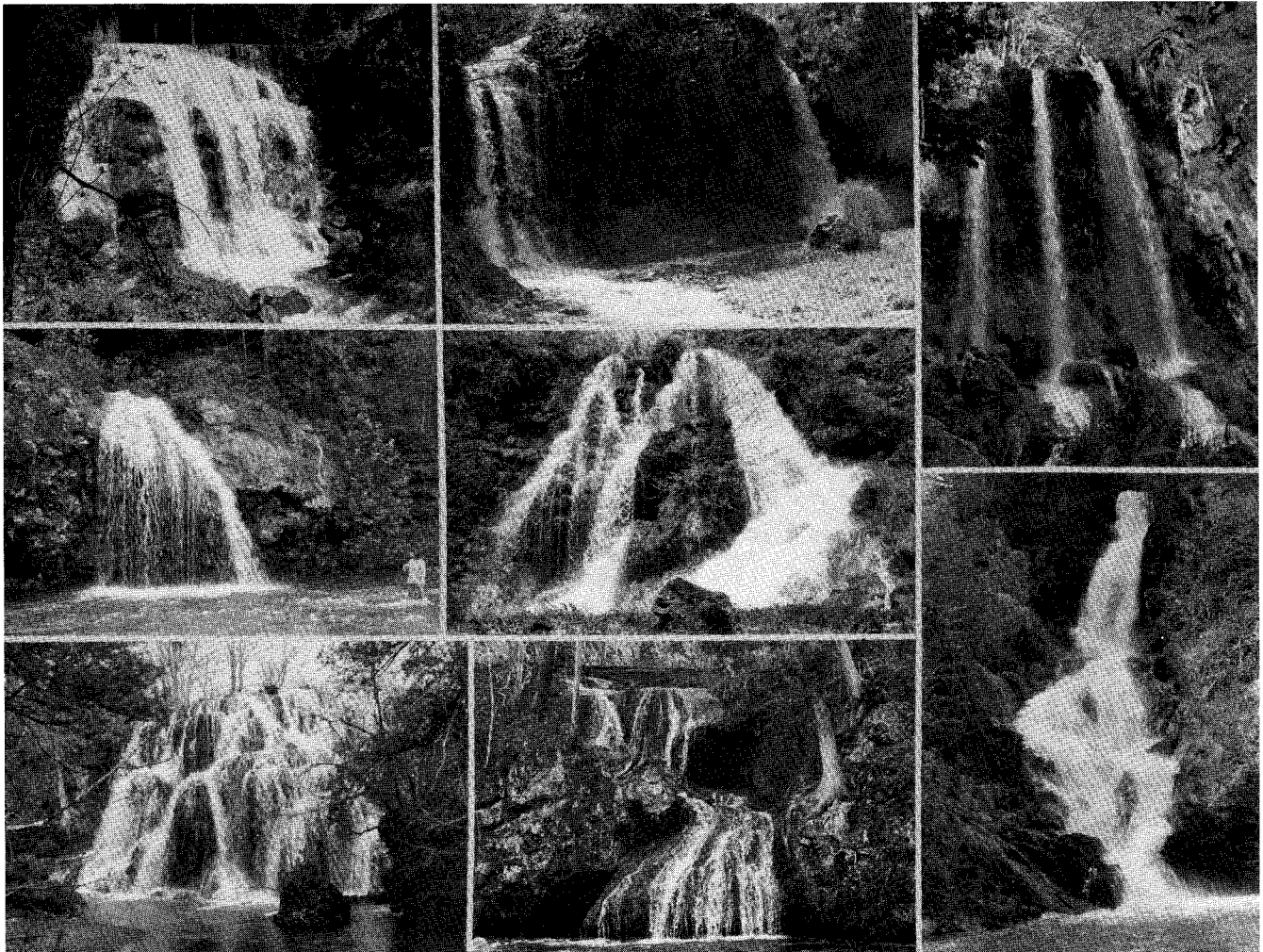


VIRGINIA DIVISION OF MINERAL RESOURCES
PUBLICATION 101

TRAVERTINE-MARL: STREAM DEPOSITS IN VIRGINIA

Janet S. Herman and David A. Hubbard, Jr., editors



COMMONWEALTH OF VIRGINIA

**DEPARTMENT OF MINES, MINERALS AND ENERGY
DIVISION OF MINERAL RESOURCES**

Robert C. Milici, State Geologist

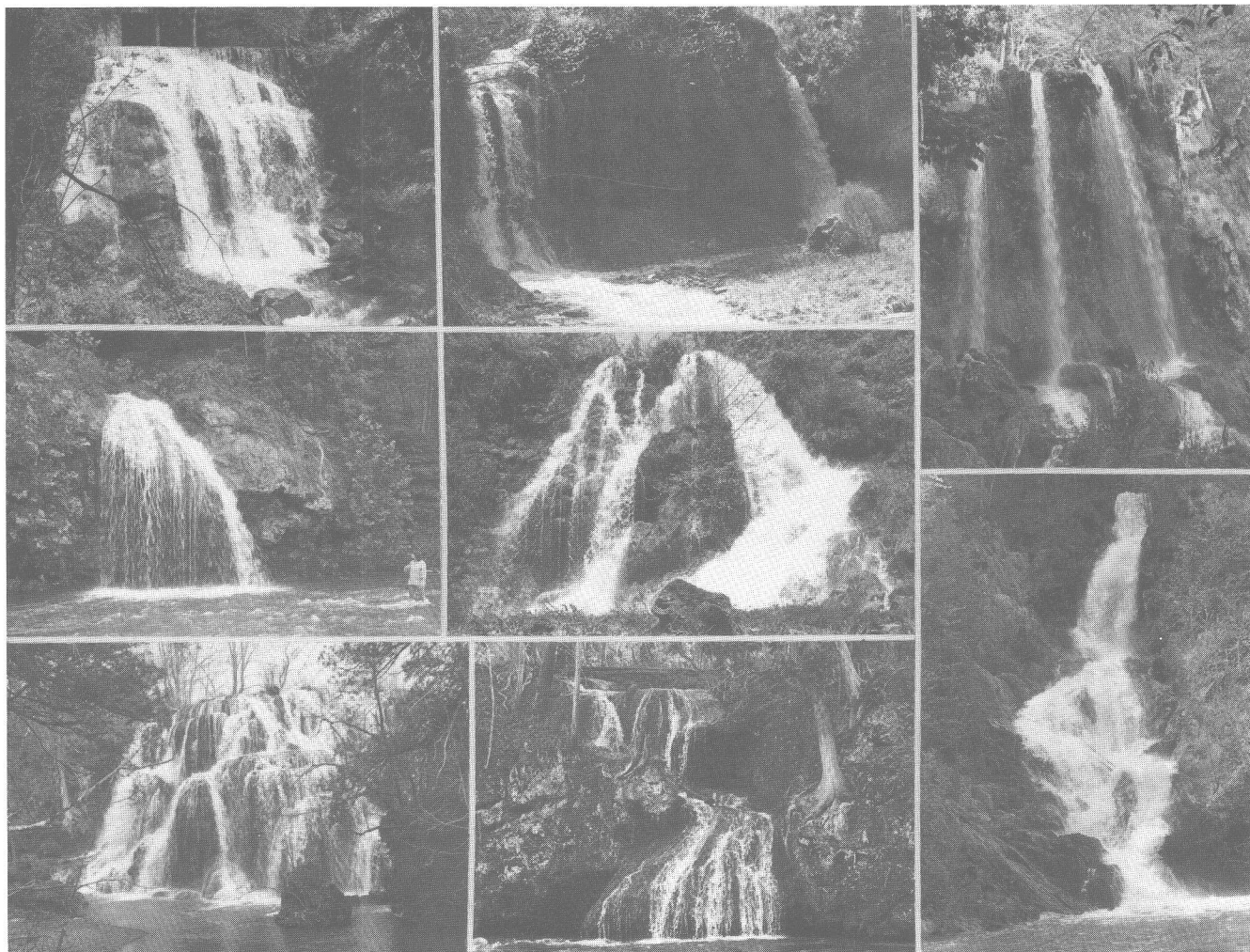
CHARLOTTESVILLE, VIRGINIA

1990

VIRGINIA DIVISION OF MINERAL RESOURCES
PUBLICATION 101

TRAVERTINE-MARL: STREAM DEPOSITS IN VIRGINIA

Janet S. Herman and David A. Hubbard, Jr., editors



COMMONWEALTH OF VIRGINIA

DEPARTMENT OF MINES, MINERALS AND ENERGY
DIVISION OF MINERAL RESOURCES

Robert C. Milici, State Geologist

CHARLOTTESVILLE, VIRGINIA

1990

FRONT COVER: Travertine waterfalls of Virginia, clockwise from top left photograph; waterfall (about 8.5 m) at the crossing of State Road 706 and Marl Creek near Riverside, Rockbridge County; Glenn Falls, twin falls (about 6 m) along Marl Creek near Steeles Tavern in Rockbridge County; 21-m waterfall, severely damaged during Hurricane Camille, on Moores Creek, Rockbridge County; Falling Spring Falls (about 21 m) along Falling Spring Creek, Alleghany County, J. S. Herman in lower left forefront; western-most terminal cascade (about 7.5 m) of Falling Spring Run at its junction with Middle River in Augusta County; Beaverdam Falls (about 8.5 m) on Sweet Springs Creek at its junction with Dunlap Creek, Alleghany County; northern-most of the Cypress Falls of Sheep Creek at its junction with South River, Rockbridge County, M. M. Lorah in right forefront; center photograph, Marlbrook Falls (about 10.5 m) along Marlbrook Creek, Rockbridge County (Photographs by David A. Hubbard, Jr.).

Please note that all of these waterfalls are on private property and permission must be obtained before visiting them.

VIRGINIA DIVISION OF MINERAL RESOURCES
PUBLICATION 101

TRAVERTINE-MARL: STREAM DEPOSITS IN VIRGINIA

Janet S. Herman and David A. Hubbard, Jr., editors

COMMONWEALTH OF VIRGINIA

DEPARTMENT OF MINES, MINERALS AND ENERGY
DIVISION OF MINERAL RESOURCES

Robert C. Milici, State Geologist

CHARLOTTESVILLE, VIRGINIA

1990

DEPARTMENT OF MINES, MINERALS AND ENERGY
RICHMOND, VIRGINIA
O. Gene Dishner, Director

Copyright 1990, Commonwealth of Virginia

Portions of this publication may be cited if credit is given to the Virginia Division of Mineral Resources.

PREFACE

The Appalachian Valley and Ridge province in Virginia, West Virginia, Maryland, and Pennsylvania has proven to be a fertile environment for developing our knowledge of the geology of travertine-marl. The deposits of travertine in Virginia, fascinating in their form and in the variety of processes that they represent, have stimulated our own research efforts for several years. We discovered that other people were similarly engaged in research on various aspects of travertine-marl, and we have learned a great deal from them through informal contacts and from their widely scattered publications. A few years ago, we decided that the scientific community, including both specialists and generalists, could benefit from the broad experience of investigators who have studied travertine-marl in the mid-Atlantic region and began to assemble a comprehensive collection of papers. To ensure broad topical coverage of the varied aspects of travertine-marl research, we also invited contributions from authors working on similar deposits in other localities. The result of the endeavor is this volume of contributed papers.

We relied heavily upon our friends and colleagues to help in the preparation of this volume. Of course the major effort was made by the authors who not only wrote manuscripts but also participated in discussions with us, educated us, and reviewed each other's contributions. We thank every one of the 21 authors for their enthusiasm for this project and for their patience with our editing.

A number of other peers supported our project through their thoughtful reviews of the manuscripts; we thank Michael B. Barber, Charles S. Bartlett, Jr., Marilyn J. Bradley, F. Howard Campbell, III, Dennis Curry, Richard V. Dietrich, Carol A. Hill, George M. Hornberger, Alan D. Howard, Walton R. Kelly, Donald C. Le Van, Aaron L. Mills, Jack E. Nolde, Bruce C. Parker, Eugene K. Rader, Sarah C. Tremaine, Michael L. Upchurch, William C. Ward, Carol M. Wicks, and Warren W. Wood. We frequently called upon George Hornberger, Dave Lasch, Aaron Mills, and Gene Rader for editorial advice and learned much in the process.

Beyond these individuals, many others have made contributions to educating us, to stimulating our interest in travertine-marl research, and to supporting our efforts to assemble this volume. Without all their help, preparation of this volume would not have been possible.

Janet S. Herman
David A. Hubbard, Jr.

Charlottesville, Virginia
April 1990

TRAVERTINE-MARL: STREAM DEPOSITS IN VIRGINIA

EDITED BY

Janet S. Herman¹ and David A. Hubbard, Jr.²

CONTENTS

	Page
Overview of travertine-marl volume, by David A. Hubbard, Jr. and Janet S. Herman.....	1
A CO ₂ outgassing model for Falling Spring Run, Augusta County, Virginia, by Kimberly J. Hoffer-French and Janet S. Herman.....	5
Geochemical evolution and calcite precipitation rates in Falling Spring Creek, Virginia, by Michelle M. Lorah and Janet S. Herman.....	17
The geology and geochemistry of the Falls Hollow travertine deposit, by Carl S. Kirby and J. Donald Rimstidt.....	33
A comparative study of travertine-marl-depositing streams in Virginia, by Janet S. Herman and David A. Hubbard, Jr.....	43
Petrology of Quaternary travertine deposits, Arbuckle Mountains, Oklahoma, by Karen M. Love and Henry S. Chafetz.....	65
The geology of the Falling Spring travertine deposit, Alleghany County, Virginia, by Kristin O. Dennen, Richard J. Diecchio, and Mark A. Stephenson.....	79
A commercial marl deposit near Winchester, Virginia, by William F. Giannini.....	93
Travertine-marl deposits and prehistoric archaeological association, by William M. Gardner.....	101
Dating travertine, by Henry P. Schwarcz.....	113
The algal flora of travertine: an overview, by Allan Pentecost.....	117
Economic legacy and distribution of Virginia's Valley and Ridge province travertine-marl deposits, by Palmer C. Sweet and David A. Hubbard, Jr.....	129
The morphology and stratigraphy of calcareous sediments in a small alluvial-colluvial fan, New Creek Mountain, Mineral County, West Virginia, by J. Steven Kite and D. Mark Allamong.....	139
Description and origin of the calcite-rich Massanetta Variant Soil Series at Mount Crawford, Virginia, by E. Randolph McFarland and W. Cullen Sherwood.....	151
Influence of CaCO ₃ dissolution and deposition on flood plain soils in the Valley and Ridge province, by William J. Edmonds and David C. Martens.....	163
Speleogenesis in a travertine scarp: observations of sulfide oxidation in the subsurface, by David A. Hubbard, Jr., Janet S. Herman, and Pamela E. Bell.....	177

¹Department of Environmental Sciences, Clark Hall, University of Virginia, Charlottesville, VA 22903

²Virginia Division of Mineral Resources, P.O. Box 3667, Charlottesville, VA 22903

OVERVIEW OF TRAVERTINE-MARL VOLUME

David A. Hubbard, Jr.¹ and Janet S. Herman²

CONTENTS

	Page
Definition of terms.....	1
Travertine-marl deposits and how they form.....	1
Papers presented in this volume.....	2
Contemporary and suggested travertine-marl research.....	3
References cited.....	4
Glossary.....	4

DEFINITION OF TERMS

The freshwater carbonate deposits of Virginia are predominantly found in the Valley and Ridge physiographic province. The majority of these deposits were precipitated by spring and stream waters and can be subdivided into two groups: carbonate materials deposited in the subsurface in caves or carbonate materials precipitated by surficial waters. The papers in this volume on travertine-marl focus on various aspects of the surficial carbonate deposits.

Calcareous materials deposited by spring and stream waters have been variously termed calcareous sinter, calcareous tufa, calc-tufa, marl, spring-sinter, travertine, tufa, and tufaceous marl. The American Geological Institute Glossary (Gary and others, 1972) lists calcareous tufa as a redundant form of the term tufa, which is defined as "A chemical sedimentary rock composed of calcium carbonate, formed by evaporation as a thin, surficial, soft, spongy, cellular or porous, semifriable incrustation around the mouth of a hot or cold calcareous spring or seep, or along a stream carrying calcium carbonate in solution It may also be precipitated by algae or bacteria." Travertine is defined as "A hard, dense, finely crystalline, compact or massive but often concretionary limestone, of white, tan, or cream color, often having a fibrous or concentric structure and splintery fracture, formed by rapid chemical precipitation of calcium carbonate from solution in surface and groundwaters, as by agitation of stream water or by evaporation around the mouth or in the conduit of a spring (esp. of a hot spring)." In Virginia, these carbonate materials are more accurately described as precipitates from spring or stream waters supersaturated with respect to calcium carbonate. In an attempt "to avoid semantic confusion," Julia (1983) suggests the use of the term travertine for freshwater "carbonate incrustations on plant remains

(in place and debris) without reference to the pore volume or density." Marl is defined as "An old term loosely applied to a variety of materials most of which occur as soft, loose, earthy, and semifriable or crumbling unconsolidated deposits consisting chiefly of an intimate mixture of clay and calcium carbonate in varying proportions, formed under either marine or esp. freshwater conditions" (Gary and others, 1972). Freshwater carbonate materials have been collectively referred to as marl by commercial operators who mined it for use as agricultural lime. The phrase "deposits of travertine marl" was used as early as 1837 by Rogers (1884) to describe stream-deposited carbonate materials for an annual report of the Geologic Survey of the State of Virginia for the State legislature. The term travertine-marl is herein advocated for general use in reference to surficial freshwater carbonate materials deposited by spring and stream water. The use of the terms marl, travertine, or tufa are appropriate when these specific components are discussed (see the glossary appended to this paper). Most of the sixty known calcareous stream deposits in Virginia contain various proportions of marl, travertine, and tufa.

TRAVERTINE-MARL DEPOSITS AND HOW THEY FORM

A considerable range in morphology is exhibited by the travertine-marl deposits of Virginia. Extensive low-relief deposits dominated by marl are typical of the sites in the northern portion of the Valley and Ridge province. Travertine buildups, forming bluffs or falls in active stream channels, are notable components in most deposits throughout the State (see cover photograph). Some deposits contain extensive broad accumulations of marl upstream from travertine

¹Virginia Division of Mineral Resources, P.O. Box 3667, Charlottesville, VA 22903

²Department of Environmental Sciences, Clark Hall, University of Virginia, Charlottesville, VA 22903

buildups. Mining of marl has altered the morphology of some deposits and resulted in a series of dissociated travertine buildups along a stream valley. Most travertine-marl deposits are recognized only because of the waterfalls created by travertine buildups in the stream channel. The marl accumulations upstream from these depositional structures are typically obscured by vegetation and soil development, but they may be exposed in the banks of entrenched streams.

The active deposition of calcite is often observed seasonally from late spring to fall. Deposition most commonly occurs as encrustations on organic surfaces, such as plants and their debris, and on inorganic surfaces, such as rock, in and along the stream or spring. The deposition of travertine-marl is highly variable both within individual sites and between different sites. Erosion appears to be exceeding accretion at the majority of Virginia's travertine-marl deposits. Marl accumulations are entrenched by streams and have developed soil profiles. Most travertine buildups are notched by the current stream channel. During high-flow events, erosive stream water can destroy travertine-marl features.

A generalized depositional model describes the development of many of these deposits (Hubbard and others, 1985). Rain water percolating through soil overlying carbonate rock dissolves CO_2 concentrated in the soil by plant root respiration and the microbial decomposition of organic matter. The high CO_2 content of the percolating water greatly increases the amount of CaCO_3 the water can dissolve. The CO_2 -rich water migrates through fractures in folded or faulted carbonate rock, and the groundwater approaches equilibrium with respect to calcite. Upon emergence from the ground as a discrete spring or as diffuse flow through a stream bed, water with an elevated level of dissolved CO_2 is driven toward equilibrium with the lower atmospheric CO_2 level. The rate of CO_2 outgassing from spring or stream water is influenced by the level of supersaturation with respect to CO_2 and the degree to which the water is agitated. Carbon dioxide outgassing results in supersaturation with respect to calcite and its subsequent precipitation in the form of travertine-marl. Travertine buildups further increase the agitation of the water and provide surfaces for calcite deposition and for growth of biologic substrates such as algae and mosses. Organic debris also provide significant surface area for calcite deposition.

Calcareous sediments accumulate upstream from aggrading travertine buildups. The aggrading stream bed forces the stream to migrate across the valley and form a broad, flat, valley bottom upstream from the lateral travertine dam structure. A series of these features result in a step-like stream valley alternating between low-gradient, broad segments of accumulated sediments and laterally transecting high-gradient cascade-bluff structures of travertine.

During the last two centuries the burial of travertine-marl deposits by noncarbonate alluvium has increased as a result of agricultural practices. The higher levels of noncarbonate sediment have diluted the carbonate mineral content of the travertine and associated marl deposited during this time.

Man-made modifications of the landscape have increased runoff and the magnitude of flooding. The combination of higher water flows with greater fractions of noncarbonate sediment has increased the erosiveness of the streams. Abrasive sediment-laden flood water erodes travertine buildups and incises marl accumulations.

PAPERS PRESENTED IN THIS VOLUME

Interest in surficial travertine-marl deposits in and around Virginia over the past decade has resulted in a number of research projects. The 15 invited papers in this volume report the results of some of those research projects and include several papers on aspects of travertine-marl research conducted outside of Virginia.

Some of the reported research focuses on the hydrogeochemical origins of travertine-marl deposits. The process of CO_2 outgassing along Falling Spring Run, Augusta County, is related to the stream-water chemistry and the hydrological agitation imparted by the stream channel morphology. The outgassing model presented by Hoffer-French and Herman describes how the stream water is driven to high degrees of supersaturation with respect to calcite and subsequently precipitates calcite. The relationship between CO_2 outgassing and calcite precipitation is quantitatively examined by Lorah and Herman. Their study of Falling Spring Creek, Alleghany County, utilized computerized geochemical models to calculate aqueous speciation and saturation indices, PCO_2 values, and mass transfer of CO_2 and calcite. Calcite precipitation rates calculated from the mass transfer results and from a published rate law are considered to be more accurate than rates obtained from growth on calcite seed crystals placed in the creek. Kirby and Rimstidt conducted a geochemical study of a travertine-depositing stream that apparently is fed by diffuse groundwater in Falls Hollow, Montgomery County. They report the greatest degassing of CO_2 occurs upstream from the waterfall and calcite precipitation is localized at the waterfall. Using assumptions of a constant stream discharge, a constant rate of CaCO_3 precipitation, no loss of travertine to erosion, and an estimated volume of travertine, these researchers have estimated a conservative age of 5500 years for the deposit. A comparative geochemical study of travertine-marl and its associated stream or spring water is presented by Herman and Hubbard. The calcium- and bicarbonate-rich water is similar in composition for each of the 12 study sites and the composition at each site changes in the downstream direction as a result of CO_2 outgassing and concomitant increases in pH and, ultimately, calcite precipitation. Stream-associated active travertine-marl generally has a smaller ratio of calcium carbonate to the noncarbonate fraction than does the erosionally isolated older travertine-marl.

The detailed petrographic study of travertine deposits in the Arbuckle Mountains of Oklahoma by Love and Chafetz

provides insight to Virginia travertine deposits. Observations of the morphology, texture, and inorganic and organically associated constituents of travertine enabled them to discuss the formation and diagenesis of the deposits.

Comprehensive examination of travertine-marl deposits are reported in the two generalized site studies in this volume. Dennen, Diecchio, and Stephenson evaluated the geologic setting of the travertine-marl deposit along Falling Spring Creek, Alleghany County. Within a geological context, hydrological and geochemical factors are shown to control the geomorphic evolution of the site. A discussion of a commercially utilized deposit of marl along Redbud Run in Frederick County is presented by Giannini. In addition to the economic history of the deposit, paleontological aspects and archaeological age associations are presented.

A number of papers examine specific aspects of travertine-marl deposits. Archaeological associations with these deposits are discussed by Gardner. The Darlington travertine-marl deposit located along Redbud Run in Frederick County was overlain and underlain by datable archaeological artifacts, and the reported dates span a range from 500 B.C. to 200 A.D. and 7200 to 6800 B.C., respectively. In addition to the dating by archaeological associations (Gardner, Giannini) and by precipitation rates (Kirby and Rimstidt), travertine may be datable by a number of other techniques. Radio-carbon, uranium series, electron spin resonance, and thermoluminescence techniques are among the dating methods described in a review paper by Schwarcz. A comparative discussion of the algal biota found worldwide is advanced by Pentecost. Biota from sample identifications as well as the literature are described. The abundant and diverse algal flora is hypothesized to play an active role in the deposition of travertine. A compendium of the commercial utilization of travertine-marl deposits in Virginia is documented by Sweet and Hubbard. Available production figures and operational details are arranged by county. The morphology and stratigraphy of a calcareous alluvial-colluvial fan along an unnamed tributary of New Creek in Mineral County, West Virginia, are described by Kite and Allamong. This unusual fan is developed along a mountain stream that receives little coarse colluvium. Recent incision of the deposit, dated by tree ring studies, is thought to be a result of local adjustment to the truncation of the fan. A carbonate mineral-rich soil, the Massanetta Variant Soil Series, is described by McFarland and Sherwood. They describe this Rockingham County deposit, situated along an unnamed tributary of the North River, and present several theories on its origin. Soil properties and classification are influenced by the secondary dissolution and deposition of calcite in the travertine-marl-soil profile according to the study of Edmonds and Martens. Secondary deposition of calcite results in the occlusion of micronutrients and the formation of insoluble phosphorous compounds in travertine-marl bearing soil near the confluence of Spout Run and the Shenandoah River in Clarke County. Sulfide oxidation is advanced as a contributory proc-

ess in the genesis of Cesspool Cave in a Quaternary travertine-marl deposit along Sweet Springs Creek, Alleghany County. The pools and stream in this cave contain three genera of sulfur-oxidizing bacteria that are apparently utilizing the sulfide that enters the cave as H_2S in the rising spring water. Cave formation is occurring as the result of dissolution by stream water and by H_2S -rich water films on walls and ceiling.

CONTEMPORARY AND SUGGESTED TRAVERTINE-MARL RESEARCH

The research reported in the 15 articles in this volume encompasses many topics of travertine-marl investigations. This comprehensive volume includes all of the studies of travertine-marl in Virginia that were made available to the editors. A few aspects of research that have been pursued are not addressed in these 15 articles.

Travertine-marl deposits have been examined in two physiographic regions of Virginia. In addition to the major sites in the Valley and Ridge province, deposits exist in the Coastal Plain province. Burmester (1987) has characterized a deposit of travertine at Burwell Bay, Isle of Wight County. Travertine precipitation occurs at springs and seeps. The high levels of dissolved $CaCO_3$ in the groundwater are the result of the dissolution of calcareous shells in the Moore House member of the Yorktown Formation.

Although numerous papers in the volume note the association of travertine-marl deposits with faults, none of the papers discuss this relationship in detail. Thornton and Gold (Thornton and others, 1987) have examined deposits associated with faults and lineaments in Virginia and Pennsylvania. They hypothesize that the fault zones are the source of $CaCO_3$ -saturated water that derives from contact with crushed limestone created during movement on the faults. Because of the generally young age of the travertine deposits relative to the origin of the faults, they conclude that recent movement along the faults is indicated and datable by the resulting travertine buildups.

All of the travertine-marl deposits discussed in this volume as well as all of those in Virginia known to the editors are surficial deposits. The various dating methods which have been employed on a few of these deposits indicate that they are of recent age. It is not likely that stream-deposited travertine-marl older than the Quaternary will be found because of the lack of preservation of that type of deposit in the older sedimentary rocks in Virginia. The recognition of pre-Quaternary travertine-marl could prove difficult, especially if it has undergone diagenetic alteration.

Two soils associated with travertine-marl are discussed in this volume. The current soil classification does not clearly identify travertine-marl as a primary or parent material. Apparently a primary travertine-marl material can undergo

dissolution and reprecipitation during soil forming processes that obscure the identity of the parent material to observers unfamiliar with these deposits. The soil classification does not distinguish between soils with high contents of calcium carbonate whether they are primarily the result of caliche formation, associated with marl precipitated in lakes, or derived from travertine-marl deposited in streams.

The published hydrochemical studies of travertine-depositing streams in Virginia rely on inorganic geochemistry. Very little work has been conducted with the stable isotopes ^{13}C , ^{18}O , and ^2H , even though the utility of these isotopes is great. The study of stable isotopes can provide information about the chemical, climatological, and hydrological processes during the genesis of travertine-marl. Isotopes also can be used as conservative tracers to verify models of equilibrium or kinetic reactions.

A few of the papers in this volume intimated that the role of flora in the deposition of travertine-marl is poorly understood. Whether the flora serve only as a substrate or if biological processes actively drive the deposition of travertine-marl has not been resolved. The study of the flora and fauna preserved in these deposits has only been briefly touched upon in this volume. Ecological and climatological information could be obtained from appropriate paleontological investigations of the Quaternary travertine deposits in Virginia.

The papers in this volume present the current state of research on travertine-marl in Virginia. These results and ideas should be more fully compared to research on stream-deposited travertine-marl and lake-deposited travertine and marl in other regions of the world. The full geological significance of travertine-marl deposits can be realized only if knowledge of the major environments and processes influencing its formation are integrated.

REFERENCES CITED

- Burmeister, J. L., 1987, A travertine deposit on the Coastal Plain in Isle of Wight County, Virginia [unpublished senior thesis]: Williamsburg, Virginia, College of William and Mary, 55 p.
- Gary, Margaret, McAfee, Robert, Jr., and Wolf, C. L., eds., 1972, Glossary of geology: Washington, D. C., American Geological Institute, 805 p.
- Hubbard, D. A., Jr., Giannini, W. F., and Lorah, M. M., 1985, Travertine-marl deposits of the Valley and Ridge province of Virginia - a preliminary report: Virginia Division of Mineral Resources, Virginia Minerals, v. 31, n. 1, p. 1-8.
- Julia, Ramon, 1983, Travertines, in Scholle, P. A., Bebout, D. G., and Moore, C. H., eds., Carbonate depositional environments: Tulsa, Oklahoma, The American Association of Petroleum Geologists Memoir 33, p. 64-72.
- Rogers, W. B., 1884, A reprint of annual reports and other papers, on the geology of the Virginias: New York, New York, D. Appleton and Company, 832 p.
- Thomton, C. P., Gold, D. P., and Herman, J. S., 1987, Tufa/marl deposits as indicators of neotectonic activity [abs.]: Norfolk, Virginia, Geological Society of America Abstracts with Programs, v. 19, n. 2, p. 133.

GLOSSARY *

calcareous sinter Travertine.

calcareous tufa Tufa.

calc-tufa Tufa.

marl Soft, loose, earthy, and semifriable or crumbling unconsolidated deposits consisting chiefly of a mixture of clay and calcium carbonate in varying proportions, formed chiefly in freshwater conditions; content can vary from a minimum of 35 percent to almost pure calcium carbonate. The term has been used commercially to apply to all spring- or stream-deposited freshwater carbonate materials including travertine and tufa.

spring-sinter Travertine.

tophus Tufa.

travertine Hard, dense, finely crystalline, compact or massive but often concretionary limestone, of white, tan, or cream color, often having a fibrous or concentric structure and splintery fracture, formed by rapid chemical precipitation of calcium carbonate from solution in surface or groundwater by agitation of stream water or other means of outgassing of CO_2 around a spring or along a stream. It may also be precipitated by or on bacteria or algae and on other plants, organic or inorganic substrate. The cellular or less compact variety is tufa.

travertine-marl Generalized term for freshwater spring or stream deposits comprised of various intermixtures of marl, travertine, and tufa.

tufa Chemical sedimentary rock composed of calcium carbonate; formed by precipitation or to a lesser degree evaporation as a thin surficial, soft, spongy, cellular or porous semifriable incrustation around or along a spring or stream. It may also be precipitated by or on bacteria or algae and on other plants or organic debris. The hard, dense variety is travertine.

tufaceous marl Tufa or travertine.

*terms modified from Gary and others (1972).

A CO₂ OUTGASSING MODEL FOR FALLING SPRING RUN, AUGUSTA COUNTY, VIRGINIA

Kimberly J. Hoffer-French¹ and Janet S. Herman²

CONTENTS

	Page
Abstract.....	6
Introduction.....	6
Location and description of study site.....	7
Methods.....	8
Field methods and sample collection.....	8
Laboratory methods.....	8
Data analysis.....	9
Saturation state calculations.....	9
Mass transfer calculations.....	9
Reaction rate calculations.....	9
Results.....	9
Stream hydrology.....	9
Stream chemistry.....	10
Discussion.....	13
Conclusions.....	13
Acknowledgments.....	14
References cited.....	14

ILLUSTRATIONS

Figure

1. Topographic map of study area showing locations of travertine cascades and water sample collection points.....	7
2. Schematic cross section of travertine terraces along Falling Spring Run.....	8
3. Average shear stress at the second cascade versus distance.....	10
4. Flow velocity at the second travertine cascade versus distance.....	10
5. Millimolar Ca ²⁺ concentration versus distance.....	10
6. Millimolar HCO ₃ ⁻ concentration versus distance.....	10
7. pH versus distance.....	11
8. CO ₂ outgassing rates between sampling points versus distance.....	12
9. Calcite precipitation rates between sampling points versus distance.....	12

TABLES

Table

1. Raw chemical concentration data for samples from Falling Spring Run collected on July 21, 1985	11
2. Theoretical partial pressure of carbon dioxide gas and calcite saturation indices	11
3. Calculated mass transfers and reaction rates	12

¹ 106 East Main Street, Leola, PA 17540

² Department of Environmental Sciences, Clark Hall, University of Virginia, Charlottesville, VA 22903

ABSTRACT

The travertine dams found along Falling Spring Run in Augusta County, Virginia, are formed through the interplay between the chemical composition of the stream water and the earth's atmosphere. A positive feedback also exists between the solution composition of the stream water and the physical morphology of the channel. Carbon dioxide outgasses from the supersaturated stream in response to the chemical gradient between the solution and the atmosphere. At the cascade sections of the stream, CO₂ outgassing is enhanced by hydrological agitation and dispersion of the water. Outgassing drives the solution to high degrees of supersaturation with respect to calcite. Yet, calcite precipitation is kinetically inhibited until the solution reaches at least five times supersaturation. Precipitation is pronounced at the cascades as a result of the rapid loss of CO₂ and a reduced kinetic inhibition to precipitation. Kinetic inhibition is less at the travertine dams due to the availability of nucleation sites and the presence of mosses and algae which provide fresh surfaces for crystal growth. Outgassing is the fundamental process that drives calcite precipitation and hence the formation of travertine dams at Falling Spring Run.

INTRODUCTION

Travertine, a sedimentary rock composed of calcite precipitated from freshwater, is commonly found in localized deposits along river and stream channels. These deposits may range in scale from rimstone dams measuring only millimeters in height to massive buildups with waterfalls cascading over a hundred meters. Falling Spring Run in Augusta County, Virginia, is a small travertine-depositing stream with a series of cascades that offer an excellent field site to study some of the chemical and physical processes contributing to the formation and localization of travertine dams. This paper focuses on the process of CO₂ outgassing and uses chemical and hydrological observations to explain the feedback mechanism that exists between the composition of the solution and the morphology of the stream channel.

Travertine deposits typically form at, or downstream from, sites where carbonate groundwaters emerge as springs (Chafetz and Folk, 1984; Hubbard and others, 1985). The partial pressure of carbon dioxide (PCO₂) in such groundwater is usually greater than levels in the atmosphere. Pearson and others (1978) report that partial pressures of CO₂ in groundwater can range from 10 to 100 times greater than the atmospheric value of 10^{-3.5} atm. When groundwater supersaturated with CO₂ emerges as a spring, CO₂ is outgassed in an attempt to equilibrate with atmospheric CO₂ (Pearson and others, 1978). Physical obstructions to flow and steep stream gradients enhance CO₂ outgassing along the channel (Chafetz

and Folk, 1984; Herman and Lorah, 1987). Outgassing was quantified along a well-defined travertine-depositing stream (Lorah and Herman, 1988 and this volume) where 10- to 30-fold increases in the rate of loss of CO₂ were reported at a 20-m-high waterfall. Lower rates of CO₂ outgassing were reported for stretches of less turbulent water downstream from the waterfall.

As CO₂ is lost from solution, the equilibrium solubility of calcite decreases, the solution becomes supersaturated with respect to calcite, and precipitation of the mineral may occur. The importance of CO₂ exchange in driving the precipitation process has been stressed by many investigators of calcite-precipitating streams (for example, Barnes, 1965; Hubbard and others, 1985; Herman and Lorah, 1987). Lorah and Herman (1988) documented the direct relationship between CO₂ outgassing and calcite precipitation. At least two other studies have reported that the greatest loss of Ca²⁺ from solution occurred at points along a channel where water velocities were the most rapid and outgassing was presumably greatest (Jacobson and Usdowski, 1975; Dandurand and others, 1982). Amundson and Kelly (1987) noted that the largest reductions in Ca²⁺ concentrations occurred where the stream gradient increased dramatically as the stream flowed over the steep face of a travertine terrace, although flow velocity and CO₂ partial pressures were not determined. Kirby and Rimstidt (this volume) report the largest decreases in PCO₂ and greatest calcite precipitation they observed were localized at a 15-m-high waterfall.

Calcite precipitation does not occur immediately as the solution reaches supersaturation due to kinetic inhibition (Jacobson and Usdowski, 1975; Usdowski and others, 1979; Dandurand and others, 1982; Suarez, 1983; Amundson and Kelly, 1987; Herman and Lorah, 1988). Calcite precipitation in two surface streams did not begin until at least five or ten times supersaturation was reached (Jacobson and Usdowski, 1975; Dandurand and others, 1982). One study reports calcite precipitation at four times supersaturation in a warm spring-fed stream (Herman and Lorah, 1988; Lorah and Herman, this volume), while another reports that no notable precipitation was found in the Colorado River even at six times supersaturation (Suarez, 1983). These studies reveal the complexity of calcite reaction kinetics in surface streams.

The main purpose of the present study is to gain a better understanding of the physicochemical processes that influence CO₂ exchange and drive calcite precipitation in a travertine-depositing stream. The effect of stream hydrology, especially hydrological agitation, on the processes of CO₂ outgassing and calcite precipitation is assessed. Previous investigators of calcite-precipitating streams have noted that CO₂ exchange influences calcite precipitation, although the relationship was not always substantiated and the underlying causes not clearly defined. This field study focuses on quantitatively defining the chemical changes occurring in a carbonate stream as they are influenced by stream hydrology.

LOCATION AND DESCRIPTION OF STUDY SITE

The field site of the present study is located in central Augusta County, Virginia. The area lies entirely within the Shenandoah Valley of the Valley and Ridge physiographic province. The region is underlain by folded and faulted limestone and dolomite of Cambrian and Ordovician age, including the Conococheague, Elbrook, and Beekmantown formations (Rader, 1967).

Falling Spring Run is a small spring-fed stream. Two large carbonate-rich springs, issuing downstream from a regional fault along the southeast limb of the Middlebrook anticline, provide most of the stream discharge. The studied section of Falling Spring Run begins at the downstream spring (Figure 1). From this point the stream flows approximately 2.5 km before it spills into the Middle River. Over most of its course, the channel is less than 5 m wide and 30 cm deep. The stream divides to form two distinct forks in the

final 240 m; both forks flow over a travertine scarp into the Middle River (see cover, bottom middle photograph is western-most terminal cascade). At least two additional sources of small amounts of discharge are located along the flow path. A small spring is located just downstream from the first cascade and a spring-fed tributary enters Falling Spring Run downstream from the second cascade.

Three distinct travertine-marl terraces have developed along the course of Falling Spring Run (Figure 2). The terraces form a gently sloping topography bounded by the steeper faces of the travertine cascades on the ascending and descending sides. The first cascade is man-made and is located 0.080 km downstream from the beginning of the studied section. The other three cascades are travertine buildups. The entire travertine-marl deposit is reported by Collins (1924) to extend for approximately 1.6 km along the stream and to have a maximum width of 135 m, thus underlying over 16 hectares of meadowland. The series of cascade and terrace deposits rise over 40 m above the Middle River.

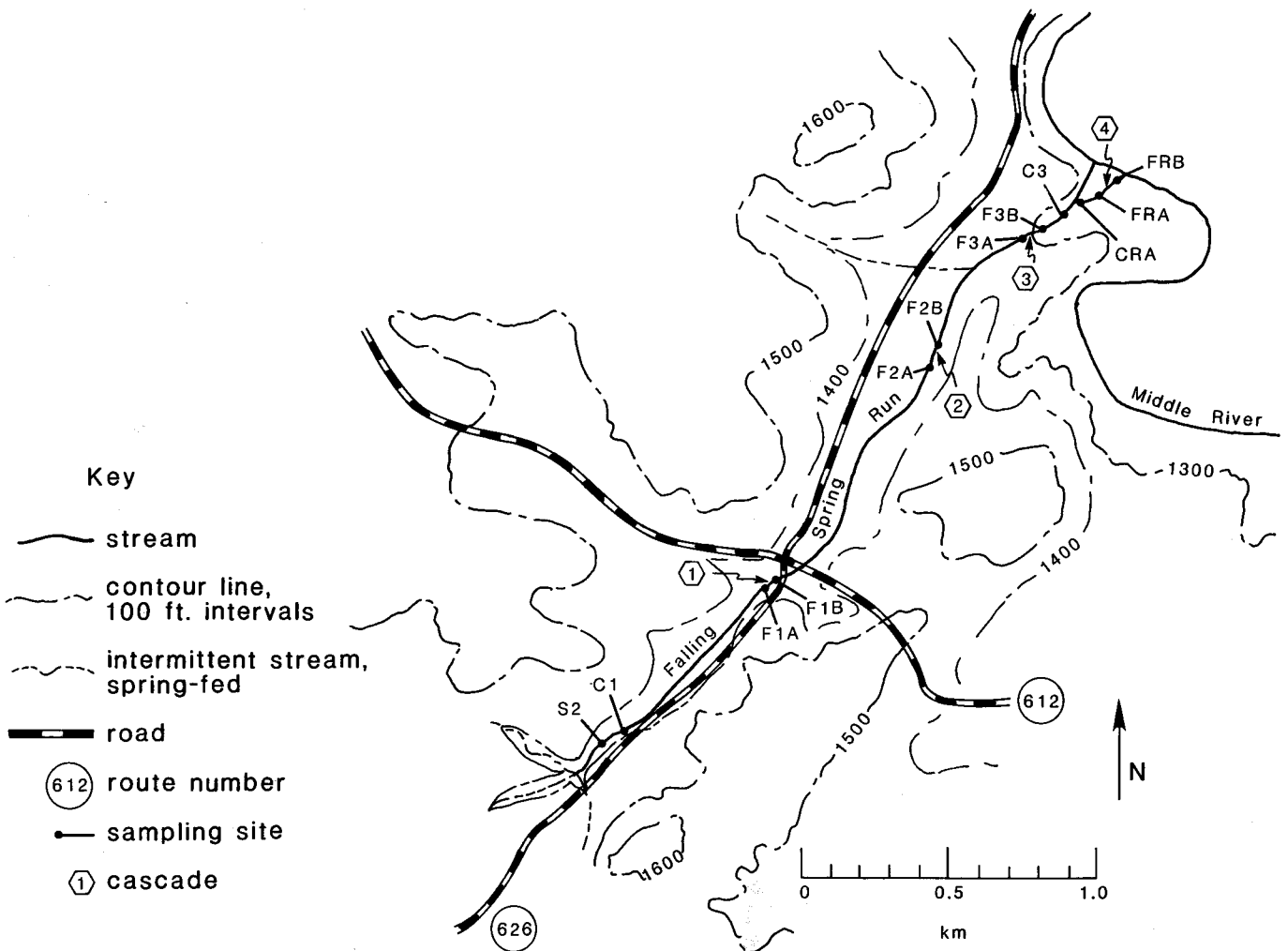


Figure 1. Topographic map of study area showing locations of travertine cascades and water sample collection points along Falling Spring Run.

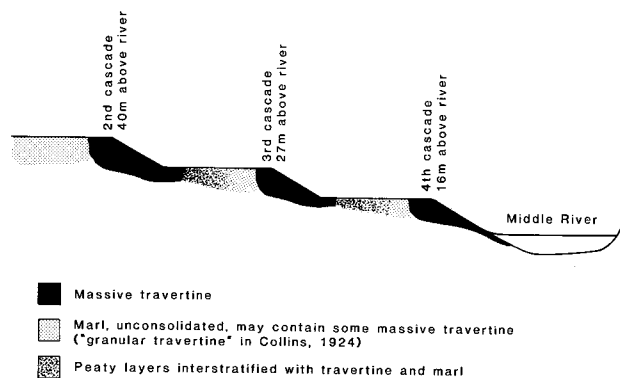


Figure 2. Schematic cross section of travertine terraces along Falling Spring Run (sketch not to scale; after Collins, 1924). The first cascade (F1A-F1B) is farther upstream and does not appear on this figure.

METHODS

FIELD METHODS AND SAMPLE COLLECTION

Water samples were collected from 12 stations along Falling Spring Run (Figure 1) on July 21, 1985. Sampling sites included one of the springs (S2), a smooth stretch of stream above the first cascade (C1), at the crest and base of each of the four cascades (F1A and F1B, F2A and F2B, F3A and F3B, FRA and FRB), a smooth section below the third cascade (C3), and above the fourth cascade on the easternmost fork (CRA).

Samples for analysis of major ions were collected in acid-washed 250-mL polyethylene bottles. Acid-washed 250-mL dissolved-oxygen bottles with ground glass stoppers were used to collect samples for alkalinity titrations. All water samples were immediately refrigerated.

Temperature, pH, and conductivity were measured in the field. Duplicate pH measurements were made with a portable Orion Model 231 pH/ion meter and an Orion Ross combination electrode. The meter was calibrated with Fisher Scientific pH 4.00 and 7.00 buffers before each measurement; pH was reproducible within ± 0.02 units. Conductivity was measured with a YSI Model 33 conductivity meter and probe; cell constants were established in the laboratory.

A Marsh-McBirney portable water-current meter was used to measure mean flow velocity at sites where cross-sectional area of the stream was determined with a measuring rod and tape. Mean flow velocities were measured at depths of 0.6 of the total depth of the water column and water depths were measured at 0.2-m intervals across the stream. Discharge was determined from mean flow velocity and cross-sectional area of the stream.

Flow velocities along the second travertine cascade were obtained using the surface float method (U.S. Geological Survey, 1977) on two dates in 1986. The travel time of a partially filled 60-mL polyethylene sample bottle was measured with a stopwatch. The travel distance was determined using a measuring tape. A coefficient of 0.85 was used to convert the average surface velocity to a mean velocity. Surface float velocity measurements can be in error by as much as 25 percent (U.S. Geological Survey, 1977).

Shear stresses along the second cascade and along the relatively quiet flow path above that cascade were approximated by using a balance between shear forces and forces due to gravity. The average bed or shear stress was calculated by

$$\tau = \rho g R S \quad (1)$$

where ρ is the density of water (1 g/cm^3), g is the acceleration due to gravity (980 cm/s^2), R (cm) is the hydraulic radius of the stream, and S represents the slope or stream gradient. The hydraulic radius can be approximated by the mean depth of the stream in relatively wide channels with approximately rectangular cross sections (Dingman, 1984). This expression applies under a case of no acceleration. Thus, the calculated shear stress values are only approximations at the cascades, where sharp acceleration occurs. The stream gradient was determined by measuring the relative change in elevation between survey points along the channel, above the cascade, with a survey level and measuring rod. A combination Suunto compass and inclinometer was used to survey elevation changes between points along the cascade. In May and June 1986, water depths were measured with a rod at 0.20-m intervals across the channel.

LABORATORY METHODS

Samples for analysis of major ions were filtered through $0.45 \mu\text{m}$ Millipore filters within 24 hours of collection. A portion of the filtered sample was acidified and later analyzed for Ca^{2+} , Mg^{2+} , Na^+ and K^+ by standard atomic absorption procedures on an Instrumentation Laboratories Model 751 atomic absorption spectrophotometer. Unacidified samples were analyzed for SO_4^{2-} , F^- , Cl^- , and NO_3^- by ion chromatography on a Dionex Advanced Chromatography Module. Replicate dilutions and quality control analyses were performed to determine analytical precision and accuracy. The relative standard deviation of Ca^{2+} concentrations ranged from 1 to 4 percent; for the 95 percent confidence interval, the concentrations were accurate within 1 to 3 percent.

Duplicate alkalinity titrations were performed with 0.02 N Baker HCl on a 50-mL unfiltered sample within 48 hours of collection. Titration endpoints were taken as the inflection points in the cumulative acid versus pH curve. The only species contributing significantly to alkalinity was as-

sumed to be HCO_3^- . The duplicate measurements agreed within 1 percent.

DATA ANALYSIS

Saturation State Calculations

The saturation state of the water with respect to carbon dioxide gas was calculated using a computerized aqueous equilibrium speciation model, WATEQF (Plummer and others, 1976), and an interactive program for generating WATEQF data input files, WATIN (Moses and Herman, 1986). The model calculates the theoretical CO_2 partial pressure (PCO_2) of a hypothetical coexistent gas phase with which the water sample is in equilibrium by

$$\text{PCO}_2 = \frac{a_{\text{HCO}_3^-} a_{\text{H}^+}}{K_1(\text{T}) K_{\text{CO}_2}(\text{T})} \quad (2)$$

where a_i indicates activity of species i , $K_1(\text{T})$ is the first dissociation constant of H_2CO_3 , and $K_{\text{CO}_2}(\text{T})$ is the Henry's Law constant at sample temperature. From previous analyses for this site (Hoffer, 1987), the discrepancy between PCO_2 values obtained from direct measurements and the values calculated from solution analyses using WATEQF was used to establish that $\log \text{PCO}_2$ values can be reported with an accuracy of ± 0.44 .

The saturation state of the water sample with respect to minerals was also calculated by WATEQF. The logarithm of the ratio of the ion activity product, $\text{IAP}(\text{T})$, to the equilibrium solubility product, $K_c(\text{T})$, at sample temperature is the saturation index for calcite

$$\text{SI}_c = \log \left[\frac{\text{IAP}(\text{T})}{K_c(\text{T})} \right] \quad (3)$$

The value of this index indicates whether the solution is undersaturated ($\text{SI}_c < 0$), supersaturated ($\text{SI}_c > 0$), or at equilibrium ($\text{SI}_c = 0$) with respect to calcite. Based on the analytical errors in pH and in Ca^{2+} and HCO_3^- concentrations and the errors in the thermodynamic data, the SI_c values can be reported to ± 0.05 units.

Although outgassing causes the stream water to become supersaturated with respect to several carbonate minerals, for example, aragonite, calcite, dolomite, and magnesite, only calcite is likely to be deposited. Other carbonate phases have not been identified as important mineralogical constituents of low-temperature freshwater travertine deposits (Hubbard, 1985). Samples were collected from a travertine deposit at a cascade. The mineralogy of the samples was identified by

powder X-ray diffraction to be calcite with a trace amount of detrital quartz (R.S. Mitchell, 1986, personal communication).

Mass Transfer Calculations

The mass transfers of chemical constituents into or out of the solution phase were determined using simple mass balance calculations (Plummer and Back, 1980). Calcite mass transfers were calculated as the change in total Ca^{2+} concentration between two consecutive sampling points along the flow path. Calcite solubility is described by



After subtracting the amount of HCO_3^- lost due to calcite precipitation, which was quantified by the mass balance on Ca^{2+} , the mass transfer of CO_2 gas was calculated as the change in total inorganic carbon concentration between two consecutive points along the flow path. Mass transfer quantities are expressed as moles of reactant per kilogram of water. Negative mass transfers indicate calcite precipitation and CO_2 outgassing while positive mass transfers indicate calcite dissolution and CO_2 ingassing. Mass transfer values are expressed as number of moles of calcite or CO_2 reacted per one kilogram of H_2O , and the units are expressed as mol/kg.

Reaction Rate Calculations

Carbon dioxide and calcite reaction rates were calculated using the mass transfer results and estimates for reaction time. The reaction times between successive sampling sites were computed from the distance between each pair of sites divided by the stream velocity. The distance between sampling sites was either surveyed or read from a topographic map. Reaction rates were computed as the mass transfer of CO_2 or calcite (in units of moles per kilogram of H_2O) divided by the reaction time (in units of seconds), and the units are expressed as mol/kg·s.

RESULTS

STREAM HYDROLOGY

The four cascades along the channel delimit broad, relatively smooth, gently sloping stretches of the stream channel referred to as terraces (Figure 2). Topographic measurements for the second travertine cascade and a small segment of the terrace upstream from it are representative of

the cascade and terrace sections of Falling Spring Run. A plot of the shear stress for the surveyed portion of the stream at the second cascade (Figure 3) reveals two distinct hydrological regimes characteristic of the cascade and terrace deposits along the stream. The relatively low-gradient channel upstream and downstream from the cascade produces a quiet flow regime in contrast to the agitated flow that occurs along the steeper gradient of the cascade (Figure 3). Figure 4 graphically illustrates the flow velocity along the surveyed segment.

STREAM CHEMISTRY

The chemical concentration data and field pH and temperature are given in Table 1. The dominant ions in the spring and stream waters are Ca^{2+} and HCO_3^- . Concentrations of Ca^{2+} and HCO_3^- decreased along the stream with notable declines occurring at the final three cascades (Figures 5 and 6). The pH values ranged from 7.01 at the spring to 8.23 at the base of the final cascade. The pH values rose along the flow path; pronounced increases were observed at each of the cascades (Figure 7).

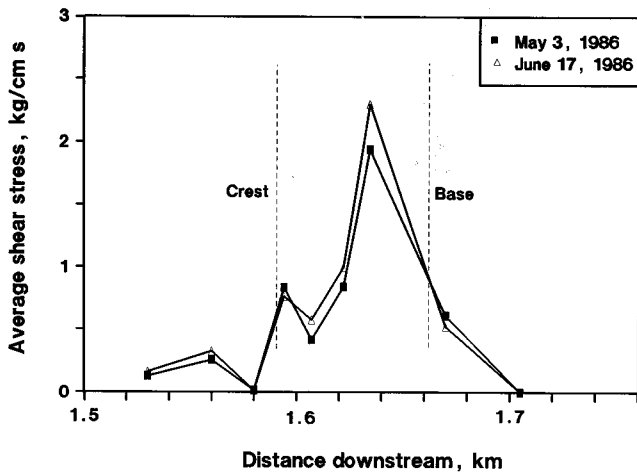


Figure 3. Average shear stress at the second cascade versus distance along the stream. Figure includes data collected as part of a larger study (Hoffer, 1987).

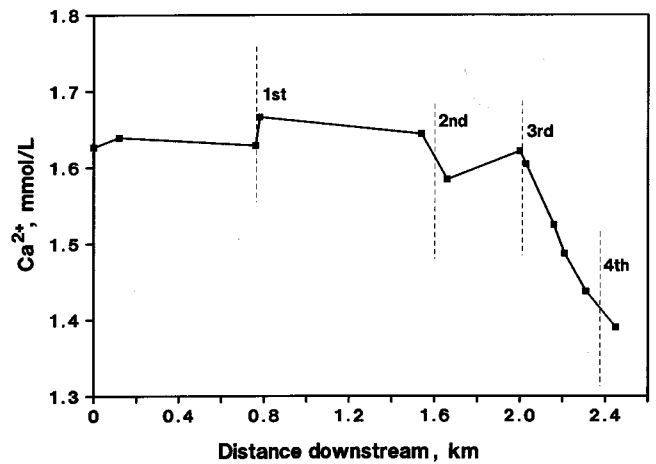


Figure 5. Millimolar Ca^{2+} concentration versus distance along the stream. Sample locations are shown in Figure 1. The origin of the studied flow path (0 km) is at the upstream spring.

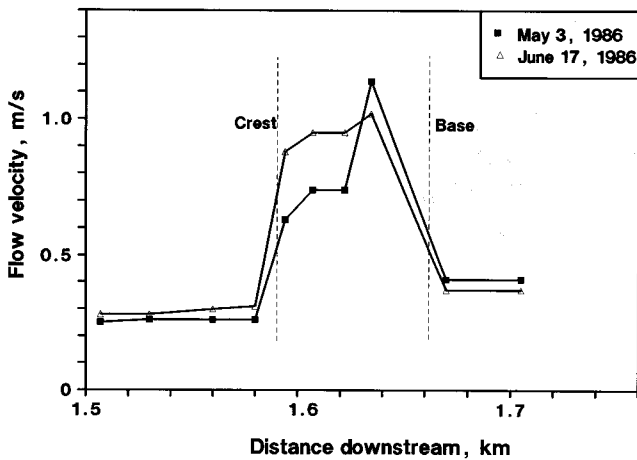


Figure 4. Flow velocity at the second travertine cascade versus distance along the stream. Figure includes data collected as part of a larger study (Hoffer, 1987).

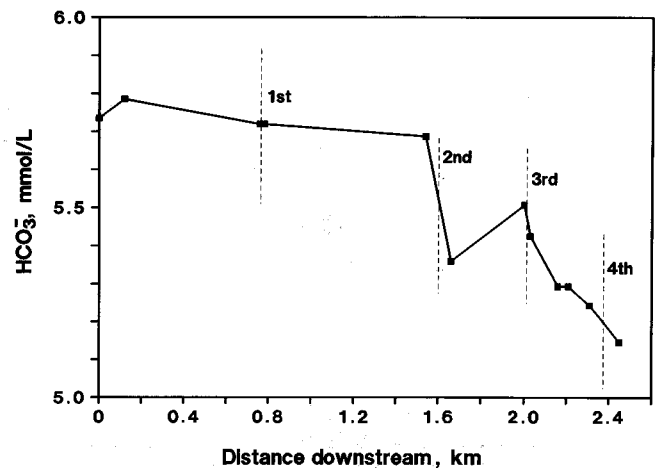


Figure 6. Millimolar HCO_3^- concentration versus distance along the stream.

The thermodynamic state of the stream water with respect to carbon dioxide and calcite is reported in Table 2. The

Table 1. Raw chemical concentration data for samples from Falling Spring Run collected on July 21, 1985. Sample locations are shown in Figure 1. Cond. is conductivity. All concentrations are expressed as mg/L.

Sample	T (°C)	Cond. ($\mu\text{S}/\text{cm}$)	pH	HCO_3^-	Ca^{2+}	Mg^{2+}	Na^+	K^+	F^-	Cl^-	SO_4^{2-}	NO_3^-
Spring sample												
S2	14.5	328	7.01	350	65.2	28.5	0.6	1.1	0.4	1.2	2.6	3.6
Stream samples												
C1	15.0	394	7.15	353	65.7	28.3	0.6	1.1	0.4	1.4	2.5	4.2
F1A	17.5	459	7.70	349	65.3	28.3	0.9	1.3	0.3	1.7	2.6	3.9
F1B	17.5	456	7.81	349	66.8	28.3	0.9	1.2	0.3	1.7	2.5	3.7
F2A	19.1	472	7.94	347	65.9	28.0	1.2	1.5	0.3	2.4	3.1	4.5
F2B	19.5	476	8.04	327	63.5	27.5	1.2	1.4	0.3	2.3	3.0	4.4
F3A	20.5	500	8.05	336	65.0	27.8	1.3	1.6	0.3	2.5	3.2	4.0
F3B	20.0	476	8.12	331	64.3	27.8	1.3	1.6	0.3	2.6	3.3	3.7
C3	22.0	505	8.14	323	61.1	27.3	1.3	1.9	0.3	2.8	3.5	4.0
CRA	21.8	500	8.14	323	59.6	27.4	1.3	1.8	0.3	2.6	3.4	4.0
FRA	21.2	492	8.19	320	57.6	27.0	1.2	1.7	0.3	2.6	3.3	4.0
FRB	21.0	481	8.23	314	55.7	27.2	1.2	1.7	0.3	2.6	3.3	4.2

PCO_2 at the spring (S2) was $10^{-1.54}$ atm, nearly 100 times greater than the atmospheric PCO_2 of $10^{-3.5}$ atm. Carbon dioxide partial pressures decreased downstream as a result of CO_2 outgassing. The spring water was undersaturated with respect to calcite ($\text{SI}_c = -0.25$). Downstream from the spring, SI_c values increased. Similar to trends observed for Ca^{2+} and HCO_3^- concentrations and pH values, the most dramatic changes in PCO_2 and SI_c values were observed at the most turbulent portions of the stream, that is, at the cascades (Table 2).

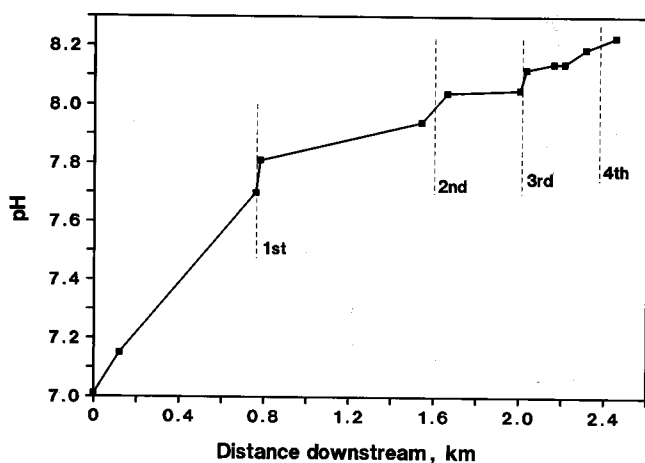


Figure 7. pH versus distance along the stream.

The chemical behavior of the water in Falling Spring Run is characterized by CO_2 outgassing and calcite precipitation (negative mass transfer, Table 3). Outgassing begins at the spring and continues along the entire length of the

channel excluding one segment above the final cascade. Calcite precipitation did not begin until the PCO_2 dropped from $10^{-1.54}$ to $10^{-2.33}$ atm, or from 100 to 15 times greater than atmospheric levels, and the solution was five times supersaturated with respect to calcite. Calcite precipitation (Table 3) was calculated for the initial portion of the stream below the first cascade and for the entire flow path downstream from the second cascade.

Table 2. Theoretical partial pressure of carbon dioxide gas (PCO_2) and calcite saturation indices (SI_c). Results were obtained from WATEQF calculations.

Sample	$\log \text{PCO}_2$	SI_c
Spring		
S2	-1.54	-0.25
Stream		
C1	-1.68	-0.10
First Cascade		
F1A	-2.22	+0.47
F1B	-2.33	+0.59
Second Cascade		
F2A	-2.46	+0.73
F2B	-2.59	+0.79
Third Cascade		
F3A	-2.58	+0.84
F3B	-2.66	+0.89
Stream		
C3	-2.68	+0.90
Fourth Cascade		
CRA	-2.68	+0.89
FRA	-2.74	+0.91
FRB	-2.79	+0.93

Table 3. Calculated mass transfers and reaction rates. All mass transfers are expressed as moles per kilogram of H₂O (mol/kg), and all reaction rates are mass transfers per second (mol/kg-s). Positive values indicate calcite dissolution and carbon dioxide ingassing; negative values denote calcite precipitation and carbon dioxide outgassing.

Sampling Sites (initial to final)	Mass Transfers		Reaction Rates	
	Calcite	CO ₂ Gas	Calcite	CO ₂ Gas
S2 to C1	+1.0 x 10 ⁻⁵	-3.3 x 10 ⁻⁴	+7.5 x 10 ⁻⁹	-2.5 x 10 ⁻⁸
C1 to F1A	+1.0 x 10 ⁻⁵	-8.0 x 10 ⁻⁴	+1.9 x 10 ⁻⁹	-1.5 x 10 ⁻⁷
F1A to F1B	+4.0 x 10 ⁻⁵	-1.1 x 10 ⁻⁴	+2.4 x 10 ⁻⁷	-6.6 x 10 ⁻⁷
F1B to F2A	-3.0 x 10 ⁻⁵	-8.0 x 10 ⁻⁵	-4.7 x 10 ⁻⁹	-1.3 x 10 ⁻⁸
F2A to F2B	-6.0 x 10 ⁻⁵	-3.1 x 10 ⁻⁴	-2.1 x 10 ⁻⁷	-1.1 x 10 ⁻⁶
F2B to F3A	+4.0 x 10 ⁻⁵	-9.0 x 10 ⁻⁵	+1.7 x 10 ⁻⁸	-3.7 x 10 ⁻⁸
F3A to F3B	-2.0 x 10 ⁻⁵	-8.0 x 10 ⁻⁵	-6.7 x 10 ⁻⁸	-2.6 x 10 ⁻⁷
F3B to C3	-7.0 x 10 ⁻⁵	-8.0 x 10 ⁻⁵	-5.4 x 10 ⁻⁸	-6.2 x 10 ⁻⁸
C3 to CRA	-4.0 x 10 ⁻⁵	+4.0 x 10 ⁻⁵	-4.0 x 10 ⁻⁸	+4.0 x 10 ⁻⁸
CRA to FRA	-5.0 x 10 ⁻⁵	-1.0 x 10 ⁻⁵	-4.5 x 10 ⁻⁸	-9.0 x 10 ⁻⁹
FRA to FRB	-5.0 x 10 ⁻⁵	-7.0 x 10 ⁻⁵	-3.2 x 10 ⁻⁸	-4.5 x 10 ⁻⁸
*C1 to F2A	+2.0 x 10 ⁻⁵	-9.9 x 10 ⁻⁴	+1.7 x 10 ⁻⁹	-8.4 x 10 ⁻⁸
*CRA to FRB	-1.0 x 10 ⁻⁴	-8.0 x 10 ⁻⁵	-3.8 x 10 ⁻⁸	-3.0 x 10 ⁻⁸

* Mass transfers and reaction rates calculated for longer stretches of the stream.

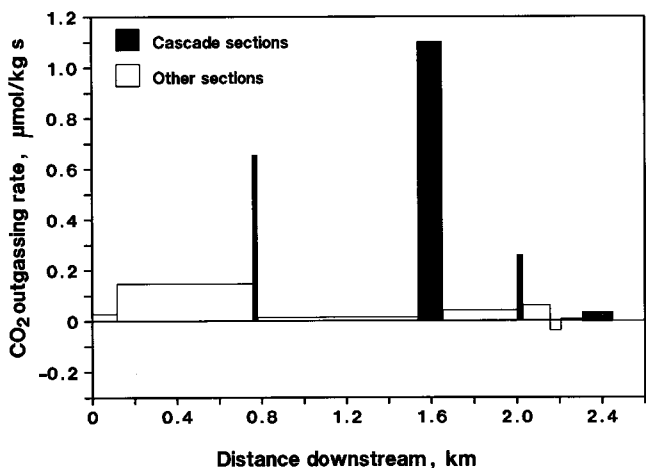


Figure 8. CO₂ outgassing rates between sampling points versus distance along the stream. Values of the reaction rate are listed in Table 3.

Rates of reaction are also reported in Table 3. Outgassing rates were rapid where the most disturbed flow was observed (Figure 8). The rate increased by almost two orders of magnitude as the stream flowed over the second cascade and decreased nearly the same amount downstream from the cascade. Calcite precipitation rates were also greater at the cascades compared to the less turbulent sections of the

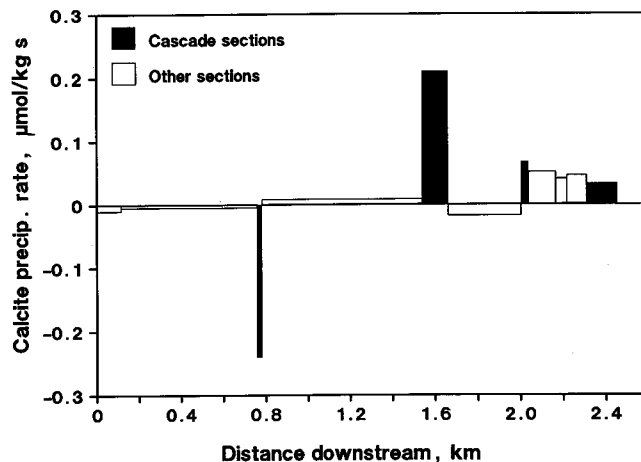


Figure 9. Calcite precipitation rates between sampling points versus distance along the stream. Values of the reaction rate are listed in Table 3.

channel (Figure 9). An exception occurs between the third and final cascades, where calcite supersaturation states resulted in high precipitation rates upstream from the final cascade. Precipitation at the second cascade exceeded the rate of all other segments of the studied flow path. Here, the rate increased by a factor of 40 over the rate immediately upstream as the water cascaded over the travertine dam.

DISCUSSION

The carbonate groundwater issuing from the spring contains elevated CO_2 concentrations with respect to the atmosphere. This disequilibrium between the supersaturated solution and atmosphere is the driving force for CO_2 outgassing (Jacobson and Usdowski, 1975; Dandurand and others, 1982). Carbon dioxide gas begins to escape to the atmosphere at the spring and outgassing continues along the entire flow path. Decreasing HCO_3^- concentration (Figure 6) and increasing pH values (Figure 7) reflect the loss of CO_2 from solution. The partial pressure of CO_2 decreases by almost a third of its original level along the initial 170 m of flow path. Although PCO_2 values drop along the entire length of the stream (Table 2), the stream water remains supersaturated with CO_2 even after 2.5 km of flow path.

The rate of CO_2 exchange along the flow path depends on the degree of hydrological agitation of the flow. High rates of outgassing were found at the cascades (Figure 8) where flow resistance was high. Outgassing along the cascades of Falling Spring Run is particularly fast relative to other segments along the channel (Figure 8), because CO_2 is able to outgas more readily where the water is hydrologically agitated (Figure 3). These findings are consistent with the observations of Lorah and Herman (1988 and this volume). They quantified the most rapid outgassing rates for the more turbulent stretches, above and at the 20-m waterfall, of Falling Spring Creek, Virginia. Although outgassing rates were not quantified, Kirby and Rimstidt (this volume) also observed large decreases in CO_2 partial pressure upstream from, and at, a 15-m-high waterfall in Falls Hollow, Virginia.

The degree of hydrological agitation along Falling Spring Run is related to the shear stress along the boundaries of the stream. Factors such as skin friction, form drag, variations in slope, and hydraulic jumps contribute to the shear stress acting on the water flowing along the channel. These factors all reduce the energy available to the main flow in the stream (Dingman, 1984) and lead to random velocity fluctuations, or turbulence. Flow resistance is higher at the cascades (Figure 3) compared to other segments of Falling Spring Run because: 1) the travertine dams have a larger surface area to resist flow, 2) the deposits have irregular surfaces, and such irregularities result in increased form drag and produce hydraulic jumps, and 3) the steep topographic gradient at the cascades causes the flow velocity to increase.

Outgassing along the cascades is also influenced by dispersion of the stream water. The surface flow disperses, or spreads out, as it flows over the travertine dams increasing the area over which CO_2 escape is possible. Dispersion under low-flow conditions resulted in rapid outgassing in a stream observed by Dandurand and others (1982). High outgassing rates were also calculated for stream water cascading and dispersing over a waterfall (Herman and Lorah, 1988).

As CO_2 escapes from solution, the equilibrium solubil-

ity of calcite decreases and the solution becomes increasingly supersaturated. Calcite precipitation is theoretically possible whenever enough CO_2 is lost from solution to shift the calcite saturation state above the equilibrium value. The saturation state with respect to calcite increases downstream from the springs which feed Falling Spring Run (Table 2), yet Ca^{2+} and HCO_3^- concentrations (Figures 5 and 6) indicate that measurable calcite precipitation does not occur until the stream water reaches the second travertine cascade. Here, the solution is between five and six times supersaturated, enough to overcome kinetic inhibition to precipitation. This threshold value is consistent with the level reported for precipitation in another travertine-depositing stream (Jacobson and Usdowski, 1975). Herman and Lorah (1988) observed small amounts of precipitation at lower degrees of supersaturation in Falling Spring Creek.

Calcite precipitation does not keep pace with outgassing, as evidenced by increasing saturation states along the flow path of Falling Spring Run (Table 2), yet rates of both reactions do show parallel trends. Precipitation rates were high at the second cascade (Figure 9) where outgassing was rapid (Figure 8). Precipitation rates were also high along the final section of the stream, which includes the fourth cascade, where high degrees of supersaturation with respect to calcite, driven by the greatest extent of outgassing, were observed (Table 3). The results for Falling Spring Run are similar to those of Lorah and Herman (1988 and this volume). They observed that most of the calcite precipitation in Falling Spring Creek occurs at the waterfall where the stream experiences the most rapid CO_2 loss. The greatest calcite precipitation in the stream in Falls Hollow was also observed at the waterfall where the CO_2 partial pressures dropped significantly, although declines in PCO_2 upstream from the waterfall were greater (Kirby and Rimstidt, this volume).

The present investigation has shown that hydrological agitation of the stream water plays a major role in the localization of calcite deposition along Falling Spring Run. Although not specifically addressed in this paper, other factors, including biological processes, may also influence travertine deposition along Falling Spring Run. The uptake of CO_2 by biological activity has been shown to be negligible for this stream (Hoffer, 1987; Hoffer-French and Herman, 1989); however, the mosses and algae which thrive at the travertine dams may lower the kinetic inhibition to calcite precipitation by providing additional fresh growth surfaces for calcite nuclei (Emeis and others, 1987). Regardless of the exact role of biological processes in this system, the present study illustrates the importance of stream hydrology on CO_2 fluxes along a calcite-precipitating stream.

CONCLUSIONS

The exchange of carbon dioxide gas between the stream and the earth's atmosphere influences calcite precipitation

along Falling Spring Run. Carbon dioxide outgasses from the carbonate-rich solution when the groundwater emerges at the springs and outgassing continues along the entire flow path in an attempt to equilibrate with atmospheric levels. Hydrological agitation and dispersion of the stream water at the travertine dams enhance CO₂ flux.

Outgassing forces the solution to high degrees of supersaturation with respect to calcite. Significant calcite precipitation begins at the second cascade where the solution is between five and six times supersaturated with respect to the mineral. In addition to the great CO₂ flux there, precipitation is further localized at the travertine dams because the deposit itself and the algae and mosses growing on it provide fresh growth surfaces which lower the inhibition to formation of stable calcite nuclei.

Today, rapid outgassing along the most turbulent sections of Falling Spring Run is associated with significant calcite deposits. It is likely that, in the past, these travertine dams were formed at points along the channel where rapid CO₂ exchange occurred because of hydrological agitation related to the outcrops of resistant rock in the stream bed or other geomorphic features. The stream hydrology influences the feedback mechanisms acting between the chemical composition of the water and morphology of the channel in this travertine-depositing stream system.

ACKNOWLEDGMENTS

We thank David Hubbard, Jr. for assisting us in identifying a field site and the Carroll family, Boyd Cupp, and Fred Cupp for allowing us access to their properties. We are grateful to those who helped with the field work for the larger study of which this study is a part, especially René Price, Carol Wicks, Jeffrey Sitler, Anne Barsanti, Connie Gold, Laura Sacks, Bill Jones, Mike Reiter, Michelle Lorah, and Diane Miller. Michelle Lorah, Isabelle Cozzarelli, Carl Moses, and John Maben provided generous assistance in the laboratory. We thank Richard Mitchell for performing the X-ray diffraction analysis. Partial funding was provided by the Department of Environmental Sciences at the University of Virginia. The ion chromatography instrument was purchased through an NSF award to JSH (EAR-84-17122). Thoughtful comments from George Hornberger, Donald Rimstidt, and Marilyn Bradley helped us improve this manuscript.

REFERENCES CITED

Amundson, Ronald, and Kelly, Eugene, 1987, The chemistry and mineralogy of a CO₂-rich travertine-depositing spring in the California Coast Range: *Geochimica et Cosmochimica Acta*, v. 51, p. 2883-2890.

Barnes, Ivan, 1965, Geochemistry of Birch Creek, Inyo County, California - a travertine depositing creek in an arid climate: *Geochimica et Cosmochimica Acta*, v. 29, p. 85-112.

Chafetz, H.S., and Folk, R.L., 1984, Travertines: depositional morphology and the bacterially constructed constituents: *Journal of Sedimentary Petrology*, v. 54, p. 289-316.

Collins, R.E.L., 1924, Travertine deposits in Virginia: *Pan-American Geology*, v. 41, p. 103-106.

Dandurand, J.L., Gout, R., Hoeffs, J., Menschel, Günther, Schott, J., and Usdowski, Eberhard, 1982, Kinetically controlled variations of major components and carbon and oxygen isotopes in a calcite-precipitating spring: *Chemical Geology*, v. 36, p. 299-315.

Dingman, S.L., 1984, *Fluvial hydrology*: New York, New York, W.H. Freeman & Co., 383 p.

Emeis, K.-C., Richnow, H.-H., and Kempe, Stephan, 1987, Travertine formation in Plitvice National Park, Yugoslavia: chemical versus biological control: *Sedimentology*, v. 34, p. 595-609.

Herman, J.S., and Lorah, M.M., 1987, CO₂ outgassing and calcite precipitation in Falling Spring Creek, Virginia, U.S.A.: *Chemical Geology*, v. 62, p. 251-262.

Herman, J.S., and Lorah, M.M., 1988, Calcite precipitation rates in the field: measurement and prediction for a travertine-depositing stream: *Geochimica et Cosmochimica Acta*, v. 52, p. 2347-2355.

Hoffer, K.J., 1987, Daily and seasonal CO₂ fluxes in a travertine-depositing stream [M.S. Thesis]: Charlottesville, University of Virginia, 157 p.

Hoffer-French, K.J., and Herman, J.S., 1989, Evaluation of hydrological and biological influences on CO₂ fluxes from a karst stream: *Journal of Hydrology*, v. 108, p. 189-212.

Hubbard, D.A., Jr., 1985, Annotated bibliography of the Valley and Ridge travertine-marl deposits of Virginia: *Virginia Division of Mineral Resources, Virginia Minerals*, v. 31, n. 1, p. 9-12.

Hubbard, D.A., Jr., Giannini, W.F., and Lorah, M.M., 1985, Travertine-marl deposits of the Valley and Ridge province of Virginia - a preliminary report: *Virginia Division of Mineral Resources, Virginia Minerals*, v. 31, n. 1, p. 1-8.

Jacobson, R.L., and Usdowski, Eberhard, 1975, Geochemical controls on a calcite precipitating stream: *Contributions in Mineralogy and Petrology*, v. 51, p. 65-74.

Lorah, M.M., and Herman, J.S., 1988, The chemical evolution of a travertine-depositing stream: geochemical processes and mass transfer reactions: *Water Resources Research*, v. 24, p. 1541-1552.

Moses, C.O., and Herman, J.S., 1986, WATIN - a computer program for generating input files for WATEQF: *Ground Water*, v. 24, p. 83-89.

Pearson, F.J., Fischer, D.W., and Plummer, L.N., 1978, Correction of ground-water chemistry and carbon isotopic composition for effects of CO₂ outgassing: *Geochimica et Cosmochimica Acta*, v. 42, p. 1799-1807.

Plummer, L.N., and Back, William, 1980, The mass balance approach: application to interpreting the chemical evolution of hydrologic systems: *American Journal of Science*, v. 280, p. 130-142.

Plummer, L.N., Jones, B.F., and Truesdell, A.H., 1976, WATEQF - a FORTRAN IV version of WATEQ, a computer program for calculating chemical equilibria of natural waters: *U.S. Geological Survey Water-Resources Investigation* 76-13, 61 p.

Rader, E.K., 1967, Geology of the Staunton, Churchville, Greenville, and Stuarts Draft quadrangles, Virginia: Virginia Division of Mineral Resources Report of Investigations 12, 43 p.

Suarez, D.L., 1983, Calcite supersaturation and precipitation kinetics in the lower Colorado River, All American Canal and East Highland Canal: Water Resources Research, v. 19, p. 653-661.

Usdowski, Eberhard, Hoefs, J., and Menschel, Günther, 1979, Relationship between ^{13}C and ^{18}O fractionation and changes in major element composition in a recent calcite-depositing spring - a model of chemical variations with inorganic CaCO_3 precipitation: Earth and Planetary Science Letters, v. 42, p. 267-276.

U.S. Geological Survey, 1977, National handbook of recommended methods for water-data acquisition: Reston, Virginia, Book 1, Chapter 1, 110 p.

GEOCHEMICAL EVOLUTION AND CALCITE PRECIPITATION RATES IN FALLING SPRING CREEK, VIRGINIA

Michelle M. Lorah¹ and Janet S. Herman²

CONTENTS

	Page
Abstract.....	18
Introduction.....	18
Field site description.....	18
Previous studies.....	19
Methods.....	20
Field and laboratory methods.....	20
Data analysis.....	21
Calculation of geochemical evolution.....	21
Calculation of calcite precipitation rates.....	22
Results.....	22
Geochemical evolution.....	22
Comparison of calcite precipitation rates.....	25
Discussion.....	27
Geochemical evolution.....	27
Carbon dioxide outgassing.....	27
Calcite precipitation.....	28
Comparison of calcite precipitation rates.....	29
Rates of mass transfer.....	29
Rate law calculations.....	29
Calcite seed crystals.....	30
Conclusions.....	30
Acknowledgments.....	31
References cited.....	31

ILLUSTRATIONS

Figure	
1. Location of Falling Spring Creek, Alleghany County, Virginia, and location of sample collection points.....	19
2. Photographs of Falling Spring Creek. (A) The waterfall showing the recent travertine deposits at its base. (B) A small recent travertine dam above the waterfall.....	20
3. Millimolar Ca ²⁺ concentration versus distance along the flow path.....	23
4. Millimolar HCO ₃ ⁻ concentration versus distance along the flow path.....	23
5. pH versus distance along the flow path.....	24
6. Calculated partial pressure of carbon dioxide gas (PCO ₂) versus distance along the flow path.....	24
7. Saturation state with respect to calcite (SI _c) versus distance along the flow path.....	24
8. CO ₂ outgassing rates versus reaction time between sampling points.....	26
9. Calcite precipitation rates versus reaction time between sampling points for the mass transfer results and the rate law results.....	26
10. Total amount of calcite precipitated along the stream for the mass transfer results and the rate law results.....	26

¹U.S. Geological Survey, 208 Carroll Bldg., 8600 La Salle Rd., Towson, MD 21204

²Department of Environmental Sciences, Clark Hall, University of Virginia, Charlottesville, VA 22903

TABLES

	Page
1. Nature of water sampling sites.....	21
2. Selected chemical analyses of Falling Spring Creek.....	23
3. Reaction rates for CO ₂ outgassing and calcite precipitation are from mass transfer results and from calculations based on the rate law of Plummer and others (1978).....	25
4. Comparison of calcite precipitation rates calculated from the calcite seed crystal measurements, from the mass transfer results, and from the rate law of Plummer and others (1978).....	27

ABSTRACT

This field study focuses on quantitatively defining the chemical changes occurring in a travertine-depositing stream and on comparing different methods of calculating calcite precipitation rates. Carbon dioxide outgassing and calcite precipitation control the chemical evolution of Falling Spring Creek, located in Alleghany County, Virginia. Mass balance calculations were used to determine the mass transfer of CO₂ and calcite. The mass transfer results were combined with reaction times, estimated from stream discharge, to calculate rates of CO₂ outgassing and calcite precipitation.

The stream, fed by a carbonate spring, is supersaturated with respect to CO₂ along the entire 5.2-km flow path that was studied. Outgassing of CO₂ drives the water to high degrees of supersaturation with respect to calcite. Calcite precipitation is relatively slow along the stream segment above the crest of a 20-m-high waterfall. At the waterfall, greater water turbulence causes the most rapid escape of CO₂, and calcite precipitation rates reach a maximum. Recent travertine deposits are located in the stream bed immediately above, at, and below the waterfall. Net calcite precipitation occurs at all times of the year but is greatest during low-flow conditions in the summer and early fall. Using an experimentally derived rate law, calcite precipitation rates were calculated and found to be within a factor of 1 to 45 of the mass transfer rates. Calcite precipitation rates could not be quantified accurately by measuring calcite accumulation on seed crystals that were placed in the stream.

INTRODUCTION

The relationship between carbon dioxide flux and calcite solubility is a critical factor in the geochemical evolution of carbonate water systems. The partial pressure of carbon dioxide in groundwater typically reaches values 10 to 100 times greater than the atmospheric value (10^{-3.5} atm, Pearson and others, 1978; Butler, 1982). As this groundwater emerges at the earth's surface, the water loses CO₂ in an attempt to equilibrate with the lower CO₂ concentration in the atmos-

phere (Jacobson and Langmuir, 1970; Langmuir, 1971). Carbon dioxide outgassing is the dominant cause of supersaturation with respect to calcite and subsequent precipitation of this mineral in many carbonate waters. Although carbon dioxide outgassing and calcite precipitation have been extensively studied from a theoretical and experimental approach, field-based investigations of the interplay of these processes and their reaction rates are still lacking.

Thermodynamic, or equilibrium, models can be used to determine if a solution will tend to evolve carbon dioxide or to precipitate calcite; however, kinetic information is required to determine the rate at which these reactions occur. One method of obtaining reaction rates is to calculate mass transfers of a mineral or gas along a flow path using observed chemical data. This method has been used to model chemical changes in carbonate groundwater systems (Plummer, 1977; Plummer and Back, 1980; Back and others, 1983). Another approach consists of theoretical and experimental study of reaction rates in the laboratory. Many laboratory studies of calcite dissolution and precipitation have been conducted (for example, Plummer and others, 1978; Reddy and others, 1981), but the rate laws that were developed require further testing in field situations (Plummer and Back, 1980).

The first objective of this field investigation was to quantify the rates of carbon dioxide outgassing and calcite precipitation in a travertine-depositing stream. Reaction rates were determined using a combination of mass balance calculations and hydrologic measurements. The second objective was to compare the calcite precipitation rates obtained from the mass transfer results to an experimentally derived rate law and to measurements of the amount of calcite growth on seed crystals placed in the stream.

FIELD SITE DESCRIPTION

The study area is located along Falling Spring Creek in Alleghany County, Virginia, and lies in the thermal springs area of the western anticlines of the Valley and Ridge province (Figure 1). The surficial geology consists of Lower Ordovician dolomite, Middle and Upper Ordovician limestone, which contains significant shale interbeds, and Si-

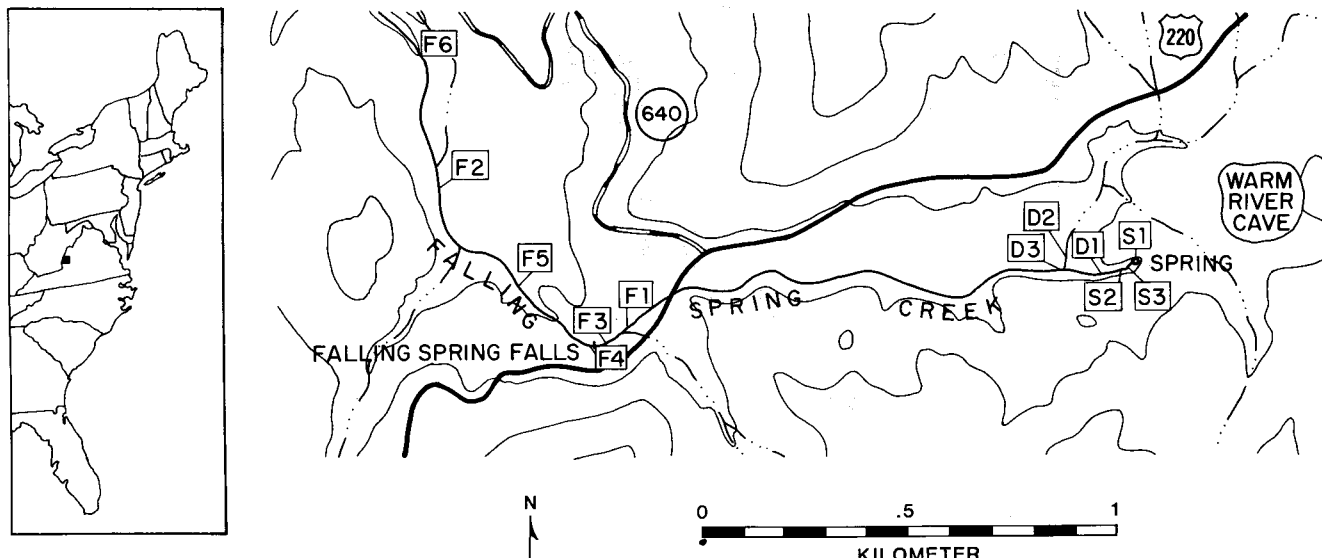


Figure 1. Location of Falling Spring Creek, Allegheny County, Virginia, and location of sample collection points. Contour interval is 30 m.

lurian sandstone, shale, and limestone (Dennen and Diecchio, 1984; Rader, 1984; Dennen and others, this volume).

Falling Spring, which feeds Falling Spring Creek, actually consists of several discrete springs emerging from a large breakdown pile downstream from Warm River Cave. Falling Spring represents a mixture of thermal and cold groundwaters. Deeply circulated meteoric water, which has been heated under a normal geothermal gradient (Severini and Huntley, 1983) to a temperature that may exceed 38°C, issues as a thermal spring inside the cave. The thermal water converges in the cave with a cold stream derived from shallow groundwater, and this mixed stream resurges as Falling Spring (Herman and Lorah, 1986).

Approximately 0.8 km downstream from Falling Spring, the stream breaches a small Tuscarora sandstone ridge (Dennen and others, this volume) and flows another 0.23 km on travertine-marl material. The stream subsequently flows over a 20-m-high travertine escarpment (Figure 2A; Figure 1 in Dennen and others, this volume; cover, top right photograph). Recent travertine deposits cover the face of the escarpment and are evident in the stream bed immediately above (Figure 2B) and below the waterfall. Over most of its course, the stream is less than 4 m wide and 40 cm deep.

PREVIOUS STUDIES

The degree of supersaturation with respect to calcite increases as the PCO_2 of the water decreases downstream from a carbonate spring (Barnes, 1965; Shuster and White, 1971; Jacobson and Usdowski, 1975); however, calcite does not precipitate immediately from supersaturated solutions. A critical degree of supersaturation must be achieved to pass the

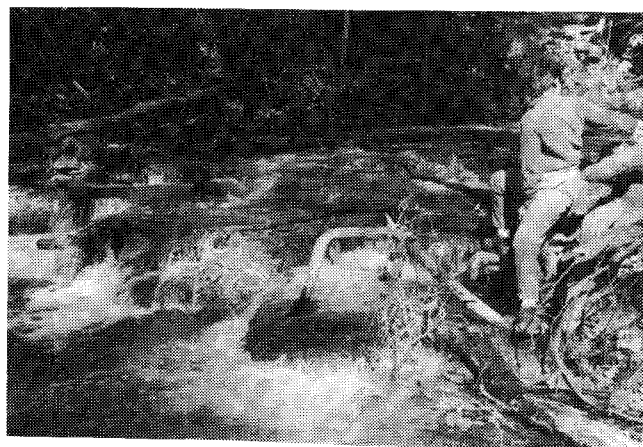
energy barrier to nucleation (Stumm and Morgan, 1981). Laboratory kinetic studies have shown that the critical concentration, above which nucleation and growth occur, can be as much as ten times the equilibrium calcite solubility value (Reddy, 1983). Foreign ions in solution, such as phosphate, magnesium, and some organic compounds, can also retard calcite growth by adsorbing to a crystal surface and blocking active growth sites (Morse, 1983). Because of one or more of these inhibiting factors, high degrees of supersaturation with respect to calcite can be maintained in a solution without noticeable calcite precipitation taking place. Two field studies of travertine-depositing streams show that five times (Jacobson and Usdowski, 1975) and ten times (Dandurand and others, 1982) supersaturation with respect to calcite must be reached before calcite precipitates. Suarez (1983) reports that calcite precipitation is not detectable in the Colorado River system although the water reaches 4.6 times supersaturation with respect to calcite.

Few researchers have quantified reaction rates in field studies. Relative rates of calcite precipitation along travertine-depositing streams have been determined by measuring changes in Ca^{2+} concentration with distance (Jacobson and Usdowski, 1975; Dandurand and others, 1982). Jacobson and Usdowski (1975) also give rates estimated from the mass of calcite that precipitated on objects placed in a stream. Although several researchers have noted that agitation of stream water at cascades allows a great amount of CO_2 outgassing to occur (Dandurand and others, 1982), no previous study has quantified the rate of removal of CO_2 in a natural field setting.

In contrast, many laboratory experiments have been conducted to investigate the reaction kinetics of calcite in CO_2 - H_2O systems. Several different rate equations have been produced, but the rate law of Plummer and others (1978) is



A



B

Figure 2. Photographs (courtesy of David A. Hubbard, Jr.) of Falling Spring Creek. (A) The waterfall showing the recent travertine deposits at its base. (B) A small recent travertine dam above the waterfall.

the only one which attempts to describe both calcite dissolution and precipitation at all solution pH and PCO_2 values (Plummer and others, 1979; Inskeep and Bloom, 1985). The equation relates the net dissolution rate (R) in units of mass

of calcite per unit surface area in a unit of time (units expressed as $\text{mol}/\text{cm}^2\cdot\text{s}$) to the activities (a) of H^+ , Ca^{2+} , HCO_3^- , and H_2CO_3^* .

$$R = k_1 a_{\text{H}^+} + k_2 a_{\text{H}_2\text{CO}_3^*} + k_3 a_{\text{H}_2\text{O}} - k_4 a_{\text{Ca}^{2+}} a_{\text{HCO}_3^-} \quad (1)$$

where H_2CO_3^* is $\text{CO}_2(\text{aq}) + \text{H}_2\text{CO}_3^0$ and the k_n are rate constants. Although the rate law has been tested and supported by several laboratory kinetic studies (House, 1981; Reddy and others, 1981; Suarez, 1983; Inskeep and Bloom, 1985), it has not been tested with field data.

METHODS

FIELD AND LABORATORY METHODS

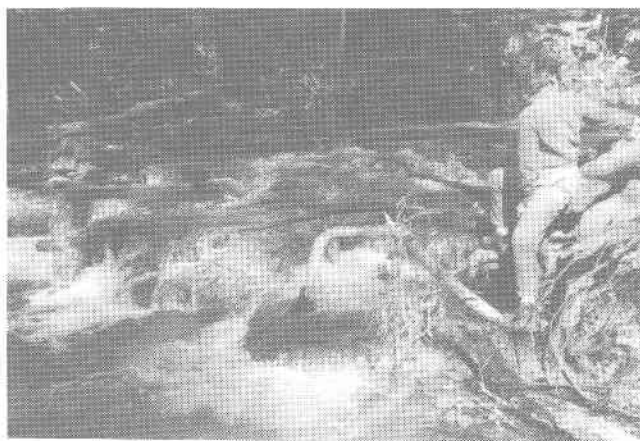
The results presented in this paper were obtained from seven field trips to collect water samples along Falling Spring Creek between June 1984 and April 1985. Twelve sampling sites were established along a 5.2-km stretch of Falling Spring Creek (Table 1, Figure 1). Three of the distinct springs emerging from the breakdown pile downstream from Warm River Cave were sampled (S-1, S-3, and S-2). All the springs combine to form Falling Spring Creek upstream from site D-1. Site D-3 is downstream from the junction of a small intermittent tributary (D-2) with Falling Spring Creek. The tributary rarely flowed and was, therefore, infrequently sampled. Samples were also collected near the crest of Falling Spring Falls (F-1 and F-3), immediately below the waterfall (F-4), and downstream from the waterfall (F-5, F-2, and F-6). The last sampling site (F-6) is approximately 4 km downstream from the waterfall.

Calcite seed crystals were placed at one location at the crest of the waterfall (F-3) and at three below the waterfall (F-4, F-5, and F-6). Calcite rhombohedrons were suspended by nylon monofilament inside cages (10-cm cube) fashioned out of 1.27-cm mesh galvanized hardware cloth. The cages were anchored to metal posts approximately 30 cm beneath the water surface during one collection trip and removed on the next trip. The amount of calcite precipitated was measured by the change in weight of the seed crystal.

Temperature, pH, and discharge were determined in the field. A portable pH meter and a combination electrode were used to measure pH after calibration with pH 4.00 and 7.00 buffers, which were allowed to reach thermal equilibrium with the stream water. Duplicate pH measurements, reproducible within ± 0.02 units, were made on samples immediately after collection in a beaker (Wood, 1976). Discharge was obtained by measuring flow velocity with a portable current meter and by determining the cross-sectional area



A



B

Figure 2. Photographs (courtesy of David A. Hubbard, Jr.) of Falling Spring Creek. (A) The waterfall showing the recent travertine deposits at its base. (B) A small recent travertine dam above the waterfall.

the only one which attempts to describe both calcite dissolution and precipitation at all solution pH and PCO_2 values (Plummer and others, 1979; Inskeep and Bloom, 1985). The equation relates the net dissolution rate (R) in units of mass

of calcite per unit surface area in a unit of time (units expressed as $mol/cm^2 \cdot s$) to the activities (a) of H^+ , Ca^{2+} , HCO_3^- , and $H_2CO_3^*$.

$$R = k_1 a_{H^+} + k_2 a_{H_2CO_3^*} + k_3 a_{H_2O} - k_4 a_{Ca^{2+}} a_{HCO_3^-} \quad (1)$$

where $H_2CO_3^*$ is $CO_2(aq) + H_2CO_3^0$ and the k_n are rate constants. Although the rate law has been tested and supported by several laboratory kinetic studies (House, 1981; Reddy and others, 1981; Suarez, 1983; Inskeep and Bloom, 1985), it has not been tested with field data.

METHODS

FIELD AND LABORATORY METHODS

The results presented in this paper were obtained from seven field trips to collect water samples along Falling Spring Creek between June 1984 and April 1985. Twelve sampling sites were established along a 5.2-km stretch of Falling Spring Creek (Table 1, Figure 1). Three of the distinct springs emerging from the breakdown pile downstream from Warm River Cave were sampled (S-1, S-3, and S-2). All the springs combine to form Falling Spring Creek upstream from site D-1. Site D-3 is downstream from the junction of a small intermittent tributary (D-2) with Falling Spring Creek. The tributary rarely flowed and was, therefore, infrequently sampled. Samples were also collected near the crest of Falling Spring Falls (F-1 and F-3), immediately below the waterfall (F-4), and downstream from the waterfall (F-5, F-2, and F-6). The last sampling site (F-6) is approximately 4 km downstream from the waterfall.

Calcite seed crystals were placed at one location at the crest of the waterfall (F-3) and at three below the waterfall (F-4, F-5, and F-6). Calcite rhombohedrons were suspended by nylon monofilament inside cages (10-cm cube) fashioned out of 1.27-cm mesh galvanized hardware cloth. The cages were anchored to metal posts approximately 30 cm beneath the water surface during one collection trip and removed on the next trip. The amount of calcite precipitated was measured by the change in weight of the seed crystal.

Temperature, pH, and discharge were determined in the field. A portable pH meter and a combination electrode were used to measure pH after calibration with pH 4.00 and 7.00 buffers, which were allowed to reach thermal equilibrium with the stream water. Duplicate pH measurements, reproducible within ± 0.02 units, were made on samples immediately after collection in a beaker (Wood, 1976). Discharge was obtained by measuring flow velocity with a portable current meter and by determining the cross-sectional area

of the stream. Discharge was measured near site D-3 on each trip and at additional sites, near F-1 and F-6, during four of the sampling trips.

Table 1. Nature of water sampling sites. Locations of sites are shown in Figure 1. The analytical and calculated results from water samples collected at these eleven sites are shown in Figures 2 to 6. Site D-2, an intermittent tributary that enters the stream at about 190 m, is not plotted.

Sample name	Distance downstream (m)	Nature of the sample
S-1	0	spring, beginning of the surface stream
S-3	29	spring
S-2	30	spring
D-1	72	well-defined surface stream established; mass transfer calculations begin here
D-3	200	downstream from occasional tributary input
F-1	1120	among travertine dams near crest of waterfall
F-3	1220	crest of waterfall
F-4	1240	directly below waterfall
F-5	1490	among travertine dams below waterfall
F-2	1790	among travertine dams below waterfall
F-6	5200	farthest downstream sampling point

Samples for chemical analyses were collected in acid-washed 250-mL polyethylene bottles. Samples for laboratory alkalinity titrations were collected in acid-washed 250-mL glass bottles with ground glass stoppers. All samples were immediately refrigerated. Within 24 hours of collection, samples were filtered through 0.45 μm filters, and a portion of each filtered sample was acidified with concentrated HNO_3 . Acidified samples were later analyzed for the cations Ca^{2+} , Mg^{2+} , Na^+ , and K^+ by standard atomic absorption procedures. Replicate dilutions and analyses were performed to determine the maximum relative standard deviations for concentration values: 4.0 percent for Ca^{2+} , 3.4 percent for Mg^{2+} , 6.8 percent for Na^+ , and 3.5 percent for K^+ . The detection limits were 0.019 mg/L Ca^{2+} , 0.0096 mg/L Mg^{2+} , 0.074 mg/L Na^+ , and 0.059 mg/L K^+ . Concentrations of SO_4^{2-} , F^- , Cl^- , NO_3^- , and PO_4^{3-} in the unacidified samples were determined by standard ion chromatographic techniques. Environmental Protection Agency standards for F^- and SO_4^{2-} were analyzed, and the concentrations were within the range given for a 95 percent confidence interval.

Duplicate alkalinity titrations were performed on each sample within 36 hours of returning to the laboratory. Titration endpoints were taken to be the inflection points in the cumulative-acid-added versus pH curve, and alkalinity values were converted to HCO_3^- concentration. Analytical errors in HCO_3^- concentrations were usually less than 1 per-

cent with a maximum error of 2 percent. Because preliminary work established that the difference in alkalinities between filtered and unfiltered samples was within the error of titration, all subsequent measurements were performed on unfiltered samples. The average error induced by performing the titrations in the laboratory rather than in the field was 4 percent, whereas the maximum error was 10 percent (Lorah, 1987).

DATA ANALYSIS

Calculation of Geochemical Evolution

To describe the geochemical evolution of Falling Spring Creek, the necessary data analysis included defining the saturation state of the waters with respect to calcite and carbon dioxide and determining the rates of mass transfer of calcite and carbon dioxide gas along the flow path. The raw chemical concentration data and the field pH and temperature for each sample were input to WATEQF, a computer program for geochemical modeling (Plummer and others, 1976). Based on thermochemical data, WATEQF calculates the activities of all species in solution and the saturation state of the water with respect to mineral phases.

The saturation index for calcite (SI_c) is the logarithm of the ratio of the ion activity product to the equilibrium solubility product at sample temperature. The value of the saturation index indicates whether the solution is undersaturated (negative SI_c), supersaturated (positive SI_c), or at equilibrium ($\text{SI}_c = 0$) with respect to calcite. Given the errors in the pH values, the Ca^{2+} and HCO_3^- concentrations, and the thermodynamic data, the SI_c values can be reported to ± 0.05 units. The theoretical CO_2 partial pressure (PCO_2) of a hypothetical gas phase with which the water sample is in equilibrium is also calculated by WATEQF, using the ionic strength, HCO_3^- concentration, and pH of the sample. The stream-water samples were considered to be supersaturated with carbon dioxide if PCO_2 values were greater than the normal atmospheric PCO_2 of $10^{-3.50}$ atm. The error in calculated log PCO_2 values is ± 0.03 .

The calcite and CO_2 mass transfers (moles of reactant per one kilogram of H_2O , herein mol/kg) were determined by using a mass balance on the total calcium concentration and the total inorganic carbon concentration between successive pairs of sampling sites. The calcite mass transfer is simply the change in calcium concentration between two points. The CO_2 mass transfer is the change in total inorganic carbon concentration minus the change in calcium concentration, which accounts for the loss or gain of HCO_3^- due to calcite precipitation or dissolution. Negative mass transfer indicates calcite precipitation and CO_2 outgassing; positive mass transfer indicates calcite dissolution and CO_2 ingassing. The mass balance calculations were performed for stream segments

beginning slightly downstream from the springs (D-1) and ending at the last site (F-6). Mass balance calculations were not attempted between the springs and site D-1, because the three springs had variable chemical composition and discharge (Lorah, 1987). Because fresh travertine from Falling Spring Creek was identified by powder X-ray diffraction to be calcite with a trace amount of detrital quartz (R.S. Mitchell, 1986, personal communication), calcite was the only CaCO_3 mineral considered for the mass transfer calculations.

Rates of calcite precipitation and carbon dioxide outgassing (moles of reactant per one kilogram of H_2O in one second, herein mol/kg-s) were calculated by dividing each mass transfer by an estimated reaction time. Reaction time between successive sampling sites was computed from distance between successive sampling sites divided by flow velocity. An average uniform velocity, which was determined from the discharge measurements, was assumed to exist along the stream for each sampling trip. The results generated a discontinuous curve with a constant reaction rate between pairs of sampling sites.

Calculation of Calcite Precipitation Rates

Calcite precipitation rates were also calculated from the rate law developed by Plummer and others (Equation 1; 1978). The activities of ions observed in the stream water at each sampling site were obtained from the WATEQF calculations. The rate constants in Equation (1) were calculated from the temperature-dependent expressions given in Plummer and others (1978); the term k_1' was assumed to be 10 times larger than k_1 (Plummer and others, 1978; Suarez, 1983); and activities of ions on the calcite surface were assumed to equal those in the bulk water sample.

The model of Plummer and others gives the rates in units of mol/cm²-s. An estimated surface area for the stream bed and the volume of water flowing between two sampling locations was used to convert these rates to mol/kg-s. If the stream bottom and sides are assumed to have smooth rectangular shapes, the surface area, A, can be calculated from

$$A = 2ld + lw \quad (2)$$

where l is the length of the stream segment, d is the maximum water depth, and w is the width of the stream. The depth and width, which were obtained at the discharge measurement sites, were considered to be constants along the stream. The mass of water (kg H_2O) flowing between successive sites was calculated by multiplying the discharge by the reaction time. Multiplying the rate in units of mol/cm²-s by the surface area and dividing by the mass of water gives the calcite precipitation rates in mol/kg-s.

Calcite precipitation rates were estimated from the mass of calcite precipitated on each seed crystal during the time it

was in the stream. The surface areas of the seed crystals, which were calculated from their measured dimensions, were between 20 and 30 cm². Calcite precipitation rates (mol/s) were normalized over the surface area of the seed crystals to give the precipitation rates in units of mol/cm²-s.

To compare the mass transfer results with the seed crystal measurements, the mass transfers of calcite (mol/kg) for the date the seed crystal was placed in the stream and for the date it was removed were averaged and multiplied by the average discharge of water (kg/s). Calcite precipitation rates were then obtained in units of mol/cm²-s by normalizing the mass transfer to the surface area of the stream bed (Equation 2).

While the mass transfer results give the amount of calcite transferred out of solution between an initial and a final sampling site, each seed crystal only measured calcite accumulation at one specific sampling site. Thus, calcite could have precipitated on a crystal with a rate comparable to those given by the mass transfer results for the stretch of stream either immediately upstream or immediately downstream from the crystal's location. For comparison here, the mass transfer results for the upstream segment were used.

RESULTS

GEOCHEMICAL EVOLUTION

The results of the chemical analyses (Table 2) show that Ca^{2+} and HCO_3^- dominate the chemical character of Falling Spring Creek. The other major ions are SO_4^{2-} and Mg^{2+} . Concentrations of K^+ are elevated relative to Na^+ , and Na/K molar ratios range from 0.5 to 0.25. Chloride and F^- are present in low concentrations. Nitrate and PO_4^{3-} concentrations were determined to be below 5 and 1 mg/L, respectively. The pH values ranged from near neutral to values as high as 8.50. The entire data set is available in Lorah (1987).

Downstream and seasonal changes were observed in the stream-water composition. For each month that samples were collected, Ca^{2+} and HCO_3^- concentrations generally decreased downstream (Figures 3 and 4). Large decreases in Ca^{2+} and HCO_3^- concentrations occurred between the crest of the waterfall (F-3) and the last sampling site (F-6). These downstream changes were more pronounced in the summer and fall than in the spring and winter months (Figures 3 and 4). For example, HCO_3^- concentrations dropped by 48 percent from site F-3 to F-6 in October 1984, whereas a 28 percent decrease was observed in April 1985. The pH generally increased downstream except for a significant drop between the last two sampling sites (Figure 5). The most rapid change in pH occurred near the crest of the waterfall (F-1 to F-3) and directly at the waterfall (F-3 to F-4). Seasonally, concentrations of dissolved ions were higher in the

Table 2. Selected chemical analyses of Falling Spring Creek. Cond. is conductivity. All concentrations are in mg/L.

Sample	T (°C)	Cond. (μS/cm)	pH	HCO ₃ ⁻	Ca ²⁺	Mg ²⁺	Na ⁺	K ⁺	F ⁻	Cl ⁻	SO ₄ ²⁻
October 14, 1984											
S-1	24.3	700	7.32	308	165	25.4	5.1	14.2	1.0	3.3	283
S-3	24.6	730	7.23	316	168	28.0	3.9	14.8	1.1	3.5	291
S-2	24.7	720	7.20	315	169	26.2	3.9	14.3	1.1	5.8	296
D-1	24.3	730	7.24	310	168	26.0	3.4	14.2	1.1	3.2	283
D-3	23.6		7.43	314	168	26.2	2.8	12.9	1.2	3.5	288
F-1	21.4	695	7.79	312	166	25.6	3.5	13.9	1.2	3.4	286
F-3	20.5	695	8.06	311	164	25.2	3.7	14.0	1.0	3.5	283
F-4	19.7	690	8.27	278	160	25.6	3.6	14.3	1.0	3.8	286
F-5	19.6	690	8.28	273	157	25.5	3.1	14.1	1.1	3.4	283
F-2	18.4	660	8.37	264	151	25.6	3.2	14.3	1.0	3.4	283
F-6	14.4	442	8.25	210	122	21.3	3.3	11.4	0.7	4.0	246
April 6, 1985											
S-1	20.0	590	6.98	234	102	17.0	2.5	6.8	0.5	3.3	150
S-3	20.0	600	6.91	239	105	17.1	2.9	7.3	0.6	3.9	159
S-2	20.0	600	6.89	240	106	16.6	2.4	6.9	0.6	3.8	159
D-1	19.5	600	7.01	237	103	17.2	3.0	7.1	0.6	3.6	158
D-3	17.0	595	7.19	237	104	16.6	2.4	6.6	0.6	3.8	158
F-1	17.0	600	7.41	235	104	16.9	2.5	6.5	0.6	3.7	160
F-3	16.5	520	7.83	234	102	16.5	2.8	6.9	0.6	3.8	162
F-4	13.0	510	7.98	224	100	16.3	2.7	6.6	0.6	3.7	162
F-5	13.5	488	7.92	220	99	16.2	2.5	6.7	0.6	3.8	162
F-2	13.5	461	7.98	209	97	16.7	2.3	6.4	0.6	3.9	164
F-6	11.0	393	8.08	183	83	15.0	2.5	5.8	0.6	4.3	142

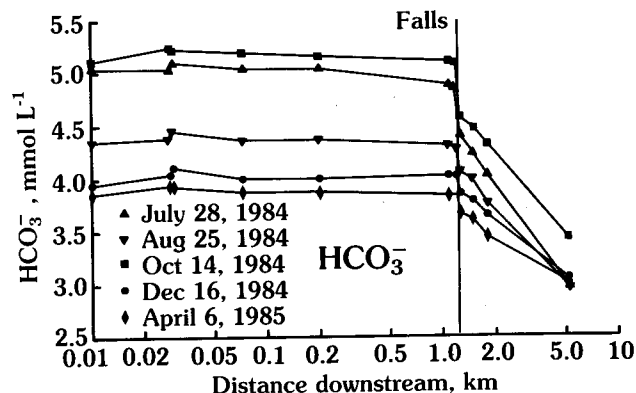
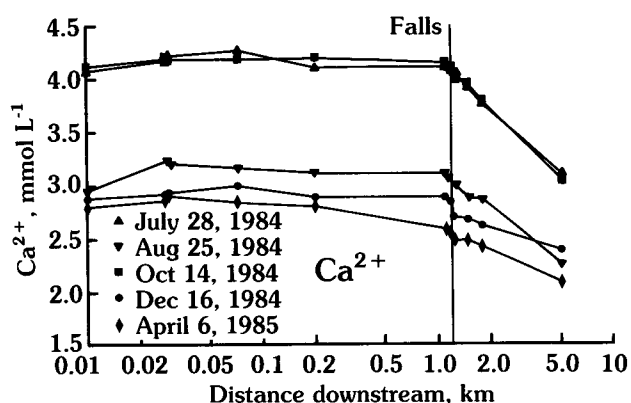


Figure 3. Millimolar Ca²⁺ concentration versus distance along the flow path. The flow path begins (0 km) at site S-1. Sample names and locations are given in Table 1.

Figure 4. Millimolar HCO₃⁻ concentration versus distance along the flow path.

summer and fall than in the spring and winter. The Ca^{2+} and HCO_3^- concentrations were highest in the July and October samples (Figures 3 and 4).

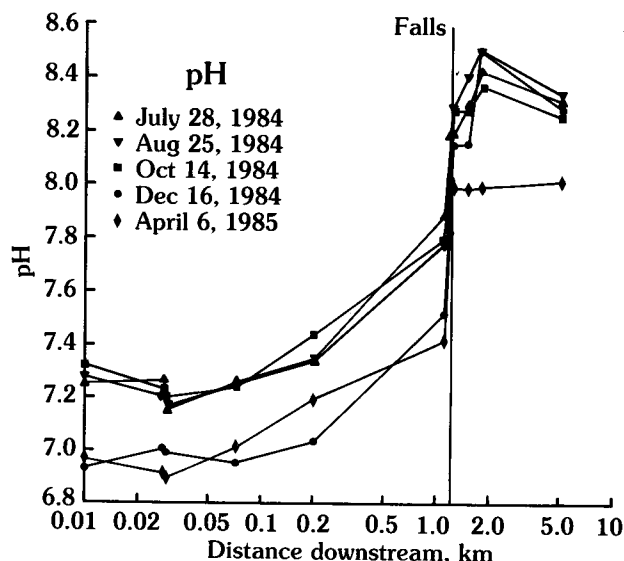


Figure 5. pH versus distance along the flow path.

The downstream changes in Ca^{2+} and HCO_3^- were much greater than the effect of dilution by inputs of groundwater to the stream. Concentrations of conservative constituents such as F^- and Cl^- , which can act as indicators of dilution, did not show a significant decrease along the flow path. In addition, discharge measurements did not indicate significant groundwater recharge or surface runoff entering the stream (Lorah, 1987; Lorah and Herman, 1988).

The results of the WATEQF calculations show that the stream was always supersaturated with CO_2 and usually supersaturated with respect to calcite. The calculated PCO_2 of the springs ranged from $10^{-2.02}$ to $10^{-1.56}$ atm throughout the year. The PCO_2 values decreased downstream except between the last two sampling sites for several of the months (Figure 6). The most rapid decrease in PCO_2 along the stream occurred in the vicinity of the waterfall on each sampling trip.

During the summer and fall, Falling Spring Creek was supersaturated with respect to calcite along the entire studied flow path (Figure 7). In contrast, the three springs were undersaturated in the spring and winter months, although the stream water reached supersaturation before site F-1 was reached. In the summer and fall the stream water was between approximately 11 and 16 times supersaturated ($\text{SI}_c = 1.0$ and 1.2) with calcite at the crest of the waterfall (F-3), but in the spring and winter months the water was only three to six times supersaturated ($\text{SI}_c = 0.5$ to 0.8) at this site. The most rapid increases in the saturation indices occurred from near the crest of the waterfall to below the waterfall (F-1 to F-4). The saturation indices generally continued to increase below the waterfall but decreased between the last two sites (F-2 to F-6).

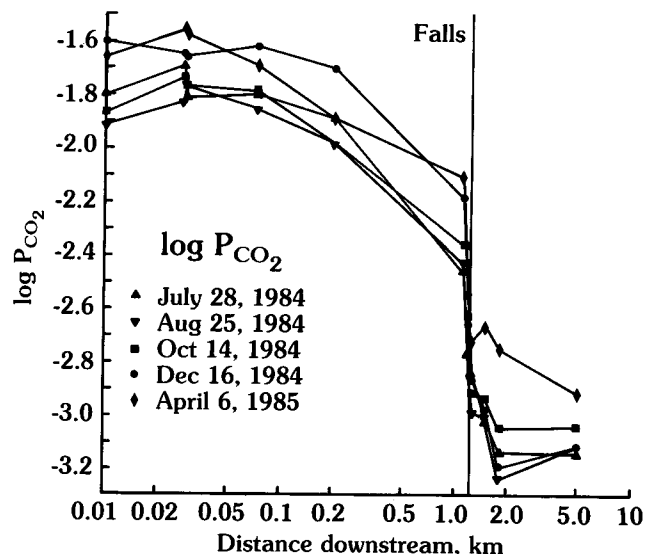


Figure 6. Calculated partial pressure of carbon dioxide gas (PCO_2) versus distance along the flow path. Normal atmospheric PCO_2 is $10^{-3.5}$ atm.

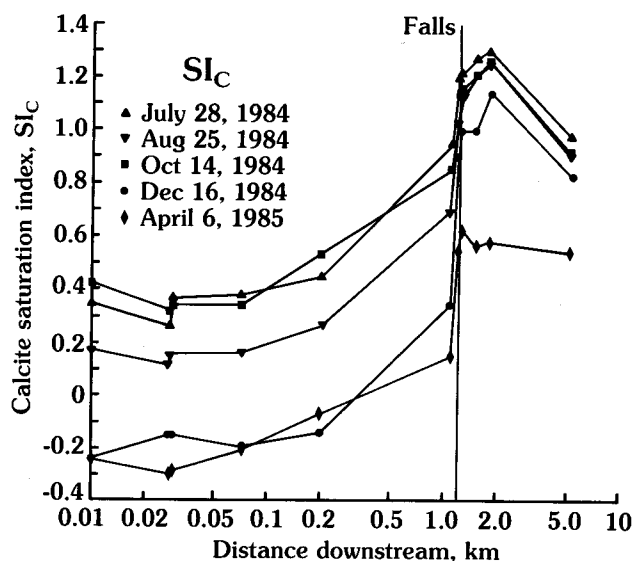


Figure 7. Saturation state with respect to calcite (SI_c) versus distance along the flow path. Positive values indicate the solution is supersaturated with respect to calcite; negative values indicate undersaturation.

The CO_2 outgassing and calcite precipitation rates varied over two or three orders of magnitude along Falling Spring Creek. The CO_2 outgassing rates increased significantly as the stream flowed over the escarpment (Table 3, Figure 8). Outgassing rates at the waterfall (F-3 to F-4) varied between 403×10^{-9} to 4180×10^{-9} mol/kg-s throughout the sampling period (Table 3). At all other sampling locations, outgassing rates were only between 0.57×10^{-9} to 781×10^{-9} mol/kg-s. Outgassing rates dropped to a minimum between the last two sites (F-2 to F-6) on each sampling date.

Table 3. Reaction rates for CO₂ outgassing and calcite precipitation are from mass transfer results and from calculations based on the rate law of Plummer and others (1978). Rate law results are reported for the initial point in each flow-path segment. All units are moles of reactant per one kilogram of H₂O in one second (herein, mol/kg·s). Negative signs denote calcite precipitation or CO₂ outgassing; positive signs denote calcite dissolution or CO₂ ingassing. Values that are marked with an asterisk (*) are suspect because they contradict the saturation state of the water with respect to calcite.

Sampling Sites (initial to final)	Mass Transfer Rates		Rate Law Rates
	Calcite	CO ₂	Calcite
June 23, 1984			
D-1 to D-3	-4.26 x 10 ⁻⁸	-8.50 x 10 ⁻⁸	-5.2 x 10 ⁻⁹
D-3 to F-1	+1.02 x 10 ^{-8*}	-7.16 x 10 ⁻⁸	-6.5 x 10 ⁻⁹
F-1 to F-3	-7.80 x 10 ⁻⁹	-2.95 x 10 ⁻⁷	-2.1 x 10 ⁻⁸
F-3 to F-4	-2.28 x 10 ⁻⁶	-1.18 x 10 ⁻⁶	-5.0 x 10 ⁻⁸
F-4 to F-5	+3.42 x 10 ^{-8*}	-1.33 x 10 ⁻⁷	-6.2 x 10 ⁻⁸
F-5 to F-2	-5.33 x 10 ⁻⁸	-8.11 x 10 ⁻⁸	-7.4 x 10 ⁻⁸
F-2 to F-6	-3.72 x 10 ⁻⁸	-5.67 x 10 ⁻¹⁰	-7.5 x 10 ⁻⁸
F-6			-2.8 x 10 ⁻⁸
July 28, 1984			
D-1 to D-3	-1.92 x 10 ⁻⁷	+6.86 x 10 ^{-8*}	-1.1 x 10 ⁻⁸
D-3 to F-1	-2.00 x 10 ⁻⁹	-1.00 x 10 ⁻⁷	-1.4 x 10 ⁻⁸
F-1 to F-3	-8.16 x 10 ⁻⁸	-2.06 x 10 ⁻⁷	-4.7 x 10 ⁻⁸
F-3 to F-4	-1.51 x 10 ⁻⁷	-4.18 x 10 ⁻⁶	-9.6 x 10 ⁻⁸
F-4 to F-5	-1.00 x 10 ⁻⁷	-4.26 x 10 ⁻⁸	-8.1 x 10 ⁻⁸
F-5 to F-2	-9.70 x 10 ⁻⁸	-6.66 x 10 ⁻⁸	-1.1 x 10 ⁻⁷
F-2 to F-6	-3.63 x 10 ⁻⁸	-1.45 x 10 ⁻⁸	-1.2 x 10 ⁻⁷
F-6			-5.7 x 10 ⁻⁸
August 25, 1984			
D-1 to D-3	-2.46 x 10 ⁻⁸	-1.84 x 10 ⁻⁷	-5.2 x 10 ⁻⁹
D-3 to F-1	-1.03 x 10 ⁻⁸	-4.79 x 10 ⁻⁸	-7.3 x 10 ⁻⁹
F-1 to F-3	-7.33 x 10 ⁻⁸	-2.98 x 10 ⁻⁷	-2.5 x 10 ⁻⁸
F-3 to F-4	-5.53 x 10 ⁻⁷	-3.31 x 10 ⁻⁶	-6.5 x 10 ⁻⁸
F-4 to F-5	-9.87 x 10 ⁻⁸	-7.97 x 10 ⁻⁸	-7.1 x 10 ⁻⁸
F-5 to F-2	-5.59 x 10 ⁻⁸	-1.12 x 10 ⁻⁷	-8.9 x 10 ⁻⁸
F-2 to F-6	-3.52 x 10 ⁻⁸	-7.19 x 10 ⁻⁹	-9.0 x 10 ⁻⁸
F-6			-4.0 x 10 ⁻⁸
October 14, 1984			
D-1 to D-3	+1.91 x 10 ^{-8*}	-1.50 x 10 ⁻⁷	-9.8 x 10 ⁻⁹
D-3 to F-1	-6.62 x 10 ⁻⁹	-2.94 x 10 ⁻⁸	-1.6 x 10 ⁻⁸
F-1 to F-3	-8.38 x 10 ⁻⁸	-8.60 x 10 ⁻⁸	-3.7 x 10 ⁻⁸
F-3 to F-4	-5.64 x 10 ⁻⁷	-3.22 x 10 ⁻⁶	-6.8 x 10 ⁻⁸
F-4 to F-5	-2.99 x 10 ⁻⁸	-1.05 x 10 ⁻⁸	-9.2 x 10 ⁻⁸
F-5 to F-2	-6.14 x 10 ⁻⁸	-8.95 x 10 ⁻⁹	-9.0 x 10 ⁻⁸
F-2 to F-6	-2.64 x 10 ⁻⁸	-2.06 x 10 ⁻⁹	-1.1 x 10 ⁻⁷
F-6			-5.1 x 10 ⁻⁸
December 16, 1984			
D-1 to D-3	-5.30 x 10 ^{-8*}	-1.29 x 10 ⁻⁷	+4.3 x 10 ⁻¹¹
D-3 to F-1	0.00	-9.36 x 10 ⁻⁸	-6.4 x 10 ⁻¹⁰
F-1 to F-3	-5.60 x 10 ⁻⁸	-2.93 x 10 ⁻⁷	-9.1 x 10 ⁻⁹
F-3 to F-4	-1.27 x 10 ⁻⁶	-4.03 x 10 ⁻⁷	-3.2 x 10 ⁻⁸
F-4 to F-5	-1.12 x 10 ⁻⁸	-2.23 x 10 ⁻⁸	-4.1 x 10 ⁻⁸
F-5 to F-2	-3.46 x 10 ⁻⁸	-9.13 x 10 ⁻⁸	-4.1 x 10 ⁻⁸
F-2 to F-6	-2.06 x 10 ⁻⁸	-5.83 x 10 ⁻⁹	-8.0 x 10 ⁻⁸
F-6			-3.6 x 10 ⁻⁸

Sampling Sites (initial to final)	Mass Transfer Rates		Rate Law Rates
	Calcite	CO ₂	Calcite
February 16, 1985			
D-1 to D-3	-1.25 x 10 ^{-8*}	-1.13 x 10 ⁻⁷	-1.0 x 10 ⁻⁹
D-3 to F-1	0.00	-4.29 x 10 ⁻⁸	-1.7 x 10 ⁻⁹
F-1 to F-3	0.00	-7.81 x 10 ⁻⁷	-3.9 x 10 ⁻⁹
F-3 to F-4	-1.63 x 10 ⁻⁷	-6.53 x 10 ⁻⁷	-1.6 x 10 ⁻⁸
F-4 to F-5	-5.88 x 10 ⁻⁹	-8.74 x 10 ⁻⁸	-2.3 x 10 ⁻⁸
F-5 to F-2	-9.49 x 10 ⁻⁹	-5.86 x 10 ⁻⁸	-3.2 x 10 ⁻⁸
F-2 to F-6	-3.88 x 10 ⁻⁸	-1.16 x 10 ⁻⁸	-4.2 x 10 ⁻⁸
F-6			-2.3 x 10 ⁻⁸
April 6, 1985			
D-1 to D-3	+2.55 x 10 ⁻⁸	-4.98 x 10 ⁻⁷	+4.4 x 10 ⁻¹⁰
D-3 to F-1	0.00	-6.88 x 10 ⁻⁸	-2.0 x 10 ⁻⁹
F-1 to F-3	-1.07 x 10 ⁻⁷	-4.67 x 10 ⁻⁷	-5.7 x 10 ⁻⁹
F-3 to F-4	-7.43 x 10 ⁻⁷	-1.70 x 10 ⁻⁶	-1.9 x 10 ⁻⁸
F-4 to F-5	-1.24 x 10 ⁻⁹	-4.59 x 10 ⁻⁸	-2.5 x 10 ⁻⁸
F-5 to F-2	-5.25 x 10 ⁻⁸	-1.07 x 10 ⁻⁷	-2.1 x 10 ⁻⁸
F-2 to F-6	-2.35 x 10 ⁻⁸	-7.64 x 10 ⁻⁹	-2.3 x 10 ⁻⁸
F-6			-2.2 x 10 ⁻⁸

The lowest calcite precipitation rates or small dissolution rates were calculated for the beginning of the stream, commonly between sites D-1 to D-3 or sites D-3 to F-1 (Table 3, Figure 9). Calcite precipitation rates reached a distinct maximum at the waterfall (F-3 to F-4) throughout the sampling period, varying between 151×10^{-9} and 2280×10^{-9} mol/kg·s (Table 3). The rates dropped again downstream from the waterfall (F-4 to F-6) but generally remained higher than those seen above the waterfall (D-1 to F-1). The total amount of calcite precipitated along Falling Spring Creek was calculated from the sum of the mass transfers for each sampling date (shaded boxes, Figure 10). Calcite precipitation reached a peak on the July trip (1.18×10^{-3} mol/kg) and remained high through October. Compared to the July trip, calcite precipitation was lower by more than 50 percent on the February and April 1985 sampling trips (0.56×10^{-3} and 0.50×10^{-3} mol/kg, respectively).

COMPARISON OF CALCITE PRECIPITATION RATES

The results obtained from the experimentally derived rate law and from the mass transfer calculations generally agreed within an order of magnitude or better (Table 3, Figure 9). Both methods also gave the same downstream trends in the reaction rates. Low precipitation rates were calculated upstream from the waterfall (D-1 to F-1), and higher rates were predicted at, and downstream from, the waterfall (F-1 to F-6). There were some discrepancies, however, between the methods. The rate law predicted much smaller precipitation rates at the waterfall and generally higher rates below the waterfall than the mass transfer results (Table 3). In a few

instances, the mass transfer calculations showed calcite dissolution, while the rate law calculations predicted calcite precipitation. These cases occurred when the calcium concentration increased along a stream segment even though the solution was supersaturated with respect to calcite.

The seed crystal results gave lower calcite precipitation rates than either the mass transfer or rate law results (Table 4). The greatest differences between the seed crystal and the mass transfer results are seen at the waterfall (F-4). At this site the mass transfer rates were 60 to 441 times higher than the seed crystal measurements. Elsewhere along the stream, the mass transfer rates were greater than the crystal growth rates by a factor of 1.3 to 166. During each measurement period, calcite precipitation rates were most rapid on the seed crystals placed at site F-5 below the waterfall; however, the mass transfer results always showed a distinct maximum at the top of the waterfall (F-4). Overall, the rate law calculations and the mass transfer results agreed better with each other (a factor of 1 to 45) than either did with the seed crystal measurements (Table 4).

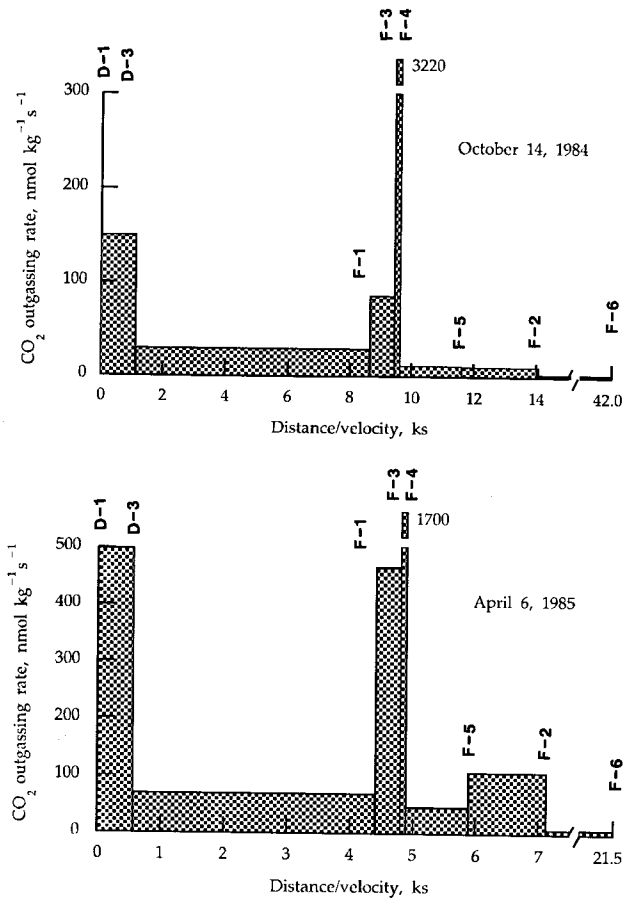


Figure 8. CO₂ outgassing rates versus reaction time (distance/velocity) between sampling points. The mass transfer rates were calculated for sequential segments of the flow path beginning at D-1. Two representative sampling dates are shown.

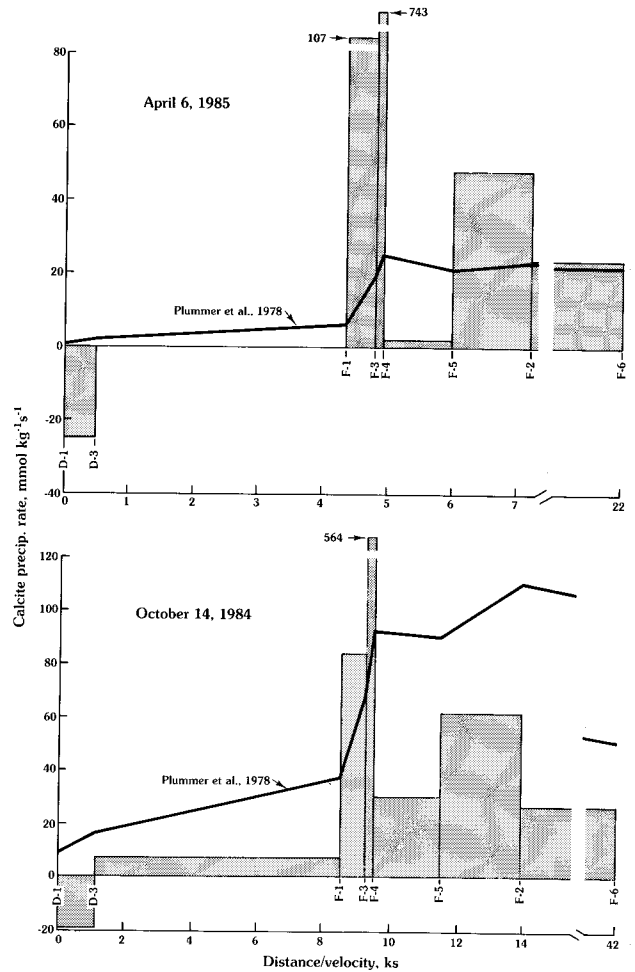


Figure 9. Calcite precipitation rates versus reaction time (distance/velocity) between sampling points for the mass transfer results (shown as shaded boxes) and the rate law results (shown as line labelled Plummer et al., 1978). Two representative sampling dates are shown.

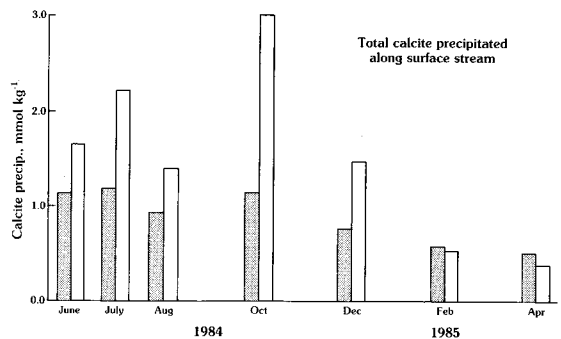


Figure 10. Total amount of calcite precipitated along the stream for the mass transfer results (shown as shaded boxes) and the rate law results (shown as unshaded boxes).

Table 4. Comparison of calcite precipitation rates calculated from the calcite seed crystal measurements, from the mass transfer results, and from the rate law of Plummer and others (1978). Rates are in units of mol/cm²·s.

Measurement Dates		Location of Crystal	Precipitation Rates		
From	To		Seed Crystal	Mass Transfer	Rate Law
6-23-84	7-28-84	F-4	7.9 x 10 ⁻¹¹	3.2 x 10 ⁻⁸	1.7 x 10 ⁻⁹
6-23-84	7-28-84	F-5	5.3 x 10 ⁻¹⁰	6.9 x 10 ⁻¹⁰	2.2 x 10 ⁻⁹
6-23-84	7-28-84	F-2	4.2 x 10 ⁻¹¹	1.8 x 10 ⁻⁹	2.3 x 10 ⁻⁹
7-28-84	8-25-84	F-4	1.2 x 10 ⁻¹⁰	7.2 x 10 ⁻⁹	1.7 x 10 ⁻⁹
7-28-84	8-25-84	F-5	3.9 x 10 ⁻¹⁰	2.2 x 10 ⁻⁹	2.2 x 10 ⁻⁹
7-28-84	8-25-84	F-2	2.1 x 10 ⁻¹⁰	1.7 x 10 ⁻⁹	2.4 x 10 ⁻⁹
8-25-84	10-14-84	F-4	9.9 x 10 ⁻¹¹	1.4 x 10 ⁻⁸	1.9 x 10 ⁻⁹
8-25-84	10-14-84	F-5	5.2 x 10 ⁻¹⁰	1.3 x 10 ⁻⁹	2.1 x 10 ⁻⁹
8-25-84	10-14-84	F-2	1.8 x 10 ⁻¹⁰	1.4 x 10 ⁻⁹	2.4 x 10 ⁻⁹
10-14-84	12-16-84	F-3	2.3 x 10 ⁻¹¹	1.8 x 10 ⁻⁹	1.2 x 10 ⁻⁹
10-14-84	12-16-84	F-4	6.2 x 10 ⁻¹¹	2.2 x 10 ⁻⁸	1.6 x 10 ⁻⁹
10-14-84	12-16-84	F-5	1.8 x 10 ⁻¹⁰	5.5 x 10 ⁻¹⁰	1.6 x 10 ⁻⁹
10-14-84	12-16-84	F-2	3.7 x 10 ⁻¹¹	1.2 x 10 ⁻⁹	2.4 x 10 ⁻⁹
12-16-84	2-16-85	F-3	5.3 x 10 ⁻¹²	8.8 x 10 ⁻¹⁰	6.2 x 10 ⁻¹⁰
12-16-84	2-16-85	F-4	5.9 x 10 ⁻¹¹	2.6 x 10 ⁻⁸	8.2 x 10 ⁻¹⁰
12-16-84	2-16-85	F-5	1.0 x 10 ⁻¹⁰	2.8 x 10 ⁻¹⁰	9.3 x 10 ⁻¹⁰
12-16-84	2-16-85	F-2	5.8 x 10 ⁻¹¹	6.6 x 10 ⁻¹⁰	1.6 x 10 ⁻⁹

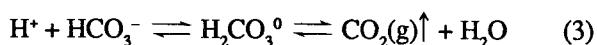
DISCUSSION

GEOCHEMICAL EVOLUTION

Carbon dioxide outgassing and calcite precipitation are the two major processes controlling the chemical changes along Falling Spring Creek. The water chemistry data, the saturation state of the waters relative to carbon dioxide gas and calcite, and the rates obtained from the mass transfer calculations substantiate this conclusion.

Carbon Dioxide Outgassing

Outgassing is evident along Falling Spring Creek. The decrease in HCO₃⁻ concentration (Figure 4) and increase in pH downstream (Figure 5) reflect the loss of CO₂:



Thus, H⁺ ions are consumed during outgassing to give a rise

in pH, and an equal amount of HCO₃⁻ is lost from solution.

Rates of CO₂ transfer out of solution (Table 3, Figure 8) are relatively high immediately downstream from the springs (sites D-1 to D-3, 140 x 10⁹ to 460 x 10⁹ mol/kg·s). No distinct decrease in HCO₃⁻ concentration is measured along this stretch of stream (Figure 4) because HCO₃⁻ concentration is a less sensitive parameter than pH to changes in the partial pressure of CO₂ (Shuster and White, 1971; Jacobson and Usdowski, 1975).

Although the water is still highly supersaturated with CO₂, outgassing rates drop significantly along the next 920 m of Falling Spring Creek (D-3 to F-1). Between these sampling locations the stream flows along a fairly smooth and straight path. As the stream encounters the small riffles near the top of the waterfall (F-1 to F-3) and the waterfall itself (F-3 to F-4), greater water turbulence leads to more rapid loss of CO₂. Near the crest of the waterfall (F-1 to F-3), pH values increase by 0.3 to 0.5 unit over the short distance of 100 m, and PCO₂ values show a corresponding sharp decrease. The solution composition changes dramatically as the stream cascades over the 20-m-high escarpment. The first distinct decrease in HCO₃⁻ concentration is seen at the waterfall (Figure 4). Carbon dioxide gas escapes from the turbulent water as fast as 4180 x 10⁹ mol/kg·s (Table 3). Thus, this

study clearly shows the direct relationship between rapid CO₂ outgassing and turbulent areas in carbonate streams.

Outgassing continues downstream from the waterfall, but rates decline below the high values seen at the waterfall. Outgassing rates generally drop to a minimum between the last two sampling sites (F-2 to F-6), because the CO₂ concentration gradient between the stream water and the air is at a minimum. Temperature is another factor that could slow the outgassing rates. Water temperatures drop by as much as 10°C along the studied flow path as the thermal spring water adjusts to the cooler air temperature and as evaporative cooling occurs (Lorah, 1987). Because CO₂ solubility increases with lower temperatures, the rate of outgassing would decrease downstream. The stream is still slightly supersaturated with respect to CO₂ at the last sampling site, which lies approximately 5.2 km downstream from the springs. Carbonate waters are known to remain supersaturated with CO₂ after many hours of contact with the open atmosphere (Barnes, 1965; Jacobson and Langmuir, 1970). Approximately 6 to 12 hours, depending on the flow velocity on a sampling date, elapse as a volume of water flows from the surface springs to the last sampling site.

Calcite Precipitation

Calcite precipitation



is extensive along Falling Spring Creek because the steep concentration gradient for CO₂ between the stream water and the atmosphere and the turbulence of the stream water allow extensive CO₂ outgassing.

Calcite does not precipitate instantaneously as supersaturation is reached. The Ca²⁺ and HCO₃⁻ concentrations remain nearly constant for the first 1.12 km of flow path (S-1 to F-1), even though the water becomes more and more supersaturated with respect to calcite. In the summer and fall months the water becomes five to nine times supersaturated (SI_c = 0.7 and 1.0) with respect to calcite before site F-1 is reached (Lorah, 1987; Lorah and Herman, 1988). But reaction rate calculations indicate that very little calcite precipitation occurs upstream from this sampling location (Table 3, Figure 9).

Further CO₂ outgassing and increase in calcite supersaturation is needed to overcome the kinetic inhibitions to calcite crystallization. In the highly turbulent areas near the crest of, and at, the waterfall, a rapid increase in the degree of supersaturation (Figure 7) occurs in response to the higher outgassing rates (Figure 8). A large decrease in the Ca²⁺ and HCO₃⁻ concentrations (Figures 3 and 4) provides chemical evidence that significant calcite precipitation begins in the vicinity of the waterfall. The HCO₃⁻ concentrations drop

more dramatically than Ca²⁺, because both calcite precipitation and CO₂ outgassing are removal mechanisms for HCO₃⁻. The calculated calcite precipitation rates (Figure 9) are large near the crest of the waterfall (F-1 to F-3), but they reach a maximum at the waterfall (F-3 to F-4).

The travertine deposits are physical evidence for calcite precipitation in the stream. Travertine is not noticeable between the springs and site F-1. Near the crest of the waterfall, buildups of travertine (Figure 2B) have formed small rimstone dams and coatings over rocks, twigs, bottles, and other materials in the stream bed. The vertical cliff at the waterfall (Figure 2A) is a thick "cascade-type" travertine deposit, characterized by draped and stalactite-like forms that are layered due to successive coatings of travertine (Chafetz and Folk, 1984; Dennen and Diecchio, 1984; Dennen and others, this volume). At the base of the waterfall, thick deposits extend above the stream's surface (Figure 2A), and fresh white calcite crusts were observed on everything in contact with the stream water, including undecomposed leaves and twigs. Travertine deposits are most obvious at, and immediately below, the waterfall (Dennen and others, this volume), but more rimstone dams are evident for at least 1.0 km downstream from the waterfall. Thus, the combined chemical and physical evidence suggests that calcite precipitation begins and reaches its maximum rate in the highly turbulent area of the waterfall.

The pattern of calcite precipitation observed along Falling Spring Creek demonstrates the kinetic inhibition that has been noted in several other travertine-depositing streams (Jacobson and Usdowski, 1975; Usdowski and others, 1979; Dandurand and others, 1982). Three factors are most often mentioned as inhibiting calcite precipitation: an energy barrier to calcite nucleation and growth (Stumm and Morgan, 1981), a lack of suitable nucleation sites (Suarez, 1983), and the presence of strongly adsorbing species such as dissolved magnesium or phosphate ions (Morse, 1983).

Ions adsorbing to the calcite surface are not likely to inhibit precipitation rates in this stream. Phosphate was not detectable in the stream water, and no relationship could be found between the magnesium concentration and the degree of supersaturation required for the onset of calcite precipitation (Lorah, 1987; Lorah and Herman, 1988). Contact with calcite as a nucleation site does not seem necessary for deposition at Falling Spring Creek, because travertine coatings are found on any material in the water's path. Particles in suspension and material on the channel bottom and sides could act as nucleation sites all along the stream. One study has shown that contact of stream water with previously deposited travertine accelerates calcite precipitation rates in the vicinity of waterfalls (Steidtmann, 1936). The possibility of an energy barrier to calcite nucleation and growth remains difficult to evaluate. The rapid outgassing of CO₂ and associated rise in pH and the calcite supersaturation state at the waterfall may allow such an energy barrier to be passed, even at the lower supersaturation levels observed during

winter and early spring.

Although the rate of precipitation is not as high as at the waterfall, calcite deposition continues along the 4 km of stream that was studied below the waterfall (Figure 9). Despite this prolonged precipitation, the water remains far from equilibrium with respect to calcite at the last sampling site. As calcite precipitates, more CO_2 is produced (Equation 4) and must be removed from solution to maintain the high level of calcite supersaturation observed. The calcite saturation index only decreases significantly between the last two sampling sites (Figure 7), showing that calcite precipitation finally begins to outpace the loss of CO_2 from the stream water. The drop in pH at the last site also indicates that more CO_2 is being added to the water by calcite precipitation than is removed by CO_2 outgassing (Figure 5). Outgassing rates reached a minimum between the last two sampling sites throughout the year. Once the driving force of CO_2 outgassing has decreased, Falling Spring Creek finally begins to approach equilibrium with respect to calcite.

Seasonally, the amount of calcite precipitated is tied to the mixing of the two carbonate-rich waters inside Warm River Cave (Herman and Lorah, 1986; Herman and Lorah, 1987). During low-flow conditions in summer and fall, less of the shallow groundwater is available to dilute the more concentrated thermal water inside the cave. The mixed stream emerges already supersaturated with respect to calcite, and outgassing of CO_2 can then drive the stream water to a higher degree of calcite supersaturation than observed during the spring and winter. Consequently, more calcite must be precipitated per unit volume of water to reach equilibrium with respect to calcite. On the July trip when travertine deposition was a maximum, the water reached 16 times supersaturation ($\text{SI}_c = 1.2$) with respect to calcite at the crest of the waterfall. On this date, a total of 1.18×10^{-3} mol/kg, or 0.118 g/kg, of calcite was precipitated along the studied section of Falling Spring Creek (shaded boxes, Figure 10). High-flow conditions during the spring and winter months cause the thermal cave stream to become greatly diluted by shallow groundwater, and the mixed water emerges from the cave undersaturated with respect to calcite. In February and April 1985 the net amount of calcite precipitated was more than 50 percent lower than observed in July. This seasonal effect of shallow groundwater dilution was also recognized by Dennen and Diecchio (1984) and Dennen and others (this volume), who expected the greatest calcite precipitation to occur in late summer when dilution would be least.

COMPARISON OF CALCITE PRECIPITATION RATES

Rates of Mass Transfer

The mass transfer rates, which are based on the observed chemical composition of Falling Spring Creek, are used to

assess how accurately calcite precipitation rates could be predicted by two other methods. Errors in the mass transfer results themselves may arise from errors in both the chemical and hydrologic data. Some of the mass balance calculations are suspect because they contradict the saturation state of the water with respect to calcite (Lorah and Herman, 1988). These contradictory results were obtained for the upper reaches of the stream where the Ca^{2+} concentrations differed only slightly between the consecutive samples. Because very small changes in Ca^{2+} concentrations were being subtracted, relatively small errors in the chemical analyses became magnified.

Errors in the reaction times, which were calculated from the discharge measurements, could also lead to errors in the rates. The analytical error in the discharge measurements was between 3 and 23 percent (Lorah, 1987; Lorah and Herman, 1988). In addition, a large error in the reaction time could occur from assuming a uniform velocity along the stream. Because the same reaction time values were used to compute the precipitation rates for all three methods, however, this common error does not need to be considered when comparing the different results.

Rate Law Calculations

The field-based mass transfer rates were compared to those calculated with an experimentally derived rate equation (Plummer and others, 1978). These two methods of determining reaction rates differ greatly. One approach applies mass balance calculations to observed chemical data from a natural water system; the other approach involves a theoretical and experimental study of the calcite dissolution/precipitation reaction. Yet, the two results agree remarkably well (Table 3, Figure 9).

The largest difference is seen at the waterfall where the rate law predicts a lower precipitation rate by a factor of 1.7 to 45 (Table 3). Other than at the waterfall, the rates agree within a factor of 1 to 18. The stream water is highly supersaturated with respect to calcite at the waterfall, and both nucleation and growth are likely to be occurring. Because the rate law only considers calcite growth, the equation could underestimate rates for the extreme conditions at the waterfall. The mass transfer rates are lower than the rate law calculations for most other segments of the stream, especially downstream from the waterfall.

Problems in estimating the surface area of the stream could account for some of the disagreement between the mass transfer and the rate law results. For comparison to the mass transfer rates, the results from the rate equation were multiplied by an estimated surface area over which the chemical reactions could be taking place in Falling Spring Creek. Although a crystal's surface area can be measured carefully for use in laboratory studies, the surface area of a stream bed

cannot be determined as easily or accurately. In this study, the stream was assumed to have a smooth rectangular shape which probably does not give the actual effective surface area of the stream bed. Factors such as roughness of the stream bed and grain size of the sediments would have a large control on the area available for precipitation to occur. At the waterfall the stream bed deviates more from a smooth, rectangular shape than at any other section of Falling Spring Creek. Because the large, irregularly shaped deposits of travertine would provide numerous nucleation sites for fresh calcite, the surface area could have been greatly underestimated in the vicinity of the waterfall. If the surface area was underestimated, the rates calculated with the equation of Plummer and others would also be underestimated. This error could contribute to the larger deviation between the mass transfer and rate law results noted at the waterfall.

To determine the overall agreement between the mass transfer results and the rate law calculations, the net amount of calcite precipitation predicted by the two methods was also compared for each sampling date. For the rate law results, the average calcite precipitation rate between each successive initial and final sampling point was calculated and then multiplied by the reaction time between the sites. All the stream segments were summed to give the predicted total amount of calcite precipitated. The agreement between the mass transfer results (shaded boxes, Figure 10) and the rate law calculations (unshaded boxes, Figure 10) is remarkable. Although the calcite precipitation rates calculated from the two methods differed by a factor of 1 to 45 (Table 3, Figure 9), the net amount of calcite precipitation given by the two methods agree within a factor of 3 for each sampling date (Figure 10). In addition, both methods show the same seasonal pattern of calcite precipitation. Considering the vastly different theoretical basis of the two methods, the agreement between the mass transfer and rate law results is too close to be fortuitous and gives some encouragement that the rate law can be used outside the laboratory.

Calcite Seed Crystals

The calcite precipitation rates determined from the seed crystal measurements were 1.3 to 441 times lower than the mass transfer results (Table 4). Many factors could have prevented calcite precipitation on the seed crystals. The cages probably disrupted water flow to the crystals, and they often became covered with debris such as twigs and leaves, which would have further blocked access of the water to the crystals. Some of the precipitated calcite could have been dislodged and transported downstream in suspension, instead of being trapped permanently on the crystal surface. Although all the losses of Ca^{2+} and HCO_3^- from the stream water were attributed to calcite precipitation in the mass transfer calculations, the seed crystal technique would not be able to account for calcite in suspension.

The location of the seed crystals and the length of time that they remained in the stream could also have influenced the rate calculations. Calcite precipitation is not uniform across the width of the stream in any one area, as seen by the irregular shape and distribution of the travertine deposits. Therefore, the crystal's location in the stream could be a factor in the amount of calcite that accumulated on it. Precipitation rates for the seed crystals were calculated as a gross average over a period of 28 to 63 days, depending on the length of time between sampling trips. Precipitation rates determined from the mass transfer calculations were based only on the chemical changes observed on a specific date.

The largest error between the mass transfer results and the seed crystal results occurs at the waterfall (F-4, Table 4). The estimated surface area of the stream bed probably accounts for the error at this site. For comparisons, the precipitation rates obtained by the mass balance calculations were normalized over the surface area of the stream bed. If the surface area was underestimated at the waterfall, the calcite precipitation rates given by the mass transfer results expressed per unit area would be too high. The results of the present study suggest that the seed crystal method does not give accurate calcite precipitation rates, although this approach may still be useful in giving qualitative information.

CONCLUSIONS

The processes of carbon dioxide outgassing and calcite precipitation control the chemical evolution of the travertine-depositing stream in this study. When the carbonate groundwater issues to the surface and feeds Falling Spring Creek, CO_2 outgassing occurs as the stream water adjusts toward equilibrium with the atmosphere. Outgassing forces the solution to high degrees of supersaturation with respect to calcite. By using mass balance calculations and estimates of reaction time, the rates of CO_2 outgassing and calcite precipitation along the flow path were quantified.

Calcite precipitation rates are low or nonexistent along the first 1.12 km of Falling Spring Creek where the stream flows along with little agitation. Rapid CO_2 outgassing and increased calcite supersaturation in the vicinity of the waterfall are needed to overcome the kinetic inhibitions on calcite nucleation and growth. At all times of the year, CO_2 outgassing and calcite precipitation occur most rapidly at the 20-m-high waterfall where water turbulence is greatest. The stream water does not attain equilibrium with respect to either CO_2 or calcite by the last sampling point 4 km downstream from the waterfall. Net calcite precipitation occurs along Falling Spring Creek throughout the year but decreases by as much as 50 percent during the high-flow conditions in the spring and winter.

Using an experimentally derived rate law developed by Plummer and others (1978), calcite precipitation rates were

predicted to within a factor of 1 to 45 of the mass transfer rates. Considering the fundamental difference between these two approaches, the agreement between the field-based mass transfer rates and the predictions from the rate law was very good. Calcite precipitation rates could not be quantified accurately by measuring calcite accumulation on seed crystals that were placed in the stream. Those rates were within a factor of 441 of agreeing with the mass transfer rates.

ACKNOWLEDGMENTS

We thank David Hubbard, Jr. for first showing us Warm River Cave and Falling Spring Creek. Burton Parker, Gusztav Asboth, and Joe West graciously allowed us access to their properties. We thank the people who assisted with field or laboratory work: Jeffrey Sitler, David Hubbard, Jr., Isabelle Cozzarelli, Carl Moses, Butler Stringfield, Kimberly Hoffer, Jeff Flanzenbaum, Rod Morris, Fred Daus, Bill Murray, Carol Wicks, Alan Howard, and Patsy Howard. We gratefully acknowledge financial support provided by the U.S. Geological Survey (United States - Spain Joint Committee for Scientific and Technological Cooperation grant number 83-007) and the University of Virginia. We thank Niel Plummer, Michael Reddy, and Lennart Sjöberg for their advice. We thank Don Rimstidt, Rick Diecchio, and Mike Upchurch for their helpful comments on an early version of this manuscript.

REFERENCES CITED

- Back, William, Hanshaw, B.B., Plummer, L.N., Rahn, P.H., Rightmire, C.T., and Rubin, Meyer, 1983, Process and rate of dedolomitization: Mass transfer and ^{14}C dating in a regional carbonate aquifer: *Geological Society America Bulletin*, v. 94, p. 1415-1429.
- Barnes, Ivan, 1965, Geochemistry of Birch Creek, Inyo County California - a travertine depositing creek in an arid climate: *Geochimica et Cosmochimica Acta*, v. 29, p. 85-112.
- Butler, J.N., 1982, Carbon dioxide equilibria and their applications: Reading, Massachusetts, Addison-Wesley Publishing Company, 259 p.
- Chafetz, H.S., and Folk, R.L., 1984, Travertines: depositional morphology and the bacterially constructed constituents: *Journal of Sedimentary Petrology*, v. 54, p. 289-316.
- Dandurand, J.L., Gout, R., Hoefs, J., Menschel, Günther, Schott, J., and Usdowski, Eberhard, 1982, Kinetically controlled variations of major components and carbon and oxygen isotopes in a calcite-precipitating spring: *Chemical Geology*, v. 36, p. 299-315.
- Dennen, K.O., and Diecchio, R.J., 1984, The Falling Spring, Alleghany County, Virginia, in Rader, E.K., and Gathright, T.M., II, eds., Stratigraphy and structure in the thermal spring area of the western anticlines: Virginia Division of Mineral Resources, Sixteenth Annual Virginia Geologic Field Conference, p. 17-19.
- Herman, J.S., and Lorah, M.M., 1986, Groundwater geochemistry in Warm River Cave Virginia: *National Speleological Society Bulletin*, v. 48, p. 54-61.
- Herman, J.S., and Lorah, M.M., 1987, CO_2 outgassing and calcite precipitation in Falling Spring Creek, Virginia, U.S.A.: *Chemical Geology*, v. 62, p. 251-262.
- Herman, J.S., and Lorah, M.M., 1988, Calcite precipitation rates in the field: measurement and prediction for a travertine-depositing stream: *Geochimica et Cosmochimica Acta*, v. 52, p. 2347-2355.
- House, W.A., 1981, Kinetics of crystallization of calcite from calcium bicarbonate solutions: *Journal of the Chemical Society, Faraday Transactions 1*, v. 77, p. 341-359.
- Inskip, W.P., and Bloom, P.R., 1985, An evaluation of rate equation for calcite precipitation kinetics at PCO_2 less than 0.01 atm and pH greater than 8: *Geochimica et Cosmochimica Acta*, v. 49, p. 2165-2180.
- Jacobson, R.L., and Langmuir, Donald, 1970, The chemical history of some spring waters in carbonate rocks: *Ground Water*, v. 8, n. 3, p. 5-9.
- Jacobson, R.L., and Usdowski, Eberhard, 1975, Geochemical controls on a calcite precipitating spring: *Contributions in Mineralogy and Petrology*, v. 51, p. 65-74.
- Langmuir, Donald, 1971, The geochemistry of some carbonate groundwaters in central Pennsylvania: *Geochimica et Cosmochimica Acta*, v. 35, p. 1023-1045.
- Lorah, M.M., 1987, The chemical evolution of a travertine-depositing stream [M.S. thesis]: Charlottesville, University of Virginia, 175 p.
- Lorah, M.M., and Herman, J.S., 1988, The chemical evolution of a travertine-depositing stream: geochemical processes and mass transfer reactions: *Water Resources Research*, v. 24, p. 1541-1552.
- Morse, J.W., 1983, The kinetics of calcium carbonate dissolution and precipitation, in Reeder, R.J., ed., Carbonates: mineralogy and chemistry: Washington, D.C., Mineralogical Society of America, *Reviews in Mineralogy*, v. 11, p. 227-264.
- Pearson, F.J., Fisher, D.W., and Plummer, L.N., 1978, Correction of groundwater chemistry and carbon isotopic composition for effects of CO_2 degassing: *Geochimica et Cosmochimica Acta*, v. 42, p. 1799-1807.
- Plummer, L.N., 1977, Defining reactions and mass transfer in part of the Floridan aquifer: *Water Resources Research*, v. 13, p. 801-812.
- Plummer, L.N., and Back, William, 1980, The mass balance approach: application to interpreting the chemical evolution of hydrologic systems: *American Journal of Science*, v. 280, p. 130-142.
- Plummer, L.N., Jones, B.F., and Truesdell, A.H., 1976, WATEQF - A FORTRAN IV version of WATEQ, a computer program for calculating chemical equilibria of natural waters: U.S. Geological Survey Water-Resources Investigations 76-13, 61 p.
- Plummer, L.N., Parkhurst, D.L., and Wigley, T.M.L., 1979, Critical review of the kinetics of calcite dissolution and precipitation, in Jenne, E.A., ed., Chemical modelling in aqueous systems: American Chemical Society Symposium, v. 93, p. 537-573.
- Plummer, L.N., Wigley, T.M.L., and Parkhurst, D.L., 1978, The kinetics of calcite dissolution in CO_2 -water systems at 5° to 60°C and 0.0 to 1.0 atm CO_2 : *American Journal of Science*, v. 278, p. 179-216.

Rader, E.K., 1984, Stratigraphy of the western anticlines - a summary, *in* Rader, E.K., and Gathright, T.M., II, eds., *Stratigraphy and structure in the thermal spring area of the western anticlines: Virginia Division of Mineral Resources, Sixteenth Annual Virginia Geologic Field Conference*, p. 1-9.

Reddy, M.M., 1983, Characterization of calcite dissolution and precipitation using an improved experimental technique: *Sciences Geologiques, Memoirs*, v. 71, p. 109-117.

Reddy, M.M., Plummer, L.N., and Busenberg, Eurybiades, 1981, Crystal growth of calcite from calcium bicarbonate solutions at constant PCO_2 and 25°C: a test of a calcite dissolution model: *Geochimica et Cosmochimica Acta*, v. 45, p. 1281-1289.

Severini, A.P., and Huntley, David, 1983, Heat convection in Warm Springs Valley, Virginia: *Ground Water*, v. 21, p. 726-732.

Shuster, E.T., and White, W.B., 1971, Seasonal fluctuations in the chemistry of limestone springs: a possible means for characterizing carbonate aquifers: *Journal of Hydrology*, v. 14, p. 93-128.

Steidtmann, Edward, 1936, Travertine-depositing waters near Lexington, Virginia: *Journal of Geology*, v. 44, p. 193-200.

Stumm, Werner, and Morgan, J.J., 1981, *Aquatic chemistry*: New York, New York, John Wiley & Sons, Inc., p. 310-317.

Suarez, D.L., 1983, Calcite supersaturation and precipitation kinetics in the lower Colorado River, All-American Canal and East Highland Canal: *Water Resources Research*, v. 19, p. 653-661.

Uzdowski, Eberhard, Hoefs, J., and Menschel, Günther, 1979, Relationship between ^{13}C and ^{18}O fractionation and changes in major element composition in a recent calcite-depositing spring - a model of chemical variations with inorganic $CaCO_3$ precipitation: *Earth and Planetary Science Letters*, v. 42, p. 267-276.

Wood, W.W., 1976, Guidelines for collection and field analysis of groundwater samples for selected unstable constituents: U.S. Geological Survey Techniques Water-Resources Investigations, Book 1, Chapter D2, 24 p.

THE GEOLOGY AND GEOCHEMISTRY OF THE FALLS HOLLOW TRAVERTINE DEPOSIT

Carl S. Kirby and J. Donald Rimstidt

CONTENTS

	Page
Abstract.....	33
Introduction.....	34
Description of site.....	34
Methods.....	36
Results.....	37
Discussion.....	38
Physical aspects.....	38
Chemistry.....	38
Conclusions.....	41
Acknowledgments.....	41
References cited.....	41

ILLUSTRATIONS

Figure	
1. Geologic map of Falls Hollow.....	35
2. Location and height of cascades.....	36
3. Schematic cross section through Falls Hollow.....	37
4. Variation of pH along the stream course.....	37
5. Variation of PCO_2 along the stream course.....	37
6. Variation of Ca^{2+} concentration along the stream course.....	38
7. Variation of HCO_3^- concentration along the stream course.....	39
8. Degree of saturation with respect to calcite along the stream course.....	39
9. Schematic cross section through a cascade.....	40

TABLE

Stream-water chemistry data.....	39
----------------------------------	----

ABSTRACT

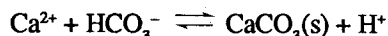
The Falls Hollow travertine deposit in Montgomery County, Virginia, shows no significant discrete spring as a source of carbonate-charged solutions. The dominant morphological characteristic of the deposit is a scarp face over which the stream plunges to form an approximately 15-m-high waterfall. This deposit contains approximately 3.46×10^8 kg of calcite. The age of the deposit is estimated at 5500 years.

Stream water sampled on two dates, November 15, 1986 and July 7, 1987, was analyzed for pH, Ca^{2+} , and HCO_3^- . These analyses show that the stream water is one to nine times supersaturated with respect to calcite. Both data sets show that significant degassing of CO_2 upstream from the waterfall leads to a high degree of supersaturation with respect to calcite. The saturation state drops rapidly as a result of extensive calcite deposition at the waterfall.

The precipitation of travertine occurs by a two-step process. First, CO_2 is lost from the solution



which causes a pH increase leading to calcite supersaturation. Then CaCO_3 precipitates



as encrustations and as cascades or rimstone dams. The stream-water chemistry appears to be closely linked to the morphology of the deposit and flow regime of the stream. Most rapid precipitation occurs at the large waterfall, although most CO_2 degassing occurs well upstream from the waterfall.

INTRODUCTION

There are numerous travertine-depositing streams in the Valley and Ridge province of Virginia (Hubbard and others, 1985). These deposits are clearly associated with carbonate-charged groundwaters that enter the stream via springs. This report describes a deposit where travertine is presently being precipitated in Montgomery County, Virginia. Groundwater which enters the stream via diffuse flow through the stream bed is the main source of carbonate-charged solutions. This study was undertaken to investigate the chemical evolution of the stream water composition and the physical characteristics of the Falls Hollow deposit.

DESCRIPTION OF SITE

The Falls Hollow travertine deposit lies within the Falls Ridge Preserve of the Nature Conservancy near Fagg, Virginia (Ironto quadrangle), along an unnamed stream in Falls Hollow (Figure 1). The rocks of the immediate area consist of the Cambrian Elbrook dolomite thrust over Ordovician, Silurian, and Devonian clastic rocks by the Salem thrust fault (McHugh, 1986). Travertine is presently being precipitated in the stream which flows across a terrace of previously deposited travertine. A less extensive travertine deposit is associated with a stream in nearby Fagg Hollow (William P. Bradley, 1986, personal communication). Sinkholes occur on the ridge crest above both deposits, however, the recharge area for the groundwater was not determined.

Dense deciduous forest covers the slopes surrounding Falls Hollow. The valley floor is relatively level (slope less than 5°) with the exception of an 18-m scarp of travertine (Figure 1). The vegetation on the valley floor consists of grasses and small deciduous trees. Some areas along the

stream are marshy, and horsetails are very abundant in these patches. The lack of mature trees on the valley floor results from earlier agricultural activities (William P. Bradley, 1986, personal communication).

The travertine deposit lies along an 800-m stretch of the stream. Downstream from sample site J (Figure 1), there is only minor encrustation of CaCO_3 on stream gravel. There is also only minor encrustation upstream from sample site B (Figure 1). The travertine forms cascades from less than 0.3 m high to a 15-m waterfall. Cascades have been divided into three orders with respect to height (Figure 2): the densely stippled area indicates cascades less than or equal to 0.3 m in height (approximately 40 additional cascades less than 0.3 m high occur in the stream but are not shown in this figure); the lightly stippled area indicates 23 cascades between 0.3 and 3.0 m high; there is only one cascade (waterfall) greater than 3 m in height. The 15-m-high waterfall is very similar, except in scale, to all other cascades in the stream, but it will be referred to as the "waterfall." The cascades have rounded crests, and the downstream sides have either undercut faces or ramps which prograde downstream.

The dominant morphological characteristic of the deposit is a scarp face approximately 18 m high that extends approximately 180 m across the valley floor. The stream presently descends over the western edge producing a waterfall, but its course has shifted back and forth across the valley through time to produce the scarp. Eroded portions of the scarp exhibit several characteristics of the travertine. The weathered rock is light gray; the fresh rock is white to light brown. The travertine exhibits both subparallel layering and a botryoidal habit. The layered travertine displays only microscopic porosity; the botryoidal material contains cavities ranging from microscopic pores to 12-m^3 cavities. Leaf and plant stem casts occur throughout the deposit. Some mosses grow on the cascades but do not appear to be incorporated into the deposit, because moss structures are not seen in the layered travertine either in hand sample or in thin section. Thin-section observation, however, shows that numerous algal filaments are incorporated into the travertine.

Historically, travertine deposits have been mined as sources of high-purity CaCO_3 (Hubbard and others, 1985). Early in this century, a previous land owner built a lime kiln (Figure 10 in Sweet and Hubbard, this volume) and truck scales intending to produce agricultural lime in Falls Hollow. This enterprise was unsuccessful because the very porous travertine absorbed most of the blasting shock so the costs of blasting outweighed the benefits of having a nearly pure CaCO_3 source (William P. Bradley, 1986, personal communication).

A small spring with minor travertine deposition flows into the stream above the waterfall (spring symbol, Figure 1). An analysis of water from this spring is reported as sample C in the Table. An intermittent spring (not shown in Figure 1) showing minor travertine deposition occurs in the drainage at the easternmost edge of the scarp. Other very small surface

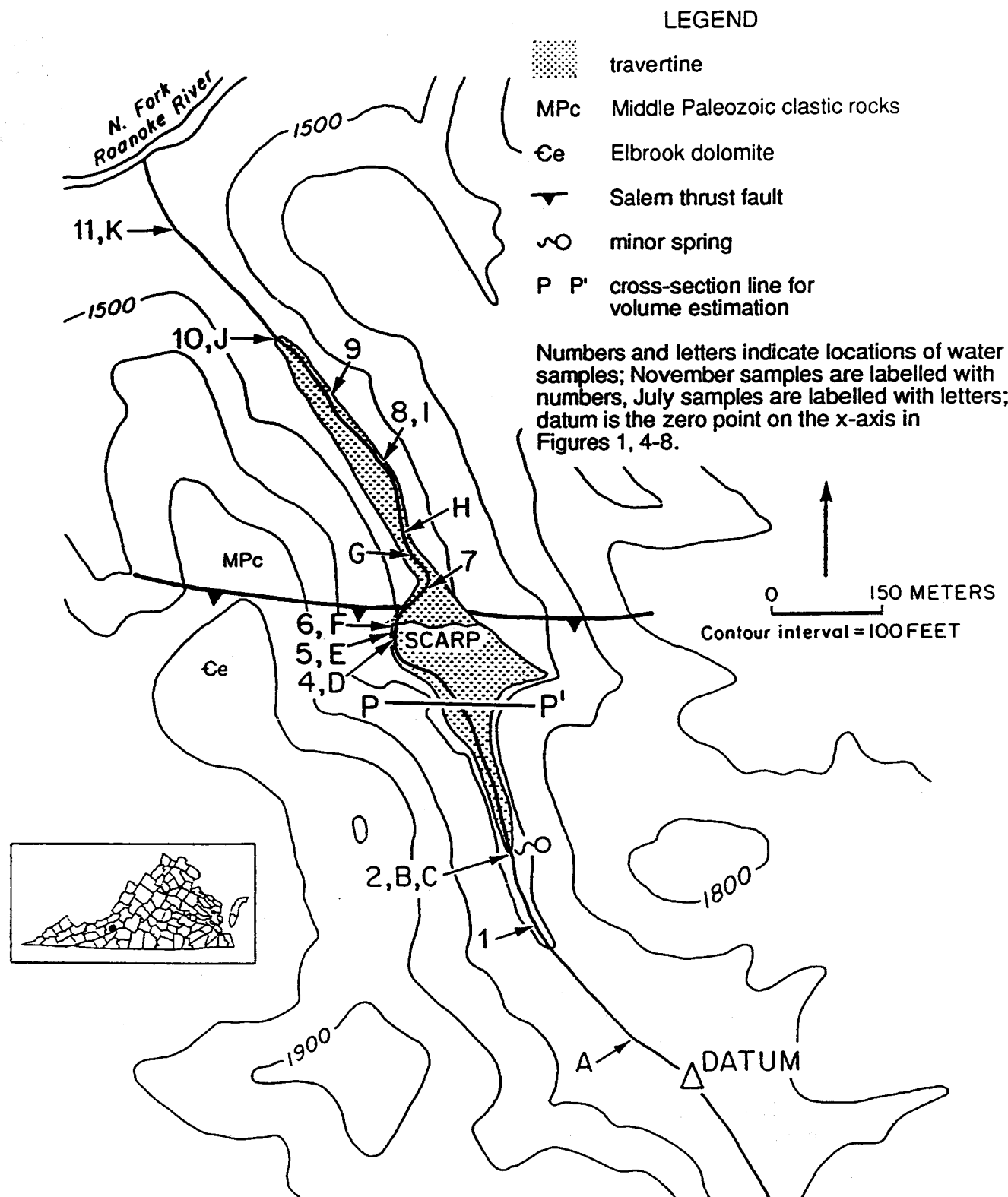


Figure 1. Geologic map of Falls Hollow.

springs were found upstream from the area mapped.

The valley floor, which is composed predominantly of travertine decomposed into soil, is slightly undulose and slopes less than 5°. The valley walls slope approximately 25°. There is a marked break in slope between the valley floor and valley walls.

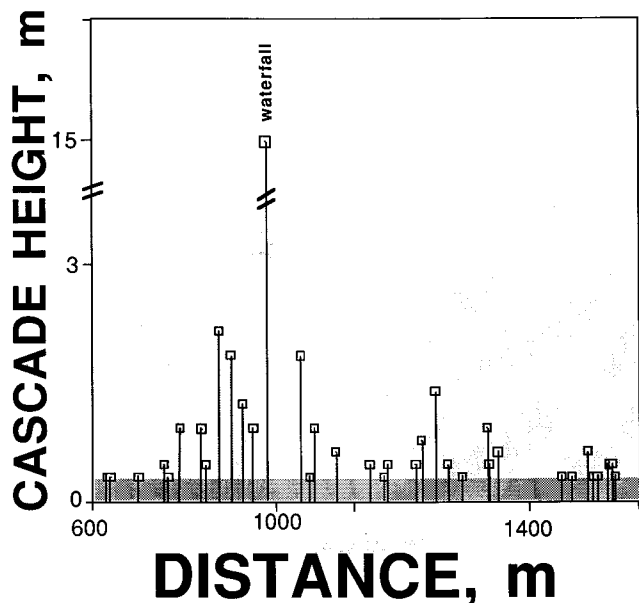


Figure 2. Location and height of cascades.

METHODS

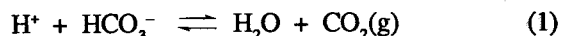
Water samples were collected from the stream on two dates: November 15, 1986 and July 7, 1987. Both dates were selected to coincide with base-flow conditions. Two water samples were taken from each of 11 locations (samples are in alphabetical and numerical order from upstream to downstream, Figure 1). The datum shown in Figure 1 is the zero point in the x-direction for all graphs, and x is positive in the downstream direction. All 125-mL polyethylene sample bottles were washed with acid and rinsed with distilled water; the bottles for Ca^{2+} and Mg^{2+} analysis were rinsed with distilled, deionized water rather than distilled water. Each bottle was filled completely, leaving no headspace. Water temperature was measured at each sample location.

For the November sampling, the pH of one set of samples was measured within 3 hours of sampling; this set of samples was subsequently acidified with 1.0 mL concentrated HNO_3 . The second set of samples was titrated with 0.1 molar HCl within eight hours of sampling to determine HCO_3^- concentration. All samples were refrigerated at approximately 0°C until analysis. Equivalence points were identified graphically; all lay near $\text{pH} = 4.4 \pm 0.5$. Calcium ion concentrations

were determined by atomic absorption spectrophotometry using an oxygen/acetylene flame and a wave length of 422.7 nm.

For the July sampling, pH was measured in the field. One set of samples was acidified with 1.0 mL concentrated HCl, and then Ca^{2+} , Mg^{2+} , Fe^{2+} , and Mn^{2+} concentrations were determined from these samples using inductively coupled activated plasma analysis. Alkalinity titrations were performed on the second set of samples within 8 hours of collection. Samples were refrigerated at approximately 0°C until analysis. Water velocity data were collected using a Pygmy meter, and velocity contours were established for stream cross sections at sample sites A and J (Figure 1). Discharge data were calculated from the weighted velocity averages per cross-sectional area.

Based on the reaction



PCO_2 was calculated as

$$\text{PCO}_2 = \frac{a_{\text{H}^+} a_{\text{HCO}_3^-}}{K_{\text{H}} K_1} \quad (2)$$

where K_{H} is the Henry's Law constant for CO_2 , and K_1 is the first dissociation constant for H_2CO_3 ; both constants are from Naumov and others (1974). The constants K_{H} and K_1 were selected to correspond to the temperatures measured at the time of sampling. Activities (a) were calculated from the Debye-Hückel equation using measured Ca^{2+} , HCO_3^- , H^+ , and Mg^{2+} concentrations to estimate ionic strength.

The degree of saturation with respect to calcite was calculated as Q/K , where Q is the ratio of the product of the activities of bicarbonate and calcium ions to the activity of hydrogen ion,

$$Q = \frac{a_{\text{HCO}_3^-} a_{\text{Ca}^{2+}}}{a_{\text{H}^+}} \quad (3)$$

and K is the temperature-dependent equilibrium constant from Stumm and Morgan (1970) for the reaction specified in the equation



The amount of CaCO_3 in the deposit was found by estimating the volume and porosity of the deposit. The porosity was estimated by two-dimensional point counting of pores; it was assumed that areal percent is equal to volume percent. Pores were divided into three size intervals. A photograph of the scarp face taken from 20-m distance was used to count pores greater than 6.5 μm^2 . A second photograph taken 1 m from the scarp face was used to count pores

between 6.5 and 0.09 cm². The contribution of pores smaller than 0.09 cm² was determined by thin-section observations. In this manner, pores of similar size were only counted once. The percentage contributions of porosity at each scale were summed to give the reported porosity.

Figure 3 illustrates the method for estimating the volume of the deposit. The x-direction of this figure is parallel to line P-P' in Figure 1; z represents the assumed depth of the deposit. The data points correspond to 20-foot topographic contours from which a linear extrapolation was made to model the valley morphology before the development of the travertine deposit. It was assumed that the volume of rock and sediment at present minus the volume of rock and sediment before the travertine deposit developed is equal to the volume of the deposit. A thickness of six meters of detrital fill was assumed to underlie the travertine at all locations. That thickness was chosen as a first approximation based on visual estimates; assuming 3 or 10 m of fill changes the total estimated volume by +15 or -26 percent, respectively. The formula for calculating the volume of each element is:

$$\text{VOLUME} = [x - (x - x')/2]zy.$$

The deposit was divided into ten such volume elements and their volumes were summed to yield the total volume of the deposit. The actual volume of calcium carbonate in the deposit was calculated by multiplying the total volume by one minus the porosity to give the total volume of CaCO₃.

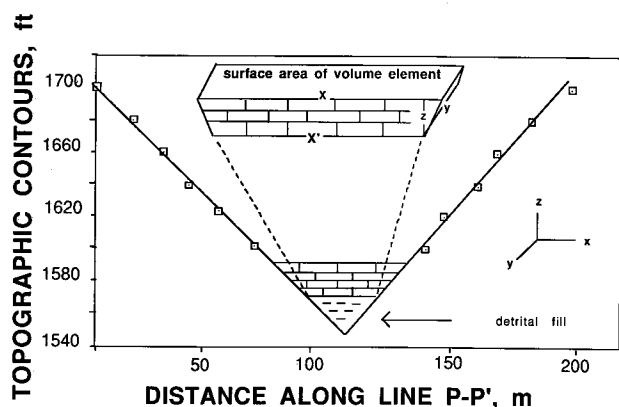


Figure 3. Schematic cross section through Falls Hollow. This figure illustrates the method for estimating the volume of the deposit. See text for details.

RESULTS

The table displays the results of chemical analyses of solutions sampled on November 15, 1986 and July 7, 1987. The graphical representations of the data (Figures 4-8) illustrate the relationship between the stream-water chemistry and the distance along the flow path.

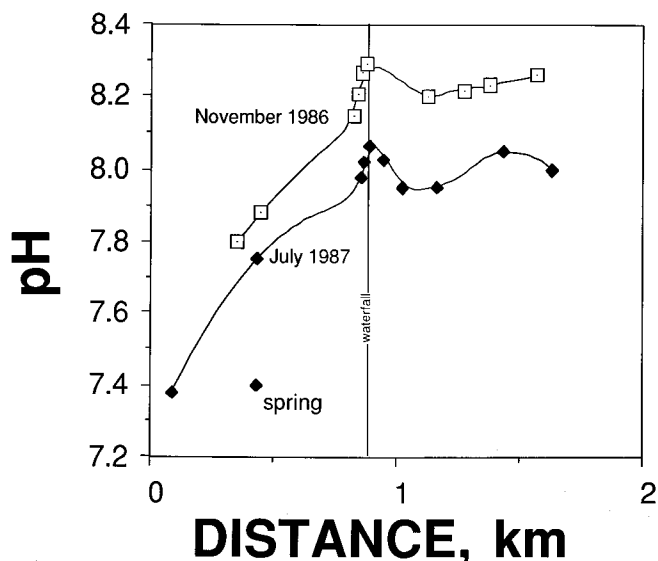


Figure 4. Variation of pH along the stream course.

Though slightly different quantitatively, the November and July data were qualitatively very similar except that there were steep positive slopes in the PCO₂ and Ca²⁺ curves for July data immediately below the waterfall (Figures 5 and 6). For the July 7, 1987 sampling, the discharge at the upstream sampling point (A, Figure 1) was 21.8 L/s; the downstream discharge (J, Figure 1) was 28.0 L/s.

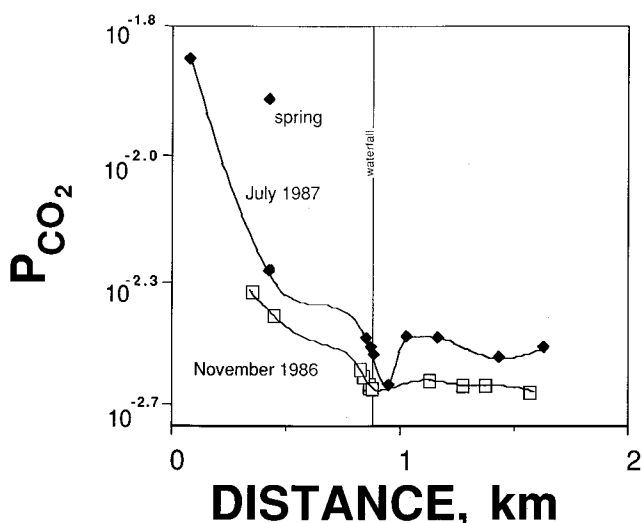


Figure 5. Variation of PCO₂ along the stream course.

Examination of the travertine from the scarp face showed that calcite is the dominant constituent of the deposit. No aragonite was found by X-ray diffraction analysis. The pores greater than 6.5 cm² in cross-sectional area account for 42

percent of the porosity, whereas pores between 6.5 cm² and 0.09 cm² account for 4 percent, and those with cross-sectional area less than 0.09 cm² account for an additional 5 percent yielding a total porosity for the deposit of 51 percent.

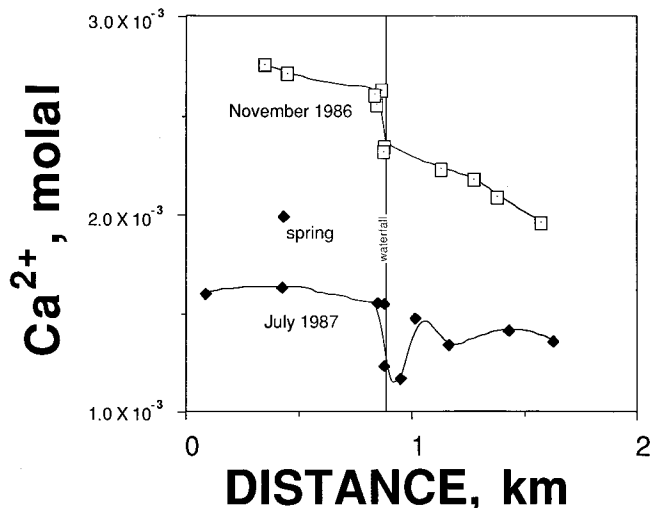


Figure 6. Variation of Ca²⁺ concentration along the stream course.

Errors for pH, Ca²⁺, HCO₃⁻, Mg²⁺, and Mn²⁺ concentrations are shown in the Table. Errors for PCO₂ and degree of saturation are less than 35 percent and 33 percent, respectively, of the value reported and are based on reported errors from the Table. The greatest contribution to these errors was from pH; a relatively small uncertainty in pH results in a large uncertainty in H⁺ concentration.

DISCUSSION

PHYSICAL ASPECTS

The morphology of the valley floor suggests that there are two travertine terraces filling the valley between the more steeply sloping valley walls. The terrace upstream from the waterfall is an area of very active travertine deposition while the terrace below the waterfall seems to be growing more slowly. The stream has migrated back and forth across the valley floor to produce the terraces. The cascades build up until the decreased gradient forces the stream to change course. The pattern of deposition is similar to a delta, for the stream migrates laterally, and the cascades prograde downstream. Near the crest of the waterfall, the stream has eroded to its present position with banks up to 2.4 m high. This

evidence suggests that erosion has outstripped precipitation in the most recent past.

The large cavities are not dissolution features, rather, they are primary porosity due to creation of open space in the travertine when cascades prograde downstream. Organic debris such as logs (Figure 9) divert the flow of water and cause the creation of a cavity behind a cascade. Some cavities also result from the decay of organic debris after travertine precipitates around it. Based on the present precipitation in the stream, it appears that layered travertine develops in the cascades and that travertine with botryoidal habit develops in the pools behind the cascades and in cavities underneath the cascades.

The total volume of the deposit was calculated as 255,000 m³. The actual volume of calcium carbonate in the deposit was estimated as 125,000 m³ after accounting for pore space. Based on a density of calcite of 2.72 g/cm³, this deposit contains approximately 3.46 x 10⁸ kg or 3.46 x 10⁹ moles of calcite.

In order to place some constraints on the age of the deposit, a mass-balance approach to modeling the age was used. This approach is intended as an order-of-magnitude approximation, therefore no error estimates have been reported. The age of the deposit was estimated by assuming: 1) a constant average discharge of 25 L/s, 2) all material in the deposit is calcite, 3) the concentration of Ca²⁺ in solution has been constant, 4) the volume and porosity calculated above, and 5) no erosion of the travertine has occurred. Another constraint is that the deposit cannot be zero years old as 100 percent error would allow. The method for age estimation is outlined below.

$$\begin{aligned} \text{A) } \text{Ca}^{2+}_{\text{deposited}} &= \text{Ca}^{2+}_{\text{upstream}} - \text{Ca}^{2+}_{\text{downstream}} \\ 8 \times 10^{-4} \text{ mol/L} &= 2.75 \times 10^{-3} \text{ mol/L} - 1.96 \times 10^{-3} \text{ mol/L} \\ &\text{(these concentrations are from the November data)} \end{aligned}$$

$$\begin{aligned} \text{B) carbonate deposition rate} &= \\ &(\text{Ca}^{2+}_{\text{deposited}})(\text{average discharge}) \\ 6.3 \times 10^5 \text{ mol/yr} &= (8 \times 10^{-4} \text{ mol/L})(7.8 \times 10^8 \text{ L/yr}) \end{aligned}$$

$$\begin{aligned} \text{C) age of deposit} &= \\ &(\text{carbonate in deposit})/(\text{carbonate deposition rate}) \\ 5500 \text{ yrs} &= (3.46 \times 10^9 \text{ mol calcite})/(6.3 \times 10^5 \text{ mol calcite/yr}) \end{aligned}$$

The most likely age of the deposit is estimated as 5500 years.

CHEMISTRY

The pH of the stream water (Figure 6) is controlled by two reactions. When the degassing reaction (Equation 1) proceeds to the right, the pH increases. When the precipitation reaction (Equation 4) proceeds to the right, pH decreases. The stream loses CO₂ over the entire sampling range, except

Table. Stream-water chemistry data. SITE indicates distance downstream from datum (see Figure 1 for location of datum and samples). All concentrations are reported in mg/L. Ca^{2+} , Mg^{2+} , and Mn^{2+} concentrations errors are 2σ . Volumetric errors, graphical determination of equivalence, and pH errors contribute to reported HCO_3^- errors.

Sample	Site (m)	T ^a (°C)	pH ^b	Ca ²⁺	HCO ₃ ⁻	Mg ²⁺	Mn ²⁺
November 15, 1986							
1	305	10.5	7.80	109.8±0.8	261.8±12.4		
2	402	10.0	7.88	108.3±2.6	257.4±12.4		
3	777	9.0	8.15	104.0±1.4	252.3±12.4		
4	796	8.5	8.21	102.3±1.2	251.6±12.4		
5	811	8.0	8.27	105.7±2.6	249.4±12.4		
6	822	7.0	8.29	93.4±3.2	250.8±12.4		
7	832	7.0	8.29	93.8±2.2	235.5±11.6		
8	1080	6.0	8.20	89.1±1.8	229.0±11.6		
9	1222	5.5	8.22	87.1±1.6	222.4±11.6		
10	1332	5.0	8.23	84.0±2.0	217.3±11.6		
11	1517	4.5	8.26	78.6±1.6	213.7±11.6		
July 7, 1987							
A	81	17.0	8.00	54.4±0.14	247.6±11.8	37.6±0.42	0.002±0.002
B	397	17.0	8.05	56.3±0.24	249.0±12.0	37.7±0.11	0.001±0.000
C	399	16.0	7.95	53.7±0.25	288.0±15.2	38.0±0.27	0.001±0.000
D	796	16.5	7.95	59.1±0.20	246.1±12.2	38.3±0.19	0.001±0.001
E	811	16.5	8.03	46.6±0.14	243.9±12.2	37.6±0.28	0.001±0.000
F	822	17.0	8.07	49.6±0.20	232.6±11.4	36.9±0.25	0.001±0.001
G	884	16.5	8.02	62.0±0.34	234.8±11.6	36.3±0.23	0.001±0.000
H	954	16.0	7.98	62.1±0.24	223.5±11.4	36.8±0.21	0.003±0.000
I	1080	12.5	7.38	78.6±0.63	228.2±12.0	43.3±0.37	0.001±0.000
J	1332	17.0	7.75	65.2±1.04	211.8±11.4	30.6±0.43	0.003±0.000
K	1517	17.0	7.38	63.8±0.31	223.5±12.4	28.4±0.08	0.003±0.000

^aError of value reported is ±0.5.
^bError of value reported is ±0.05.

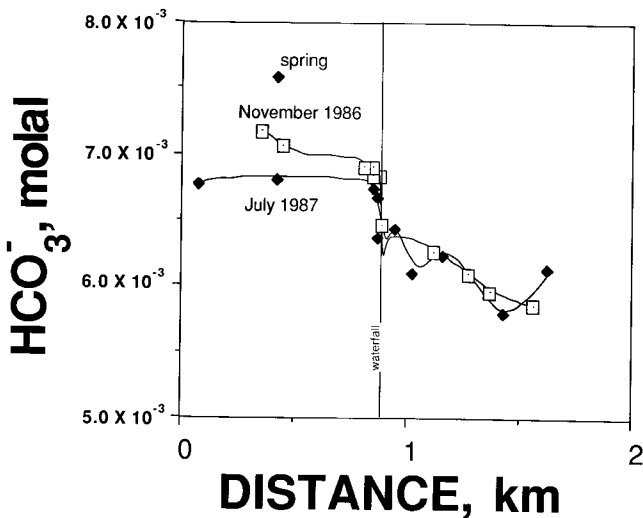


Figure 7. Variation of HCO_3^- concentration along the stream course.

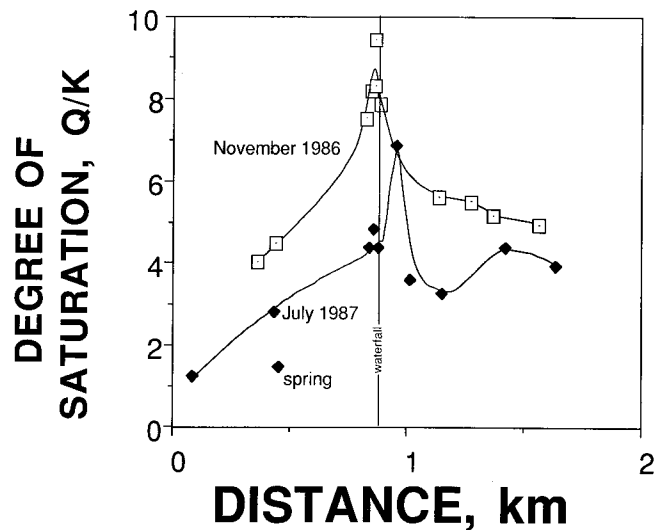


Figure 8. Degree of saturation with respect to calcite along the stream course.

in the July data where there is an increase in PCO_2 immediately below the waterfall, in an attempt to reach equilibrium with atmospheric PCO_2 (approximately $10^{-3.5}$ atm; Figure 5). The pH decrease below the waterfall indicates that this is the only area where the precipitation reaction predominates over the degassing reaction in controlling pH.

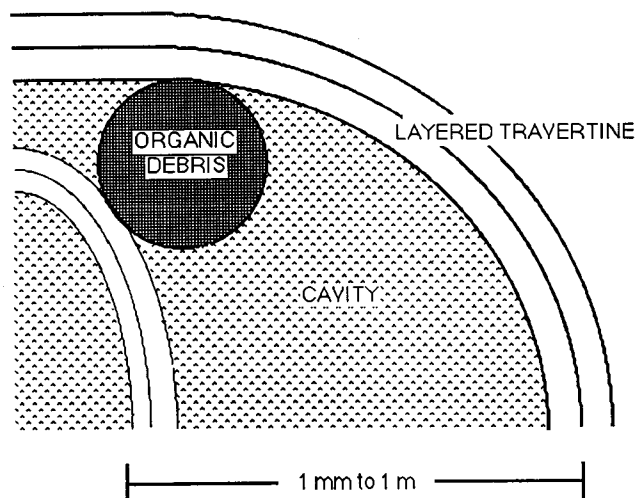


Figure 9. Schematic cross section through a cascade.

Figure 6 shows that the Ca^{2+} concentration decreases relatively slowly above the waterfall indicating low CaCO_3 precipitation rates, where the term rate refers to the change of the concentration variable (pH, PCO_2 , Ca^{2+} , HCO_3^- , degree of saturation) with respect to distance along the flow path. These rates are indicated by the slopes of the curves. Calcium ions only enter the stream through groundwater, and their only sink is travertine deposition. Calcium leaves the stream slowly except at the waterfall, indicating that most rapid deposition in the system takes place around the waterfall. The rapid decline in Ca^{2+} coupled with the rapid pH drop near the waterfall is caused by CaCO_3 precipitation (Equation 4). The precipitation rate downstream from the waterfall is relatively slow. This observation is consistent with the studies of Herman and Lorah (1987) and Lorah and Herman (this volume), who found that the highest precipitation rate occurred near a large waterfall in Falling Spring Creek.

The behavior of the bicarbonate ion in solution roughly parallels the behavior of Ca^{2+} , as shown in Figure 7. Downstream from the waterfall, the HCO_3^- concentration varies more than Ca^{2+} . The HCO_3^- concentration is controlled by both CO_2 loss (Equation 1) and CaCO_3 precipitation (Equation 4).

A degree of saturation value of one indicates saturation, and values greater than one indicate supersaturation. The stream water is supersaturated from one to nine times in the study area (Figure 8). The continual loss of CO_2 in the upstream reach results in the constantly increasing levels of

supersaturation upstream from the waterfall. Herman and Lorah (1987) found similar behavior in a stream they examined, although they did not measure a significant decrease in saturation below the waterfall. The rapidly decreasing supersaturation at and below the waterfall at Falls Hollow indicates that the solution precipitates a significant amount of CaCO_3 as it flows over the waterfall.

The steep slope of the Ca^{2+} concentration curve (Figure 6) near the waterfall shows that the greatest amount of precipitation occurs near the waterfall. Visual inspection of the deposit also shows that the greatest precipitation has occurred at the waterfall in the past, for the thickest portion of the deposit is located at the scarp face where the waterfall was located in the past. The greatest amount of degassing occurs well above the waterfall as shown in Figure 5. Because the PCO_2 does not change as much near the waterfall as it does upstream, the precipitation of travertine is not localized by removal of CO_2 from the solution either by degassing to the atmosphere or by removal by photosynthetic organisms. Thus, the algal filaments found in the travertine appear simply to be passively incorporated rather than to be a cause of precipitation. This conclusion is consistent with the observation by Hoffer-French and Herman (1989) that the travertine at Falling Spring Run precipitates just as fast at night, when CO_2 is not taken up by algae, as in the daytime. It does allow the possibility that secretions from plants might trap CaCO_3 particles that can furnish abundant substrate onto which more calcite can precipitate from solution as suggested by Emeis and others (1987), although no evidence was observed in hand sample or thin section that mosses were incorporated into the travertine.

The precipitation of travertine occurs by a two-step process. First, carbon dioxide is lost from the solution according to Equation (1) which causes a pH increase leading to supersaturation with respect to calcite. Then CaCO_3 precipitates according to Equation (4) as encrustations and as cascades or rimstone dams. Though the precipitation of some travertine deposits appear to be significantly influenced by biological agents (Chafetz and Folk, 1984; Weijermars and others, 1986; Emeis and others, 1987; Dennen and others, this volume; Love and Chafetz, this volume; Pentecost, this volume), the main control on precipitation in the stream in this study appears to be physicochemical rather than biological. Chafetz and Folk (1984) suggest that lake travertines are biologically precipitated. Weijermars and others (1986) claim that a travertine terrace in central Spain is being formed by biogenic processes, with mosses responsible for removing CO_2 to produce CaCO_3 supersaturation. No evidence of significant biological removal of CO_2 was found at Falls Hollow; most of the CO_2 is degassed upstream from the large waterfall. The sharp decline in dissolved calcium and in the degree of saturation (Figures 6 and 8) show that the waterfall is the site of most of the calcite deposition. Figure 5 shows that degassing of CO_2 at the waterfall is insignificant, and therefore biological removal of CO_2 is probably not a major

cause of rapid precipitation.

Emeis and others (1987) argue that supersaturation with respect to calcite by itself is insufficient, in some cases, to initiate precipitation of travertine. They suggest that the Ca^{2+} ions require a suitable (biological) substrate in order to precipitate even from a supersaturated solution. Although no evidence was found in the stream or in the travertine at Falls Hollow that biological agents provide a substrate for CaCO_3 nucleation, we do agree that a calcite surface is an excellent substrate for precipitation. Little CaCO_3 precipitates from less turbulent slow-moving water where contact of the water with the calcite in the sides or bed of the stream is minimal. More turbulent flow at cascades, however, allows most of the solution to contact the calcite substrate, thus accelerating precipitation.

CONCLUSIONS

Although the carbonate-charged solutions apparently enter this stream via diffuse groundwater flow through the stream bed, the chemical behavior and morphological characteristics of this deposit are quite similar to other deposits produced by solutions from springs. The large waterfall is the dominant morphological feature of this deposit, and waterfalls which are considerably larger than nearby cascades occur at many travertine deposits (Herman and Lorah, 1987; Goff and Shevenell, 1987; Herman and Hubbard, this volume). At this deposit, the greatest amount of precipitation occurs at the waterfall resulting in a dramatic change in the water chemistry in the immediate area of the waterfall. The changes in the solution chemistry of the stream at this site are qualitatively similar to those documented by Lorah and Herman (this volume) for Falling Spring Creek and Hoffer-French and Herman (this volume) for Falling Spring Run. The localization of calcite precipitation at the cascades is probably controlled by the turbulent flow regime at these sites.

Erosion presently predominates over precipitation of travertine in Falls Hollow and also seems to be significant at other travertine deposits in Virginia (Hubbard and others, 1985). It is not clear whether this erosion is the result of a climatic change or a result of human activities such as clearing land in the upstream reaches of a stream which produces higher flood discharges. It seems likely that preservation of some travertine deposits may be enhanced by curbing surface water runoff in the upstream area.

ACKNOWLEDGMENTS

We would like to thank Mr. William P. Bradley and the Nature Conservancy for their cooperation in this study.

REFERENCES CITED

- Chafetz, H.S., and Folk, R.L., 1984, Travertines: depositional morphology and the bacterially constructed constituents: *Journal of Sedimentary Petrology*, v. 54, p. 289-316.
- Emeis, K.-C., Richnow, H.-H., and Kempe, Stephan, 1987, Travertine formation in Plitvice National Park, Yugoslavia: chemical versus biological control: *Sedimentology*, v. 34, p. 595-609.
- Goff, Fraser, and Shevenell, Lisa, 1987, Travertine deposits of Soda Dam, New Mexico, and their implications for the age and evolution of the Valles caldera hydrothermal system: *Geological Society of America Bulletin*, v. 99, p. 292-302.
- Herman, J.S., and Lorah, M.M., 1987, CO_2 outgassing and calcite precipitation in Falling Spring Creek, Virginia, U.S.A.: *Chemical Geology*, v. 62, p. 251-262.
- Hoffer-French, K.J., and Herman, J.S., 1989, Evaluation of hydrological and biological influences on CO_2 fluxes from a karst stream: *Journal of Hydrology*, v. 108, p. 189-212.
- Hubbard, D.A., Jr., Giannini, W.F., and Lorah, M.M., 1985, Travertine-marl deposits of the Valley and Ridge province of Virginia – a preliminary report: *Virginia Division of Mineral Resources, Virginia Minerals*, v. 31, n. 1, p. 1-8.
- McHugh, M.L., 1986, Reevaluation of the southwestern end of the Salem synclinorium [M.S. thesis]: Blacksburg, Virginia Polytechnic Institute and State University, 111 p.
- Naumov, G.B., Ryzhenko, B.N., and Khodakovsky, I.L., 1974, *Handbook of thermodynamic data: National Technical Information Service Report No. USGS-WRD-74-001*, 328 p.
- Stumm, Werner, and Morgan, J.J., 1970, *Aquatic chemistry: an introduction emphasizing chemical equilibria in natural waters*: New York, New York, Wiley-Interscience, 583 p.
- Weijermars, Rudd, Mulder-Blanken, C.W., and Wiegers, Jaap, 1986, Growth rate observation from the moss-built Checa travertine terrace, central Spain: *Geological Magazine*, v. 123, n. 3, p. 279-286.

A COMPARATIVE STUDY OF TRAVERTINE-MARL-DEPOSITING STREAMS IN VIRGINIA

Janet S. Herman¹ and David A. Hubbard, Jr.²

CONTENTS

	Page
Abstract.....	44
Introduction.....	44
Site descriptions.....	45
Methods.....	51
Field methods and sample collection.....	51
Sample site description.....	51
Geochemical data analysis.....	52
Results.....	53
Travertine-marl.....	53
Biota.....	53
Water.....	53
Discussion.....	59
Travertine-marl.....	59
Biota.....	60
Water.....	60
Testing the model of critical groundwater input.....	61
Conclusions.....	62
Acknowledgments.....	63
References cited.....	63

ILLUSTRATIONS

Figure	
1. Locations of travertine-depositing streams in Virginia.....	45
2. A portion of the Ashby Gap 7.5-minute quadrangle illustrating the James site (JAM), Clarke County.....	45
3. A portion of the Hamburg 7.5-minute quadrangle illustrating the Hamburg site (HAM), Page County.....	46
4. A portion of the Timberville 7.5-minute quadrangle illustrating the Arbagast site (ARB), Rockingham County....	46
5. A portion of the Staunton 7.5-minute quadrangle illustrating the Quicks Mill site (QUI), Augusta County.....	46
6. Portions of the Greenville and Stuarts Draft 7.5-minute quadrangles illustrating the Folly Mills site (MIL), Augusta County.....	48
7. A portion of the Warm Springs 7.5-minute quadrangle illustrating the Warm Springs site (WAR), Bath County...	48
8. A portion of the Vesuvius 7.5-minute quadrangle illustrating the Glenn Falls site (GLE) in Augusta and Rock- bridge counties.....	49
9. A portion of the Vesuvius 7.5-minute quadrangle illustrating the Moores Creek site (MOO), Rockbridge County.....	49
10. A portion of the Ironto 7.5-minute quadrangle illustrating the Falls Hollow site (FAL), Montgomery County.....	50
11. A portion of the Ironto 7.5-minute quadrangle illustrating the mound site (MOU), Montgomery County.....	50
12. Portions of the Ironto and Elliston 7.5-minute quadrangles illustrating the Shawsville site (SHA), Montgomery County.....	50

¹Department of Environmental Sciences, Clark Hall, University of Virginia, Charlottesville, VA 22903

²Virginia Division of Mineral Resources, P. O. Box 3667, Charlottesville, VA 22903

TABLES

Table	Page
1. Chemical composition of travertine-marl samples.....	54
2. The biota of several travertine-depositing streams.....	55
3. Chemical composition of water samples.....	56
4. Calculated parameters describing the chemical composition of the travertine-depositing waters.....	57
5. Chemical composition of water samples collected for isotopic analysis.....	58
6. Isotopic composition and calculated parameters of the travertine-depositing waters.....	58

ABSTRACT

A survey of 12 travertine-depositing streams in Virginia established the chemical nature of the waters and their travertine-marl deposits. The waters are primarily Ca-HCO₃-type and evolve in a downstream direction by CO₂ outgassing, concomitant increases in pH, and calcite precipitation. The greatest calcite precipitation, localized at the travertine buildups, occurs just downstream from the greatest CO₂ losses. More recent travertine-marl has lower CaCO₃ contents than the older materials isolated from active deposition. Petrographic examination of some travertine showed a range of textures from fresh micritic material to significantly neomorphosed calcite. Abundant algae were identified on a number of travertine samples. Chemical and hydrological processes, however, can adequately explain the precipitation of calcite from the streams in this study. Input of carbonate-rich water from discrete springs or tributaries or from diffuse groundwater flow through stream beds usually is determined structurally by the location of fractures or faults. This input of carbonate-rich water is a critical control on the ultimate formation of travertine.

INTRODUCTION

The deposition of calcium carbonate by freshwater springs and streams has received attention from researchers around the world. Chemical, hydrological, and biological studies of travertine deposits in Europe and North America, including some studies in Virginia, have been widely published. Our work in Virginia includes an inventory of the travertine-marl deposits in the State (Hubbard, 1985; Hubbard and others, 1985) and detailed geochemical and hydrological studies conducted from 1984 to 1986 at two streams (Lorah and Herman, 1988 and this volume; Hoffer-French and Herman, 1989 and this volume).

With these earlier studies as a basis, we developed a conceptual model of travertine-marl deposition in Virginia streams. Travertine-marl deposits are found downstream

from locations of groundwater discharge from carbonate bedrock. This groundwater discharge may take the form of discrete springs that fully or partially feed the stream flow or it may be in the form of diffuse input through the stream bed. The emergence of groundwater, whether it is discrete or diffuse, commonly is controlled structurally by faults and fractures that provide permeable pathways for the upward migration of groundwater in folded rock.

Groundwater that has circulated through carbonate rocks at depth issues onto the surface nearly in equilibrium with respect to calcite and with a partial pressure of CO₂ that is elevated relative to the atmosphere. Carbon dioxide outgasses from the water; the outgassing is enhanced by the hydrological agitation of the flowing stream. The continued loss of CO₂ as the water flows downstream causes the solution to become increasingly supersaturated with respect to calcite.

Calcite precipitation occurs at some distance downstream from the emergence of carbonate-rich groundwater. A combination of factors influence the deposition of travertine. Primarily, the water must reach a high degree of supersaturation before significant calcite precipitation occurs. This condition is typically met at a waterfall or cascade where increased turbulence of the stream causes the highest CO₂ outgassing rates. Additionally, an appropriate substrate seems to be a factor in localizing calcite precipitation. Substrates can be previously precipitated calcite, mosses or algae, or other inorganic or organic surfaces occurring in the stream bed.

Travertine initially forms on an obstruction in the stream bed, such as a bedrock ledge or a fallen tree, that increases the turbulence of stream flow. Travertine accumulation on the obstruction causes even more turbulence and further enhances travertine deposition. Thus, travertine buildups are formed by a self-perpetuating process. Deposition of travertine on a buildup and the simultaneous accumulation of carbonate-rich sediments (marl) immediately upstream from the buildup reduce the gradient of the upstream segment until it is unable to accommodate high stream flow. High stream flow either erodes the travertine buildup or results in the lateral migration of the stream to form a channel with a steeper gradient. Thus, the migrating stream forms a series of transverse travertine buildups with associated upstream marl

accumulations.

The present investigation is a synoptic examination of 12 travertine-depositing streams in Virginia (Figure 1). Sampling of water was designed to test our hypothesis that the input of carbonate-rich water, whether from a discrete spring or from diffuse flow, has a critical effect on the formation of travertine and that the location of the input is commonly determined by faults or fractures. Sampling of travertine-marl materials was designed to elucidate the constancy of depositional conditions over time. Some additional information on the isotopic composition of the stream waters, the petrographic description of travertine, and the identification of algae from several sites was provided by our colleagues. This information is included to describe further the travertine-depositing stream systems in Virginia.

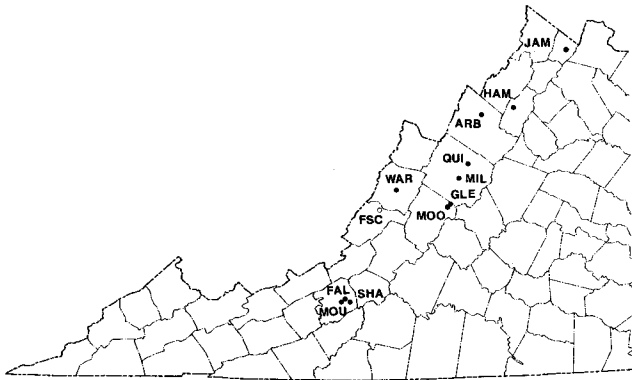


Figure 1. Locations of travertine-depositing streams in Virginia sampled in the course of this study (dots). The Falling Spring Creek (FSC) site (open circle) was sampled only for petrographic, isotopic, and biologic analyses.

SITE DESCRIPTIONS

The James site (JAM, Figure 2) is located in the Ashby Gap quadrangle in Clarke County. Travertine-depositing waters rise from a spring in interbedded limestone and dolomite rocks mapped as the Elbrook Formation and situated on the eastern limb of the Franklinton syncline (Gathright and Nystrom, 1974). Intermittent surface drainage originating upstream from the spring is present only after extended periods of precipitation (James, 1987, personal communication). The first of the travertine buildups is situated approximately 460 m downstream from the spring. Marl accumulations that extend upstream from this travertine buildup result in a broad, flat valley fill. Travertine can be observed along the stream from State Road 621 to the Shenandoah River and approximately 80 m east of the stream in an embankment along State Road 621.

The Hamburg site (HAM, Figure 3) is located in the Hamburg quadrangle in Page County. Carbonate-rich waters

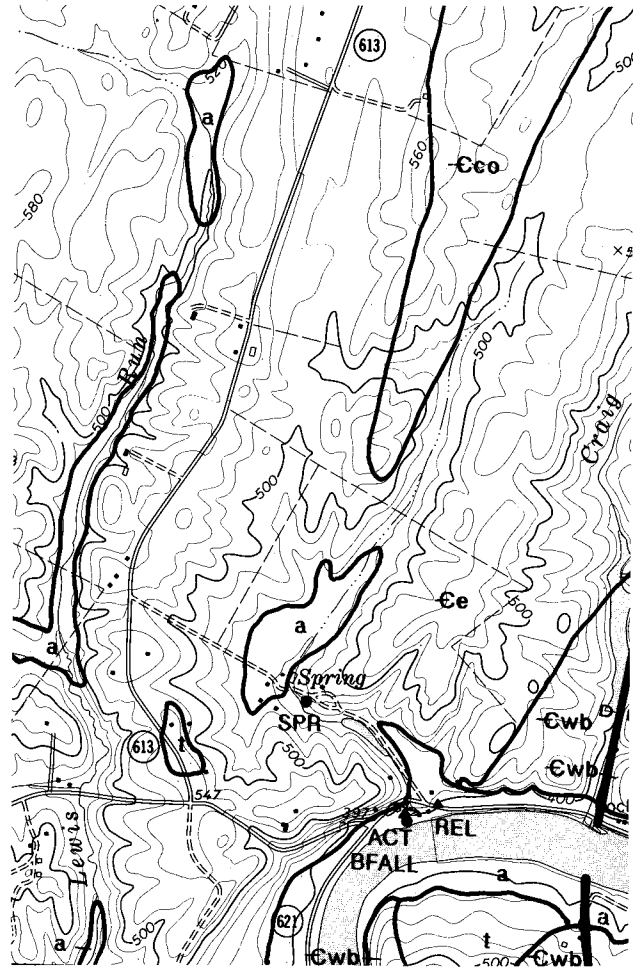


Figure 2. A portion of the Ashby Gap 7.5-minute quadrangle illustrating the James site (JAM), Clarke County. Water-sample locations are indicated by dots, travertine-sample locations by triangles, and the travertine buildup by a double-pointed arrow. The geology is modified from Gathright and Nystrom (1974): **a** alluvium; **t** terrace deposit; **Cco** Conococheague Formation; **Ee** Elbrook Formation; **Cwb** Waynesboro Formation; **—** fault trace with D - downthrown side and U - upthrown side.

enter Mill Creek at a few small springs and by diffuse flow from the folded and faulted carbonate rocks of the Beekmantown Formation. Travertine can be seen in the form of highly eroded ledges and rimstone dams in Mill Creek (described in Allen, 1967). A few oncolites have been observed in this stream.

The Arbagast site (ARB, Figure 4) is located in the Timberville quadrangle in Rockingham County. Carbonate-rich waters rise from a spring in the Chepultepec Dolomite (Brent, 1960). The spring waters mix with a very small surface stream which flows along the strike of the bedrock to the Shenandoah River. The small stream has incised marl and an associated travertine buildup approximately 230 m down-

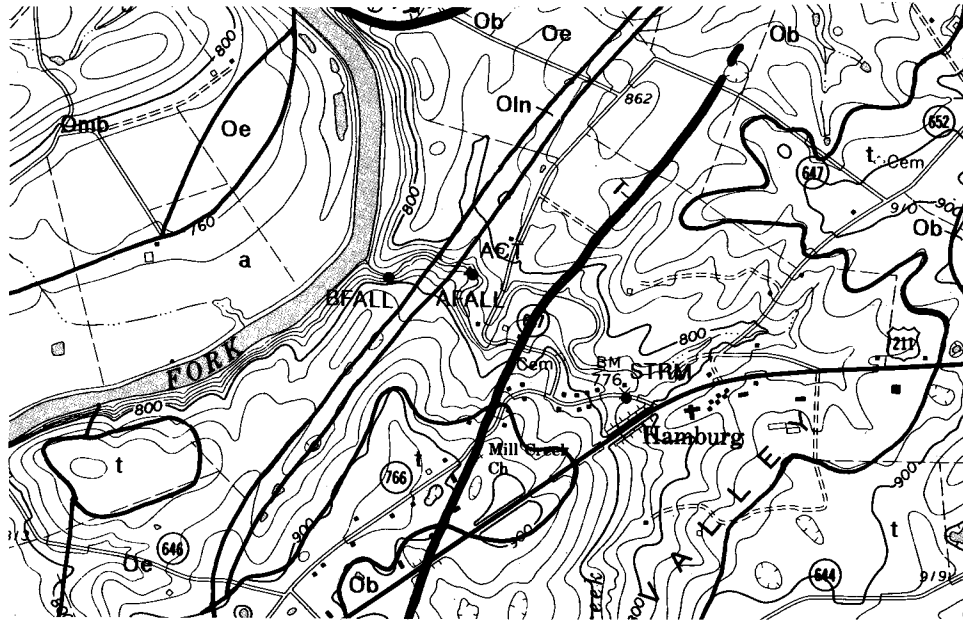


Figure 3. A portion of the Hamburg 7.5-minute quadrangle illustrating the Hamburg site (HAM), Page County. Water-sample locations are indicated by dots and the travertine-sample location by a triangle. The geology is modified from Allen (1967): a alluvium; t terrace deposit; Omb Martinsburg Formation; Oe Edinburg Formation; Oln Lincolnshire and New Market formations; Ob Beekmantown Formation; **—** fault trace with T - hanging-wall rocks.

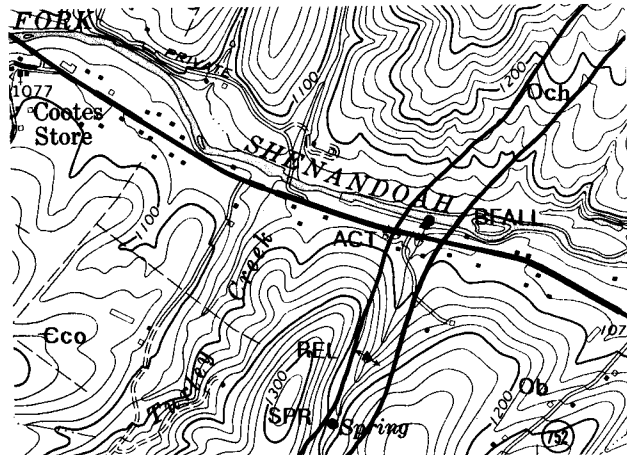


Figure 4. A portion of the Timberville 7.5-minute quadrangle illustrating the Arbagast site (ARB), Rockingham County. Water-sample locations are indicated by dots, travertine-sample locations by triangles, and the large travertine buildup by a double-pointed arrow. The geology is modified from Brent (1960): Ob Beekmantown Formation; Och Chepultepec Dolomite; Eco Conococheague Formation.

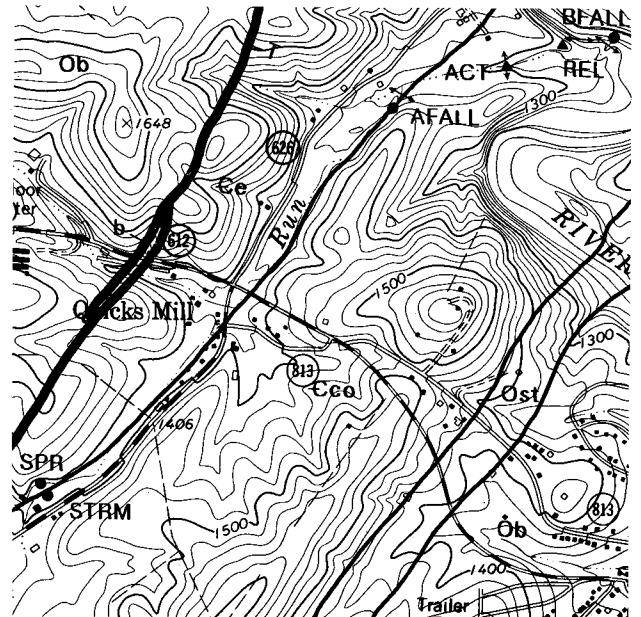


Figure 5. A portion of the Staunton 7.5-minute quadrangle illustrating the Quicks Mill site (QUI), Augusta County. Water-sample locations are indicated by dots, travertine-sample locations by triangles, and travertine buildups by double-pointed arrows. The geology is modified from Rader (1967): Ob Beekmantown Formation; Ost Stonehenge Limestone; Eco Conococheague Formation; Ce Elbrook Formation; b breccia; **—** fault trace with T - hanging-wall rocks.

stream from the spring. Other smaller travertine buildups occur along the remaining 490 m of the stream course to the Shenandoah River.

The Quicks Mill site (QUI, Figure 5) occurs along Falling Spring Run in the Staunton quadrangle in Augusta County. Carbonate-rich waters rise from springs in the carbonate rocks mapped at the contact of the Elbrook and Conococheague formations. These rocks comprise the hanging wall of the Staunton fault (referred to as the Pulaski-Staunton fault by Rader, 1967). A number of small tributaries mix with the spring waters along the course of Falling Spring Run (Hoffer-French and Herman, this volume). There are three major travertine buildups and associated marl accumulations (Collins, 1924). An incised travertine remnant stands 3 m above the current stream level approximately 150 m above the stream's junction with the Middle River. The remnant structure is the former site of the final cascade series into the Middle River and caps a wide shelter cave overlooking the river. The current stream tract bifurcates and forms twin cascades into the Middle River to the east of the shelter cave (see cover, bottom middle photograph for western-most terminal cascade). Travertine-marl materials were commercially worked for agricultural lime from 1921 to 1945 (Sweet and Hubbard, this volume).

The Folly Mills site (MIL, Figure 6) is situated in the Stuarts Draft and Greenville quadrangles in Augusta County. Carbonate-rich waters move up along the Staunton fault and enter Folly Mills Creek by small springs and diffuse flow through the stream bed. Some carbonate-rich waters enter the creek as it flows across carbonate footwall rocks mapped as the Conococheague, Stonehenge (Chepultepec Dolomite of Rader, 1967), and Beekmantown formations. Travertine-marl materials are deposited along 640 m of Folly Mills Creek in the vicinity of Folly Mills (Rader, 1967).

The Warm Springs site (WAR, Figure 7) is located in the Warm Springs quadrangle in Bath County. Travertine-depositing waters with temperatures in excess of 35°C rise at springs in the Middle Ordovician limestone in the core of the Warm Springs anticline. The Warm Springs are situated along a transverse lineament visible on LANDSAT imagery (Gathright, 1981). Gathright (1981) suggested that the thermal springs are a result of deep groundwater circulation in vertical fracture zones that are expressed as lineaments. A small travertine buildup, formerly evident at the junction of the discharge from the Warm Springs and Warm Springs Run in early 1985, was destroyed by the November 1985 flood. Thin travertine coatings were observed within the last three years on rocks in the run from Warm Springs.

The Glenn Falls site (GLE, Figure 8) is located in the Vesuvius quadrangle in Augusta and Rockbridge counties. Carbonate-rich water associated with the Fairfield fault enters Marl Creek by diffuse flow and small springs from the folded carbonate rocks of the Conococheague Formation in the hanging wall. Travertine buildups and associated marl deposits are situated approximately 530 m downstream along

Marl Creek from U.S. Highway 11. There are one 7-m and two 3-m buildups; the largest one is known locally as Glenn Falls (see cover, top middle photograph). These deposits were extensively altered by flood waters resulting from Hurricane Camille in 1969 (T. M. Gathright, II, 1984, personal communication) which also destroyed an old mill located at the top of Glenn Falls.

The Moores Creek site (MOO, Figure 9; see cover, bottom right photograph) is situated in the Vesuvius quadrangle in Rockbridge County. Carbonate-rich water rises from springs and by diffuse flow from folded carbonate rocks of the Stonehenge and Conococheague formations in the hanging wall of the Fairfield fault. Travertine-marl features include a 6-m-thick incised deposit of marl located 300 m southwest of the intersection of State Road 706 and Moores Creek. Incised marls are just upstream from travertine buildups that are 3 m and 20 m high. Approximately 180 m farther downstream is a travertine buildup that is 14 m high. Downstream from it, incised banks of travertine and marl as much as 6 m thick are exposed for 120 m along Moores Creek. Both the 20- and 14-m-high buildups are developed on pre-existing cascades of Conococheague Formation rocks. These falls were largely stripped of their travertine deposits by flood waters associated with Hurricane Camille in 1969. P.C. Lucas (1984, personal communication) estimated that only 20 percent of the travertine remains at the Moores Creek Falls after this destructive event. Extensive research on this site was carried out prior to this storm event by Steidtmann (1934a, 1934b, 1935a, 1935b, 1935c, 1936), who referred to the site as Wilson Creek or Wilson Falls Creek. The stream is named Wilson Falls Run on the 1894 Lexington 30-minute topographic map.

The Falls Hollow site (FAL, Figure 10) is located in the Ironto quadrangle in Montgomery County. Carbonate-rich waters rise in small springs and as diffuse flow from Max Meadows-type breccias in the hanging-wall rocks of the Pulaski fault (Salem fault of Cooper, 1961). Numerous small travertine rimstone buildups are found along the stream in addition to a 15-m-high buildup that extends across the valley 730 m up Falls Hollow from its intersection with the North Fork of the Roanoke River. Agricultural lime was commercially produced by calcining travertine from the site during 1939 to 1940 (Sweet and Hubbard, this volume). Additional research was carried out on this deposit by Kirby and Rimstidt (this volume).

The mound site (MOU, Figure 11) is located above Den Creek in the Ironto quadrangle in Montgomery County. Travertine-depositing waters rise as a small spring along State Road 641 and have deposited a 9-m-high hemi-dome buildup. The spring issues from Max Meadows-type breccias in the hanging-wall rocks of the Pulaski fault (Salem fault of Cooper, 1961). This site was apparently a part of the Montgomery White Sulfur Springs resort in the 1880s. These travertine-marl materials were commercially worked for agricultural lime in the 1930s by R.N. Lantz (Sweet and Hub-

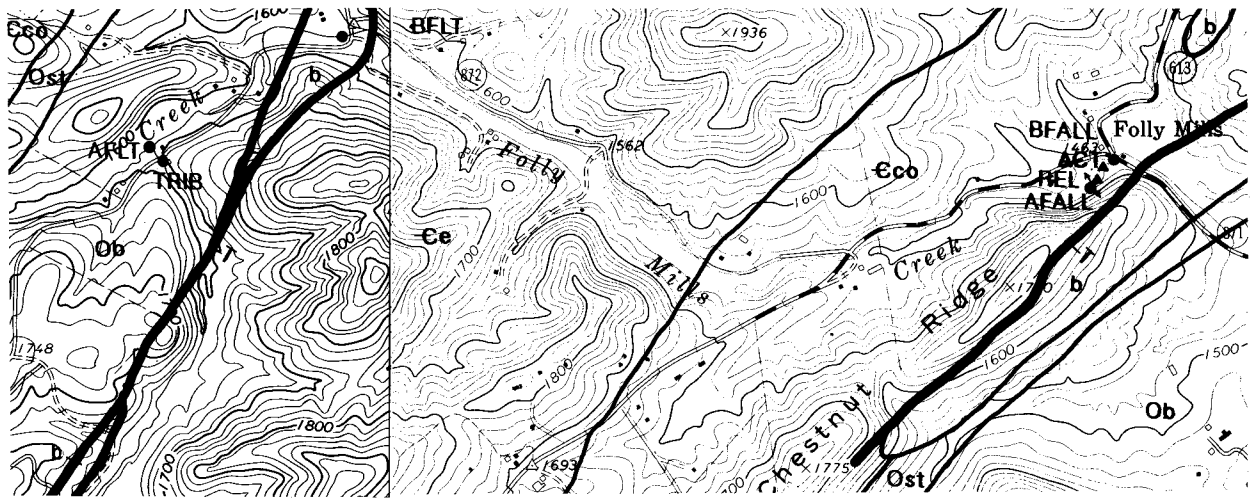


Figure 6. Portions of the Greenville and Stuarts Draft 7.5-minute quadrangles illustrating the Folly Mills site (MIL), Augusta County. Water-sample locations are indicated by dots, travertine and marl sample locations by triangles, and the large travertine buildup by a double-pointed arrow. The geology is modified from Rader (1967): **Ob** Beekmantown Formation; **Ost** Stonehenge Limestone; **Eco** Conococheague Formation; **Ce** Elbrook Formation; **b** breccia; **—** fault trace with T - hanging-wall rocks.

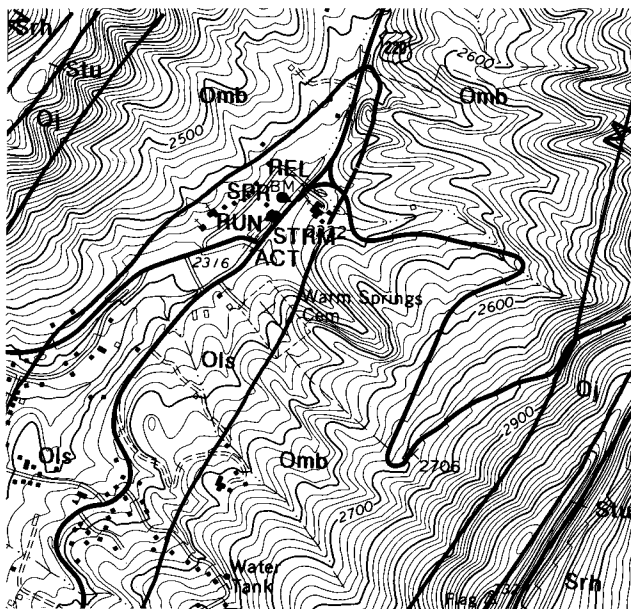


Figure 7. A portion of the Warm Springs 7.5-minute quadrangle illustrating the Warm Springs site (WAR), Bath County. Water-sample locations are indicated by dots and travertine-sample locations by triangles. The geology is modified from R. S. Edmundson (1935, Virginia Division of Mineral Resources Field Map Files): **Srh** Rose Hill Formation; **Stu** Tuscarora Sandstone; **Oj** Juniata Formation; **Omb** Martinsburg Formation; **Ols** Middle Ordovician limestones.

bard, this volume).

The Shawsville site (SHA, Figure 12) is located along Spring Branch in the Elliston and Ironto quadrangles in Montgomery County. Carbonate-rich waters rise in springs and by diffuse flow from the Max Meadows-type breccias comprising the hanging wall of the Pulaski fault (Salem fault of Cooper, 1961). The breccia ranges from large fractured blocks of massive dolomite to autobrecciated shaley dolomite to thoroughly crushed and macerated carbonate rock. The upper reaches of Spring Branch traverse the fault that defines the Christiansburg window (Broughton, 1971; not shown in Figure 12). Travertine-marl features include small rimstone buildups and a 3.6-m-high travertine buildup located 381 m upstream from its junction with the South Fork of the Roanoke River. Downstream from the travertine buildup the stream crosses a fault (Figure 12) where the Rome shale is in contact with the breccia.

The Falling Spring Creek site (FSC, Figure 1) is located in Alleghany County in the Covington quadrangle. Falling Spring Creek originates at Falling Spring, a series of springs, where the carbonate-rich waters of Warm River Cave rise to the surface through breakdown downstream from the cave. Warm River Cave and Falling Spring have developed in the Middle Ordovician limestone at the southwestern end of the Warm Spring anticline (Rader and Gathright, 1984). Travertine-marl deposits occur approximately 0.95 km downstream from Falling Spring where the stream breaches steeply dipping beds of the Tuscarora sandstone. Falling Spring Creek has deposited travertine-marl along the 4.3-km flow path from the sandstone beds to the Jackson River. The largest of the travertine buildups is a 20-m waterfall located 229 m downstream from the Tuscarora sandstone knickpoint (cover,

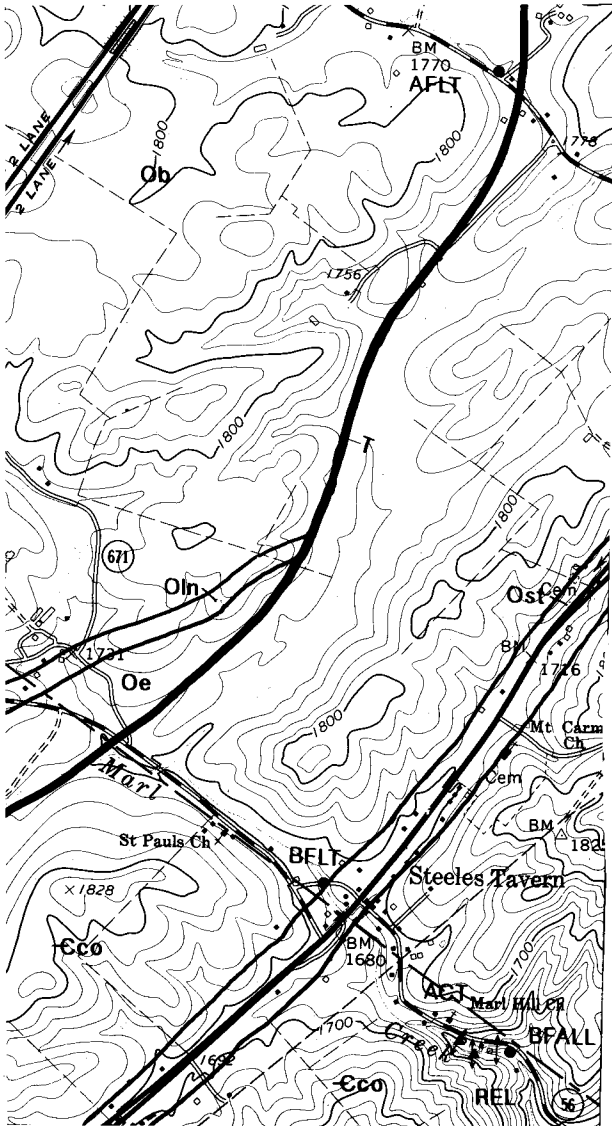


Figure 8. A portion of the Vesuvius 7.5-minute quadrangle illustrating the Glenn Falls site (GLE) in Augusta and Rockbridge counties. Water-sample locations are indicated by dots, travertine-sample locations by triangles, and travertine buildups by double-pointed arrows. The geology is modified from Werner (1966) by E. K. Rader: **Oe** Edinburg Formation; **Oln** Lincolnshire and New Market limestones; **Ob** Beekmantown Formation; **Ost** Stonehenge Limestone; **Cco** Conococheague Formation; **■** fault trace with T - hanging-wall rocks.

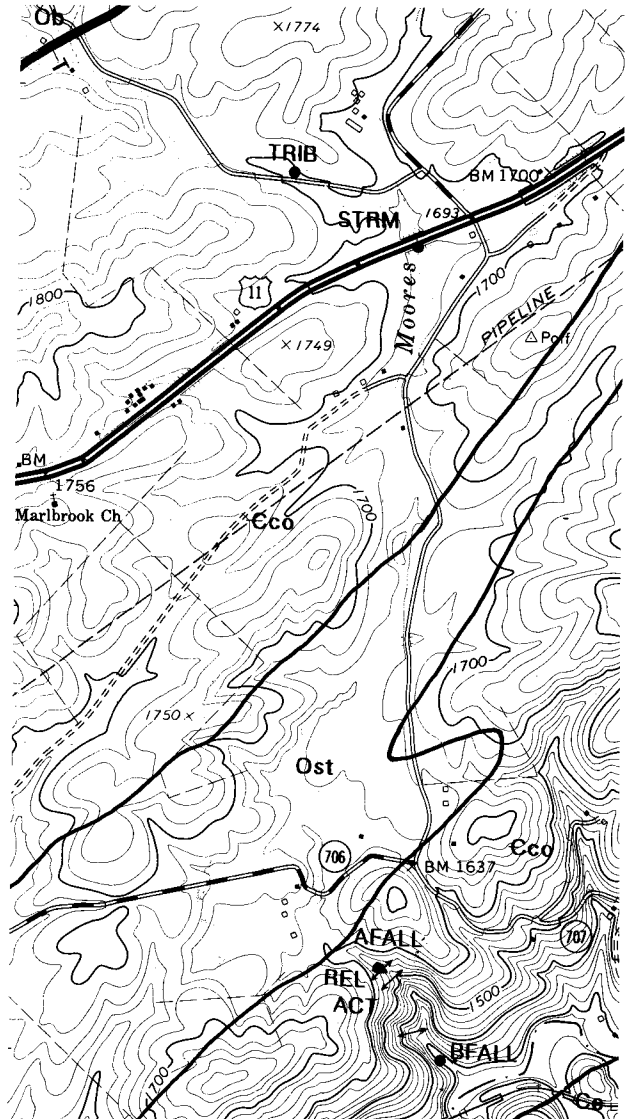


Figure 9. A portion of the Vesuvius 7.5-minute quadrangle illustrating the Moores Creek site (MOO), Rockbridge County. Water-sample locations are indicated by dots, travertine-sample locations by triangles, and travertine buildups by double-pointed arrows. The geology is modified from Werner (1966) by E. K. Rader: **Ob** Beekmantown Formation; **Ost** Stonehenge Limestone; **Cco** Conococheague Formation; **Ce** Elbrook Formation; **■** fault trace with T - hanging-wall rocks.

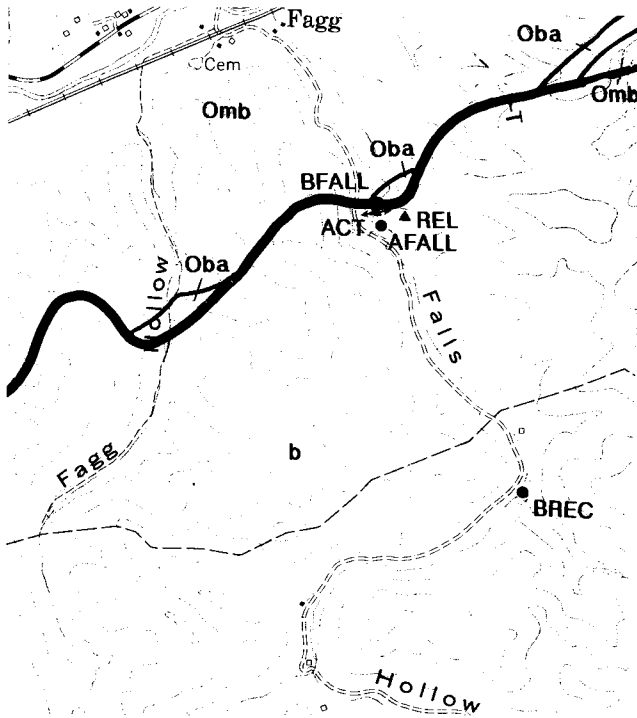


Figure 10. A portion of the Ironto 7.5-minute quadrangle illustrating the Falls Hollow site (FAL), Montgomery County. Water-sample locations are indicated by dots, travertine-sample locations by triangles, and the major travertine buildup by a double-pointed arrow. The geology is modified from Broughton (1971): **Omb** Martinsburg Formation; **Oba** Bays Formation; **b** Max Meadows type breccia; **—** fault trace with T - hanging-wall rocks.

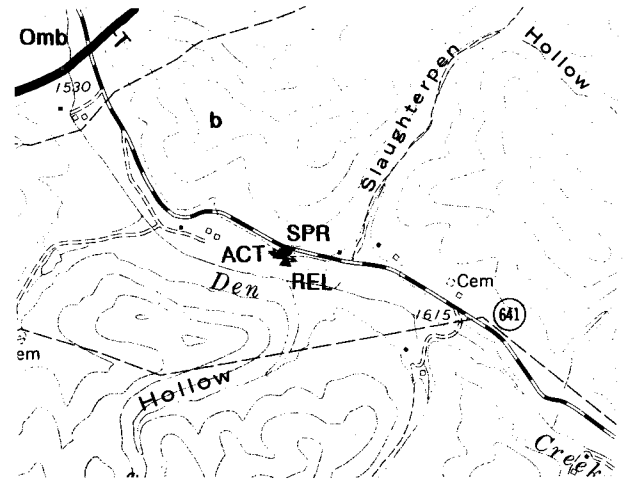


Figure 11. A portion of the Ironto 7.5-minute quadrangle illustrating the mound site (MOU), Montgomery County. The water-sample locations are indicated by dots, travertine-sample locations by triangles, and the travertine buildup by a double-pointed arrow. The geology is modified from Broughton (1971): **Omb** Martinsburg Formation; **b** Max Meadows type breccia; **—** fault trace with T - hanging-wall rocks.

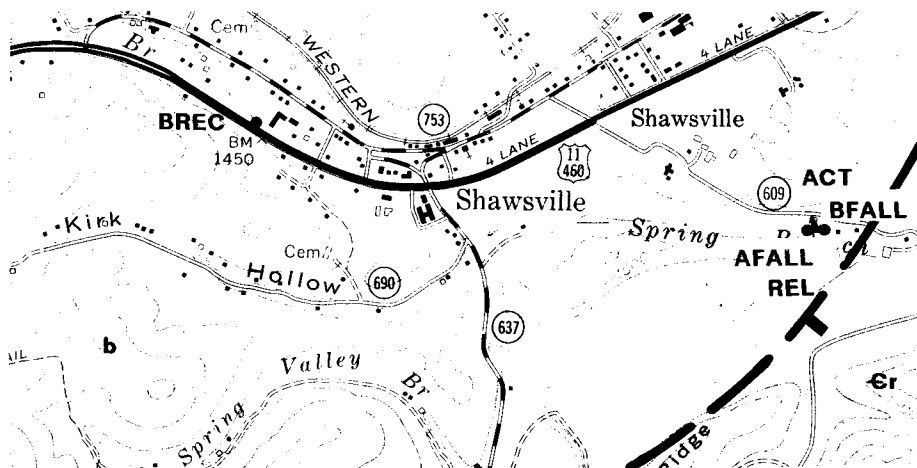


Figure 12. Portions of the Ironto and Elliston 7.5-minute quadrangles illustrating the Shawsville site (SHA), Montgomery County. The water-sample locations are indicated by dots, the travertine-sample locations by triangles, and the travertine buildup by a double-pointed arrow. The geology is modified from Broughton (1971) and Butts (1933): **Cr** Rome Formation; **b** Max Meadows type breccia; **—** fault trace with tick mark indicating the direction of dip.

top right photograph). A hydrogeochemical study by Lorah and Herman (this volume) and a geological study by Dennen and others (this volume) focus on this site.

METHODS

FIELD METHODS AND SAMPLE COLLECTION

Two types of travertine-marl materials, here defined as "active" and "relict," were sampled for chemical analysis. Active travertine-marl material generally was undergoing active deposition and was located in the stream. Relict travertine-marl was isolated above stream waters by stream entrenchment, and sampling for relict material was biased toward material located farthest from the water.

Sample locations for water were selected to test our hypothesized model of the chemical evolution of the stream water. The water samples were collected from springs, whenever discrete springs could be identified, and from major tributary inputs immediately upstream from travertine deposits. Sampling was conducted upstream and downstream from fault traces where diffuse input of groundwater to the stream was hypothesized to be influencing travertine formation. Additionally, samples were collected above and below waterfalls formed by travertine. Because similar hydrological and seasonal conditions were sought for the comparative study of the different streams, all the water samples for our survey were collected within one eight-week period in the fall of 1986.

Water samples for analyses of major ions were collected in acid-washed 250-mL polyethylene bottles. Acid-washed 250-mL dissolved-oxygen bottles with ground glass stoppers were used to collect samples for alkalinity titrations. All water samples were immediately refrigerated. Temperature, pH, and conductivity were measured in the field. Duplicate pH measurements were made with a portable Orion model 231 pH/ion meter and an Orion Ross combination electrode. The meter was calibrated with Fisher Scientific pH 4.00 and 7.00 buffers; pH was reproducible within ± 0.02 units. Conductivity was measured with a YSI model 33 conductivity meter and probe.

In addition to the samples of travertine-marl and water that formed the basis for our survey, we also collected samples of travertine for petrographic analysis and for identification of associated biota and water samples for stable isotopic analysis. At each site, two water samples for carbon and oxygen isotopic analysis were collected in 40-mL glass bottles with polyseal caps. A few grains of mercuric chloride were added to each of the carbon isotope samples in order to inhibit biological activity. These additional samples were obtained from only a few of the sites.

Sample Site Description

JAM (Figure 2): A sample of active travertine precipitated on algae was taken from a cascade within 30 m of the stream's junction with the Shenandoah River. A relict travertine sample was collected from a weathered buildup exposed along State Road 618 about 80 m east of the stream. Water samples were collected at the spring (spr) feeding the stream and downstream from the waterfalls (bfall). A sample was obtained for algal identification from the same cascade as the active travertine specimen.

HAM (Figure 3): A small rimstone dam was sampled in Mill Creek approximately 335 m east of its junction with the Shenandoah River. The rimstone buildup was highly burrowed and eroded, but was considered to be active due to its location in the stream. No travertine-marl materials were observed isolated from the creek waters. Water samples were collected upstream from the first travertine deposition in the main stream (strm), immediately above the first of the rimstone dams (afall), and downstream from the rimstone dams (bfall). A spring feeds into the stream just above the rimstone dams, but the spring water was not sampled.

ARB (Figure 4): A sample of active travertine was collected from a small rimstone dam within 15 m of the junction of an unnamed stream with the Shenandoah River. A relict sample was obtained from an eroded travertine buildup entrenched by the stream and located 455 m south-southwest from its junction with the Shenandoah River. Water samples were collected at the spring (spr) and downstream from the travertine buildups (bfall).

QUI (Figure 5): A sample of active travertine was taken from the base of the third cascade, a 4.5-m-high buildup on Falling Spring Run 335 m upstream from the junction with Middle River. A relict-travertine specimen was collected from an incised buildup remnant that is 3 m high located approximately 150 m upstream from the river. Water samples were collected from the main stream above any obvious spring inputs (strm) and from one of the major springs (spr; S2 of Hoffer-French and Herman, this volume). There are three significant cascades between the springs and the junction of the creek with the Middle River. Stream water samples were collected above the first cascade (afall; close to site F2A of Hoffer-French and Herman, this volume) and below the third cascade (bfall; close to site FRB of Hoffer-French and Herman, this volume).

The water samples for isotopic analysis were collected separately at the spring (spr) and the base of the third cascade (bfall). An additional isotope sample was obtained from the second cascade (mid; close to site F3A of Hoffer-French and Herman, this volume). A sample of travertine in contact with the water at the second cascade (mid) and a sample from the base of the third cascade (bfall) were collected for petrographic analysis. Two travertine-biota specimens were collected from the second travertine buildup. One specimen

(named A in Table 2) consisted of a travertine-encrusted pendant of algae which was suspended from an overhanging ledge of travertine in the waterfall. The second specimen (named B in Table 2) consisted of botryoidal travertine coated with light and dark patches of algae.

MIL (Figure 6): Active travertine and marl were sampled from Folly Mills Creek approximately 45 m upstream from the bridge on State Road 671. A specimen of relict travertine was taken from an extremely eroded travertine buildup located 76 m upstream from the highway bridge. Water samples were collected from the main stream above (aft) and on the breccia (brec) of a fault, both upstream from the buildups. A tributary (trib) that feeds the main stream between these two locations was also sampled. The main stream was sampled again immediately upstream (afall) and downstream (bfall) from the travertine buildup that forms the waterfall.

A travertine-biota specimen was taken from a 0.6-m-high rimstone buildup approximately 48 m upstream from the bridge. A thin coating of calcareous mud covered the travertine and algae.

WAR (Figure 7): An active-travertine specimen, a 0.3-cm-thick coating, was scraped from rocks in the spring run below the Warm Springs bathhouses and just above the confluence with Warm Springs Run. A relict travertine sample was taken from a block of travertine in the bank of the run just below the upper bathhouse. A spring-water (spr) sample was collected just outside of the first spring house. Samples from the combined run were obtained just below the input of the second spring house to the combined run (run) and downstream from another spring input but before the spring waters mixed with Warm Springs Run (strm).

GLE (Figure 8): An active-travertine sample was collected from the stream at the upper falls on Marl Creek; however, this sample was highly eroded and did not show signs of active deposition. A relict-travertine specimen was collected 5 to 10 m downstream from the middle falls on the north bank of the creek at a level about equal with the creek upstream from the falls. Two water samples were collected above (aft) and below (bft) a fault upstream from the series of waterfalls. A third water sample was collected below Glenn Falls (bfall).

Algal specimens were collected at two locations along Marl Creek. A specimen (named A in Table 2) of algae was collected at a small rimstone buildup downstream from the site where the active-travertine specimen was obtained. This specimen contained calcareous mud trapped between its strands. A second algal specimen (named B in Table 2) was collected at the base of Glenn Falls.

MOO (Figure 9): An active-travertine sample was collected in the stream from the upper 3-m-high cascade on Moores Creek. A relict-travertine sample was collected from the 6-m-high incised bank above the active sample site. A tributary (trib) and the main creek (strm) were sampled at some distance above the waterfalls. The main stream was

sampled again at the top of the falls (afall) and downstream from the last observed travertine deposition (bfall).

FAL (Figure 10): A specimen of travertine showing features indicative of active deposition was collected from the face of the 15-m falls in Falls Hollow. A relict-travertine specimen was collected from the eastern end of the 15-m-high buildup approximately 90 m from the present stream position. The stream was sampled upstream from the main travertine buildup (brec) and just above (afall) and below (bfall) the buildup.

The water samples collected for isotopic analysis were obtained above (afall) and below (bfall) the buildup. A sample of travertine in contact with the water was collected from the base of the falls (bfall) for petrographic analysis. A specimen of algae that coated botryoidal travertine was collected from a section of the 15-m cascade.

MOU (Figure 11): An active-travertine specimen, a fragment of a small rimstone feature, was collected. This travertine was very porous and contained organic material. A relict specimen was collected from a large block of travertine on the southeastern edge of a mound buildup above Den Creek. The spring water was sampled. A sample was obtained for algal identification from the rimstone feature from which the active-travertine specimen was collected.

SHA (Figure 12): An active-travertine sample was taken from a small rimstone dam near the base of a 3.6-m travertine buildup in Spring Branch. A relict specimen was collected from a travertine block located below the 3.6-m buildup behind an old mill. Water samples were collected along the stream from locations in the brecciated rocks (brec) and above (afall) and below (bfall) the travertine buildup.

FSC: Water samples were obtained for isotopic analysis. Samples were collected at the spring (named spr in Tables 5 and 6; near site S2 of Lorah and Herman, this volume), at the crest of the falls (named afall in Tables 5 and 6; near site F3 of Lorah and Herman, this volume), and near the base of the falls (named bfall in Tables 5 and 6; near site F4 of Lorah and Herman, this volume). Travertine was collected from active rimstone features at locations in the stream above (afall) and below (bfall) the 20-m-high waterfall. Several well-lithified samples were obtained from a relict travertine feature exposed along State Road 640 approximately 200 m northwest of the present stream course. During 1985, travertine was deposited on seed crystals or their enclosing cages that were located downstream from the waterfalls (Lorah and Herman, this volume). Samples of this travertine were examined for algae.

GEOCHEMICAL DATA ANALYSIS

The raw chemical concentration data and the field pH and temperature for each water sample were entered into WATEQF, a computerized geochemical model (Plummer

and others, 1976), by means of an interactive program for generating input files (Moses and Herman, 1986). Based on thermochemical data, WATEQF calculates the activities of all species in solution and the saturation state of the water with respect to mineral phases.

The saturation index for calcite (SI_c) is the logarithm of the ratio of the ion activity product to the equilibrium solubility product at the sample temperature. The value of the saturation index indicates whether the solution is undersaturated (negative SI_c), supersaturated (positive SI_c), or at equilibrium ($SI_c = 0$) with respect to calcite. Given the errors in the pH values, the Ca^{2+} and HCO_3^- concentrations, and the thermodynamic data, the SI_c values can be reported to ± 0.05 units. The theoretical CO_2 partial pressure (PCO_2) of a hypothetical gas phase with which the water sample is in equilibrium is also calculated by WATEQF, using the ionic strength, HCO_3^- concentration, and pH of the sample. The stream samples are considered to be supersaturated with carbon dioxide if PCO_2 values are greater than the normal atmospheric PCO_2 of $10^{-3.50}$ atm. The error in calculated $\log PCO_2$ values is ± 0.03 .

RESULTS

TRAVERTINE-MARL

The two types of travertine samples, active and relict, collected at each site have different compositions (Table 1). The active travertine and marl materials have an average calcium carbonate ($CaCO_3$) content of 89.84 percent by weight, with values ranging from 75.56 to 97.12 percent, and an average magnesium carbonate ($MgCO_3$) content of 1.53 percent, with values ranging from 0.84 to 2.00 percent. Relict travertine averages 94.95 percent $CaCO_3$ content by weight, with a range of values from 90.45 to 98.14 percent; the average $MgCO_3$ content is 1.44 percent, with a range of values from 0.47 to 2.07 percent. In general, the relict travertines are higher in $CaCO_3$ and contain less noncarbonate detrital constituents (SiO_2 , Al_2O_3 , Fe_2O_3 , K_2O and TiO_2) than more recent travertine and marl materials.

BIOTA

A number of algae, including diatoms, that live on travertine were identified from several Virginia streams (Table 2; Allan Pentecost, 1988, written communication). The samples from FAL and FSC showed only sparse life. Algae were significant in the MOU and JAM samples but diversity was limited. Diatoms and algae were abundant in QUI, MIL, and GLE samples. Mosses were significant in one sample from MIL.

WATER

Temperatures of travertine-depositing waters range from a high value of 33°C, for the thermal waters at WAR, to intermediate values of 13.0 to 21.0°C, measurements made in September, to low values of 9.0 to 12.0°C, measurements made in November (Table 3). The differences in temperatures among the samples collected at each site are always less than 4°C.

Spring and stream waters all have pH values between 7.09 and 8.42 (Table 3). The lowest values are observed at springs: 7.56 at QUI, 7.62 at WAR, 7.28 at JAM, 7.25 at ARB, and 7.09 at MOU. All non-thermal stream waters have pH values greater than 8.04 except the upstream sample at QUI and the tributary sample at MIL. The pH values for the run below Warm Springs are lower at 7.72 to 7.85. The general trend for samples from the same site is an increase in pH in the downstream direction.

Conductivity values (Table 3) and total dissolved solids concentrations (Table 4) indicate that many of these water samples are grossly similar. The thermal waters at the WAR site are distinctly different from all the others; they are the most concentrated of all of the waters. The waters at FAL and MOU are almost as concentrated as the WAR samples. The waters at the other eight study sites are less concentrated, and roughly in order of decreasing solute concentrations they are: SHA, ARB, JAM, QUI, MIL, HAM, GLE, and MOO.

All the non-thermal waters sampled in this study are of the calcium-bicarbonate type (Table 3). Calcium, the dominant cation, averages 72.9 mg/L and has a range from 58.2 to 90.5 mg/L in the 30 non-thermal samples. In general, waters at JAM, SHA, MOU, and FAL have slightly higher concentrations of Ca^{2+} than samples from QUI, MIL, GLE, MOO, HAM, and ARB. The WAR samples, at 107.4 to 114.5 mg/L, have the highest Ca^{2+} concentration of all the samples. Magnesium is the second most abundant cation, ranging from 15.8 to 43.3 mg/L. Samples from QUI, MIL, ARB, SHA, MOU, and FAL have higher concentrations of Mg^{2+} than those from GLE, MOO, WAR, JAM, and HAM.

Sodium concentrations range from 0.51 mg/L at MOU to 8.43 mg/L at GLE, but all the rest of the samples fall between 1.55 and 7.77 mg/L (Table 3). In general, GLE, MOO, and JAM have the highest Na^+ concentrations, MIL, WAR, HAM, and SHA are intermediate, and QUI, ARB, and FAL are lowest. Potassium values for the non-thermal samples span a range from 0.93 to 4.68 mg/L, again from MOU and GLE, respectively. Waters from MIL, GLE, and MOO have greater concentrations of K^+ than the other non-thermal samples. The samples from WAR, at 10.52 to 11.34 mg/L, have more than twice as much K^+ in them than any other samples.

Bicarbonate is the dominant anion in all samples except those from WAR in which sulfate is more abundant (Table 3). The HCO_3^- concentration averages 322.6 mg/L for the non-thermal samples and ranges from 232.8 to 435.1 mg/L.

Table 1. Chemical composition of travertine-marl samples. The site names are defined in the text. Active or recently deposited material is labelled act; relict or old material is labelled rel. Travertine samples are indicated by T; the marl sampled is labelled M. Analyses were obtained by wavelength dispersive X-ray fluorescence using National Bureau of Standards reference compounds as standards. The analyses are reported in units of weight percent.

	JAM		HAM	ARB		QUI		MIL		
	act T	rel T		act T	rel T	act T	rel T	act T	act M	rel T
CaCO ₃	88.96	97.89	94.09	85.66	91.35	85.51	95.29	88.67	75.56	95.56
MgCO ₃	0.84	0.47	1.49	1.50	1.39	1.64	2.07	2.19	2.10	1.92
SiO ₂	7.55	1.09	2.71	10.05	5.28	10.10	1.58	6.58	18.04	1.59
Fe ₂ O ₃	0.57	0.09	1.14	0.82	0.50	0.67	0.20	0.86	2.32	0.34
Al ₂ O ₃	1.26	0.18	0.30	1.43	0.96	1.47	0.36	1.25	1.43	0.35
K ₂ O	0.63	0.07	0.05	0.37	0.31	0.38	0.15	0.29	0.38	0.10
Na ₂ O	0.00	0.13	0.08	0.00	0.08	0.00	0.04	0.00	0.00	0.00
TiO ₂	0.11	0.01	0.05	0.11	0.06	0.16	0.02	0.09	0.11	0.02
P ₂ O ₅	0.05	0.05	0.09	0.05	0.05	0.06	0.07	0.06	0.06	0.03
S	0.03	0.02	0.01	0.00	0.02	0.02	0.22	0.01	0.01	0.09

	WAR		GLE		MOO		FAL		MOU		SHA	
	act T	rel T										
CaCO ₃	92.73	90.45	96.55	92.15	97.12	98.14	92.48	96.83	92.67	95.44	88.07	96.44
MgCO ₃	1.77	1.39	0.89	1.04	0.88	0.91	1.70	2.07	1.30	1.33	2.00	1.82
SiO ₂	3.70	5.35	1.88	5.11	1.40	0.66	3.51	0.67	4.33	2.13	6.62	1.01
Fe ₂ O ₃	0.41	1.02	0.18	0.46	0.21	0.11	0.57	0.11	0.33	0.22	0.86	0.20
Al ₂ O ₃	0.50	1.15	0.38	0.93	0.31	0.13	1.06	0.20	0.82	0.48	1.52	0.23
K ₂ O	0.15	0.27	0.07	0.19	0.05	0.03	0.36	0.07	0.42	0.23	0.65	0.10
Na ₂ O	0.00	0.00	0.00	0.00	0.00	0.00	0.16	0.00	0.00	0.00	0.00	0.15
TiO ₂	0.05	0.07	0.02	0.06	0.02	0.01	0.07	0.01	0.07	0.03	0.12	0.02
P ₂ O ₅	0.04	0.07	0.02	0.04	0.01	0.01	0.01	0.00	0.02	0.04	0.10	0.02
S	0.65	0.24	0.01	0.01	0.01	0.01	0.08	0.03	0.03	0.10	0.07	0.02

Waters from MOU and FAL have the highest HCO₃⁻ concentrations, whereas QUI, MIL, JAM, ARB, and SHA have intermediate concentrations, and GLE, MOO, and HAM have the lowest concentrations. The thermal waters at WAR have the lowest HCO₃⁻ concentrations of all the samples.

Sulfate concentrations in the non-thermal waters range from 2.19 to 49.29 mg/L. The samples from FAL have the highest concentrations by at least a factor of 2.5. Waters at JAM, SHA, and MOU have relatively elevated SO₄²⁻ concentrations. Samples from MIL, GLE, MOO, HAM, and ARB have lower concentrations, and QUI samples have the lowest concentrations of all the non-thermal waters. The samples from WAR have very high SO₄²⁻ concentrations of 254.4 to 262.6 mg/L. Chloride concentrations range from 1.37 to 16.18 mg/L. In general, the relative concentrations of Cl⁻ follow the relative concentrations of Na⁺ so that GLE, MOO, JAM, and SHA have the highest, MIL, HAM, and ARB have the intermediate, and QUI, WAR, MOU, and FAL have the lowest concentrations.

Nitrate concentrations range from less than 0.50 to 21.16 mg/L in all the waters sampled (Table 3). Waters at JAM and

ARB have very high concentrations. Waters collected at QUI, MIL, GLE, MOO, HAM, and SHA all have distinctly lower concentrations, somewhat less than half the values observed for JAM and ARB. The samples from WAR, MOU, and FAL have very low concentrations.

The molar Ca/Mg ratios of all the waters are between 1.02 and 3.03 (Table 4). Reflecting their lower Mg²⁺ concentrations, waters collected at GLE, MOO, JAM, and HAM have the larger Ca/Mg ratios. The samples from WAR also have large ratios reflecting the high Ca²⁺ concentrations in those samples. The molar Na/K ratios for the WAR samples are 0.498 to 0.616. Only two non-thermal samples, the tributary stream at MIL (trib) and the spring at MOU (spr), have molar Na/K ratios less than 1.0. All other non-thermal waters have ratios between 1.13 and 4.30. The molar Cl/SO₄ ratios are greater than 1.32 for all samples except those collected at WAR, MOU, and FAL.

All the waters sampled are supersaturated with respect to the CO₂ content of the atmosphere (10^{-3.5} atm; Table 4). The calculated values span a range of nearly two orders of magnitude from 10^{-1.55} to 10^{-3.11} atm. The largest values are

Table 2. The biota of several travertine-depositing streams. All identifications were provided by Allan Pentecost (1988, written communication).

Name	Type	Occurrence
The James site (JAM)		
<i>Phoridium</i> <i>Vaucheria</i>	green alga Xanthophyceae	(empty sheaths only) (no live material)
Falling Spring Run, Quicks Mill site (QUI)		
Sample A		
<i>Phormidium incrustatum</i>	blue-green alga	major component
<i>Schizothrix calcicola</i>	blue-green alga	
<i>Oocardium stratum</i>	green alga	abundant
<i>Cymbella</i>	diatom	
<i>Achnanthes</i>	diatom	
Sample B		
<i>Phormidium incrustatum</i>	blue-green alga	major component
<i>Navicula angusta</i>	diatom	abundant
<i>Vaucheria</i>	Xanthophyceae	(sterile)
Folly Mills Creek (MIL)		
moss	moss	predominant
<i>Phormidium incrustatum</i>	blue-green alga	abundant
<i>Cymbella naviculiformis</i>	diatom	abundant
<i>Nitzschia</i> sp.	diatom	
Marl Creek, Glenn Falls (GLE)		
Samples A and B		
<i>Cladophora glomerata</i>	green alga	abundant
<i>Gongrosira incrustans</i>	green alga	
<i>Phormidium incrustatum</i>	blue-green alga	(epiphytic on <i>Cladophora</i>)
<i>Gomphonema</i>	diatom	
<i>Diatoma</i>	diatom	
The Falls Hollow site (FAL)		
<i>Phormidium incrustatum</i>	blue-green alga	minor
The mound site (MOU)		
<i>Vaucheria</i>	Xanthophyceae	(no live material)
Falling Spring Creek (FSC)		
<i>Cocconeis</i> sp.	diatom	very scarce
<i>Synedra</i> sp.	diatom	very scarce

Table 3. Chemical composition of water samples. Site names are defined in the text. Within each site group, the samples are ordered upstream to downstream. The inflection points in potentiometric titrations determined HCO_3^- , assumed to be the only species contributing significantly to alkalinity. Samples were filtered through 0.45 μm Millipore filters, an acidified portion was analyzed for Ca^{2+} , Mg^{2+} , Na^+ , and K^+ by standard atomic absorption procedures, and an unacidified portion was analyzed for SO_4^{2-} , F^- , Cl^- , and NO_3^- by ion chromatography. All ion concentrations are reported in units of mg/L.

Sample name	Collection date	Temp. (°C)	Cond. ($\mu\text{S}/\text{cm}$)	pH	HCO_3^-	Ca	Mg	Na	K	SO_4	Cl	NO_3
JAM spr	9-21-86	13.0	258	7.28	315.1	90.5	18.1	5.38	2.13	18.24	9.45	16.29
JAM bfall	9-21-86	16.0	318	8.29	302.6	85.2	18.3	4.32	2.12	18.52	9.45	15.30
HAM strm	9-21-86	19.0	352	8.04	279.9	63.2	24.6	3.51	4.27	9.43	6.51	7.46
HAM afall	9-21-86	19.5	-	8.07	288.0	70.5	20.8	3.38	2.23	6.65	6.01	5.56
HAM bfall	9-21-86	19.0	341	8.18	289.2	64.1	25.5	4.02	2.72	9.72	7.60	6.84
ARB spr	9-21-86	14.0	352	7.25	332.4	68.7	29.3	2.07	1.34	7.44	4.74	21.16
ARB bfall	9-21-86	18.0	390	8.11	331.2	81.2	26.5	2.31	3.48	8.72	5.91	16.80
QUI strm	9-6-86	15.0	335	7.55	350.7	61.1	30.7	3.39	2.42	2.19	1.88	3.98
QUI spr	9-6-86	14.0	344	7.56	354.9	70.7	29.2	3.08	1.80	2.47	1.46	3.74
QUI afall	9-6-86	14.7	355	8.14	350.7	79.2	28.2	2.60	1.92	3.18	2.21	3.98
QUI bfall	9-6-86	16.0	342	8.41	325.8	67.7	28.3	2.39	2.14	3.33	2.55	3.86
MIL aflt	9-6-86	19.5	375	8.40	303.6	62.9	29.2	4.49	3.51	8.58	6.76	5.23
MIL trib	9-6-86	15.5	340	7.87	309.7	67.4	26.8	1.55	2.99	6.02	3.23	6.22
MIL brec	9-6-86	17.0	349	8.26	314.6	69.8	27.4	3.42	2.96	7.16	4.91	5.47
MIL afall	9-6-86	16.5	345	8.38	316.7	68.9	26.8	2.88	2.96	7.30	4.82	4.61
MIL bfall	9-6-86	16.0	340	8.42	315.1	64.8	28.7	4.54	3.97	7.16	4.91	4.48
WAR spr	9-7-86	33.0	780	7.62	189.9	110.9	23.5	3.81	10.52	254.4	1.76	<0.50
WAR run	9-7-86	33.0	790	7.72	188.7	107.4	23.8	3.70	10.59	262.6	1.76	0.49
WAR strm	9-7-86	33.0	800	7.85	188.7	114.5	24.7	3.32	11.34	257.0	2.31	<0.50
GLE aflt	9-6-86	21.0	395	8.18	271.9	58.2	19.1	5.87	4.41	9.78	11.30	6.72
GLE bflt	9-6-86	20.0	382	8.25	273.3	65.1	21.3	6.50	4.68	9.57	12.48	8.58
GLE bfall	9-6-86	16.7	350	8.28	274.1	71.9	18.6	8.43	4.27	8.30	12.73	6.22
MOO trib	9-6-86	16.0	368	8.12	290.9	74.1	20.4	7.47	4.09	10.59	13.07	5.23
MOO strm	9-6-86	20.0	329	8.07	233.6	74.4	18.0	7.77	4.09	8.07	16.18	2.61
MOO afall	9-6-86	19.7	318	8.42	243.8	71.3	16.3	6.86	4.01	7.23	12.73	3.48
MOO bfall	9-6-86	17.0	300	8.38	232.8	62.9	15.8	6.91	3.75	7.44	13.40	3.24
FAL brec	11-1-86	9.0	332	8.09	401.2	78.9	30.1	2.47	2.36	10.28	1.96	0.75
FAL afall	11-1-86	11.0	412	8.05	441.7	86.5	43.3	3.06	1.94	49.29	1.46	0.87
FAL bfall	11-1-86	10.0	401	8.18	400.4	71.1	42.3	2.05	1.58	48.58	1.37	0.87
MOU spr	11-1-86	12.0	389	7.09	435.1	89.2	35.9	0.51	0.93	15.54	1.37	0.50
SHA brec	11-1-86	11.5	343	8.12	375.9	85.1	38.7	4.06	2.96	19.23	9.40	3.62
SHA afall	11-1-86	11.0	372	8.23	363.0	81.0	38.7	4.66	3.04	18.66	10.22	2.97
SHA bfall	11-1-86	11.0	348	8.21	360.3	80.5	37.3	4.69	2.99	18.66	10.22	3.19

Table 4. Calculated parameters describing the chemical composition of the travertine-depositing waters. Charge error indicates the quality of the analyses. TDS stands for total dissolved solids. Saturation indices are reported for calcite (SI_C), aragonite (SI_A), dolomite (SI_D), and gypsum (SI_G). All ratios are molar ratios.

Sample	Charge name	TDS error (%)	log PCO_2 (mg/L)	SI_C	SI_A	SI_D	SI_G	Ca/Mg	Na/K	Cl/SO ₄
JAM spr	1.78	475.2	-1.87	+0.08	-0.07	-0.36	-2.19	3.03	4.30	1.40
JAM bfall	1.19	455.8	-2.90	+1.07	+0.92	+1.70	-2.22	2.82	3.47	1.38
HAM strm	3.34	398.9	-2.65	+0.72	+0.58	+1.31	-2.62	1.56	1.40	1.87
HAM afall	2.99	403.1	-2.67	+0.82	+0.67	+1.39	-2.73	2.06	2.58	2.45
HAM bfall	2.54	409.7	-2.79	+0.87	+0.73	+1.62	-2.61	1.52	2.51	2.12
ARB spr	-0.95	467.2	-1.81	-0.03	-0.18	-0.23	-2.69	1.42	2.63	1.73
ARB bfall	3.00	476.1	-2.66	+0.94	+0.79	+1.65	-2.58	1.86	1.13	1.84
QUI strm	-1.08	456.4	-2.08	+0.26	+0.11	+0.44	-3.27	1.21	2.38	2.33
QUI spr	1.17	467.4	-2.09	+0.32	+0.17	+0.45	-3.16	1.47	2.91	1.60
QUI afall	3.99	472.0	-2.69	+0.94	+0.78	+1.63	-3.02	1.70	2.30	1.88
QUI bfall	2.82	436.1	-2.99	+1.12	+0.97	+2.09	-3.06	1.45	1.90	2.07
MIL aflt	3.53	424.3	-2.99	+1.09	+0.94	+2.14	-2.69	1.31	2.18	2.13
MIL trib	2.88	423.9	-2.46	+0.58	+0.43	+0.97	-2.79	1.53	0.882	1.45
MIL brec	3.74	435.7	-2.85	+0.99	+0.84	+1.82	-2.72	1.55	1.97	1.86
MIL afall	2.55	435.0	-2.97	+1.09	+0.94	+2.01	-2.71	1.56	1.65	1.79
MIL bfall	3.24	433.7	-3.02	+1.09	+0.94	+2.02	-2.75	1.37	1.94	1.86
WAR spr	-3.40	594.8	-2.32	+0.47	+0.34	+0.71	-1.10	2.86	0.616	0.0187
WAR run	-5.30	599.0	-2.43	+0.55	+0.42	+0.89	-1.10	2.74	0.594	0.0182
WAR strm	-1.97	601.9	-2.56	+0.71	+0.57	+1.18	-1.09	2.81	0.498	0.0244
GLE aflt	-2.45	387.3	-2.80	+0.84	+0.70	+1.51	-2.63	1.85	2.26	3.13
GLE bflt	2.21	401.5	-2.88	+0.94	+0.79	+1.69	-2.61	1.85	2.36	3.53
GLE bfall	4.39	404.6	-2.92	+0.97	+0.82	+1.59	-2.62	2.34	3.36	4.16
MOO trib	3.24	425.9	-2.74	+0.84	+0.69	+1.35	-2.51	2.20	3.11	3.34
MOO strm	11.26	364.7	-2.76	+0.76	+0.62	+1.20	-2.62	2.51	3.23	5.43
MOO afall	7.49	365.7	-3.11	+1.09	+0.94	+1.83	-2.68	2.65	2.91	4.77
MOO bfall	4.71	346.2	-3.09	+0.95	+0.80	+1.55	-2.70	2.41	3.13	4.88
FAL brec	-2.05	528.0	-2.61	+0.85	+0.70	+1.39	-2.50	1.59	1.78	0.517
FAL afall	-1.58	628.1	-2.52	+0.89	+0.74	+1.63	-1.84	1.21	2.68	0.0803
FAL bfall	-3.17	568.3	-2.70	+0.89	+0.73	+1.68	-1.90	1.02	2.21	0.0764
MOU spr	-0.34	579.1	-1.55	-0.01	-0.16	-0.26	-2.30	1.51	0.933	0.239
SHA brec	5.48	539.0	-2.66	+0.91	+0.76	+1.63	-2.23	1.33	2.33	1.32
SHA afall	5.87	522.3	-2.79	+0.98	+0.82	+1.78	-2.26	1.27	2.61	1.48
SHA bfall	5.24	517.9	-2.77	+0.95	+0.80	+1.72	-2.26	1.31	2.67	1.48

Table 5. Chemical composition of water samples collected for isotopic analysis. Site names are defined in the text. Within each site group, the samples are ordered upstream to downstream. All ion concentrations are reported in units of mg/L.

Sample name	Collection date	Temp. (°C)	Cond. (µS/cm)	pH	HCO ₃	Ca	Mg	Na	K	SO ₄	Cl	NO ₃
QUI spr	10-7-87	14.8	309	7.42	361.2	71.9	29.3	1.70	1.42	2.51	1.53	5.02
QUI mid	10-7-87	14.7	335	8.37	350.2	67.1	28.4	2.95	2.19	3.61	4.44	4.26
QUI bfall	10-7-87	14.4	-	8.43	339.1	63.5	28.4	3.16	2.06	3.75	4.75	4.59
FAL afall	10-10-87	14.0	410	7.94	438.1	87.0	40.0	2.26	1.87	47.05	1.40	0.80
FAL bfall	10-10-87	13.0	391	8.39	405.7	72.2	41.5	2.32	1.81	46.35	1.30	0.75
FSC sp	10-10-87	26.3	975	7.45	339.2	159.2	32.1	4.58	16.02	315.4	3.60	<0.50
FSC afall	10-10-87	23.6	890	8.32	328.2	155.1	32.1	4.05	16.94	312.0	3.50	<0.50
FSC bfall	10-10-87	21.8	850	8.37	305.1	148.4	31.5	4.46	16.48	316.8	3.62	<0.50

Table 6. Isotopic composition and calculated parameters of the travertine-depositing waters. Isotopic compositions are reported in the standard δ notation; carbon is expressed relative to the PDB standard and oxygen is expressed relative to the SMOW standard. The isotopic analyses were provided by Henry S. Chafetz (1988, written communication). Charge error indicates the quality of the analyses. TDS stands for total dissolved solids. Saturation indices are reported for calcite (SI_c), aragonite (SI_A), dolomite (SI_D), and gypsum (SI_G). All ratios are molar ratios.

Sample name	¹³ C (‰)	¹⁸ O (‰)	Charge error (%)	TDS (mg/L)	log PCO ₂	SI _c	SI _A	SI _D	SI _G	Ca/Mg	Na/K	Cl/SO ₄
QUI spr	-11.950	-7.798	0.10	474.6	-1.94	+0.21	+0.06	+0.24	-3.15	1.49	2.04	1.65
QUI mid	-11.459	-7.752	-1.17	463.2	-2.92	+1.09	+0.93	+2.01	-3.03	1.43	2.29	3.33
QUI bfall	-10.401	-7.972	-1.29	449.3	-3.00	+1.10	+0.95	+2.06	-3.03	1.36	2.61	3.43
FAL afall	-11.051	-7.451	-2.76	618.5	-2.40	+0.83	+0.68	+1.53	-1.86	1.32	1.41	0.0806
FAL bfall	-10.148	-7.372	-3.37	571.9	-2.90	+1.14	+0.99	+2.22	-1.93	1.06	2.18	0.0760
FSC spr	n.a.	-8.061	-4.41	870.1	-1.95	+0.58	+0.44	+0.85	-0.93	3.01	0.486	0.0309
FSC afall	-2.697	-8.213	-4.28	851.9	-2.88	+1.35	+1.21	+2.37	-0.94	2.93	0.407	0.0304
FSC bfall	-3.065	-8.223	-4.87	826.3	-2.97	+1.33	+1.18	+2.31	-0.94	2.86	0.460	0.0308

observed for the non-thermal spring samples at QUI (10^{-2.09} atm), JAM (10^{-1.87} atm), ARB (10^{-1.81} atm), and MOU (10^{-1.55} atm). In general, within a set of samples collected at one site, the PCO₂ decreases for downstream samples. The smallest values are observed from the samples collected below the waterfalls.

Thirty-one of the water samples collected for this study are supersaturated with respect to calcite (Table 4). The remaining two samples, the springs at the ARB and MOU

sites, are in equilibrium with calcite. Saturation indices (SI_c) for the supersaturated samples range from +0.08 to +1.12, or from 1.2 to 13 times supersaturated. The springs at QUI, WAR, and JAM have some of the lowest supersaturation values. For most sets of samples collected from a single site, the waters become more supersaturated in the downstream direction. For two sites, MOO and SHA, the stream composition has shifted back toward equilibrium in the sample farthest downstream.

The spring waters at JAM, ARB, and MOU are slightly undersaturated with respect to aragonite and dolomite; all the other samples are supersaturated (Table 4). All the waters are undersaturated with respect to gypsum, although the samples from WAR are the least undersaturated, reflecting their high Ca^{2+} and SO_4^{2-} concentrations.

The water samples collected for isotopic analysis at QUI, FAL, and FSC in 1987 (Table 5) are chemically similar to other samples collected at those sites in the past (Table 3, this study; Hoffer-French and Herman, this volume; Kirby and Rimstidt, this volume; Lorah and Herman, this volume). The isotopic composition (Table 6) of dissolved carbon is distinctly heavier at FSC ($\delta^{13}\text{C}$ from -2.697 to -3.065 ‰), which is fed by thermal springs, than at QUI (-11.950 to -10.401 ‰) and at FAL (-11.051 to -10.148 ‰). The non-thermal water samples have carbon isotopic compositions that are typical for groundwaters in carbonate bedrock. Their composition ($\delta^{13}\text{C} \approx -11$ ‰) reflects approximately equal input of carbon from the dissolution of calcite in marine limestones ($\delta^{13}\text{C} = 0$ ‰) and from dissolution of CO_2 generated from the microbial degradation of organic matter in soils ($\delta^{13}\text{C} = -22$ ‰) (Pearson and Hanshaw, 1970). The oxygen isotope ratios in the three stream waters are more similar to one another. The $\delta^{18}\text{O}$ values all ranged between -7.372 and -8.223 ‰, with FSC samples being the lightest and FAL samples being the heaviest (Table 6).

DISCUSSION

TRAVERTINE-MARL

The generalized trend of higher carbonate contents in the relict travertine specimens and higher amounts of noncarbonate detrital constituents in the active, or more recent, travertine-marl specimens is contrary to expectations. One would expect older materials, which have been removed from contact with the depositional system, to have undergone a loss of carbonate through weathering and a relative apparent increase in the concentrations of the less soluble noncarbonate detrital constituents. Current findings (Table 1) suggest a decreased level of carbonate precipitation occurring in the streams, a higher level of noncarbonate clastic sediment in the streams, or a combination of both conditions. Unfortunately we have no data on precipitation rates or composition of Virginia's stream-deposited travertine-marls from 5000 or even 100 years ago.

The geochemical observations of this study and of several other reports in this volume (Hoffer-French and Herman; Kirby and Rimstidt; Lorah and Herman) indicate that considerable amounts of calcite are being deposited by a number of streams at the present time. Active travertine deposition has been quantified at Falling Spring Creek, Alleghany County,

Virginia (Lorah and Herman, this volume). As much as 0.6 cm of calcite precipitated on calcite seed crystals and hardware cloth cages that were left in Falling Spring Creek for a two-month period in the late summer of 1984. Calcite also precipitated during other months. Banded travertine was collected from a relict deposit of travertine located in the vicinity of Falling Spring Falls along State Road 640, 180 m west of the intersection of State Road 640 and U.S. Highway 220. The travertine bands, ranging from 0.5 to 1.4 cm in thickness, are thought to represent yearly cycles of carbonate deposition.

Most travertine deposits show the predominance of erosion over deposition today. Steidtmann (1934b and 1936) suggested that the advent of land cultivation is responsible for the demise of travertine deposition at the Moores Creek site. He hypothesized that muddy waters reduce the extent of algae and moss that provided a framework for calcite deposition and that subsequent floods have entrenched the deposits.

The idea that the character of the travertine-marl deposits has drastically changed in the last 200 years is plausible. There are reports of extensive damage to certain deposits by floods associated with Hurricane Camille in 1969. The writers witnessed extensive damage to travertine-marl sites as a result of storms during 1984 and 1985. If travertine-marl deposition has declined since a different climatic period 500, 1000, or more years in the past, a number of sites would have been all but lost to flood damage.

Even more pervasive than flood damage are the effects of agricultural activities in Virginia. Soil erosion provides an increased load of non-carbonate clastic debris to streams. This clastic sediment has buried travertine-marl deposits locally, diluted carbonate precipitates actively forming deposits, and abrasively scoured other deposits. Among the sites we have studied, we have not found the contemporary deposition of extensive marl materials containing more than 85 percent carbonate. All significant active marl deposits contain lenses and interlayers rich in non-carbonate sediments. Extensive relict marl deposits of more than 85 percent CaCO_3 , however, are common (Sweet and Hubbard, this volume).

Agriculture and other human activities have extensively altered runoff patterns, which have greatly increased the magnitudes of local floods. These floods, with their highly abrasive non-carbonate sediment loads, are actively downcutting travertine-marl accumulations. Between flood events the growth of travertine buildups can be impressive; however, the associated accumulations of sediment behind these structures contain considerable quantities of non-carbonate allogenic sediment.

The few exceptions to the general trend of higher levels of non-carbonate detrital material in the more recently deposited travertine are noted for the Hamburg (HAM), Warm Springs (WAR), and Glenn Falls (GLE) samples (Table 1). The only travertine found at the Hamburg site was extensively eroded and burrowed rimstone dams located in the

stream. The relatively high CaCO_3 content and the relatively low SiO_2 , Al_2O_3 , Fe_2O_3 , K_2O , and TiO_2 values may indicate that the rimstone structures are considerably older than their in-stream location might suggest.

The travertine specimens collected from the Warm Springs site yielded some unusual results. Thin (0.3 cm) active travertine coatings were removed from cobbles in the spring run. No other active travertine material was observed. Relict travertine was found in the bank of the 0.3-m-wide run only a few meters from one of the bath houses. Thus, the relict sample was not strictly isolated from the stream although it did appear to have been somewhat weathered.

The two travertine samples selected at the Glenn Falls site were both weathered. The sample of active travertine showed no evidence of recent deposition, and no other travertine in the vicinity appeared to have been recently deposited. The relict travertine sample was collected from a corroded but not highly weathered shelf of travertine at the same elevation as the stream level upstream from the falls. This ledge could have been part of the stream course prior to the 1969 flood in the area. Thus, the relict specimen actually could be younger than the extensively eroded samples collected from the stream. The travertine sampled in the stream may have been exhumed by the same storm event that isolated the more recent "relict" sample.

The petrologic analysis of the small number of travertine samples collected from QUI, FAL, and FSC proved inconclusive (H. S. Chafetz, 1988, written communication). Some samples have undergone significant neomorphism from micritic material to coarse bladed spar. Without many more samples to cover a complete gradation from very fresh material to thoroughly indurated rock, it is impossible to distinguish reliably between typical inorganically precipitated travertine and diagenetically altered algal laminated travertines (Love and Chafetz, this volume). Most of the samples looked like algal laminated material, suggesting that algae formed a substrate that aided the precipitation of calcite (H. S. Chafetz, 1988, written communication).

BIOTA

Many of the algae, including diatoms, identified from travertine in several streams in Virginia (Table 2) are the same species that have been identified in similar environments elsewhere in the world (see Pentecost, this volume). Not all of the seven streams had comparable abundances of algae. The samples from FAL and FSC, the most impressive of the travertine-depositing streams, have only sparse algae. Algae were significant enough to serve as a framework for travertine deposition at a number of sites. Samples from MOU and JAM contained one and two genera of algae, respectively. Travertine from several of the streams sampled, QUI, MIL, and GLE, exhibited abundant, diverse life, espe-

cially blue-green algae and diatoms.

It is unlikely that travertine material from a surface stream would not have some indication of associated algae. The genetic relationship, however, is unclear and cannot be resolved from this type of examination. Some researchers have found evidence of active involvement of algae and bacteria in travertine deposition (Dennen and others, this volume; Love and Chafetz, this volume), whereas others have shown that physical and chemical processes cause the observed travertine precipitation (Hoffer-French and Herman, this volume; Kirby and Rimstidt, this volume; Lorah and Herman, this volume). This study is a brief examination of many streams and does not resolve this issue.

WATER

The waters of the 12 travertine-depositing streams studied have many chemical similarities. The 10 non-thermal streams are Ca-HCO_3 -type waters, the thermal stream at FSC is a $\text{Ca-HCO}_3, \text{SO}_4$ -type water, and the thermal stream at WAR is a Ca-SO_4 -type water (Tables 3 and 5). All the waters have a large dissolved solids content for surface waters, especially rich in Ca^{2+} and Mg^{2+} , reflecting the input of groundwaters from carbonate rocks. The Ca/Mg molar ratios (Tables 4 and 6) show that most of the waters have come in contact with dolomite as well as limestone at some point in their flow path (White, 1988). The thermal waters are chemically distinguished from the non-thermal waters by their high SO_4^{2-} concentrations, their small Cl/SO_4 molar ratios, their high K^+ concentrations, and their small Na/K molar ratios (Tables 4 and 6). Interestingly, two non-thermal waters show some of these characteristics: FAL has high absolute SO_4^{2-} concentrations, and MOU has a high SO_4^{2-} concentration relative to Cl^- and a high K^+ concentration relative to Na^+ .

The saturation states of the waters with respect to CO_2 and calcite (Tables 4 and 6) are comparable to values observed in more detailed studies of individual streams (Hoffer-French and Herman, this volume; Lorah and Herman, this volume). The springs are supersaturated by as much as two orders of magnitude with respect to the CO_2 levels of the atmosphere. This elevated PCO_2 causes the spring-water pH values to be relatively low. The stream waters have lower partial pressures than the springs because the CO_2 progressively outgasses from the streams along their flow paths, but the streams still remain supersaturated with respect to CO_2 for a significant distance downstream from the major spring inputs. The higher values of pH for the stream water relative to the springs can be attributed to the CO_2 outgassing.

Two springs (ARB and MOU) are near equilibrium with respect to calcite, but all the stream waters are supersaturated (Tables 4 and 6). In previous studies that spanned several seasons, stream waters undersaturated with respect to calcite

were only observed during very wet conditions such as in the winter or early spring (Hoffer-French and Herman, this volume; Lorah and Herman, this volume). The calcite saturation indices become increasingly positive in a downstream direction as outgassing occurs.

Eight of the streams (JAM, HAM, QUI, MIL, MOO, FAL, SHA, FSC; Tables 3 and 5) exhibit decreasing Ca^{2+} concentrations in the segment of flow path from above the travertine waterfall to below it; thus, the Ca^{2+} loss is localized at the waterfalls. No loss of Ca^{2+} is observed at ARB and GLE, although they are morphologically similar to the other waterfall sites. There was no flow segment sampled at MOU. There was no travertine buildup at WAR.

Two types of processes could cause the decreased Ca^{2+} concentrations: dilution by input of a water with lower Ca^{2+} concentration or loss of Ca^{2+} from solution through formation of or reaction with a solid. One sample in each set was collected upstream from any obvious input of other water, such as discrete springs or tributaries, that could dilute the Ca^{2+} concentration. The diffuse input of diluting water, however, cannot be completely ruled out. The concentrations of unreactive species such as Cl^- do not decrease in the same stream segments as the Ca^{2+} concentrations do, however, as would be expected if dilution were important (Herman and Lorah, 1987). Of these streams, four show a small decrease in Mg^{2+} over the same flow segments. The Na^+ and K^+ concentrations do not show any consistent change. Calcium is the only cation being removed from solution.

The presence of recent travertine and the supersaturation of the stream waters with respect to calcite both indicate that the most likely removal mechanism for Ca^{2+} is calcite precipitation. Samples were not collected along a great enough length of the flow path for most streams in this study to show downstream adjustment toward equilibrium ($\text{SI}_c = 0$). In a study of Falling Spring Creek, Lorah and Herman (1988) found that saturation indices continued to increase downstream although maximum calcite precipitation occurred at the waterfalls because of the concurrent CO_2 outgassing and increase in pH. Decreased saturation indices are finally observed 4 km downstream from the waterfalls which is a greater distance than covered in the samples of this study.

Testing the Model of Critical Groundwater Input

Water samples were collected to provide a general description of the nature of travertine-depositing streams in Virginia and to examine the effect of discrete or diffuse input of carbonate-rich water to these streams. Groundwater is the hypothesized input, although no direct observation of groundwater collected from wells is part of this study. The chemical composition of spring water is interpreted as an indication of the groundwater composition. The discrete input of carbonate-rich water may occur as springs or as tributary streams. In

either case, these inputs can be sampled directly as discrete water sources. The contrasting condition is diffuse input of carbonate-rich water, which, in our hypothesized scenario, occurs as diffuse flow of groundwater through a stream bed and cannot be sampled.

Several sites appeared to be hydrologically simple: discrete springs are contributing significant volumes of water to the stream not far above the site of travertine deposition. The samples from JAM (Figure 2) are a simple pair collected from a discrete spring (spr) that is the headwater of the stream and from below the travertine waterfalls (bfall). Our model of CO_2 outgassing and CaCO_3 deposition at the falls explains the increase in pH and the decrease in Ca^{2+} and HCO_3^- concentrations between the two samples. The other major ions show some minor changes in concentrations, but there is no consistent pattern.

The ARB site (Figure 4) is physically similar to JAM, although there is a very small stream above the major spring input. The two samples are from the spring (spr) and the stream below the travertine buildup (bfall). The pH increases and the HCO_3^- concentration drops slightly as at many of the other waterfalls, but the Ca^{2+} concentration increases significantly. Even though the stream water is significantly supersaturated with respect to calcite, the increasing Ca^{2+} concentration indicates that calcite precipitation is probably not occurring. The Mg^{2+} concentration decreases, but the other cations increase. This observation cannot be explained by our model.

No clear picture emerges for WAR (Figure 7) where all the samples have similar overall compositions. The spring (spr) has a higher Ca^{2+} concentration than the run (run), but the concentration in the stream (strm) is highest. Negligible travertine deposition occurs in Warm Springs Run.

QUI (Figure 5) is hydrologically more complex than the other discrete spring sites. A major spring (spr) is higher in Ca^{2+} and HCO_3^- than the main stream (strm) above the spring input. The spring water is also lower in Na^+ , K^+ , Cl^- , and NO_3^- , reflecting its more pristine state than the surface stream that can be easily influenced by various sources of chemical contamination. Other significant inputs of calcium-rich water, including small tributaries, are more fully described by Hoffer-French and Herman (this volume) and are indicated by the relatively high Ca^{2+} concentration at the top of the first cascade (afall). This elevated Ca^{2+} concentration may be necessary to drive significant calcite precipitation. A pattern of the loss of dissolved CO_2 occurring slightly upstream from the loss of Ca^{2+} is established in previous studies (Hoffer-French and Herman, 1989) and at other sites (Kirby and Rimstidt, this volume; Lorah and Herman, 1988). Again, it is clear in our samples from this site. The HCO_3^- concentration begins to decrease upstream from the crest of the cascade, and the Ca^{2+} concentration drops at the cascade. Near the base of the final cascade (bfall), both Ca^{2+} and HCO_3^- concentrations are much lower.

Several of our study sites were selected to examine the

effects of suspected diffuse inputs of groundwater into the stream. We hypothesize that such diffuse input of Ca-HCO₃⁻ rich groundwater is as important to triggering the onset of travertine precipitation as the discrete input of water from tributaries or springs. MIL (Figure 6), with five samples, is a good site to test our model. The tributary (trib) contributes water that is higher in Ca²⁺ and HCO₃⁻, lower in pH, and cooler than the main stream (afIt). The mixed-stream composition overlying the fault (brec) is even higher in Ca²⁺ and HCO₃⁻, although there is no obvious gain of water from a discrete source. We infer diffuse input of carbonate-rich groundwater to the stream bed in the vicinity of the fault. Near the crest of the falls (afall), where there is minor travertine, Ca²⁺ concentration decreases slightly. The small increase in HCO₃⁻ in the same sample is not consistent with the common pattern of a loss of dissolved CO₂ preceding a measurable loss of Ca²⁺. Below the falls (bfall), the Ca²⁺ concentration is significantly lower and is lower than any upstream sample except from the original main stream; HCO₃⁻ is only slightly lower. None of the other chemical constituents give clear or consistent evidence for the input, either discrete or diffuse, of water of a different composition. We believe all these waters to be very similar in their major ion chemistry and that they differ only slightly in the parameters that most directly affect calcite precipitation: Ca²⁺ and HCO₃⁻ concentration, pH, and temperature.

The effect that the composition of the tributary has on the main stream at MOO (Figure 9) cannot be quantified because we do not have a sample above the junction. From the tributary (trib) and the mixed sample (strm), we can infer that the stream and tributary have similar Ca²⁺ concentrations and that the tributary has a distinctly higher HCO₃⁻ concentration. From their junction to the crest of the falls (afall), there is a slight loss of Ca²⁺ and, again, an unexpected gain of HCO₃⁻. The concentration of every other constituent except NO₃⁻ decreases. The role of diffuse groundwater input is not clear here. As in the other paired waterfall samples, Ca²⁺ and HCO₃⁻ concentrations decrease significantly at the waterfalls (bfall).

At HAM (Figure 3) stream samples were collected from above (strm), immediately above (afall), and below (bfall) the rimstone dams. There are significant increases in Ca²⁺ and HCO₃⁻ concentrations in the first segment of the flow path. There also are decreases in all the other major ions. This chemical pattern suggests an input of diffuse Ca-HCO₃⁻-type groundwater to the stream. Whereas there are slight increases in the concentrations of the rest of the constituents at the rimstone dams, there is a large decrease in Ca²⁺ concentration.

Stream samples were collected at SHA (Figure 12) from brecciated rocks above (brec), immediately above (afall), and below (bfall) the falls. There is an obvious input of surface water along this reach of stream. Concentrations of Ca²⁺ and HCO₃⁻ decrease along the sampled segment of stream, and the decrease is greater above the falls than at them. These observations suggest that dilution occurs at the site.

Two upstream samples, above (afIt) and below a fault (bfIt), and one sample below the falls (bfall) were collected at GLE (Figure 8). The pH increases slightly, as it does near the end of all the sampled stream segments in this study. The HCO₃⁻ concentration increases slightly, though, whereas the Ca²⁺ increases significantly. The other major anions show no consistent pattern. As at ARB, although the saturation index for calcite increases along the flow path, the increasing Ca²⁺ concentrations show that calcite precipitation is probably not occurring.

At site FAL (Figure 10) stream samples were collected from above (brec), immediately above (afall), and below (bfall) the waterfalls. There is no obvious input of surface or groundwater along this reach of stream. FAL is notable for the large increases of Ca²⁺, HCO₃⁻, Mg²⁺, and SO₄²⁻ concentrations with little change in pH between the two upstream samples (Table 3). Of all the samples collected in this study, these two yield the clearest chemical evidence of diffuse input of groundwater to a stream. Kirby and Rimstidt (this volume) also argue for the premise of the input of carbonate-rich groundwater via diffuse flow through the stream bed above the falls. The notably high Mg²⁺ and SO₄²⁻ concentrations for the two samples near the falls are confirmed in samples collected by us one year later for isotopic analysis (Table 5) and by the Mg²⁺ analyses reported by Kirby and Rimstidt (this volume). Large decreases in HCO₃⁻ (from 441.7 to 400.4 mg/L; Table 3) and Ca²⁺ (from 86.5 to 71.1 mg/L; Table 3) concentrations and increased pH are observed concurrently with no other significant changes in chemical composition between samples at the falls. Kirby and Rimstidt (this volume) also observed the large mass losses of HCO₃⁻ and Ca²⁺ in the vicinity of the waterfalls, although their absolute concentration values are different than our measurements. The stream in Falls Hollow is losing more Ca²⁺ and HCO₃⁻ than Falling Spring Creek, which was previously shown to deposit large amounts of calcite (Lorah and Herman, this volume). On a simple mass-balance basis, the Falls Hollow stream appears to be precipitating significant amounts of calcite (Kirby and Rimstidt, this volume). The chemical evolution of this stream is evidence in support of the model that carbonate-rich groundwater input, irrespective of whether it is from a discrete spring or from diffuse groundwater inflow, is the critical control on travertine precipitation from streams.

CONCLUSIONS

The chemical composition of travertine-marl collected from streams in Virginia shows a general trend that the active, younger materials contain a greater complement of noncarbonate detrital constituents than the older carbonate-rich travertine-marl that is presently isolated from active precipitation. It is possible that the composition of travertine-marl

deposits has changed in very recent geologic time to become less carbonate-rich as more clastic material is carried by streams as a result of an increase in soil erosion from agricultural and other human activities.

Petrographic examination of travertine samples from several sites shows a range in materials from fresh micritic calcite to neomorphosed coarse-bladed spar. Although some of the sparry material collected appeared to be diagenetically altered, algally laminated travertine, other sparry material cannot be clearly distinguished from inorganically precipitated travertine.

Although abundant algae, including diatoms, were identified on many samples of travertine from these streams, their genetic relationship to the travertine is unresolved. Our model for travertine precipitation relies upon chemical and hydrological processes with algae providing a physical framework or substrate for deposition.

Many common features among the travertine-depositing streams of Virginia are identified. Observations of the chemical composition of stream waters show that they are usually Ca-HCO₃-type waters. The processes of CO₂ outgassing and calcite precipitation account for most of the chemical changes seen along the short segments of flow path that were sampled. Greatest CO₂ losses most often are measured immediately upstream from or at a travertine buildup. The greatest losses of Ca²⁺, indicating calcite precipitation, are observed at the buildup. Dilution is not a significant factor in determining Ca²⁺ concentration.

The streams studied were selected to examine the hypothesis that input of carbonate-rich water is a critical control on travertine deposition. Some stream compositions are influenced by discrete inputs from springs or tributaries. In other streams, chemical evidence indicates there is diffuse groundwater input through the stream bed. Structural control on the localization of this input is apparent in streams that cross known faults. From our examination of the chemical evolution of these streams, we conclude that the input of carbonate-rich water is essential to the formation of travertine.

Our resulting genetic model for travertine deposits requires input of carbonate-rich groundwater to the stream. Fractures and faults control the upward migration of that groundwater. Outgassing of CO₂ is driven by chemical gradients and hydrological agitation. The greatest loss of CO₂ from solution precedes the greatest Ca²⁺ mass transfer. Calcite precipitation is localized at the waterfalls. Travertine buildups grow by a self-perpetuating process that can be interrupted by erosive floods or by land-use practices that increase the clastic load of streams in the limestone valleys of Virginia.

ACKNOWLEDGMENTS

Marilyn Bradley, Carol Wicks, and René Price per-

formed the chemical analyses; without their tireless efforts this paper would not have been possible. We thank Jeffrey Sittler, Charles Thornton, and David Gold for their assistance in the field. Thomas M. Gathright, II, and Eugene K. Rader contributed numerous insights into the structural and stratigraphic interpretations of the geology of the field sites. We thank the many landowners that allowed us access to their properties. Henry Chafetz kindly performed analyses of water and travertine samples that we sent to him. Allan Pentecost graciously performed analyses of travertine samples that we sent to him. Jackie Kennamer performed analyses of travertine and marl samples. Walt Kelly and Don Le Van provided helpful comments on the manuscript.

REFERENCES CITED

- Allen, R.M., Jr., 1967, Geology and mineral resources of Page County: Virginia Division of Mineral Resources Bulletin 81, 78 p.
- Brent, W.B., 1960, Geology and mineral resources of Rockingham County: Virginia Division of Mineral Resources Bulletin 76, 174 p.
- Broughton, P.L., 1971, The Pulaski-Salem thrust sheet and the eastern part of the Christiansburg window, southwestern Virginia [M. S. thesis]: Blacksburg, Virginia Polytechnic Institute and State University, 126 p.
- Butts, Charles, 1933, Geologic map of the Appalachian Valley in Virginia: Virginia Geological Survey Bulletin 42, 1:250,000 scale map.
- Collins, R.E.L., 1924, Travertine deposits in Virginia: Pan-American Geology, v. 41, p. 103-106.
- Cooper, B.N., 1961, Grand Appalachian field excursion: Virginia Polytechnic Institute, Engineering Extension Series, Geological Guidebook No. 1, 187 p.
- Gathright, T.M., II, 1981, Road log to the structures of the thermal springs area of western Virginia: Virginia Division of Mineral Resources, 13 p.
- Gathright, T.M., II, and Nystrom, P.G., Jr., 1974, Geology of the Ashby Gap quadrangle, Virginia: Virginia Division of Mineral Resources Report of Investigations 36, 55 p.
- Herman, J.S., and Lorah, M.M., 1987, CO₂ outgassing and calcite precipitation in Falling Spring Creek, Virginia, U.S.A.: Chemical Geology, v. 62, p. 251-262.
- Hoffer-French, K.J., and Herman, J.S., 1989, Evaluation of hydrological and biological influences on CO₂ fluxes from a karst stream: Journal of Hydrology, v. 108, p. 189-212.
- Hubbard, D.A., Jr., 1985, Annotated bibliography of the Valley and Ridge travertine-marl deposits of Virginia: Virginia Division of Mineral Resources, Virginia Minerals, v. 31, n. 1, p. 9-12.
- Hubbard, D.A., Jr., Giannini, W.F., and Lorah, M.M., 1985, Travertine-marl deposits of the Valley and Ridge province of Virginia - a preliminary report: Virginia Division of Mineral Resources, Virginia Minerals, v. 31, n. 1, p. 1-8.
- Lorah, M.M., and Herman, J.S., 1988, The chemical evolution of a travertine-depositing stream: geochemical processes and mass transfer reactions: Water Resources Research, v. 24, p. 1541-1552.

Moses, C.O., and Herman, J.S., 1986, WATIN - a computer program for generating input files for WATEQF: *Ground Water*, v. 24, p. 83-89.

Pearson, F.J., Jr., and Hanshaw, B.B., 1970, Sources of dissolved carbonate species in ground water and their effects on carbon-14 dating: Vienna, Austria, Proceedings of the International Atomic Energy Agency Symposium on Isotopes in Hydrology, p. 271-286.

Plummer, L.N., Jones, B.F., and Truesdell, A.H., 1976, WATEQF - a FORTRAN IV version of WATEQ, a computer program for calculating chemical equilibria of natural waters: U.S. Geological Survey Water-Resources Investigation 76-13, 61 p.

Rader, E.K., 1967, Geology of the Staunton, Churchville, Greenville, and Stuarts Draft quadrangles, Virginia: Virginia Division of Mineral Resources Report of Investigations 12, 43 p.

Rader, E.K., and Gathright, T.M., II, 1984, Stratigraphy and structure in the thermal springs area of the western anticlines: Charlottesville, Virginia Division of Mineral Resources, Sixteenth Annual Virginia Geologic Field Conference, 58 p.

Steidtmann, Edward, 1934a, Travertine deposits near Lexington, Virginia [abs.]: Proceedings of the Virginia Academy of Science, p. 56.

Steidtmann, Edward, 1934b, Travertine deposits near Lexington, Virginia: *Science*, v. 80, n. 2068, p. 162-163.

Steidtmann, Edward, 1935a, Travertine near Lexington, Virginia [abs.]: *American Mineralogist*, v. 20, n. 3, p. 206.

Steidtmann, Edward, 1935b, Travertine depositing waters near Lexington [abs.]: Proceedings of the Virginia Academy of Science, p. 70.

Steidtmann, Edward, 1935c, Travertine depositing waters near Lexington, Virginia: *Science*, v. 82, n. 2127, p. 333-334.

Steidtmann, Edward, 1936, Travertine-depositing waters near Lexington, Virginia: *Journal of Geology*, v. 44, n. 2, p. 193-200.

Werner, H.J., 1966, Geology of the Vesuvius quadrangle, Virginia: Virginia Division of Mineral Resources Report of Investigations 7, 53 p.

White, W.B., 1988, Geomorphology and hydrology of karst terrains: New York, New York, Oxford University Press, 464 p.

PETROLOGY OF QUATERNARY TRAVERTINE DEPOSITS, ARBUCKLE MOUNTAINS, OKLAHOMA

Karen M. Love and Henry S. Chafetz

CONTENTS

	Page
Abstract.....	66
Introduction.....	66
Field location.....	66
Methods.....	67
Results and discussion.....	68
Morphology.....	68
Constituents.....	69
Organic material and associated deposits.....	69
Algally laminated crusts.....	69
Algally coated grains.....	70
Moss-rich deposits.....	70
Inorganic deposits.....	71
Spelean-like deposits.....	71
Vadose pisoids.....	72
General calcite crystal petrography.....	73
Cement morphologies.....	76
Conclusions.....	77
Acknowledgments.....	77
References cited.....	77

ILLUSTRATIONS

Figure	
1. Location map.....	67
2. Overview of Turner Falls.....	67
3. Small buildup of travertine.....	68
4. Travertine strata dip vertically.....	68
5. Moderately lithified algally laminated crusts.....	69
6. Slab of algally laminated crust.....	69
7. Photomicrograph of a light layer composed of filamentous cyanophyte bushes.....	69
8. Photomicrograph of cyanoids.....	70
9. Photomicrograph of a moss-rich travertine.....	70
10. Layer of cave popcorn.....	71
11. Scanning electron micrograph of a cave pearl cortex.....	72
12. Scanning electron micrograph of neomorphic spar.....	72
13. Photomicrograph showing cortices of vadose pisoids.....	72
14. Scanning electron micrograph of spar.....	73
15. Photomicrograph of fibrous spar crystals.....	73
16. Photomicrograph of fibrous, feathery fans of inorganically formed calcite crystals.....	73
17. Photomicrograph reveals triangular cross sections of elongate crystals.....	74
18. Photomicrograph of bladed crystals.....	74
19. Photomicrograph showing radiating bundles of fibrous crystals.....	74

	Page
20. Scanning electron micrograph of ribbon crystals.....	75
21. Scanning electron micrographs of calcite spikes. A. Overview. B. Close-up.....	75
22. Photomicrograph of inclusion-rich zones within crystals.....	75
23. Photomicrograph of inclusion-rich zones within bladed crystals.....	75
24. Photomicrographs. A. Rhombohedral crystals. B. Hexagonal crystals.....	76
25. Photomicrograph of gravitational cement.....	76
26. Photomicrograph of meniscus cement.....	76
27. Photomicrograph of clear, rhombohedral crystals filling a pore.....	76

ABSTRACT

INTRODUCTION

Travertine deposits, freshwater carbonates precipitated from spring and stream waters, are abundant in the Arbuckle Mountains region of Oklahoma at past and present sites of waterfalls and cascades. These irregular, wedge-shaped, low-magnesian calcite deposits exhibit a great diversity of structure, texture, and morphology and contain a wide variety of inorganic and organic constituents.

Organically associated components of travertine include algally laminated crusts and coated grains and moss-rich deposits. Algally laminated crusts consist of an alternation of layers of *Phormidium* bushes encased in elongate, sparry calcite crystals and *Schizothrix* filaments surrounded by equidimensional crystals. These crusts commonly undergo aggradational neomorphism, resulting in layers composed almost entirely of coarse, columnar crystals. Mosses act as highly favorable surfaces for encrustation, commonly resulting in deposits resembling a string of beads that are composed of equidimensional crystals enveloping leaves and elongate spar deposited on the stems.

Inorganic travertine mainly consists of spelean-like deposits which precipitated in cavernous areas. These inorganic accumulations include stalactites, flowstone, cave popcorn, and cave pearls. Inorganically coated grains (vadose pisoids) form in small cavities within the deposits; many of these pisoid accumulations are inversely graded and contain gravitational cements. Some of the pisoids have a coarsely crystalline structure, whereas others are composed of an alternation of layers of micrite and spar.

Both the organically associated and the inorganic travertine deposits are composed of calcite crystals displaying a wide range of morphologies and sizes. Euhedral to anhedral equidimensional crystals range from several micrometers to several millimeters in diameter. Bladed to fibrous and columnar crystals are common and are aligned with their long axes oriented perpendicular to the substrate. Unusual crystal morphologies include parallel "ribbon" crystals, parallel "spikes," and "nested" crystals. These unusual morphologies may result from either partial dissolution or unusual geochemical conditions during growth. Cement morphologies in travertine include vadose (gravitational and meniscus) and phreatic (isopachous) forms.

Waterfall and cascade travertine deposits are irregular, low-magnesian calcite accumulations which form predominantly in streams at sites of waterfalls and rapids (herein referred to as waterfall travertines). These deposits exhibit a great diversity of structure, texture, and morphology and contain a wide variety of constituents, both inorganic and organic. cursory examination of a number of these deposits and a review of the literature pertaining to waterfall travertine accumulations indicate that these deposits share many characteristic features (Chafetz and Folk, 1984). Consequently, petrographic descriptions of waterfall travertine deposits from one area contribute significantly to the understanding of other waterfall travertine accumulations. More specifically, analyses of waterfall travertine deposits from the Arbuckle Mountains of south-central Oklahoma should prove valuable to investigators of waterfall travertines from Virginia, as indicated by gross similarities between the Arbuckle Mountains deposits and those from western Virginia (Hubbard and others, 1985).

Although a number of articles have dealt specifically with waterfall travertines, these articles usually presented overall morphological descriptions or descriptions of the organisms associated with the deposits (Branner, 1901 and 1911; Gregory, 1911; Steidtmann, 1934; Golubic, 1969; Ordonez and Garcia del Cura, 1983), or the articles focused on the chemistry of the waters or associated waterfall deposits (Steidtmann, 1935; Jacobson and Usdowski, 1975). Few petrographic studies of travertine have been conducted (Emig, 1917; Irion and Muller, 1968; Braithwaite, 1979), and Emig (1917) published the only previous study of the Arbuckle Mountains travertine.

FIELD LOCATION

Two principal travertine locations, along Honey Creek and Falls Creek (Figure 1) in the southwestern portion of the Arbuckle Mountains of south-central Oklahoma, comprised the primary field sites for this investigation. Honey Creek, in southwestern Murray County, flows in a northeasterly direc-

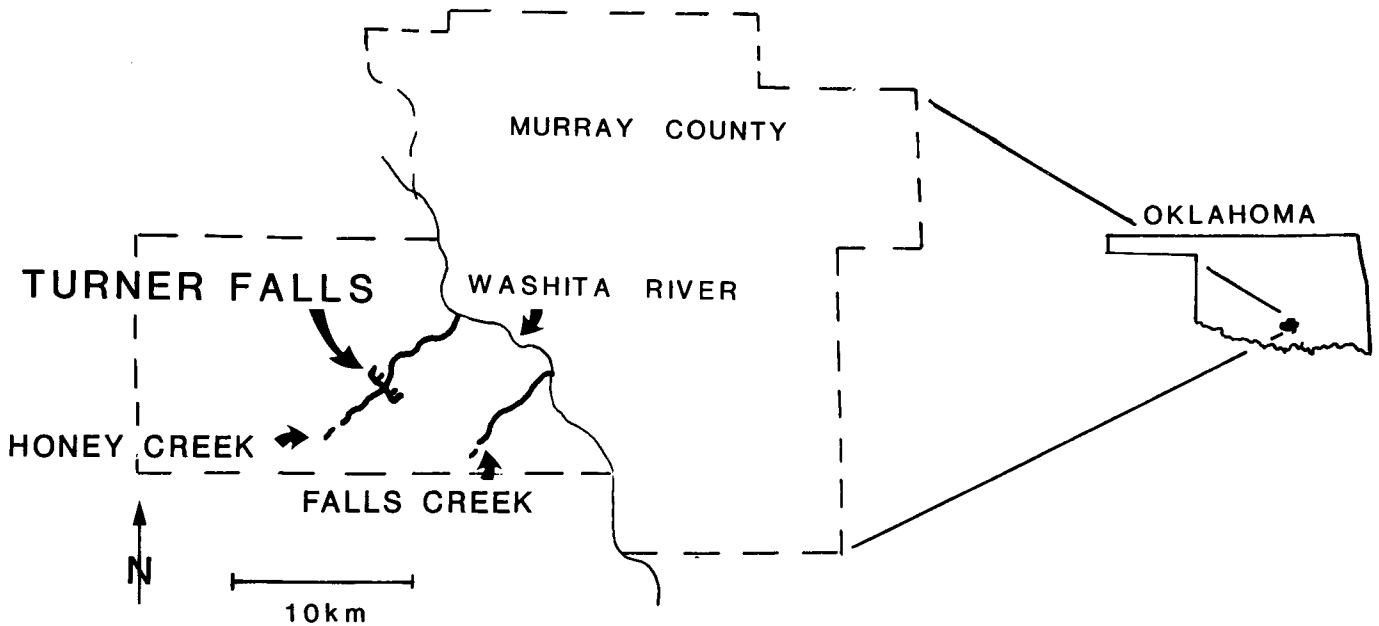


Figure 1. Location map of Honey Creek, Turner Falls, Falls Creek, and the Washita River in southwestern Murray County, south-central Oklahoma.

tion to its confluence with the Washita River (Figure 1). Numerous springs nourish the intermittent tributaries and the perennial stream of Honey Creek. The stream cascades over small travertine dams "to the very end of the canyon, where there is a sheer drop of 60 feet to the valley beyond" (Emig, 1917, p. 16-17). This "sheer drop" is Turner Falls (Figure 2), the main buildup of travertine along the creek and the focus of this study.

Falls Creek also lies in southwestern Murray County, approximately 3 km southeast of Honey Creek, which it parallels (Figure 1). Falls Creek joins with the Washita River about 6.5 km downstream from the Honey Creek confluence. Both the perennial stream and the intermittent tributaries of Falls Creek are spring-fed. Travertine deposits have modified the stream; notable is the 6-m-high Upper Price Falls, approximately 0.5 km upstream from the Washita River.

METHODS

Oriented samples of travertine were collected from the beds and banks of the streams. Samples of living algae and mosses were collected and preserved in glass containers with a mixture of 90 percent formalin, 5 percent acetic acid, and 5 percent alcohol. Binocular and petrographic microscopes were used to study hand specimens and thin sections. In order to examine crystal morphologies of unconsolidated travertine, loose grain mounts were made. A scanning electron microscope (SEM) was used to study crystal morphologies, microtextures, and microorganisms.



Figure 2. Overview of Turner Falls on Honey Creek. Cliffs to right and left of waterfall are composed of travertine and represent an "ancestral" Turner Falls. The stream broke through these older travertine deposits and is aggrading the present falls. Total height of travertine is approximately 25 m.

Bulk mineralogy and $MgCO_3$ content of the travertine deposits were determined using X-ray powder diffraction. To estimate $MgCO_3$ content, a CaF_2 standard was used to determine the position of the (104) calcite maximum. The $MgCO_3$ content was then estimated by measuring the 2θ of the calcite, and subsequently using a curve (Goldsmith and others, 1961) for relating the position of the calcite peak to mole percent $MgCO_3$ (Milliman, 1974).

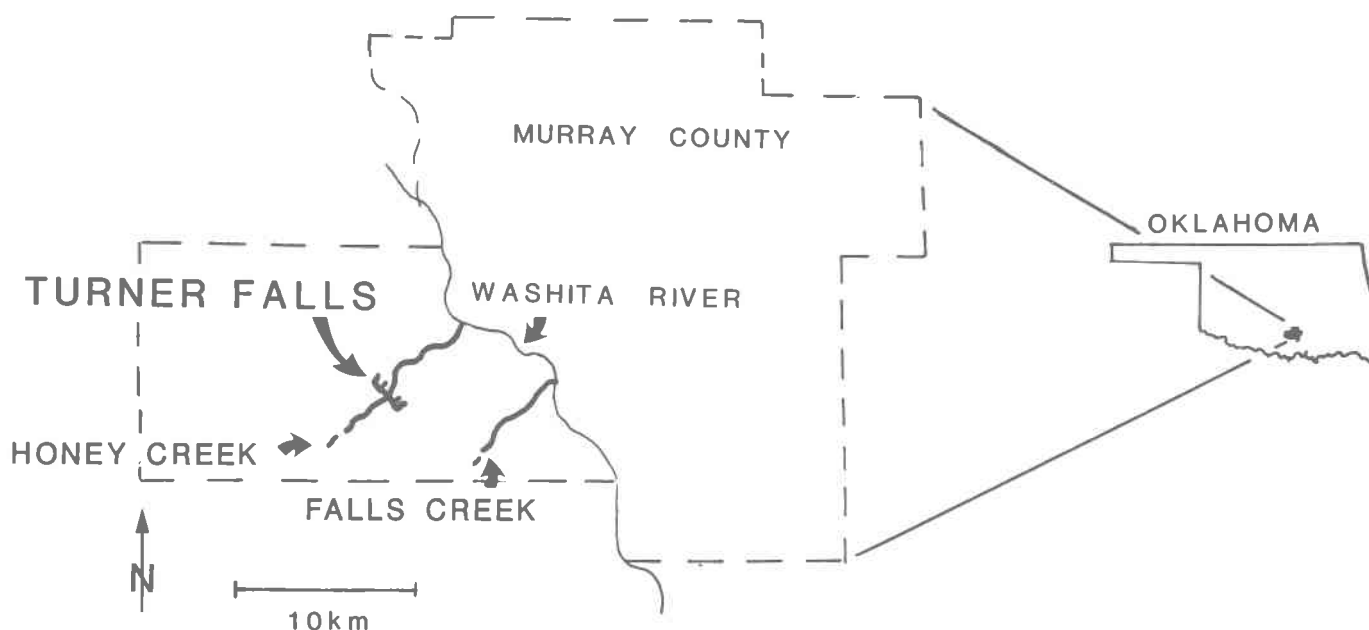


Figure 1. Location map of Honey Creek, Turner Falls, Falls Creek, and the Washita River in southwestern Murray County, south-central Oklahoma.

tion to its confluence with the Washita River (Figure 1). Numerous springs nourish the intermittent tributaries and the perennial stream of Honey Creek. The stream cascades over small travertine dams “to the very end of the canyon, where there is a sheer drop of 60 feet to the valley beyond” (Emig, 1917, p. 16-17). This “sheer drop” is Turner Falls (Figure 2), the main buildup of travertine along the creek and the focus of this study.

Falls Creek also lies in southwestern Murray County, approximately 3 km southeast of Honey Creek, which it parallels (Figure 1). Falls Creek joins with the Washita River about 6.5 km downstream from the Honey Creek confluence. Both the perennial stream and the intermittent tributaries of Falls Creek are spring-fed. Travertine deposits have modified the stream; notable is the 6-m-high Upper Price Falls, approximately 0.5 km upstream from the Washita River.

METHODS

Oriented samples of travertine were collected from the beds and banks of the streams. Samples of living algae and mosses were collected and preserved in glass containers with a mixture of 90 percent formalin, 5 percent acetic acid, and 5 percent alcohol. Binocular and petrographic microscopes were used to study hand specimens and thin sections. In order to examine crystal morphologies of unconsolidated travertine, loose grain mounts were made. A scanning electron microscope (SEM) was used to study crystal morphologies, microtextures, and microorganisms.



Figure 2. Overview of Turner Falls on Honey Creek. Cliffs to right and left of waterfall are composed of travertine and represent an “ancestral” Turner Falls. The stream broke through these older travertine deposits and is aggrading the present falls. Total height of travertine is approximately 25 m.

Bulk mineralogy and $MgCO_3$ content of the travertine deposits were determined using X-ray powder diffraction. To estimate $MgCO_3$ content, a CaF_2 standard was used to determine the position of the (104) calcite maximum. The $MgCO_3$ content was then estimated by measuring the 2θ of the calcite, and subsequently using a curve (Goldsmith and others, 1961) for relating the position of the calcite peak to mole percent $MgCO_3$ (Milliman, 1974).

RESULTS AND DISCUSSION

MORPHOLOGY

The morphological irregularity of the waterfall travertine deposits of the Arbuckle Mountains area documents one characteristic of waterfall travertine in general: few types of deposits, including other kinds of travertine, are so diverse. On a large scale, the deposits of the Arbuckle Mountains are wedge-shaped with the thickest parts of the accumulations occurring at past or present sites of waterfalls. At these sites, the travertine widens laterally in a downstream direction and narrows and thins upstream from the waterfalls. On waterfall faces, the overhanging travertine forms a fan-shaped deposit with cavernous areas inside and underneath the accumulations. The travertine fans usually do not extend to the surface of the pool present at the base of the falls. Along the bottoms of such deposits, rounded tongue-like lobes of travertine resemble dripping wax. In some places along Honey Creek, the lower edges of the travertine fans have grown downward onto dipping Ordovician limestone ledges which project upward from the stream (Figure 3). The cascading travertine that forms waterfall faces in the Arbuckle Mountains commonly has an irregular, undulatory appearance caused by outwardly or upwardly convex surfaces which are separated by narrower troughs. Along the tops of some falls, a row of laterally convex protrusions of travertine creates a scalloped outline.



Figure 3. Small buildup of travertine a short distance upstream from Turner Falls. Height of individual travertine ledges along the stream course rapidly decreases in the upstream direction. In some areas, the travertine fans are suspended over the water below (white arrow), whereas in other areas, the travertine extends downward to older limestone deposits in the stream (black arrow). Cavernous areas are created behind and beneath such overhanging fans.

Overall dimensions of the deposits range from thin (millimeter) coatings on rocks to a mass approximately 25 m in vertical thickness. This mass, located along Honey Creek, extends approximately 140 m laterally and thins to a thickness of a few centimeters. Comparable dimensions have been reported for waterfall travertine deposits in other areas (Gregory, 1911; Steidtmann, 1934; Ordonez and Garcia del Cura, 1983), although larger deposits exist such as sites in the Plitvice Lakes area, Yugoslavia (Srdoc and others, 1985).

Much of the travertine is bedded. Beds are nearly horizontal above the falls, but dips increase at waterfall edges until the beds are nearly vertical on the faces of falls (Figures 3 and 4). Not all of the falls along Honey Creek and Falls Creek have steep faces; a number of areas along the streams contain a series of low-angle (about 15 to 24°) cascades, forming successions of rapids. The change from horizontal to increasingly vertical faces results in a vast array of bed orientations and configurations, including curved layers. Such erratic depositional orientations complicate thickness measurements because depositional thickness and vertical thickness of a deposit are not the same. Some individual beds range in thickness from approximately 1 cm to more than 50 cm (most commonly they are 2 to 10 cm thick).

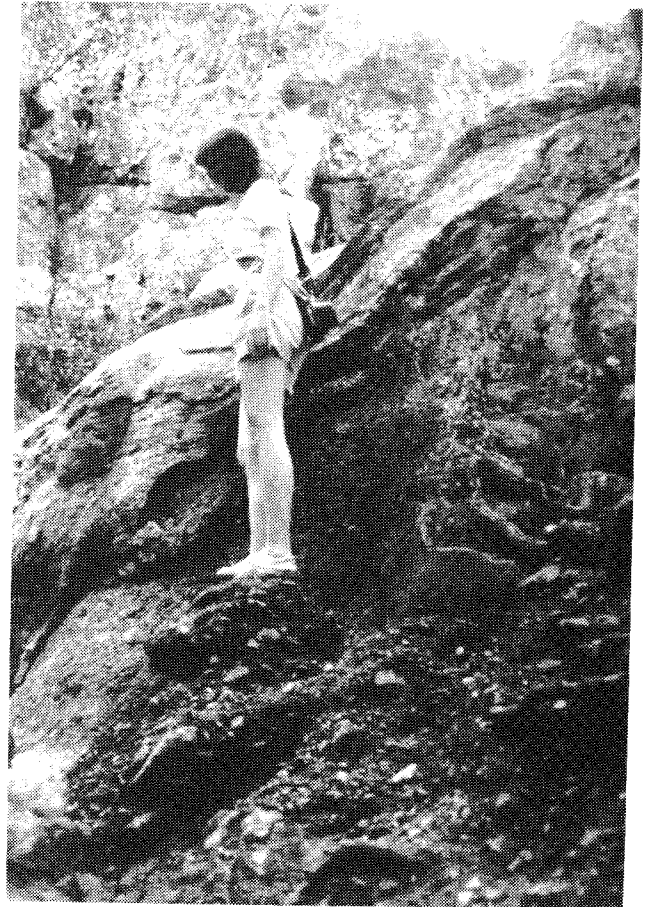


Figure 4. Travertine strata dip vertically along front of high cliff shown in Figure 2.

RESULTS AND DISCUSSION

MORPHOLOGY

The morphological irregularity of the waterfall travertine deposits of the Arbuckle Mountains area documents one characteristic of waterfall travertine in general: few types of deposits, including other kinds of travertine, are so diverse. On a large scale, the deposits of the Arbuckle Mountains are wedge-shaped with the thickest parts of the accumulations occurring at past or present sites of waterfalls. At these sites, the travertine widens laterally in a downstream direction and narrows and thins upstream from the waterfalls. On waterfall faces, the overhanging travertine forms a fan-shaped deposit with cavernous areas inside and underneath the accumulations. The travertine fans usually do not extend to the surface of the pool present at the base of the falls. Along the bottoms of such deposits, rounded tongue-like lobes of travertine resemble dripping wax. In some places along Honey Creek, the lower edges of the travertine fans have grown downward onto dipping Ordovician limestone ledges which project upward from the stream (Figure 3). The cascading travertine that forms waterfall faces in the Arbuckle Mountains commonly has an irregular, undulatory appearance caused by outwardly or upwardly convex surfaces which are separated by narrower troughs. Along the tops of some falls, a row of laterally convex protrusions of travertine creates a scalloped outline.



Figure 3. Small buildup of travertine a short distance upstream from Turner Falls. Height of individual travertine ledges along the stream course rapidly decreases in the upstream direction. In some areas, the travertine fans are suspended over the water below (white arrow), whereas in other areas, the travertine extends downward to older limestone deposits in the stream (black arrow). Cavernous areas are created behind and beneath such overhanging fans.

Overall dimensions of the deposits range from thin (millimeter) coatings on rocks to a mass approximately 25 m in vertical thickness. This mass, located along Honey Creek, extends approximately 140 m laterally and thins to a thickness of a few centimeters. Comparable dimensions have been reported for waterfall travertine deposits in other areas (Gregory, 1911; Steidtmann, 1934; Ordonez and Garcia del Cura, 1983), although larger deposits exist such as sites in the Plitvice Lakes area, Yugoslavia (Srdoc and others, 1985).

Much of the travertine is bedded. Beds are nearly horizontal above the falls, but dips increase at waterfall edges until the beds are nearly vertical on the faces of falls (Figures 3 and 4). Not all of the falls along Honey Creek and Falls Creek have steep faces; a number of areas along the streams contain a series of low-angle (about 15 to 24°) cascades, forming successions of rapids. The change from horizontal to increasingly vertical faces results in a vast array of bed orientations and configurations, including curved layers. Such erratic depositional orientations complicate thickness measurements because depositional thickness and vertical thickness of a deposit are not the same. Some individual beds range in thickness from approximately 1 cm to more than 50 cm (most commonly they are 2 to 10 cm thick).

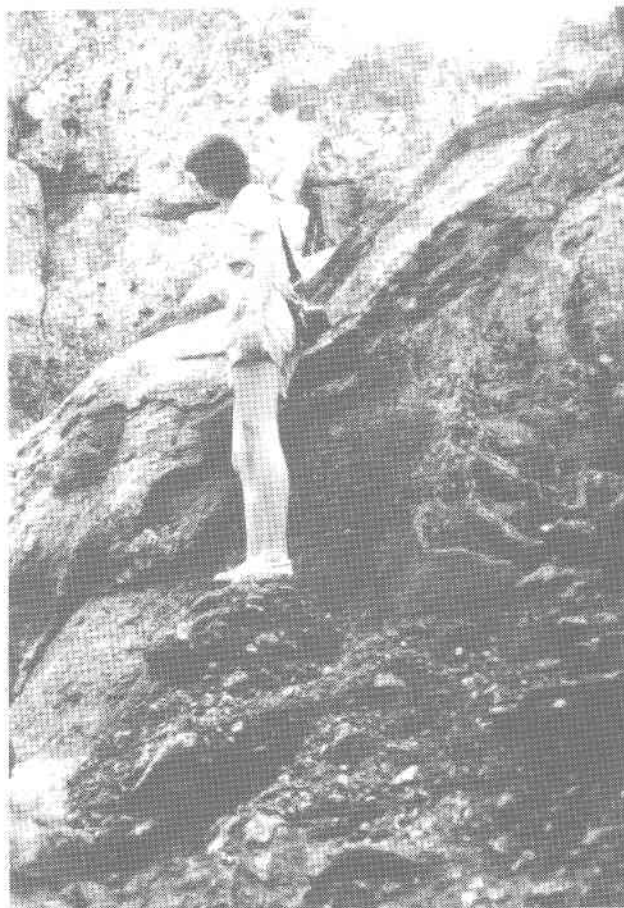


Figure 4. Travertine strata dip vertically along front of high cliff shown in Figure 2.

CONSTITUENTS

Organic Material and Associated Deposits

The waterfall travertine of the Arbuckle Mountains can contain abundant organic material. Algae (particularly blue-green, green, and golden (diatoms)) and mosses, which constitute the largest percentage of organic material in the travertine, are often incorporated, while still living, into the deposits. On the overhanging deposits forming fall faces, algae and mosses are ubiquitous. Both the mosses and the algae are encrusted near their bases, imparting a color transition ranging from light brown near the bases, where the thickest coating of calcium carbonate exists, to bright green at the unencrusted, actively growing apices. Once the organisms have been completely coated, they begin to decay, and, in older deposits, only molds remain. In addition to the algae and mosses, some living vascular plants become incorporated into the deposits. Near the stream banks, partially exposed roots of ferns, grasses, and trees are encrusted.

Clastic organic remains, such as algae, mosses, and grasses, frequently are entombed in the travertine, and tree leaves and twigs which fall into the streams are encrusted. "If objects of any kind, branches, twigs, leaves, are immersed in such waters, they are speedily incrustated, often in the most beautiful manner" (Le Conte, 1892, p. 78). Unlike the downstream-oriented plants encrusted in life position, these organic remnants occur in random orientations in the deposits.

Algally Laminated Crusts: Laminated algal crusts are a common constituent of waterfall travertine deposits (Figure 5). These stratified deposits form as drapes over wet surfaces and display a wide range of orientations. A high percentage of these crusts are vertically or nearly vertically oriented. Laminated crusts range from a few millimeters to over a meter in aggregate thickness, whereas individual laminae range from 0.5 to 2 mm thick. The laminae occur as couplets, with a light and dark layer comprising each couplet (Figure 6). The light layers are composed of filamentous cyanophyte "bushes", probably *Phormidium*, with their long axes oriented perpendicularly to the laminae, whereas the dark layers are composed of individual cyanophyte filaments, probably *Schizothrix*. The alternation of light and dark layers represents summer (*Phormidium*) and winter (*Schizothrix*) growth.

The cyanophyte bushes are encased in one or several large elongate sparry calcite (spar) crystals, which are parallel to the long axis of the filaments (Figure 7). In contrast, the individual filaments comprising the dark layers are surrounded by anhedral to euhedral equidimensional calcite crystals from several to 50 μm in length. Neomorphism (in this case, calcite-to-calcite recrystallization) of the crusts results in dense laminated strata composed of coarse columnar crystals. Individual neomorphic crystals are oriented

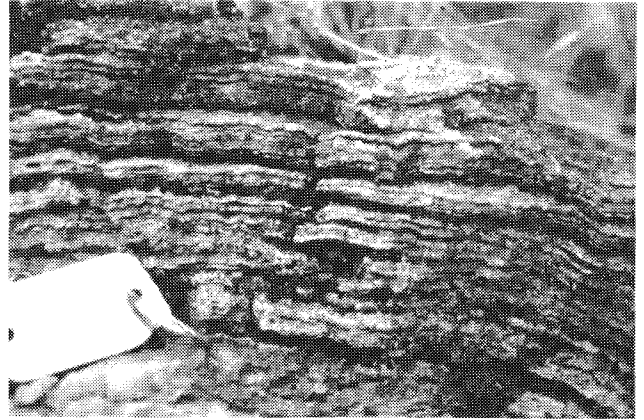


Figure 5. Moderately lithified algally laminated crusts. The alternation of thin and thick laminae is accentuated by weathering. Key ring for scale.



Figure 6. Slab of algally laminated crust is well lithified and displays differential diagenesis along the laminae. The darker (left) part of the sample is primarily composed of coarse columnar sparry calcite which is a product of aggradational neomorphism within the crust and which has partially obliterated many of the finer laminae. The original laminae are more evident on the relatively non-neomorphosed light (right) part of the sample. (Centimeter scale shown at the bottom left of the photograph.)

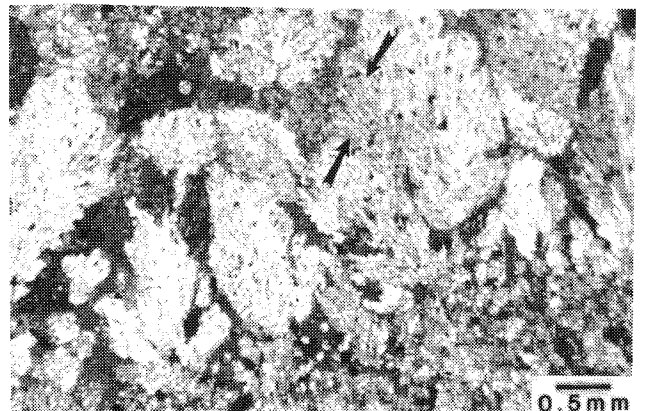


Figure 7. Photomicrograph (crossed nicols) of a light layer composed of filamentous cyanophyte bushes (arrows point to filaments) encased in spar crystals.

CONSTITUENTS

Organic Material and Associated Deposits

The waterfall travertine of the Arbuckle Mountains can contain abundant organic material. Algae (particularly blue-green, green, and golden (diatoms)) and mosses, which constitute the largest percentage of organic material in the travertine, are often incorporated, while still living, into the deposits. On the overhanging deposits forming fall faces, algae and mosses are ubiquitous. Both the mosses and the algae are encrusted near their bases, imparting a color transition ranging from light brown near the bases, where the thickest coating of calcium carbonate exists, to bright green at the unencrusted, actively growing apices. Once the organisms have been completely coated, they begin to decay, and, in older deposits, only molds remain. In addition to the algae and mosses, some living vascular plants become incorporated into the deposits. Near the stream banks, partially exposed roots of ferns, grasses, and trees are encrusted.

Clastic organic remains, such as algae, mosses, and grasses, frequently are entombed in the travertine, and tree leaves and twigs which fall into the streams are encrusted. "If objects of any kind, branches, twigs, leaves, are immersed in such waters, they are speedily incrustated, often in the most beautiful manner" (Le Conte, 1892, p. 78). Unlike the downstream-oriented plants encrusted in life position, these organic remnants occur in random orientations in the deposits.

Algally Laminated Crusts: Laminated algal crusts are a common constituent of waterfall travertine deposits (Figure 5). These stratified deposits form as drapes over wet surfaces and display a wide range of orientations. A high percentage of these crusts are vertically or nearly vertically oriented. Laminated crusts range from a few millimeters to over a meter in aggregate thickness, whereas individual laminae range from 0.5 to 2 mm thick. The laminae occur as couplets, with a light and dark layer comprising each couplet (Figure 6). The light layers are composed of filamentous cyanophyte "bushes", probably *Phormidium*, with their long axes oriented perpendicularly to the laminae, whereas the dark layers are composed of individual cyanophyte filaments, probably *Schizothrix*. The alternation of light and dark layers represents summer (*Phormidium*) and winter (*Schizothrix*) growth.

The cyanophyte bushes are encased in one or several large elongate sparry calcite (spar) crystals, which are parallel to the long axis of the filaments (Figure 7). In contrast, the individual filaments comprising the dark layers are surrounded by anhedral to euhedral equidimensional calcite crystals from several to 50 μm in length. Neomorphism (in this case, calcite-to-calcite recrystallization) of the crusts results in dense laminated strata composed of coarse columnar crystals. Individual neomorphic crystals are oriented

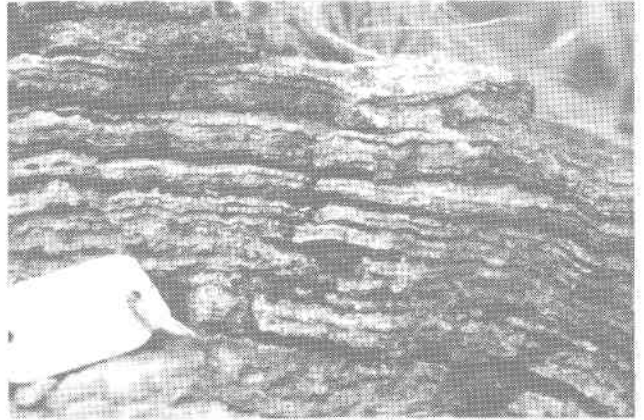


Figure 5. Moderately lithified algally laminated crusts. The alternation of thin and thick laminae is accentuated by weathering. Key ring for scale.

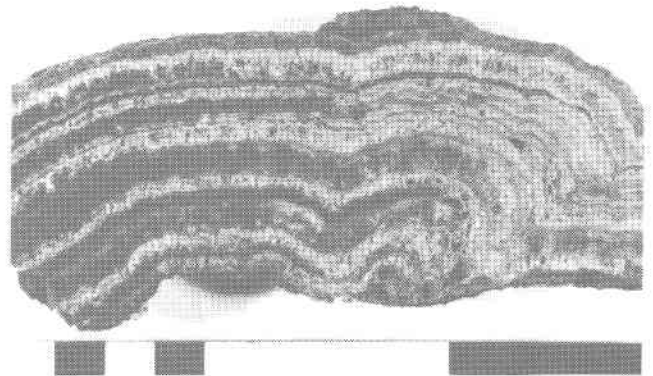


Figure 6. Slab of algally laminated crust is well lithified and displays differential diagenesis along the laminae. The darker (left) part of the sample is primarily composed of coarse columnar sparry calcite which is a product of aggradational neomorphism within the crust and which has partially obliterated many of the finer laminae. The original laminae are more evident on the relatively non-neomorphosed light (right) part of the sample. (Centimeter scale shown at the bottom left of the photograph.)



Figure 7. Photomicrograph (crossed nicols) of a light layer composed of filamentous cyanophyte bushes (arrows point to filaments) encased in spar crystals.

perpendicularly to the light and dark laminae, cross laminae boundaries, and commonly are up to 1 cm long and 0.5 cm wide. These crusts, in which algae served as the framework material, are very similar in appearance to crusts which lack any organic framework, such as cave flowstone. Algally laminated crusts are discussed in detail by Love and Chafetz (1988).

Algally Coated Grains: Cyanoids tend to be subspherical and range in diameter from less than 1 mm to greater than 12 cm. They have irregular, bumpy surface textures similar to the surfaces of the algally laminated crusts and are internally laminated (Figure 8). The coating-to-nucleus thickness ratio ranges from approximately 1:8 to 7:1. In most cases, the coatings (cortices) are thinner along the bases of the cyanoids. This phenomenon occurs commonly among the specimens several centimeters or greater in diameter and probably results from the inability of currents to roll the larger grains. Consequently, algal coatings develop mostly on the tops and sides of cyanoids. The laminations of the cortices resemble those in the organic, laminated crusts, consisting of alternating light and dark layers.

Nuclei of these coated grains range in size due to the diversity of particles which may be coated in the streams. Many nuclei are fragments of Paleozoic rocks (principally rhyolites and limestones). Other coated grains contain nuclei such as travertine clasts and organic material.

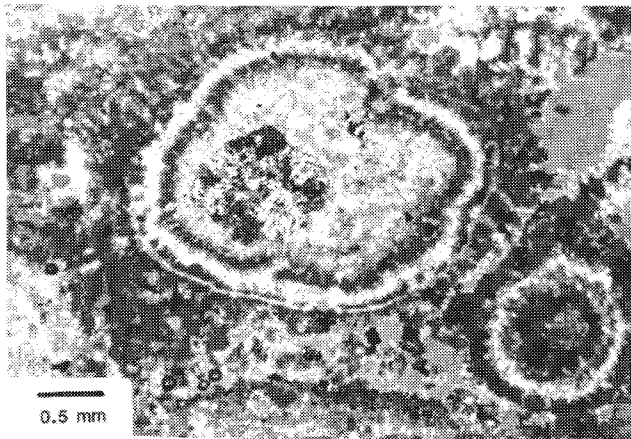


Figure 8. Photomicrograph (crossed nicols) of cyanoids; darker layers in coatings contain cyanophyte filaments, whereas lighter layers contain relatively clear micrite and spar. Large cyanoid displays volcanic rock-fragment nucleus; nucleus of smaller cyanoid is a micritic clast. Notice thicker outer coating of algae (dark layers) on top and sides of grains in contrast with the base. (Top of sample is to the left; large cyanoid is approximately 3 mm in diameter.)

Moss-rich Deposits: Aquatic mosses (Class Musci) have been noted as important constituents in waterfall travertine deposits (Emig, 1918 and 1921; Herlinger, 1981; Richardson,

1981; Ordonez and Garcia del Cura, 1983). They flourish on waterfall faces and occupy the bulk of the organic deposits in the Arbuckle Mountains travertine. The conspicuous, decorative mosses occur predominantly as tufted aggregates and pendent bunches. Wherever sufficient water flows over these mosses, they indicate the current direction by bending downstream from their places of attachment. Consequently, mosses above falls are oriented subhorizontally, whereas those on waterfall faces are oriented more nearly vertically, approximating the slopes of the travertine deposits. As a result of the dimensions of these plants, their morphologies are reflected much more visibly in the deposits than are morphologies of the algae. The mosses form highly porous deposits (up to about 75 percent porosity) in which the stems or molds are usually oriented parallel to one another even as the overall orientations range from vertical to horizontal.

The encrusted moss stems range in length from several millimeters to greater than 1 cm and are typically unbranched. Diameters of the stems range from approximately 0.1 to 0.3 mm. The leaves, which average 1 mm in length and 0.3 mm in width, have a single, thick midrib which extends nearly to the tip of the leaf. Cells assume a long hexagonal shape and are the same from the margins to the tips of the leaves, but are slightly swollen at the bases of the leaves.

The mosses and their algal epiphytes (Figure 9) are progressively encrusted from their bases while growth proceeds at the apices. Following encrustation, the mosses begin to decay, turning reddish-orange and finally black. Following decay, molds (Figure 9) may subsequently be infilled with sparry calcite. The mosses also act as filters, trapping calcite crystals and other material such as organic debris, rock, and mineral fragments washed from upstream. Coarse-silt-sized quartz grains commonly occur between mosses, and sand-sized grains are less commonly present.

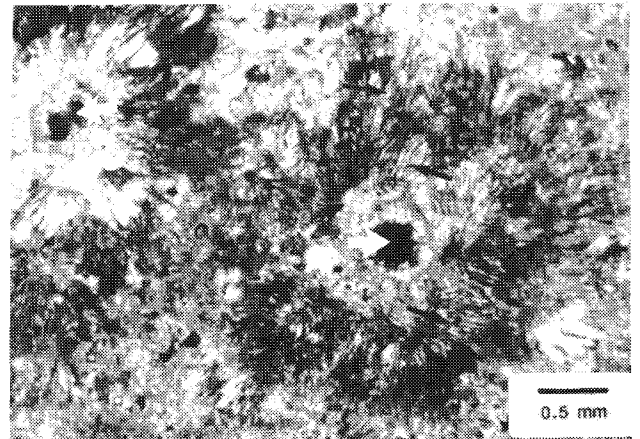


Figure 9. Photomicrograph (transverse section in plane light) of a moss-rich travertine showing mold of moss stem (white arrow) and algal epiphytes surrounded by spar (black arrow).

perpendicularly to the light and dark laminae, cross laminae boundaries, and commonly are up to 1 cm long and 0.5 cm wide. These crusts, in which algae served as the framework material, are very similar in appearance to crusts which lack any organic framework, such as cave flowstone. Algally laminated crusts are discussed in detail by Love and Chafetz (1988).

Algally Coated Grains: Cyanoids tend to be subspherical and range in diameter from less than 1 mm to greater than 12 cm. They have irregular, bumpy surface textures similar to the surfaces of the algally laminated crusts and are internally laminated (Figure 8). The coating-to-nucleus thickness ratio ranges from approximately 1:8 to 7:1. In most cases, the coatings (cortices) are thinner along the bases of the cyanoids. This phenomenon occurs commonly among the specimens several centimeters or greater in diameter and probably results from the inability of currents to roll the larger grains. Consequently, algal coatings develop mostly on the tops and sides of cyanoids. The laminations of the cortices resemble those in the organic, laminated crusts, consisting of alternating light and dark layers.

Nuclei of these coated grains range in size due to the diversity of particles which may be coated in the streams. Many nuclei are fragments of Paleozoic rocks (principally rhyolites and limestones). Other coated grains contain nuclei such as travertine clasts and organic material.

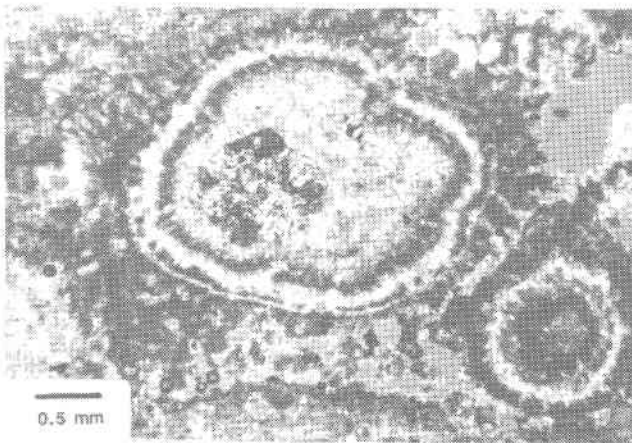


Figure 8. Photomicrograph (crossed nicols) of cyanoids; darker layers in coatings contain cyanophyte filaments, whereas lighter layers contain relatively clear micrite and spar. Large cyanoid displays volcanic rock-fragment nucleus; nucleus of smaller cyanoid is a micritic clast. Notice thicker outer coating of algae (dark layers) on top and sides of grains in contrast with the base. (Top of sample is to the left; large cyanoid is approximately 3 mm in diameter.)

Moss-rich Deposits: Aquatic mosses (Class Musci) have been noted as important constituents in waterfall travertine deposits (Emig, 1918 and 1921; Herlinger, 1981; Richardson,

1981; Ordonez and Garcia del Cura, 1983). They flourish on waterfall faces and occupy the bulk of the organic deposits in the Arbuckle Mountains travertine. The conspicuous, decorative mosses occur predominantly as tufted aggregates and pendent bunches. Wherever sufficient water flows over these mosses, they indicate the current direction by bending downstream from their places of attachment. Consequently, mosses above falls are oriented subhorizontally, whereas those on waterfall faces are oriented more nearly vertically, approximating the slopes of the travertine deposits. As a result of the dimensions of these plants, their morphologies are reflected much more visibly in the deposits than are morphologies of the algae. The mosses form highly porous deposits (up to about 75 percent porosity) in which the stems or molds are usually oriented parallel to one another even as the overall orientations range from vertical to horizontal.

The encrusted moss stems range in length from several millimeters to greater than 1 cm and are typically unbranched. Diameters of the stems range from approximately 0.1 to 0.3 mm. The leaves, which average 1 mm in length and 0.3 mm in width, have a single, thick midrib which extends nearly to the tip of the leaf. Cells assume a long hexagonal shape and are the same from the margins to the tips of the leaves, but are slightly swollen at the bases of the leaves.

The mosses and their algal epiphytes (Figure 9) are progressively encrusted from their bases while growth proceeds at the apices. Following encrustation, the mosses begin to decay, turning reddish-orange and finally black. Following decay, molds (Figure 9) may subsequently be infilled with sparry calcite. The mosses also act as filters, trapping calcite crystals and other material such as organic debris, rock, and mineral fragments washed from upstream. Coarse-silt-sized quartz grains commonly occur between mosses, and sand-sized grains are less commonly present.



Figure 9. Photomicrograph (transverse section in plane light) of a moss-rich travertine showing mold of moss stem (white arrow) and algal epiphytes surrounded by spar (black arrow).

Inorganic Deposits

Some of the travertine deposits in the field area show no evidence of having precipitated around an organic framework and contain no visible organic material (herein referred to as inorganic travertine). The bulk of such deposits consists of the spelean-like material precipitated within cavernous areas. This travertine tends to be more dense than the travertine precipitated in association with organisms.

In most cases, the inorganic deposits show some type of layering. Nearly vertical layers predominate and range in thickness from 2 to 6 cm. These deposits are typically laminated; laminae generally parallel the substrate and exhibit a wide range of color, thickness, and morphology. Individual laminae range in thickness from approximately 0.1 to 8 mm and are not of uniform thickness.

Spelean-like Deposits: Waterfall deposits contain a number of constructional cavities housing travertine forms similar to spelean deposits. Due to this similarity, it is practical to describe these features using speleological terminology; therefore, the travertine forms associated with cavities are herein termed stalactites, flowstone, cave popcorn, cave pearls, and rimstone dams.

Stalactites are common in the waterfall travertine cavities and frequently occur in groups clinging to ceilings. Shapes are slender to stocky cones with elliptical to circular cross sections. Sizes range from about 3 to 50 cm in length and from about 3 to 15 cm in diameter.

Flowstone deposits usually occur on cave walls and consist of smooth or folded sheet-like layers (Warwick, 1953; Wells, 1971; White, 1976). One type of flowstone, often referred to as draperies or curtains, is analogous to travertine forms in the field area. Along Honey Creek, a nearly vertical wall of travertine associated with a cavernous structure displays sinuous layers of vertically oriented folds. Individual folds average 30 cm in height and 15 cm in width; layers average 1 cm in thickness.

Another spelean-like form associated with the cavities has been termed cave popcorn (Thraikill, 1965; White, 1976), cave coral, and cave grapes (Thraikill, 1976; White, 1976; Bögli, 1980). In the Arbuckle Mountains area, this botryoidal form consists of hemispherical mounds, ranging in diameter from 3 mm to 3 cm, which protrude in clusters from cavity walls. Commonly, the cave popcorn occurs along a single horizon or shelf. The largest such horizon, measured along Honey Creek, extends approximately 6 m laterally and is 30 cm thick (Figure 10). Cave popcorn is also found in small cavities (approximately 2 to 10 cm in diameter) in the travertine.

Cave pearls (Bögli, 1980) constitute another spelean-like deposit associated with cavities in the Arbuckle Mountains travertine deposits. They have been described as unattached, usually highly polished, spherical to ellipsoidal to

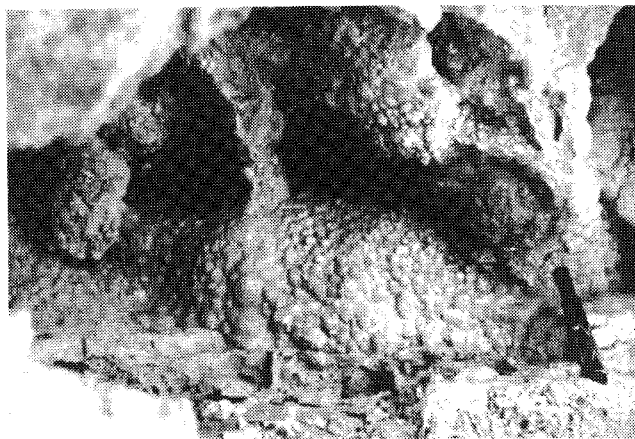


Figure 10. Layer of cave popcorn alongside Honey Creek; marking pen at right provides a scale.

polyhedral concretionary forms found in shallow pools in caves and mines (Davidson and McKinstry, 1931; Thraikill, 1976). In the Arbuckle Mountains, cave pearls are present in a few very localized areas. They usually occur as non-touching particles that have highly polished, whitish surfaces and range in shape from spherules to four- or five-sided polyhedrons. Cave pearls range in size from 2 mm to 3 cm in diameter. The average diameter of the spherules is 1 cm, whereas the polyhedrons average 8 mm in width, 13 mm in length, and 7 mm in height (although some of the polyhedral forms are flattened).

In thin section, cave pearls display a radial-fibrous structure which creates a pseudo-uniaxial cross under crossed nicols. The radial-fibrous crystal boundaries range from planar to feathery. Where the crystal boundaries are feathery, the radial texture is less distinctive. The crystals range in length from 0.25 to 14 mm and in width from 0.02 to 2 mm.

In addition to the radial structure, cave pearls have well-developed concentric laminae defined in plane light by color changes from tan to brown to dark brown. Laminae range in thickness from 0.05 to 0.2 mm, and individual laminae maintain a fairly constant thickness. Some of the laminae, however, are discordant (Figure 11), and parts of some cave pearls have undergone partial neomorphism to coarse spar (Figure 12; Bathurst, 1975, Fig. 335, p. 482). Nuclei of the cave pearls, which may be single or multiple, range in diameter from 0.5 to 3 mm, and are composed of micrite (microcrystalline calcite, less than about 5 μm in diameter) which occasionally has a clotted appearance.

Several theories of cave pearl formation have been proposed. The unifying factor in these theories is the formation of cave pearls in a splash cup, which is a bowl-shaped depression into which water drips and accumulates (Davidson and McKinstry, 1931; Black, 1951). The underlying conflict in the different formational theories concerns the necessity of agitation of the cave pearls within the splash cups. The cave pearls from the Arbuckle Mountains field area were probably formed in an agitated splash cup in which they were turned

Inorganic Deposits

Some of the travertine deposits in the field area show no evidence of having precipitated around an organic framework and contain no visible organic material (herein referred to as inorganic travertine). The bulk of such deposits consists of the spelean-like material precipitated within cavernous areas. This travertine tends to be more dense than the travertine precipitated in association with organisms.

In most cases, the inorganic deposits show some type of layering. Nearly vertical layers predominate and range in thickness from 2 to 6 cm. These deposits are typically laminated; laminae generally parallel the substrate and exhibit a wide range of color, thickness, and morphology. Individual laminae range in thickness from approximately 0.1 to 8 mm and are not of uniform thickness.

Spelean-like Deposits: Waterfall deposits contain a number of constructional cavities housing travertine forms similar to spelean deposits. Due to this similarity, it is practical to describe these features using speleological terminology; therefore, the travertine forms associated with cavities are herein termed stalactites, flowstone, cave popcorn, cave pearls, and rimstone dams.

Stalactites are common in the waterfall travertine cavities and frequently occur in groups clinging to ceilings. Shapes are slender to stocky cones with elliptical to circular cross sections. Sizes range from about 3 to 50 cm in length and from about 3 to 15 cm in diameter.

Flowstone deposits usually occur on cave walls and consist of smooth or folded sheet-like layers (Warwick, 1953; Wells, 1971; White, 1976). One type of flowstone, often referred to as draperies or curtains, is analogous to travertine forms in the field area. Along Honey Creek, a nearly vertical wall of travertine associated with a cavernous structure displays sinuous layers of vertically oriented folds. Individual folds average 30 cm in height and 15 cm in width; layers average 1 cm in thickness.

Another spelean-like form associated with the cavities has been termed cave popcorn (Thraillkill, 1965; White, 1976), cave coral, and cave grapes (Thraillkill, 1976; White, 1976; Bögli, 1980). In the Arbuckle Mountains area, this botryoidal form consists of hemispherical mounds, ranging in diameter from 3 mm to 3 cm, which protrude in clusters from cavity walls. Commonly, the cave popcorn occurs along a single horizon or shelf. The largest such horizon, measured along Honey Creek, extends approximately 6 m laterally and is 30 cm thick (Figure 10). Cave popcorn is also found in small cavities (approximately 2 to 10 cm in diameter) in the travertine.

Cave pearls (Bögli, 1980) constitute another spelean-like deposit associated with cavities in the Arbuckle Mountains travertine deposits. They have been described as unattached, usually highly polished, spherical to ellipsoidal to

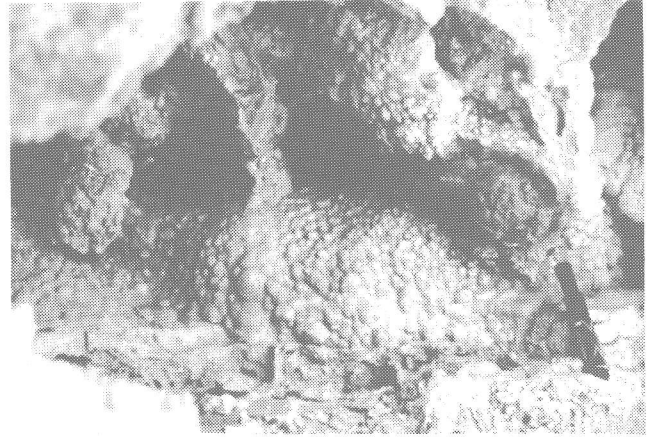


Figure 10. Layer of cave popcorn alongside Honey Creek; marking pen at right provides a scale.

polyhedral concretionary forms found in shallow pools in caves and mines (Davidson and McKinstry, 1931; Thraillkill, 1976). In the Arbuckle Mountains, cave pearls are present in a few very localized areas. They usually occur as non-touching particles that have highly polished, whitish surfaces and range in shape from spherules to four- or five-sided polyhedrons. Cave pearls range in size from 2 mm to 3 cm in diameter. The average diameter of the spherules is 1 cm, whereas the polyhedrons average 8 mm in width, 13 mm in length, and 7 mm in height (although some of the polyhedral forms are flattened).

In thin section, cave pearls display a radial-fibrous structure which creates a pseudo-uniaxial cross under crossed nicols. The radial-fibrous crystal boundaries range from planar to feathery. Where the crystal boundaries are feathery, the radial texture is less distinctive. The crystals range in length from 0.25 to 14 mm and in width from 0.02 to 2 mm.

In addition to the radial structure, cave pearls have well-developed concentric laminae defined in plane light by color changes from tan to brown to dark brown. Laminae range in thickness from 0.05 to 0.2 mm, and individual laminae maintain a fairly constant thickness. Some of the laminae, however, are discordant (Figure 11), and parts of some cave pearls have undergone partial neomorphism to coarse spar (Figure 12; Bathurst, 1975, Fig. 335, p. 482). Nuclei of the cave pearls, which may be single or multiple, range in diameter from 0.5 to 3 mm, and are composed of micrite (microcrystalline calcite, less than about 5 μm in diameter) which occasionally has a clotted appearance.

Several theories of cave pearl formation have been proposed. The unifying factor in these theories is the formation of cave pearls in a splash cup, which is a bowl-shaped depression into which water drips and accumulates (Davidson and McKinstry, 1931; Black, 1951). The underlying conflict in the different formational theories concerns the necessity of agitation of the cave pearls within the splash cups. The cave pearls from the Arbuckle Mountains field area were probably formed in an agitated splash cup in which they were turned

during growth. Evidence for this mode of formation includes 1) their localization in small, bowl-shaped areas, 2) their highly polished appearance, 3) evidence of abrasion or at least movement (discordant laminae observed during SEM analysis), and 4) uniform lamina thickness.

Associated with the cave pearls in the field area are tiny rimstone dams. The dams are analogous to "microgours" found in caves on flowstones and stalactites bordering trickling waters or pools (Hill, 1976; Bögli, 1980). The dams, on the order of 1 to 2 mm in height and width, form an anastomosing network.

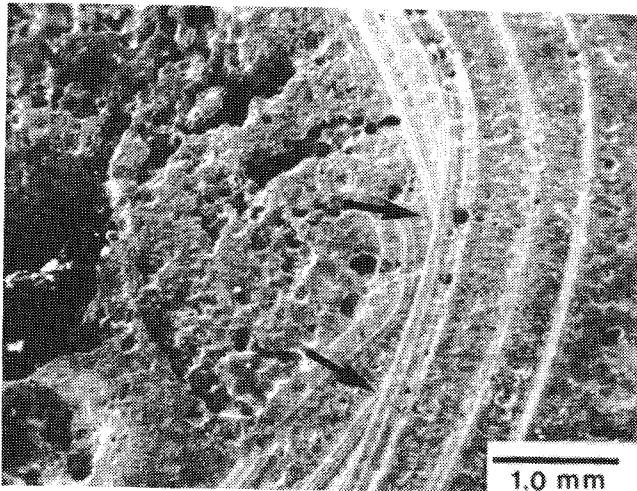


Figure 11. Scanning electron micrograph of a cave pearl cortex reveals discordant laminae (arrows).

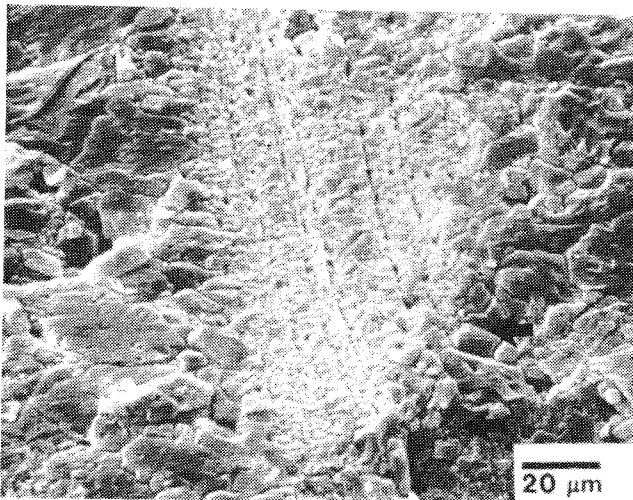


Figure 12. Scanning electron micrograph of neomorphic spar (arrows) terminating cortex laminae, obliterating original structure.

Vadose Pisoids: In addition to cave pearls and cyanoids, coated grains occur which most closely resemble caliche or vadose pisoids (referred to collectively as "vadoids" by Peryt, 1983). Similar grains have been reported from other traver-

tine deposits (Chafetz and Meredith, 1983; Folk and Chafetz, 1983). In the Arbuckle Mountains, these coated grains usually occur in distinct, nearly horizontal layers up to approximately 8 mm in thickness, sometimes separated by erosional surfaces. Each deposit contains a maximum of five such layers and is very localized (usually less than 10 cm across). Two samples were collected in which the upper surfaces were currently exposed. In one of these samples, the uppermost layer of coated grains is inversely graded. Inverse grading is usually less distinct or non-existent in the lower layers; one sample contains a layer which appears to be normally graded. Some layers which are not graded show lateral variations in grain size.

Shapes of the vadose pisoids range from spherical to ellipsoidal to polyhedral and are largely determined by the shapes of the nuclei. Pisoid diameters range from less than 0.1 mm to approximately 3 mm. Cortical thicknesses range from 0.03 to 1.5 mm and may be either of equal thickness all around a nucleus or slightly thicker on the top, bottom, or one or more sides of a grain. Within some cortices, a well-developed concentric structure is evident, commonly composed of two to five laminae. These laminae are composed of micrite or spar or both (Figure 13).

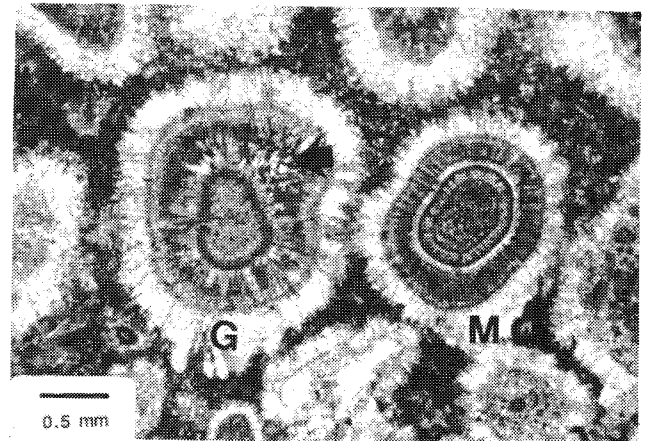


Figure 13. Photomicrograph (crossed nicols) showing cortices of vadose pisoids composed of alternating micrite and spar laminations. Pisoid at left center shows triangular cross sections (arrow) of elongate crystals, and gravitational cement (G) at base. Pisoid at right center shows development of meniscus cement (M).

Many of the coated grains display a well-developed radial structure. This radial structure may either be original or due to radiating neomorphic spar. Neomorphism is evident in many of the grains in which fibrous to bladed crystals terminate and destroy concentric laminae. Some grains appear to have undergone intense neomorphism which has obliterated any original structure. Where radial structure appears to be original, no disruption can be seen where radial crystals pass through concentric laminae. Some cortices have alternating concentric layers of radiating and non-radiating

during growth. Evidence for this mode of formation includes 1) their localization in small, bowl-shaped areas, 2) their highly polished appearance, 3) evidence of abrasion or at least movement (discordant laminae observed during SEM analysis), and 4) uniform lamina thickness.

Associated with the cave pearls in the field area are tiny rimstone dams. The dams are analogous to "microgours" found in caves on flowstones and stalactites bordering trickling waters or pools (Hill, 1976; Bögli, 1980). The dams, on the order of 1 to 2 mm in height and width, form an anastomosing network.

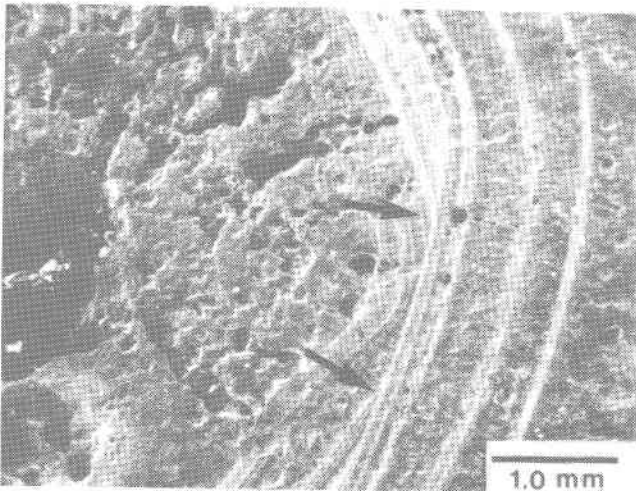


Figure 11. Scanning electron micrograph of a cave pearl cortex reveals discordant laminae (arrows).

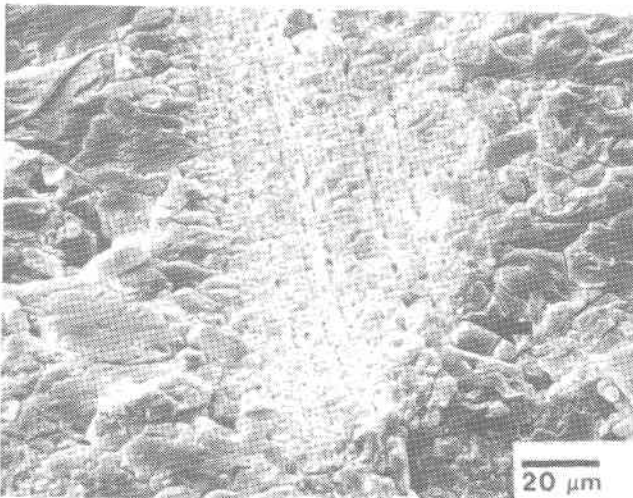


Figure 12. Scanning electron micrograph of neomorphic spar (arrows) terminating cortex laminae, obliterating original structure.

Vadose Pisoids: In addition to cave pearls and cyanoids, coated grains occur which most closely resemble caliche or vadose pisoids (referred to collectively as "vadoids" by Peryt, 1983). Similar grains have been reported from other traver-

tine deposits (Chafetz and Meredith, 1983; Folk and Chafetz, 1983). In the Arbuckle Mountains, these coated grains usually occur in distinct, nearly horizontal layers up to approximately 8 mm in thickness, sometimes separated by erosional surfaces. Each deposit contains a maximum of five such layers and is very localized (usually less than 10 cm across). Two samples were collected in which the upper surfaces were currently exposed. In one of these samples, the uppermost layer of coated grains is inversely graded. Inverse grading is usually less distinct or non-existent in the lower layers; one sample contains a layer which appears to be normally graded. Some layers which are not graded show lateral variations in grain size.

Shapes of the vadose pisoids range from spherical to ellipsoidal to polyhedral and are largely determined by the shapes of the nuclei. Pisoid diameters range from less than 0.1 mm to approximately 3 mm. Cortical thicknesses range from 0.03 to 1.5 mm and may be either of equal thickness all around a nucleus or slightly thicker on the top, bottom, or one or more sides of a grain. Within some cortices, a well-developed concentric structure is evident, commonly composed of two to five laminae. These laminae are composed of micrite or spar or both (Figure 13).

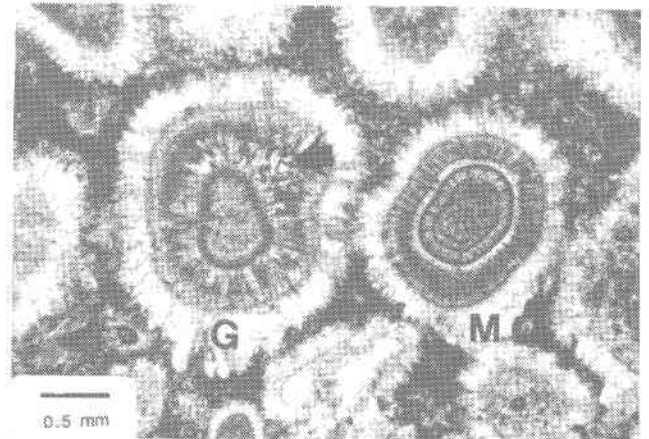


Figure 13. Photomicrograph (crossed nicols) showing cortices of vadose pisoids composed of alternating micrite and spar laminations. Pisoid at left center shows triangular cross sections (arrow) of elongate crystals, and gravitational cement (G) at base. Pisoid at right center shows development of meniscus cement (M).

Many of the coated grains display a well-developed radial structure. This radial structure may either be original or due to radiating neomorphic spar. Neomorphism is evident in many of the grains in which fibrous to bladed crystals terminate and destroy concentric laminae. Some grains appear to have undergone intense neomorphism which has obliterated any original structure. Where radial structure appears to be original, no disruption can be seen where radial crystals pass through concentric laminae. Some cortices have alternating concentric layers of radiating and non-radiating

crystals; the radiating crystals do not extend into the overlying laminae.

The nuclei of vadose pisoids commonly consist of some type of carbonate material, although quartz, chert, and volcanic rock-fragment nuclei occur, probably from Cambrian rhyolites in the area. Some of the nuclei, usually silicic, are wholly or partially dissolved or replaced by carbonate. Carbonate nuclei consist of micrite (often clotted), spar (often rhombic), micritic clasts with quartz sand and silt, and calcified algal filaments. The coated grains may have more than one nucleus, resulting in an oblong grain.

Coated grains may have formed by one of two *in situ* processes: 1) the grains formed in a small area, but were subjected to periodic rolling (analogous to cave pearls), or 2) the grains formed without rolling (analogous to some caliche pisoids). The first of these two processes, *in situ* growth accompanied by some rolling, could occur as a result of alternating wet and dry conditions. For example, clastic grains wash into small pools where they become coated while undergoing slight agitation, and inverse grading develops as smaller grains sift downward between larger grains. Following development of such a layer, a dry interval may occur, during which an erosional surface develops. During the next wet interval, another coated grain layer develops. This scenario explains how the algal coatings which grew predominantly on upper surfaces are found in diverse orientation and on multiple surfaces. Most grain movement appears to have ceased by the time the final coating formed, because some of the coatings have a polygonal fit. The non-parallel orientation of some of the subsequent gravitational cement may suggest slight later movement. The second *in situ* hypothesis, involving formation without rolling, cannot explain the thicker occurrence of algal coating on some lower grain surfaces.

GENERAL CALCITE CRYSTAL PETROGRAPHY

Both the inorganic and the organically associated travertine deposits contain a wide range of morphologies and sizes of low-magnesian (approximately 2 mole percent $MgCO_3$) calcite crystals. Equidimensional micritic crystals occur frequently as euhedral, subhedral, and anhedral crystals. The euhedral micritic crystals are flattened or unit rhombohedrons. Prismatic spar (up to 0.2 mm in diameter) occurs as anhedral, subhedral, and euhedral (rhombohedral and hexagonal) crystals (Figure 14), with many of the anhedral crystals forming mosaics of sparry calcite.

Bladed to fibrous calcite comprises one of the most common crystal morphologies. These crystals nearly always occur with their long axes oriented perpendicular to the surfaces from which they precipitated, whether the surfaces are organic (Figure 15) or inorganic (Figure 16). The crystals, which extend up to 1 cm in length, often increase in width

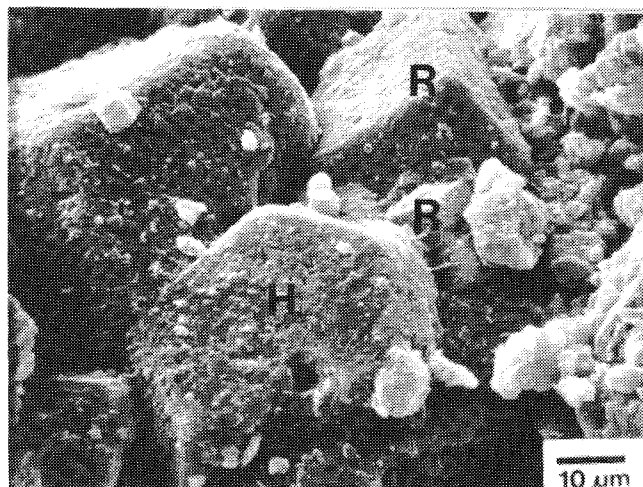


Figure 14. Scanning electron micrograph of spar shows rhombohedral (R) and hexagonal (H) crystals. (Hexagonal crystal is approximately 40 μm across.)

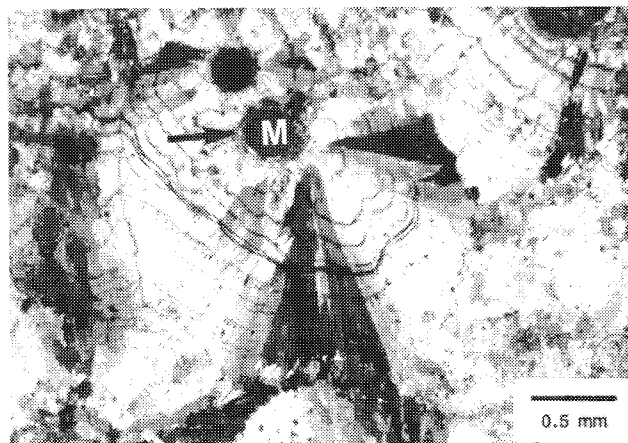


Figure 15. Photomicrograph (crossed nicols) of fibrous spar crystals that radiate away from circular voids; moss stem molds (M) rimmed with organic material (arrow).



Figure 16. Photomicrograph (crossed nicols) of fibrous, feathery fans of inorganically formed calcite crystals oriented perpendicularly to an inorganic substrate.

crystals; the radiating crystals do not extend into the overlying laminae.

The nuclei of vadose pisoids commonly consist of some type of carbonate material, although quartz, chert, and volcanic rock-fragment nuclei occur, probably from Cambrian rhyolites in the area. Some of the nuclei, usually silicic, are wholly or partially dissolved or replaced by carbonate. Carbonate nuclei consist of micrite (often clotted), spar (often rhombic), micritic clasts with quartz sand and silt, and calcified algal filaments. The coated grains may have more than one nucleus, resulting in an oblong grain.

Coated grains may have formed by one of two *in situ* processes: 1) the grains formed in a small area, but were subjected to periodic rolling (analogous to cave pearls), or 2) the grains formed without rolling (analogous to some caliche pisoids). The first of these two processes, *in situ* growth accompanied by some rolling, could occur as a result of alternating wet and dry conditions. For example, clastic grains wash into small pools where they become coated while undergoing slight agitation, and inverse grading develops as smaller grains sift downward between larger grains. Following development of such a layer, a dry interval may occur, during which an erosional surface develops. During the next wet interval, another coated grain layer develops. This scenario explains how the algal coatings which grew predominantly on upper surfaces are found in diverse orientation and on multiple surfaces. Most grain movement appears to have ceased by the time the final coating formed, because some of the coatings have a polygonal fit. The non-parallel orientation of some of the subsequent gravitational cement may suggest slight later movement. The second *in situ* hypothesis, involving formation without rolling, cannot explain the thicker occurrence of algal coating on some lower grain surfaces.

GENERAL CALCITE CRYSTAL PETROGRAPHY

Both the inorganic and the organically associated travertine deposits contain a wide range of morphologies and sizes of low-magnesian (approximately 2 mole percent $MgCO_3$) calcite crystals. Equidimensional micritic crystals occur frequently as euhedral, subhedral, and anhedral crystals. The euhedral micritic crystals are flattened or unit rhombohedrons. Prismatic spar (up to 0.2 mm in diameter) occurs as anhedral, subhedral, and euhedral (rhombohedral and hexagonal) crystals (Figure 14), with many of the anhedral crystals forming mosaics of sparry calcite.

Bladed to fibrous calcite comprises one of the most common crystal morphologies. These crystals nearly always occur with their long axes oriented perpendicular to the surfaces from which they precipitated, whether the surfaces are organic (Figure 15) or inorganic (Figure 16). The crystals, which extend up to 1 cm in length, often increase in width

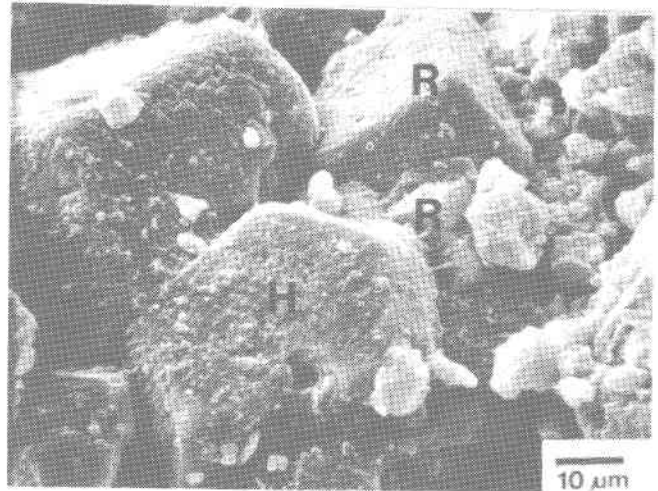


Figure 14. Scanning electron micrograph of spar shows rhombohedral (R) and hexagonal (H) crystals. (Hexagonal crystal is approximately 40 μm across.)



Figure 15. Photomicrograph (crossed nicols) of fibrous spar crystals that radiate away from circular voids; moss stem molds (M) rimmed with organic material (arrow).



Figure 16. Photomicrograph (crossed nicols) of fibrous, feathery fans of inorganically formed calcite crystals oriented perpendicularly to an inorganic substrate.

from base to top and have triangular cross sections (many showing curved surfaces, Figure 17), plane boundaries, and sharp crystal terminations (Figure 18). Prisms having triangular cross sections have been reported from several other non-marine carbonate deposits (Binkley and others, 1980; Chafetz and Butler, 1980; Schreiber and others, 1981). Columnar crystals are quite common, ranging in length from less than 1 mm to greater than 1 cm and in width from 0.2 to 3 mm. Crystal boundaries range from planar to jagged or feathery. Crystal terminations are frequently rounded or squared, although rhombohedral terminations occur.

Crystals associated with algal material are most commonly equidimensional and micritic. Columnar spar crystals, however, commonly precipitate around algal bushes. The crystals surrounding the leaves and stems of mosses vary greatly in size and form. Euhedral to anhedral micritic equidimensional crystals are common, as are bladed to fibrous, radially oriented spar crystals which are analogous to the "rosettes" of crystals described by Irion and Muller (1968). Elongate crystals usually radiate from stems, whereas leaves are surrounded by smaller, equidimensional crystals.

Most of the crystals in the inorganic deposits tend to be larger and more inclusion-free than the crystals precipitated in association with organic material. Columnar, fibrous, and bladed crystals occur most frequently and tend to be clustered into radiating bundles and fans (Figure 19). Individual elongate crystals range from approximately 0.1 mm to 1 cm in length and from 0.01 to 3 mm in width. Some of these crystals have sharp terminations, although the majority display feathery ends. Crystal edges often appear ragged and irregular.

Many of the crystal irregularities arise from the fact that the crystals are actually composed of smaller crystallites which fuse into one crystal or remain as separate entities. Kendall and Broughton (1978), Braithwaite (1979), and Chafetz and Butler (1980) attributed crystallites to precipitation from films of water. The thickness of these water films is proportional to the degree to which the crystallites coalesce into larger crystals, with thicker films producing more complete coalescence.

In laminated samples, crystals usually transgress the laminae, although differences in crystal development sometimes occur above and below a lamina (Figure 19). This difference in crystals across a lamina probably reflects some change in precipitational conditions.

Unusual crystal morphologies observed with the SEM in inorganic specimens are parallel "ribbon" crystals (Figure 20) and parallel "spikes" (Figure 21; Folk and others, 1985). Ribbon crystals usually occur in clusters, with individuals ranging from 30 to 150 μm in length and 3 to 12 μm in width. Each ribbon repeatedly narrows and widens and may even twist helically. Calcite spikes are often associated with the ribbon crystals and range in length from 4 to 30 μm , whereas widths range from 1 to 10 μm . Both the ribbon crystals and the calcite spikes may be attributable to partial dissolution or



Figure 17. Photomicrograph (crossed nicols) reveals triangular cross sections of elongate crystals; many of the crystal edges are curved.

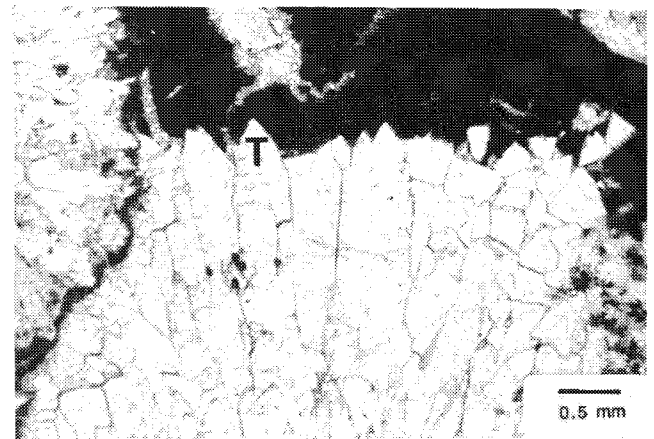


Figure 18. Photomicrograph (plane light) of bladed crystals with sharp crystal terminations (T) abutting micritic crystals (dark area at top right).



Figure 19. Photomicrograph (crossed nicols) showing radiating bundles of fibrous crystals and crystallites. Notice the difference in crystal development above versus below the thickest lamina (arrows).

from base to top and have triangular cross sections (many showing curved surfaces, Figure 17), plane boundaries, and sharp crystal terminations (Figure 18). Prisms having triangular cross sections have been reported from several other non-marine carbonate deposits (Binkley and others, 1980; Chafetz and Butler, 1980; Schreiber and others, 1981). Columnar crystals are quite common, ranging in length from less than 1 mm to greater than 1 cm and in width from 0.2 to 3 mm. Crystal boundaries range from planar to jagged or feathery. Crystal terminations are frequently rounded or squared, although rhombohedral terminations occur.

Crystals associated with algal material are most commonly equidimensional and micritic. Columnar spar crystals, however, commonly precipitate around algal bushes. The crystals surrounding the leaves and stems of mosses vary greatly in size and form. Euhedral to anhedral micritic equidimensional crystals are common, as are bladed to fibrous, radially oriented spar crystals which are analogous to the "rosettes" of crystals described by Irion and Muller (1968). Elongate crystals usually radiate from stems, whereas leaves are surrounded by smaller, equidimensional crystals.

Most of the crystals in the inorganic deposits tend to be larger and more inclusion-free than the crystals precipitated in association with organic material. Columnar, fibrous, and bladed crystals occur most frequently and tend to be clustered into radiating bundles and fans (Figure 19). Individual elongate crystals range from approximately 0.1 mm to 1 cm in length and from 0.01 to 3 mm in width. Some of these crystals have sharp terminations, although the majority display feathery ends. Crystal edges often appear ragged and irregular.

Many of the crystal irregularities arise from the fact that the crystals are actually composed of smaller crystallites which fuse into one crystal or remain as separate entities. Kendall and Broughton (1978), Braithwaite (1979), and Chafetz and Butler (1980) attributed crystallites to precipitation from films of water. The thickness of these water films is proportional to the degree to which the crystallites coalesce into larger crystals, with thicker films producing more complete coalescence.

In laminated samples, crystals usually transgress the laminae, although differences in crystal development sometimes occur above and below a lamina (Figure 19). This difference in crystals across a lamina probably reflects some change in precipitational conditions.

Unusual crystal morphologies observed with the SEM in inorganic specimens are parallel "ribbon" crystals (Figure 20) and parallel "spikes" (Figure 21; Folk and others, 1985). Ribbon crystals usually occur in clusters, with individuals ranging from 30 to 150 μm in length and 3 to 12 μm in width. Each ribbon repeatedly narrows and widens and may even twist helically. Calcite spikes are often associated with the ribbon crystals and range in length from 4 to 30 μm , whereas widths range from 1 to 10 μm . Both the ribbon crystals and the calcite spikes may be attributable to partial dissolution or



Figure 17. Photomicrograph (crossed nicols) reveals triangular cross sections of elongate crystals; many of the crystal edges are curved.

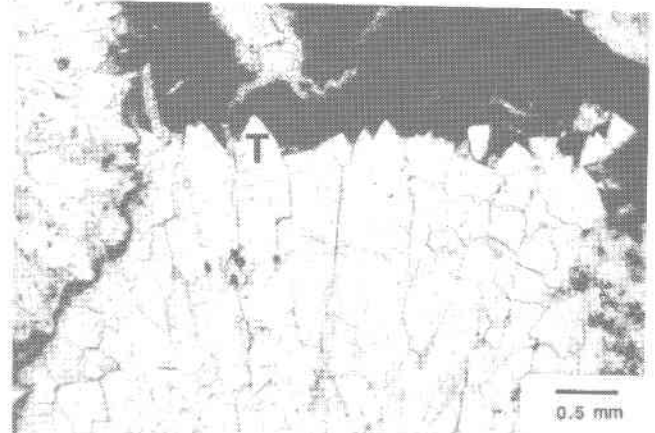


Figure 18. Photomicrograph (plane light) of bladed crystals with sharp crystal terminations (T) abutting micritic crystals (dark area at top right).



Figure 19. Photomicrograph (crossed nicols) showing radiating bundles of fibrous crystals and crystallites. Notice the difference in crystal development above versus below the thickest lamination (arrows).

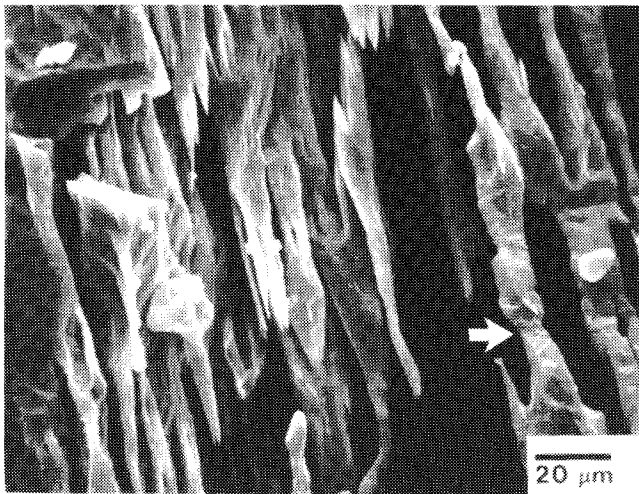


Figure 20. Scanning electron micrograph of ribbon crystals; some of the crystals appear to twist (arrow).

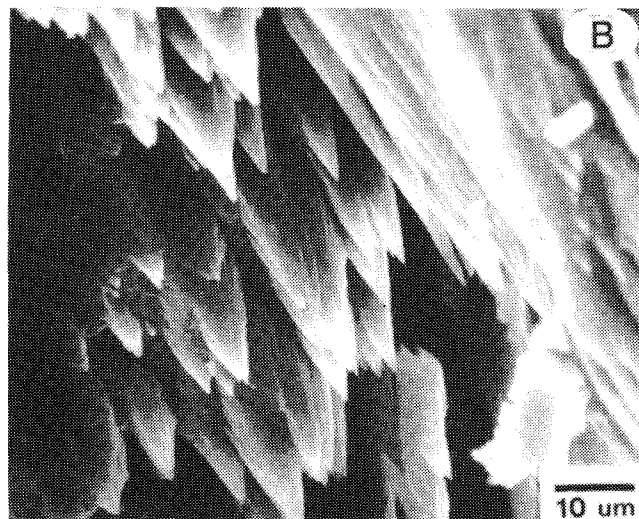
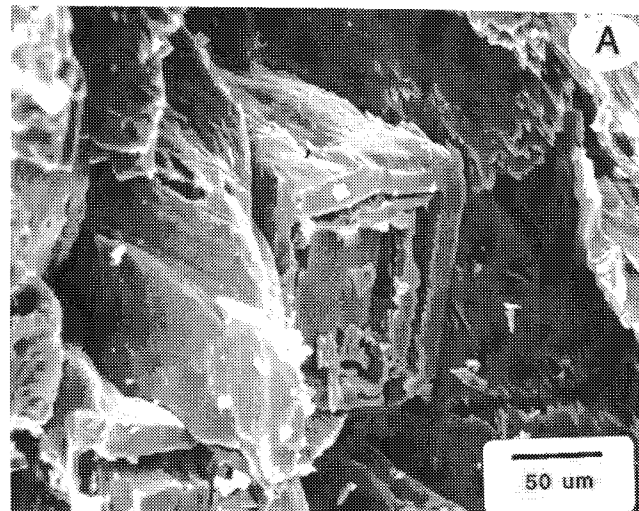


Figure 21. Scanning electron micrographs of calcite spikes. A. Overview of area of spiked forest. B. Close-up view of spikes.

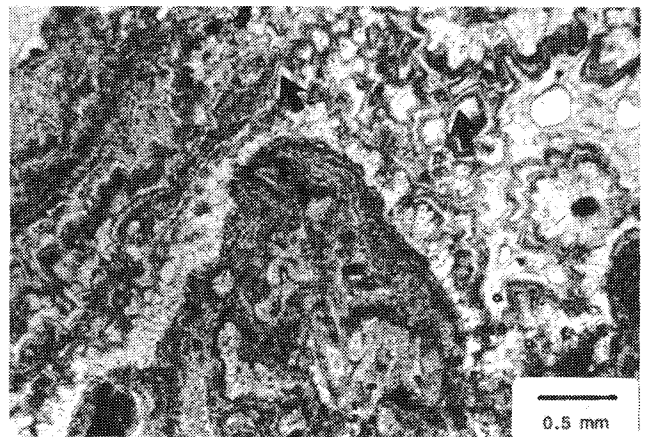


Figure 22. Photomicrograph (plane light) of inclusion-rich zones within crystals (arrows) which give the deposits a laminated appearance.

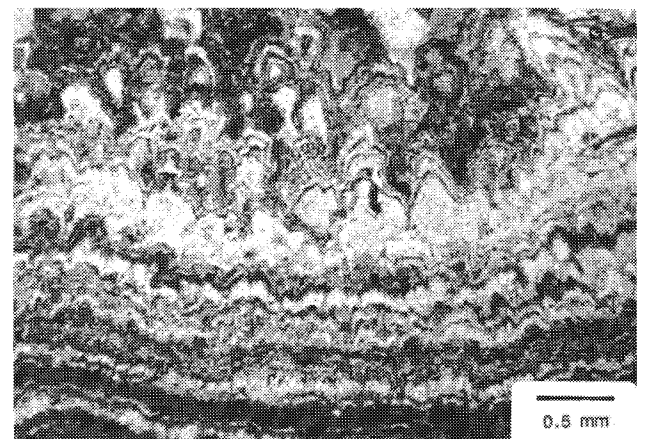


Figure 23. Photomicrograph (plane light) of inclusion-rich zones within bladed crystals.

variations in geochemical conditions during precipitation.

Many crystals in the waterfall travertine contain inclusion-rich zones (Figure 22). Bladed (Figure 23) and equant (Figure 24) crystals may display one or more of these zones. The zones have been interpreted as pauses in growth and have been reported in calcite crystals in many freshwater carbonate deposits (Folk and Assereto, 1976; Kendall and Broughton, 1978; Braithwaite, 1979; Meredith, 1980). Kendall and Broughton (1978, p. 524) reasoned that "Inclusions are trapped by the advancing growth surface and variations in either the supply, or the rates of absorption, of impurities give rise to variations in impurity concentration which thus come to define a growth-layering."

Several samples containing zoned crystals were observed with the SEM. The inclusion-rich zones appear to have been partially dissolved. In thin section, however, this is usually not observed. This discrepancy may be explained by the fact that the crystals observed with the SEM occurred near large (millimeter-sized) pore spaces, where meteoric water probably flowed, resulting in the preferential dissolution of the inclusion-rich layers.

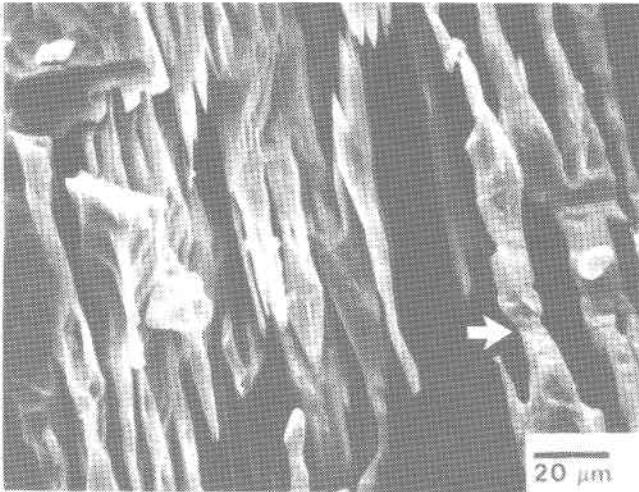


Figure 20. Scanning electron micrograph of ribbon crystals; some of the crystals appear to twist (arrow).

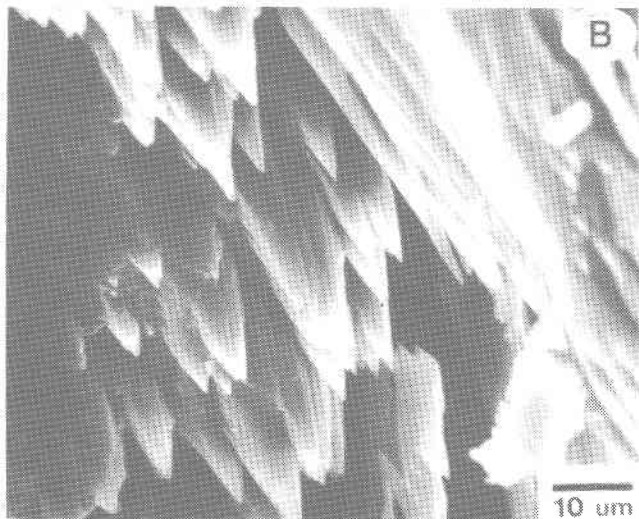
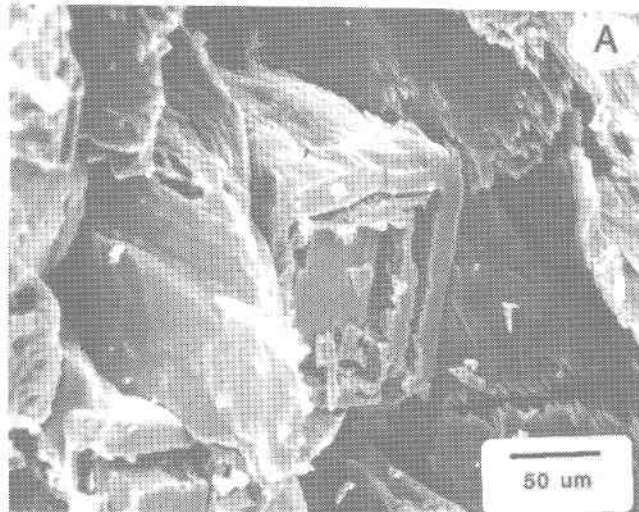


Figure 21. Scanning electron micrographs of calcite spikes. A. Overview of area of spiked forest. B. Close-up view of spikes.

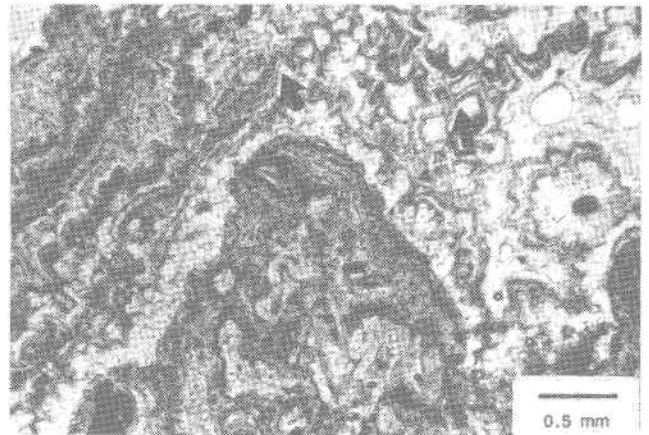


Figure 22. Photomicrograph (plane light) of inclusion-rich zones within crystals (arrows) which give the deposits a laminated appearance.

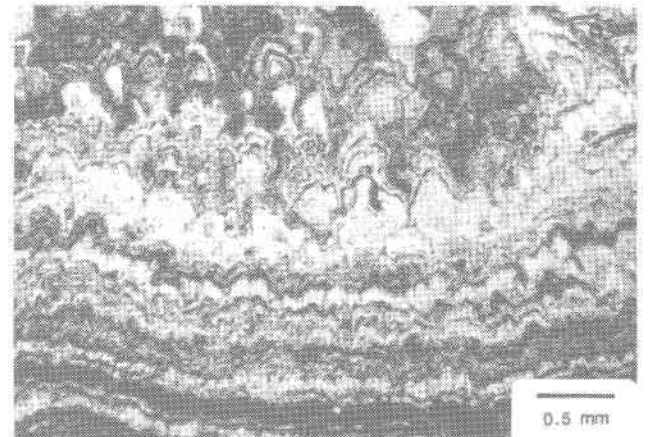


Figure 23. Photomicrograph (plane light) of inclusion-rich zones within bladed crystals.

variations in geochemical conditions during precipitation.

Many crystals in the waterfall travertine contain inclusion-rich zones (Figure 22). Bladed (Figure 23) and equant (Figure 24) crystals may display one or more of these zones. The zones have been interpreted as pauses in growth and have been reported in calcite crystals in many freshwater carbonate deposits (Folk and Assereto, 1976; Kendall and Broughton, 1978; Braithwaite, 1979; Meredith, 1980). Kendall and Broughton (1978, p. 524) reasoned that "Inclusions are trapped by the advancing growth surface and variations in either the supply, or the rates of absorption, of impurities give rise to variations in impurity concentration which thus come to define a growth-layering."

Several samples containing zoned crystals were observed with the SEM. The inclusion-rich zones appear to have been partially dissolved. In thin section, however, this is usually not observed. This discrepancy may be explained by the fact that the crystals observed with the SEM occurred near large (millimeter-sized) pore spaces, where meteoric water probably flowed, resulting in the preferential dissolution of the inclusion-rich layers.

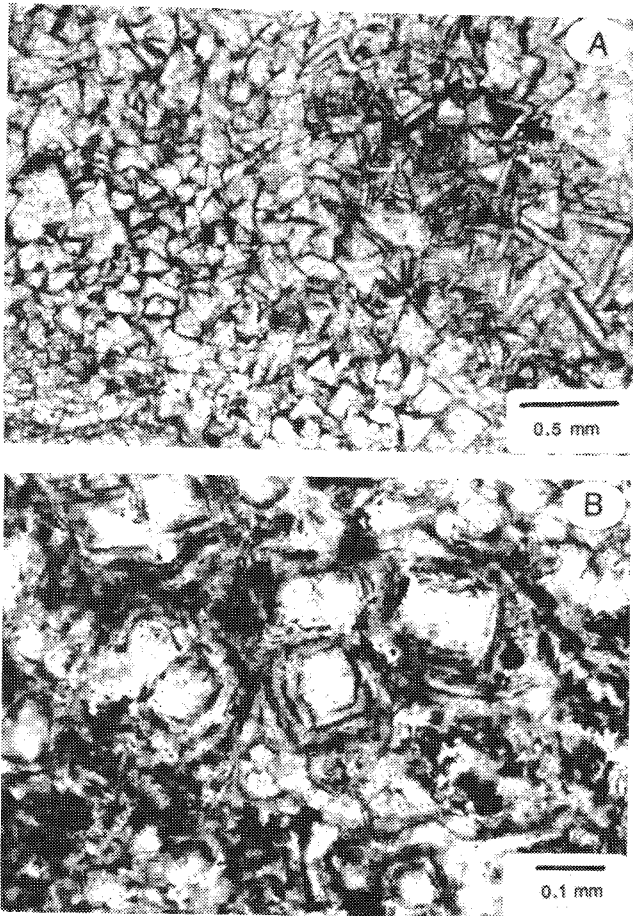


Figure 24. Photomicrographs (crossed nicols). A. Rhombohedral crystals; crystals in right half of photograph show one or more inclusion-rich layers (arrow) paralleling crystal outlines. B. Hexagonal crystals; crystals show several inclusion-rich zones paralleling crystal outlines.

Cement Morphologies

Many different types of cements occur in the travertine deposits including gravitational, meniscus, isopachous, random mosaic, and poikilotopic cements. Gravitational cement occurs in several samples (Figure 25), but it is most abundant in samples containing vadose pisoids. The bladed or fibrous crystals comprising this cement type range in length from 0.2 to 4 mm and in width from 0.05 to 1 mm. Meniscus cements (Figure 26) also occur in association with the vadose pisoids. The meniscus cement crystals range from euhedral (rhombohedral) to anhedral and range in size from several micrometers to approximately 0.5 mm.

Isopachous cements are common. Isopachous rims surround both organic and inorganic constituents and are composed of either equant (anhedral and/or rhombohedral) or bladed crystals. Many coated grains have an outer isopachous rim of radial calcite crystals which is thickest on grains nearer the deposit's surface and becomes progressively thinner with increasing depth.

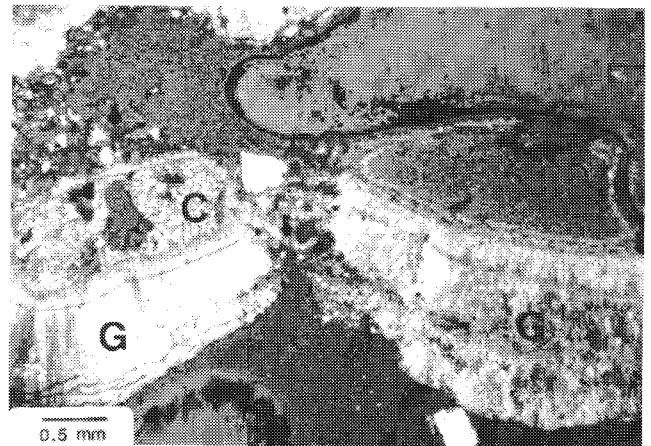


Figure 25. Photomicrograph (crossed nicols) showing gravitational cement (G) suspended from chert grains (C).

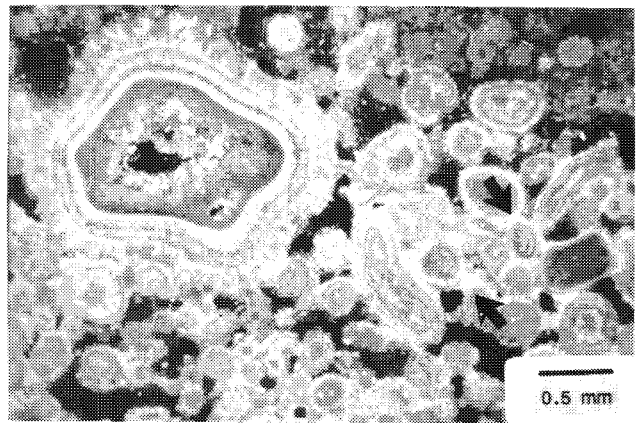


Figure 26. Photomicrograph (crossed nicols) of meniscus cement (arrows) around coated grains.

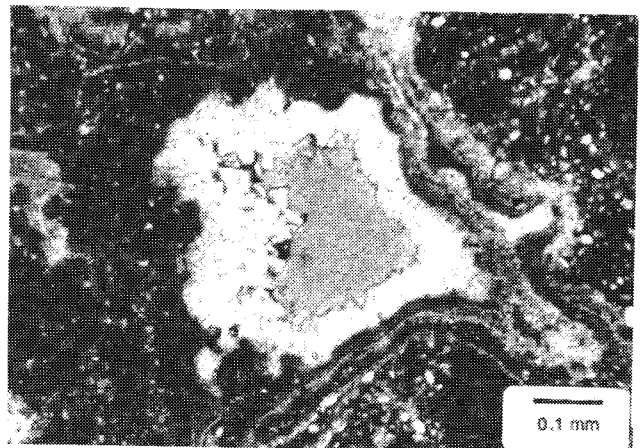


Figure 27. Photomicrograph (plane light) of clear, rhombohedral crystals filling a pore; crystals increase in size toward the center of the pore.

Many pisoids display well-developed gravitational cement superimposed on isopachous rims. The gravitational cement, up to 1 mm in thickness, occurs along the tops of pore

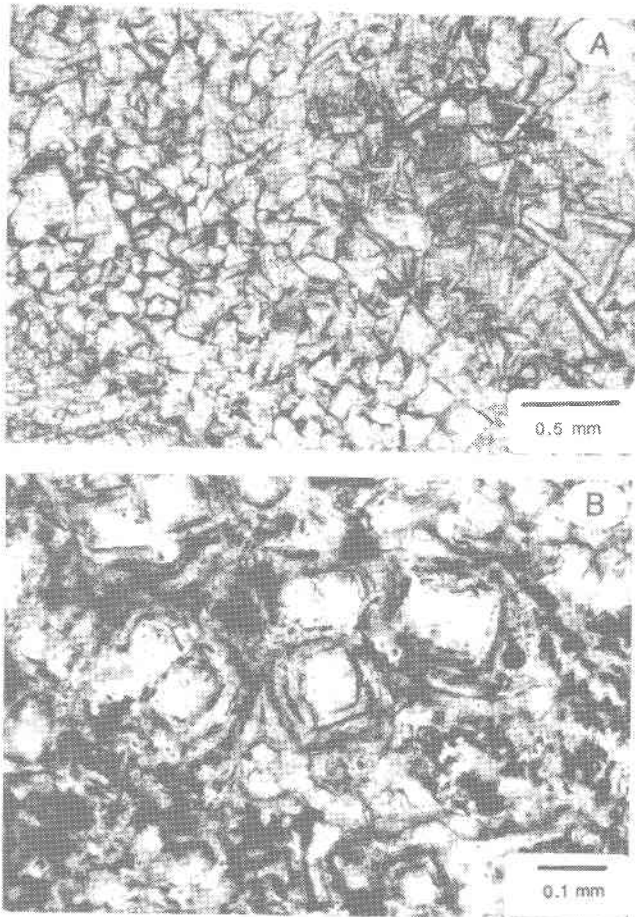


Figure 24. Photomicrographs (crossed nicols). A. Rhombohedral crystals; crystals in right half of photograph show one or more inclusion-rich layers (arrow) paralleling crystal outlines. B. Hexagonal crystals; crystals show several inclusion-rich zones paralleling crystal outlines.

Cement Morphologies

Many different types of cements occur in the travertine deposits including gravitational, meniscus, isopachous, random mosaic, and poikilotopic cements. Gravitational cement occurs in several samples (Figure 25), but it is most abundant in samples containing vadose pisoids. The bladed or fibrous crystals comprising this cement type range in length from 0.2 to 4 mm and in width from 0.05 to 1 mm. Meniscus cements (Figure 26) also occur in association with the vadose pisoids. The meniscus cement crystals range from euhedral (rhombohedral) to anhedral and range in size from several micrometers to approximately 0.5 mm.

Isopachous cements are common. Isopachous rims surround both organic and inorganic constituents and are composed of either equant (anhedral and/or rhombohedral) or bladed crystals. Many coated grains have an outer isopachous rim of radial calcite crystals which is thickest on grains nearer the deposit's surface and becomes progressively thinner with increasing depth.

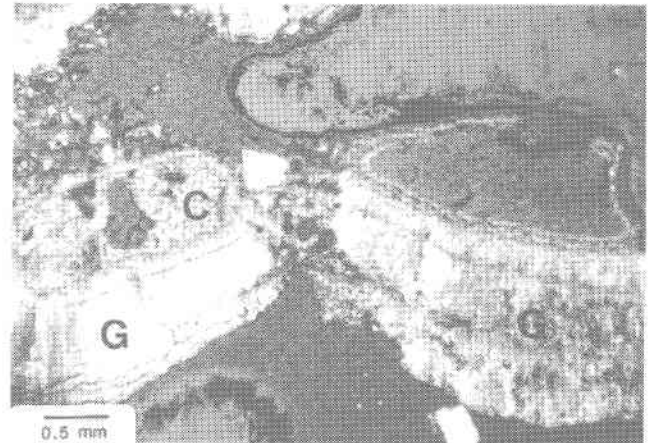


Figure 25. Photomicrograph (crossed nicols) showing gravitational cement (G) suspended from chert grains (C).

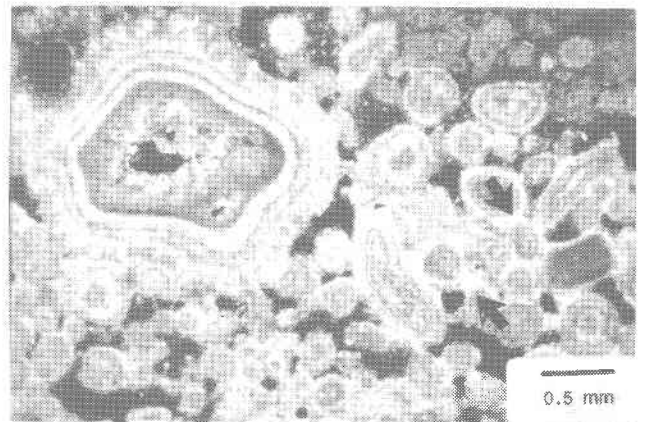


Figure 26. Photomicrograph (crossed nicols) of meniscus cement (arrows) around coated grains.

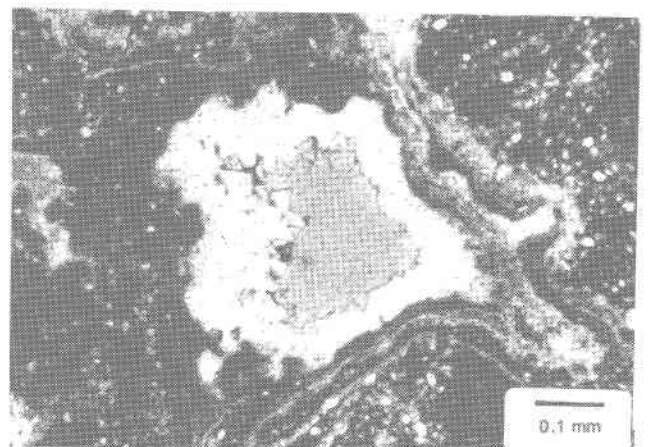


Figure 27. Photomicrograph (plane light) of clear, rhombohedral crystals filling a pore; crystals increase in size toward the center of the pore.

Many pisoids display well-developed gravitational cement superimposed on isopachous rims. The gravitational cement, up to 1 mm in thickness, occurs along the tops of pore

spaces, occasionally extending to the bottoms. An unusual aspect of the gravitational cement is that the hanging groups of crystals do not parallel each other. Although the clusters are all oriented approximately downwards, variations in orientation of up to 45° occur between groups of crystals. Both meniscus cement (Figure 13) and blocky spar cement are also found between some of the coated grains.

Euhedral crystals often occur as pore-filling cements, increasing in size toward pore centers (Figure 27). Equant, random-mosaic cements usually occur as secondary cements. Poikilotopic cements, individual crystals encasing several grains, are relatively uncommon but do occur in several samples and range in size from 0.5 to 3 mm in length.

This diversity of cement types indicates a range of depositional microenvironments. Meniscus and gravitational cements are indicative of precipitation in vadose conditions (Dunham, 1969; Muller, 1971), whereas isopachous cements indicate phreatic conditions (Land, 1971). The fact that both vadose and phreatic cements occur in close association illustrates both the rapid flux of conditions during a relatively short period of time and the diversity of conditions throughout the area at any given time.

Although the order of cement formation varies within individual samples, isopachous cements most commonly precipitated first, followed by random mosaic, poikilotopic, and vadose cements. This progression reflects initial formation of cement under phreatic conditions (travertine fully saturated by stream or groundwaters); variation in water levels or the diversion of water flow results in the subaerial exposure of these deposits and the development of vadose cements (this sequence can be repeated numerous times).

CONCLUSIONS

The waterfall travertine deposits of the Arbuckle Mountains are remarkably diverse. This diversity extends from macroscopic constituents, such as spelean-like deposits and algal crusts, to a plethora of organic and inorganic microscopic constituents, reflecting the diversity of microenvironments present within the travertine-depositing environment.

Abundant organic material occurs in the waterfall travertine, especially algae and mosses. Algally laminated crusts and algally coated grains are composed of alternating layers of spar-encased *Phormidium* bushes and encrusted *Schizothrix* filaments. Some of the crusts undergo aggradational neomorphism in which the spar surrounding *Phormidium* bushes grows upward at the expense of overlying layers. Diagenesis of this type results in dense crusts composed almost exclusively of coarse, columnar crystals. These diagenetic crusts retain virtually no evidence of their organic origin.

Inorganic deposits dominate in constructional cavities within the travertine accumulations and include spelean forms such as stalactites, flowstone, and cave pearls. Inor-

ganically coated grains (vadose pisoids) also occur.

The low-magnesian calcite crystals comprising the deposits include equidimensional, bladed, and fibrous forms. Several peculiar morphologic types occur (ribbons, spikes, and nested crystals). The calcite crystals form a variety of cement types, including vadose (meniscus and gravitational) and phreatic (isopachous) cements.

ACKNOWLEDGMENTS

We gratefully acknowledge the financial support of the Geology Foundation, University of Houston, and student grants to KML from the American Association of Petroleum Geologists and Sigma Xi.

REFERENCES CITED

- Bathurst, R.G.C., 1975, Carbonate sediments and their diagenesis: Amsterdam, Netherlands, Elsevier Publishing Company, Developments in Sedimentology No. 12, 658 p.
- Binkley, K.L., Wilkinson, B.H., and Owen, R.M., 1980, Vadose beachrock cementation along a southeastern Michigan marl lake: *Journal of Sedimentary Petrology*, v. 50, p. 953-962.
- Black, D.M., 1951, Loose carbonate accretions from Carlsbad Caverns, New Mexico: *Science*, v. 114, p. 126-127.
- Bögli, Alfred, 1980, Karst hydrology and physical speleology: Berlin, West Germany, Springer-Verlag, 284 p.
- Braithwaite, C.J.R., 1979, Crystal textures of recent fluvial pisolites and laminated crystalline crusts in Dyfed, South Wales: *Journal of Sedimentary Petrology*, v. 49, p. 181-194.
- Branner, J.C., 1901, The origin of travertine falls and reefs: *Science*, new series, v. 14, p. 184-185.
- Branner, J.C., 1911, Aggraded limestone plains of the interior of Bahia and climatic changes suggested by them: *Geological Society of America Bulletin*, v. 22, p. 187-206.
- Chafetz, H.S., and Butler, J.C., 1980, Petrology of recent caliche pisolites, spherulites, and speleothem deposits from central Texas: *Sedimentology*, v. 27, p. 497-518.
- Chafetz, H.S., and Folk, R.L., 1984, Travertines: depositional morphology and the bacterially constructed constituents: *Journal of Sedimentary Petrology*, v. 54, p. 289-316.
- Chafetz, H.S., and Meredith, J.C., 1983, Recent travertine pisoliths (pisoids) from southeastern Idaho, U.S.A., in Peryt, T.M., ed., *Coated grains*: Berlin, West Germany, Springer-Verlag, p. 450-455.
- Davidson, S.C., and McKinsty, H.E., 1931, "Cave pearls," oolites, and isolated inclusions in veins: *Economic Geology*, v. 26, p. 289-294.

- Dunham, R.J., 1969, Vadose pisolites in the Capitan Reef (Permian), New Mexico and Texas, in Friedman, G.M., ed., Depositional environments in carbonate rocks: Tulsa, Oklahoma, Society of Economic Paleontologists and Mineralogists, Special Publication 14, p. 182-191.
- Emig, W.H., 1917, Travertine deposits of Oklahoma: Oklahoma Geological Survey Bulletin 29, p. 9-76.
- Emig, W.H., 1918, The travertine deposits of the Arbuckle Mountains, Oklahoma, with reference to the plant agencies concerned in their formation: Science, new series, v. 47, p. 468.
- Emig, W.H., 1921, Mosses as rock builders: Proceedings of the Oklahoma Academy of Science, v. 1, p. 38-40.
- Folk, R.L., and Assereto, R., 1976, Comparative fabrics of length-slow and length-fast calcite and calcitized aragonite in a Holocene speleothem, Carlsbad Caverns, New Mexico: Journal of Sedimentary Petrology, v. 46, p. 486-496.
- Folk, R.L., and Chafetz, H.S., 1983, Pisoliths (pisoids) in Quaternary travertines of Tivoli, Italy, in Peryt, T.M., ed., Coated grains: Berlin, West Germany, Springer-Verlag, p. 474-487.
- Folk, R.L., Chafetz, H.S., and Tiezzi, Pamela, 1985, Bizarre forms of depositional and diagenetic calcite in hot-spring travertines, central Italy, in Schneidermann, N., and Harris, P.M., eds., Carbonate cements: Tulsa, Oklahoma, Society of Economic Paleontologists and Mineralogists, Special Publication 36, p. 349-369.
- Goldsmith, J.R., Graf, D.L., and Heard, H.C., 1961, Lattice constants of the calcium-magnesium carbonates: American Mineralogist, v. 46, p. 453-457.
- Golubic, Stjepko, 1969, Cyclic and noncyclic mechanisms in the formation of travertine: International Association of Theoretical and Applied Limnology, Proceedings, v. 17, p. 956-961.
- Gregory, J.W., 1911, Constructive waterfalls: Scottish Geographical Magazine, v. 27, p. 537-546.
- Herlinger, D.L., 1981, Petrology of the Fall Creek travertine, Bonneville County, Idaho [M.S. thesis]: Houston, Texas, University of Houston, 172 p.
- Hill, C.A., 1976, Cave minerals: Huntsville, Alabama, National Speleological Society, 137 p.
- Hubbard, D.A., Jr., Giannini, W.F., and Lorah, M.M., 1985, Travertine-marl deposits of the Valley and Ridge province of Virginia - a preliminary report: Virginia Division of Mineral Resources, Virginia Minerals, v. 31, n. 1, p. 1-8.
- Irion, G., and Muller, G., 1968, Mineralogy, petrology, and chemical composition of some calcareous tufa from the Schwabische Alb, Germany, in Muller, G., and Friedman, G.M., eds., Recent developments in carbonate sedimentology in central Europe: Berlin, West Germany, Springer-Verlag, p. 157-171.
- Jacobson, R.L., and Uzdowski, Eberhard, 1975, Geochemical controls on a calcite precipitating spring: Contributions to Mineralogy and Petrology, v. 51, p. 65-74.
- Kendall, A.C., and Broughton, P.L., 1978, Origin of fabrics in speleothems composed of columnar calcite crystals: Journal of Sedimentary Petrology, v. 48, p. 519-538.
- Land, L.S., 1971, Phreatic versus meteoric diagenesis of limestones: Evidence from a fossil water table in Bermuda, in Bricker, O.P., ed., Carbonate cements: Baltimore, Maryland, The Johns Hopkins Press, p. 133-136.
- Le Conte, J., 1892, Elements of geology: New York, New York, Appleton and Company, 640 p.
- Love, K.M., and Chafetz, H.S., 1988, Diagenesis of laminated travertine crusts, Arbuckle Mountains, Oklahoma: Journal of Sedimentary Petrology, v. 58, p. 441-445.
- Meredith, J. C., 1980, Diagenesis of Holocene-Pleistocene (?) travertine deposits: Fritz Creek, Clark County and Fall Creek, Bonneville County, Idaho [M.S. thesis]: Houston, Texas, University of Houston, 263 p.
- Milliman, J.D., 1974, Marine carbonates: Berlin, West Germany, Springer-Verlag, 375 p.
- Muller, G., 1971, "Gravitational" cement: an indicator for the vadose zone of the subaerial diagenetic environment, in Bricker, O.P., ed., Carbonate cements: Baltimore, Maryland, The Johns Hopkins Press, p. 301-302.
- Ordonez, S., and Garcia del Cura, M.A., 1983, Recent and Tertiary fluvial carbonates in central Spain, in Collinson, J.D., and Lewin, J., eds., Modern and ancient fluvial systems: London, England, International Association of Sedimentologists Special Publication 6, p. 485-497.
- Peryt, T.M., 1983, Vadoids, in Peryt, T.M., ed., Coated grains: Berlin, West Germany, Springer-Verlag, p. 437-449.
- Richardson, D.H.S., 1981, The biology of mosses: New York, New York, John Wiley & Sons, Inc., 220 p.
- Schreiber, B.C., Smith, D., and Schreiber, E., 1981, Spring peas from New York State: Nucleation and growth of freshwater hollow ooliths and pisoliths: Journal of Sedimentary Petrology, v. 51, p. 1341-1346.
- Srdoc, D., Horvatincic, N., Obelic, B., Krajcar, I., and Sliepcevic, A., 1985, Procesl talozenja kalcita u krskim vodama s posebnim osvrtom na Plitvicka jezera, Krs Jugosl. (Calcite deposition processes in karstwaters with special emphasis on Plitvice Lakes, Yugoslavia): Zagreb, 11/4-6, p. 1-104, (English Summary, p. 98-104).
- Steidtmann, Edward, 1934, Travertine deposits near Lexington, Virginia: Science, v. 80, p. 162-163.
- Steidtmann, Edward, 1935, Travertine depositing waters near Lexington, Virginia: Science, v. 82, p. 333-334.
- Thraillkill, J.V., 1965, Origin of cave popcorn: National Speleological Society Bulletin, v. 27, p. 59.
- Thraillkill, J.V., 1976, Speleothems, in Walter, M.R., ed., Stromatolites: Amsterdam, Netherlands, Elsevier Publishing Company, p. 73-86.
- Warwick, G.T., 1953, Calcite bubbles - a new cave formation?: National Speleological Society Bulletin 12, p. 38-42.
- Wells, A.W., 1971, Cave calcite: Studies in speleology, v. 2, parts 3-4, p. 129-148.
- White, W.B., 1976, Cave minerals and speleothems, in Ford, T.D., and Cullingford, C.H.D., eds., The science of speleology: London, England, Academic Press, p. 267-327.

THE GEOLOGY OF THE FALLING SPRING TRAVERTINE DEPOSIT, ALLEGHANY COUNTY, VIRGINIA

Kristin O. Dennen¹, Richard J. Diecchio², and Mark A. Stephenson³

CONTENTS

	Page
Abstract.....	80
Introduction.....	80
Geologic and topographic setting.....	80
Stream characteristics.....	82
Methods.....	84
Travertine.....	84
Modern travertine.....	84
Discussion of modern travertine deposition.....	85
Ancient travertine.....	86
Discussion of ancient travertine deposition.....	87
Geomorphic development of Falling Spring Creek.....	89
Acknowledgments.....	90
References cited.....	91

ILLUSTRATIONS

Figure	
1. Falling Spring Creek waterfall.....	80
2. Geology of Warm Springs anticline.....	81
3. Falling Spring Creek drainage system.....	82
4. Profile along Falling Spring Creek.....	83
5. Twig coated with travertine.....	84
6. Travertine-coated boulders of Tuscarora sandstone.....	84
7. Travertine terraces.....	85
8. Algal curtains at top of waterfall.....	85
9. Nearly horizontally bedded travertine.....	86
10. Steeply dipping travertine.....	87
11. Layered travertine.....	87
12. Travertine breccias.....	87
13. Photomicrograph of coated lithic fragments.....	88
14. Tree molds.....	88
15. Porous travertine.....	88
16. Photomicrograph of travertine lamination.....	89
17. Procaryotic filamentous material.....	89
18. Profile A-B through Little Mountain.....	90

¹Department of Geology, University of North Carolina, Chapel Hill, NC 27514

²Department of Geology, George Mason University, Fairfax, VA 22030

³Coastal Oil and Gas Corporation, Jackson, MS 39201

ABSTRACT

Falling Spring is a mixture of mineral-enriched thermal water and shallow groundwater that forms Falling Spring Creek. A waterfall along Falling Spring Creek is the site of pronounced CO₂ degassing, an increase in pH, and a decrease in calcite solubility in the creek water. Active, observable travertine deposition in Falling Spring Creek occurs in the vicinity of the waterfall, especially at the bottom of the waterfall, and is much more rapid during times of low flow.

Modern travertine consists mainly of layered deposits and encrustations and forms dams, terraces, and cascades. Precipitation is controlled by the amount of dilution by shallow groundwater and surface runoff and chemical changes along the flow path that affect calcite solubility, particularly those associated with stream turbulence. Biological agents play an important role in the deposition of the travertine.

The escarpment over which the water cascades is itself an ancient travertine deposit. Part of this ancient deposit exists at elevations above the top of the waterfall and above the elevation of the present-day spring. The ancient deposit contains many of the same features observable in the modern travertine deposits of the stream bed itself. Ancient cascade deposits at these higher elevations probably formed in the vicinity of a knickpoint that was elevated relative to the present knickpoint. The change in the position and elevation of the knickpoint may be due to headward erosion of Falling Spring Valley or may be due to the existence of an ancient travertine dam.

INTRODUCTION

The waterfall at Falling Spring Falls (Figure 1; cover, top right photograph), Alleghany County, Virginia, is probably the highest waterfall in the Appalachian Valley and Ridge physiographic province. In fact, Thomas Jefferson (1825) described Falling Spring Falls as a 61-m-high cascade that in his day was higher than Niagara Falls. Today the waterfall is less than half that height.

Falling Spring Creek contains a mixture of surficial runoff and water that issues from a thermal spring. In the vicinity of the waterfall, active travertine deposition can be observed. The waterfall escarpment itself is an ancient travertine deposit.

The thermal spring and waterfall provide an excellent field laboratory for the study of travertine deposition. The two-fold purpose of our study was: 1) to investigate the controlling factors for travertine deposition in the stream, in particular, the relationship of the waterfall to the formation of travertine, and 2) to apply our findings on the Falling Spring Creek system to a geologic and geomorphic investigation of the ancient travertine deposit which forms the travertine es-

carpment beneath and behind the waterfall (Figure 1). This paper represents an expansion of a preliminary report (Dennen and Diecchio, 1984).



Figure 1. Falling Spring Creek waterfall. Photograph taken from overlook along U.S. Highway 220.

GEOLOGIC AND TOPOGRAPHIC SETTING

Falling Spring emanates from the Middle Ordovician Lowville limestone (lower Black River Group) (Reeves, 1932) near the southern end of Warm Springs anticline, one of a number of anticlines that expose Ordovician limestone in the western part of the Valley and Ridge. Falling Spring is the most southerly of four thermal spring areas (Warm Springs, Hot Springs, Healing Springs, and Falling Spring) within the anticline (Figure 2). The oldest stratum exposed in the anticline is the Lower Ordovician Beekmantown Formation, which is unconformably overlain by Middle Ordovician limestones (Butts, 1940).

Falling Spring Valley is a topographic feature coincident with the exposure of Ordovician limestones in the core of the southern end of the Warm Springs anticline (Figure 2). The valley is surrounded on all sides by a resistant ridge that is formed by the Lower Silurian Tuscarora Sandstone (Figure 3). Little Mountain comprises the western flank of the

ABSTRACT

Falling Spring is a mixture of mineral-enriched thermal water and shallow groundwater that forms Falling Spring Creek. A waterfall along Falling Spring Creek is the site of pronounced CO₂ degassing, an increase in pH, and a decrease in calcite solubility in the creek water. Active, observable travertine deposition in Falling Spring Creek occurs in the vicinity of the waterfall, especially at the bottom of the waterfall, and is much more rapid during times of low flow.

Modern travertine consists mainly of layered deposits and encrustations and forms dams, terraces, and cascades. Precipitation is controlled by the amount of dilution by shallow groundwater and surface runoff and chemical changes along the flow path that affect calcite solubility, particularly those associated with stream turbulence. Biological agents play an important role in the deposition of the travertine.

The escarpment over which the water cascades is itself an ancient travertine deposit. Part of this ancient deposit exists at elevations above the top of the waterfall and above the elevation of the present-day spring. The ancient deposit contains many of the same features observable in the modern travertine deposits of the stream bed itself. Ancient cascade deposits at these higher elevations probably formed in the vicinity of a knickpoint that was elevated relative to the present knickpoint. The change in the position and elevation of the knickpoint may be due to headward erosion of Falling Spring Valley or may be due to the existence of an ancient travertine dam.

INTRODUCTION

The waterfall at Falling Spring Falls (Figure 1; cover, top right photograph), Alleghany County, Virginia, is probably the highest waterfall in the Appalachian Valley and Ridge physiographic province. In fact, Thomas Jefferson (1825) described Falling Spring Falls as a 61-m-high cascade that in his day was higher than Niagara Falls. Today the waterfall is less than half that height.

Falling Spring Creek contains a mixture of surficial runoff and water that issues from a thermal spring. In the vicinity of the waterfall, active travertine deposition can be observed. The waterfall escarpment itself is an ancient travertine deposit.

The thermal spring and waterfall provide an excellent field laboratory for the study of travertine deposition. The two-fold purpose of our study was: 1) to investigate the controlling factors for travertine deposition in the stream, in particular, the relationship of the waterfall to the formation of travertine, and 2) to apply our findings on the Falling Spring Creek system to a geologic and geomorphic investigation of the ancient travertine deposit which forms the travertine es-

carpment beneath and behind the waterfall (Figure 1). This paper represents an expansion of a preliminary report (Den-
nen and Diecchio, 1984).

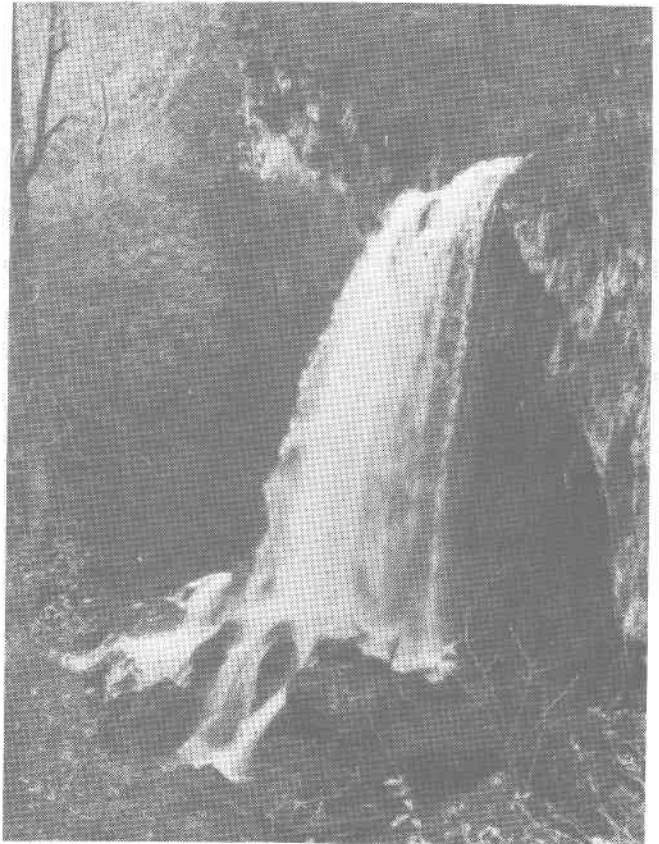


Figure 1. Falling Spring Creek waterfall. Photograph taken from overlook along U.S. Highway 220.

GEOLOGIC AND TOPOGRAPHIC SETTING

Falling Spring emanates from the Middle Ordovician Lowville limestone (lower Black River Group) (Reeves, 1932) near the southern end of Warm Springs anticline, one of a number of anticlines that expose Ordovician limestone in the western part of the Valley and Ridge. Falling Spring is the most southerly of four thermal spring areas (Warm Springs, Hot Springs, Healing Springs, and Falling Spring) within the anticline (Figure 2). The oldest stratum exposed in the anticline is the Lower Ordovician Beekmantown Formation, which is unconformably overlain by Middle Ordovician limestones (Butts, 1940).

Falling Spring Valley is a topographic feature coincident with the exposure of Ordovician limestones in the core of the southern end of the Warm Springs anticline (Figure 2). The valley is surrounded on all sides by a resistant ridge that is formed by the Lower Silurian Tuscarora Sandstone (Figure 3). Little Mountain comprises the western flank of the

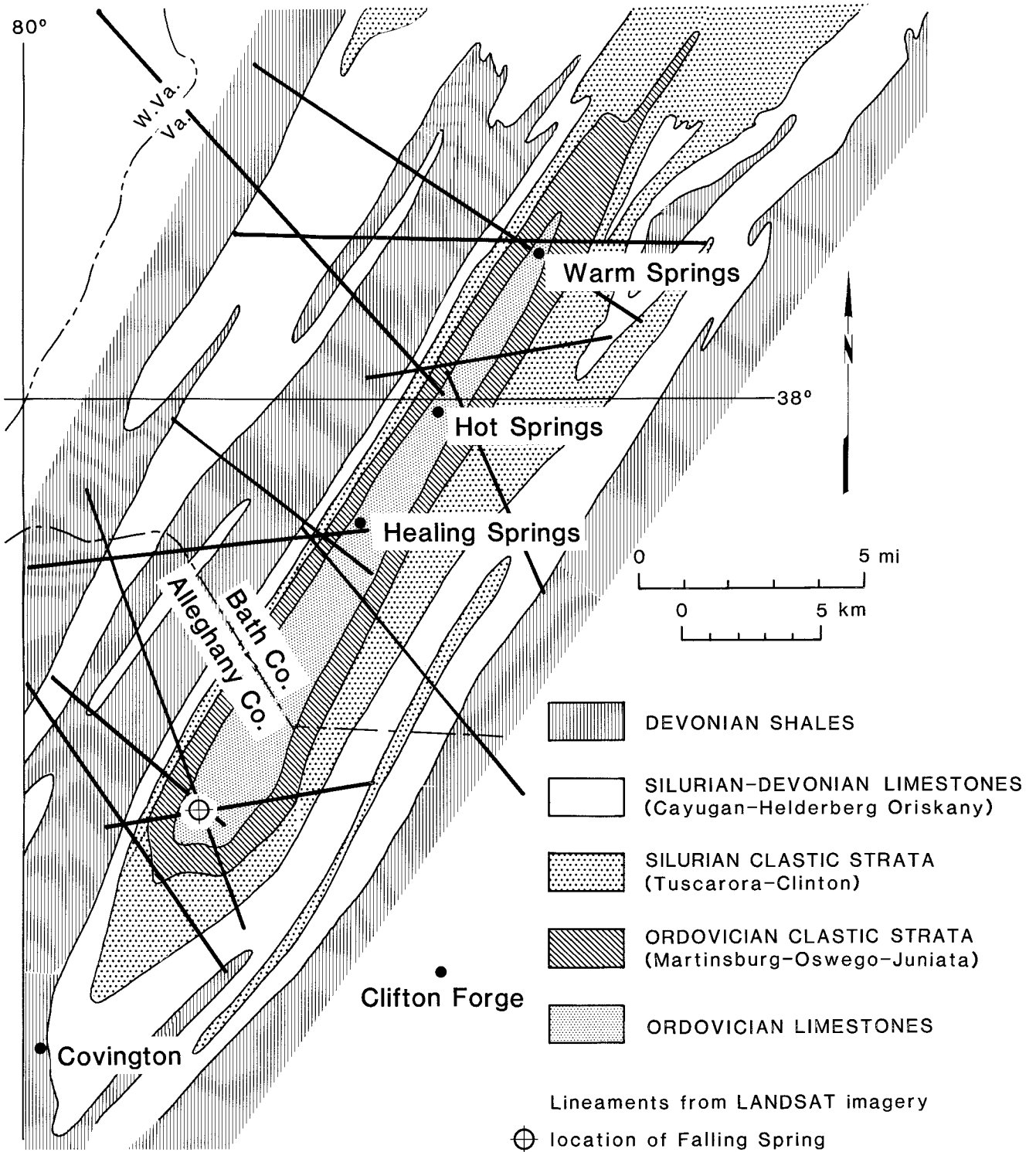


Figure 2. Geology of Warm Springs anticline.

anticline, and Warm Springs Mountain is the eastern flank. All of the surface drainage in the southern end of Falling Spring Valley flows through a water gap cut into the Tuscarora sandstone ridge. The travertine escarpment over which the waterfall of Falling Spring Creek flows occurs about 300 m downstream from the water gap (Figure 4).

As illustrated in Figure 2, the thermal spring areas in the Warm Springs anticline all occur near the intersection of surface lineaments within the anticline (Hobba and others, 1979; Geiser, 1979; Gathright, 1984). Apparently, these lineaments are the surficial expression of fracture zones which facilitate the upward movement of the thermal water.

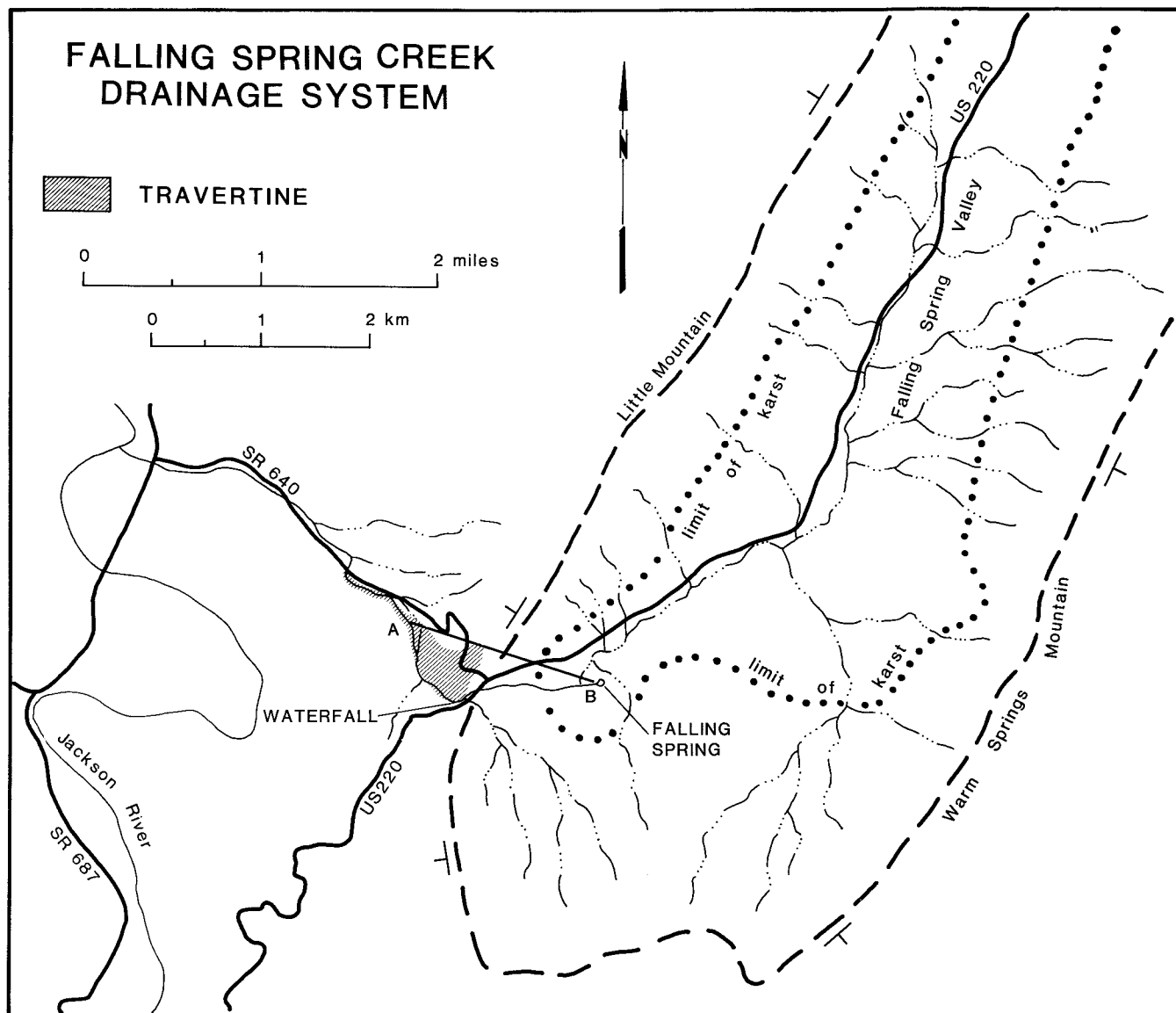


Figure 3. Falling Spring Creek drainage system. Heavy dashed line represents approximate outcrop of Tuscarora Sandstone.

The Tuscarora sandstone is well jointed and displays about 9 m of left lateral displacement at the water gap of Falling Spring Creek (Geiser, 1979).

Different theories for the source of the heat in the thermal springs have been advanced. Chemical similarity between the thermal spring waters and non-thermal spring waters is the basis for the theory that the thermal springs are deeply circulated surface-derived water (Reeves, 1932; Helz and Sinex, 1974; Hobba and others, 1979). On the basis of down-hole heat flow measurements and the observation that a near normal geothermal gradient exists in the thermal springs area, Perry and others (1979) propose that the thermal springs result from deep circulation of meteoric water along steeply-dipping fractured strata and recirculation back to the surface along fracture zones. Dennison and Johnson (1971) have

pointed out the spatial coincidence between the maximum temperature thermal springs in Bath County (adjacent to and north of Alleghany County) and the location of a Tertiary dike swarm in Highland County (adjacent to and north of Bath County) and the proximity of both features to the proposed 38th parallel fracture zone. They propose a slowly cooling Tertiary pluton as the heat source.

STREAM CHARACTERISTICS

Falling Spring is a mixture of thermal and normal temperature spring waters that emanate and mix within Warm River Cave before they reach the surface (Holsinger, 1975).

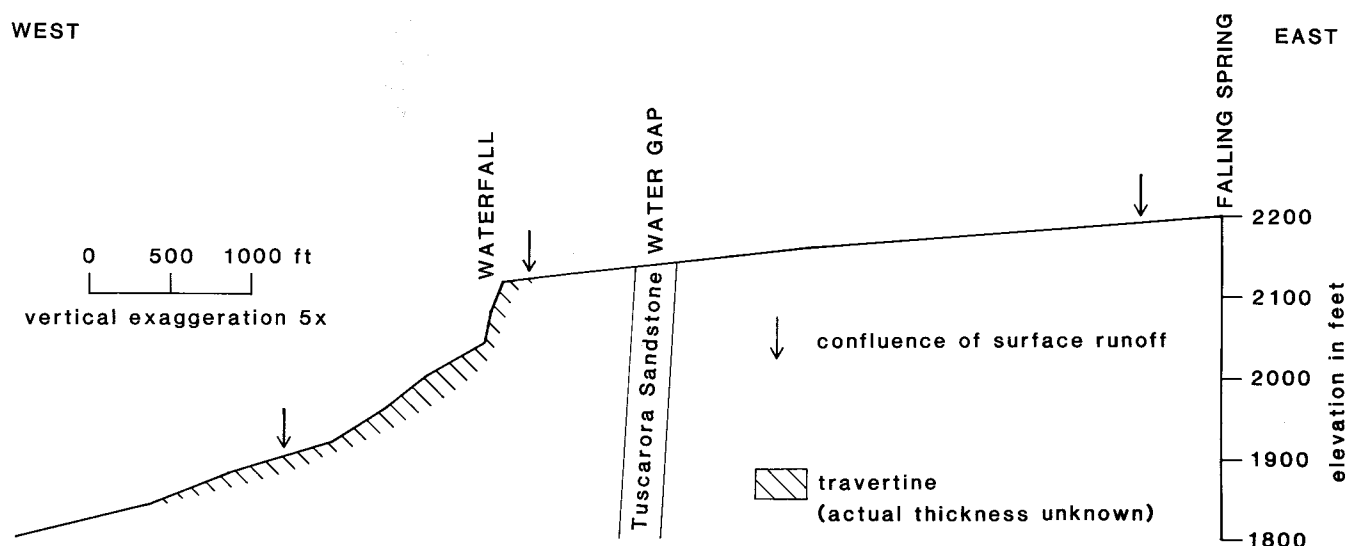


Figure 4. Profile along Falling Spring Creek.

Falling Spring Creek mixes with normal temperature surface streams, most of which drain a karst area, before cascading over Falling Spring Falls (Figures 3 and 4). Downstream from the waterfall, other tributaries from outside the karst area mix with the water of Falling Spring Creek. The Falling Spring Creek drainage system is a tributary of the Jackson River (Figure 3).

Rogers (1884) measured the temperature of Falling Spring some time between 1834 and 1838 and reported 17°C. Reeves (1932) reported slight seasonal variations in the temperature of Falling Spring, ranging from 18°C in the winter to 23°C in autumn. Helz and Sinex (1974) recorded 22.2°C, but they did not make clear whether this measurement was taken during their July or February visit. Hobba and others (1979) reported 25°C at the spring in December. Lorah (1987) recorded temperatures at the spring and at several sites along the stream for the period of a year. She reported a high of 35°C for the warm cave stream in July and a low of 27.5°C in December. Temperatures of the surface spring and stream ranged from 15°C in April to 25°C in July.

Reeves (1932) noted that Falling Spring had the highest discharge rate of all springs in the area, averaging 380 to 450 L/s and that this varied sharply during the year. He proposed that the variation in discharge in addition to the temperature fluctuations at the spring indicated mixing with shallow groundwater. Lorah (1987) charted the discharge rates of Falling Spring Creek over the period of a year. She reported a high of 1200 L/s in April and a low of about 250 L/s in 1984 between October and December.

After issuing onto the surface at Falling Spring, the mixed waters of Falling Spring Creek flow over the gently sloping valley floor at the southern end of Falling Spring Valley (Figure 4). The water gap cut into the Tuscarora sandstone represents a knickpoint between the valley of the

Jackson River and the elevated segment of Falling Spring Valley. Falling Spring Creek cascades over a travertine escarpment about 300 m downstream from the place where it passes over the Tuscarora sandstone.

Immediately below the waterfall, Falling Spring Valley has a convex profile. This is the area where travertine dams are most prominent, and where travertine deposition occurs at the greatest rate during the late summer and early fall. Farther downstream, where less travertine deposition occurs, travertine dams are much less prominent, and the stream profile is more gently sloping and concave.

Reeves (1932) presented geochemical analyses of water collected at the spring. Helz and Sinex (1974) studied chemical equilibria of the waters from ten thermal springs in the vicinity, including Falling Spring, and concluded that the waters were not similar to brines that formed nearby lead-zinc ore deposits, even though both the thermal springs and the ore deposits are found in Ordovician limestones. Hobba and others (1979) studied Falling Spring as part of a geochemical and hydrological study of wells and springs in thermal-spring areas of the entire Appalachian mountain system. Their report included chemical, isotope, and dissolved gas analyses.

Dennen and Diecchio (1984) reported preliminary results of some chemical observations of Falling Spring Creek. Lorah and Herman (Herman and Lorah, 1987; Lorah, 1987; Lorah and Herman, this volume) present detailed chemical measurements taken in Warm River Cave and along Falling Spring Creek. These sources report that an important chemical aspect of Falling Spring Creek is the change in solubility of calcite along the stream course. From the mouth of the spring and continuing downstream, there is an increase in pH due to outgassing of CO₂. This change in pH causes the water to become supersaturated with respect to calcite. The in-

creased CO₂ outgassing is due to the increased turbulence of the water, particularly as it goes over the falls.

METHODS

Our study of the Falling Spring area consisted of field observations made from 1979 to 1987. Visits were made at various times during the year, including low-flow periods (late summer) and high-flow periods (winter and early spring). Visual observations of the modern and ancient travertine were made. The visually apparent state of travertine deposition within the stream at the time of the visit was also noted qualitatively. Samples of both modern and ancient travertine were collected for petrographic analysis.

TRAVERTINE

MODERN TRAVERTINE

Travertine that has formed in the present stream bed is referred to as modern travertine. In Falling Spring Creek, modern travertine deposits are much more common and more extensive downstream from Falling Spring Falls. During the summer and early fall, when stream flow is greatly reduced, it is relatively easy to find new travertine encrusting any debris in the stream below the falls. The encrustation is hard and dense and coats everything in the stream, including glass bottles, twigs (Figure 5), roots, leaves, and rocks (Figure 6).



Figure 5. Twig coated with travertine.

Travertine dams build up over tree roots, fallen limbs, and resistant rock in the stream, where the water flow is more turbulent. Pools of water form behind the dams and some of the pools near the falls are several meters deep. Downstream the pools become shallower. Some of the pools contain



Figure 6. Travertine-coated boulders of Tuscarora sandstone in a recently abandoned part of the stream channel. Photograph taken on slope leading from overlook to the base of the waterfall.

leaves, sticks, and pebbles, which are commonly encrusted with travertine, with the result that the leaves become very brittle. This pool filling is particularly apparent during the autumn when flow is low and fallen leaves accumulate in the pools. There are many areas in the stream, associated with travertine dams, that appear to be terraced (Figure 7).

A soft, crumbly form of modern travertine is associated with algae and mosses. This travertine appears as a muddy brown layer ranging from 0.05 to 2 cm thick and is found forming beneath growing algal mats and encrusting mosses. It is more commonly found during times of low flow. Throughout the year, algae hang in long curtains from the top of the falls (Figure 8) and covers the debris in the stream directly below the falls. Algae and mosses also grow on rocks, roots, and tree limbs in quieter water and pools to the side and downstream from the falls, and on any damp surface in the vicinity of the creek. Modern travertine can be found in almost all these places.

Water seeps from the top of the travertine escarpment to the lower part. The surface of the lower part of the escarpment is set back, and the travertine here takes on a dripstone-like

creased CO₂ outgassing is due to the increased turbulence of the water, particularly as it goes over the falls.

METHODS

Our study of the Falling Spring area consisted of field observations made from 1979 to 1987. Visits were made at various times during the year, including low-flow periods (late summer) and high-flow periods (winter and early spring). Visual observations of the modern and ancient travertine were made. The visually apparent state of travertine deposition within the stream at the time of the visit was also noted qualitatively. Samples of both modern and ancient travertine were collected for petrographic analysis.

TRAVERTINE

MODERN TRAVERTINE

Travertine that has formed in the present stream bed is referred to as modern travertine. In Falling Spring Creek, modern travertine deposits are much more common and more extensive downstream from Falling Spring Falls. During the summer and early fall, when stream flow is greatly reduced, it is relatively easy to find new travertine encrusting any debris in the stream below the falls. The encrustation is hard and dense and coats everything in the stream, including glass bottles, twigs (Figure 5), roots, leaves, and rocks (Figure 6).

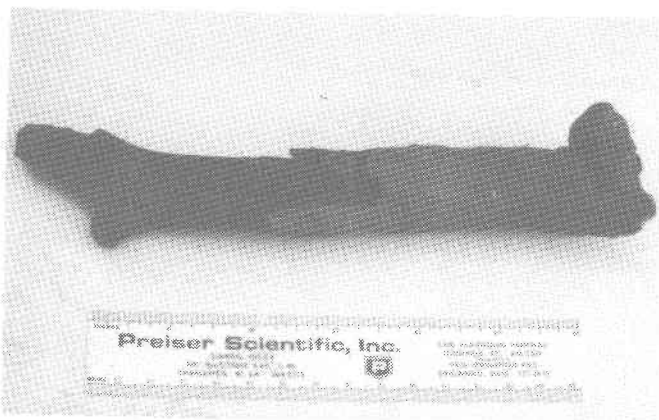


Figure 5. Twig coated with travertine.

Travertine dams build up over tree roots, fallen limbs, and resistant rock in the stream, where the water flow is more turbulent. Pools of water form behind the dams and some of the pools near the falls are several meters deep. Downstream the pools become shallower. Some of the pools contain

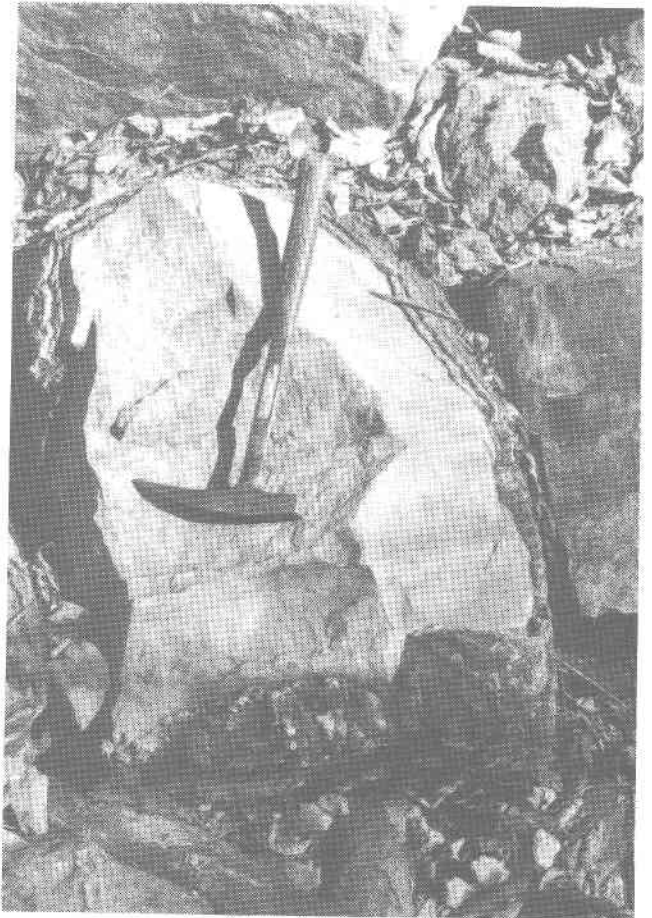


Figure 6. Travertine-coated boulders of Tuscarora sandstone in a recently abandoned part of the stream channel. Photograph taken on slope leading from overlook to the base of the waterfall.

leaves, sticks, and pebbles, which are commonly encrusted with travertine, with the result that the leaves become very brittle. This pool filling is particularly apparent during the autumn when flow is low and fallen leaves accumulate in the pools. There are many areas in the stream, associated with travertine dams, that appear to be terraced (Figure 7).

A soft, crumbly form of modern travertine is associated with algae and mosses. This travertine appears as a muddy brown layer ranging from 0.05 to 2 cm thick and is found forming beneath growing algal mats and encrusting mosses. It is more commonly found during times of low flow. Throughout the year, algae hang in long curtains from the top of the falls (Figure 8) and covers the debris in the stream directly below the falls. Algae and mosses also grow on rocks, roots, and tree limbs in quieter water and pools to the side and downstream from the falls, and on any damp surface in the vicinity of the creek. Modern travertine can be found in almost all these places.

Water seeps from the top of the travertine escarpment to the lower part. The surface of the lower part of the escarpment is set back, and the travertine here takes on a dripstone-like

appearance and grows downward in bulbous, stalactite-like forms.



Figure 7. Travertine terraces in Falling Spring Creek a few hundred feet downstream from waterfall.

DISCUSSION OF MODERN TRAVERTINE DEPOSITION

Lorah and Herman (Lorah, 1987; Lorah and Herman, this volume) have succeeded in measuring much of what we concluded from visual observations. They found that the calcite precipitation rate in Falling Spring Creek is low to non-existent until the water reaches the vicinity of the waterfall and that the calcite precipitation rate reaches a maximum during low-flow conditions in the summer and early fall. We observed that noticeable travertine deposition occurs below the waterfall and is most prominent during times of low stream flow.

Golubic (1969) describes how objects in a travertine-depositing stream can become cemented together by travertine and, in a relatively short time, become part of a large porous deposit. The travertine dams may illustrate the

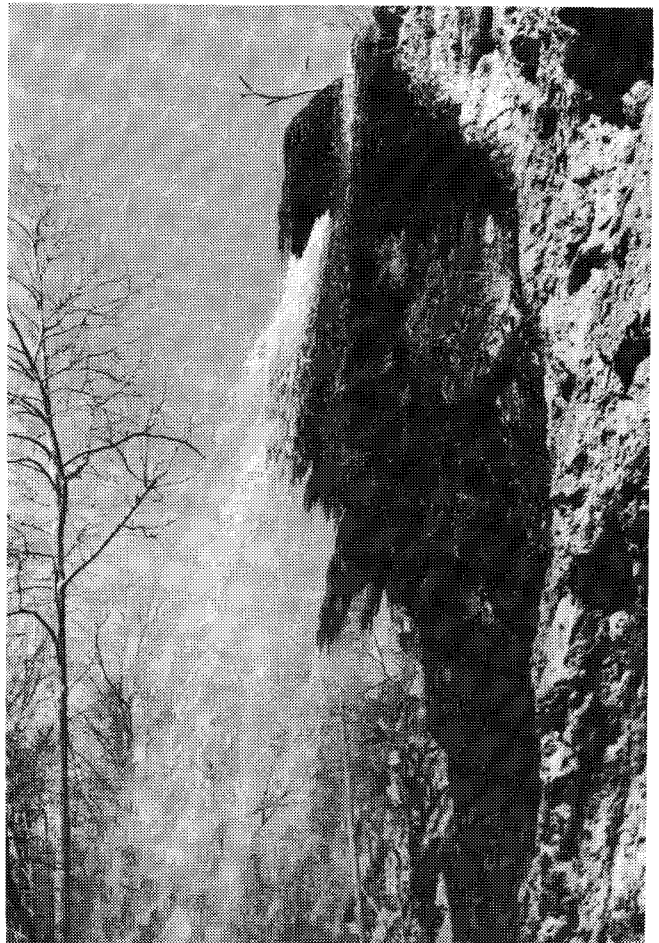


Figure 8. Algal curtains at top of waterfall. Photograph taken during a time of reduced flow.

beginning of this process. As the travertine collects on the dams, the flow of the water is impeded more and more, and pools begin to form behind the dams. As debris collects in the pools and becomes encrusted, the pools begin to fill. This pool filling is particularly apparent during the autumn when fallen leaves accumulate in the pools and when flow is low and the calcite precipitation rate is high. Eventually over a period of years, the pools are filled with coated debris and form terraces. The force of the falling water, which slows or prevents accumulation of debris, probably causes the pools underneath the falls to be the deepest.

The intimate association of algae, mosses, and travertine suggests that biologic agents play an important part in the deposition of some of the travertine. Many authors have described this close association and suggested several ways in which the biologic agents interact with the chemical environment. Chafetz and Folk (1984) describe travertine deposited by bacteria in chemically harsh hot springs as an end-member in a series which includes travertines associated with algae and mosses living in less severe conditions. Pentecost (1985) provides a discussion of how calcite particles might be trapped or nucleated by algal filaments. In our

appearance and grows downward in bulbous, stalactite-like forms.



Figure 7. Travertine terraces in Falling Spring Creek a few hundred feet downstream from waterfall.

DISCUSSION OF MODERN TRAVERTINE DEPOSITION

Lorah and Herman (Lorah, 1987; Lorah and Herman, this volume) have succeeded in measuring much of what we concluded from visual observations. They found that the calcite precipitation rate in Falling Spring Creek is low to non-existent until the water reaches the vicinity of the waterfall and that the calcite precipitation rate reaches a maximum during low-flow conditions in the summer and early fall. We observed that noticeable travertine deposition occurs below the waterfall and is most prominent during times of low stream flow.

Golubic (1969) describes how objects in a travertine-depositing stream can become cemented together by travertine and, in a relatively short time, become part of a large porous deposit. The travertine dams may illustrate the



Figure 8. Algal curtains at top of waterfall. Photograph taken during a time of reduced flow.

beginning of this process. As the travertine collects on the dams, the flow of the water is impeded more and more, and pools begin to form behind the dams. As debris collects in the pools and becomes encrusted, the pools begin to fill. This pool filling is particularly apparent during the autumn when fallen leaves accumulate in the pools and when flow is low and the calcite precipitation rate is high. Eventually over a period of years, the pools are filled with coated debris and form terraces. The force of the falling water, which slows or prevents accumulation of debris, probably causes the pools underneath the falls to be the deepest.

The intimate association of algae, mosses, and travertine suggests that biologic agents play an important part in the deposition of some of the travertine. Many authors have described this close association and suggested several ways in which the biologic agents interact with the chemical environment. Chafetz and Folk (1984) describe travertine deposited by bacteria in chemically harsh hot springs as an end-member in a series which includes travertines associated with algae and mosses living in less severe conditions. Pentecost (1985) provides a discussion of how calcite particles might be trapped or nucleated by algal filaments. In our

preliminary report (Dennen and Diecchio, 1984) we suggested that bacteria which form sticky fibrous networks can act as sediment traps and, along with algae and mosses, provide an ideal substrate for nucleating calcite crystals. Emeis and others (1987) did a detailed organic and geochemical study of mosses living in travertine-depositing streams and lakes and discovered that epiphytic diatoms and algae inhabiting mosses secrete a sticky mucous which traps suspended calcite particles. These authors propose that the presence of biological activity and mucous traps is a prerequisite for the initiation and maintenance of travertine buildups.

The area at the base of the escarpment is similar to the "calcified vaults" described by Golubic (1969). He described a process in which the encrustation of growing algae and mosses is accompanied by the bacterial decomposition of the entrapped plants. During this process, CO_2 concentrations increase locally in the water seeping through the porous travertine deposits, causing the dissolution of some of the travertine and enriching the water in dissolved CaCO_3 . When this supersaturated water seeps down through the deposit and contacts the outside air, some of the CO_2 escapes, and the surfaces of the travertine vault are coated with the resulting calcite precipitate, similar to the way dripstone is formed in a cave. The supersaturated spray from the falls adds to the coating process.

The two separate processes of calcite precipitation and travertine deposition can be distinguished. Lorah (1987) found that photosynthesis by plants in Falling Spring Creek had no measurable effect on the rate of calcite precipitation and ruled out biological activity as a primary factor in the precipitation of calcite in the stream. In view of the studies by Emeis and others (1987) and based upon the close association of travertine and algal buildups, however, we suggest that biological activity is an important factor in the deposition of travertine at Falling Spring Creek. It appears, therefore, that calcite precipitation is controlled largely by inorganic factors and that travertine deposition is controlled largely by organic factors.

ANCIENT TRAVERTINE

For the purposes of this paper, we define ancient travertine as any travertine which was not formed in the existing stream bed. The ancient travertine deposit is located on the western side of Little Mountain and north of Falling Spring Creek (Figure 3). The oldest travertine outcrops occur along State Road 640, at elevations higher than the falls. The topography of the area adjacent to the waterfall has been modified by quarrying of the ancient travertine deposit. Between 1914 and 1941, 387,760 tons of lime were produced, and quarrying continued for a few years after that (Hubbard and others, 1985; Sweet and Hubbard, this volume).

The outcrop of the ancient travertine displays bedding or layering of varied orientations. Figure 9 shows part of the outcrop which has very gently dipping bedded travertine (up to 5°). Figure 10 shows more steeply dipping travertine (dips of 75° or more). Steeply dipping sections such as this are flanked by sections of randomly oriented bedding. Successive layers or coatings of travertine are evident in many places in the ancient deposit (Figure 11). Toward the north end of the outcrop are what appear to be solution or collapse breccias of layered travertine (Figure 12). Some deposits consist of travertine-coated, rounded and flattened pebbles of Ordovician and Silurian clastic strata which underlie the travertine. Figure 13 is a photomicrograph of such a deposit in which small, rounded pebbles of quartzarenite, probably from the Tuscarora Sandstone, and siltstone, probably from the Rose Hill Formation, are cemented together with two different laminations of travertine. Most of the ancient travertine is very porous and contains molds of various types and sizes. Many are molds of tree limbs (Figure 14), leaves, and rootlets. Figure 15 shows a detail of the layering in Figure 11. The layering ranges from 0.5 to 2 cm thick, similar in size to that described for the modern travertine, and consists of porous bands oriented parallel to the substrate.

Petrographically, the ancient travertine commonly appears laminated and vuggy. Figure 16 is a photomicrograph of a single lamination, taken from the part of the outcrop shown in Figure 13. The laminations are composed of microspar with vuggy porosity parallel to the lamination and long bladed calcite crystals which have extended themselves by a series of overgrowths radiating outward from the microspar.

Figure 17 is a scanning electron micrograph of what is probably a filamentous prokaryote (bacteria or blue-green algae) fossilized in the ancient deposit.

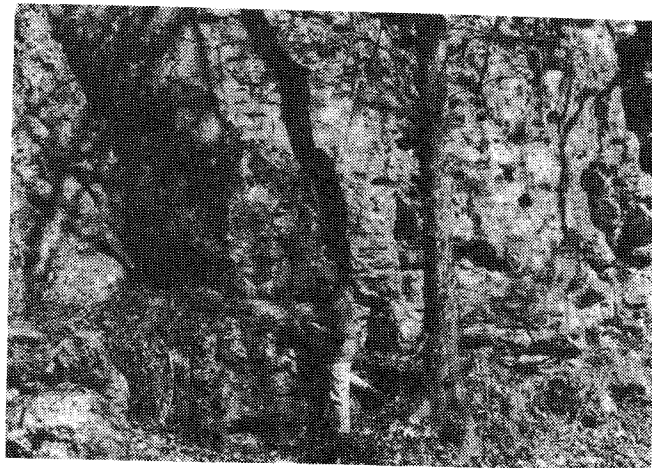


Figure 9. Nearly horizontally bedded travertine, ancient travertine deposit. Photograph taken along State Road 640.

preliminary report (Dennen and Diecchio, 1984) we suggested that bacteria which form sticky fibrous networks can act as sediment traps and, along with algae and mosses, provide an ideal substrate for nucleating calcite crystals. Emeis and others (1987) did a detailed organic and geochemical study of mosses living in travertine-depositing streams and lakes and discovered that epiphytic diatoms and algae inhabiting mosses secrete a sticky mucous which traps suspended calcite particles. These authors propose that the presence of biological activity and mucous traps is a prerequisite for the initiation and maintenance of travertine buildups.

The area at the base of the escarpment is similar to the "calcified vaults" described by Golubic (1969). He described a process in which the encrustation of growing algae and mosses is accompanied by the bacterial decomposition of the entrapped plants. During this process, CO_2 concentrations increase locally in the water seeping through the porous travertine deposits, causing the dissolution of some of the travertine and enriching the water in dissolved CaCO_3 . When this supersaturated water seeps down through the deposit and contacts the outside air, some of the CO_2 escapes, and the surfaces of the travertine vault are coated with the resulting calcite precipitate, similar to the way dripstone is formed in a cave. The supersaturated spray from the falls adds to the coating process.

The two separate processes of calcite precipitation and travertine deposition can be distinguished. Lorah (1987) found that photosynthesis by plants in Falling Spring Creek had no measurable effect on the rate of calcite precipitation and ruled out biological activity as a primary factor in the precipitation of calcite in the stream. In view of the studies by Emeis and others (1987) and based upon the close association of travertine and algal buildups, however, we suggest that biological activity is an important factor in the deposition of travertine at Falling Spring Creek. It appears, therefore, that calcite precipitation is controlled largely by inorganic factors and that travertine deposition is controlled largely by organic factors.

ANCIENT TRAVERTINE

For the purposes of this paper, we define ancient travertine as any travertine which was not formed in the existing stream bed. The ancient travertine deposit is located on the western side of Little Mountain and north of Falling Spring Creek (Figure 3). The oldest travertine outcrops occur along State Road 640, at elevations higher than the falls. The topography of the area adjacent to the waterfall has been modified by quarrying of the ancient travertine deposit. Between 1914 and 1941, 387,760 tons of lime were produced, and quarrying continued for a few years after that (Hubbard and others, 1985; Sweet and Hubbard, this volume).

The outcrop of the ancient travertine displays bedding or layering of varied orientations. Figure 9 shows part of the outcrop which has very gently dipping bedded travertine (up to 5°). Figure 10 shows more steeply dipping travertine (dips of 75° or more). Steeply dipping sections such as this are flanked by sections of randomly oriented bedding. Successive layers or coatings of travertine are evident in many places in the ancient deposit (Figure 11). Toward the north end of the outcrop are what appear to be solution or collapse breccias of layered travertine (Figure 12). Some deposits consist of travertine-coated, rounded and flattened pebbles of Ordovician and Silurian clastic strata which underlie the travertine. Figure 13 is a photomicrograph of such a deposit in which small, rounded pebbles of quartzarenite, probably from the Tuscarora Sandstone, and siltstone, probably from the Rose Hill Formation, are cemented together with two different laminations of travertine. Most of the ancient travertine is very porous and contains molds of various types and sizes. Many are molds of tree limbs (Figure 14), leaves, and rootlets. Figure 15 shows a detail of the layering in Figure 11. The layering ranges from 0.5 to 2 cm thick, similar in size to that described for the modern travertine, and consists of porous bands oriented parallel to the substrate.

Petrographically, the ancient travertine commonly appears laminated and vuggy. Figure 16 is a photomicrograph of a single lamination, taken from the part of the outcrop shown in Figure 13. The laminations are composed of microspar with vuggy porosity parallel to the lamination and long bladed calcite crystals which have extended themselves by a series of overgrowths radiating outward from the microspar.

Figure 17 is a scanning electron micrograph of what is probably a filamentous prokaryote (bacteria or blue-green algae) fossilized in the ancient deposit.



Figure 9. Nearly horizontally bedded travertine, ancient travertine deposit. Photograph taken along State Road 640.

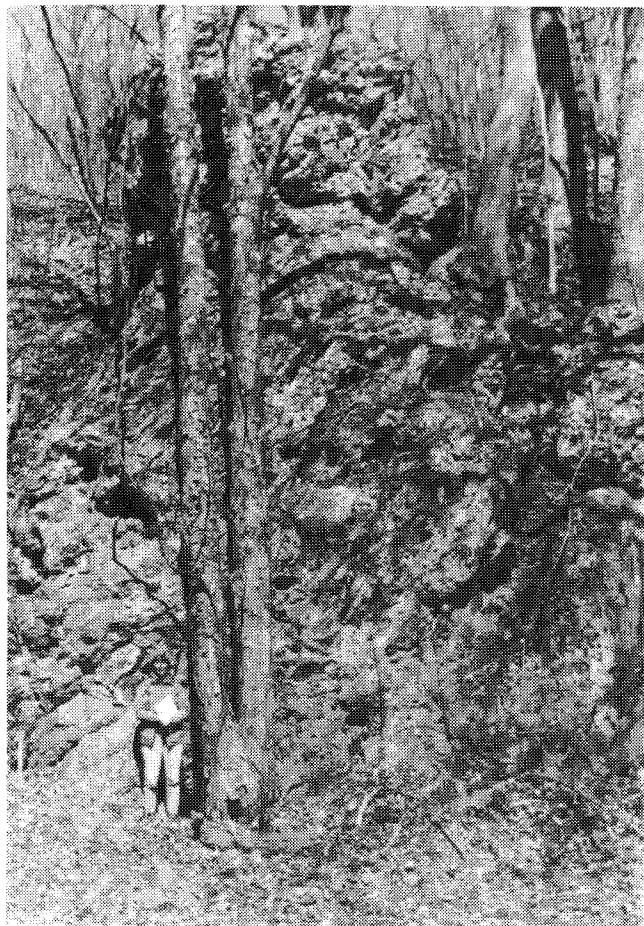


Figure 10. Steeply dipping travertine, ancient travertine deposit. Photograph taken along State Road 640.

DISCUSSION OF ANCIENT TRAVERTINE DEPOSITION

The travertine deposits (modern and ancient) are characteristic of the "waterfall or cascade deposits" described by Chafetz and Folk (1984). The morphology of the deposits is determined mostly by the force of the water and the shape of the algal- and moss-covered surfaces upon which the travertine collects. In the ancient travertine, this has resulted in the wide range of orientations of the layering (Figures 11 and 14). In the modern travertine, the most steeply dipping sections are found on steeply sloping surfaces directly under the waterfall, where the water is most turbulent. The steeply dipping sections in the ancient deposit may therefore show positions of ancient waterfall sites. The pebbly part of the deposit is shown in Figure 13, and the point at which it was found in the ancient travertine most likely marks a stream channel.

The two crystal sizes in the laminations seen in thin section (Figure 16) may be a result of the combination of inorganic and organic processes described by Emeis and



Figure 11. Layered travertine, ancient travertine deposit. Photograph taken along State Road 640. Probably representative of a coated surface.

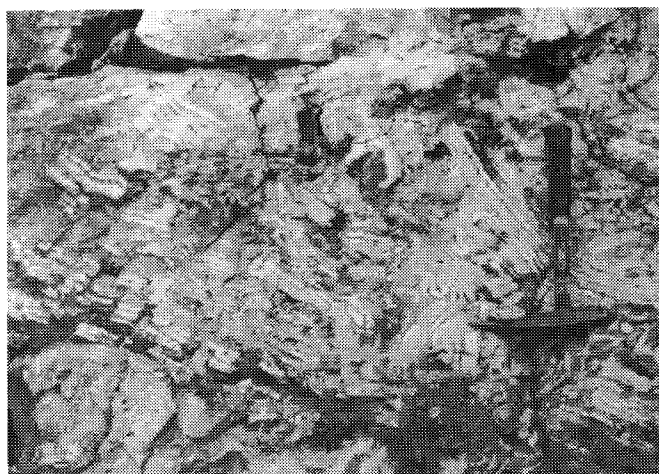


Figure 12. Travertine breccias, ancient deposit. Photograph taken along State Road 640. Probably representative of collapse of a layered accumulation.

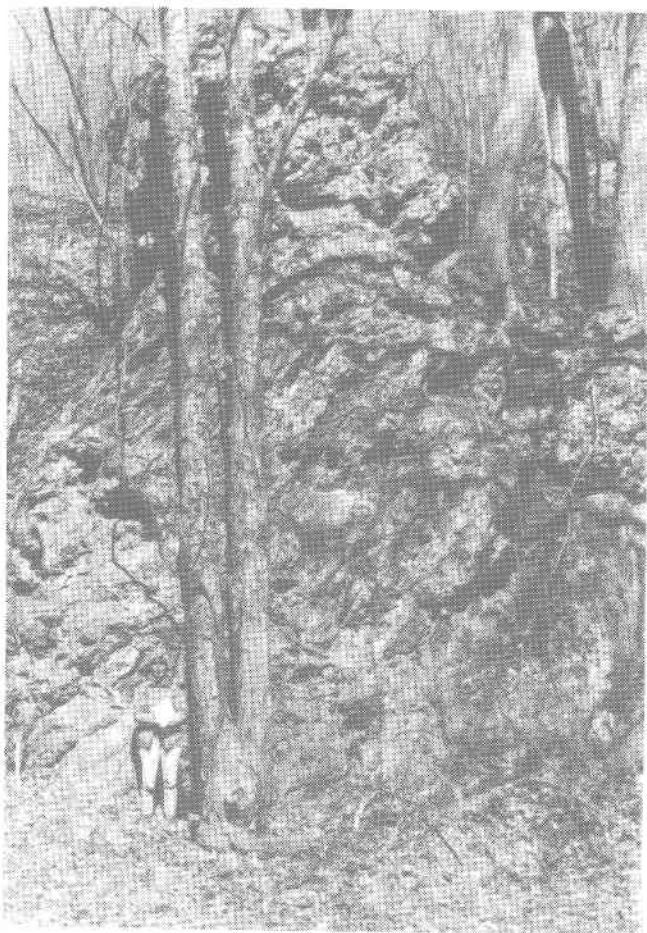


Figure 10. Steeply dipping travertine, ancient travertine deposit. Photograph taken along State Road 640.

DISCUSSION OF ANCIENT TRAVERTINE DEPOSITION

The travertine deposits (modern and ancient) are characteristic of the "waterfall or cascade deposits" described by Chafetz and Folk (1984). The morphology of the deposits is determined mostly by the force of the water and the shape of the algal- and moss-covered surfaces upon which the travertine collects. In the ancient travertine, this has resulted in the wide range of orientations of the layering (Figures 11 and 14). In the modern travertine, the most steeply dipping sections are found on steeply sloping surfaces directly under the waterfall, where the water is most turbulent. The steeply dipping sections in the ancient deposit may therefore show positions of ancient waterfall sites. The pebbly part of the deposit is shown in Figure 13, and the point at which it was found in the ancient travertine most likely marks a stream channel.

The two crystal sizes in the laminations seen in thin section (Figure 16) may be a result of the combination of inorganic and organic processes described by Emeis and



Figure 11. Layered travertine, ancient travertine deposit. Photograph taken along State Road 640. Probably representative of a coated surface.



Figure 12. Travertine breccias, ancient deposit. Photograph taken along State Road 640. Probably representative of collapse of a layered accumulation.



Figure 13. Photomicrograph of coated lithic fragments. Tuscarora sandstone fragment (T) and siltstone fragment from Rose Hill Formation (R), coated with two layers of travertine. Sampled from ancient travertine deposit exposed along State Road 640. Crossed nicols. Scale bar represents 1 mm.

others (1987). These authors proposed two different phases of moss encrustation during fresh-water travertine formation. During the first phase, micritic calcite settles and is trapped by mucous strands secreted by diatoms inhabiting the moss. In waters supersaturated with respect to calcite, this initiates more rapid calcite precipitation at the site of entrapment and massive, sparry calcite (the second phase) buries the moss surface. The moss then grows above the crust, is again inhabited by diatoms, which secrete mucous strands, and the process repeats itself. In Figure 16, the microspar may be the trapped precipitate, and the sparry calcite may represent the second phase. In Figure 13, two complete cycles of this process may be visible in the two layers of travertine.

Golubic and Fischer (1975) found that crystal size zonation in algae fossilized in fresh-water travertine were inversely correlated to the content of entrapped Fe-rich clays. They suggested that the crystal formation recorded changes in water levels and the amount of suspended material. The fact that the smaller crystal sizes in their study are correlated with a higher amount of entrapped clays reinforces the idea proposed by Emeis and others (1987) that the process of

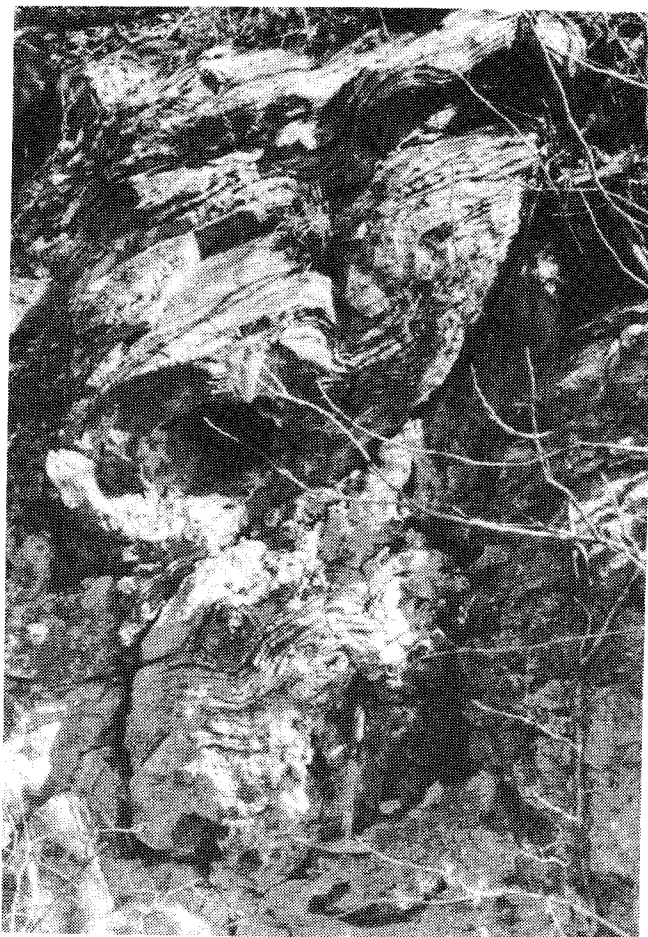


Figure 14. Tree molds, ancient travertine deposit. Photograph taken along State Road 640.

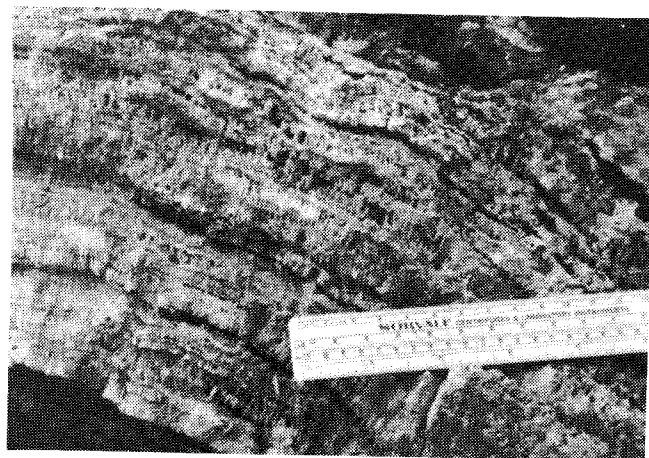


Figure 15. Porous travertine. Enlarged portion of Figure 11.

travertine deposition begins by entrapment of very small particles. Golubic and Fischer's study may also provide an explanation for the differing hues of the travertine layers in Figure 13 (and on a larger scale, in Figure 15). If the amount of entrapped Fe-rich clays is responsible for the color differ-



Figure 13. Photomicrograph of coated lithic fragments. Tuscarora sandstone fragment (T) and siltstone fragment from Rose Hill Formation (R), coated with two layers of travertine. Sampled from ancient travertine deposit exposed along State Road 640. Crossed nicols. Scale bar represents 1 mm.

others (1987). These authors proposed two different phases of moss encrustation during fresh-water travertine formation. During the first phase, micritic calcite settles and is trapped by mucous strands secreted by diatoms inhabiting the moss. In waters supersaturated with respect to calcite, this initiates more rapid calcite precipitation at the site of entrapment and massive, sparry calcite (the second phase) buries the moss surface. The moss then grows above the crust, is again inhabited by diatoms, which secrete mucous strands, and the process repeats itself. In Figure 16, the microspar may be the trapped precipitate, and the sparry calcite may represent the second phase. In Figure 13, two complete cycles of this process may be visible in the two layers of travertine.

Golubic and Fischer (1975) found that crystal size zonation in algae fossilized in fresh-water travertine were inversely correlated to the content of entrapped Fe-rich clays. They suggested that the crystal formation recorded changes in water levels and the amount of suspended material. The fact that the smaller crystal sizes in their study are correlated with a higher amount of entrapped clays reinforces the idea proposed by Emeis and others (1987) that the process of

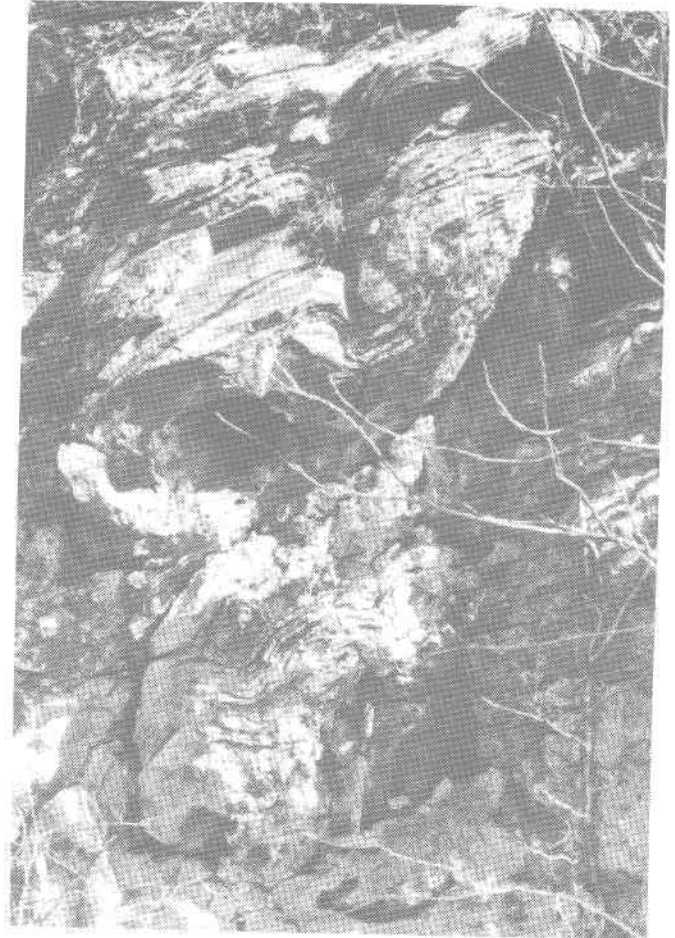


Figure 14. Tree molds, ancient travertine deposit. Photograph taken along State Road 640.

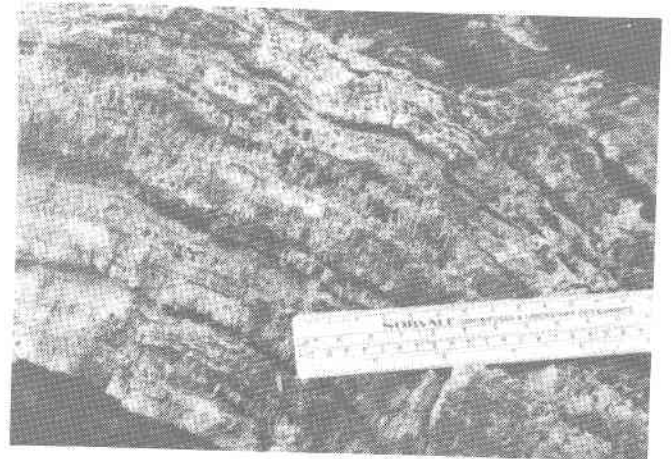


Figure 15. Porous travertine. Enlarged portion of Figure 11.

travertine deposition begins by entrapment of very small particles. Golubic and Fischer's study may also provide an explanation for the differing hues of the travertine layers in Figure 13 (and on a larger scale, in Figure 15). If the amount of entrapped Fe-rich clays is responsible for the color differ-

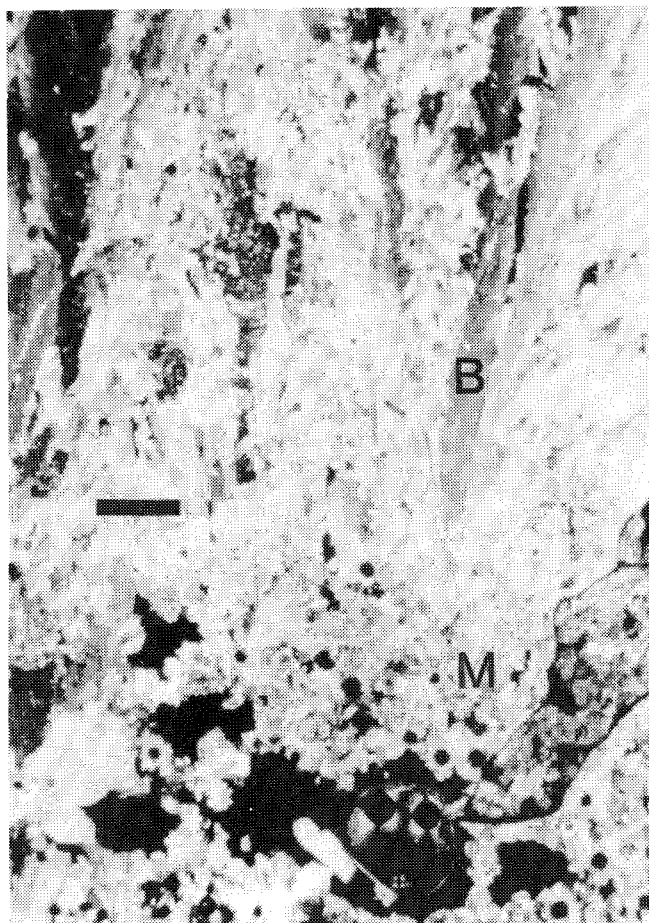


Figure 16. Photomicrograph of travertine lamination. Bladed calcite crystals (B) growing on microspar (M). Small round holes are probably molds of filamentous material. Crossed nicols. Scale bar represents 0.1 mm.

ences, the darker layers may record high-flow conditions in Falling Spring Creek during the winter and early spring, when the water would be carrying larger amounts of suspended Fe-rich sediments weathered from surrounding bedrock (the Juniata and Rose Hill formations are iron-rich).

Figure 17 shows what may be algal filaments which, according to Emeis and others (1987), are critical in providing nucleating sites for precipitating travertine. Calcareous molds of these filaments are visible in the photomicrograph. The underlying travertine appears to be full of small holes. These may be the micropores described by Chafetz and Folk (1984), which are formed when bacterial colonies, surrounded by freshly forming travertine, die and decay. This photomicrograph emphasizes the intimate association and intricate combination of organic and inorganic processes in the formation of travertine.

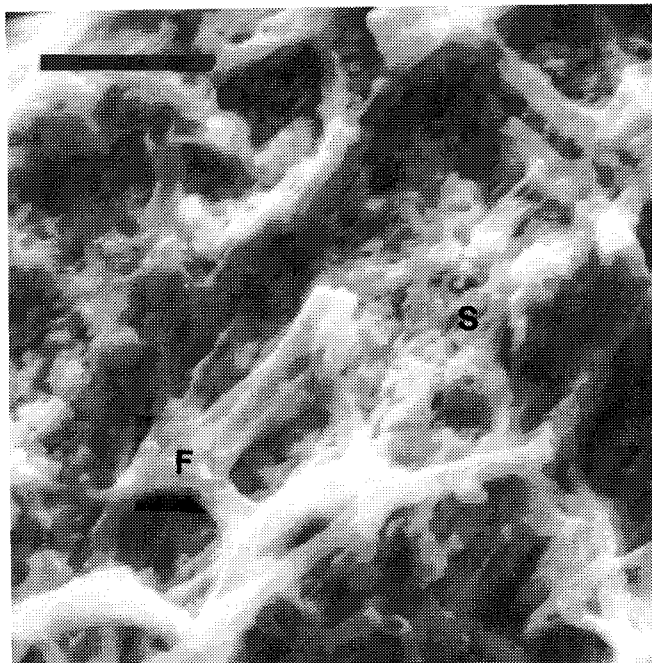


Figure 17. Procaryotic (?) filamentous material (F) on a porous substrate (S). Scanning electron micrograph of travertine coating found on a fossilized tree limb. Scale bar represents 10 μ m.

GEOMORPHIC DEVELOPMENT OF FALLING SPRING CREEK

The ancient travertine deposit near Falling Spring Falls occurs on the dip slope of Little Mountain, in the same general position with regard to the Tuscarora Sandstone as the modern travertine deposits (Figures 3 and 18). In either case (modern or ancient), the travertine occurs on a Tuscarora dip-slope and contains cascade deposits. The highest topographic position of the ancient travertine deposit is at least 6 m higher than the present elevation of the Falling Spring and more than 30 m above the elevation of the waterfall (Figure 18).

The Tuscarora sandstone forms a ridge that surrounds many of the anticlines and synclines in the Appalachian Valley and Ridge province. Other streams (not thermal or travertine depositing) that flow over the Tuscarora sandstone exhibit disturbed flow in the form of rapids, cascades, or waterfalls (for example, at Narrows and at Goodwins Ferry on the New River and at Meadow Creek Falls at the northeast nose of the Sinking Creek anticline). The disturbed flow that occurs in Falling Spring Creek as it passes over the travertine ledge is influential in the outgassing of carbon dioxide and the increased deposition of travertine. The resistant ridge of Tuscarora sandstone most likely played a crucial role in the location of the travertine deposits, perhaps serving as the original cause of the turbulence associated with travertine deposition. The ancient deposit must have formed when

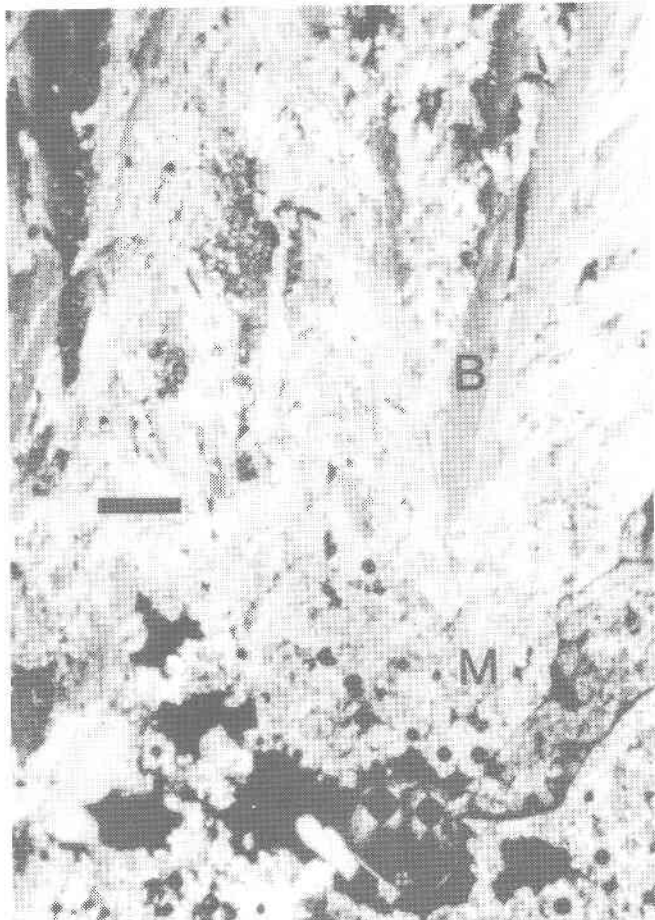


Figure 16. Photomicrograph of travertine lamination. Bladed calcite crystals (B) growing on microspar (M). Small round holes are probably molds of filamentous material. Crossed nicols. Scale bar represents 0.1 mm.

ences, the darker layers may record high-flow conditions in Falling Spring Creek during the winter and early spring, when the water would be carrying larger amounts of suspended Fe-rich sediments weathered from surrounding bedrock (the Juniata and Rose Hill formations are iron-rich).

Figure 17 shows what may be algal filaments which, according to Emeis and others (1987), are critical in providing nucleating sites for precipitating travertine. Calcareous molds of these filaments are visible in the photomicrograph. The underlying travertine appears to be full of small holes. These may be the micropores described by Chafetz and Folk (1984), which are formed when bacterial colonies, surrounded by freshly forming travertine, die and decay. This photomicrograph emphasizes the intimate association and intricate combination of organic and inorganic processes in the formation of travertine.

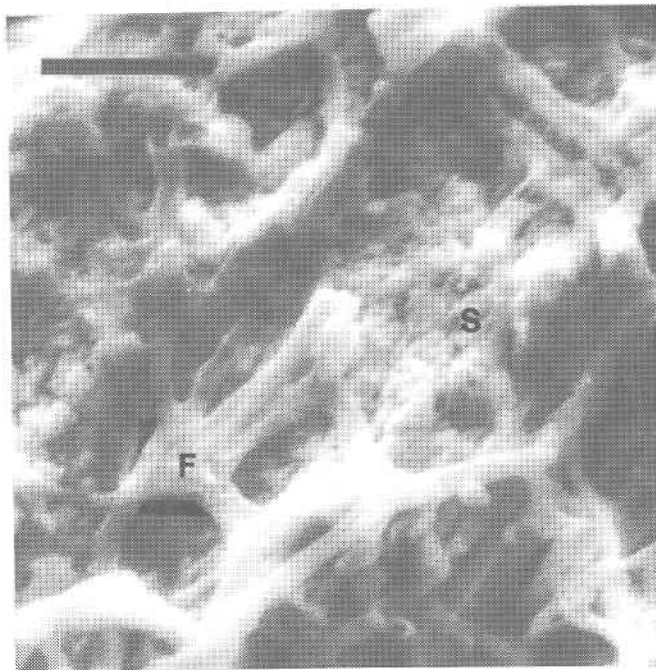


Figure 17. Procaryotic (?) filamentous material (F) on a porous substrate (S). Scanning electron micrograph of travertine coating found on a fossilized tree limb. Scale bar represents 10 μ m.

GEOMORPHIC DEVELOPMENT OF FALLING SPRING CREEK

The ancient travertine deposit near Falling Spring Falls occurs on the dip slope of Little Mountain, in the same general position with regard to the Tuscarora Sandstone as the modern travertine deposits (Figures 3 and 18). In either case (modern or ancient), the travertine occurs on a Tuscarora dip-slope and contains cascade deposits. The highest topographic position of the ancient travertine deposit is at least 6 m higher than the present elevation of the Falling Spring and more than 30 m above the elevation of the waterfall (Figure 18).

The Tuscarora sandstone forms a ridge that surrounds many of the anticlines and synclines in the Appalachian Valley and Ridge province. Other streams (not thermal or travertine depositing) that flow over the Tuscarora sandstone exhibit disturbed flow in the form of rapids, cascades, or waterfalls (for example, at Narrows and at Goodwins Ferry on the New River and at Meadow Creek Falls at the northeast nose of the Sinking Creek anticline). The disturbed flow that occurs in Falling Spring Creek as it passes over the travertine ledge is influential in the outgassing of carbon dioxide and the increased deposition of travertine. The resistant ridge of Tuscarora sandstone most likely played a crucial role in the location of the travertine deposits, perhaps serving as the original cause of the turbulence associated with travertine deposition. The ancient deposit must have formed when

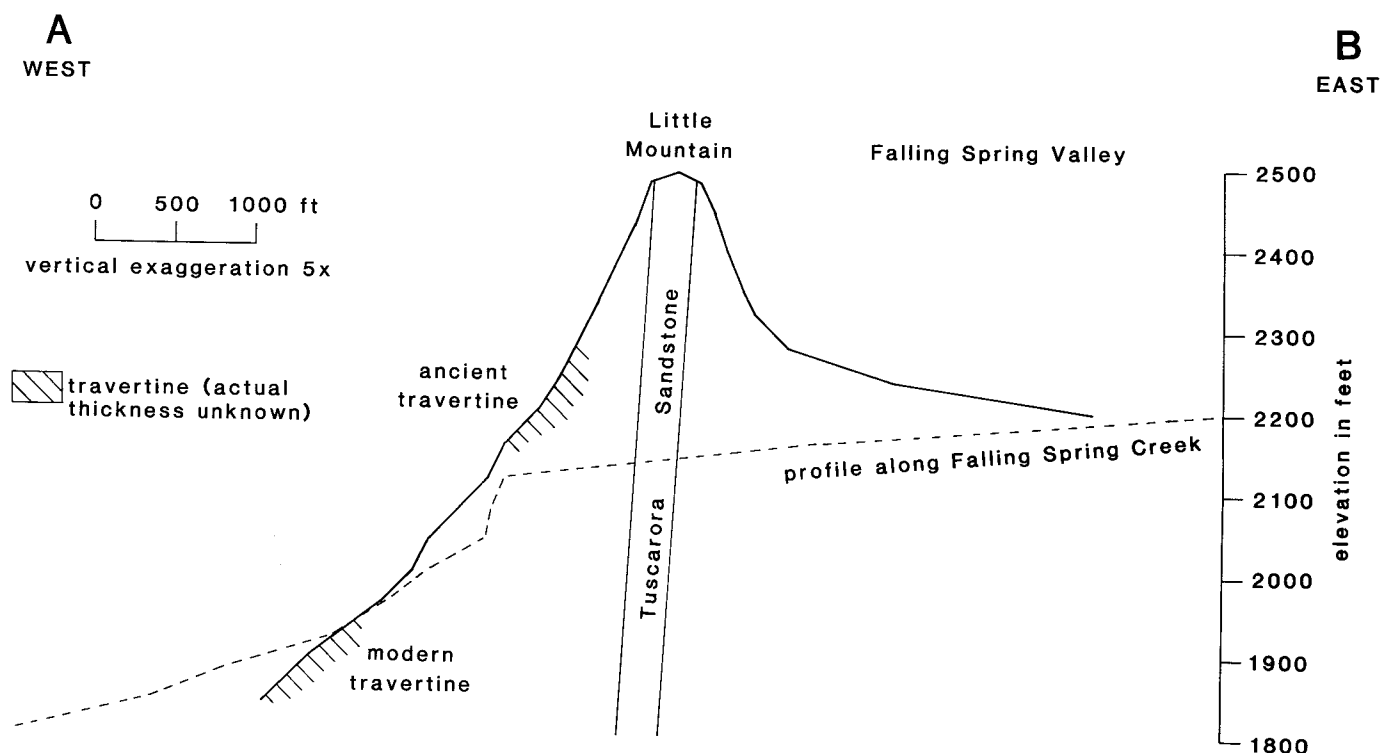


Figure 18. Profile A-B, solid line, through Little Mountain. Location of profile is indicated on Figure 3. Dashed-line profile is same as Figure 4. Both profiles are aligned with respect to the position of the Tuscarora Sandstone.

Falling Spring Creek had a profile that was elevated relative to today and probably flowed over a different path. The ancient profile, however, must still have crossed a ledge of Tuscarora sandstone.

The water gap cut into the Tuscarora represents a knickpoint between the valley of the Jackson River and the elevated upper segment of Falling Spring Valley. The elevation of the knickpoint is controlled by the elevation of Falling Spring Creek where it crosses the Tuscarora sandstone. The ancient cascade deposits that occur above the present spring and waterfall had probably formed when the knickpoint was elevated. In the Falling Spring area, therefore, there may be evidence of the continuing headward erosion of Falling Spring Valley (Figure 18), the elevation of which is controlled by the water gap.

Alternatively, Golubic (1969) describes how travertine buildup can dam a stream, causing the formation of a lake behind the dam. Flood waters can cause the collapse of the travertine dam and completely change the stream profile. In the case of Falling Spring, travertine could have formed a dam, pooling the waters of the creek behind it, and elevating the base level of Falling Spring Valley. The creek could have spilled over the ridge at a different location, and formed another travertine deposit at a different, higher elevation. A subsequent flood may have washed away the dam and once again lowered the base level of the valley.

Even within historical times, there have been noticeable changes in the travertine escarpment. The convex profile of the stream directly below the waterfall is most likely due to travertine accumulation. This may account for some of the difference between the height of Falling Spring Falls in Thomas Jefferson's day (61 m) and the present height (less than 30 m). According to David Hubbard (1988, personal communication), the stream was diverted to its present location at the southeastern end of the travertine ledge by early quarrying operations. He suggests that if the water were now flowing over the escarpment which extends to the far west end of the travertine deposit (Figure 3), the cascade would be about 0.4 km long and would approach the height that Thomas Jefferson described.

ACKNOWLEDGMENTS

We would like to thank the following people for their assistance in this project. Eugene Rader, Gregory Zielinski, an anonymous reviewer, and the editors of this volume provided very useful critical reviews of this manuscript. Richard Bullock assisted with some of the fieldwork. Elizabeth Swinsky helped with the photography. Richard Larson and Deborah Dwornik helped with the scanning electron microscope.

REFERENCES CITED

- Chafetz, H.S., and Folk, R.L., 1984, Travertines: depositional morphology and the bacterially constructed constituents: *Journal of Sedimentary Petrology*, v. 54, p. 289-316.
- Dennen, K.O., and Diecchio, R.J., 1984, The Falling Spring, Alleghany County, Virginia, *in* Rader, E.K., and Gathright, T.M., II, eds., *Stratigraphy and structure in the thermal springs area of the western anticlines*: Virginia Division of Mineral Resources, Sixteenth Annual Virginia Geologic Field Conference, p. 17-22.
- Dennison, J.M., and Johnson, R.W., 1971, Tertiary intrusions and associated phenomena near the thirty-eighth parallel fracture zone in Virginia and West Virginia: *Geological Society of America Bulletin*, v. 82, p. 501-508.
- Emeis, K.-C., Richnow, H.-H., and Kempe, Stephan, 1987, Travertine formation in Plitvice National Park, Yugoslavia: chemical versus biological control: *Sedimentology*, v. 34, p. 595-609.
- Gathright, T.M., II, 1984, Geologic environment of the thermal springs of western Virginia, *in* Rader, E.K., and Gathright, T.M., II, eds., *Stratigraphy and structure in the thermal springs area of the western anticlines*: Virginia Division of Mineral Resources, Sixteenth Annual Virginia Geologic Field Conference, p. 13-15.
- Geiser, P.A., 1979, Field trip guide to selected thermal springs of western Virginia: Guidebook for symposium on geothermal energy and its direct uses in the Eastern United States, April, 1979, Hot Springs, Virginia: Davis, California, Geothermal Resources Council, 14 p.
- Golubic, Stjepko, 1969, Cyclic and noncyclic mechanisms in the formation of travertine: *International Association of Theoretical and Applied Limnology, Proceedings*, v. 17, p. 956-961.
- Golubic, Stjepko, and Fischer, A.G., 1975, Ecology of calcareous nodules forming in Little Conestoga Creek near Lancaster, Pennsylvania: *International Association of Theoretical and Applied Limnology, Proceedings*, v. 19, p. 2315-2323.
- Helz, G.R., and Sinex, S.A., 1974, Chemical equilibria in the thermal spring waters of Virginia: *Geochimica et Cosmochimica Acta*, v. 38, p. 1807-1820.
- Herman, J.S., and Lorah, M.M., 1987, CO₂ outgassing and calcite precipitation in Falling Spring Creek, Virginia, U.S.A.: *Chemical Geology*, v. 62, p. 251-262.
- Hobba, W.A., Jr., Fisher, D.W., Pearson, F.J., Jr., and Chemerys, J.C., 1979, Hydrology and geochemistry of thermal springs of the Appalachians: U.S. Geological Survey Professional Paper 1044-E, 36 p.
- Holsinger, J.R., 1975, Description of Virginia caves: Virginia Division of Mineral Resources Bulletin 85, 450 p.
- Hubbard, D.A., Jr., Giannini, W.F., and Lorah, M.M., 1985, Travertine-marl deposits of the Valley and Ridge Province of Virginia - a preliminary report: Virginia Division of Mineral Resources, Virginia Minerals, v. 31, p. 1-8.
- Jefferson, Thomas, 1825, Notes on the State of Virginia: Philadelphia, H.C. Carey and I. Lea, 344 p.
- Lorah, M.M., 1987, The chemical evolution of a travertine-depositing stream [M.S. thesis]: Charlottesville, University of Virginia, 175 p.
- Pentecost, Allan, 1985, Association of cyanobacteria with tufa deposits: identity, enumeration, and nature of the sheath material revealed by histochemistry: *Geomicrobiology Journal*, v. 4, p. 285-298.
- Perry, L.D., Costain, J.K., and Geiser, P.A., 1979, Heat flow in western Virginia and a model for the origin of thermal springs in the folded Appalachians: *Journal of Geophysical Research*, v. 84, n. B12, p. 6875-6883.
- Reeves, Frank, 1932, Thermal springs of Virginia: Virginia Geological Survey Bulletin 36, 56 p.
- Rogers, W.B., 1884, Connection of thermal springs in Virginia with anticlinal axes and faults, *in* A reprint of annual reports and other papers on the geology of the Virginias: New York, D. Appleton & Co., p. 575-597.

A COMMERCIAL MARL DEPOSIT NEAR WINCHESTER, VIRGINIA

William F. Giannini

CONTENTS

	Page
Abstract.....	93
Introduction.....	94
Description of the deposit.....	94
Setting.....	94
Carbonate materials at the Redbud Run site.....	95
Paleontological associations.....	97
Archaeological associations.....	97
Age of deposit.....	98
Commercial aspects.....	98
Discussion.....	98
Acknowledgments.....	98
References cited.....	99

ILLUSTRATIONS

Figure	
1. Index map of Holocene travertine-marl deposits in Virginia.....	94
2. Geologic map of the abandoned Redbud Run commercial marl pit and associated spring.....	95
3. Travertine near the base of the Redbud Run deposit.....	96
4. Loose, earthy marl along Redbud Run.....	96
5. Concretions and encrustations of precipitated CaCO ₃ on plant stems and roots.....	96
6. Typical mollusk shells from the Redbud Run travertine-marl deposit.....	97
7. Indian artifacts from the top of the Redbud Run deposit.....	97
8. View of travertine-marl deposit immediately after mining began.....	98
9. Redbud Run deposit after removal of unconsolidated calcareous material.....	98

TABLE

Mollusks from the Redbud Run travertine-marl deposit	97
--	----

ABSTRACT

Significant marl deposits of Holocene age have been mined in Frederick and Clarke counties, Virginia. The Redbud Run deposit, located 1.6 km north of Winchester, Frederick County, was partially removed by surface mining. The portion of the deposit removed, about 460 m long, 75 m wide, and 4 m deep, was located on the south side of Redbud Run and was oriented parallel to the direction of the present

stream flow. An unmined portion with similar composition, size, shape, and tonnage of marl occurs on the north side of Redbud Run. The marl was nearly pure CaCO₃ (mostly calcite) containing less than 5 weight percent insolubles. The unmined lower travertine portion is approximately 0.9 m thick and contains up to 97.08 percent CaCO₃. The upper commercial-marl portion of the deposit attained thicknesses as great as 2.7 m of mostly loose, very fine- to coarse-grained material containing up to 96.69 percent CaCO₃. An abun-

dance of land-dwelling and freshwater mollusk (gastropod) shells and shell fragments composed of aragonite (CaCO₃) occurred throughout the marl and travertine. Major travertine-marl deposition at the Redbud Run site probably occurred during the last 10,000 years as estimated from Indian artifacts included in the deposit and under it. A total volume of about 70,000 short tons of marl, or about 80 percent of the south-side deposit, was removed and sold for use as a soil fertility enhancer.

INTRODUCTION

High-purity travertine-marl deposits with greater than 95 percent CaCO₃ are common Holocene sediments in carbonate-rock areas of the Valley and Ridge province of Virginia (Figure 1). These deposits are composed of two principal types of materials: 1) travertine - massive and indurated CaCO₃ materials which formed as falls and rapids in streams and 2) marl - unconsolidated accumulations of CaCO₃ deposited upstream from travertine materials. Locations of the waterfall-type travertine-marl deposits are more widely distributed than those predominantly composed of marl. Deposits of travertine as thick as 18 m are known in the State (Helz and Sinex, 1974). Extensive, predominantly marl-type deposits, occur in Frederick and Clarke counties. Travertine-marl deposits are commonly associated with major Paleozoic thrust faults (Thornton, 1953; Hubbard and others, 1985 and 1986).

This study, focused on the travertine-marl deposit along Redbud Run in Frederick County, Virginia (Figure 2), was conducted to determine the physical setting of the site, to ascertain the type of materials comprising the deposit, to describe the paleontological and archaeological associations, to establish the time of major travertine-marl deposition, and also to record information about the commercial development of the deposit.

DESCRIPTION OF THE DEPOSIT

SETTING

The travertine-marl deposit lies downstream from extensive faults (Figure 2) mapped by Butts and Edmundson (1966). Water percolating along the fault zones appears as a spring, flowing at least 103 L/s from rocks of the Conococheague Formation. This spring, having an annual average temperature between 12°C and 13°C, forms Redbud Run about 70 m upstream from the travertine-marl deposit. Redbud Run traverses the deposit parallel to its long axis dividing it into almost equal portions with relatively flat surfaces along the north and south sides of the stream. The Redbud Run travertine-marl deposit is about 460 m long, 150 m wide, with maximum thicknesses of 4 m.

A layer of calcareous soil containing organic material covered the deposit prior to mining. The deposit overlies a

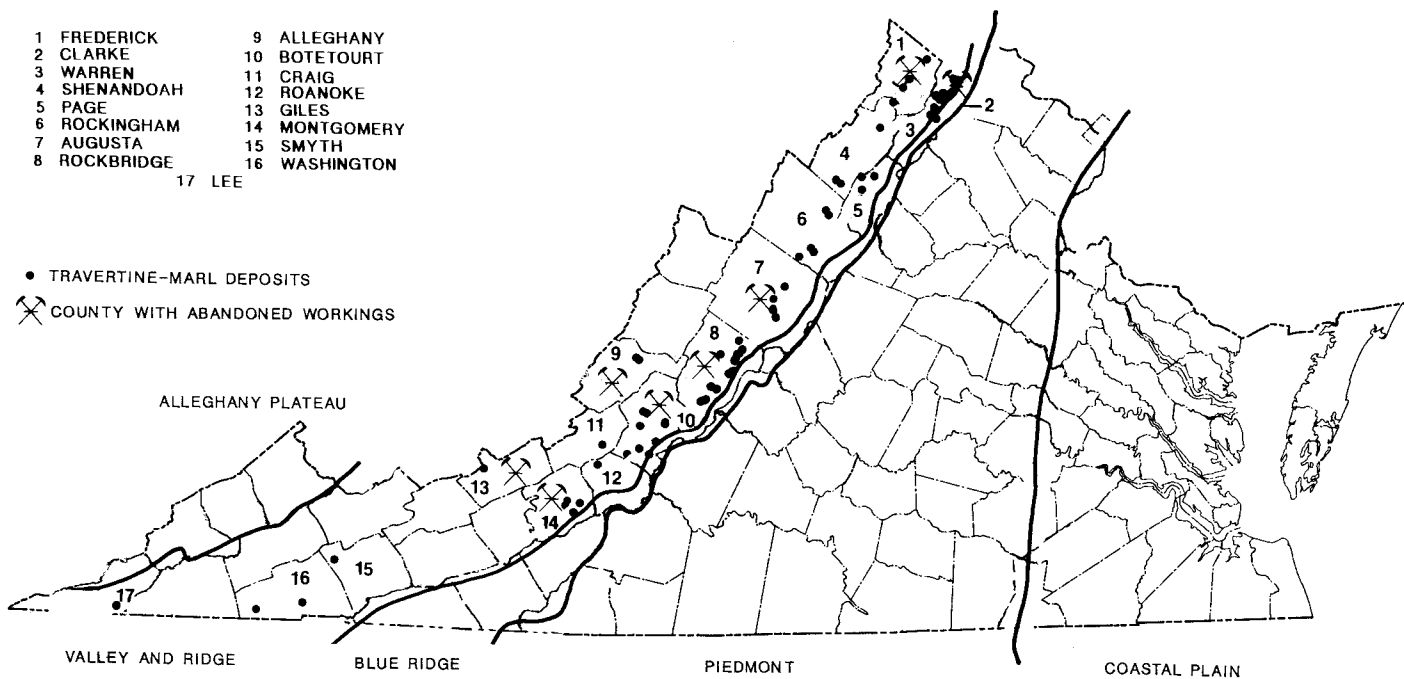


Figure 1. Index map of Holocene travertine-marl deposits in Virginia; counties in the Valley and Ridge province with sites worked for agricultural products used to enhance soil fertility (modified from Hubbard and others, 1985).

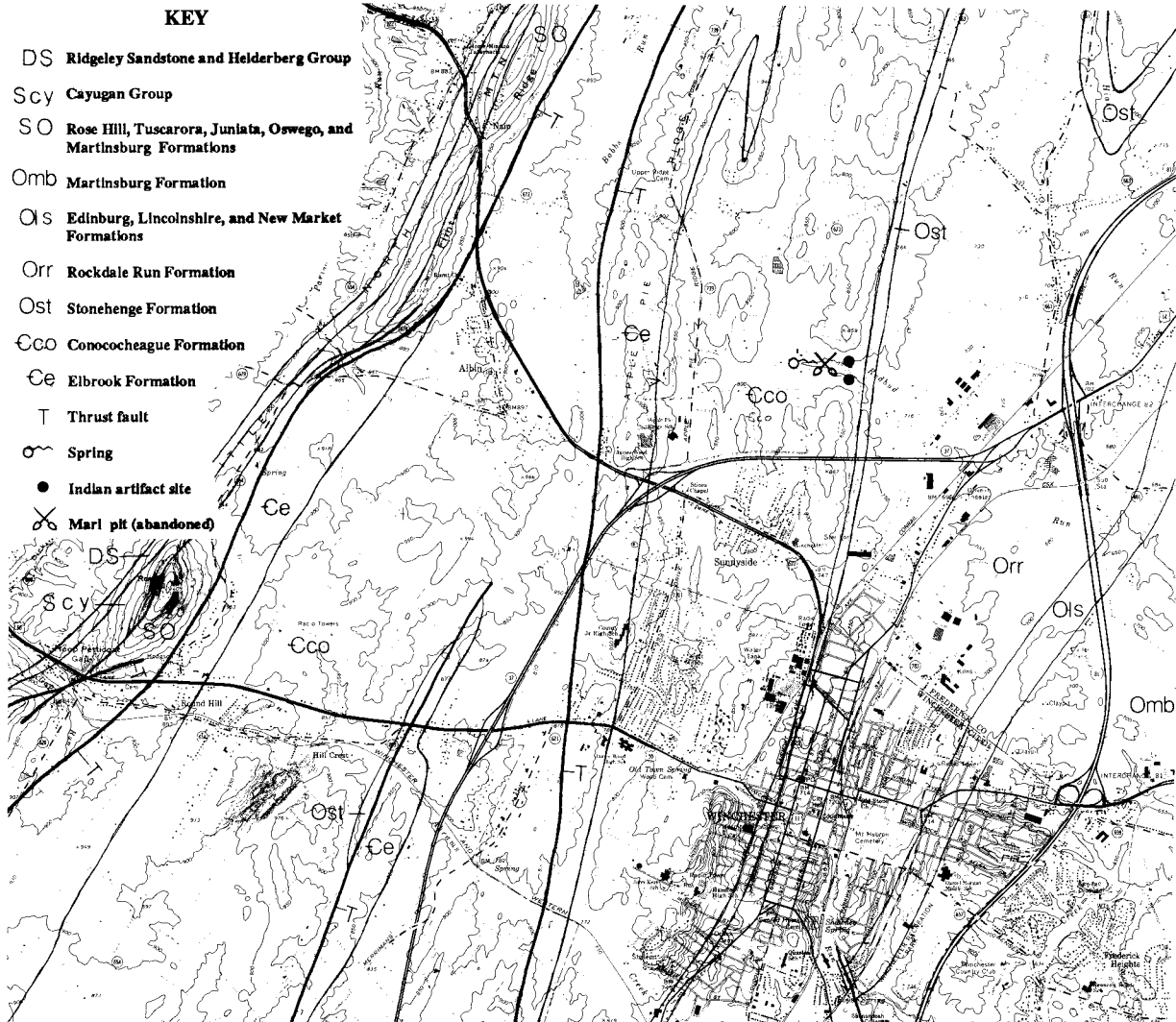


Figure 2. Geologic map of the abandoned Redbud Run commercial marl pit and associated spring in the Conococheague Formation of Cambrian age (geologic map modified from Butts and Edmundson, 1966). Location 1.6 km north of Winchester, Frederick County, Virginia.

coarse channel-lag or fine saprolitic material in a broad saucer-shaped stream valley in carbonate rock of the Upper Cambrian Conococheague Formation. This formation contains mostly bluish-gray limestone with interbedded magnesian limestone, dolostone, and coarse-grained sandstone. The lag, when present, consists of slightly rounded to angular sandstone pebbles and sand, mostly derived from the Conococheague Formation, and covers yellowish-orange (10 YR 6/6) clay to a thickness as large as 0.3 m. The marl contact with the underlying material is sharp, and occasionally marl occurs on knobs of carbonate rock that lack a lag or saprolitic covering. The saprolite was probably removed by erosion prior to travertine-marl deposition.

CARBONATE MATERIALS AT THE REDBUD RUN SITE

The travertine occurs as massive, concretionary, or encrusting, mostly yellowish-brown (10 YR 6/4) to very pale brown (10 YR 8/3), freshwater carbonate deposits. It contains as high as 97.08 percent CaCO_3 , mostly calcite, and a maximum of 1.69 percent MgCO_3 . Encrustations on freshwater and land-snail shells, shell fragments, and plant parts are common. The larger masses of consolidated material, which attain thicknesses of 0.9 m, are more common in the base of the deposit (Figure 3).



Figure 3. Travertine near the base of the Redbud Run deposit; approximately 1.2 m of loose material has been removed for use as an agricultural soil-conditioning product (1983).

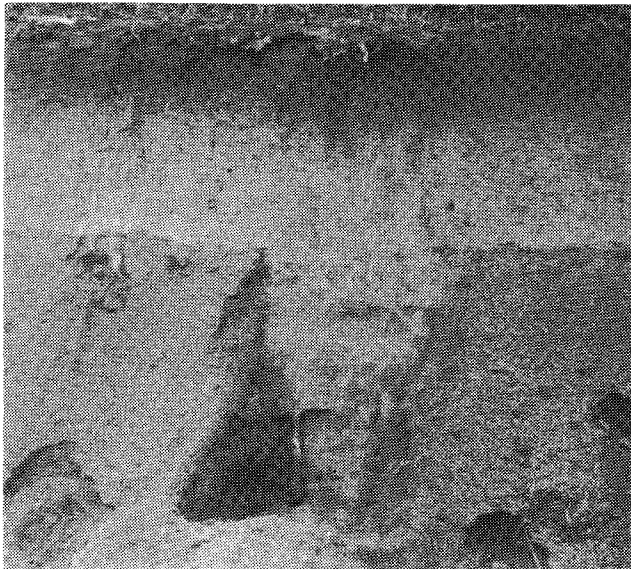


Figure 4. Loose, earthy marl along Redbud Run, exposure is 2.7 m thick; predominantly yellowish-brown, deposit is greater than 95 percent CaCO_3 ; note darker brown, organic-rich zone near top of deposit.

The marl is a loose, earthy, fine- to coarse-texture material, mostly calcite, with compositions as high as 96.69 percent CaCO_3 and 1.30 percent MgCO_3 and minor amounts of clay, silt, and sand (Figure 4). The color is predominately pale yellowish-brown (10 YR 6/2) but ranges from light-gray (10 YR 7/1) when dry to dark yellowish-brown (10 YR 4/4) when wet. Darker material typically contains more organic material and occurs at the top of the deposit. This highly calcareous soil attains thicknesses of 0.3 m.

Calcareous concretions and encrustations are common (Figure 5). Encrustations of CaCO_3 on plant stems and roots have resulted in hollow-tube segments. Pisoliths formed from fragments of encrustations acting as nuclei for further concentric encrustation. Concretions, encrustations, pisoliths, and fragments of these materials and travertine occur within the marl. Snail shells and shell fragments are also found throughout the deposit. All the shells that were examined are composed of the mineral aragonite (CaCO_3).

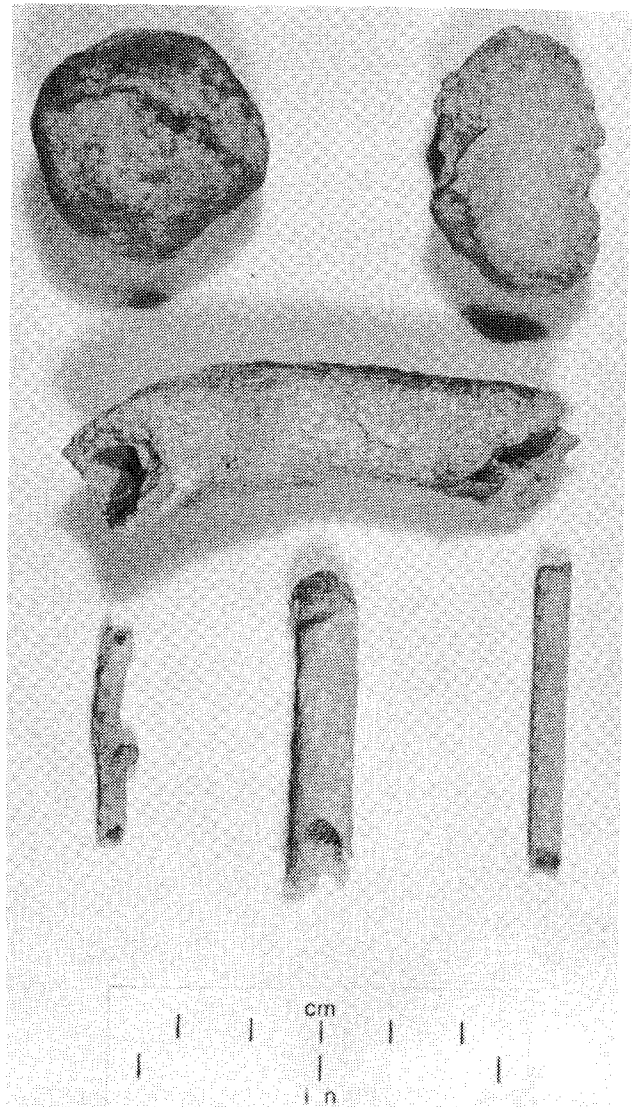


Figure 5. Concretions and encrustations of precipitated CaCO_3 on plant stems and roots resulting in hollow tube fragments are common in the Redbud Run travertine-marl deposit (photograph by T. M. Gathright, II).



Figure 3. Travertine near the base of the Redbud Run deposit; approximately 1.2 m of loose material has been removed for use as an agricultural soil-conditioning product (1983).

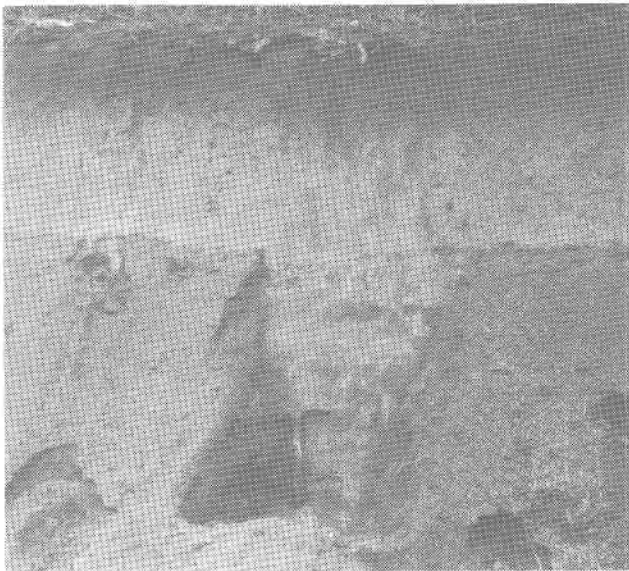


Figure 4. Loose, earthy marl along Redbud Run, exposure is 2.7 m thick; predominantly yellowish-brown, deposit is greater than 95 percent CaCO_3 ; note darker brown, organic-rich zone near top of deposit.

The marl is a loose, earthy, fine- to coarse-texture material, mostly calcite, with compositions as high as 96.69 percent CaCO_3 and 1.30 percent MgCO_3 and minor amounts of clay, silt, and sand (Figure 4). The color is predominately pale yellowish-brown (10 YR 6/2) but ranges from light-gray (10 YR 7/1) when dry to dark yellowish-brown (10 YR 4/4) when wet. Darker material typically contains more organic material and occurs at the top of the deposit. This highly calcareous soil attains thicknesses of 0.3 m.

Calcareous concretions and encrustations are common (Figure 5). Encrustations of CaCO_3 on plant stems and roots have resulted in hollow-tube segments. Pisoliths formed from fragments of encrustations acting as nuclei for further concentric encrustation. Concretions, encrustations, pisoliths, and fragments of these materials and travertine occur within the marl. Snail shells and shell fragments are also found throughout the deposit. All the shells that were examined are composed of the mineral aragonite (CaCO_3).

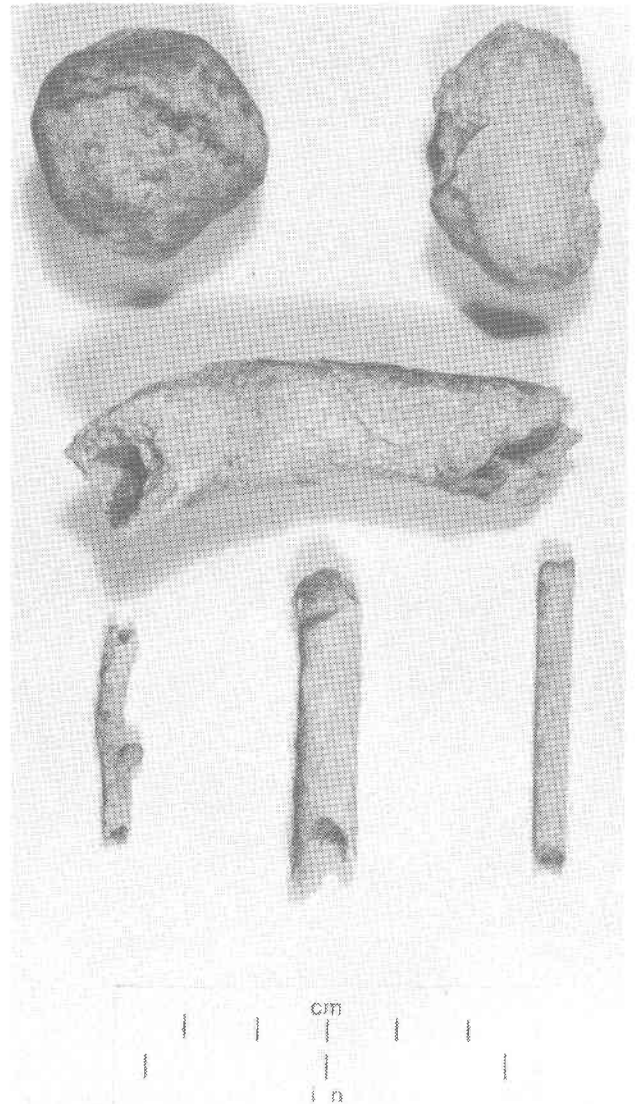


Figure 5. Concretions and encrustations of precipitated CaCO_3 on plant stems and roots resulting in hollow tube fragments are common in the Redbud Run travertine-marl deposit (photograph by T. M. Gathright, II).

PALEONTOLOGICAL ASSOCIATIONS

Seven species of land-dwelling mollusks and three species of freshwater-dwelling mollusks were identified from shell remains from the Redbud Run travertine-marl deposit (Table). Shells and shell fragments commonly constituted about 10 percent of the marl material (Figure 6). Most shells in the travertine and some shells in the marl were encrusted with calcite. The most commonly occurring shells in the deposit were the land-dwelling *Triodopsis* sp. and the freshwater *Lymnaea* sp.

Land-dwelling species are known to inhabit a wide variety of environments including swamps and marshes as well as forests and rock surfaces (Burch, 1962 and 1982). The freshwater snails inhabit springs and ponds as well as rivers and lakes and are found in very shallow water.

Table. Mollusks from the Redbud Run travertine-marl deposit.

Species	Estimated Abundance*	Habitat note
Subclass Pulmonata		
Order Stylommatophora		
Family Pupillidae		
<i>Gastrocopta</i> sp.	M	land-dwelling
Family Polygyridae		
<i>Stenotrema hirsutum?</i> (Say)	H	land-dwelling
<i>Triodopsis fallax</i> (Say)	H	land-dwelling
<i>T. albolabris?</i> (Say)	M	land-dwelling
<i>T. sp. a</i>	L	land-dwelling
<i>T. sp. b</i>	L	land-dwelling
? <i>Polygyra</i> sp.	L	land-dwelling
Order Limnophila		
Family Lymnaeidae		
<i>Lymnaea palustris? alustris?</i> Mull.	H	freshwater
Family Physidae		
<i>Physa gyrina</i>	M	freshwater
Family Planorbidae		
<i>Heliosoma</i> sp.	L	freshwater

*Estimated Abundance: H = high, M = medium, L = low.

ARCHAEOLOGICAL ASSOCIATIONS

A number of Indian artifacts were found by the writer and David A. Hubbard, Jr. near the eastern end of the Redbud Run deposit in the top of the marl at a site on each side of the stream (Figure 2). Two projectile points and 24 pieces of pottery were collected near a fire pit containing small cobbles of sandstone at the north-side site and a point was collected from the south side of Redbud Run (Figure 7). William Gardner, from the Thunderbird Museum, Front Royal, Virginia, collected additional artifacts including a sandstone pestal near

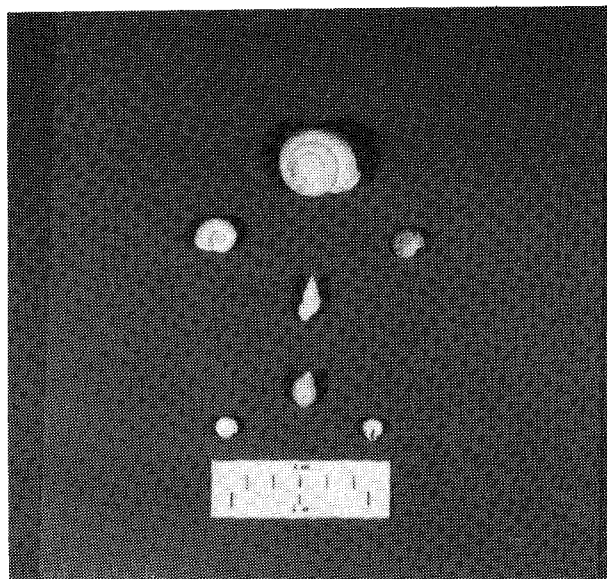


Figure 6. Typical mollusk (gastropod or snail) shells from the Redbud Run travertine-marl deposit.

the fire pit. He determined the artifacts from the top of the marl to be from the period between 500 B.C. to 200 A.D. Gardner also collected points beneath the deposit after mining had ceased. The artifacts were on the surface of the channel-lag material along the contact zone with the travertine-marl. The age range of these artifacts was determined as being from 6800 and 7200 B.C. (Gardner, this volume).

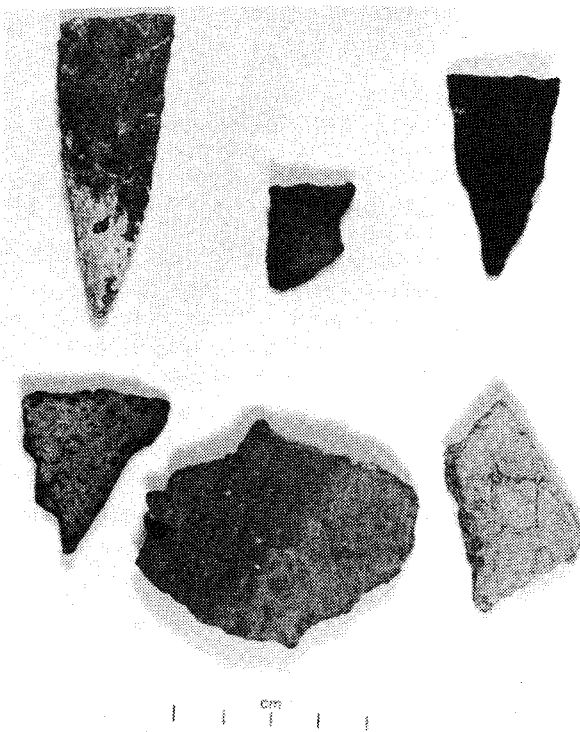


Figure 7. Indian artifacts from the top of the Redbud Run deposit date to as recent as 500 A.D. or 1490 years B.P. (photograph by T. M. Gathright, II).

PALEONTOLOGICAL ASSOCIATIONS

Seven species of land-dwelling mollusks and three species of freshwater-dwelling mollusks were identified from shell remains from the Redbud Run travertine-marl deposit (Table). Shells and shell fragments commonly constituted about 10 percent of the marl material (Figure 6). Most shells in the travertine and some shells in the marl were encrusted with calcite. The most commonly occurring shells in the deposit were the land-dwelling *Triodopsis* sp. and the freshwater *Lymnaea* sp.

Land-dwelling species are known to inhabit a wide variety of environments including swamps and marshes as well as forests and rock surfaces (Burch, 1962 and 1982). The freshwater snails inhabit springs and ponds as well as rivers and lakes and are found in very shallow water.

Table. Mollusks from the Redbud Run travertine-marl deposit.

Species	Estimated Abundance*	Habitat note
Subclass Pulmonata		
Order Stylommatophora		
Family Pupillidae		
<i>Gastrocopta</i> sp.	M	land-dwelling
Family Polygyridae		
<i>Stenotrema hirsutum?</i> (Say)	H	land-dwelling
<i>Triodopsis fallax</i> (Say)	H	land-dwelling
<i>T. albolabris?</i> (Say)	M	land-dwelling
<i>T. sp. a</i>	L	land-dwelling
<i>T. sp. b</i>	L	land-dwelling
? <i>Polygyra</i> sp.	L	land-dwelling
Order Limnophila		
Family Lymnaeidae		
<i>Lymnaea palustris? alustris?</i> Mull.	H	freshwater
Family Physidae		
<i>Physa gyrina</i>	M	freshwater
Family Planorbidae		
<i>Heliosoma</i> sp.	L	freshwater

*Estimated Abundance: H = high, M = medium, L = low.

ARCHAEOLOGICAL ASSOCIATIONS

A number of Indian artifacts were found by the writer and David A. Hubbard, Jr. near the eastern end of the Redbud Run deposit in the top of the marl at a site on each side of the stream (Figure 2). Two projectile points and 24 pieces of pottery were collected near a fire pit containing small cobbles of sandstone at the north-side site and a point was collected from the south side of Redbud Run (Figure 7). William Gardner, from the Thunderbird Museum, Front Royal, Virginia, collected additional artifacts including a sandstone pestal near

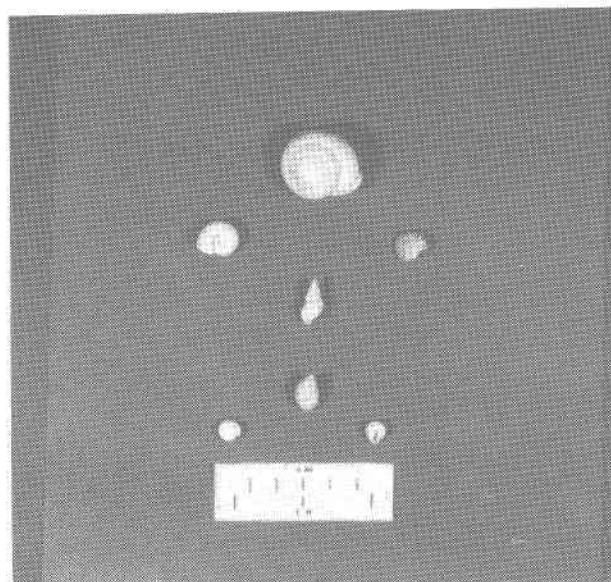


Figure 6. Typical mollusk (gastropod or snail) shells from the Redbud Run travertine-marl deposit.

the fire pit. He determined the artifacts from the top of the marl to be from the period between 500 B.C. to 200 A.D. Gardner also collected points beneath the deposit after mining had ceased. The artifacts were on the surface of the channel-lag material along the contact zone with the travertine-marl. The age range of these artifacts was determined as being from 6800 and 7200 B.C. (Gardner, this volume).

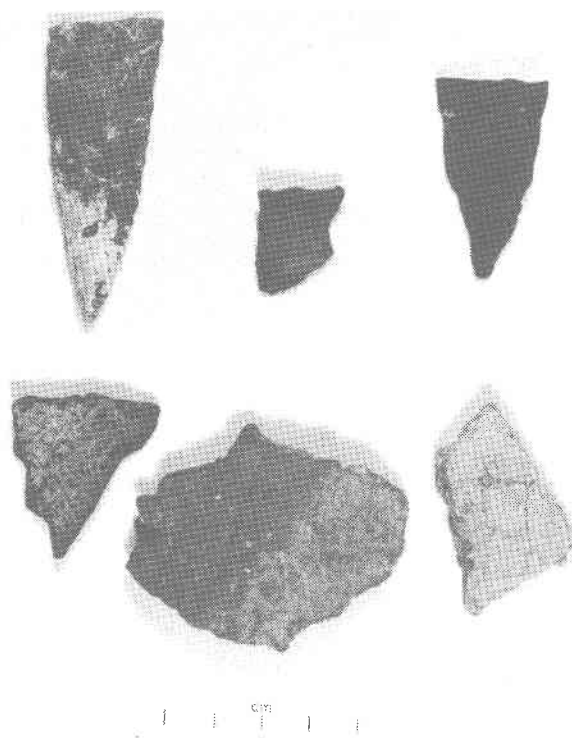


Figure 7. Indian artifacts from the top of the Redbud Run deposit date to as recent as 500 A.D. or 1490 years B.P. (photograph by T. M. Gathright, II).

AGE OF DEPOSIT

The data most useful to determine an approximate time of major travertine-marl deposition at the Redbud Run site are the ages of Indian artifacts collected from the top and underneath the deposit. William Gardner's (1987, personal communication) age determinations of the artifacts fix the time of major deposition to be between approximately 8800 years B.P., based on artifacts underneath, and 1490 years B.P., based on those from the top of the deposit.

Identification of the freshwater and land-dwelling mollusk species found in the Redbud Run deposit do not contribute useful information about the age of the deposit, because these species have existed throughout the Holocene Epoch.

COMMERCIAL ASPECTS

The study of the commercial marl deposit began in 1981 just prior to its mining for use as a soil-fertility enhancing material. Less than 1 m of a dark-brown, calcareous, organic-rich soil had been removed with the grass cover along the northern and southern sides of Redbud Run in 1978. About 70,000 short tons of high purity marl, greater than 95 percent CaCO_3 , was exposed along each side of the stream. Mining began on the southern side of Redbud Run, during October 1981, utilizing a pan scraper and a front-end loader to pile and load the loose marl (Figure 8). Mining proceeded until indurated travertine was encountered near the base of the deposit. The travertine could not be removed with the scraper or loader, and mining ceased late in 1982 (Figure 9). This factor ended the mining of travertine-marl in Frederick County and the era, from 1838 (Rogers, 1844), of mining Holocene marl deposits in the Valley and Ridge province of Virginia.

Environmental concerns, zoning changes, increased land values, and population growth in Frederick and Clarke counties will probably preclude the development of the marl deposit along the north side of Redbud Run or any others in the area.

DISCUSSION

The origin of the Redbud Run and similar deposits in Frederick and Clarke counties is similar to other travertine-marl deposits described by Hubbard and others (1985) and Herman and Lorah (1987). The deposits originated by precipitation of calcite (CaCO_3) from spring waters associated with fault systems in carbonate rocks. Travertine and marl precipitated as the waters became supersaturated with respect to calcite upon CO_2 outgassing. The conditions that were responsible for the onset of travertine-marl deposition, the

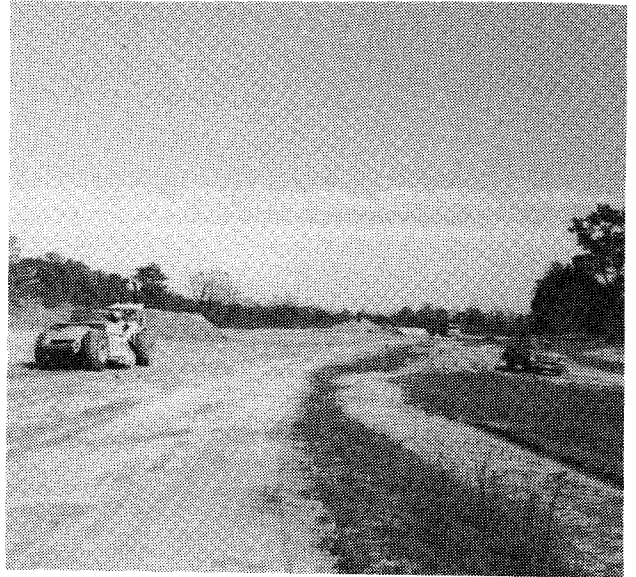


Figure 8. View of travertine-marl deposit immediately after mining began (October 1981).



Figure 9. Redbud Run deposit after removal of unconsolidated calcareous material (marl); the remaining travertine shows an undulating surface (February 1983).

role of climatic change, and the effects of agricultural activities during the past 200 years are all topics that require additional research for a better understanding.

ACKNOWLEDGMENT

Samuel O. Bird helped in the preparation of this paper through discussions on the origin of the deposits, measurements of spring discharge, and the identification and ecology of the gastropods of the Redbud Run deposit.

AGE OF DEPOSIT

The data most useful to determine an approximate time of major travertine-marl deposition at the Redbud Run site are the ages of Indian artifacts collected from the top and underneath the deposit. William Gardner's (1987, personal communication) age determinations of the artifacts fix the time of major deposition to be between approximately 8800 years B.P., based on artifacts underneath, and 1490 years B.P., based on those from the top of the deposit.

Identification of the freshwater and land-dwelling mollusk species found in the Redbud Run deposit do not contribute useful information about the age of the deposit, because these species have existed throughout the Holocene Epoch.

COMMERCIAL ASPECTS

The study of the commercial marl deposit began in 1981 just prior to its mining for use as a soil-fertility enhancing material. Less than 1 m of a dark-brown, calcareous, organic-rich soil had been removed with the grass cover along the northern and southern sides of Redbud Run in 1978. About 70,000 short tons of high purity marl, greater than 95 percent CaCO_3 , was exposed along each side of the stream. Mining began on the southern side of Redbud Run, during October 1981, utilizing a pan scraper and a front-end loader to pile and load the loose marl (Figure 8). Mining proceeded until indurated travertine was encountered near the base of the deposit. The travertine could not be removed with the scraper or loader, and mining ceased late in 1982 (Figure 9). This factor ended the mining of travertine-marl in Frederick County and the era, from 1838 (Rogers, 1844), of mining Holocene marl deposits in the Valley and Ridge province of Virginia.

Environmental concerns, zoning changes, increased land values, and population growth in Frederick and Clarke counties will probably preclude the development of the marl deposit along the north side of Redbud Run or any others in the area.

DISCUSSION

The origin of the Redbud Run and similar deposits in Frederick and Clarke counties is similar to other travertine-marl deposits described by Hubbard and others (1985) and Herman and Lorah (1987). The deposits originated by precipitation of calcite (CaCO_3) from spring waters associated with fault systems in carbonate rocks. Travertine and marl precipitated as the waters became supersaturated with respect to calcite upon CO_2 outgassing. The conditions that were responsible for the onset of travertine-marl deposition, the



Figure 8. View of travertine-marl deposit immediately after mining began (October 1981).



Figure 9. Redbud Run deposit after removal of unconsolidated calcareous material (marl); the remaining travertine shows an undulating surface (February 1983).

role of climatic change, and the effects of agricultural activities during the past 200 years are all topics that require additional research for a better understanding.

ACKNOWLEDGMENT

Samuel O. Bird helped in the preparation of this paper through discussions on the origin of the deposits, measurements of spring discharge, and the identification and ecology of the gastropods of the Redbud Run deposit.

REFERENCES CITED

- Burch, J.B., 1962, The eastern land snails: Dubuque, Iowa, Brown Company, 214 p.
- Burch, J.B., 1982, Freshwater snails (Mollusca: Gastropoda) of North America: Cincinnati, Ohio, U.S. Environmental Protection Agency, 294 p.
- Butts, Charles, and Edmundson, R.S., 1966, Geology and mineral resources of Frederick County: Virginia Division of Mineral Resources Bulletin 80, 142 p.
- Helz, G.R., and Sinex, S.A., 1974, Chemical equilibria in the thermal spring waters of Virginia: *Geochimica et Cosmochimica Acta*, v. 38, p. 1807-1820.
- Herman, J.S., and Lorah, M.M., 1987, CO₂ outgassing and calcite precipitation in Falling Spring Creek, Virginia, U.S.A.: *Chemical Geology*, v. 62, p. 251-262.
- Hubbard, D.A., Jr., Giannini, W.F., and Lorah, M.M., 1985, Travertine-marl deposits of the Valley and Ridge province of Virginia - a preliminary report: Virginia Division of Mineral Resources, Virginia Minerals, v. 31, n. 1, p. 1-8.
- Hubbard, D.A., Jr., Giannini, W.F., and Lorah, M.M., 1986, Quaternary travertine-marl deposits of Virginia (abs.), in McDonald, J.N., and Bird, S.O., eds., The Quaternary of Virginia-a symposium volume: Virginia Division of Mineral Resources Publication 75, p. 126.
- Rogers, W.B., 1884, A reprint of the geology of the Virginias: New York, New York, D. Appleton and Company, 832 p.
- Thornton, C.P., 1953, The geology of the Mount Jackson quadrangle, Virginia [Ph.D. dissert.]: New Haven, Connecticut, Yale University, 211 p.

TRAVERTINE-MARL DEPOSITS AND PREHISTORIC ARCHAEOLOGICAL ASSOCIATION

William M. Gardner

CONTENTS

	Page
Abstract.....	101
Introduction.....	102
Archaeological background.....	102
The archaeological sites: their settings and associations.....	105
The Williams Spring complex.....	105
44Fk13 to 15.....	105
44FkA.....	105
44Fk49.....	106
The Falling Springs Run site.....	108
Chapel Run.....	108
Maryland.....	109
Climate and time.....	109
Summary and conclusions.....	109
References cited.....	110

ILLUSTRATIONS

Figure		
1. Portion of Winchester 7.5-minute quadrangle showing location of Williams Spring complex.....		103
2. Schematic cross section of Darlington marl pit.....		104
3. Projectile points from site 44Fk49.....		106

TABLE

Artifact analysis of site 44Fk49 Locus A.....	107
---	-----

ABSTRACT

Prehistoric artifacts were first reported in association with travertine-marl deposits in a 1924 study of the Falling Springs Run deposit near Verona, Virginia. In 1985, a second discovery was reported in a similar context along Redbud Run near Winchester, Virginia. This latter location subsequently produced projectile points dating to 7200 to 6800 B.C., the earliest prehistoric artifacts recorded in association with marl deposits. Analysis of artifacts from the Redbud

Run site and the topographic setting indicate a transient, limited-activity camp, along the edge of an old pond or still-water stream. Lithic materials employed by the inhabitants include both local material and metarhyolite from the Maryland Blue Ridge. At least a portion of the archaeological site was covered with marl by post-occupation deposition. Between 500 B.C. and A.D. 200, another prehistoric group briefly visited the Redbud Run marl pit location, encamping on the opposite side of the stream on previously formed marl in what was apparently a stream-side setting. These artifacts were later covered with calcium carbonate-rich soil but no

marl. The presence of pottery at the Falling Springs Run site indicates that the reported cultural remains date after 1000 B.C., but more precise dating is not possible based on current information. The encampment at Falling Springs Run was also on a previously formed marl. Other travertine-marl pits in the Shenandoah Valley have been reported to contain prehistoric artifacts, but these reports cannot be corroborated. Studies in the Hagerstown Valley in Washington County, Maryland, have noted artifacts in extinct ponds in both floodplain and non-stream settings in which calcium carbonate was precipitated as marl at various stages in the history of the ponds. Ranges for the dates of occupation of these sites were estimated to be between 8000 and 700 B.C., a span which agrees with the Virginia evidence. The primary attraction of both the Virginia and Maryland locations seems to have been water and the associated flora and fauna. The juxtaposition of calcium carbonate precipitates and prehistoric artifacts in both cases appears coincidental.

INTRODUCTION

While reports of prehistoric artifacts in association with travertine-marl deposits in the Shenandoah Valley of Virginia have been minimal, at least two reports (Collins, 1924; Hubbard and others, 1985) of such an association have been published. In addition, a recent review (Curry and Stewart, 1986) addressed associations of prehistoric cultural materials and extinct ponds containing marl deposits in the adjacent Hagerstown Valley of Washington County, Maryland. In these studies, the artifacts were reported to be within the deposits, in soils which have built up on top of the deposits, or adjacent to the deposits. In 1985, William F. Giannini, of the Virginia Division of Mineral Resources, recovered prehistoric pottery fragments, or sherds, from the commercially mined Darlington marl pit on Redbud Run (Figures 1 and 2), just north of Winchester, in Frederick County, Virginia. These finds were published in a general review article (Hubbard and others, 1985) and are reported by Giannini (this volume). Subsequent visits to this area revealed the presence of two distinct and spatially separated artifact-bearing localities dating from different times and situated on surfaces which had different formational histories. Because of the temporally diagnostic nature of the ceramics, the period of habitation of the originally reported location could be placed between 500 B.C. and A.D. 200 (not A.D. 750-1000 as originally reported in Hubbard and others, 1985). The absence of pottery at the second location, plus other lines of information such as the high incidence of lithic artifacts of metarhyolite, a material rarely employed after 1000 B.C. by the prehistoric inhabitants of the Shenandoah Valley, indicated an earlier culture. A single temporally diagnostic spear point (Figure 3b), known as Kirk Stemmed (Coe, 1964), dating to approximately 7200 to 6800 B.C., was later recov-

ered from this locality. A more detailed study of this second locality involving intensive artifact collecting procedures and analysis of the recovered material was subsequently undertaken. The initial discovery area and other exposed surfaces of the entire deposit were examined. No additional artifacts were recovered. Other sites from the nearby springs, which are the headwaters of the stream in which the travertine-marl formed, are known.

The purpose of this presentation is to report the results of the archaeological studies at the Darlington marl pit, to compare these results to the other reports or studies of prehistoric archaeological remains and travertine-marl deposits in the Shenandoah Valley of Virginia and the Hagerstown Valley of Maryland, and to offer general observations and tentative conclusions concerning what the archaeology/travertine-marl pit associations can contribute to our knowledge. The analysis of the Darlington marl pit collection represents the first detailed study of an archaeological site in association with a travertine-marl deposit and is designed to situate in time the archaeological evidence at this location and delimit the functional nature of the occupation at the site. Observations are also made on the environmental setting before, during, and after the periods of occupation. The comparative review of the admittedly scanty available data addresses differences and similarities in the nature of the sites.

ARCHAEOLOGICAL BACKGROUND

The Shenandoah Valley and surrounding area have been inhabited for at least 11,000 to 11,500 years (Carr and Gardner, 1978; Gardner and Boyer, 1978; Hoffman and others 1979; Stewart, 1981; Wall, 1981; Gardner, 1986). Within this time span, archaeologists recognize several divisions. Of pertinence to this study, because of the temporal range of the artifacts associated with the travertine-marl deposits, are the Archaic (8000-1000 B.C.) and Woodland (1000 B.C. to ca. A.D. 1700) periods. The Early (8000-6800 B.C.), Middle (6800-2500 B.C.), and Late (2500-1000 B.C.) Archaic, and Early (1000-500 B.C.), Middle (500 B.C.-A.D. 900), and Late (A.D. 900-1700) Woodland divisions (Gardner, 1986) are further divided into phases such as the Early Archaic I, II, and III. Ceramics are associated only with the Woodland period. An example of the Kirk Stemmed projectile point type (Coe, 1964) was found at a Darlington marl pit locus. This point type is bracketed between 7200 and 6800 B.C. by radiocarbon dates for the "Fifty" site in the Flint Run Paleoindian-Early Archaic complex along the South Fork of the Shenandoah River. This temporal range is in agreement with dates reported by Chapman (1976) and places the projectile point style in the third and final phase of the Early Archaic (Early Archaic III). Prehistoric ceramics with net-impressed surfaces and tempered with crushed rock, such as those found at the other Darlington marl pit locus by Gian-

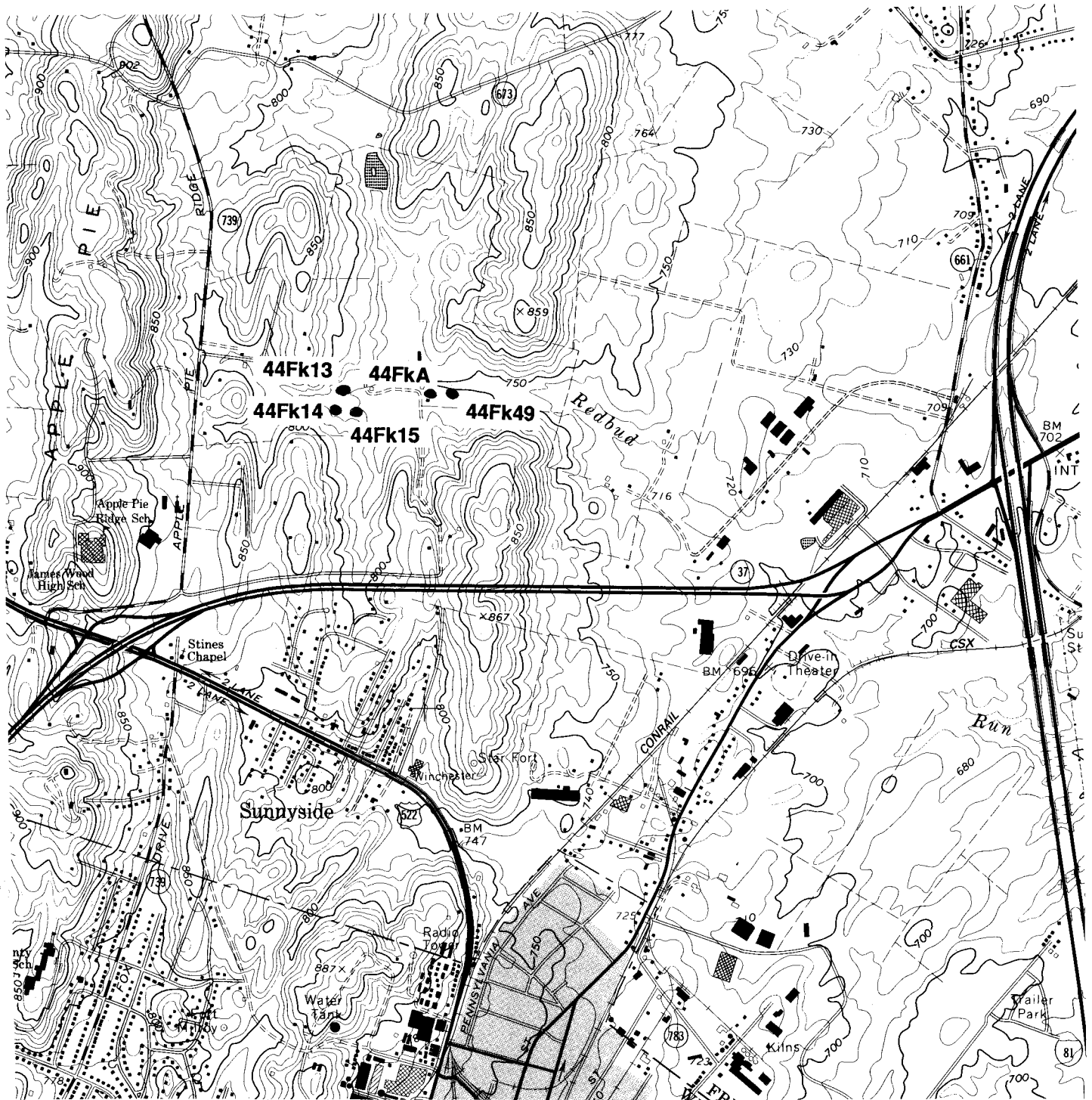
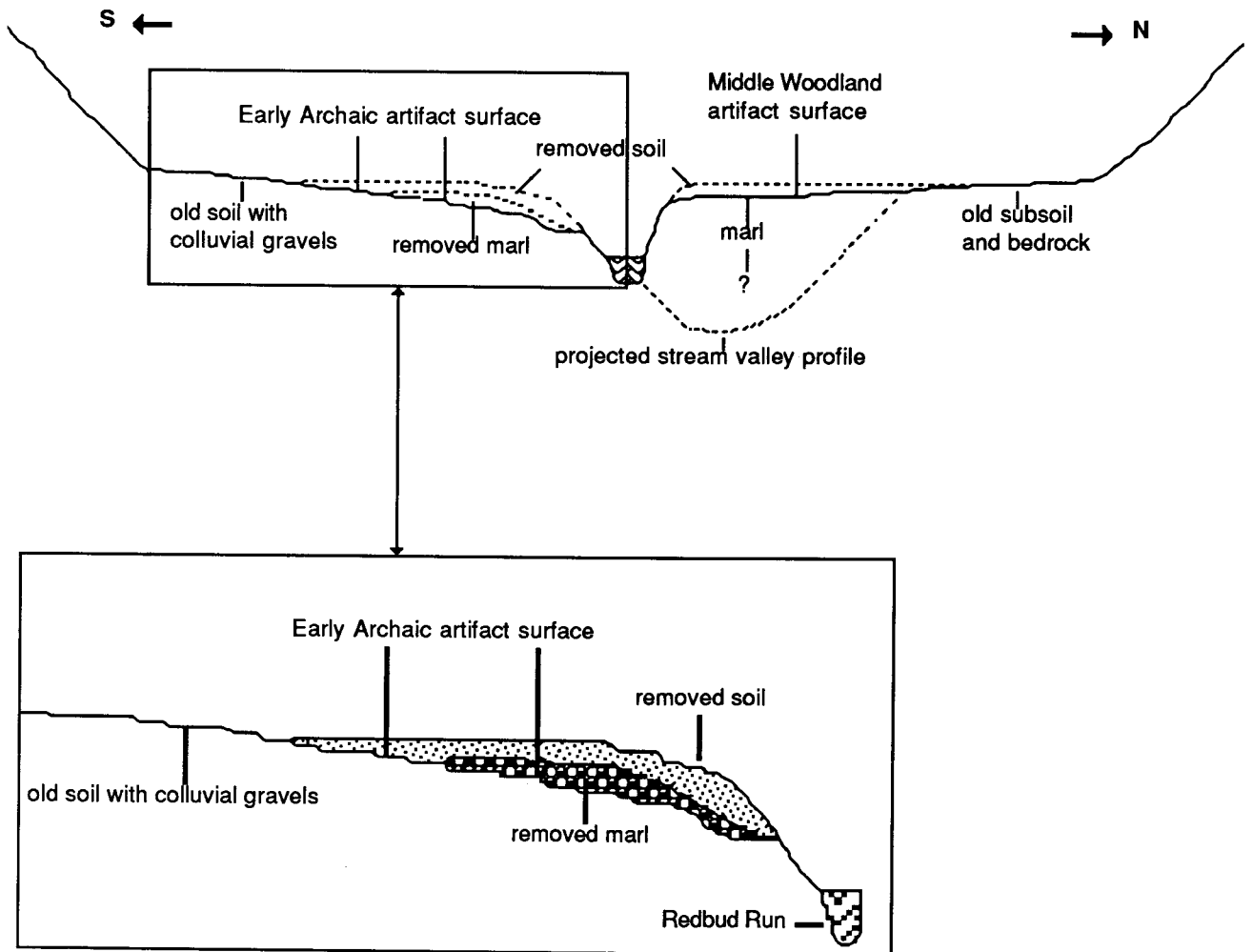


Figure 1. Portion of Winchester 7.5-minute quadrangle showing location of Williams Spring complex of archaeological sites.

nini, have not been found in radiocarbon-dated contexts in the Shenandoah Valley. Recent unpublished research has shown that ceramics of this type date to post-750 B.C. Similar ceramics from the Potomac Piedmont and Coastal Plain provinces have age dates between 500 B.C. and A.D. 200. Crushed-rock-tempered, net-impressed ceramics are considered the

major diagnostic artifact of the earlier of the two Middle Woodland phases (Gardner, 1982).

Lithic materials provided the basic element in the technology of the area's prehistoric populations. The primary lithic materials employed were chert, or flint (including chalcedony and jasper), quartzite, quartz, and metarhyolite.



not to scale

Figure 2. Schematic cross section of Darlington marl pit showing prehistoric site locations.

The natural distribution of these materials is only partly known. Chert of varying knapping quality is widespread in the carbonate rocks of the Valley and Ridge province. Jasper, as that material is defined by archaeologists, is restricted to widely separated outcrops along the western edge of the Blue Ridge Mountains. The primary quartzites employed also occur along the western edge of the Blue Ridge Mountains but are much more widely and continuously distributed than jasper. Knapping-quality quartzite similar to the Blue Ridge Mountains varieties apparently occurs in other areas of the Valley and Ridge province and is relatively common in cobble form. The distribution of quartz is not fully known but is apparently relatively widespread. The metarhyolite used by the prehistoric populations in the area is assumed to be derived from the nearest available source, located in a region of the Blue Ridge Mountains from just north of Harper's Ferry, West Virginia, to Gettysburg, Pennsylvania.

Patterns of lithic selection can be clearly distinguished at

different periods in prehistory. During the earliest period (Paleoindian, circa 9200-8000 B.C.), a restricted range of microcrystalline lithic materials was employed. This material was often transported great distances, and its occurrence at a locality is a clue to Late Pleistocene or Early Holocene human activity. The local material most often selected by these early groups was jasper. The almost exclusive use of this material began to wane by 7500 B.C. as a broader range of lithic materials was increasingly employed. By Early Archaic III, diversity in choice prevailed. Some long-distance transport of raw material reflecting the extent of population movements continued, but this was increasingly augmented by expedient use of local materials. By 6800 B.C., commensurate with a major reduction in size of territorial ranges, proximity rather than the type of raw material controlled what was utilized.

Metarhyolite projectile points are commonly found at archaeological sites dating from 7500 B.C. as far south as the

mid-reaches of the North and South Forks of the Shenandoah River. At sites dating from 6000 B.C., metarhyolite artifacts within the Shenandoah Valley become rare more than a few kilometers south of the outcrops indicating a reduction in the geographic extent of exploitative forays. Near the outcrops, in the Hagerstown Valley, metarhyolite remains the primary raw material at sites dating from 7000 B.C. (Stewart, 1981). South along the Shenandoah Valley, metarhyolite use appears again at sites dating between 1800 and 1200 B.C. Ongoing investigations indicate this brief metarhyolite reappearance coincides with groups whose lithic mainstay was metarhyolite and who periodically shifted their settlements from the Potomac River south to the mid-reaches of the forks of the Shenandoah River. Quartzite was a preferred lithic material from 2500 to 1800 B.C. but was used at all times. Use of small quantities of jasper recurs during the Middle and Late Woodland. None of these patterns are inflexible and can only be used as guidelines, but with other lines of evidence they are supportive of chronological placement and population movements.

THE ARCHAEOLOGICAL SITES: THEIR SETTINGS AND ASSOCIATIONS

THE WILLIAMS SPRING COMPLEX

The Darlington marl pit is discussed in an earlier review of marl pits (Hubbard and others, 1985) and by Giannini (this volume). The archaeological site associated with the pit is 44Fk49. It is located within a few hundred meters of the head of Redbud Run (Figure 1), a tributary of Opequon Creek, which flows into the Potomac River. The head of Redbud Run consists of a series of springs known as Williams Spring. Associated with these springs are a number of archaeological sites, 44Fk13, 44Fk14, 44Fk15, and an unrecorded site, herein referred to as 44FkA. Together, these five sites form the Williams Spring complex. The artifacts from 44Fk13 to 15 were collected in 1979 and are reported in general terms on the state site inventory forms, copies of which are contained in Thunderbird Research Corporation (TRC) files in Woodstock, Virginia. The artifacts were not available for study. The artifacts from 44Fk49 and 44FkA are on repository with TRC and were available for study and are reported here in more detail.

44Fk13 to 15

The information on the form for 44Fk13 indicates the collection contained chert flakes, chert biface fragments, a chert core fragment, and a chert projectile point fragment of

a temporally non-diagnostic small-stemmed type. The reported inventory for 44Fk14 consists of metarhyolite, chalcedony, chert, and jasper flakes, two chert bifaces, a chalcedony biface, a quartz projectile point or biface, a chert projectile point, and a metarhyolite biface (45 mm long and 30 mm wide). Prehistoric artifacts reported for 44Fk15 include quartz and chert flakes, two jasper flakes, three chert biface fragments, and one chert projectile point. The chert projectile point is actually a preform rather than a point. It is probable that the reported jasper flakes are from Blue Ridge Mountains sources, but available information is inadequate for a positive identification.

All three of these sites are directly associated with the complex of springs at this locality as opposed to the stream. Because they were found as part of a site-location study, the sites were not examined thoroughly. Vegetation cover resulted in relatively poor visibility, which created adverse collecting conditions. This bias in the artifact collection made it impossible to determine the intensity of occupation or the site function.

44FkA

Site 44FkA was found in the course of the study of the Darlington marl pit. The collected inventory consists of one bifacially worked irregularly shaped chert block, probably a core fragment; two relatively thick and short fragments of chert, possibly from bifaces; one complete chalcedony flake 22 mm in length and 14 mm in width with multiple dorsal flake scars from biface reduction; one distal end of a chert biface; one small quartz chunk or core fragment; one complete jasper flake 30 mm long by 25 mm wide with multiple dorsal flake scars from biface reduction; two metarhyolite flakes; and a steep-angled chert end-scraper. It appears that the local blocky chert was selected, preliminarily shaped into bifacial cores, and then further reduced. The chert bifaces and comparatively thick chert flakes recovered are all products of early steps in the tool-making process, and it is possible that unifacial flake tools as opposed to bifacial core tools were the desired end product. Even though the metarhyolite flakes are incomplete it is worth noting they are larger and thinner than the chert flakes. One of the metarhyolite flakes has multiple dorsal scars indicating biface reduction. The thinness of the flake indicates a relatively late stage in the reduction process.

The chert is of the mottled, grayish variety which is common throughout the Shenandoah Valley and is presumed to be local, if not immediately contiguous to the site area. Chalcedony is also known to occur locally. The local chert occurs in two forms, bedded and nodular. The bedded chert is usually found along ridges, while nodular deposits occur in a variety of locations on valley floors. The nodules are often small angular chunks. The bedded chert often occurs in layers less than 60 mm in thickness. The size of the nodule

or thickness of the bed is a limiting factor in flake and finished-artifact size. The scraper contains areas of crust on its dorsal surface indicative of bedding thus suggesting that it was made of the local chert. The jasper flake is non-local and is probably Blue Ridge Mountains jasper. It is as thin as the metarhyolite flakes, which suggests it was removed from a bifacial tool as a result of resharpening. Although the site was only partially studied, field observations and the material collected suggest that it may represent a transient exploitative camp.

44Fk49

Site 44Fk49 (the Darlington marl pit) contains two temporally distinct and spatially separated areas of cultural activity (Figure 2). The earliest activity area, designated Locus A, is situated on the south side of Redbud Run. This area has produced no ceramics and it is here that a Kirk Stemmed projectile point (Figure 3b), partially coated with marl, was found during an earlier visit. Artifacts in Locus A were distributed along the edge of what appears to be an old terrace of Redbud Run (Figure 2 and see discussion below). The size of the activity locus was relatively small with maximum west-east dimensions of 42.1 m and north-south dimensions of 6.1 m. The eastern and western limits are defined by topographically lower areas, probably erosional scars of Redbud Run or a pond which formed along the stream.

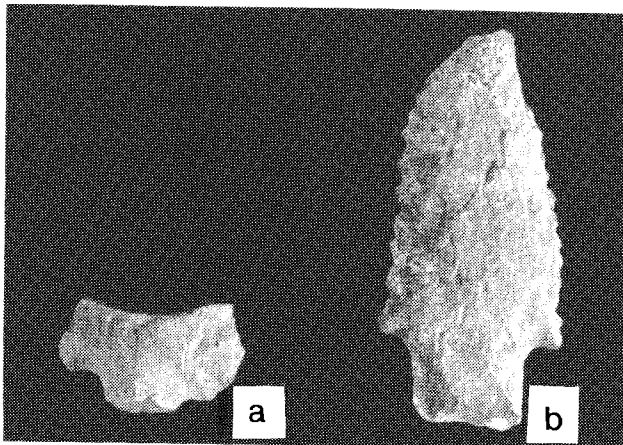


Figure 3. Projectile points from site 44Fk49: (a) Early Archaic metarhyolite point base, heavily resharpened; (b) diagnostic (point on right).

A surface collection in which every observed artifact was collected was conducted at Locus A. Surface visibility in the collecting area was excellent. Prior to the initiation of the surface collection, the site area was divided into two collecting units separated by an erosional low which appears to

have formed after mining of marl had ceased (post-1978). While the division was arbitrary, differences in artifacts did exist between the east and west collecting units, indicating that the erosional declivity may have been extant during the period(s) of prehistoric occupation. The eastern unit was 19.1x6.1 m. The western unit was 16.5x5.5 m. The northern perimeter of the collecting area was defined by the edge of a slope, presumably a terrace edge and the original boundary of the site. The southern margin was defined, in part, by a film of calcium carbonate washed downslope from piles of overburden surrounding the marl pit. Artifacts were scarce to absent before reaching this area, and it is presumed the collecting area as defined represents the southern boundary of the cultural activity.

The Table presents the results of the artifact collection. The use of the category "with bulb of percussion" provides the most accurate representation of flake totals (in the sense of minimum number of flakes); debitage amounts are quite low, indicating limited activity and occupation(s) of short duration. The absence of tools other than projectile points further supports this interpretation. Metarhyolite is the most prevalent raw material and is also the material which can be conclusively determined to be non-local. The absence of metarhyolite cores and the presence of a number of flakes with multiple flake scars on the dorsal surface indicate the material was brought to the site in the form of late-stage bifaces. More detailed analysis indicates that the metarhyolite flakes occur in two broad size clusters: 20x25 mm (to a maximum of 35x40 mm) and less than 15x15 mm. In the east unit, there were only three of the larger flakes. In the west unit, there were 10 flakes in the larger category. Overall, the flakes from the eastern unit were thinner. This type of evidence suggests somewhat different activities: tool resharpening in the eastern unit and tool production in the western section. Whether use of the two units was concurrent or representative of different episodes of occupation cannot be determined. The point recovered from the west collecting unit (Figure 3a) has been heavily resharpened showing a long history of use prior to being discarded. This use modification also altered the shape making it difficult to determine the actual form. The point, however, is Early Archaic and may be corner notched, and, thus, it may predate by a few hundred years the point collected earlier and illustrated in Figure 3b. It is probable that all of the metarhyolite flakes belong to the Early Archaic period.

The chert from the two collecting units is quite similar to the local material and is probably representative of expedient tool manufacture as opposed to the transport of previously prepared tools into the site. The chert is black and comes from small angular nodules. One of the chert bifaces is informative about how tools were made from this material. In attempting to reduce the raw material, the stone worker was constrained to the thickness of the chert nodule. The thickness of 23 mm is smaller than many of the larger sized flakes of the metarhyolite. A knapper starting from a core of such small size is

or thickness of the bed is a limiting factor in flake and finished-artifact size. The scraper contains areas of crust on its dorsal surface indicative of bedding thus suggesting that it was made of the local chert. The jasper flake is non-local and is probably Blue Ridge Mountains jasper. It is as thin as the metarhyolite flakes, which suggests it was removed from a bifacial tool as a result of resharpening. Although the site was only partially studied, field observations and the material collected suggest that it may represent a transient exploitative camp.

44Fk49

Site 44Fk49 (the Darlington marl pit) contains two temporally distinct and spatially separated areas of cultural activity (Figure 2). The earliest activity area, designated Locus A, is situated on the south side of Redbud Run. This area has produced no ceramics and it is here that a Kirk Stemmed projectile point (Figure 3b), partially coated with marl, was found during an earlier visit. Artifacts in Locus A were distributed along the edge of what appears to be an old terrace of Redbud Run (Figure 2 and see discussion below). The size of the activity locus was relatively small with maximum west-east dimensions of 42.1 m and north-south dimensions of 6.1 m. The eastern and western limits are defined by topographically lower areas, probably erosional scars of Redbud Run or a pond which formed along the stream.

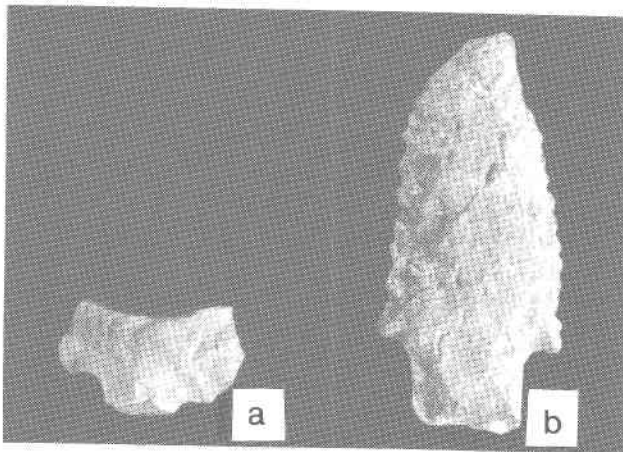


Figure 3. Projectile points from site 44Fk49: (a) Early Archaic metarhyolite point base, heavily resharpened; (b) diagnostic (point on right).

A surface collection in which every observed artifact was collected was conducted at Locus A. Surface visibility in the collecting area was excellent. Prior to the initiation of the surface collection, the site area was divided into two collecting units separated by an erosional low which appears to

have formed after mining of marl had ceased (post-1978). While the division was arbitrary, differences in artifacts did exist between the east and west collecting units, indicating that the erosional declivity may have been extant during the period(s) of prehistoric occupation. The eastern unit was 19.1x6.1 m. The western unit was 16.5x5.5 m. The northern perimeter of the collecting area was defined by the edge of a slope, presumably a terrace edge and the original boundary of the site. The southern margin was defined, in part, by a film of calcium carbonate washed downslope from piles of overburden surrounding the marl pit. Artifacts were scarce to absent before reaching this area, and it is presumed the collecting area as defined represents the southern boundary of the cultural activity.

The Table presents the results of the artifact collection. The use of the category "with bulb of percussion" provides the most accurate representation of flake totals (in the sense of minimum number of flakes); debitage amounts are quite low, indicating limited activity and occupation(s) of short duration. The absence of tools other than projectile points further supports this interpretation. Metarhyolite is the most prevalent raw material and is also the material which can be conclusively determined to be non-local. The absence of metarhyolite cores and the presence of a number of flakes with multiple flake scars on the dorsal surface indicate the material was brought to the site in the form of late-stage bifaces. More detailed analysis indicates that the metarhyolite flakes occur in two broad size clusters: 20x25 mm (to a maximum of 35x40 mm) and less than 15x15 mm. In the east unit, there were only three of the larger flakes. In the west unit, there were 10 flakes in the larger category. Overall, the flakes from the eastern unit were thinner. This type of evidence suggests somewhat different activities: tool resharpening in the eastern unit and tool production in the western section. Whether use of the two units was concurrent or representative of different episodes of occupation cannot be determined. The point recovered from the west collecting unit (Figure 3a) has been heavily resharpened showing a long history of use prior to being discarded. This use modification also altered the shape making it difficult to determine the actual form. The point, however, is Early Archaic and may be corner notched, and, thus, it may predate by a few hundred years the point collected earlier and illustrated in Figure 3b. It is probable that all of the metarhyolite flakes belong to the Early Archaic period.

The chert from the two collecting units is quite similar to the local material and is probably representative of expedient tool manufacture as opposed to the transport of previously prepared tools into the site. The chert is black and comes from small angular nodules. One of the chert bifaces is informative about how tools were made from this material. In attempting to reduce the raw material, the stone worker was constrained to the thickness of the chert nodule. The thickness of 23 mm is smaller than many of the larger sized flakes of the metarhyolite. A knapper starting from a core of such small size is

performer limited in what can be produced. It is therefore probable that the goal of local tool production was small unifacial informal flake tools which could be discarded after a brief use. Such short term use would not necessarily be discernible unless the edges had been used on, or against, hard material. The chalcedony is apparently also from local sources and some of the coloration of the flakes grades into the black chert. The chalcedony debitage occurred in a small locus in the eastern unit and is probably representative of a

Table. Artifact analysis of site 44Fk49 Locus A.

	West Unit			
	metarhyolite	chert	quartz	
without bulb of percussion	96	21	10	
with bulb of percussion	25	5	0	
chunks/core fragments	0	1	0	
preforms/biface fragments	1	2	0	
point fragments	1	0	0	
total	123	29	10	
	East Unit			
	metarhyolite	chert	quartz	chalcedony
without bulb of percussion	37	9	0	7
with bulb of percussion	14	1	0	2
chunks/core fragments	0	4	4	2
preforms/biface fragments	0	0	1	0
point fragments	1	0	0	0
total	52	14	5	11

single tool manufacturing episode. The quartz is probably local. It was not possible to determine when the chert, chalcedony, and quartz artifacts were produced. Expedient use of local materials, however, is common in Archaic period sites even when non-local materials were imported.

Conspicuous by their absence are Blue Ridge Mountains jasper, or other types of high knapping quality chert, and quartzite. The absence of jasper is good evidence that Locus A was not used by pre-7500 B.C. populations, whereas the absence of quartzite is equally good evidence for non-use by cultures dating to 2500-1200 B.C. The absence of pottery is supportive evidence for non-use of Locus A after 1000 B.C. Taken as a whole, the indications are that the entire occupation of Locus A can be placed before 6000 B.C. The non-occurrence of local Blue Ridge Mountains lithic materials suggests that the users of the site were moving south down Opequon Creek and not the Shenandoah River.

The artifacts were found resting on the surface of an old B horizon of a soil. The amount of clay on the individual peds and color indicate this horizon is older than the 10,000-years-B.P. surface at the Thunderbird and Fifty sites along the South Fork of the Shenandoah River. The formation of these horizons may coincide with the cool and wet episodes at the close of the last Wisconsin glacial advance (Gardner, 1974; Segovia, 1974). This time also was coincident with a downcutting episode of the South Fork of the Shenandoah River and

may be the time when the terrace on which the artifacts found at Locus A was formed. The absence of a soil profile beneath the prehistoric horizon dated between 9200 and 8800 B.P. may indicate a period(s) of erosion. Colluvium derived from the nearby slopes was also present on the same surface as the artifacts and may have resulted from the postulated erosional episode. At Fifty and other sites on the South Fork, an increase in slope erosion can be documented during the period around 9200 to 8800 B.P.

Some of the artifacts were coated with calcareous material. Many artifacts were coated with a thin calcareous deposit, almost like a whitewash, whereas an even greater number were only slightly stained. At least some of these latter artifacts were coated as a result of post-mining erosion of waste piles. Other artifacts appear to have been in calcium carbonate-rich soils and others appear to have actually been in a setting in which calcium carbonate encrusted them. In the interpretation offered here, the artifacts were deposited on a single surface. The artifacts at the northern, or lowest, portion of the site along the edge of the stream terrace were subsequently included in an environment in which calcium carbonate could encrust them. Those artifacts slightly further south were in a setting in which calcium carbonate-rich soil developed over them. They were coated with calcareous material by water percolating through the soil. The southern-most artifacts lay far enough from the terrace edge to be beyond the influence of the marl development and growth of the thin coat of calcium carbonate developed after they were exposed in the 1960s.

The overall interpretation suggests a very small group of people, possibly even an individual or two, stopping briefly along the banks of Redbud Run, Locus A, at two or more intervals during the period from circa 7500 to 6800 B.C. The inhabitants were engaged in limited activities on an exploitative foray from a longer term base camp which was probably located along Opequon Creek. The configuration of the apparent terrace edge on which the site is located, the coincidence of the termination of artifact distribution with this edge, and the known propensity (Gardner, 1987) for prehistoric groups to camp close to the water's edge on well-drained surfaces indicates that water was immediately contiguous. It is unclear if the adjacent setting at this juncture was that of a fast-flowing stream, sluggish stream, partially ponded stream, fully ponded stream, or some combination. Calcium carbonate encrustations around plant stems immediately adjacent to the site indicate relatively still water at some juncture but this need not have been coterminous with the prehistoric occupation. Except for the extensively resharpened and discarded projectile points, the only artifacts recovered were metarhyolite flakes from modification of previously prepared bifaces and flakes from knapping of local materials. This assemblage is suggestive of activities involved in the processing of vegetation as opposed to hunting, fishing, or birding, and it suggests a relatively still-water environment adjacent to the area of occupation.

At a time after the artifacts were developed, the extreme northern edge of the site was inundated. The absence of indications of artifact movement points toward a low-energy environment which would indicate a pond edge. Calcium carbonate subsequently was precipitated, burying this portion of the site and coating the artifacts. Calcareous soil developed in at least the middle section of the site. The southern extreme seems to have been outside of the marl/calcareous soil environment. The chronological range of the projectile points indicates that the inundation could have taken place only after 6800 B.C. The site remained buried until 1978, when soil was removed to build a lake at the site. The mining of marl in 1981 and 1982 does not seem to have destroyed any of the site at Locus A.

The second component at 44Fk49, Locus B, lies on the north side of Redbud Run (Figure 2). The artifacts consisted of less than a dozen pottery fragments, all of which were recovered during Giannini's visit. The surfaces of the pottery had been malleated with net and the paste mixed with crushed rock prior to firing. The crushed-rock-tempered, net-impressed pottery in the Shenandoah Valley dates to the first part of the Middle Woodland, between approximately 500 B.C. to A.D. 200. During subsequent visits to the location, no other evidence of human occupation was found even by scraping with trowel and shovel. Only a few rocks broken by fire, remnants of a stone-lined camp hearth, were noted. The artifacts were found at the interface of the soil zone and the underlying marl deposit, indicating the marl at this location had formed by 500 B.C. to A.D. 200. The depth of the soil removed by the heavy machinery during lake construction and mining operations is not known. The distance from the reported artifact finds to the current creek channel is approximately 12 m; however, there could have been a channel in the intervening area.

There is little information available for an interpretation of the function of the Middle Woodland component of site 44Fk49. The small number of ceramics and the absence of other recovered tools indicate a short-term occupation. The hearth rocks do indicate at least an overnight stay.

THE FALLING SPRING RUN SITE

Collins (1924) discusses the Falling Springs Run marl deposit and notes an association of Indian artifacts. Falling Springs Run is a first- or second-order tributary of the Middle River and joins that river northwest of Verona, Virginia. Like Redbud Run, a number of springs occur upstream from the deposits. Three terraces of travertine-marl materials occur along the stream valley. Collins notes that at the upstream end of each terrace, contiguous with and upstream of the travertine-marl are peat deposits. The reported vegetation buried in the peat includes chestnut oak and sycamore which is consistent with Holocene deposits (Gardner, 1974; Carbone, 1976).

Similar vegetation was found in a buried meander loop or a backwater swamp, dating to 7200 B.C., in the flood plain of the South Fork of the Shenandoah River. This does not preclude a Pleistocene date for the Falling Springs Run deposits since the hydrophytic sere may well have been the primary deciduous "relict" in the terminal Late Glacial vegetal mosaic (Carbone, 1976).

On the third terrace, Collins (1924) reports that "fragments of Indian pottery and pieces of charcoal were found buried to a depth of several feet." He further notes "the owner of the property stated that 'several rings of fire discolored stones with charcoal in their midst' were uncovered when the thin overburden of yellow clay was removed from the travertine." The occurrence of prehistoric remains at the interface of the soil and travertine-marl deposits is much like the situation at the later component of site 44Fk49, where occupation took place after the travertine-marl deposits had formed. The presence of several hearths suggests a rather large site, perhaps a base camp or hamlet, or a smaller, but frequently revisited site. Since no other information is provided about the pottery, all that can be stated with assurance is that the hearths date to after 1000 B.C. when ceramics first appear in the prehistoric record of the area. The presence of ceramics to a depth of a meter in what can only be interpreted as the underlying travertine-marl deposits can be accounted for in two ways. First, pits into which refuse was deposited could have been excavated into the underlying travertine by the groups responsible for the hearths, in which case, the ceramics would have to be concurrent in age with those at the interface of the soil and the travertine. Pits are common in riverine-associated base camps during the Woodland era. Second, it is possible that the site may have had occupation levels from different ceramic phases superimposed over one another. If this were the case, a sequence of events would be necessary in which there was periodic marl deposition, occupation of this surface, followed by abandonment, subsequent marl deposition, and utilization of the new surface by other prehistoric groups. The available data are insufficient to evaluate either interpretation. Had the latter occurred, however, it is probable Collins (1924) would have commented on calcium carbonate coatings on the ceramics.

CHAPEL RUN

Chapel Run is a tributary of the Shenandoah River in Clarke County. In the area near the mouth of the stream marl deposits of considerable depth have formed. Their lateral extent is not known. Viewed from the bank of Chapel Run, the depth in this location appears to be close to 6 m. The deposits were mined in the past (Sweet and Hubbard, this volume), but the area is now overgrown. Several different people (Julian Hammond, 1976, personal communication; C. Lanier Rodgers, 1987, personal communication) have re-

ported artifacts from this location. The reports are vague and little other than "lots of axes" is known about these artifacts. Given the setting, a significant stream near its junction with a major river, the presence of an archaeological site is not surprising. It is probable that most of the artifacts came from the soil overlying the marl.

MARYLAND

Curry and Stewart (1986) report on archaeological sites and a type of extinct pond in the Valley and Ridge province of Maryland. The particular ponds which were the focus of their study can often be determined by the occurrence of marl. In the definition employed in their work, marl "is a calcareous clay or mixture of clay and particles of calcite or dolomite, usually with fragments of shell" and "is a direct result of previously ponded water in limestone regions" (Curry and Stewart, 1986). They further note that in many instances an alternating sequence of marl and silt can be observed and that the deposits are thin. This description differs from the deposits described by Hubbard and others (1985) and Collins (1924), and it does not correspond with observations at the Williams Spring complex or Chapel Run. In each of these cases, the entire stream valley is filled with marl. A similarity does exist, however, because many of the ponds observed by Curry and Stewart (1986) formed in an alluvial setting. The Maryland and Virginia sites represent two different kinds of deposits. These differences are probably more important from the geological than the archaeological perspective, because it was the water and the associated flora and fauna that attracted humans, not the specifics of the chemical or hydrological setting.

In the Curry and Stewart (1986) archaeological overview, five types of sites are reported: pond-edge, pond-oriented, stray points in marl, pond-oriented sites in marl dating to dry intervals, and sites atop marl. Their pond-edge sites correspond to the Early Archaic component at 44Fk49, while the Middle Woodland component as well as the hearths at Falling Spring Run fall into the site-atop-marl category. The remainder of the Williams Spring complex could be considered pond-oriented, but they could also simply be spring-oriented. Of the sites they discuss, 18Wa281 is the only pond-edge site. This site is located on a spur just above flood-plain marl. Artifacts recovered at the site consisted of approximately three dozen metarhyolite flakes (the study area is on the Hagerstown Valley floor near the metarhyolite quarries and the presence of metarhyolite in this setting is not as time sensitive). On the spur the artifacts came from the interface of the clay soil and the marl. Site 18Wa282 produced metarhyolite bifaces and flakes on well-drained soil contiguous with marl. The artifacts came from the clay soil/marl interface. Both sites would be classified in the short-term-use category. A small base camp dating from the

Middle Archaic was reported on a low knoll overlooking one of these deposits. Isolated projectile points were found on the surface of now cultivated extinct ponds. These represent the stray-points-in-marl category. The points dated from the Late Archaic and, possibly, the terminal Early Archaic or early Middle Archaic. A Late Woodland (post A.D. 1000) village or hamlet site, 18Wa163, was found within brown clay loam overlying marl.

CLIMATE AND TIME

Curry and Stewart (1986) attempt to correlate the history of the Maryland ponds with the climatic sequence for the area put forth by Carbone (1976). This does not seem to be feasible for the type of stream-valley marl deposits discussed for the Virginia area because stream order, location along stream, and other factors vary too widely, and, if Hubbard and others (1985) are correct, the dynamics of the travertine-marl deposits of stream valleys are continuous with growth both across the stream valley and downstream. Hubbard and his associates and Curry and Stewart (1986) all place the development of the respective deposits in the Holocene. This seems to be the case at site 44Fk49. It is also possible that the relative warmth of the post-glacial era, whether seasonal as Hubbard and others (1985) suggest, or long term as Curry and Stewart (1986) indicate, may have been necessary for this kind of development to take place. Hubbard and his colleagues indicate continuing growth of the stream-associated travertine-marl deposits up to the historic period, with such growth decreasing as a result of the accelerated erosion of the post-17th century. Curry and Stewart (1986) feel the marl ponds in Washington County, Maryland, had all but dried up by 700 B.C.

SUMMARY AND CONCLUSIONS

The earliest prehistoric material collected from a travertine-marl deposit in the Shenandoah Valley of Virginia, or other types of marl deposits in Maryland, comes from the Darlington marl pit site (44Fk49) in Frederick County, Virginia. Locus A at this site produced one definite and one possible Kirk Stemmed projectile point datable from 7200 to 6800 B.C. This places it within the Holocene, the time assumed by most workers to be when travertine-marl deposits first began to form. In the Virginia area, travertine-marl deposits formed along streams which had their origins as carbonate-rich springs or which had a significant portion of their course through carbonate bedrock. Where travertine-marl deposits formed, they may be as wide as the valley and can reach considerable depths.

Arbitrary division of Locus A at site 44Fk49 into two

collecting units in order to determine if activity or chronological differences existed across the site demonstrated the existence of patterned cultural differences. Although the cultural significance of this is not of particular import, the patterning does indicate minimal post-deposition movement. Use of the location took place prior to its being covered by marl and on a land surface which probably was formed after 15,000 B.P. The artifact distribution at the site is associated with what appears to have been a low terrace, probably associated with an episode of ponding of the stream. The location of the archaeological site was near the extreme southern limits of the pond. Following inundation, calcium carbonate was precipitated from solution, creating a thin covering of marl. Many of the artifacts were partially coated with a carbonate material, presumably a result of deposition by water percolating from above. Only a few artifacts were coated with calcium carbonate, indicative of inundation by water. Collecting procedures were not sufficiently controlled to determine the location of the calcium carbonate-coated artifacts. An attempt to develop a lake and commercial mining of the marl deposit resulted in the removal of most of the overburden. The remainder was eroded, thereby exposing the artifacts.

Site 44Fk49 also yielded a Middle Woodland occupation at Locus B dating to somewhere between 500 B.C. and A.D. 200. This occupation was defined by a small hearth on the surface of, but not within, the marl. Between 0.3 and 0.7 m of soil had covered the artifacts and the associated hearth. There was no evident post-habitation inundation by water, and the carbonate coating of the artifacts appears to be the result of movement of calcium carbonate in solution through the overlying soil horizon.

The two occupation loci at 44Fk49, although separated by several millenia, fall into the generalized category of transient camps. Sites of similar function but unknown time periods (the Williams Spring complex) are found around the series of springs which form the head of Redbud Run a hundred meters upstream. At the time of the Early Archaic occupation at 44Fk49, the immediate environmental setting seems to have been that of a pond edge or other low-energy aquatic environment. The Middle Woodland component appears to have been associated with a stream-side habitat.

Reviews of other locations with reported travertine-marl and prehistoric sites only provided indirect data. The Falling Spring Run site contained ceramic-bearing fire hearths sitting on marl deposits at the base of the overlying soil zone (Collins, 1924). Ceramics found by Collins (1924) at depths of less than a meter into the marl could either be the result of intrusive pits dug during prehistoric occupation or from a series of occupations sitting on alternating layers of marl. In this latter case, it would be necessary to postulate repeated episodes of ponding and marl formation, occupation by prehistoric groups on the dry and hardened surface, and inundation of this surface. All of this had to have occurred after 1000 B.C., because pottery is present throughout.

A study of prehistoric artifacts in various associations with extinct ponds containing marl in the Great Valley of Maryland (Curry and Stewart, 1986) revealed a similar cultural picture as that observed in Virginia. The geological setting, however, differs. The Maryland marl deposits are reported as low areas which were once ponds, ponded streams, or ponded meander scars. The deposits are thin and occasionally interbedded with soil accumulations suggesting recurrent episodes of ponding, drying, and calcium carbonate precipitation. Although no artifacts have been found in direct association with any of these deposits, prehistoric artifact scatters have been found along the edges of these ponds, on higher ground overlooking the ponds, and in extinct ponds which have been cultivated. The context of these latter sites cannot be stated with assurance because cultivation in the historic period has mixed the deposits. The type of sites include short term, base camps, and stray projectile point finds. Based on climatic and settlement pattern models for the area, Curry and Stewart (1986) predicted that the earliest components would date to the Early Archaic, whereas the latest would be prior to 300 B.C. Both ends of this time range are in accord with the evidence available from the sites in Virginia.

At least some of the marl deposits are post-Pleistocene, based on the archaeological evidence and a lack of reported Pleistocene faunal remains coated with calcium carbonate. It would be premature to generalize this chronology to all deposits. There have been only two archaeological studies and one of these (the present study) has been incidental rather than systematic. In order to address specific research questions, a systematic study of the Virginia travertine-marl deposits most likely to contain archaeological sites is needed. Detailed studies of several travertine-marl deposits might also allow correlation of episodes of major travertine-marl development with Holocene climatic episodes as suggested for the Hagerstown Valley deposits studied by Curry and Stewart (1986). In any of these studies, however, it is necessary to remember that it was the flora and fauna of the riparian setting at different periods in its evolution which attracted prehistoric populaces and not the travertine-marl, because no evidence exists of pre-Columbian use of this material.

REFERENCES CITED

- Carbone, V.A., 1976, Environment and prehistory in the Shenandoah Valley [Ph.D. dissert.]: Washington, D.C., The Catholic University of America, 227 p.
- Carr, K.R., and Gardner, W.M., 1978, A preliminary archaeological resources reconnaissance of Berkeley County, West Virginia (unpublished manuscript): Martinsburg, West Virginia, Berkeley County Historic Commission, 98 p.
- Chapman, Jefferson, 1976, The Archaic period in the lower Little Tennessee River valley-the radio-carbon dates: *Tennessee Anthropologist*, v. 1, p. 1-12.

- Coe, J.L., 1964, The formative cultures of the Carolina Piedmont: Philadelphia, Pennsylvania, Transactions of the American Philosophical Society, new series, v. 54, 130 p.
- Collins, R.E.L., 1924, Travertine deposits in Virginia: Pan-American Geology, v. 41, p. 103-106.
- Curry, D.C., and Stewart, R.M., 1986, Extinct ponds and prehistoric site distribution: implications for paleoenvironments in the Ridge and Valley province: draft copy of paper presented to the 1986 Middle Atlantic Archaeological Conference, 7 p.
- Gardner, W.M., 1974, The Flint Run complex: pattern and process during the Paleo-Indian to Early Archaic, in Gardner, W.M., ed., The Flint Run Paleo-Indian complex: a preliminary report 1971-1973 seasons: Washington, D.C., The Catholic University of America, Archaeology Laboratory, Occasional Publication No. 1, p. 5-47.
- Gardner, W.M., 1982, Early and Middle Woodland in the Middle Atlantic: an overview, in Moeller, R. W., ed., Practicing environmental archaeology: methods and interpretations: Washington, Connecticut, American Indian Archaeological Institute, Occasional Paper No. 3, p. 53-86.
- Gardner, W.M., 1986, Lost arrowheads and broken pottery: Woodstock, Virginia, Thunderbird Museum, 98 p.
- Gardner, W.M., 1987, Comparison of Ridge and Valley, Blue Ridge, Piedmont, and Coastal Plain Archaic period site distribution: an idealized transect (preliminary model): Journal of Middle Atlantic Archaeology, v. 3, p. 49-80.
- Gardner, W.M., and Boyer, W.P., 1978, A cultural resources reconnaissance of the northern segment of Massanutten Mountain in George Washington National Forest, Page, Warren, and Shenandoah Counties, Virginia: Atlanta, Georgia, U.S. Department of Agriculture, Forest Service, Southeastern Region, Archaeological Report No. 2, 120 p.
- Hoffman, M.A., Foss, R.W., van Atta, J., and Vernon, R.W., 1979, Patterns in time: human adaptation in the Blue Ridge from 7000 B.C. to 1930 A.D. (unpublished manuscript): Philadelphia, Pennsylvania, U.S. National Park Service, 420 p.
- Hubbard, D.A., Jr., Giannini, W.F., and Lorah, M.M., 1985, Travertine-marl deposits of the Valley and Ridge province of Virginia - a preliminary report: Virginia Division of Mineral Resources, Virginia Minerals v. 31, n. 1, p. 1-8.
- Segovia, A.F., 1974, Geology and geochronology of the Shenandoah Valley in the Flint Run area, in Gardner, W. M., ed., The Flint Run Paleo-Indian complex: A preliminary report 1971-73 seasons: Washington, D.C., The Catholic University of America, Archaeology Laboratory, Occasional Publication No. 1, p. 48-65.
- Stewart, R.M., 1981, Prehistoric settlement/subsistence patterns and the testing of predictive site locations models in the Great Valley of Maryland [Ph.D. dissert.]: Washington, D.C., The Catholic University of America, 438 p.
- Wall, R.D., 1981, An archaeological study of the western Maryland coal mining region: the prehistoric resources: Baltimore, Maryland Geological Survey, Division of Archaeology, 183 p.

DATING TRAVERTINE

Henry P. Schwarcz

CONTENTS

	Page
Introduction.....	113
Methods of dating travertine.....	113
Radiocarbon.....	113
Uranium series.....	114
Electron spin resonance.....	114
Thermoluminescence.....	114
Paleomagnetism.....	114
Paleontology.....	115
Acknowledgments.....	115
References cited.....	115

INTRODUCTION

Travertine is a form of limestone, formed from freshwater by chemical and biological processes. Most travertine deposits that have been studied are relatively young in a geological sense, dating from the Cenozoic Era and largely from the last parts of it, the Pleistocene or Holocene epochs. The age of a limestone is generally obtained paleontologically, by the study of the fauna and flora enclosed in it and which were, in many cases, responsible for its deposition. Travertine is not generally datable by this means, but various physical methods of dating do exist that are applicable to them, depending on the actual time range over which they were deposited. This chapter presents a brief summary of the principal methods of absolute dating which are applicable to travertine.

Dating travertine is interesting not only because it gives an age for a geological deposit, but because travertine serves as geological markers that can give dates to other phenomena such as erosion, faunal assemblages, faulting, and clastic sedimentation. Techniques of dating travertine are essential to the development of a timescale for a wide variety of surficial processes, including biological evolution. Much of the development of absolute dating of travertine has been motivated by the fact that they are the loci of important archaeological sites such as Bilzingsleben, DDR (Schwarcz and others, 1988).

For each of the dating methods described, there are certain general precautions and limitations to consider when collecting samples for dating. Most importantly, the travertine should not show obvious signs of diagenesis, or having

been recrystallized, since it was initially deposited. The "age" obtained from diagenetically altered travertine might give the time of diagenesis, but, even more likely, the age could be entirely meaningless.

METHODS OF DATING TRAVERTINE

RADIOCARBON

Radiocarbon (^{14}C) is present in the atmosphere and is assumed to have been there at about the same concentration for many millenia. Any carbonate material, such as travertine, which is deposited at the earth's surface will contain a certain amount of ^{14}C fixed from the dissolved inorganic carbon of the water from which the travertine is precipitated (Taylor, 1987). The ^{14}C enters the water largely through direct absorption (exchange) from CO_2 in the atmosphere, through photosynthesis and respiration of plants, and by decomposition of plants and animals in the water. The measurement of a ^{14}C age requires a knowledge of the ^{14}C activity in the carbonate at the time it was deposited. For travertine, we can only assume that the activity in the past was the same as for modern travertine being deposited at the same spot today, given that the spring is still active. The emergent spring waters which typically deposit travertine usually contain much "dead" (non-radioactive) carbon from their limestone aquifer (Fontes, 1980). This dead carbon dilutes the "live" (^{14}C -bearing) atmospheric carbon, and, therefore, freshly deposited travertine has a low ^{14}C activity. Failure to correct

for this low initial activity can lead to excessively old apparent ages for travertine. When no modern equivalent is present, ^{14}C dating is risky. It is also unsafe to date fossil organic matter enclosed in travertine deposits because the plants will have been respiring CO_2 escaping from the stream water which is also depleted in ^{14}C compared with the atmosphere. Carbon-14 dates of travertine, therefore, should be treated with caution.

The potential time range for ^{14}C dates is from a few hundred years up to about 60,000 years. The limit is defined by the half-life of ^{14}C (5700 years). The new methods of accelerator dating are not particularly helpful, because they do not extend the time range. They are useful for small samples, but limited sample size is not a common problem in the dating of travertine.

URANIUM SERIES

Traces of uranium (U) are always deposited in the carbonate mineral of travertine. Thorium (Th) is not very soluble in spring waters and is usually absent from freshly deposited travertine. Uranium-234 undergoes radioactive decay to an isotope of thorium (^{230}Th) with a half-life of 75,000 years. We can determine the age of a travertine by measuring the amount of ^{230}Th that has formed from the radioactive decay of the ^{234}U in the rock. This result is called a $^{230}\text{Th}/^{234}\text{U}$ or, simply, a Th/U date (Gascoyne and Schwarcz, 1982). The age range is up to about 400,000 years. The isotope protactinium-231 (^{231}Pa) can also be used to date travertine in the same way over approximately the same time range (up to 300,000 years), but the travertine must contain at least 1 ppm U.

For both Th/U and Pa/U dating, we have to avoid travertine containing detrital contaminants (sand, silt, and mud), because this material contains Th (and Pa) and can lead to an apparently old age. Detrital Th can be detected, however, because it is always accompanied by the isotope ^{232}Th , which is not a product of radioactive decay. It is usually possible to find thin layers of travertine that are relatively detritus-free. There are various methods that can be used to correct for the detrital contamination, but these procedures are tedious and costly.

A few tens of grams of travertine are needed to obtain a Th/U date. Most dating is done using the alpha-spectrometric method and has a precision of about ± 5 percent. A newer method of mass spectrometric dating allows a precision of about ± 1 percent, comparable to that of ^{14}C (Li and others, 1989).

Radium (^{226}Ra) is also found in travertine and might be useful for dating younger deposits, because it has a half-life of 1600 years. One can measure the Ra content of modern deposits. Assuming that the older deposits started out with the same amount of Ra, the age back to about 10,000 years can

be estimated based on the radioactive decay of the radium. The ages from this technique are not very precise.

The $^{234}\text{U}/^{238}\text{U}$ isotope ratio of uranium in travertine also provides a kind of clock. This ratio approaches a value of 1.000 in infinitely old materials. If the isotope ratios in modern travertine at a given site are greater or less than 1.0 and if it is safe to assume that the initial ratio was always the same, then we can estimate ages back to about a million years. Establishing that the initial ratio was constant is best done by using the Th/U method (see above) to date the younger deposits. Then by back-calculating from the present-day $^{234}\text{U}/^{238}\text{U}$ ratio of each travertine layer, its initial ratio can be evaluated for constancy. The method works especially well where the spring depositing the travertine has emerged from a major, long-lived aquifer, in which case the uranium isotope ratio will probably have been the same for millions of years.

ELECTRON SPIN RESONANCE

Electron spin resonance (ESR) dating is based on the measurement of a type of radiation damage that the carbonate crystals experience as a result of bombardment by cosmic rays and natural radioactivity from their own atoms of uranium, thorium, and potassium (Grün and others, 1988). The method has been shown to work well on relatively clean, well-crystallized calcite that forms a minor part of some travertine, especially the overhangs (stalactites) on dam-like deposits that line the edges of pools. The time range is from a few thousand years up to a few hundred thousand years. Calcite exhibits many ESR signals, each characterized by its "g" value. This number determines where the signal occurs in an ESR spectrum. Only the signal with a g value of 2.0007 appears to be reliable for dating. Some samples also contain humic matter which gives a signal that appears to be datable.

THERMOLUMINESCENCE

Thermoluminescence (TL) dating ought to be applicable to travertine since it has been shown to work on stalagmites (Debenham and Aitken, 1984). There do not appear to be any published reports of attempts at TL dating of travertine. Thermoluminescence is applicable over the same time range as ESR, but it is probably somewhat less reliable. It is also extremely sensitive to detrital contamination.

PALEOMAGNETISM

When calcite is chemically precipitated in the form of stalagmites or travertine, it usually traps a weak magnetic

signal that records the direction and intensity of the earth's magnetic field at the time it was deposited (Latham and others, 1979). This remnant field can be used to learn something about the age of a travertine. For example, travertine older than 720,000 years may have a reversed magnetic orientation, because this was the date of the last reversal of the earth's field. The ages between then and now can be determined less precisely from measurement of secular variation (SV) which is due to the slow drift of the magnetic pole around the geographic (spin) pole. Age measurements can only be done by comparison with a dated record from somewhere else. Paleomagnetism of travertine is probably more interesting for its geophysical record than as a dating method.

PALEONTOLOGY

Many travertine deposits contain fossils, and these can often be used to give some clue to the age of the travertine. When combined with an absolute age method such as U-series, we can learn about the possible date of deposition. For example, the climatic cycles from glacial to interglacial conditions that North America has experienced have caused changes in faunal populations that should be clearly recorded in the travertine faunal assemblages. These can be correlated to particular glacial/interglacial stages (isotope stages) by one of the physical methods described above.

ACKNOWLEDGMENTS

The author acknowledges the assistance of grants from the Natural Sciences and Engineering Research Council (Canada) and the Social Sciences and Humanities Research Council (Canada).

REFERENCES CITED

- Debenham, N.C., and Aitken, Martin, 1984, Thermoluminescence dating of stalagmitic calcite: *Archaeometry*, v. 26, p. 155-170.
- Fontes, J.Ch., 1980, Environmental isotopes in groundwater hydrology, *in* Fritz, Peter, and Fontes, J.Ch., eds., *Handbook of environmental isotope geochemistry*: Amsterdam, The Netherlands, Elsevier Scientific Publishing Company, v. 1, p. 75-140.
- Gascoyne, Melvyn, and Schwarcz, H.P., 1982, Carbonates and sulphates, *in* Ivanovich, Miro, and Harmon, R.S., eds., *Uranium series disequilibrium dating*: Oxford, England, Oxford University Press, p. 268-301.
- Grün, Rainer, Schwarcz, H.P., Ford, D.C., and Hentsch, Barbara, 1988, ESR dating of spring deposited travertines: *Quaternary Science Reviews*, v. 7, p. 429-432.
- Latham, A.G., Schwarcz, H.P., Ford, D.C., and Pearce, G.W., 1979, The paleomagnetism of stalagmite deposits: *Nature*, v. 280, p. 282-284.
- Li, W.-X., Lundberg, J., Dickin, A.P., Ford, D.C., Schwarcz, H.P., McNutt, R.H., and Williams, D., 1989, High-precision mass-spectrometric uranium-series dating of cave deposits and implications for paleoclimate studies: *Nature*, v. 339, p. 534-536.
- Schwarcz, H.P., and Blackwell, Bonnie, 1983, Uranium series disequilibrium dating, *in* Rutter, Nathaniel, ed., *Dating methods of Pleistocene deposits and their problems*: Geoscience Canada Reprint Series No. 2, p. 9-18.
- Schwarcz, H.P., Grün, Rainer, Latham, A.G., Mania, Dietrich, and Brunacker, Karl, 1988, The Bilzingsleben archaeological site: New dating evidence: *Archaeometry*, v. 30, p. 5-17.
- Taylor, R.E., 1987, *Radiocarbon dating: an archaeological perspective*: Orlando, Florida, Academic Press, 212 p.

THE ALGAL FLORA OF TRAVERTINE: AN OVERVIEW

Allan Pentecost

CONTENTS

	Page
Abstract.....	117
Introduction.....	118
The algae and their distribution.....	118
Cyanobacteria (blue-green algae).....	118
Eukaryotic algae.....	119
The biota of Virginia travertine.....	122
Ecology.....	122
Significance in travertine deposition.....	125
References cited.....	126

ILLUSTRATIONS

Figure	
1. Illustrations of algal genera associated with travertine.....	120
2. Scanning electron micrographs of <i>Oocardium</i> and <i>Vaucheria</i> from Turner Falls, Oklahoma.....	121
3. Distribution of <i>Oocardium stratum</i> worldwide.....	123
4. Colony of <i>Cladophora glomerata</i> along Marl Creek, Rockbridge County, Virginia.....	124

TABLES

Table	
1. Algae frequently recorded from travertine.....	118
2. Plant-related factors favorable to travertine deposition.....	125

ABSTRACT

Most active travertine possesses a rich algal flora, with the majority of algae belonging to the classes Cyanophyceae (cyanobacteria), Chlorophyceae (green algae), and Bacillariophyceae (diatoms). Two filamentous genera of cyanobacteria, *Phormidium* and *Schizothrix* are abundant and widely distributed, often forming nodular, calcified growths. The commonest encrusted green algae are *Gongrosira* and *Oocardium*. Diatoms belonging to the genera *Achnanthes*, *Cymbella*, and *Gomphonema* are also abundant. Ecologically, the algae can be divided roughly into two groups: 1) a perennial, usually encrusted community which include many cyanobacteria, *Oocardium*, and *Vaucheria*,

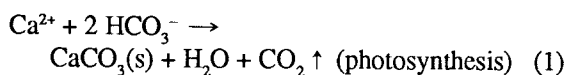
and the remains of these often become incorporated into the travertine matrix; 2) a seasonal community composed of superficial growths of diatoms, green, and other algae which do not normally become encrusted or preserved within the travertine.

The formation of travertine is sometimes the result of water alkalization promoted by algal photosynthesis. The significance of algae in this respect depends mainly upon the ratio of algal biomass to the rate of water discharge, irradiance, and temperature. Some algae, especially cyanobacteria, can trap and bind suspended calcite. Although evidence is limited, this process could initiate the extensive precipitation of calcite at some travertine surfaces.

INTRODUCTION

Most active travertine possesses a rich surface flora of algae and bacteria (including cyanobacteria), bryophytes, and sometimes spermatophytes. Since Ferdinand Cohn (1862) first drew attention to the growth of algae on such deposits, a substantial literature has developed describing the flora of individual travertines, mainly in Europe and North America. There have also been attempts to demonstrate specific plant associations (Frey and Probst, 1974), because a specialized flora is frequently found on travertine.

The deposition of travertine has also been attributed to the metabolic activities of these plants. The importance of algae in travertine formation has been long debated, because the number of algae present can vary widely, and they occasionally may be virtually absent (Pia, 1933 and 1934; Golubic, 1973; Pentecost, 1985a). Algal photosynthesis results in the removal of carbon dioxide from the surrounding water, which, for the sake of simplicity, may be regarded as a dilute calcium bicarbonate solution. The removal of carbon dioxide alters the equilibrium of the CO₂-bicarbonate-carbonate system (Equation 1) leading to the precipitation of calcium carbonate.



The amount of carbon dioxide removed by photosynthesis depends upon many factors, chief among them are the algal biomass present, the light intensity, and temperature. The extent to which photosynthesis can lead to the precipitation of calcium carbonate will vary, and may not always be a significant factor when compared with the outgassing of carbon dioxide to the atmosphere.

Many algae secrete mucilaginous substances capable of trapping and binding small particles of calcium carbonate. Thus, algae may have an important role in the stabilization, consolidation, and, perhaps, the initiation of travertine deposition, by providing centers of nucleation leading to general precipitation (Pentecost and Riding, 1986; Emeis and others, 1987).

This paper will review the distribution and ecology of travertine algae and consider their influence upon deposition processes.

THE ALGAE AND THEIR DISTRIBUTION

CYANOBACTERIA (BLUE-GREEN ALGAE)

The most frequently recorded genera of algae from travertine are listed in Table 1. Of these, the cyanobacteria are usually the most conspicuous members, often imparting a bluish-green or orange-yellow tinge to the deposits. Many

Table 1. Algae frequently recorded from travertine (author's observations).

1. Cyanobacteria (blue-green algae)	
<i>Aphanocapsa</i>	*
<i>Calothrix</i>	*
<i>Chamaesiphon</i>	
<i>Dichothrix</i>	*
<i>Hydrococcus</i>	
<i>Gloeocapsa</i>	*
<i>Homoeothrix</i>	*
<i>Lyngbya</i>	*
<i>Nostoc</i>	
<i>Phormidium</i>	**
<i>Plectonema</i>	
<i>Rivularia</i>	
<i>Schizothrix</i>	**
<i>Scytonema</i>	
2. Chlorophyceae (green algae)	
<i>Chaetophora</i>	
<i>Chlorotylum</i>	
<i>Cladophora</i>	*
<i>Cosmarium</i>	
<i>Gongrosira</i>	**
<i>Oocardium</i>	*
<i>Spirogyra</i>	
<i>Zygnema</i>	
3. Rhodophyceae (red algae)	
<i>Batrachospermum</i>	
<i>Chantransia</i>	
4. Xanthophyceae	
<i>Vaucheria</i>	*
5. Chrysophyceae	
<i>Chrysonobula</i>	
6. Bacillariophyceae (diatoms)	
<i>Achnanthes</i>	**
<i>Amphora</i>	
<i>Cocconeis</i>	*
<i>Cymbella</i>	**
<i>Diatoma</i>	*
<i>Didymosphenia</i>	
<i>Diploneis</i>	
<i>Epithemia</i>	
<i>Eunotia</i>	*
<i>Fragilaria</i>	
<i>Gomphonema</i>	*
<i>Meridion</i>	
<i>Navicula</i>	*
<i>Nitzschia</i>	*
<i>Rhoicosphenia</i>	
<i>Rhopalodia</i>	
<i>Synedra</i>	*

** Most commonly recorded.

* Frequently recorded.

species have been recorded from travertine by Prát (1929) and Pia (1933 and 1934), who reviewed the earlier literature. The number of species regularly recorded from travertine is, however, small. Most species are encrusted with calcite and the pattern of calcification is often similar to that found in certain stromatolites. For example, modern *Rivularia* bears a striking resemblance to late Proterozoic stromatolites exposed in the Sahara Desert (Janet Bertrand-Sarfati, 1987, personal communication). The occurrence of stromatolite-like structures in travertine may result from reduced burrowing activity by animals and seasonal changes in water chemistry leading to regular deposit laminations.

A small number of species, such as *Phormidium incrustatum* and *Homoeothrix crustacea*, seem to occur exclusively in carbonate-depositing environments (Fritsch, 1950; Golubic, 1967 and 1973; Kann, 1973; Pentecost and Riding, 1986). *P. incrustatum* (Figure 1a), a filamentous species exhibiting gliding motility, is probably the most frequently recorded species on travertine. The trichomes are of indefinite length, 4 to 6 μm in diameter and sometimes grow together in fascicles, forming small botryoidal colonies, particularly in quiet, shaded areas. (A trichome is a single row of cells, not to be confused with a filament, which in cyanobacterium terminology, consists of one or more trichomes enclosed by a sheath of polysaccharide). These cyanobacteria form a calcite-encrusted mat a few millimeters in thickness on the surface of travertine and their dependence upon light for growth limits the depth at which they can survive beneath the precipitated calcite (Pentecost, 1978).

Closely related to *Phormidium* is *Schizothrix*, a genus distinguished by its compound sheath (Figure 1b) enclosing several parallel trichomes. The number of trichomes enclosed is variable, and *Schizothrix* can be difficult to distinguish from *Phormidium*. The commonest species, *S. fasciculata* (= *S. calcicola* s. lato), is fairly easy to distinguish on account of its very narrow trichomes, 1 to 2 μm in diameter. *Lyngbya* may also occur and is distinguished by its rigid sheath enclosing a single trichome. In other respects, species of *Lyngbya* resemble those of *Phormidium*.

The remaining important genera belong to the Rivulariaceae, which are characterized by their tapering trichomes and the frequent production of heterocysts, specialized thick-walled nitrogen-fixing cells. There are four common genera distinguished mainly by their morphology (Geitler, 1932). *Rivularia* forms gelatinous colonies up to 15 mm across (Figure 1c), which often extend to form a thin stratum in flowing water. The colonies are remarkable for their copious mucilage, within which calcite is precipitated as regular bands. *Dichothrix* is similar, but it is non-gelatinous and usually forms much smaller tufts. In *Calothrix*, the filaments are unbranched. All three genera possess heterocysts at their broad bases. *Homoeothrix* is distinguished by its lack of heterocysts. Like other genera, the colonies are usually densely encrusted with calcite, giving the travertine a characteristic botryoidal appearance.

The remaining commonly reported cyanobacteria, although frequently encountered, are not normally major components (Golubic, 1973). Several are non-filamentous, consisting of groups of rounded cells contained within a mucilaginous coat and include *Aphanocapsa* (Figure 1d), *Hydrococcus*, and *Gloeocapsa*. *Aphanocapsa* species are often reported (Pia, 1934), but the range of cell size within the colonies makes identification to species difficult.

Of the genera listed in Table 1, only *Nostoc* is regularly found uncalcified (Figure 1e). This cyanobacterium forms dark-brown, rubbery growths on the surface of travertine. Occasionally, growths of *Phormidium*, *Plectonema*, and *Tolypothrix* may also be found free of calcite, particularly during cold periods.

EUKARYOTIC ALGAE

These algae are invariably found growing on travertine where there is sufficient illumination. Representatives from five algal classes are frequently reported. Among the green algae, the desmid *Oocardium stratum* has only been found in carbonate-depositing environments (Golubic and Marcenko, 1958). *Oocardium* (Figure 1f) is a distinctive plant and is the best example of an alga known to be specifically associated with travertine formation. *Oocardium* forms pale-green colonies or crusts in flowing water, frequently where there is rapid calcite precipitation. The colonies consist of columns of mucilage, which support at their apices spheroidal, usually bilobate, green cells containing two chloroplasts. The mucilage is densely encrusted with calcite microspar (Figure 2A and B), and when the colonies are dried, the travertine surface is found to consist of a myriad of crystal faces, resembling a crust of sugar. The distribution of *Oocardium stratum*, the only species in the genus, is shown in Figure 3. Although infrequently reported, the species occurs in tropical to cool-temperate environments and appears to be more common in warmer regions such as the southern United States. In Europe the species has not been found north of latitude 55°. While it is common in parts of Belgium (van Oye, 1937), it is very rare in the United Kingdom where it grows in a few streams with temperatures averaging about 10°C (Whitton, 1974).

The most frequently reported green alga is *Gongrosira* (Pentecost, 1988) which is a small, richly branched cushion-forming plant (Figure 1g) easily mistaken in the field for *Oocardium*. About ten species of *Gongrosira* have been found on travertine but some species characteristics are known to be variable and the genus requires taxonomic revision. Most material in Europe conforms to *G. incrustans*. *Gongrosira* forms densely calcified crusts or cushions, 1 to 5 mm wide, which are found worldwide. Frequently, decalcified colonies reveal a mixture of *Gongrosira* and several filamentous cyanobacteria forming "composite" cushions. Closely related to *Gongrosira* is *Chlorotylum*, which is

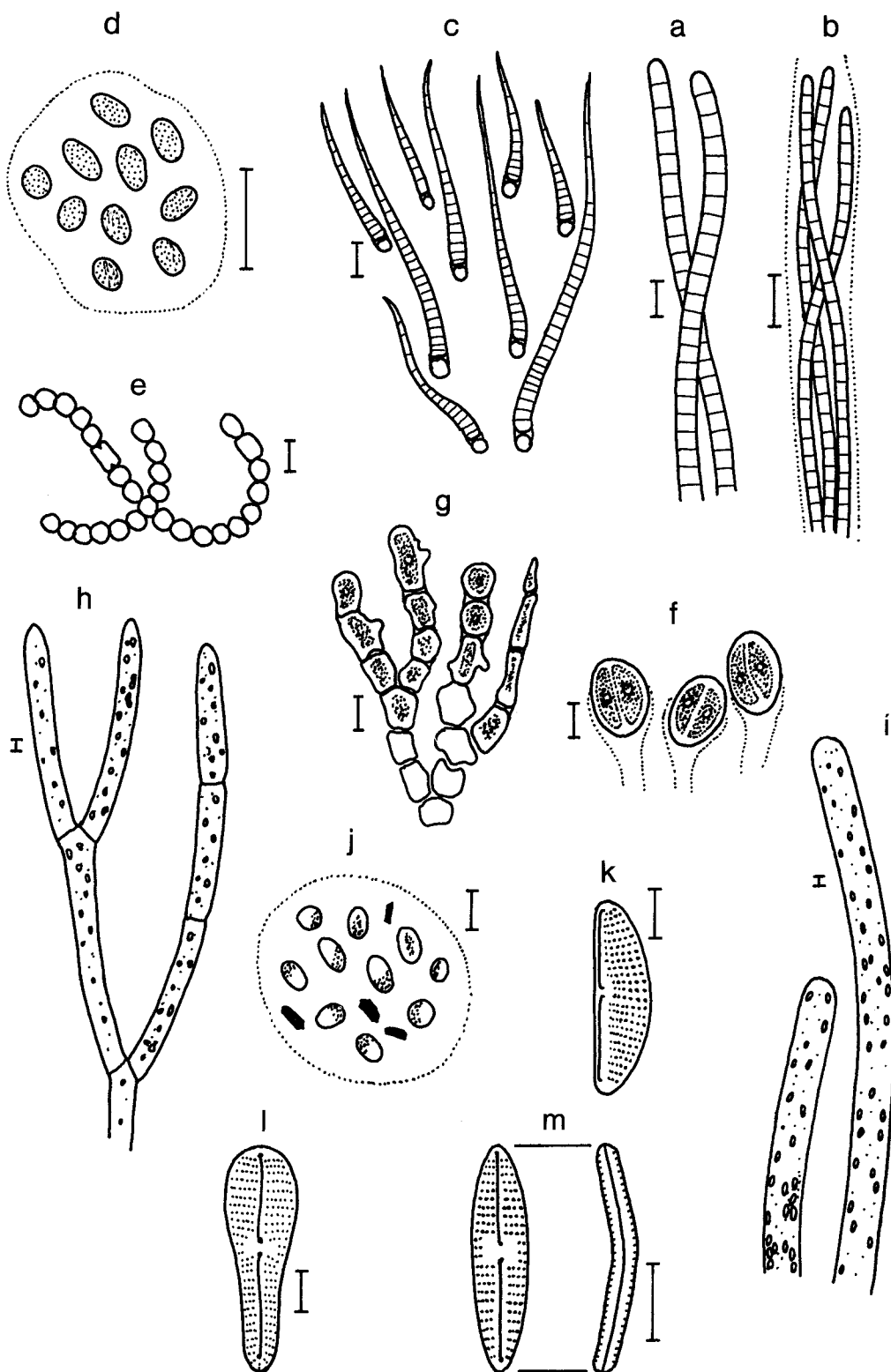
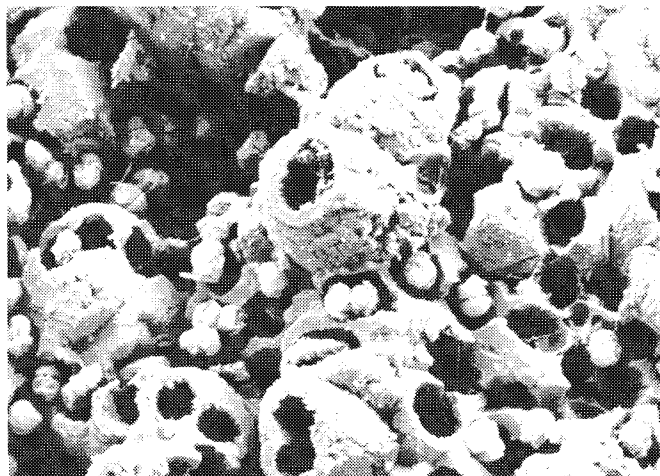
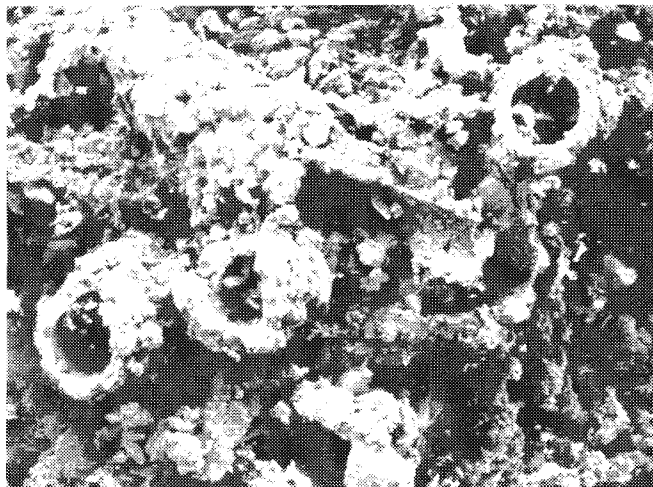


Figure 1. Illustrations of algal genera commonly associated with travertine: (a) *Phormidium*, (b) *Schizothrix*, (c) *Rivularia* with basal heterocysts, (d) *Aphanocapsa*, (e) *Nostoc*, (f) *Oocardium*, (g) *Gongrosira*, (h) *Cladophora*, (i) *Vaucheria*, (j) *Chrysonobula*, (k) *Cymbella*, (l) *Gomphonema*, (m) *Achnanthes*. Scale bar 10 μm .

Figure 2. Scanning electron micrographs of travertine algae.



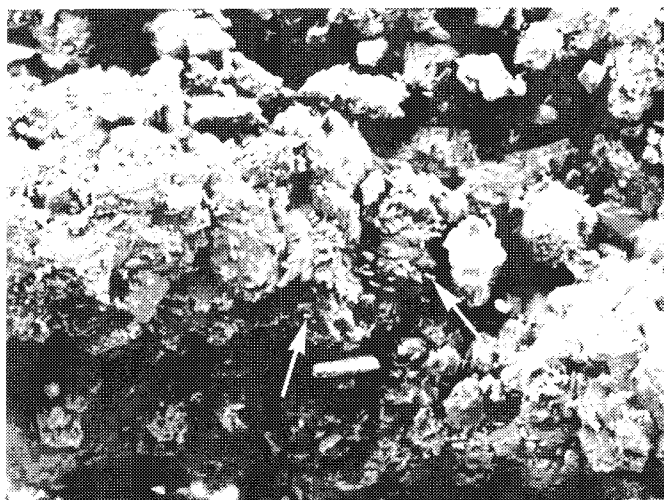
A. Colony of *Oocardium stratum* from Honey Creek, above Turner Falls, Arbuckle Mountains, Oklahoma. Many of the bilobate cells which measure $18\ \mu\text{m}$ in diameter, have become dislodged from their calcite tubes, leaving a honeycomb structure. Critical-point dried in ethanol series and Au-Pd coated. Collected January 1, 1988. Magnification 400X.



C. Fossil cf. *Vaucheria* from the travertine cliff overlooking Turner Falls, Arbuckle Mountains, about 20 m down the cliff. The smooth inner surface of one tube is exposed and was probably originally in contact with the cell wall. Inner tube diameter is $65\ \mu\text{m}$ and the encrustation thickness is 15 to $20\ \mu\text{m}$. Air-dried and Au-Pd coated. Collected January 1, 1988. Magnification 200X.

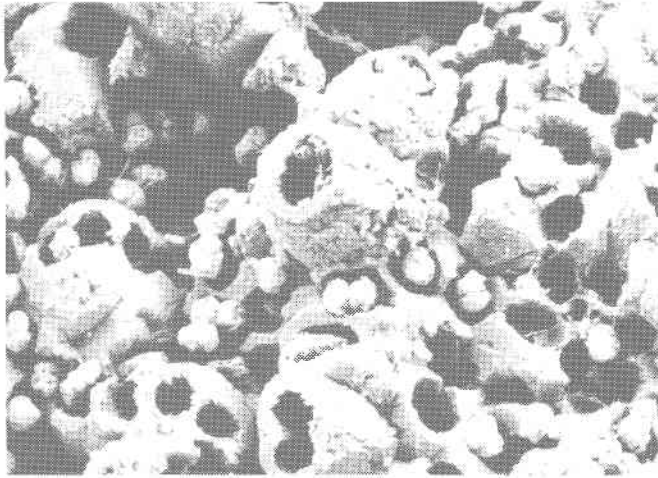


B. Detail of *Oocardium* colony. The calcite tubes form around each cell and traces of mucilage can be seen along the inner margin and within the body of the tubes. The flat tube ends are part of a single crystal face which can extend across hundreds of cells. Bacteria may be seen on this face. Note the ornamented cell wall of *Oocardium*, typical of the family to which the species belongs. Magnification 1600X.

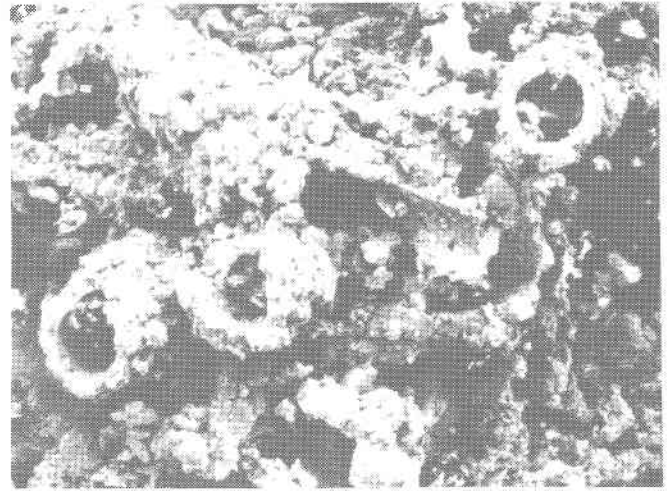


D. Detail of the surface encrustation on *Vaucheria* showing the comparatively coarse, randomly orientated crystals on the outer tube surface. Crystals measure 20 to $40\ \mu\text{m}$ in diameter and are covered in small coccoid structures (arrows), possibly bacteria. Magnification 375X.

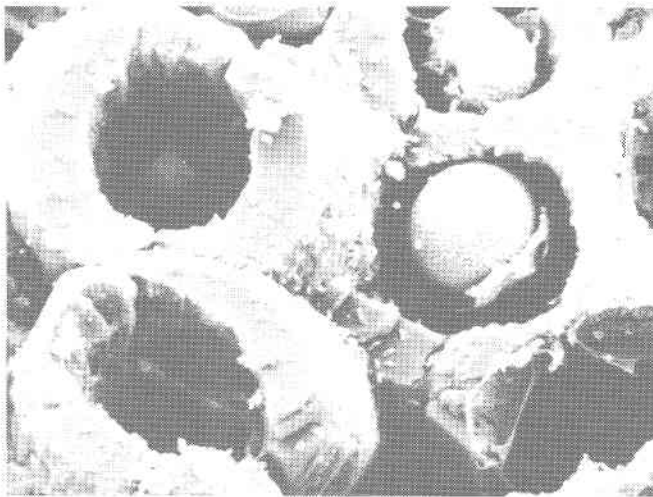
Figure 2. Scanning electron micrographs of travertine algae.



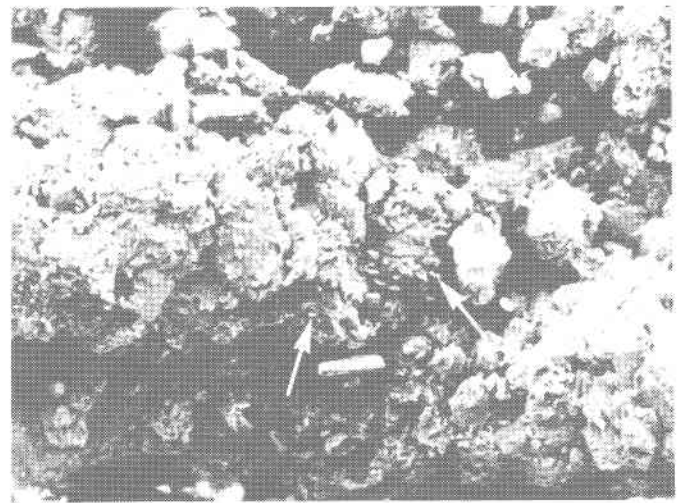
A. Colony of *Oocardium stratum* from Honey Creek, above Turner Falls, Arbuckle Mountains, Oklahoma. Many of the bilobate cells which measure $18\ \mu\text{m}$ in diameter, have become dislodged from their calcite tubes, leaving a honeycomb structure. Critical-point dried in ethanol series and Au-Pd coated. Collected January 1, 1988. Magnification 400X.



C. Fossil cf. *Vaucheria* from the travertine cliff overlooking Turner Falls, Arbuckle Mountains, about 20 m down the cliff. The smooth inner surface of one tube is exposed and was probably originally in contact with the cell wall. Inner tube diameter is $65\ \mu\text{m}$ and the encrustation thickness is 15 to $20\ \mu\text{m}$. Air-dried and Au-Pd coated. Collected January 1, 1988. Magnification 200X.



B. Detail of *Oocardium* colony. The calcite tubes form around each cell and traces of mucilage can be seen along the inner margin and within the body of the tubes. The flat tube ends are part of a single crystal face which can extend across hundreds of cells. Bacteria may be seen on this face. Note the ornamented cell wall of *Oocardium*, typical of the family to which the species belongs. Magnification 1600X.



D. Detail of the surface encrustation on *Vaucheria* showing the comparatively coarse, randomly orientated crystals on the outer tube surface. Crystals measure 20 to $40\ \mu\text{m}$ in diameter and are covered in small coccoid structures (arrows), possibly bacteria. Magnification 375X.

Closely related to *Gongrosira* is *Chlorotylum*, which is rarely reported but is known from the United States (New York State), Europe, and North Africa (Smith, 1933). The species are distinguished by their alternate long and short cells but are otherwise similar to *Gongrosira*. Probably the most conspicuous green alga of active travertine is *Cladophora* (Figure 1h), which consists of dense, green, matted filaments. They are frequently branched and have a coarse texture but are generally uncalcified. Species of *Cladophora* are also common worldwide in flowing hard waters and are often present where there is some organic pollution, such as the travertine falls at Tivoli, Italy. The remaining Chlorophyceae are of minor importance and growths of *Chaetophora*, *Zygnema*, *Spirogyra*, and *Cosmarium* are only occasionally encrusted with calcite (Prát, 1929; Pia, 1933 and 1934; Wallner, 1935a).

The red algae (Rhodophyceae) *Batrachospermum* and *Chantransia* are frequently reported from travertine, but they are not normally present in large numbers and rarely become encrusted with calcite (Fritsch and Pantin, 1946). These algae are members of a lotic community thriving in clean, hard water. Characteristic pale-green, densely encrusted tufts of *Vaucheria* (*Xanthophyceae*) are widespread on travertine and sometimes produce a distinctive matted fabric, readily indentifiable in old deposits (Figure 2C and D). *Vaucheria* is immediately distinguished from *Cladophora* by its lack of internal septation and lack of branching (Figure 1i). Material collected from travertine is usually infertile, but Emig (1917) found *V. geminata* and *V. sessilis* in Oklahoma.

In common with *Oocardium*, colonies of *Chrysonobula* (*Chrysophyceae*) have so far only been found associated with travertine. In the United Kingdom, *Chrysonobula* forms masses of thick, white, polysaccharide jelly attached to travertine in fast-flowing streams. The jelly surrounds small brown-yellow cells (Figure 1j), and numerous modified calcite crystals grow within the gel (Lund, 1961). The jelly is readily detached from the travertine so most of the precipitated calcite does not become consolidated.

The diatom flora of travertine is not well known even though diatoms are usually easy to identify to species level, which is not the case in many algal groups. Many diatoms are known to inhabit specialized niches, making them good "indicator" species (Patrick, 1977). There are 15 widely reported genera on travertine (Table 1, Figure 1k-m), but some of the species, such as *Achnanthes microcephala*, *Diatoma hiemale*, and *Didymosphenia geminata*, are widely distributed in hard waters. In a recent study of stromatolitic travertine, Winsborough and Golubic (1987) identified several diatoms associated with calcification, including *Gomphonema olivaceum* var. *calcareum* and *Nitzschia denticula*. The former may be characteristic of travertine and is possibly restricted to them. Diatoms rarely form distinctive encrusted bioherms and usually produce an irregular, often seasonal, growth on top of the perennial cyanobacterium/chlorophyte flora. Diatom frustules, which are made of silica,

are infrequently preserved in carbonate matrices, so comparatively little use can be made of them as paleoenvironmental indicators in travertine, although this does not imply that they are insignificant in carbonate deposition. In common with many cyanobacteria, the diatoms found on travertine exhibit gliding motility associated with mucilage secretion. This mucilage may assist in the consolidation of some travertine (Wallner, 1935b; Emeis and others, 1987; Winsborough and Golubic, 1987).

THE BIOTA OF VIRGINIA TRAVERTINE

The algal flora of Virginia travertine has been studied briefly by several workers. Steidtmann (1934, 1936) drew attention to algae and bryophytes on deposits at Lexington and noted their significance as frameworks upon which calcite is deposited. In two brief notes, Mathews (1962a, 1962b) mentioned the occurrence of *Oocardium stratum* in deposits of Montgomery County and considered the species an important carbonate-depositing agent. The cyanobacterium *Calothrix viguieri* and charophyte alga *Chara vulgaris* were also reported. Charophytes often precipitate considerable quantities of calcium carbonate as a result of their photosynthetic activity (Pentecost, 1984; Raven and others, 1986), and they can be important marl producers in shallow hard-water lakes, but they are not generally found growing directly upon travertine, preferring deep, calm waters. Gillespie and Clendenning (1964) list eighteen algae from deposits in Hardy County, West Virginia. *Oocardium* was not noted, but *Cladophora glomerata*, *Phormidium incrustatum*, *Synedra rumpens*, and *Diatoma hiemale* were found to be abundant.

More recently, samples collected by D.A. Hubbard, Jr. were examined briefly from three sites in Virginia: Falling Spring Run and Folly Mills Creek in Augusta County and Glenn Falls, Marl Creek, Rockbridge County. Material collected from Falling Spring Run revealed the cyanobacterium *Schizothrix calcicola* s. lato, with *Oocardium stratum*, *Vaucheria*, and the diatoms *Achnanthes*, *Cymbella*, and *Navicula angusta*. Surface scrapes from Folly Mills Creek were rich in diatoms, with *Cymbella naviculiformis* and species of *Gomphonema* and *Nitzschia*. At Glenn Falls, unencrusted tufts of *Cladophora glomerata* were common (Figure 4) with the epiphytic diatoms *Gomphonema* and *Diatoma*. Encrusted growths of *Gongrosira incrustans* and *Vaucheria* were also present. The cyanobacterium *Phormidium incrustatum* was common at all three sites, and uncalcified mats of this species occurred in Folly Mills Creek.

ECOLOGY

Light and temperature exert a controlling influence on the establishment and growth of algae, although extremes of

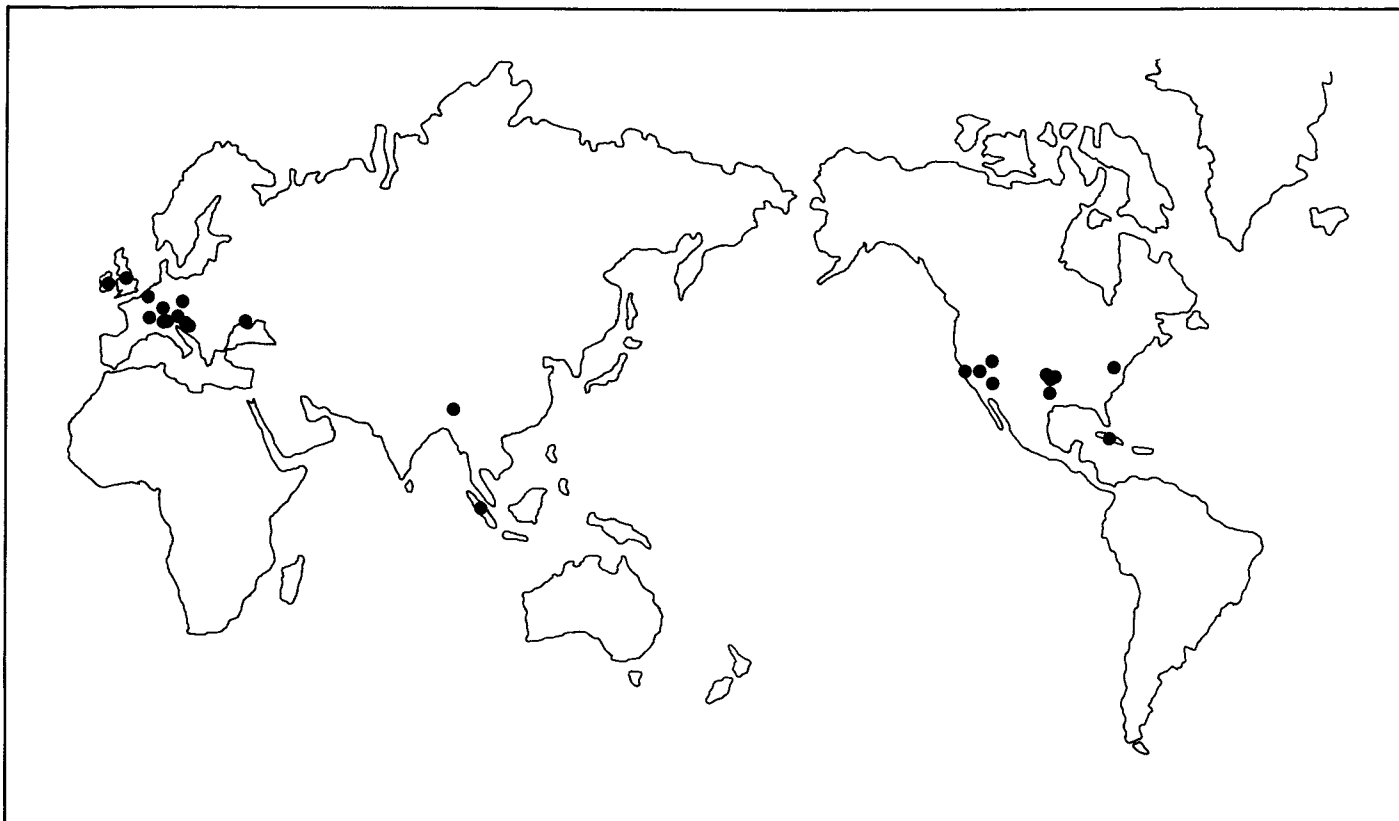


Figure 3. The distribution of *Oocardium stratum*. Sources consulted: Carter (1926), West and Fritsch, (1927), Ruttner (1931), Smith (1933), Wallner (1933), van Oye (1937), Golubic and Marcenko (1958), Mathews (1962a, 1962b), Golubic (1967), Hindak (1978), and Whitton (1974).

temperature are rarely encountered on moist travertine since excess heat is rapidly conducted and convected away. For algae, travertine deposits represent an ever-changing environment with respect to light, and evidence for extremes of intensity can be found in the upper 1 to 4 mm of the deposits (Pentecost, 1978). The problems encountered are similar to those in unencrusted algal mats, but the efficiency of light utilization is lower because some light is absorbed and some is reflected by the deposit, leaving less for photosynthesis. Whether algae are more efficient at harvesting light in such unadvantageous situations is still uncertain. Cyanobacteria are known to grow under extremely low illumination and can survive heterotrophically in the complete absence of light (Smith, 1982). Recently, seasonal growth-rate measurements have been made for three calcified cyanobacteria: *Calothrix*, *Homoeothrix*, and *Rivularia* (Pentecost, 1987 and 1988b). The measurements revealed in every case maximum growth during summer and minimum growth in winter. In *Rivularia* and *Calothrix* growth was significantly correlated with stream-water temperature. The measurements were made in northern England where water temperatures averaged 7 to 10°C and radial growth rates of 0.4 to 2.5 mm per year were obtained. Higher rates of growth would be expected at lower latitudes although many cyanobacteria are

remarkably slow-growing, even under apparently optimal conditions. Studies by Livingstone and others (1984) suggest that light intensity is the most important factor for the growth of *Rivularia*. Both light and temperature, however, are important, and their relative significance may depend upon the local environment. Light has other effects on growth, as filamentous cyanobacteria are phototactic. Sometimes, the colonies assume bizarre shapes as a result (Golubic, 1973), and this is often seen in growths of *Rivularia* and *Homoeothrix* on the vertical sides of encrusted stones.

High levels of organic pollution are inhibitory to carbonate precipitation and may alter the algal flora. *Phormidium incrustatum* deposits, once a notable feature of some chalk streams in the United Kingdom (Fritsch and Pantin, 1946), have now disappeared as a result of dredging and eutrophication, with levels of dissolved nitrate-nitrogen and phosphate-phosphorus now exceeding 6 and 1 mg/L, respectively. Edwards and Heywood (1960) found that pollution by domestic sewage destroyed calcite encrustations on shells of gastropods in England, but the algal flora was unaffected, consisting of *Cocconeis* and *Chantransia* both above and below the sewage outfall. High levels of phosphates are known to inhibit calcite nucleation (Raistrick, 1949), but low levels of organic pollution appear to have a minimal effect on

travertine deposits. For example, at Falls Creek, Oklahoma, untreated sewage discharge occurs from a village, whose population reaches 2000 on weekends, but active deposition of calcite and a rich algal flora still occur on the lower falls. Emig (1917) reported that pollution by cattle may have affected the algal flora of the upper reaches of a creek, but no evidence of this remains today. Acidic pollution has been deemed responsible for the destruction of the deposits along Little Conestoga Creek, Pennsylvania (Golubic, 1973), where increasing levels of pollution led to the total inhibition of precipitation and loss of the associated cyanobacteria while the green alga *Gongrosira* remained but in a morphologically altered state (Golubic and Fischer, 1975).



Figure 4. Colony of *Cladophora glomerata* along Marl Creek, Rockbridge County, Virginia. *Cladophora* is a coarse, hair-like, green alga which is very conspicuous and common worldwide in flowing hard waters (Photograph by D. A. Hubbard, Jr.).

Fluctuating water levels have a considerable effect on the algal flora. Discharge over travertine dams and falls is normally reduced during the warmer months, resulting in the exposure of deposits at the stream edge. Complete desiccation may occur and this sometimes can be recognized in the flora, since several cyanobacteria are adapted to regimes of

wetting and drying, notably species of *Scytonema* and *Gloeo-capsa*. These algae are common in seepages, particularly where there is high evaporation (Jaag, 1945; Pentecost, 1982 and 1985a). Other species, such as *Rivularia* can survive desiccation (Pentecost, 1987), but *Schizothrix*, *Gongrosira*, and many benthic diatoms, which grow in deeper water, appear to be less tolerant (Pentecost, 1982). Flow rate is also known to affect species composition. Rates of flow exceeding 1 m/s restrict the development of trailing filamentous forms and favor the development of small cushions of *Homoeothrix* and *Gongrosira*. Where gradients are steep and the flow rate incessantly high, the algal flora may be extremely sparse.

Travertine-depositing rivers are well known for their downstream concentration gradients of carbon dioxide, calcium, and pH (Gruninger, 1965; Usdowski and others, 1979; Pentecost, 1981; Thorpe, 1981). Although calcium is an important structural component of plant cells and a regulator of metabolism (Campbell, 1983), the effect of calcium concentration on the ecology of algae has received little attention. The result of falling levels of calcium, typical of those occurring in travertine-depositing streams, has not been investigated. There are problems designing experiments to measure this effect because the decrease in calcium concentration is accompanied by a decrease and change in the speciation of the total dissolved carbon, and there is also a rise in pH. Thus, observed changes in the algal flora could be due to any combination of these factors. Furthermore, pH affects the ionic speciation of dissolved phosphate and silica, which could alter the uptake rates of these important algal nutrients.

The hydrogen ion concentration can fall by an order of magnitude over distances of a hundred meters in travertine-depositing streams, a much greater change in concentration than that occurring in dissolved calcium or carbon dioxide. In an English travertine-depositing stream, Waterfall Beck, quantitative algal sampling has demonstrated downstream changes in the algal flora (Pentecost, 1982). A significant positive correlation was obtained between *Schizothrix calcicola* numbers and pH, and *Achnanthes* species were more abundant when the pH rose above 8.0 and travertine was deposited.

Stream algae can be divided into two groups: those which become abundant only at particular times of the year, then die or become rare or impossible to find, and those which are abundant throughout the year. Perennial components of travertine-depositing waters include most of the cyanobacteria species which have been mentioned together with *Oocardium*, *Gongrosira*, and *Vaucheria*. Other algae may also be perennial, but there have been few seasonal observations on such streams. In Waterfall Beck, the algae *Chrysonobula holmesii*, *Didymosphenia geminata*, *Fragilaria virescens*, and *Nostoc* spp. have their growth optimum in early summer. Other diatoms also appear to show seasonal growth patterns because *Homoeothrix* colonies become covered with a thin, brown diatom stratum during the winter months in this stream. Differences between the two groups may not always be so clear-

travertine deposits. For example, at Falls Creek, Oklahoma, untreated sewage discharge occurs from a village, whose population reaches 2000 on weekends, but active deposition of calcite and a rich algal flora still occur on the lower falls. Emig (1917) reported that pollution by cattle may have affected the algal flora of the upper reaches of a creek, but no evidence of this remains today. Acidic pollution has been deemed responsible for the destruction of the deposits along Little Conestoga Creek, Pennsylvania (Golubic, 1973), where increasing levels of pollution led to the total inhibition of precipitation and loss of the associated cyanobacteria while the green alga *Gongrosira* remained but in a morphologically altered state (Golubic and Fischer, 1975).



Figure 4. Colony of *Cladophora glomerata* along Marl Creek, Rockbridge County, Virginia. *Cladophora* is a coarse, hair-like, green alga which is very conspicuous and common worldwide in flowing hard waters (Photograph by D. A. Hubbard, Jr.).

Fluctuating water levels have a considerable effect on the algal flora. Discharge over travertine dams and falls is normally reduced during the warmer months, resulting in the exposure of deposits at the stream edge. Complete desiccation may occur and this sometimes can be recognized in the flora, since several cyanobacteria are adapted to regimes of

wetting and drying, notably species of *Scytonema* and *Gloeocapsa*. These algae are common in seepages, particularly where there is high evaporation (Jaag, 1945; Pentecost, 1982 and 1985a). Other species, such as *Rivularia* can survive desiccation (Pentecost, 1987), but *Schizothrix*, *Gongrosira*, and many benthic diatoms, which grow in deeper water, appear to be less tolerant (Pentecost, 1982). Flow rate is also known to affect species composition. Rates of flow exceeding 1 m/s restrict the development of trailing filamentous forms and favor the development of small cushions of *Homoeothrix* and *Gongrosira*. Where gradients are steep and the flow rate incessantly high, the algal flora may be extremely sparse.

Travertine-depositing rivers are well known for their downstream concentration gradients of carbon dioxide, calcium, and pH (Gruninger, 1965; Usdowski and others, 1979; Pentecost, 1981; Thorpe, 1981). Although calcium is an important structural component of plant cells and a regulator of metabolism (Campbell, 1983), the effect of calcium concentration on the ecology of algae has received little attention. The result of falling levels of calcium, typical of those occurring in travertine-depositing streams, has not been investigated. There are problems designing experiments to measure this effect because the decrease in calcium concentration is accompanied by a decrease and change in the speciation of the total dissolved carbon, and there is also a rise in pH. Thus, observed changes in the algal flora could be due to any combination of these factors. Furthermore, pH affects the ionic speciation of dissolved phosphate and silica, which could alter the uptake rates of these important algal nutrients.

The hydrogen ion concentration can fall by an order of magnitude over distances of a hundred meters in travertine-depositing streams, a much greater change in concentration than that occurring in dissolved calcium or carbon dioxide. In an English travertine-depositing stream, Waterfall Beck, quantitative algal sampling has demonstrated downstream changes in the algal flora (Pentecost, 1982). A significant positive correlation was obtained between *Schizothrix calcicola* numbers and pH, and *Achnanthes* species were more abundant when the pH rose above 8.0 and travertine was deposited.

Stream algae can be divided into two groups: those which become abundant only at particular times of the year, then die or become rare or impossible to find, and those which are abundant throughout the year. Perennial components of travertine-depositing waters include most of the cyanobacteria species which have been mentioned together with *Oocardium*, *Gongrosira*, and *Vaucheria*. Other algae may also be perennial, but there have been few seasonal observations on such streams. In Waterfall Beck, the algae *Chrysonobula holmesii*, *Didymosphenia geminata*, *Fragilaria virescens*, and *Nostoc* spp. have their growth optimum in early summer. Other diatoms also appear to show seasonal growth patterns because *Homoeothrix* colonies become covered with a thin, brown diatom stratum during the winter months in this stream. Differences between the two groups may not always be so clear-

cut, however. Marker and Casey (1982) observed irregular fluctuations in the abundance of *Gongrosira incrustans* and *Phormidium incrustatum* in an experimental stream depositing travertine. The algal flora of some calcareous European streams (not all depositing travertine) has been studied by Golubic (1967) who has provided a list of the common species.

Aquatic bryophytes frequently become covered with a dense growth of algae below their growing tips. Diatoms (particularly species of *Achnanthes*, *Cocconeis*, and *Eunotia*) are particularly well represented and may be seen colonizing the surfaces of bryophyte leaves, often almost covering them. These epiphytes may play an important role in the early stages of travertine formation by providing a large surface area for the nucleation of calcite crystals (Emeis and others, 1987). Bryophytes also provide a wide range of microhabitats for algae, for example, flat, illuminated leaf surfaces and shaded leaf axils and stems. In addition, bryophytes shelter a rich invertebrate fauna including herbivores, such as *Tinodes*, which feed on encrusted *Homoeothrix* and *Phormidium*.

SIGNIFICANCE IN TRAVERTINE FORMATION

The formation of travertine is unlikely to occur in the total absence of microorganisms. Microscopic algae and bacteria are ubiquitous on the earth's surface and have been found wherever they have been searched for.

The presence of algae can influence the precipitation of calcium carbonate in several ways, but the most obvious process is by the net removal of aqueous carbon dioxide by photosynthesis. There is no doubt that such a process occurs in marine algae, such as *Halimeda*, which possesses a specialized anatomy designed to enhance photosynthetic calcification (Borowitzka, 1982). Freshwater algae do not possess such an anatomy, but any photosynthetic activity will be favorable for travertine formation. There have been no detailed field studies directly measuring photosynthesis rates and degassing rates simultaneously in travertine-depositing waters, and photosynthetic uptake is frequently ignored in geochemical studies. Barnes (1965) and Hoffer-French and Herman (1989) obtained evidence of photosynthetic activity, whilst other investigators have either failed to obtain conclusive evidence (Cole and Bachelder, 1969; Jacobson and Usdowski, 1975) or failed to detect any photosynthetic activity at all (Usdowski and others, 1979; Lorah and Herman, 1988).

The important factors affecting aquatic plant growth are summarized in Table 2. Maximum growth of a particular species is observed under optimum levels of insolation, temperature, and essential nutrients. Optimum is not necessarily the same as maximum. For example, extreme levels of irradiance and temperature can be detrimental to growth

(Soeder and Stengel, 1974). Because travertine supports a diverse algal community, and not a single species, the optimum conditions for one species do not necessarily coincide with the optima for others. The role played by phosphorus is particularly interesting as this element is often the major limiting nutrient for algal growth (Healey, 1973), but many phosphates are known to be effective inhibitors of calcite nucleation (Raistrick, 1949). High levels of dissolved phosphates may thus encourage plant growth but discourage travertine formation. Thus, in the absence of a detailed vegetation survey, all that can be said is that the contribution of photosynthesis to calcium carbonate precipitation will range from negligible to highly significant.

Table 2. Plant-related factors favorable to travertine deposition.

<u>LOW LEVELS</u>	<u>HIGH LEVELS</u>
discharge	insolation
water pollution	water temperature
plant-secreted nucleation-inhibitors	available nitrogen
	available Si (diatoms)
	CO ₂ and HCO ₃ ⁻
	mucilage secretion
	biomass/unit area

Algae may also influence deposition in other ways. The construction of a physical framework for precipitation has already been noted. Bryophytes in particular make possible the exposure of a large surface area of water which facilitates carbon dioxide exchange and the evaporation of water. The algae *Oocardium*, *Chrysonobula*, and *Rivularia* produce copious mucilage within which calcite appears to be preferentially nucleated (Pentecost and Riding, 1986; Emeis and others, 1987). The nucleation of calcite may occur upon or within the gelatinous sheaths or cell walls at favorable low-energy organopolymer sites or upon bacteria, clay, silt, or calcite which has become trapped among the cells or adhered to the mucilage. Once crystals have formed, further precipitation may be rapid through secondary nucleation on the calcite already present. These processes are difficult to distinguish because the particles responsible for nucleation may be of colloidal dimensions and would be hard to detect in an experimental system. A wide range of bacteria has been isolated from active travertine, but it has not yet been possible to demonstrate calcite deposition under apparently favorable conditions (Pentecost and Terry, 1989).

Other mechanisms, such as the osmotic uptake of water (Pia, 1934; Hubbard and others, 1985), may occur, but they would have a negligible effect in flowing waters because the amount of water required by algae is extremely small compared to the amount available.

In conclusion, it is noted that although many algae have been found growing on travertine, only a small number seem

to be confined to this substratum. The algal flora of travertine is incompletely known and there are few records from tropical and polar sites. The diatom flora of travertine would repay further study considering the proven value of diatoms as sensitive environmental indicators.

The deposition of travertine is known to be influenced by algae in at least two ways, namely by the photosynthetic uptake of carbon dioxide, promoting water alkalization, and the production of calcite-trapping, or, nucleating mucilages. Studies of biologically influenced nucleation are difficult to perform but some progress is being made. One simple line of enquiry would be the careful observation of natural and artificial substrates using scanning electron microscopy to observe the development of calcite associated with the attached microorganisms.

REFERENCES CITED

- Barnes, Ivan, 1965, Geochemistry of Birch Creek, Inyo County, California; a travertine-depositing creek in an arid climate: *Geochimica et Cosmochimica Acta*, v. 29, p. 85-112.
- Borowitzka, M.A., 1982, Morphological and structural aspects of algal calcification: *International Review of Cytology*, v. 74, p. 127-162.
- Campbell, A.K., 1983, Intracellular calcium. Its universal role as regulator: Chichester, England, J. Wiley & Sons, 556 p.
- Carter, Nellie, 1926, Freshwater algae from India: *Records of the Botanical Survey of India*, v. 9, p. 263-302.
- Cohn, Ferdinand, 1862, Über die Algen des Karlsbader Sprudels, mit Rücksicht auf die Bildung des Sprudelsinters: *Jahresbericht des Schlesischen Gesellschaft für Vaterländische Kultur*, Bd. 2, p. 35-55.
- Cole, G.A., and Bachelder, G.L., 1969, Dynamics of an Arizona travertine-forming stream: *Journal of the Arizona Academy of Science*, v. 5, p. 271-283.
- Edwards, R.W., and Heywood, J., 1960, Effect of a sewage effluent discharge on the deposition of calcium carbonate on shells of the snail *Potamopyrgus jenkinsii* (Smith): *Nature*, v. 186, p. 492-493.
- Emeis, K.-C., Richnow, H.-H., and Kempe, Stephan, 1987, Travertine formation in Plitvice National Park, Yugoslavia: chemical versus biological control: *Sedimentology*, v. 34, p. 595-610.
- Emig, W. H., 1917, The travertine deposits of the Arbuckle Mountains, Oklahoma, with reference to the plant agencies concerned in their formation: *Oklahoma Geological Survey Bulletin*, v. 29, 75 p.
- Frey, Wolfgang, and Probst, Wilfried, 1974, Morphologische und vegetationsanalytische Untersuchungen an rezenten Kalktuffen im Keupergebiet des Suedlichen Schoenbuchs: *Beitrage zur Naturkundlichen Forschung in Sudwestdeutschland*, Bd. 33, p. 59-80.
- Fritsch, F.E., 1950, *Phormidium incrustatum*, (Naeg.) Gom., an important member of the lime-encrusting communities of flowing water: *Biologische Jahrbuch*, v. 70, p. 27-39.
- Fritsch, F.E., and Pantin, C.F.A., 1946, Calcareous concretions in a Cambridgeshire stream: *Nature*, v. 157, p. 397-399.
- Geitler, Lothar, 1932, Cyanophyceae, in Kolkwitz, R., ed., *Rabenhorst's Kryptogamenflora von Deutschland, Österreich und der Schweiz*: Leipzig, West Germany, Akademische Verlagsgesellschaft, Bd. 14, 1196 p.
- Gillespie, W.H., and Clendening, J.A., 1964, An interesting marl deposit in Hardy County, West Virginia: *Proceedings of the West Virginia Academy of Science*, v. 36, p. 147-151.
- Golubic, Stjepko, 1967, *Algenvegetation der Felsen*: Stuttgart, West Germany, Die Binnengewässer, E. Schweizerbart'sche Verlagbuchhandlung, Bd. 23, 183 p.
- Golubic, Stjepko, 1973, The relationship between blue-green algae and carbonate deposits, in Carr, N.G., and Whitton, B.A., eds., *The biology of blue-green algae*: Oxford, England, Blackwell, p. 434-472.
- Golubic, Stjepko, and Marcenko, E., 1958, Zur Morphologie und Taxonomie der Desmidiaceengattung *Oocardium*: *Schweizerische Zeitschrift für Hydrobiologie*, Bd. 20, p. 177-185.
- Golubic, Stjepko, and Fischer, A. G., 1975, Ecology of calcareous nodules forming in Little Conestoga Creek near Lancaster, Pennsylvania: *Verhandlungen der Internationalen Vereinigung für Theoretische und Angewandte Limnologie*, Bd. 19, p. 2315-2323.
- Gruninger, Werner, 1965, Rezent Kalktuffbildung im Bereich der Uracher Wasserfälle: *Abhandlung zur karst und Höhlenkunde*, E2, p. 1-113.
- Healey, F.P., 1973, Inorganic nutrient uptake and deficiency in algae: *Critical Reviews in Microbiology*, v. 3, p. 69-113.
- Hindak, Frantisek, 1978, *Sladkovodne Riasy*: Bratislava, Slovenske, Pedagogicke Nakladotel'stvo, 724 p.
- Hoffer-French, K.J., and Herman, J.S., 1989, Evaluation of hydrological and biological influences on CO₂ fluxes from a karst stream: *Journal of Hydrology*, v. 108, p. 189-212.
- Hubbard, D.A., Jr., Giannini, W.F., and Lorah, M.M., 1985, Travertine-marl deposits of the Valley and Ridge province of Virginia - a preliminary report: *Virginia Division of Mineral Resources, Virginia Minerals*, v. 31, n. 1, p. 1-8.
- Jaag, Otto, 1945, Untersuchungen über die Vegetation und Biologie der Algen des nackten Gesteins in den Alpen, im Jura und im schweizerischen Mittelland: *Beitrage zur Kryptogamenflora der Schweiz*, Bd. 9, p. 1-560.
- Jacobson, R.L., and Usdowski, Eberhard, 1975, Geochemical controls on a calcite precipitating spring: *Contributions to Mineralogy and Petrology*, v. 51, p. 65-74.
- Kann, Edith, 1973, Bemerkungen zur Systematik und Ökologie einiger mit Kalk inkrustierter *Phormidium* arten: *Schweizerische Zeitschrift für Hydrologie*, Bd. 35, p. 141-151.
- Livingstone, David, Pentecost, Allan, and Whitton, B.A., 1984, Diel variations in nitrogen and carbon dioxide fixation by the blue-green alga *Rivularia* in an upland stream: *Phycologia*, v. 23, p. 125-133.
- Lorah, M.M., and Herman, J.S., 1988, The chemical evolution of a travertine-depositing stream: *Geochemical processes and mass transfer reactions*: *Water Resources Research*, v. 24, p. 1541-1552.
- Lund, J.W.G., 1961, The algae of the Malham Tarn district: *Field Studies*, v. 1, p. 58-72.
- Marker, A.F.H., and Casey, H., 1982, The population and production dynamics of benthic algae in an artificial re-circulating hardwater stream: *Philosophical Transactions of the Royal Society of London B, Biological Sciences*, v. 298, p. 265-308.

- Mathews, H.L., 1962a, Marl deposition by the algae *Oocardium stratum* and *Chara vulgaris* in Montgomery County, Virginia: Proceedings of the Virginia Academy of Science, v. 13, n. 4, p. 250.
- Mathews, H.L., 1962b, The formation of calcareous tufa deposits in Montgomery County, Virginia: Proceedings of the Virginia Academy of Science, v. 13, n. 4, p. 283.
- Patrick, Ruth, 1977, The ecology of freshwater diatoms and diatom communities, in Werner, Dietrich, ed., The biology of diatoms: London, England, Blackwell, p. 284-332.
- Pentecost, Allan, 1978, Blue-green algae and freshwater carbonate deposits: Proceedings of the Royal Society of London, B200, p. 43-61.
- Pentecost, Allan, 1981, The tufa deposits of the Malham district, North Yorkshire: Field Studies, v. 5, p. 365-387.
- Pentecost, Allan, 1982, A quantitative study of calcareous stream and Tintenstriche algae from the Malham district, Northern England: British Phycological Journal, v. 17, p. 443-456.
- Pentecost, Allan, 1984, The growth of *Chara globularis* and its relationship to calcium carbonate deposition in Malham Tarn: Field Studies, v. 6, p. 53-58.
- Pentecost, Allan, 1985a, Association of cyanobacteria with tufa deposits: identity, enumeration and nature of the sheath material revealed by histochemistry: Geomicrobiology Journal, v. 4, p. 285-298.
- Pentecost, Allan, 1985b, Photosynthetic plants as intermediary agents between environmental bicarbonate and carbonate deposition, in Lucas, W.J., and Berry, J.A., eds., Inorganic carbon uptake by aquatic photosynthetic organisms: Rockville, Maryland, American Society of Plant Physiologists, p. 459-480.
- Pentecost, Allan, 1987, Growth and calcification of the cyanobacterium *Rivularia haematites*: Proceedings of the Royal Society of London, B232, p. 125-136.
- Pentecost, Allan, 1988, Observations on growth rates and calcium carbonate deposition in the green alga *Gongrosira*: New Phytologist, v. 110, p. 249-253.
- Pentecost, Allan, and Riding, Robert, 1986, Calcification in Cyanobacteria, in Leadbeater, B. S. C., and Riding, Robert, eds., Biomineralization in lower plants and animals: Oxford, England, Clarendon Press, p. 73-90.
- Pentecost, Allan, and Terry, Catherine, 1989, Inability to demonstrate calcite precipitation by bacterial isolates from travertine: Geomicrobiology Journal, v. 6, p. 185-194.
- Pia, Julius, 1933, Die rezenten Kalksteine: Mineralogische und Petrologische Mitteilung, Ergänzungsband 1, p. 1-419.
- Pia, Julius, 1934, Die Kalkbildung durch Pflanzen, Eine Übersicht: Beihefte zum Botanischen Zentralblatt, A52, p. 1-72.
- Prát, Silvestr, 1929, Studie o Biolithogenesi, Vapinite Rasy a Cyanophyceae pri tvoreni travertinu: Étude sur la biolithogenese, Nakladem Ceske Akademie ved a umeni, V. Praze, 167 p.
- Raistrick, B., 1949, The stabilization of the supersaturation of calcium carbonate solutions by anions possessing O-P-O-P-O chains: Discussions of the Faraday Society, v. 5, p. 234-237.
- Raven, J.A., Smith, F.A., and Walker, N.A., 1986, Biomineralization in the Charophyceae *sensu lato*, in Leadbeater, B.S.C., and Riding, Robert, eds., Biomineralization in lower plants and animals: Oxford, England, Clarendon Press, p. 125-140.
- Ruttner, F.A., 1931, Hydrographische und Hydrochemische Beobachtungen auf Java, Sumatra und Bali: Archive für Hydrobiologie Supplement Band 8, Tropische Binnengewasser, p. 197-454.
- Smith, A.J., 1982, Modes of cyanobacterial carbon metabolism, in Carr, N.G., and Whitton, B.A., eds., The biology of cyanobacteria: Oxford, England, Blackwell, p. 47-86.
- Smith, G.M., 1933, The fresh-water algae of the United States: New York, New York, McGraw-Hill, 716 p.
- Soeder, C., and Stengel, E., 1974, Physico-chemical factors affecting metabolism and growth rate, in Stewart, W.D.P., ed., Algal physiology and biochemistry: Oxford, England, Blackwell, p. 714-740.
- Steidtmann, Edward, 1934, Travertine-deposits near Lexington, Virginia: Science, v. 80, n. 2068, p. 162-163.
- Steidtmann, Edward, 1936, Travertine-depositing waters near Lexington, Virginia: Journal of Geology, v. 44, p. 193-200.
- Thorpe, P.M., 1981, Isotope studies on U.K. tufa deposits and associated source waters [Ph.D. dissert.]: England, University of Oxford, School of Geography, 314 p.
- Uzdowski, Eberhard, Hoef, J., and Menschel, Günther, 1979, Relationship between ^{13}C and ^{18}O fractionation and changes in major element composition in a recent calcite-depositing stream - a model of chemical variations with inorganic calcium carbonate precipitation: Earth and Planetary Science Letters, v. 42, p. 267-276.
- van Oye, Paul, 1937, Biologie et écologie des formations calcaires du Jurassique Belge: Biologische Jaarboek, v. 4 p. 236-265.
- Wallner, J., 1933, *Oocardium stratum* Naeg, Eine wichtige tuffbildende Alge Südbayerns: Planta, Bd. 20, p. 287-293.
- Wallner, J., 1935a, Über die Kalkbildung in der Gattung *Cosmarium*: Beihefte zum Botanischen Zentralblatt Abt. A, p. 586-590.
- Wallner, J., 1935b, Diatomeen als Kalkbildner: Hedwigia, Bd. 75, p. 137-141.
- West, G.S., and Fritsch, F.E., 1927, A treatise on the British freshwater algae: England, Cambridge University Press, 534 p.
- Whitton, B.A., 1974, Changes in the British freshwater algae, in Hawksworth, D.L., ed., The changing flora and fauna of Britain: London, England, Academic Press, p. 115-141.
- Winsborough, B.M., and Golubic, Stjepko, 1987, The role of diatoms in stromatolite growth: two examples from modern freshwater settings: Journal of Phycology, v. 23, p. 195-201.

ECONOMIC LEGACY AND DISTRIBUTION OF VIRGINIA'S VALLEY AND RIDGE PROVINCE TRAVERTINE-MARL DEPOSITS

Palmer C. Sweet and David A. Hubbard, Jr.

CONTENTS

	Page
Abstract.....	130
Introduction.....	130
Counties with documented production.....	130
Alleghany.....	130
Augusta.....	130
Botetourt.....	133
Clarke.....	133
Frederick.....	135
Giles.....	135
Montgomery.....	136
Rockbridge.....	136
Counties without documented production.....	137
Bath.....	137
Rockingham.....	137
Warren.....	137
Washington.....	137
Potential outlook.....	138
Acknowledgments.....	138
References cited.....	138

ILLUSTRATIONS

Figure	
1. Distribution of travertine-marl deposits.....	131
2. Jordan marl bed.....	131
3. Old plant at Jordan marl-bed site.....	133
4. Newspaper clipping advertising auction of machinery and tools that were used at the Jordan marl bed.....	133
5. Location of travertine-marl production sites on Old Chapel Run, Clarke County.....	134
6. Location of travertine-marl production sites on Spout Run, Clarke County.....	134
7. View of Digges' marl operation on Redbud Run.....	135
8. Location of travertine-marl production sites near Narrows, Giles County.....	136
9. Marl plant of Gatewood and Talbott in middle 1940s.....	136
10. Lime kiln.....	137

TABLE

Travertine-marl production by producer in each county.....	132
--	-----

ABSTRACT

Travertine-marl deposits are reported in eighteen counties in the Valley and Ridge province of Virginia. Production figures are reported for eight counties, and reports of operations are noted for four other counties. The earliest production was in Rockbridge County in the mid 1800s, and the most recent was in Frederick County in 1985. Most of the production was from Alleghany, Clarke, and Giles counties for agricultural lime. A total production of greater than 1,570,000 short tons of Virginia travertine-marl is documented by U. S. Bureau of Mines and mining company records for the period 1880 to 1985.

Raw material from deposits ranged from marl (unconsolidated carbonate sediment) to travertine, which required crushing. Deposits in some areas may be excluded from future use because of zoning restrictions, residential development, other sources of agricultural liming materials, and environmental considerations.

INTRODUCTION

Travertine-marl deposits are known along 60 streams in 18 counties of the Valley and Ridge province of Virginia. The earliest reference to a travertine-marl deposit in the province is an account of the Falling Spring Falls recorded by Thomas Jefferson (1825). These freshwater carbonates range in form from bluffs bearing waterfalls or cascades (cover photographs to volume) to broad, flat valley fills. Generally, as travertine builds up along a stream, marl concurrently accumulates upstream from the travertine buildup structure. The resulting morphology is a series of cascading travertine buildups bounding marl-rich terraces deposited along a section of the stream. Travertine-marl deposits are commonly associated with springs related to faults or highly fractured and folded rocks (Hubbard and others, 1985).

Available chemical analyses of travertine, free from contamination of noncarbonate sediments, show that it is composed of more than 97 percent calcium carbonate (CaCO_3). Generally, the marl that occupies the flood plains of streams is mixed with variable amounts of noncarbonate clastic sediment, resulting in CaCO_3 contents ranging from as little as 35 percent (Pettijohn, 1957) to as much as 96 percent (William F. Giannini, 1988, personal communication). Magnesium carbonate (MgCO_3) content is typically less than two percent in both travertine and marl materials (Herman and Hubbard, this volume).

Travertine-marl materials have been utilized as a flux in iron processing and for agricultural lime. An early reference noted the use of marl from Hamilton's marl bank as a flux at the Amherst iron furnace (Hotchkiss, 1880). The use of travertine-marl as a flux probably ceased in the early 1900s.

Travertine-marl materials commercially utilized as an agricultural lime must have a minimum total carbonate content of 85 percent. Current commercial trends are toward limes with high magnesium carbonate content. The term marl has been used by commercial operators to describe all travertine-marl materials worked for agricultural lime. The last Virginia production of travertine-marl for agricultural lime was in Frederick County in early 1985. Only one case is known where travertine-marl was burned or calcined to produce a quicklime for agricultural use (see section on Montgomery County). This paper provides a summary of descriptive information of known travertine-marl deposits in the Valley and Ridge province of Virginia.

COUNTIES WITH DOCUMENTED PRODUCTION

Travertine-marl deposits were commercially utilized in 12 of 18 counties in which deposits are known (Figure 1). The travertine mining history, including producers, production figures, and pit locations, is discussed for each of the eight counties with documented production and is summarized in the Table. No production figures are available for sites in four other counties which are discussed in a subsequent section.

ALLEGHANY

Travertine from Falling Spring Falls was worked for agricultural lime from 1914 to the mid-1940s. A brochure indicates that agricultural lime from this site was marketed as Barbers "Fallingsprings" Lime in the early to middle 1920s (Ohio C. Barber Fertilizer Company, circa 1926; Table, Alleghany 1a). In 1944 the Falling Springs Lime Company was quarrying travertine just west of the present falls location. Raw material was hauled three kilometers by narrow gauge railroad to the town of Falling Springs where it was ground for agricultural use. A travertine sample from the locality contained 97.85 percent CaCO_3 , 0.90 percent MgCO_3 , and 0.48 percent SiO_2 (Edmundson, 1958). The scenic 20-m Falling Spring Falls (see cover, top right photograph) can be viewed from an overlook on U.S. Highway 220. This site is described further by Dennen and others, Herman and Hubbard, and Lorah and Herman (all in this volume).

AUGUSTA

It was noted that "tufaceous marl" was abundant along Marl Run near Midway, Lewis Creek near Staunton, Poague Run near Millbrook, and elsewhere in the county (Hotchkiss, 1885). Midway was the old name for Steeles Tavern where

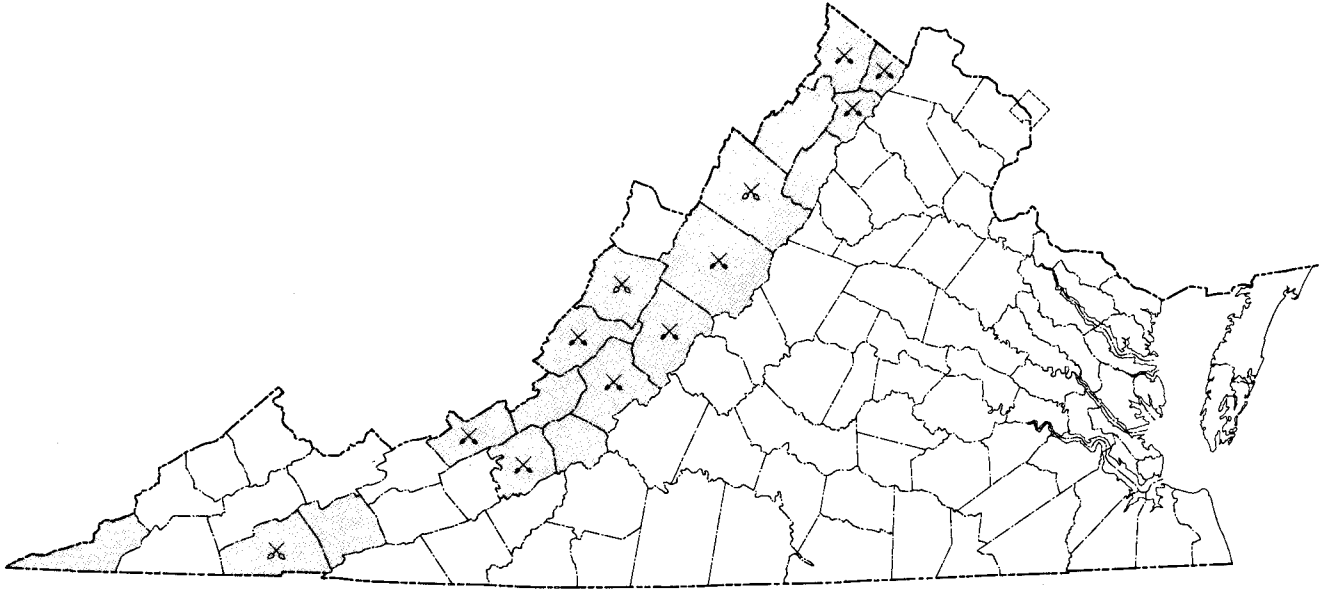


Figure 1. Distribution of travertine-marl deposits (shaded) in the Valley and Ridge province. Counties that contain inactive travertine-marl workings (\otimes) or sites which were formerly in preparation for travertine-marl production (\otimes) are indicated.

U.S. Highway 11 crosses Marl Creek. A number of travertine buildups occur downstream from this intersection. Gum Springs Branch, a tributary of Lewis Creek, flows under the town of Staunton. Marl and clay accumulations 6 to 18 m thick were reported along this branch. A number of sinkhole collapses developed in this deposit in 1910 (Van Horn, 1910; Kindle, 1911). The Poague Run occurrence was near the present day Mayfield Farm just south of the Ingleside golf course along U.S. Highway 11.

Marl was recovered commercially along Falling Spring Run near Quicks Mill at the Jordan marl-bed site. Collins (1924) noted that the site was being worked when he visited the area (Table, Augusta 5a). Marl was extracted for agricultural use at the site from the early 1900s until the 1940s (Mrs. A. LaPort, 1984, personal communication). David J. Carroll (1987, personal communication) stated that the site was first worked by Mr. Jordan around 1917 (Figure 2). Falling Spring Run was diverted to the east-southeast side of the drainage by a berm built up from topsoil stripped from the valley. A concrete dam was constructed downstream to impound water to power a water wheel, 6 m in diameter and 0.9 m wide, manufactured by the Friz Water Wheel Company of Hanover, Pennsylvania (Figure 3). This wheel, which powered the conveyors, was reportedly obtained second-hand from travertine-marl operations in Rockbridge County. Marl removed from the valley (Figure 2) was loaded into trucks and transported to the plant site, where it was screened to remove sticks, pebbles, and other coarse materials. After screening, the marl was transported by conveyors to several loading ramps. The marl was loaded into trucks that were weighed on a Frame Pitless Scale with a 15-ton capacity. The scales remain on the site. In 1936, more than 5700 short tons



Figure 2. Jordan marl bed, with overburden removed, ready for mining, Falling Spring Run, Augusta County (circa early 1920s).

of marl were sold for \$0.93/short ton. Several years later Mr. Jordan died and his foster-son C. F. Marshall worked the site from late 1941 until 1945, when the equipment was sold at auction (Figure 4). During the early 1940s most of the loose marl had been extracted and the use of hammer mills to pulverize the travertine was investigated. From 1941 to 1945 it was difficult to obtain labor and machine parts because of World War II. Subsequently, a flood ruined some of the machinery and caused alluvium to be mixed into the marl deposit. Data from a 1947 sample analysis indicated the site was no longer commercially viable. From 1945 to 1947 the Verona Marl Company (Table, Augusta 7) operated a site upstream from the Jordan marl bed and about 30 m south of the intersection of State Roads 612 and 626. Boyd F. Cupp

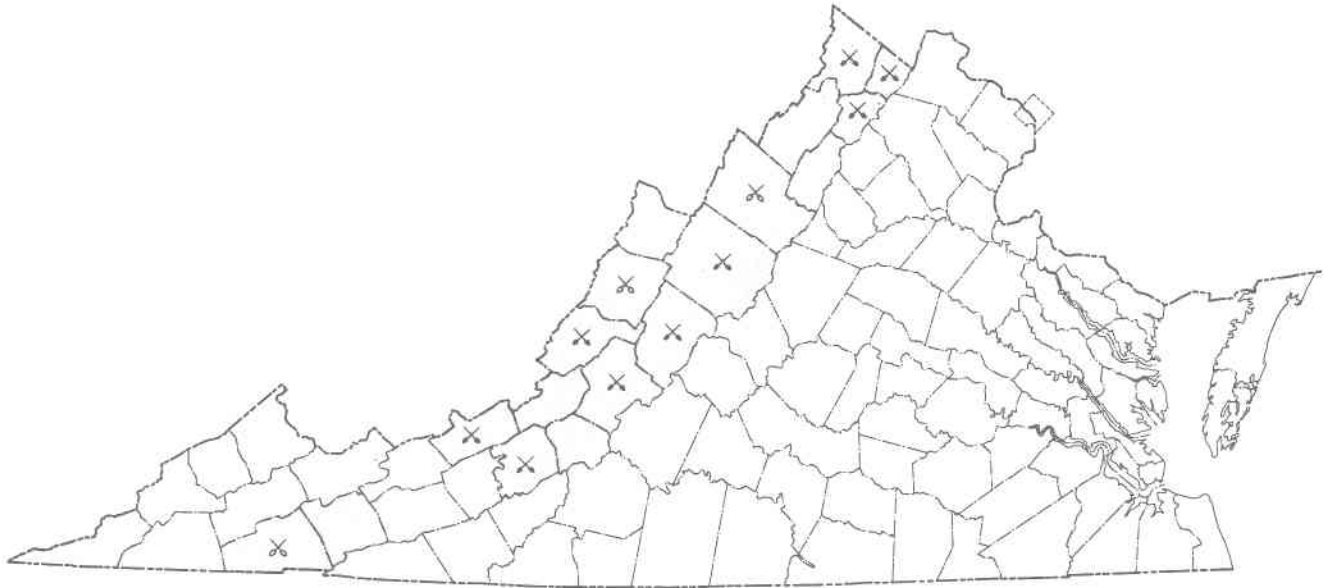


Figure 1. Distribution of travertine-marl deposits (shaded) in the Valley and Ridge province. Counties that contain inactive travertine-marl workings (X) or sites which were formerly in preparation for travertine-marl production (X) are indicated.

U.S. Highway 11 crosses Marl Creek. A number of travertine buildups occur downstream from this intersection. Gum Springs Branch, a tributary of Lewis Creek, flows under the town of Staunton. Marl and clay accumulations 6 to 18 m thick were reported along this branch. A number of sinkhole collapses developed in this deposit in 1910 (Van Horn, 1910; Kindle, 1911). The Poague Run occurrence was near the present day Mayfield Farm just south of the Ingleside golf course along U.S. Highway 11.

Marl was recovered commercially along Falling Spring Run near Quicks Mill at the Jordan marl-bed site. Collins (1924) noted that the site was being worked when he visited the area (Table, Augusta 5a). Marl was extracted for agricultural use at the site from the early 1900s until the 1940s (Mrs. A. LaPort, 1984, personal communication). David J. Carroll (1987, personal communication) stated that the site was first worked by Mr. Jordan around 1917 (Figure 2). Falling Spring Run was diverted to the east-southeast side of the drainage by a berm built up from topsoil stripped from the valley. A concrete dam was constructed downstream to impound water to power a water wheel, 6 m in diameter and 0.9 m wide, manufactured by the Friz Water Wheel Company of Hanover, Pennsylvania (Figure 3). This wheel, which powered the conveyors, was reportedly obtained second-hand from travertine-marl operations in Rockbridge County. Marl removed from the valley (Figure 2) was loaded into trucks and transported to the plant site, where it was screened to remove sticks, pebbles, and other coarse materials. After screening, the marl was transported by conveyors to several loading ramps. The marl was loaded into trucks that were weighed on a Frame Pitless Scale with a 15-ton capacity. The scales remain on the site. In 1936, more than 5700 short tons



Figure 2. Jordan marl bed, with overburden removed, ready for mining, Falling Spring Run, Augusta County (circa early 1920s).

of marl were sold for \$0.93/short ton. Several years later Mr. Jordan died and his foster-son C. F. Marshall worked the site from late 1941 until 1945, when the equipment was sold at auction (Figure 4). During the early 1940s most of the loose marl had been extracted and the use of hammer mills to pulverize the travertine was investigated. From 1941 to 1945 it was difficult to obtain labor and machine parts because of World War II. Subsequently, a flood ruined some of the machinery and caused alluvium to be mixed into the marl deposit. Data from a 1947 sample analysis indicated the site was no longer commercially viable. From 1945 to 1947 the Verona Marl Company (Table, Augusta 7) operated a site upstream from the Jordan marl bed and about 30 m south of the intersection of State Roads 612 and 626. Boyd F. Cupp

VIRGINIA DIVISION OF MINERAL RESOURCES

Table. Travertine-marl production by producer in each county.

County	Producer	Address	Deposit Name/Town	Years of Production ^a	Tonnage Sold ^a	Total Yield of Deposit (S.T.)	
Alleghany	1a. Ohio C. Barber Fert. Co.	Barber, VA		1914-1926	201,570	387,760	
	1b. Falling Springs Lime Co.	Barber, VA		1927-1941	186,190		
Augusta	1a. A. S. Bailey	Mount Sidney, VA		1929	30	42	
	1b. G. S. Bailey	Mount Sidney, VA		1940	12		
	2. James L. Coffey	Staunton, VA		1941-1944	285	285	
	3. Farmers	Marl Lime Co.		1921-1922	2,250	2,250	
	4. Bennett W. Huff	Fort Defiance, VA		1921-1929	865	865	
	5a. J. S. Jordan	Staunton, VA	Verona	1921-1945 (excl. 1932, '33, '42)	76,234	76,234	
	5b. leased to Carver F. Marshall			1942	13,394	13,394	
	6a. Arthur B. Kerr			1940-1941	205	1,205	
	6b. Wilson & Taylor	Staunton, VA	Kerr Pit	1942-1945	1,000		
	6c. leased to Verona Marl Co.			1946-1947			
7. Verona Marl Co. Inc.	Alexandria, VA	Kerr Pit & Verona Marl Pit	1945-1947	24,328	24,328		
Botetourt	1a. Daleville Lime Marl Co.	Roanoke, VA	Daleville	1919-1921	4,170	12,072	
	1b. Botetourt Lime Marl Co.	Roanoke, VA	Daleville	1922-1930	7,902		
	2. Roanoke Lime Co.	Roanoke, VA	Springfield	1919-1920	4,189	4,189	
Clarke	3. Robinson Lime Marl Co.	Fincastle, VA		1947	No production reported		
	1. Clarke Farmers Coop, Inc.	Berryville, VA	Millwood	1940 ^b -1950	137,497	137,497	
	2a. W. R. Thompson	White Post, VA	Old Chapel Marl Pits	1946	18,545	293,345	
	2b. J. C. Digges & Sons	White Post, VA	Old Chapel Marl Pits	1947-1981 (excl. 1951-1955)	274,800		
	3. Fincham Marl Plant	Berryville, VA	Old Chapel Marl Pits	1947-1949	26,272	26,272	
	4. A. Golightly & Burkner		Old Chapel Marl Pits	1950	13,000	13,000	
	5. Aimee Strother & Bro.	Berryville, VA		1952-1957 ^c (excl. 1952-1955)	1,500	1,500	
	6. Elmer Kinney	Berryville, VA		1958-1962 ^c	11,515	11,515	
	Frederick	1. Cornwall Lime Marl	Winchester, VA		1923	1,942	1,942
		2. J. C. Digges & Sons	White Post, VA	Redbud Run	1982-1985	80,000	80,000
Giles	1. Blankenship			1950	No production reported		
	2. Gatewood & Talbott Co. (sold to Langhorne & Langhorne-1948)	Huntington, WV	Narrows	1945-1948	84,242	84,242	
	3. Rufus C. Hale	Narrows, VA		1941-1947	2,650	2,650	
	4. Langhorne & Langhorne	Huntington, WV	Narrows	1942-1947	141,056	141,056	
	5a. Wolf Creek Marl	Narrows, VA	Narrows	1945-1946	42,640	84,571	
	5b. leased to Narrows Contracting Company	Narrows, VA	Narrows	1947-1950 (1952 ^c)	41,931		
Montgomery	1a. J. N. Lantz	Salem, VA		1930-1938 (excl. 1932, '33 & '35-'37)	911	911	
Rockbridge	1b. J. Gilbert Cox	Elliston, VA		1948-1949	No production reported		
	1. unnamed		Hamilton's marl bank	1880	0.5	0.5	
	2a. Calcium-Phosphate & Fertilizer Company	Roanoke, VA	Riverside	1918-1923	16,540	29,121	
	2b. Farmers Marl Lime Co.(name change)		Riverside	1925-1930	12,581		
	3. Dupont Chemical	Wilmington, DE	Riverside	1918	6,000	6,000	
	4. F. M. Hughson	Roanoke, VA	Riverside	1922-1923	No production reported		
	5. Marlbrook Lime Co.	Marlbrook, VA	Marlbrook	1913-1931 (excl. 1916-1917)	109,205	109,205	
6. United Chemical Prod. Co.	Buena Vista, VA		1923-1931	24,951	24,951		
Total:					1,570,313 (S.T.)		

^aProduction data from U.S. Bureau of Mines^bVirginia Division of Mineral Resources file data^cData from miscellaneous sources

(1987, personal communication) stated that competition from the lime-grinding plant in Staunton hurt the local marl operations. The property that Cupp now owns (about 400 m downstream from the Jordan marl bed) was reportedly explored by a fertilizer company just before World War I. The Falling Spring Run deposits are further described by Herman and Hubbard and Hoffer-French and Herman (both in this volume).



Figure 3. Old plant at Jordan marl-bed site with Friz water wheel, water pipe, and block of travertine, Augusta County (photo taken November, 1987).

BOTETOURT

A marl deposit northwest of Daleville was worked for "fertilizer" before 1920 (Woodward, 1932). The Spreading Spring Branch site at Springwood (apparently mislabeled Springfield in U. S. Bureau of Mines production records as reported in Table, Botetourt 2), was worked with a two-horse scraper (George L. Hayth, 1984, personal communication). Travertine-marl was put through a drier and then a crusher before being screened. Mr. Hayth reported his wages as a general laborer in 1919 or 1920 as \$0.90 a day; the scraper operator made \$2.50 a day. U. S. Bureau of Mines data indicate that agricultural lime produced from this deposit sold for about \$3.00/short ton (Hubbard and others, 1985).

CLARKE

Travertine-marl deposits have been worked extensively, and production records indicate that a total 483,000 short tons of material were produced from 1940 through 1981 in Clarke County. The earliest commercial production was by Snowden Strother in the mid-1930s. This operation was situated near Old Chapel on Chapel Run just south of Briggs. Strother

CLAY P. McCLURE, Auctioneer
PUBLIC SALE
 OF
All Kinds of Valuable Machinery and Tools

Due to closing the Jordan Marl bed we will sell at public auction on

Thursday, June 21, 1945

at 10 o'clock a. m., 2 miles northwest of Verona, Va., just off of the Valley Pike and one-half mile north of Quick's Mill right on the road, the following valuable personal property:

1938 D-30 International dump truck with dual speed, Farmall F-30 tractor, steel wheels on rear, McCormick-Deering 10-20 tractor, Austin-Western Rotary-Fresno scraper, 1931 Chevrolet portable motor, New Holland B-24 Stone Hammermill, one set of new hammers included; Hocking Valley Limestone Hammermill, Cleveland Jackhammer, portable air compressor, Climax Jaw Crusher, '10x'18 feed opening (wheels included), Flink's Self-feeding Limespreader (will fit 5 1/2 ft. wide dump truck bed), two-wheeled trailer on rubber, 1 horsepower gasoline engine, 1/3 horsepower electric motor, 3/4 inch United States electric drill, large wall drill, 2 forges, portable steel tool box, anvil, vise, 3 grease guns, lot of end wrenches, box wrenches, socket wrenches and assorted wrenches, 2 large pipe wrenches, several small pipe wrenches, pipe vise, pipe threader, pipe cutter, 2 large metal boxes, 3 small metal boxes, electric soldering iron, wood screws, bolts, nuts and washers, lot of small tools including hammers, punches, chisels, etc., 3/8 inch log chain; 2 1/2 inch log chain, log chain tighteners, grab hooks, swivels, house jack, 2 8-ton hydraulic truck jacks, utility jack, 2 truck tire gauges, tractor tire pump, anti-freeze tester, 2 lengths of 1 inch rubber hose, flat pulleys, small V pulleys, 4", 6" and 8" drive belting, small boxings and shafts, conveyor belt idlers, metal rods, work bench, barrels, metal barrel, wire winder, used and unused wire, metal stand with sections, 2 International 32x6 truck tire rims, 2 small gas tanks, wood saw to fit F-30 tractor, several tons of scrap iron, Remington portable typewriter, Barrett adding machine, metal typewriter table, 3 filing cabinets, coal stove, McCormick-Deering tractor hitch disc harrow, Oliver tractor turning plow, McCormick-Deering trailer limespreader on rubber, many other articles too numerous to mention.

TERMS:—CASH.

JORDAN MARL BED.

By Carver F. Marshall.
 Lunch will be served.

Figure 4. Newspaper clipping advertising auction (June 21, 1945) of machinery and tools that were used at the Jordan marl bed, Augusta County.

(1987, personal communication) stated that competition from the lime-grinding plant in Staunton hurt the local marl operations. The property that Cupp now owns (about 400 m downstream from the Jordan marl bed) was reportedly explored by a fertilizer company just before World War I. The Falling Spring Run deposits are further described by Herman and Hubbard and Hoffer-French and Herman (both in this volume).



Figure 3. Old plant at Jordan marl-bed site with Friz water wheel, water pipe, and block of travertine, Augusta County (photo taken November, 1987).

BOTETOURT

A marl deposit northwest of Daleville was worked for "fertilizer" before 1920 (Woodward, 1932). The Spreading Spring Branch site at Springwood (apparently mislabeled Springfield in U. S. Bureau of Mines production records as reported in Table, Botetourt 2), was worked with a two-horse scraper (George L. Hayth, 1984, personal communication). Travertine-marl was put through a drier and then a crusher before being screened. Mr. Hayth reported his wages as a general laborer in 1919 or 1920 as \$0.90 a day; the scraper operator made \$2.50 a day. U. S. Bureau of Mines data indicate that agricultural lime produced from this deposit sold for about \$3.00/short ton (Hubbard and others, 1985).

CLARKE

Travertine-marl deposits have been worked extensively, and production records indicate that a total 483,000 short tons of material were produced from 1940 through 1981 in Clarke County. The earliest commercial production was by Snowden Strother in the mid-1930s. This operation was situated near Old Chapel on Chapel Run just south of Briggs. Strother

CLAY P. McCLURE, Auctioneer
PUBLIC SALE
 OF
**All Kinds of Valuable
 Machinery and Tools**

Due to closing the Jordan Marl bed we will sell at public auction on

**Thursday, June 21,
 1945**

at 10 o'clock a. m., 2 miles northwest of Verona, Va., just off of the Valley Pike and one-half mile north of Quick's Mill right on the road, the following valuable personal property:

1938 D-30 International dump truck with dual speed, Farmall F-30 tractor, steel wheels on rear, McCormick-Deering 10-20 tractor, Austin-Western Rotary-Fresno scraper, 1931 Chevrolet portable motor, New Holland B-24 Stone Hammermill, one set of new hammers included; Hocking Valley Limestone Hammermill, Cleveland Jackhammer, portable air compressor, Climax Jaw Crusher, 10x18 feed opening (wheels included), Flink's Self-feeding Limespreader (will fit 5 1/2 ft. wide dump truck bed), two-wheeled trailer on rubber, 1 horsepower gasoline engine, 1/3 horsepower electric motor, 3/4 inch United States electric drill, large wall drill, 2 forges, portable steel tool box, anvil, vise, 3 grease guns, lot of end wrenches, box wrenches, socket wrenches and assorted wrenches, 2 large pipe wrenches, several small pipe wrenches, pipe vise, pipe threader, pipe cutter, 2 large metal boxes, 3 small metal boxes, electric soldering iron, wood screws, bolts, nuts and washers, lot of small tools including hammers, punches, chisels, etc., 3/8 inch log chain; 2 1/2 inch log chain, log chain tighteners, grab hooks, swivels, horse jack, 2 8-ton hydraulic truck jacks, utility jack, 2 truck tire gages, tractor tire pump, anti-freeze tester, 2 lengths of 1 inch rubber hose, flat pulleys, small V pulleys, 4", 6" and 8" drive belting, small boxings and shafts, conveyor belt idlers, metal rods, work bench, barrels, metal barrel, wire winder, used and unused wire, metal stand with sections, 2 International 32x6 truck tire rims, 2 small gas tanks, wood saw to fit F-30 tractor, several tons of scrap iron, Remington portable typewriter, Barrett adding machine, metal typewriter table, 3 filing cabinets, coal stove, McCormick-Deering tractor hitch disc harrow, Oliver tractor turning plow, McCormick-Deering trailer limespreader on rubber, many other articles too numerous to mention.

TERMS:—CASH.
JORDAN MARL BED.
 By Carver F. Marshall.
 Lunch will be served.

Figure 4. Newspaper clipping advertising auction (June 21, 1945) of machinery and tools that were used at the Jordan marl bed, Augusta County.

sold his operation to W. R. Thompson in the mid-1940s, but retained the rights to haul with one truck from the Old Chapel site (Figure 5, location 1). In 1947, J. C. Digges and Sons bought out W. R. Thompson's operations at Old Chapel Run and worked these deposits until about 1970 (Table, Clarke 2a and 2b; Figure 5, locations 1 and 2). In 1970, the Meade pit was opened by J. C. Digges and Sons and worked until about 1981 (Figure 5, location 3). The southern-most of the Old Chapel marl pits was known as the Fincham marl plant pit and was operated by Simon Newland in the late 1940s (Table, Clarke 3; Figure 5, location 4). A. Golightly and a Mr. Burkner took over operations of the Fincham site in 1950 (Table, Clarke 4). Aimee Strother, son of Snowden, operated at the Fincham site from 1952 until 1958 (Table, Clarke 5).

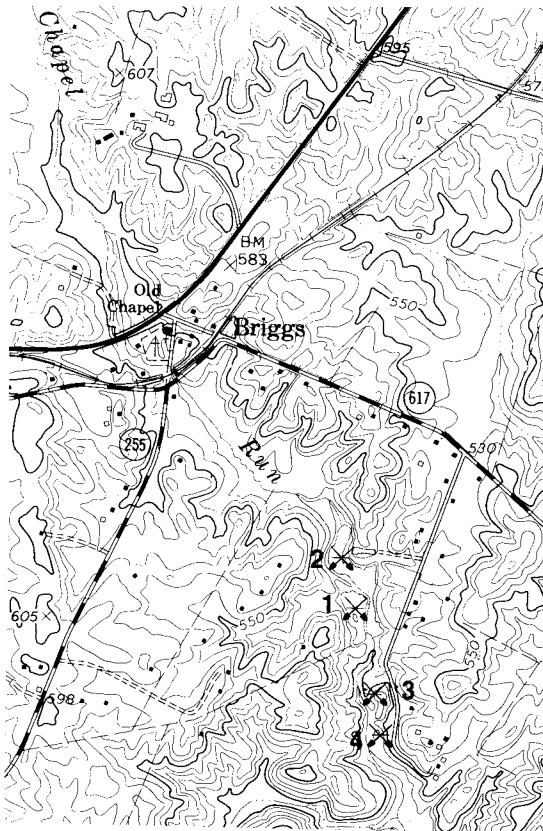


Figure 5. Location of travertine-marl production sites on Old Chapel Run, Clarke County: (1) and (2) Old Chapel pits, (3) Meade pit, and (4) Fincham marl plant pit (scale 1:24,000).

The second oldest travertine-marl operation in the county was situated on Spout Run just above its confluence with the Shenandoah River at Calmes Neck. The Clarke Farmers Cooperative opened this site about 1940 and operated here until 1950 (Table, Clarke 1; Figure 6, location 2). A. Golightly was the manager of this operation until he took over the Fincham site at Old Chapel noted above. Other operators on Spout Run included Winston and Nelson Sipes (1947 to 1950), who worked a site on the west side of the run (Figure

6, location 1). Upstream from the Sipes and Cooperative workings, J. C. Digges and Sons developed the Hollis pit in 1953 (Figure 6, location 3) which operated until September 1960. Approximately 3.2 km to the west, Elmer G. Kinney opened a site on Spout Run at Millwood in 1958. Kinney's operation continued until 1962 (Table, Clarke 6).

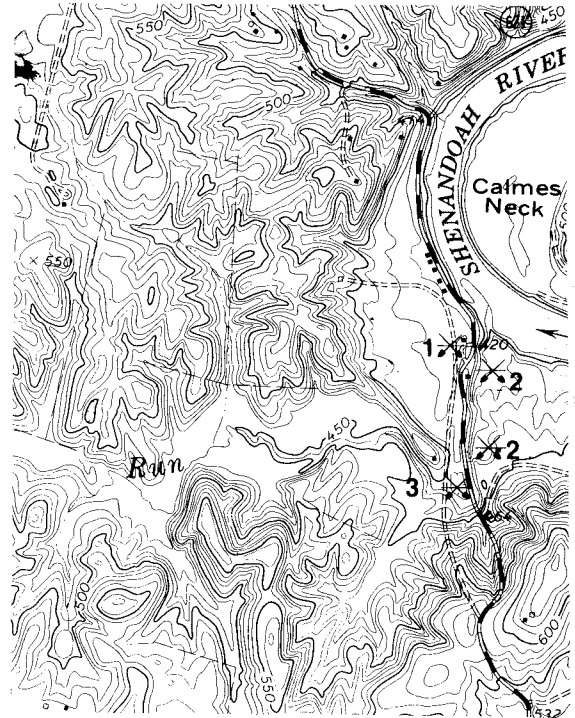


Figure 6. Location of travertine-marl production sites on Spout Run, Clarke County: (1) Sipes pit, (2) Clarke Farmers Cooperative pits, and (3) Hollis pit (scale 1:24,000).

The Weir Brothers' site on Dry Marsh Run, situated about 2.0 km east of Burnt Factory, was operated from about 1948 until the 1950s with the Sipes brothers doing most of the hauling. A West Virginia firm reportedly hauled some of this material in the 1960s and 1970s.

The Huyett pit at Gaylord on Long Marsh Run was worked by Paul Chapman in the late 1940s and early 1950s. About 1.6 km east, on Long Marsh Run, Elmer Kinney worked the Wolfe pit in 1958 and 1959. Much of the marl at this site was borderline material, being only about 85 percent total carbonate.

Clarke County travertine-marl materials range in texture from fine-grained and friable marl to "very hard ridges" of travertine with leaf impressions, such as sycamore, tree trunks, and root casts. Snail and small freshwater clam shells are abundant. Marl materials are much more abundant than travertine in the Clarke County deposits. Winston Sipes (1985, oral communication) reported one of the best marls he had seen was the Clarke Farmers Cooperative's "fine-grained red marl." This material reportedly contained 98 percent

marl. On the west side of Spout Run, the Sipes operation worked marl as thick as 6 m. The Weir deposit is believed to have only been about 1.5 m thick.

FREDERICK

Marl has been produced by two operators in the county. In 1923, marl was produced by Cornwall Lime Marl in Winchester. The company may have operated the pit on Abrams Creek near the western edge of Winchester. The most recent production was 80,000 short tons of 90 percent or greater CaCO_3 along Redbud Run, just northwest of Winchester (Figure 7). This deposit, worked from 1981-1982 and marketed from 1982-1985, is further described by Giannini (this volume).



Figure 7. View of Digges' marl operation on Redbud Run showing marl exposure and loading of trucks, Frederick County (photo taken by S. O. Bird, 1984).

GILES

Marl was dug by hand from 1935 to 1939 from the hillside (Figure 8, location 1) southeast of Wolf Creek along present State Road 724. Travertine was mined from this site using dynamite shots placed in hand-drilled holes. In the early 1940s, another pit and a plant were opened up in this area (Figure 8, location 2) by Hale Brown and Link Buckland. Later, this site was taken over by the railroad building company of Langhorne and Langhorne, Inc., of Huntington, West Virginia, whose subsidiary, Gatewood and Talbott, set up an operation on the site to extract, pulverize, and screen the material (Table, Giles 4). Deterioration of grade of the material led to the closing of this operation around 1947. A marl site on the north side of present State Highway 61 and Wolf Creek was hand dug by Rufus Hale in the late 1930s

(Figure 8, location 3; Table, Giles 3).

A hand-dug pit was opened on the Shepherd property (Figure 8, location 4) in the late 1930s, and marl was hauled by wagon for use on local farms. In the early 1940s, Willie W. Wood of Oakwood Coal and Coke, from Vansant, along with George and Frank Rosenbaum of Rosenbaum Brothers, a heavy equipment construction company from Tazewell, set up the Wolf Creek Marl Company (Table, Giles 5a). They negotiated with James Shepherd's father, who sold the mineral rights to 1012 hectares of land for \$1000 cash; the site was up the ridge from the older hand-dug pit (Figure 8, location 5). James Shepherd (1987, personal communication) remarked that if his father had accepted the proffered \$0.05/short ton royalty, instead of cash, he would have received more than \$2000 in the first 18 months of operation.

Processing at the Wolf Creek marl operation included crushing in a jaw crusher and screening. Some materials required additional pulverizing in two hammer mills. James Shepherd hauled marl in the mid-1940s to both the Norfolk and Western and the Virginian railroads. The marl was loaded into 70-ton hopper cars as well as into low-sided 0.9-m and 15-m gondolas. Some days as many as 12 hopper cars of marl were shipped at \$1.37/short ton, compared to values of \$2.50-\$3.00/short ton at other sites in the state. The product was marketed in the eastern part of Virginia, especially in Nottoway County, and in West Virginia. Floyd Graley (Wolf Creek Marl Company) bought the operation in the early 1950s when the price of marl was up to \$1.50/short ton. The operation (Figure 8, location 5) was subsequently bought by a group, which included Wetzel Brammer and Major Lilley from Beckley, West Virginia, and was renamed Virginia Marl Company. The mineral rights were retained by the former Wolf Creek Marl Company and today are split up in thirds between heirs of Wood and the Rosenbaum brothers. The Virginia Marl Company ceased operations in the mid-1960s.

The Blankenship property, in the area of Shumate, was acquired by Berman Blankenship in December 1941 (Figure 8, location 6). Production was from a marl pit in the hillside behind the present-day Turner house. This marl was reportedly processed at the Wolf Creek Marl operation. In the middle to late 1940s, a plant was set up near the present site of the Turner house by the Gatewood and Talbott Company (Figure 9; Table, Giles 2). Material from this plant was trucked across Wolf Creek and loaded on the Virginian Railroad; production continued into the early 1950s. The property subsequently was sold and broken up into subdivision lots and renamed Marlville. The marl deposits remaining along the hillside near Shumate represent potential reserves of agricultural lime.

The Giles County travertine-marl deposits described above are associated with the Narrows fault or the Piney Ridge fault (T. M. Gathright, II, 1986, personal communication).

marl. On the west side of Spout Run, the Sipes operation worked marl as thick as 6 m. The Weir deposit is believed to have only been about 1.5 m thick.

FREDERICK

Marl has been produced by two operators in the county. In 1923, marl was produced by Cornwall Lime Marl in Winchester. The company may have operated the pit on Abrams Creek near the western edge of Winchester. The most recent production was 80,000 short tons of 90 percent or greater CaCO_3 along Redbud Run, just northwest of Winchester (Figure 7). This deposit, worked from 1981-1982 and marketed from 1982-1985, is further described by Giannini (this volume).



Figure 7. View of Digges' marl operation on Redbud Run showing marl exposure and loading of trucks, Frederick County (photo taken by S. O. Bird, 1984).

GILES

Marl was dug by hand from 1935 to 1939 from the hillside (Figure 8, location 1) southeast of Wolf Creek along present State Road 724. Travertine was mined from this site using dynamite shots placed in hand-drilled holes. In the early 1940s, another pit and a plant were opened up in this area (Figure 8, location 2) by Hale Brown and Link Buckland. Later, this site was taken over by the railroad building company of Langhorne and Langhorne, Inc., of Huntington, West Virginia, whose subsidiary, Gatewood and Talbott, set up an operation on the site to extract, pulverize, and screen the material (Table, Giles 4). Deterioration of grade of the material led to the closing of this operation around 1947. A marl site on the north side of present State Highway 61 and Wolf Creek was hand dug by Rufus Hale in the late 1930s

(Figure 8, location 3; Table, Giles 3).

A hand-dug pit was opened on the Shepherd property (Figure 8, location 4) in the late 1930s, and marl was hauled by wagon for use on local farms. In the early 1940s, Willie W. Wood of Oakwood Coal and Coke, from Vansant, along with George and Frank Rosenbaum of Rosenbaum Brothers, a heavy equipment construction company from Tazewell, set up the Wolf Creek Marl Company (Table, Giles 5a). They negotiated with James Shepherd's father, who sold the mineral rights to 1012 hectares of land for \$1000 cash; the site was up the ridge from the older hand-dug pit (Figure 8, location 5). James Shepherd (1987, personal communication) remarked that if his father had accepted the proffered \$0.05/short ton royalty, instead of cash, he would have received more than \$2000 in the first 18 months of operation.

Processing at the Wolf Creek marl operation included crushing in a jaw crusher and screening. Some materials required additional pulverizing in two hammer mills. James Shepherd hauled marl in the mid-1940s to both the Norfolk and Western and the Virginian railroads. The marl was loaded into 70-ton hopper cars as well as into low-sided 0.9-m and 15-m gondolas. Some days as many as 12 hopper cars of marl were shipped at \$1.37/short ton, compared to values of \$2.50-\$3.00/short ton at other sites in the state. The product was marketed in the eastern part of Virginia, especially in Nottoway County, and in West Virginia. Floyd Graley (Wolf Creek Marl Company) bought the operation in the early 1950s when the price of marl was up to \$1.50/short ton. The operation (Figure 8, location 5) was subsequently bought by a group, which included Wetzel Brammer and Major Lilley from Beckley, West Virginia, and was renamed Virginia Marl Company. The mineral rights were retained by the former Wolf Creek Marl Company and today are split up in thirds between heirs of Wood and the Rosenbaum brothers. The Virginia Marl Company ceased operations in the mid-1960s.

The Blankenship property, in the area of Shumate, was acquired by Berman Blankenship in December 1941 (Figure 8, location 6). Production was from a marl pit in the hillside behind the present-day Turner house. This marl was reportedly processed at the Wolf Creek Marl operation. In the middle to late 1940s, a plant was set up near the present site of the Turner house by the Gatewood and Talbott Company (Figure 9; Table, Giles 2). Material from this plant was trucked across Wolf Creek and loaded on the Virginian Railroad; production continued into the early 1950s. The property subsequently was sold and broken up into subdivision lots and renamed Marlville. The marl deposits remaining along the hillside near Shumate represent potential reserves of agricultural lime.

The Giles County travertine-marl deposits described above are associated with the Narrows fault or the Piney Ridge fault (T. M. Gathright, II, 1986, personal communication).



Figure 8. Location of travertine-marl production sites near Narrows, Giles County: (1) unnamed hand-dug pit, (2) Langhorne and Langhorne pit, (3) Rufus C. Hale pit, (4) Shepherd pit, (5) Wolf Creek Marl Company (Virginia Marl Company pit), and (6) Gatewood and Talbot pit (scale 1:24,000).

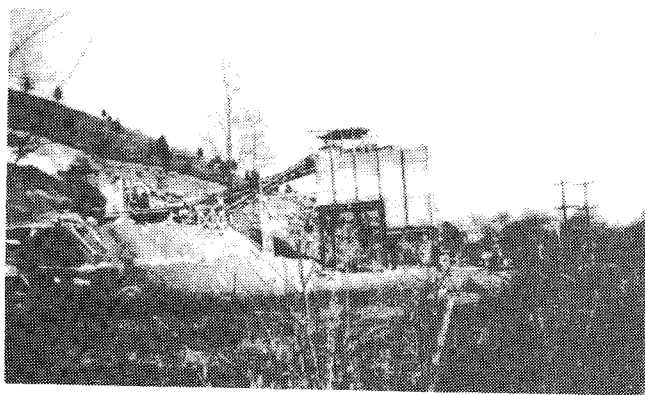


Figure 9. Marl plant of Gatewood and Talbot in middle 1940s showing hopper, screens, and storage bins on Blankenship property, Giles County.

MONTGOMERY

Schubert (circa 1921) states that a sample of marl from Montgomery County contained 94.35 percent CaCO_3 and 4.20 percent MgCO_3 , however, the source of the sample remains unknown. The Falls Hollow travertine deposit (Kirby and Rimstidt, this volume; Herman and Hubbard, this volume) is located about 4.3 km east of Ellett. A Mr. Dudley produced lime from this massive travertine buildup in 1939 and 1940; a lime kiln (Figure 10) and scale pit remain. This

is the only known Virginia operation that burned travertine-marl to produce quicklime.

The J. N. Lantz deposit is located about 3.2 km southeast of Ellett and 3.2 km west of Montgomery between Den Creek and State Road 641 (also see Herman and Hubbard, this volume). W. F. Wall (1921, written communication) estimated the presence of more than 850,000 short tons of marl at this site; a sample contained 96.7 percent CaCO_3 . A 4- to 6-m cliff of travertine is present above Den Creek along the road, west of Slaughterpen Hollow. This deposit was not worked until 1930. Production was low and the area still contains a large reserve (Table, Montgomery 1a and 1b).

ROCKBRIDGE

The earliest documented economic use of Valley and Ridge province travertine-marl materials was a marl from Marl Run (now, Marl Creek; see cover, top left photograph of waterfall upstream from marl deposit) which was used as a flux in iron production at the Buena Vista Furnace (Ruffner, 1889; Gilham, circa 1858). This furnace was in operation between 1848 and 1864 (Capron, 1967). Another Rockbridge County "tufaceous marl" was utilized as a flux in iron production in 1880. One-half short ton of marl from Hamilton's marl bank was obtained at the rate of \$0.25/short ton, including the \$0.125/short ton royalty, for the Amherst Furnace in



Figure 8. Location of travertine-marl production sites near Narrows, Giles County: (1) unnamed hand-dug pit, (2) Langhorne and Langhorne pit, (3) Rufus C. Hale pit, (4) Shepherd pit, (5) Wolf Creek Marl Company (Virginia Marl Company pit), and (6) Gatewood and Talbot pit (scale 1:24,000).

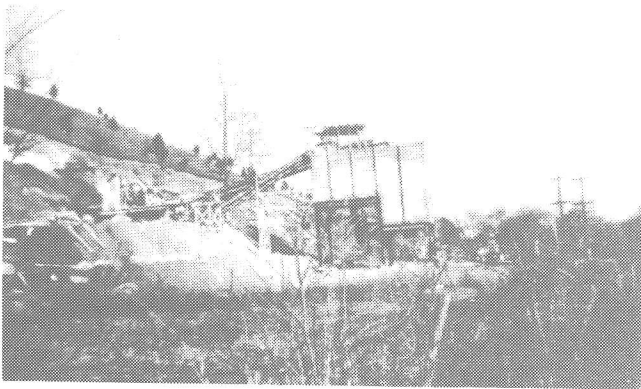


Figure 9. Marl plant of Gatewood and Talbot in middle 1940s showing hopper, screens, and storage bins on Blankenship property, Giles County.

MONTGOMERY

Schubert (circa 1921) states that a sample of marl from Montgomery County contained 94.35 percent CaCO_3 and 4.20 percent MgCO_3 , however, the source of the sample remains unknown. The Falls Hollow travertine deposit (Kirby and Rimstidt, this volume; Herman and Hubbard, this volume) is located about 4.3 km east of Ellett. A Mr. Dudley produced lime from this massive travertine buildup in 1939 and 1940; a lime kiln (Figure 10) and scale pit remain. This

is the only known Virginia operation that burned travertine-marl to produce quicklime.

The J. N. Lantz deposit is located about 3.2 km southeast of Ellett and 3.2 km west of Montgomery between Den Creek and State Road 641 (also see Herman and Hubbard, this volume). W. F. Wall (1921, written communication) estimated the presence of more than 850,000 short tons of marl at this site; a sample contained 96.7 percent CaCO_3 . A 4- to 6-m cliff of travertine is present above Den Creek along the road, west of Slaughterpen Hollow. This deposit was not worked until 1930. Production was low and the area still contains a large reserve (Table, Montgomery 1a and 1b).

ROCKBRIDGE

The earliest documented economic use of Valley and Ridge province travertine-marl materials was a marl from Marl Run (now, Marl Creek; see cover, top left photograph of waterfall upstream from marl deposit) which was used as a flux in iron production at the Buena Vista Furnace (Ruffner, 1889; Gilham, circa 1858). This furnace was in operation between 1848 and 1864 (Capron, 1967). Another Rockbridge County "tufaceous marl" was utilized as a flux in iron production in 1880. One-half short ton of marl from Hamilton's marl bank was obtained at the rate of \$0.25/short ton, including the \$0.125/short ton royalty, for the Amherst Furnace in



Figure 10. Lime kiln, approximately 5.5 m high, at Falls Hollow travertine deposit, Montgomery County (photo taken June, 1987).

Amherst County (Hotchkiss, 1880 and 1881; Table, Rockbridge 1). Hamilton's marl bank is located along the canal on the Maury River, 1.2 km east of the intersection of Interstate 81 and U.S. Highway 60, east of Lexington. The Westham Iron Furnace in Richmond was also reported to have used marl hauled by canal boats from Buena Vista (T. T. Brady, 1987, personal communication).

The Marlbrook Lime Company of Marlbrook produced marl for agricultural liming from their site in the vicinity of the South River from 1913 to 1931 (Table, Rockbridge 5). A company brochure guaranteed that their marl would be 90 percent carbonate of lime; analyses in the brochure noted as much as 97 percent carbonate of lime. A number of other companies produced agricultural material from sites near Riverside, located approximately 11.3 km downstream from Marlbrook on the South River (Table, Rockbridge 2-4).

COUNTIES WITHOUT DOCUMENTED PRODUCTION

Operations, in preliminary stages for mining marl, are known to have existed in Bath, Rockingham, Warren, and Washington counties, but no production figures are available. Information is presented on these counties in order to document available historical information.

BATH

Watson (1913) noted that an operation was being prepared for mining of marl in 1912.

ROCKINGHAM

In 1912, preparations were underway in Rockingham County to develop marl for agricultural purposes (Watson, 1913). Correspondence of June 28, 1912 from C. C. Conger, Jr., of Penn Laird in Rockingham County, to then State Geologist T. L. Watson requested a value for the marl which Mr. Conger was putting on the market. Mr. Conger also noted that F. A. Schubert, "a mineralogist from Roanoke," said it was an extremely valuable deposit. According to a 1911 Rockingham County deed book (95, p. 14), Mr. Conger acquired a water pipe and right-of-way on Meadow View farm, above a spring north of Mill Creek farm and southeast to Keezletown road. This farm property is apparently located on the present-day Grottoes 7.5-minute quadrangle along Congers Creek just southwest of Penn Laird. The barrel of marl which Mr. Schubert took back to Roanoke in 1913 was tested and found to contain 51.12 percent CaO (91.24 percent CaCO_3). In a Norfolk and Western Railway brochure on freshwater marl in the Virginias, Schubert (circa 1921) noted that a marl sample from the county contained 97.75 percent CaCO_3 and 0.73 percent MgCO_3 .

WARREN

A marl pit, located 3.1 km east of Cedarville, off the south side of State Road 658 along Willow Brook, is evidence of marl production in Warren County.

WASHINGTON

Watson (1919, Virginia Geologic Survey Field Notes) indicated that a deposit of travertine with potential commer-



Figure 10. Lime kiln, approximately 5.5 m high, at Falls Hollow travertine deposit, Montgomery County (photo taken June, 1987).

Amherst County (Hotchkiss, 1880 and 1881; Table, Rockbridge 1). Hamilton's marl bank is located along the canal on the Maury River, 1.2 km east of the intersection of Interstate 81 and U.S. Highway 60, east of Lexington. The Westham Iron Furnace in Richmond was also reported to have used marl hauled by canal boats from Buena Vista (T. T. Brady, 1987, personal communication).

The Marlbrook Lime Company of Marlbrook produced marl for agricultural liming from their site in the vicinity of the South River from 1913 to 1931 (Table, Rockbridge 5). A company brochure guaranteed that their marl would be 90 percent carbonate of lime; analyses in the brochure noted as much as 97 percent carbonate of lime. A number of other companies produced agricultural material from sites near Riverside, located approximately 11.3 km downstream from Marlbrook on the South River (Table, Rockbridge 2-4).

COUNTIES WITHOUT DOCUMENTED PRODUCTION

Operations, in preliminary stages for mining marl, are known to have existed in Bath, Rockingham, Warren, and Washington counties, but no production figures are available. Information is presented on these counties in order to document available historical information.

BATH

Watson (1913) noted that an operation was being prepared for mining of marl in 1912.

ROCKINGHAM

In 1912, preparations were underway in Rockingham County to develop marl for agricultural purposes (Watson, 1913). Correspondence of June 28, 1912 from C. C. Conger, Jr., of Penn Laird in Rockingham County, to then State Geologist T. L. Watson requested a value for the marl which Mr. Conger was putting on the market. Mr. Conger also noted that F. A. Schubert, "a mineralogist from Roanoke," said it was an extremely valuable deposit. According to a 1911 Rockingham County deed book (95, p. 14), Mr. Conger acquired a water pipe and right-of-way on Meadow View farm, above a spring north of Mill Creek farm and southeast to Keezletown road. This farm property is apparently located on the present-day Grottoes 7.5-minute quadrangle along Congers Creek just southwest of Penn Laird. The barrel of marl which Mr. Schubert took back to Roanoke in 1913 was tested and found to contain 51.12 percent CaO (91.24 percent CaCO_3). In a Norfolk and Western Railway brochure on freshwater marl in the Virginias, Schubert (circa 1921) noted that a marl sample from the county contained 97.75 percent CaCO_3 and 0.73 percent MgCO_3 .

WARREN

A marl pit, located 3.1 km east of Cedarville, off the south side of State Road 658 along Willow Brook, is evidence of marl production in Warren County.

WASHINGTON

Watson (1919, Virginia Geologic Survey Field Notes) indicated that a deposit of travertine with potential commer-

cial value was located near Vance's Mill, 3.2 km south of Abingdon. The site was owned by R. C. Copenhaver, and analysis of a sample yielded results of 92 to 95 percent CaCO_3 . Schubert (circa 1921) noted an analytical result of 93.00 percent CaCO_3 and 1.34 percent MgCO_3 for the county and listed a manufacturer named R. C. Copenhaver located along the railway in Abingdon.

POTENTIAL OUTLOOK

The outlook for production of travertine-marl materials for both new and old uses is not encouraging. Recent testing of a travertine-marl material for reactivity with SO_2 gas has shown that even though the CaCO_3 percentage is greater than 97 percent, the clay content inhibits the reactivity for desulfurization of emissions from coal-fired power plants (Sweet and others, 1988). Travertine deposits with less clay and inorganic material may prove to be more reactive.

The outlook for production of travertine-marl materials for use as agricultural lime is not promising. Many of the prime sites have been worked out. At least one other high-quality marl site is known in Clarke County but county regulations make its utilization unlikely. Some lower quality deposits may be of local use for production of agricultural material. Other travertine-marl deposits are appreciated aesthetically by their current owners so commercial utilization is not a consideration. Further restrictions include inaccessibility due to residential, commercial, and industrial development over and adjacent to deposits and competition from established agricultural lime producers, which utilize limestone-dolomite as a raw material.

ACKNOWLEDGMENTS

The historical account of travertine production in Clarke County was compiled from interviews with Paul Chapman, John and Dudley Digges, Winston Sipes, and Cecil Wolfe.

REFERENCES CITED

- Capron, J.D., 1967, Virginia iron furnaces of the Confederacy: Virginia Cavalcade, v. 17, n. 2, p. 10-18.
- Collins, R.E.L., 1924, Travertine deposits in Virginia: Pan-American Geology, v. 41, p. 103-106.
- Gilham, William, circa 1858, Map of the County of Rockbridge, Virginia: Lexington, Virginia, VMI Museum Collection, one sheet.
- Edmundson, R.S., 1958, Industrial limestones and dolomites in Virginia: James River district west of the Blue Ridge: Virginia Division of Mineral Resources Bulletin 73, 137 p.
- Hotchkiss, Jed, 1880, Marl as a blast furnace flux: The Virginias, v. 1, n. 2, p. 173.
- Hotchkiss, Jed, 1881, Untitled: The Virginias, v. 2, n. 2, p. 17.
- Hotchkiss, Jed, 1885, Historical atlas of Augusta County - Virginia: Chicago, Illinois, 93 p.
- Hubbard, D.A., Jr., Giannini, W.F., and Lorah, M.M., 1985, Travertine-marl deposits of the Valley and Ridge province of Virginia - a preliminary report: Virginia Division of Mineral Resources, Virginia Minerals, v. 31, n. 1, p. 1-8.
- Jefferson, Thomas, 1825, Notes on the State of Virginia: Philadelphia, Pennsylvania, H.C. Carey and I. Lea, 344 p.
- Kindle, E.M., 1911, The collapse of recent beds at Staunton, Va.: Proceedings of the Washington Academy of Science, v. 13, n. 2, p. 35-49.
- Ohio C. Barber Fertilizer Company, circa 1926, Facts concerning Barbers "Fallingsprings" lime: Barber, Virginia, 16 p.
- Pettijohn, F.J., 1957, Sedimentary Rocks: New York, New York, Harper & Brothers, 718 p.
- Ruffner, W.H., 1889, Report on the landed property of the Buena Vista Company: Philadelphia, Pennsylvania, Dando Printing and Publishing Co., 354 p.
- Schubert, F.A., circa 1921, Fresh water marl in the Virginias: Norfolk and Western Railway, 6 p.
- Sweet, P.C., Fordham, O.M., Jr., and Giannini, W.F., 1987, Carbonate materials suitable for desulfurization of flue gas: Virginia Division of Mineral Resources, Virginia Minerals, v. 33, n. 4, p. 33-36.
- Van Horn, F.B., 1910, A cave-in caused by an underground stream at Staunton, Va.: Engineering News, v. 64, p. 238-239.
- Watson, T.L., 1913, Biennial report on the mineral production of Virginia during the calendar years 1911 and 1912: Virginia Geological Survey Bulletin 8, 76 p.
- Woodward, H.P., 1932, Geology and mineral resources of the Roanoke area, Virginia: Virginia Geological Survey Bulletin 34, 172 p.

THE MORPHOLOGY AND STRATIGRAPHY OF CALCAREOUS SEDIMENTS IN A SMALL ALLUVIAL-COLLUVIAL FAN, NEW CREEK MOUNTAIN, MINERAL COUNTY, WEST VIRGINIA

J. Steven Kite¹ and D. Mark Allamong^{1,2}

CONTENTS

	Page
Abstract.....	139
Introduction.....	140
Bedrock geology and topography.....	141
Sediments within the deposit.....	142
Geochemistry.....	144
Dendrochronology.....	144
Discussion.....	147
Acknowledgments.....	148
References cited.....	149

ILLUSTRATIONS

Figure	
1. Location of the New Creek Mountain fan deposit.....	140
2. Map of second-order drainage basin.....	141
3. Topographic map of the travertine-marl deposit.....	143
4. Two deformed <i>Acer</i> (maple) trunks.....	145
5. Trunk deformation and subaerial root exposure.....	146
6. <i>Platanus</i> (sycamore) with 0.9 m of subaerial root exposure	146
7. Typical trees at the margins of the stream channel.....	147

TABLES

Table	
1. Water-chemistry data.....	145
2. Tree-ring data.....	146

ABSTRACT

The New Creek Mountain travertine-marl deposit occurs in a fan at the mouth of a second-order stream. Devonian Oriskany sandstone and Helderberg cherty limestone underlie the fan, and the carbonate rocks of the Silurian Tonoloway and Wills Creek formations underlie the stream. Unlike most basins draining New Creek Mountain, the headwaters receive little coarse colluvium. The fan can be differentiated into two parts. The upper fan is dominated by loose marl with travertine inclusions, whereas the lower fan is dominated by inter-

bedded marl, colluvium, and silty alluvium.

The second-order stream has incised the fan surface 2 to 6 m, despite the fact that travertine encrustations are forming currently in the stream channel. Tree-ring studies show that the incision predates the 1936 growing season, but the stream banks have been very unstable in the last few decades. At least four explanations have been offered as to why incision has occurred at so many travertine-marl deposits in the region, but local adjustment resulting from truncation of the lower fan is the simplest explanation for the New Creek Mountain locality.

¹Department of Geology and Geography, West Virginia University, Morgantown, WV 26506

²Sturm Environmental Services, P.O. Box 650, Bridgeport, WV 26330

INTRODUCTION

Investigations of colluvial and alluvial deposits in New Creek Valley, West Virginia (Kite and others, 1986), have resulted in the discovery of a deposit containing organic-rich marl and fossiliferous travertine. The calcareous sediments occur in an incised fan at the mouth of an unnamed second-order stream. The fan is located near the town of New Creek, Mineral County, 4.0 km south of Keyser, West Virginia (Figure 1). The unnamed second-order stream flows into a much larger stream named New Creek, but very little secondary calcium carbonate occurs in the latter stream. The calcareous deposit is herein referred to as the New Creek Mountain deposit to make it clear that the marl and travertine do not occur on New Creek, a tributary to the North Branch of the Potomac River.

Marl and related deposits have been reported from various localities throughout the upper Potomac River basin, but they are much less common than in the Shenandoah Valley. The only comprehensive geological report covering Mineral County stated that there were "only a few beds of marl" (Reger, 1924). Reger (1924) did not report specific travertine-marl sites in Mineral County but did describe three deposits in adjacent Grant County. The closest site, at Williamsport, is 22.4 km south of the New Creek Mountain locality. Gillespie and Clendening (1964) described a marl deposit in Hardy County, West Virginia, 22.9 km south of the locality discussed in this paper. The 20-m-thick marl deposit in Hardy County yielded remains of 20 plant genera, several types of mollusca, and fossil pollen and leaves indicative of a modern flora (Gillespie and Clendening, 1964). Marl is discussed briefly in geological reports for all counties in eastern West Virginia (Grimsley, 1916; Tilton, Prouty, and Price, 1927; Tilton, Prouty, Tucker, and Price, 1927).

The terminology used to describe sediments discussed in this paper follows Bates and Jackson (1987) and may differ from the usage in other papers in this volume. Travertine refers to relatively hard, dense, finely crystalline massive or concretionary deposits composed of calcite with minor inclusions of clastic sediments. Marl is restricted to loose, earthy deposits containing 35 to 65 percent calcium carbonate and 65 to 35 percent clay or silt. Tufa (a minor constituent of this deposit) is a soft, spongy, cellular, or porous, semifriable deposit composed of greater than 65 percent calcite. Diamicton is a nongenetic term for poorly sorted, matrix-supported, noncalcareous or very slightly calcareous sediment with a wide range in particle size; diamictons in the study area are either colluvium or debris-flow deposits. Bates and Jackson (1987) restrict diamicton and diamictite, its lithified equivalent, to noncalcareous sediment, so diamictic sediment cemented with calcium carbonate is called a matrix-supported breccia.

Research on the New Creek Mountain deposit continues as part of an M.S. thesis in geology at West Virginia Univer-

sity by the second writer. The status of this project precludes presentation of this research as a finished work. Additional research is planned on the distribution of different sediments within the deposit and analyses of sediment geochemistry and particle-size distribution. This paper is a preliminary report on research to date. The main purpose of the paper is to discuss the first travertine-marl deposit reported from Mineral County, West Virginia, a deposit with an unusual morphology and a sediment distribution that differs significantly from the model of typical travertine-marl deposits formed in Virginia (Hubbard and others, 1985).

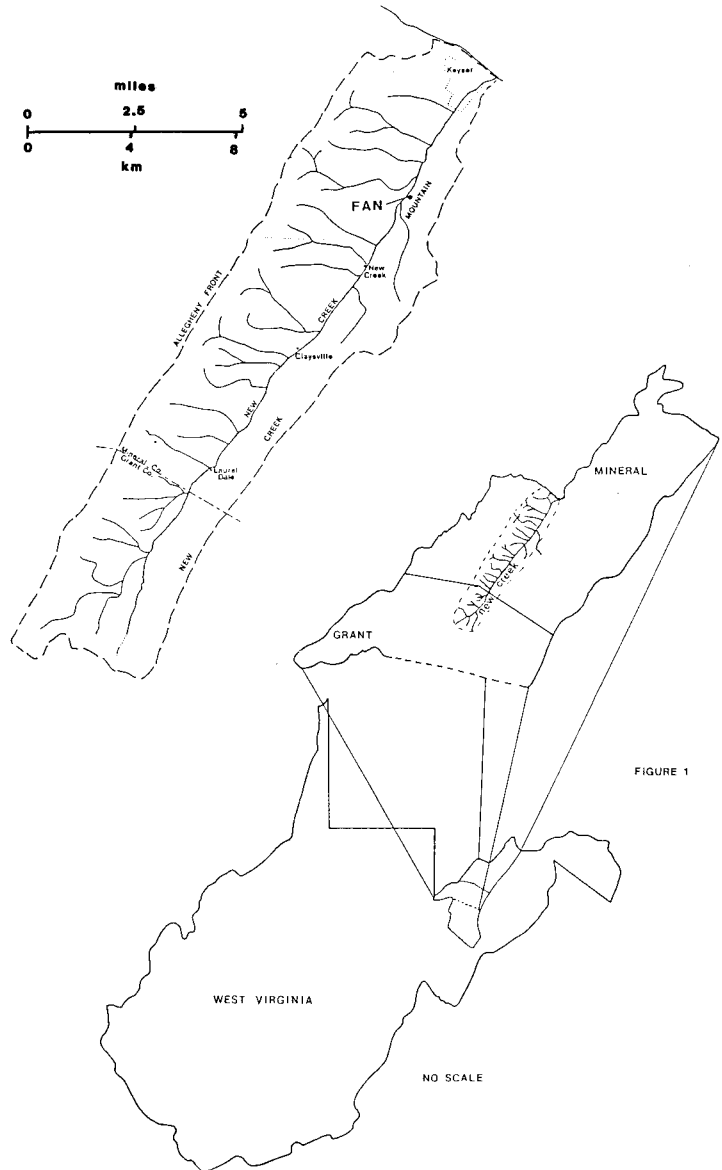


Figure 1. Location of the New Creek Mountain fan deposit. The deposit is located on the Westport MD-WV 1:24,000 topographic map (UTM coordinates: Zone 17 671866E 4363110N).

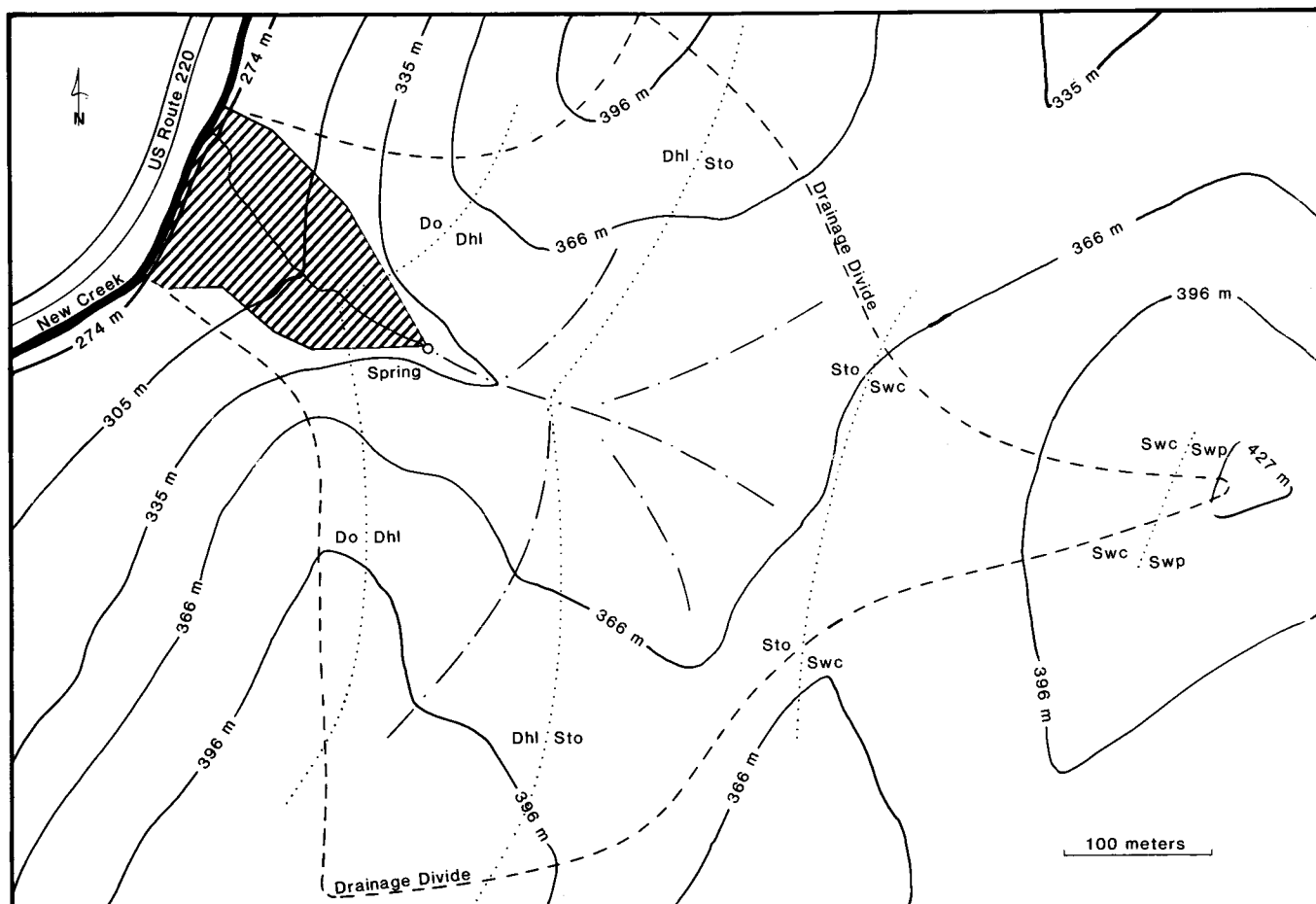


Figure 2. Map of the second-order drainage basin. Topography is after U.S. Geological Survey Westernport and Keyser 1:24,000 topographic maps. Contour interval is 30.5 m. Top of Abrams Ridge (elevation: about 490 m) lies 500 m east of the map area. The travertine-marl deposit is indicated by the cross-hatched pattern and is shown in more detail on Figure 3. Dashed line denotes drainage divide; dot-dashed lines denote ephemeral drainage. Dotted lines represent bedrock contacts. Bedrock symbols: (Do) Devonian Oriskany Sandstone; (Dhl) Devonian Helderberg Group; (Sto) Silurian Tonoloway Limestone; (Swc) Silurian Wills Creek Formation; (Swp) Silurian Williamsport Sandstone. Tonoloway-Wills Creek contact generally follows Dennison (1963).

BEDROCK GEOLOGY AND TOPOGRAPHY

The calcareous deposit occurs at the mouth of a second-order stream that drains a 0.26-km² basin (Figure 2) on the west limb of the Wills Mountain anticline, the westernmost major fold in the Valley and Ridge physiographic province (Reger, 1923; Cardwell and others, 1986). The mouth of the stream has an elevation of 270 m. A maximum elevation in excess of 427 m occurs on the easternmost knoll, but most of the steep slopes in the basin are on New Creek Mountain (Figure 2). Slopes range from less than 10 percent in upper reaches of the stream to over 70 percent on New Creek Mountain near the fan. Although its tributaries have concave profiles, the second-order stream has a generally convex profile.

Bedrock geology is an important control on the nature

and location of travertine-marl deposits. Bedrock on New Creek Mountain generally dips steeply to the west-northwest. Devonian Oriskany sandstone and Helderberg Group cherty limestone are the resistant units of this portion of New Creek Mountain. Oriskany sandstone underlies the mouth of the stream and most of the fan (Figure 2). The Helderberg rocks are exposed in the stream bed near the upper part of the fan and on adjacent steep slopes. These two resistant bedrock lithologies are the sources of all angular colluvial clasts within the calcareous deposit. Colluvium derived from the Oriskany sandstone is composed mostly of angular sandstone cobbles and boulders, whereas colluvium derived from the Helderberg Group is largely angular chert pebbles and cobbles, commonly with limestone boulders. Most of the colluvium on New Creek Mountain is texturally a diamicton with a fine-grained loamy matrix, but some outcrops of Helderberg-derived colluvium are composed entirely of angular, clast-sup-

ported chert gravel.

The Silurian Tonoloway limestone and calcareous shales of the Wills Creek Formation underlie nearly all of the headwaters of the basin. Most of the headwaters are in a topographic saddle between New Creek Mountain and the next ridge to the east, Abrams Ridge (Figure 2). It is unusual for non-resistant lithologies to underlie a drainage divide. Residual soils developed on the Tonoloway and Wills Creek are silty and yield few coarse colluvial clasts. Silty alluvium with scattered limestone cobbles occurs in low areas in the upper basin. Portions of the silty alluvium have been incised by shallow, discontinuous gullies.

Various resistant Silurian formations, such as the Tuscarora Sandstone, underlie Abrams Ridge (Reger, 1923; Dennison, 1963), but none have significant outcrops in the second-order drainage basin. Water and sediment runoff from Abrams Ridge are directed into either of two subsequent stream basins developed in narrow valleys underlain by the Tonoloway Limestone. Largely because of this diversion of colluvium from the resistant Silurian rocks into adjacent drainage basins, the upper end of the basin receives little coarse sediment. A small outcrop of Williamsport sandstone occurs at the eastern limit of the basin (Figure 2), but clasts from this outcrop weather into angular pebbles and smaller clasts before being transported more than a few meters downslope from the outcrop.

There is ample evidence of groundwater flow in the second-order drainage basin. Karst features are well developed in the upper part of the basin. The largest of several dolines is 50 m wide and 10 m deep. Two small, first-order solutional valleys are aligned with two large dolines, probably reflecting the strike of easily dissolved Tonoloway limestone. The solutional valleys have poorly developed to nonexistent stream channels, indicating that most runoff is lost into subsurface conduits during periods of normal flow. Despite average slopes of about 12 percent, the headwaters of the basin contribute water and sediment runoff directly to the stream only as the result of high-runoff events.

Down valley, the second-order stream is perennial. Normal flow is maintained by a spring issuing from the base of a steeply dipping Helderberg outcrop (Figure 3). Spring flow was measured at 1.13 L/s in January 1988 and at 0.7 L/s during early stages of a drought in July 1988. No other discharge measurements have been made at the spring, but our qualitative observations at the spring suggest that discharge has varied little from one visit to the next. Considerable downstream variation in stream flow has been noted below the spring because of recharge into and discharge out of permeable deposits within the fan.

The spring occurs just above the fan, at an elevation of 335 m (Figure 3). The stream bed becomes significantly steeper below the spring. The fan covers about 0.02 km² and is obvious in the field, but it is too small to be identified clearly on 1:24,000 scale topographic maps. The fan is not shown as a distinct soil map unit in the comprehensive soil survey

report of Mineral County (Curry and others, 1978).

The second-order stream has incised into the fan surface and has a 30 percent gradient downstream from the spring. Exposed roots and deformed trunks show channel erosion has occurred within the life-span of trees growing on the stream banks; however, the deposition of calcium carbonate has occurred on recently disturbed surfaces, freshly fallen tree trunks, and introduced clasts.

The fan can be divided into upper and lower parts. A narrow constriction in the channel (site A, Figure 3) separates the two fan segments. The uneroded fan surface has a gradient of 38 percent near the spring, but flattens downstream to only 20 percent on the lower fan. The stream channel is incised up to 6 m into the lower fan surface (site B, Figure 3). The distal end of the fan has been truncated by New Creek, so that the fan terminates in a steep, 14-m-high scarp.

SEDIMENTS WITHIN THE DEPOSIT

The upper fan is dominated by marl and travertine, but marl, coarse colluvium, and silty alluvium tend to dominate the lower fan. Travertine encrusts objects in all parts of the stream bed along the fan. Much of the freshly deposited travertine is associated with mosses and algae. The role that plants play in the deposition of calcium carbonate has not been assessed.

A mound of loose, pisolitic, very pale-brown (10YR 8/3 to 10YR 7/4) marl, with lenses of porous, white (10YR 8/2) tufa occurs just downstream from the spring (site C, Figure 3). Boulders of hard, white (10YR 8/2), botryoidal travertine lie scattered over the surface of the mound; augering with an AMS "Dutch" auger revealed pebble-sized travertine clasts at depth. The travertine is 98 percent calcium carbonate and contains molds of leaves and twigs of trees found in the modern hardwood forest. These fossil plants are similar to those found in the Hardy County marl deposit (William H. Gillespie, 1986, personal communication).

Similar sediments are characteristic of the rest of the upper fan, but most of the deposits in this reach are eroded. The average depth of augering before hitting an impenetrable layer was just over 1.0 m, with a maximum of 1.57 m; it was not clear whether the impenetrable material was travertine, coarse colluvium, or bedrock. Stream bank exposures show that the calcareous deposits in the upper fan locally exceed 2 m in thickness. Coarse colluvium overlaps the margins of the calcareous deposits at the upper fan, but only a few colluvial clasts occur scattered throughout the marl.

The mound and other calcareous deposits at the upper fan may be erosional remnants of a terrace. The calcareous sediment is very incoherent, and slight disturbances of the slope during field work triggered perceptible erosion of the stream bank. Little vegetation grows on these deposits, possibly because of their inherent instability. Although some

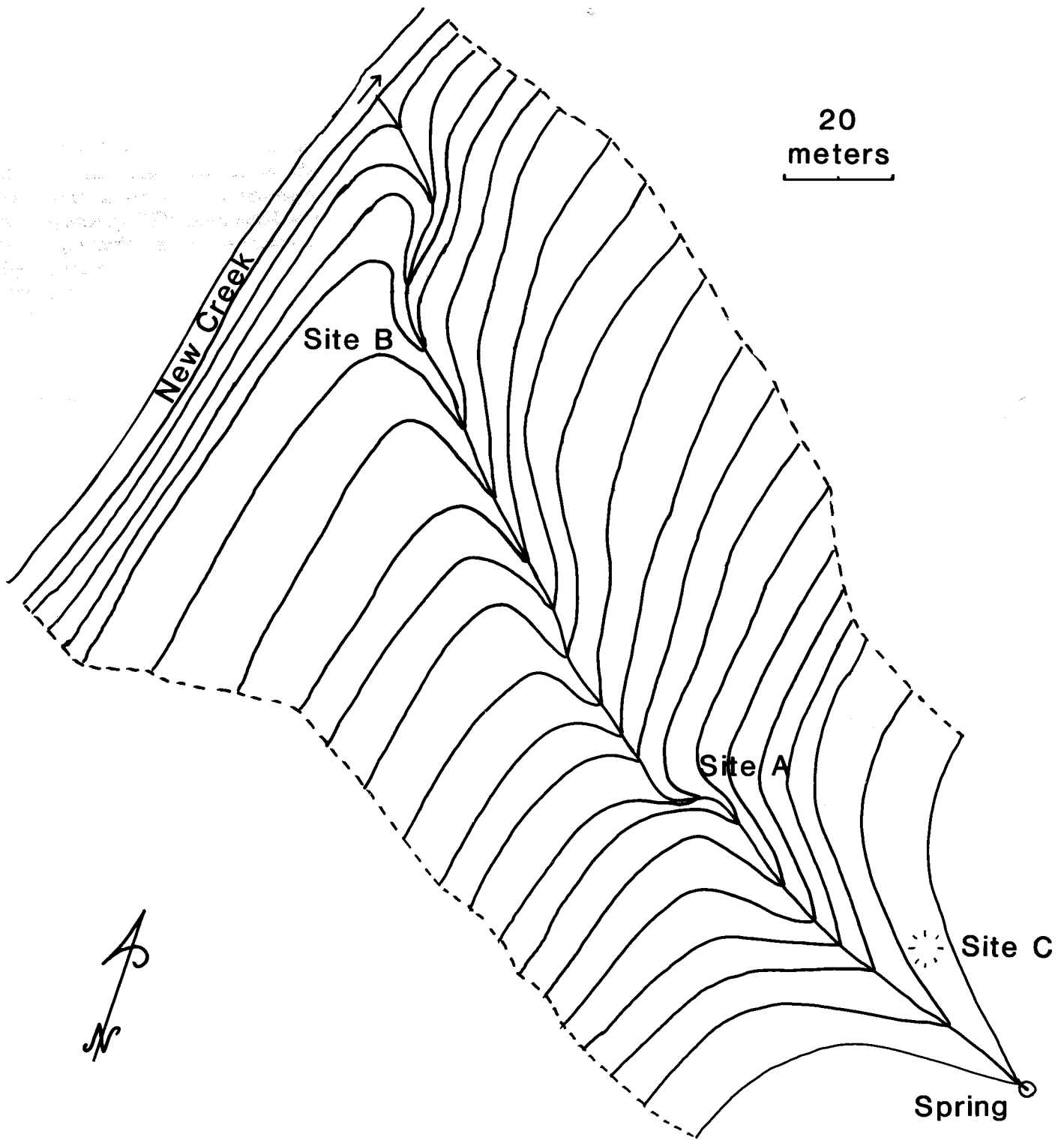


Figure 3. Topographic map of the travertine-marl deposit and second-order drainage basin. Dashed line marks limit of calcareous sediments. Topography within this limit is based on tape-and-compass mapping. Datum is confluence of unnamed stream and New Creek; contour interval is 3.05 m. See text for discussion of sites.

of the sediment eroded from the upper fan accumulates in small (less than 50 cm long) ephemeral bars along the stream channel, most of the eroded carbonate material is flushed into New Creek. There is no significant aggradation of transported calcium carbonate clasts on the lower fan.

Some encrusting travertine occurs in the channel at the constriction between the upper and lower fan, but other carbonate materials are not well developed here. Below this constriction, the fan widens and the stream is confined to a prominent incised channel.

A variety of sediments is characteristic of the lower fan. Marl is the most abundant sediment in the incised stream banks, but coarse colluvium and silty alluvium are also important. Minor travertine deposits also are exposed in the stream bank. Small-scale stratification is not apparent in most sediments in the lower fan, but crude layering can be discerned in portions of the stream bank. Like those at the upper fan, most of the sediments in the lower fan are incoherent. The stream bank is unstable except where covered by continuous root mat. Devegetation of the locality would result in accelerated erosion of the fan.

The nature of the marl in the lower fan is variable. One sample of marl was composed of 58 percent calcium carbonate, but additional analyses are needed to determine the range of calcium carbonate content in the lower fan. Silty alluvium derived from soils developed on the Tonoloway and Wills Creek formations is the main non-calcareous constituent of the marl. Silty alluvium is not apparent along the modern stream channel. Most of the marl and silty alluvium were deposited prior to fan incision. Although it was derived from the upper basin, the silty alluvium bypassed the relatively narrow, steep upper fan and was deposited on the wide, gently sloping surface of the lower fan.

Soil augering is difficult over much of the surface of the lower fan because of large, angular colluvial clasts. Large clasts are most abundant on the margins of the fan and at the top of the stratigraphic sequence exposed in the stream bank. Other bouldery concentrations occur at depth, interbedded with loose marl and travertine. Some colluvium has a fine-grained matrix and may be cemented into either clast-supported or matrix-supported breccia. Other colluvial layers lack a fine-grained clastic matrix, but the interstitial voids may be filled with relatively pure, very pale-brown (10YR 7/4) travertine. Locally, colluvial gravel is cemented into a resistant breccia. More typically, the coarse colluvial clasts are uncemented and collect as lag in the stream channel wherever marl and other fine-grained sediments have been eroded. Some colluvial cobbles and pebbles probably are transported in the channel during extreme runoff events.

The distal end of the fan is truncated by a steep scarp and appears to be composed of a variety of unconsolidated sediments, including marl and coarse colluvium. The scarp is well vegetated and wet from groundwater discharge throughout the year. Sediments are poorly exposed in the scarp, so little is known about their exact nature.

GEOCHEMISTRY

Autochthonous calcareous deposits precipitate when aqueous solutions are exposed to the atmosphere and become supersaturated with respect to carbonate minerals (White, 1976). The mechanism for CO₂ outgassing and calcite precipitation is described elsewhere (Sweeting, 1973; Hoffer-French and Herman, this volume; Lorah and Herman, this volume; Kirby and Rimstidt, this volume). Calcium carbonate deposition is frequently the result of carbon dioxide outgassing because of differences in CO₂ partial pressures between the groundwater and the atmosphere (Jennings, 1971). Carbon dioxide outgassing occurs most commonly in areas of stream turbulence, resulting in calcite deposition in the stream channel (Hubbard and others, 1985; Hoffer-French and Herman, this volume).

Water samples were taken from the stream in January 1988 and in July 1988. On both occasions, one sample was obtained from the spring and another from the unnamed tributary a few meters above its confluence with New Creek. Table 1 contains the results of chemical analyses of all four samples. All analyses were performed in accordance with Standard Methods for the Examination of Water and Wastewaters, Methods for Chemical Analysis of Water and Wastes (Environmental Protection Agency, 1979), or Standard Methods for Examination of Waste Water (Greenberg and others, 1985). The chemical analyses show that conductivity, alkalinity, total dissolved solids, calcium, magnesium, and carbon dioxide are higher in samples from the spring than farther downstream. These data indicate that carbon dioxide outgassing and carbonate mineral deposition may occur along the flow path.

DENDROCHRONOLOGY

A variety of hardwood species grow on the fan surface. *Quercus* (oak) and *Acer* (maple) are the dominant species; minor species include *Platanus* (sycamore), *Carya* (hickory), *Ulmus* (elm), *Cercis* (redbud), *Cornus* (dogwood), and numerous shrub species. Arboreal vegetation is sparse where relatively pure travertine underlies the surface, but scattered trees, such as *Cercis*, *Platanus*, and *Carpinus* (hornbeam), are established on these sites. Increment borings and cross-sectional slabs were taken from selected trees throughout the fan to determine age, growth rate, and growth abnormalities. Table 2 summarizes information obtained from these samples.

Trees growing on the undissected surfaces of the lower fan show no trunk deformation and are relatively old. Increment borings show that the larger trees growing on this surface are over 150 years old (borings 5 and 6, Table 2), suggesting that this surface has been stable over that time span.

Table 1. Water-chemistry data. Samples were taken from the stream either at the spring or a few meters upstream from the confluence with New Creek. Flow was measured in the field with a calibrated beaker and stopwatch, but all other data were determined in the lab. The following analyses were performed in accordance with the Environmental Protection Agency (1979): alkalinity (Alk.) - titrametric to pH 4.5 (method 310.1); total dissolved solids (TDS) - gravimetric, dried to 180°C (160.1); conductivity (Cond.) - specific conductance (120.1); calcium (Ca) - atomic absorption, direct aspiration (215.1); and magnesium (Mg) - atomic absorption, direct aspiration (242.1). Carbon dioxide (CO₂) was determined by titrametric methods (method 406B, Greenberg and others, 1985). All concentrations are expressed in units of mg/L.

Sample Site (Date)	Flow (L/s)	pH	Alk.	TDS	Cond. (μS/cm)	Ca	Mg	CO ₂
Spring (Jan. 1988)	1.13	7.5	282	371	588	108	12.2	43.3
Near mouth (Jan. 1988)	1.0	8.1	246	329	547	94	11.7	6.6
Spring (July 1988)	0.7	8.1	277	429	686	116	16.4	4.6
Near mouth (July 1988)	0.1	8.2	212	344	547	103	11.3	2.9

Extreme tree-trunk deformities, including overturned trunks, occur along the banks of the incised stream channel (Figures 4 and 5). Such deformities develop when trees adjust to keep near-vertical boles in response to slope instability. Cross-sectional slabs of trunks show elliptical growth patterns, with compression rings on the upslope side of the trunks. A small *Acer* (2E, Table 2) exhibited trunk rotation of approximately 135° since the tree began growing in 1941. Periods of slow growth for this tree are recorded from 1951 through 1958 and since 1966. Increment borings on a nearby *Acer* (2D, Table 2) show trunk rotation of 120° since 1952. Growth has been slow since 1964. A third *Acer* (2B, Table 2) showed less than a 90° trunk rotation since 1954. This is the youngest tree growing on the channel bank for which we have identified significant trunk deformation. The two younger trees began growing when the older tree (2E, Table 2) was under stress that was probably caused by bank instability. It is plausible that a single post-1954 event caused most of the trunk rotation, but the variations in growth rates suggest it is more likely that several episodes of instability have occurred in recent decades.

Bank instability also is shown by a large *Platanus* (1A-A", Table 2) with 0.9 m of subaerial root exposure near the top



Figure 4. Two deformed *Acer* (maple) trunks along the banks of the incised stream channel. Note exposed roots on top of the rotated bole. The tree in the foreground (2D, Table 2) shows trunk rotation of 120° since 1952. The tree behind it (2E, Table 2) exhibits trunk rotation of 135° since 1941. Leaves obscure most of the stream bed in this January 1988 photograph. Boulders of Oriskany sandstone occur as a lag in the channel.

of the incised stream bank (Figure 6). The exposed roots indicate at least 0.9 m of erosion from this section of the channel bank since 1936. Many other trees growing on the incised stream bank exhibit trunk deformation and root exposure (Figure 7).

Although tree morphology and growth rings show ample evidence that some channel-bank instability has occurred since 1936, a similar-aged *Platanus* (4, Table 2) growing in the stream channel on the lower fan exhibited no subaerial root exposure or trunk deformation. This *Platanus* shows that most of the channel incision in the distal end of the fan predates the 1936 growing season. Later slope instability recorded by deformed tree trunks and exposed roots must be attributed to lateral channel instability or local bank adjustments, not to the direct result of vertical incision.

Two trees growing on the calcareous deposits on the upper fan have been stable for over two decades, a surprising observation considering the sparse vegetation on this surface. A *Platanus* (3A, Table 2) adjacent to the stream channel at the

Table 1. Water-chemistry data. Samples were taken from the stream either at the spring or a few meters upstream from the confluence with New Creek. Flow was measured in the field with a calibrated beaker and stopwatch, but all other data were determined in the lab. The following analyses were performed in accordance with the Environmental Protection Agency (1979): alkalinity (Alk.) - titrametric to pH 4.5 (method 310.1); total dissolved solids (TDS) - gravimetric, dried to 180°C (160.1); conductivity (Cond.) - specific conductance (120.1); calcium (Ca) - atomic absorption, direct aspiration (215.1); and magnesium (Mg) - atomic absorption, direct aspiration (242.1). Carbon dioxide (CO₂) was determined by titrametric methods (method 406B, Greenberg and others, 1985). All concentrations are expressed in units of mg/L.

Sample Site (Date)	Flow (L/s)	pH	Alk.	TDS	Cond. (μ S/cm)	Ca	Mg	CO ₂
Spring (Jan. 1988)	1.13	7.5	282	371	588	108	12.2	43.3
Near mouth (Jan. 1988)	1.0	8.1	246	329	547	94	11.7	6.6
Spring (July 1988)	0.7	8.1	277	429	686	116	16.4	4.6
Near mouth (July 1988)	0.1	8.2	212	344	547	103	11.3	2.9

Extreme tree-trunk deformities, including overturned trunks, occur along the banks of the incised stream channel (Figures 4 and 5). Such deformities develop when trees adjust to keep near-vertical boles in response to slope instability. Cross-sectional slabs of trunks show elliptical growth patterns, with compression rings on the upslope side of the trunks. A small *Acer* (2E, Table 2) exhibited trunk rotation of approximately 135° since the tree began growing in 1941. Periods of slow growth for this tree are recorded from 1951 through 1958 and since 1966. Increment borings on a nearby *Acer* (2D, Table 2) show trunk rotation of 120° since 1952. Growth has been slow since 1964. A third *Acer* (2B, Table 2) showed less than a 90° trunk rotation since 1954. This is the youngest tree growing on the channel bank for which we have identified significant trunk deformation. The two younger trees began growing when the older tree (2E, Table 2) was under stress that was probably caused by bank instability. It is plausible that a single post-1954 event caused most of the trunk rotation, but the variations in growth rates suggest it is more likely that several episodes of instability have occurred in recent decades.

Bank instability also is shown by a large *Platanus* (1A-A", Table 2) with 0.9 m of subaerial root exposure near the top



Figure 4. Two deformed *Acer* (maple) trunks along the banks of the incised stream channel. Note exposed roots on top of the rotated bole. The tree in the foreground (2D, Table 2) shows trunk rotation of 120° since 1952. The tree behind it (2E, Table 2) exhibits trunk rotation of 135° since 1941. Leaves obscure most of the stream bed in this January 1988 photograph. Boulders of Oriskany sandstone occur as a lag in the channel.

of the incised stream bank (Figure 6). The exposed roots indicate at least 0.9 m of erosion from this section of the channel bank since 1936. Many other trees growing on the incised stream bank exhibit trunk deformation and root exposure (Figure 7).

Although tree morphology and growth rings show ample evidence that some channel-bank instability has occurred since 1936, a similar-aged *Platanus* (4, Table 2) growing in the stream channel on the lower fan exhibited no subaerial root exposure or trunk deformation. This *Platanus* shows that most of the channel incision in the distal end of the fan predates the 1936 growing season. Later slope instability recorded by deformed tree trunks and exposed roots must be attributed to lateral channel instability or local bank adjustments, not to the direct result of vertical incision.

Two trees growing on the calcareous deposits on the upper fan have been stable for over two decades, a surprising observation considering the sparse vegetation on this surface. A *Platanus* (3A, Table 2) adjacent to the stream channel at the

Table 2. Tree-ring data. Borings 1A, 1A', and 1A" are from the same tree, shown in Figure 6; ages given for 1A' and 1A" are for the roots alone, not whole tree. Borings 2A and 2C are not listed because of poor recovery. O. B. diam. stands for outside bole (trunk) diameter.

Boring No.	Genus	Total Age (years)	O.B. Diam. (cm)	Comments
1A	<i>Platanus</i>	51	32	trunk
1A'	<i>Platanus</i>	36	5	exposed root; compression rings
1A"	<i>Platanus</i>	40	12	exposed root; compression rings
2B	<i>Acer</i>	33	6.2	deformed trunk; compression rings
2D	<i>Acer</i>	35	9.8	deformed trunk; compression rings
2E	<i>Acer</i>	46	5	deformed trunk; compression rings
3A	<i>Platanus</i>	50	46	trunk
3B	<i>Cercis</i>	21	11	trunk
4	<i>Platanus</i>	51	48	trunk
5	<i>Acer</i>	>175	122	trunk
6	<i>Quercus</i>	>150	125	trunk

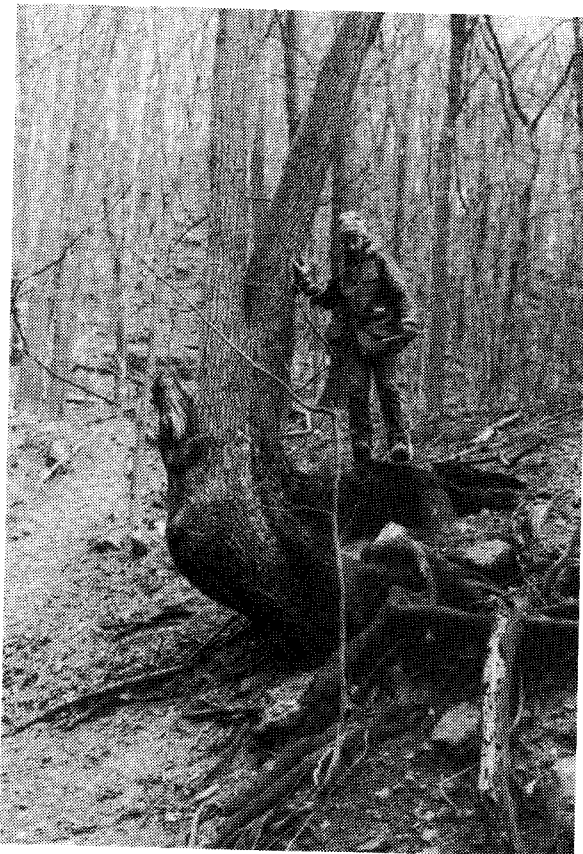


Figure 5. Trunk deformation and subaerial root exposure. Such deformities develop when trees adjust to keep near-vertical boles in response to slope instability. The two trees share a common root system.

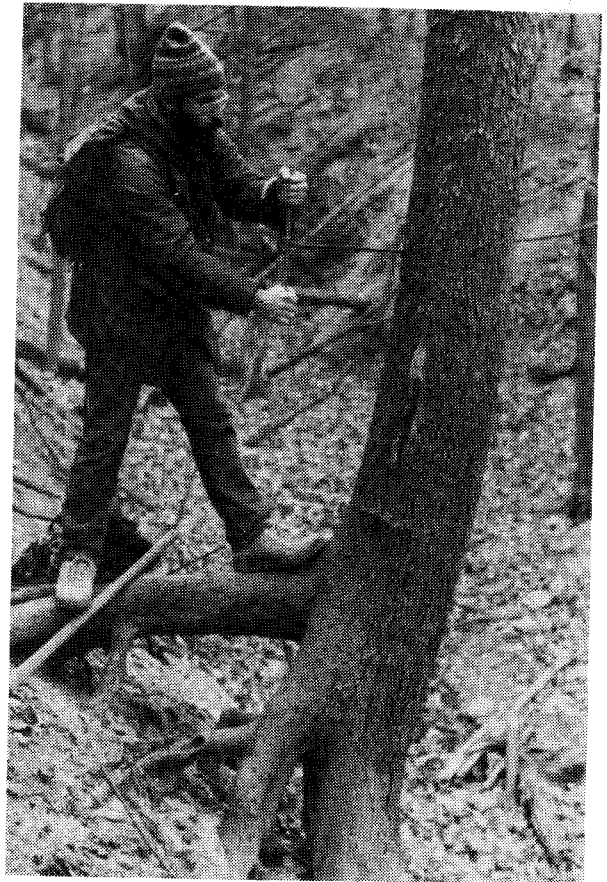


Figure 6. *Platanus* (sycamore) with 0.9 m of subaerial root exposure (1A-A", Table 2). Tree occurs at the top of the stream bank, on the lower fan. The exposed roots indicate at least 0.9 m of erosion from this section of the channel bank since the tree began to grow in 1936.

Table 2. Tree-ring data. Borings 1A, 1A', and 1A'' are from the same tree, shown in Figure 6; ages given for 1A' and 1A'' are for the roots alone, not whole tree. Borings 2A and 2C are not listed because of poor recovery. O. B. diam. stands for outside bole (trunk) diameter.

Boring No.	Genus	Total Age (years)	O.B. Diam. (cm)	Comments
1A	<i>Platanus</i>	51	32	trunk
1A'	<i>Platanus</i>	36	5	exposed root; compression rings
1A''	<i>Platanus</i>	40	12	exposed root; compression rings
2B	<i>Acer</i>	33	6.2	deformed trunk; compression rings
2D	<i>Acer</i>	35	9.8	deformed trunk; compression rings
2E	<i>Acer</i>	46	5	deformed trunk; compression rings
3A	<i>Platanus</i>	50	46	trunk
3B	<i>Cercis</i>	21	11	trunk
4	<i>Platanus</i>	51	48	trunk
5	<i>Acer</i>	>175	122	trunk
6	<i>Quercus</i>	>150	125	trunk



Figure 5. Trunk deformation and subaerial root exposure. Such deformities develop when trees adjust to keep near-vertical boles in response to slope instability. The two trees share a common root system.

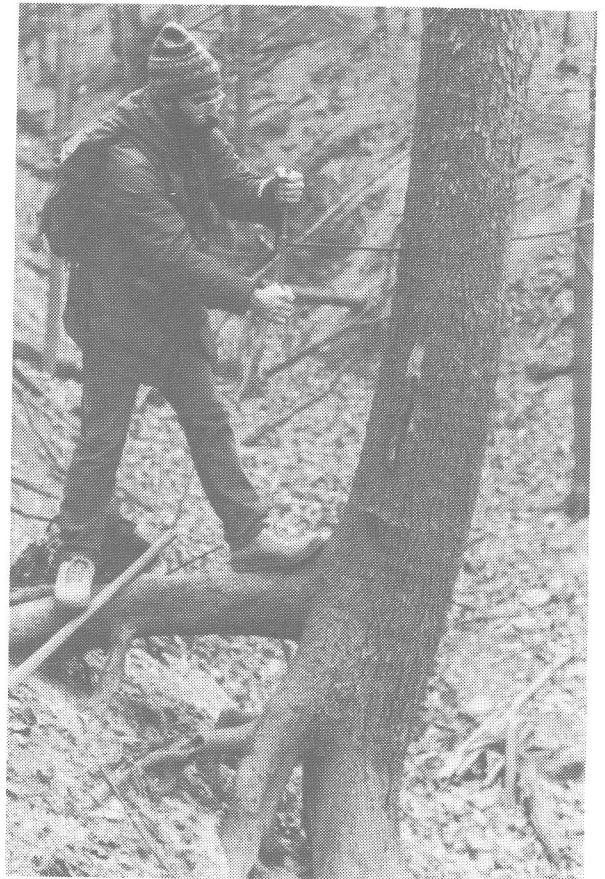


Figure 6. *Platanus* (sycamore) with 0.9 m of subaerial root exposure (1A-A'', Table 2). Tree occurs at the top of the stream bank, on the lower fan. The exposed roots indicate at least 0.9 m of erosion from this section of the channel bank since the tree began to grow in 1936.

marl-travertine mound near the spring revealed no anomalies since the tree began growing in 1937. A *Cercis* (3B, Table 2) has grown on top of the mound since 1966 with no growth anomalies. The general lack of trees may indicate that the surface of the mound has been so unstable that most saplings have been unable to adjust rapidly enough to survive. Alternatively, the lack of vegetation may be caused by the high alkalinity of the soil developed on the deposit.

The major generalization that can be drawn from our limited study of tree rings is that the banks of the stream channel have been unstable for at least one episode in the last 50 years, but most of the channel incision predates the growing season of 1936. All trees studied along the stream channel or on the upper fan surface started growing during or since 1936. Three trees began growing in that year or the next, suggesting that the fan was severely eroded during the devastating flood of March 1936 (Hoyt and Langbein, 1955), but more corroborating tree-ring data are needed before we can assign dates to specific erosion events at the New Creek Mountain site.



Figure 7. Typical trees at the margins of the stream channel. At least four trees in this photograph show trunk deformation. The fan surface is mantled by angular colluvium in the foreground. Marl is the dominant sediment exposed in the stream bank in the background.

DISCUSSION

Other fans occur at the mouths of small streams draining New Creek Mountain, but all of the others are largely composed of bouldery diamictos and poorly sorted gravel. None of the other fans visited to date have significant travertine-marl deposits. Reconnaissance study of the other fans shows several important differences in bedrock geology and topography. Most of the other fans occur at the mouths of streams draining basins with greater vertical relief, so these fans are more likely to experience erosive floods that preclude thick marl accumulation. Many of the fans occur at the mouths of streams that drain basins underlain by carbonate bedrock, but the drainage basin above the New Creek Mountain travertine-marl deposit is the only one deficient in coarse colluvium. The larger fans are fed by stream basins that extend into resistant Silurian clastic rocks east of the Tonoloway-Wills Creek outcrop belt. Several smaller fans between the site of this fan and Keyser, West Virginia, have small drainage basins that do not extend far enough to reach the Silurian rocks. The Oriskany sandstone and cherty Helderberg units in these small basins are duplicated by parasitic folds on the west limb of the Wills Mountain anticline, so that abundant coarse sediment is derived from the two folded resistant units.

Abundant coarse clasts appear to hinder the accumulation of travertine-marl through abrasion and dilution. Abrasion occurs when angular clasts are washed down the stream bed as tractive load. Dilution occurs on other fans when a greater volume of clastic sediments is deposited than on the New Creek Mountain travertine-marl deposit. Disseminated calcite may precipitate in other fans, but the carbonate mineral is minor in proportion to the clastic sediments.

No fresh deposits of silty alluvium were identified along the modern stream channel at the New Creek Mountain locality, and it appears that the silty alluvium was deposited prior to fan incision. The silty alluvium bypassed the relatively narrow, steep upper fan but was deposited on the wide, gently sloping lower fan surface.

Like almost all travertine-marl deposits in the Virginias, the deposit is eroded deeply, although there are irrefutable signs of ongoing calcium carbonate precipitation. Many explanations have been offered to explain this incongruity. The New Creek Mountain deposit can shed some insight on which of these explanations is more plausible.

An early explanation was that the ubiquitous incision occurred because of Holocene climate change. Thornton (1953) suggested that travertine-marl deposits in the Shenandoah Valley expanded during a warm, dry episode in the middle Holocene, but were reduced under cool, moist conditions in the late Holocene. This response to climatic change is plausible, because stream waters would more commonly be supersaturated with respect to calcite during dry episodes than during moist episodes. Pollen studies in the middle-Atlantic states have not identified major climatic changes

marl-travertine mound near the spring revealed no anomalies since the tree began growing in 1937. A *Cercis* (3B, Table 2) has grown on top of the mound since 1966 with no growth anomalies. The general lack of trees may indicate that the surface of the mound has been so unstable that most saplings have been unable to adjust rapidly enough to survive. Alternatively, the lack of vegetation may be caused by the high alkalinity of the soil developed on the deposit.

The major generalization that can be drawn from our limited study of tree rings is that the banks of the stream channel have been unstable for at least one episode in the last 50 years, but most of the channel incision predates the growing season of 1936. All trees studied along the stream channel or on the upper fan surface started growing during or since 1936. Three trees began growing in that year or the next, suggesting that the fan was severely eroded during the devastating flood of March 1936 (Hoyt and Langbein, 1955), but more corroborating tree-ring data are needed before we can assign dates to specific erosion events at the New Creek Mountain site.



Figure 7. Typical trees at the margins of the stream channel. At least four trees in this photograph show trunk deformation. The fan surface is mantled by angular colluvium in the foreground. Marl is the dominant sediment exposed in the stream bank in the background.

DISCUSSION

Other fans occur at the mouths of small streams draining New Creek Mountain, but all of the others are largely composed of bouldery diamictons and poorly sorted gravel. None of the other fans visited to date have significant travertine-marl deposits. Reconnaissance study of the other fans shows several important differences in bedrock geology and topography. Most of the other fans occur at the mouths of streams draining basins with greater vertical relief, so these fans are more likely to experience erosive floods that preclude thick marl accumulation. Many of the fans occur at the mouths of streams that drain basins underlain by carbonate bedrock, but the drainage basin above the New Creek Mountain travertine-marl deposit is the only one deficient in coarse colluvium. The larger fans are fed by stream basins that extend into resistant Silurian clastic rocks east of the Tonoloway-Wills Creek outcrop belt. Several smaller fans between the site of this fan and Keyser, West Virginia, have small drainage basins that do not extend far enough to reach the Silurian rocks. The Oriskany sandstone and cherty Helderberg units in these small basins are duplicated by parasitic folds on the west limb of the Wills Mountain anticline, so that abundant coarse sediment is derived from the two folded resistant units.

Abundant coarse clasts appear to hinder the accumulation of travertine-marl through abrasion and dilution. Abrasion occurs when angular clasts are washed down the stream bed as tractive load. Dilution occurs on other fans when a greater volume of clastic sediments is deposited than on the New Creek Mountain travertine-marl deposit. Disseminated calcite may precipitate in other fans, but the carbonate mineral is minor in proportion to the clastic sediments.

No fresh deposits of silty alluvium were identified along the modern stream channel at the New Creek Mountain locality, and it appears that the silty alluvium was deposited prior to fan incision. The silty alluvium bypassed the relatively narrow, steep upper fan but was deposited on the wide, gently sloping lower fan surface.

Like almost all travertine-marl deposits in the Virginias, the deposit is eroded deeply, although there are irrefutable signs of ongoing calcium carbonate precipitation. Many explanations have been offered to explain this incongruity. The New Creek Mountain deposit can shed some insight on which of these explanations is more plausible.

An early explanation was that the ubiquitous incision occurred because of Holocene climate change. Thornton (1953) suggested that travertine-marl deposits in the Shenandoah Valley expanded during a warm, dry episode in the middle Holocene, but were reduced under cool, moist conditions in the late Holocene. This response to climatic change is plausible, because stream waters would more commonly be supersaturated with respect to calcite during dry episodes than during moist episodes. Pollen studies in the middle-Atlantic states have not identified major climatic changes

during the last 10,000 years (Delcourt and Delcourt, 1986), although a warm, dry middle Holocene has been documented in New England (Davis and others, 1980) and in the upper Mississippi River drainage basin (Knox, 1983).

Alternatively, travertine-marl accumulation may depend more upon style of precipitation than temperature or mean annual rainfall. A single low-frequency, high-magnitude flood may virtually destroy a travertine-marl deposit (Hubbard and others, 1985), so an alternate climatic control would be variation in the frequency of extreme flood events, such as tropical cyclones. The ubiquitous erosion of travertine-marl deposits may result from a late Holocene episode of extreme rainfalls. Pollen studies do not yield information on the recurrence of extreme rainfalls, so we do not know if this hypothesis is consistent with actual Holocene climatic events.

Artificial devegetation, such as the clearing of farmland and logging, can increase flood severity without climatic change. Accelerated erosion of many travertine-marl deposits in the Virginias may stem from deforestation since the onset of European settlement. Poor soil conservation throughout most of the post-settlement interval has introduced great volumes of clastic sediment into streams throughout the region (Costa, 1975; Trimble, 1975; Jacobson and Coleman, 1986). These clastic sediments may have reduced carbonate mineral precipitation through dilution, and eroded existing carbonate deposits through abrasion (David A. Hubbard, Jr., 1987, personal communication).

The specific post-settlement vegetation history of the drainage basin above the New Creek Mountain deposit is not known. Much of the basin is cleared today, and gullies show that there has been some post-settlement erosion of potentially abrasive silty alluvium in the upper drainage basin. The volume of calcareous sediments eroded from the fan exceeds the volume of material lost in upland gullies by at least an order of magnitude, so the role of abrasion by post-settlement sediments transported by the stream is probably minor at this site.

The simplest explanation for the incision of the New Creek Mountain travertine-marl deposit is site specific and cannot be extrapolated as a major regional cause of the ubiquitous erosion. New Creek has truncated the extreme distal end of the fan, creating a steep scarp. All of the incision at the site can be explained by upstream erosion as the second-order stream adjusted its channel gradient in response to this truncation. We have no specific data to show when truncation occurred, but it is a likely factor contributing to erosion at this site.

The general pattern of sediment distribution at this locality shows that carbonate-rich sediments predominantly occur on the upper fan, whereas the silty marl and clastic sediments dominate the lower fan. This pattern contrasts with the general model for travertine-marl deposits in Virginia (Hubbard and others, 1985), wherein marls are most commonly found upstream from travertine dams. The deviation from this model can be explained by the setting in which the

New Creek Mountain travertine-marl occurs. The deposit occurs on a much steeper stream than most travertine-marl deposits in the region, so the turbulence essential to carbon dioxide outgassing occurs immediately below the spring; thus, carbonate-rich deposits dominate the upper fan. Marly sediments do not accumulate upstream from the site of maximum travertine development because this reach is also upstream from the spring (the source of supersaturated water) and because the surface of the travertine is too steep to serve as a dam. Farther downstream, carbonate deposits are diluted by colluvium derived from the western slope of New Creek Mountain. Prior to incision of the fan, carbonate sediments were further diluted by silty alluvium deposited on the relatively gentle surface of the lower fan, forming marl in lieu of travertine wherever calcium carbonate precipitated.

The necessity that water be supersaturated with respect to calcium carbonate causes virtually all travertine-marl deposits to be formed in basins underlain by carbonate bedrock. Most streams in the Virginias that drain basins underlain by carbonate bedrock, and therefore most travertine-marl deposits, are less steep than the stream that built the New Creek Mountain fan. The model developed by Hubbard and others (1985) undoubtedly is appropriate to explain the distribution of sediments in most travertine-marl deposits in the Virginias, especially those formed in low-relief basins underlain by Cambrian and Ordovician carbonate rocks in the Shenandoah Valley. The New Creek Mountain deposit shows that travertine-marl deposits in relatively steep basins underlain by Silurian and Devonian limestones may have atypical sediment distributions.

Possibly the most important conclusion resulting from the study of the New Creek Mountain locality is that travertine-marl deposits can occur in landforms normally associated with other types of sediments. Surficial geologists and soil scientists may encounter travertine-marl deposits obscured by bouldery colluvial deposits in hybrid landforms. The first evidence of calcium carbonate deposition noted at the New Creek Mountain deposit was encrusting travertine in the channel at the mouth of the stream. Any investigator searching for travertine-marl deposits in mountainous terrain should be aware that minor amounts of calcium carbonate in a stream bed may indicate significant calcareous deposits upstream.

ACKNOWLEDGMENTS

We are in debt to Janet Herman and David Hubbard for sharing their insights into travertine-marl deposits in numerous conversations and for their enthusiastic support for completion of this paper. The paper was improved significantly because of review comments by Eugene K. Rader, Donald C. Le Van, and W. Cullen Sherwood. William Gillespie graciously examined plant fossils in a sample of

travertine from this deposit. Geochemical analyses discussed in this paper were performed by Rex Tennant in the analytical laboratory at Sturm Environmental Services.

REFERENCES CITED

- Bates, R.L., and Jackson, J.A., 1987, Glossary of geology, third edition: Alexandria, Virginia, American Geological Institute, 788 p.
- Cardwell, D.H., Erwin R.B., and Woodward, W.P., 1986, 1968 geologic map of West Virginia (slightly revised 1986): West Virginia Geological and Economic Survey, 1:250,000 scale, 2 sheets.
- Costa, J.E., 1975, Effects of agriculture on erosion and sedimentation in the Piedmont province, Maryland: Geological Society of America Bulletin, v. 86, p. 1281-1286.
- Curry, W.H., Becker, R.B., Doonan, F.A., McKinney, D.E., and Pyle, R.E., 1978, Soil survey of Hampshire, Mineral, and Morgan counties, West Virginia: U.S. Department of Agriculture, Soil Conservation Service, 131p., 99 maps.
- Davis, M.B., Spears, R.W., and Shane, L.C.K., 1980, Holocene climate of New England: Quaternary Research, v. 14, p. 240-250.
- Delcourt, H.R., and Delcourt, P.A., 1986, Late Quaternary vegetational change in the central Atlantic states, in McDonald, J.N., and Bird, S.O., eds., The Quaternary of Virginia - a symposium volume: Virginia Division of Mineral Resources Publication 75, p. 23-35.
- Dennison, J.M., 1963, Geology of the Keyser quadrangle: West Virginia Geological and Economic Survey Geologic Map GM-1, 1:24,000 scale, 1 sheet.
- Environmental Protection Agency, 1979, Standard methods for the examination of water and waste-waters, and methods for chemical analysis of water and wastes: EPA 600/4-79-202, 490 p.
- Gillespie, W.H., and Clendening, J.A., 1964, An interesting marl deposit in Hardy County, West Virginia: Proceedings of the West Virginia Academy of Science, v. 36, p. 147-151.
- Greenberg, A.E., Trussel, R.R., Clesceri, L.S., and Franson, M.A.H., eds., 1985, Standard methods for examination of water and waste water, 16th edition: Washington, D.C., American Public Health Association, 1268 p.
- Grimsley, G.P., 1916, Jefferson, Berkeley, and Morgan counties: West Virginia Geological Survey, 644 p.
- Hoyt, W.G., and Langbein, W.B., 1955, Floods: Princeton, New Jersey, Princeton University Press, 468 p.
- Hubbard, D.A., Jr., Giannini, W.F., and Lorah, M.M., 1985, Travertine-marl deposits of the Valley and Ridge province of Virginia - a preliminary report: Virginia Division of Mineral Resources, Virginia Minerals, v. 31, n.1, p. 1-8.
- Jacobson, R.B., and Coleman, D.J., 1986, Stratigraphy and recent floodplain evolution of Maryland Piedmont flood plains: American Journal of Science, v. 286, p. 617-637.
- Jennings, J.N., 1971, Karst: Cambridge Massachusetts, The M.I.T. Press, 252 p.
- Kite, J.S., Bell, Alison, and Allamong, D.M., 1986, Preliminary observations on floodplain, terrace, and fan deposits in the upper Potomac River basin of Virginia and West Virginia, in McDonald, J.N., and Bird, S.O., eds., The Quaternary of Virginia - a symposium volume: Virginia Division of Mineral Resources Publication 75, p. 121-123.
- Knox, J.C., 1983, Responses of river systems to Holocene climates, in Wright, H.E., Jr., ed., Late-Quaternary environments of the United States, v. 2 The Holocene: Minneapolis, University of Minnesota Press, p. 26-41.
- Reger, D.B., 1923, Map II, Mineral County, showing general and economic geology: West Virginia Geological Survey, 1:62,500 scale, 1 sheet.
- Reger, D.B., 1924, Mineral and Grant counties: West Virginia Geological Survey, 866 p.
- Sweeting, M.M., 1973, Karst landforms: New York, New York, Columbia Press, 362 p.
- Thornton, C.P., 1953, The geology of the Mount Jackson quadrangle, Virginia [Ph. D. dissert.]: New Haven, Connecticut, Yale University, 221 p.
- Tilton, J.L., Prouty, W.F., and Price, P.H., 1927, Pendleton County: West Virginia Geological Survey, 384 p.
- Tilton, J.L., Prouty, W.F., Tucker, R.C., and Price, P.H., 1927, Hampshire and Hardy counties: West Virginia Geological Survey, 624 p.
- Trimble, S.W., 1975, Unsteady state denudation: Science, v. 198, p. 1207.
- White, W.B., 1976, Cave minerals and speleothems, in Ford, T.D. and Cullingford, C.H.D., eds., The science of speleology: London, England, Academic Press, p. 267-327.

DESCRIPTION AND ORIGIN OF THE CALCITE-RICH MASSANETTA VARIANT SOIL SERIES AT MOUNT CRAWFORD, VIRGINIA

E. Randolph McFarland¹ and W. Cullen Sherwood²

CONTENTS

	Page
Abstract.....	152
Introduction.....	152
Physical setting.....	153
Geology.....	153
Massanetta Variant Soil Series.....	153
Procedures.....	153
Field.....	154
Laboratory.....	154
Description of the Massanetta Variant Soil Series.....	154
Carbonate material.....	157
Noncarbonate material.....	157
Origin of the Massanetta Variant Soil Series.....	157
Relation of soil calcite to stream-water chemistry.....	159
Formation of the soil.....	160
Summary and conclusions.....	160
Acknowledgments.....	160
References cited.....	160

ILLUSTRATIONS

Figure		
1. Location of study area.....		152
2. Geologic structure of Burketown klippe.....		153
3. Geology of study area and stream-sampling locations.....		154
4. Topography of study area and soil-sampling locations.....		155
5. Cross sections showing profile development and calcite distribution in the Massanetta Variant Series at Mount Crawford.....		156
6. Soil-calcite layers exposed in stream bank.....		156
7. Sample of soil-calcite layer.....		156

TABLES

1. Analysis of calcite in soil.....		157
2. Textural comparisons of the noncarbonate materials in the Ap and B-C horizons.....		157
3. Stream-sample analyses.....		158

¹U.S. Geological Survey, Water Resources Division, 208 Carroll Building, 8600 La Salle Road, Towson, MD 21204

²Department of Geology and Geography, James Madison University, Harrisonburg, VA 22807

ABSTRACT

The Massanetta Variant Soil Series is a Mollisol which is atypical of soils normally developed in the humid-temperate climate of Virginia. In order to describe this soil and develop a theory on its origin, field and laboratory studies were conducted on a 1.5-hectare site of Massanetta Variant soil located 400 m southwest of Mount Crawford in Rockingham County, Virginia. The soil occupies a relatively flat area along a small, unnamed, deeply incised tributary to North River, just downstream from its intersection with faulted carbonate rock. Soil samples for laboratory analyses were collected from the A, B, and C horizons at nine soil-auger stations and from an excavated pit. Samples of indurated carbonate material were collected from the C horizon at one auger station and from semicontinuous layers exposed in the stream bank. Water samples were collected at 10 stream stations.

All of the carbonate material in the analyzed soil is calcite. The calcite content of the soil increases with depth, ranging from 0 to 80 percent; the calcite content of the C horizon soil exceeds 50 percent at all but one station. Molar Mg/Ca and Sr/Ca ratios were determined at two stations. Ratios are relatively constant with depth at one station, whereas both ratios decrease with depth at the other station. Stream-water pH ranges from 7.9 to 8.9; and Ca^{2+} , Mg^{2+} , and Sr^{2+} concentrations range from 120 to 170 mg/L, 37.4 to 63.6 mg/L, and 0.8 to 1.2 mg/L, respectively. Molar Mg/Ca and Sr/Ca ratios in the stream water are 219 and 25 times greater, respectively, than in the soil calcite. Concentrations and partitioning at this level are consistent with results found in the literature for springs and streams actively precipitating carbonate minerals. The texture and sand-grain morphology of the noncarbonate material in the Massanetta Variant Series was compared to that of local residuum and alluvium deposited by the nearby North River. The noncarbonate material in the soil strongly resembles the local residuum; only a small fraction of river-derived grains is present. It is proposed that marl was deposited over the study area by precipitation of calcite from the small stream that crosses the Burketown klippe border fault. Semicontinuous layers of indurated calcite found in the soil could have formed around plant roots at or near vegetated surfaces during pauses in active marl formation or within the soil that developed over the marl after its formation.

INTRODUCTION

Soils mapping in Augusta and Rockingham counties, Virginia (Hockman and others, 1978 and 1982), resulted in the discovery of a carbonate-mineral-rich Mollisol, which

has been named the Massanetta Variant Soil Series. Mollisols usually form in response to semiarid, grassland conditions, so they are common on the Great Plains but are relatively rare in the more humid eastern portion of the United States. This paper presents results of a study of the Massanetta Variant Series at a specific site and discusses possible origins of the soil. Descriptions are made of the distribution and composition of the carbonate material in the soil and of the texture and sand-grain morphology of the noncarbonate material. Stream-water chemistry is related to the formation of the soil.

The 1.5-hectare site chosen for study is approximately 400 m southwest of Mount Crawford, Virginia, at approximate latitude $38^{\circ}21' \text{ N}$, longitude $78^{\circ}57' \text{ W}$ (Figure 1). This study area was chosen because of the presence of the well-developed Mollisol over marl and because a small stream draining the deposit is deeply incised, providing an opportunity for observing changes with depth within the deposit. The site is adjacent to the northeastern edge of the Burketown klippe (Figure 2). The bedrock units consist of Upper Cambrian to Ordovician limestone, dolomite, and slate. The Massanetta Variant Series is developed over a marl deposit, which overlies a mixture of sandy gravel and yellowish-brown, clay-rich residuum. The small stream that drains the deposit originates in the steep topography over the klippe, crosses the fault (Figure 2), and proceeds across what appears to be a low terrace and empties into the North River. The Massanetta Variant Series is present on this terrace-like feature.

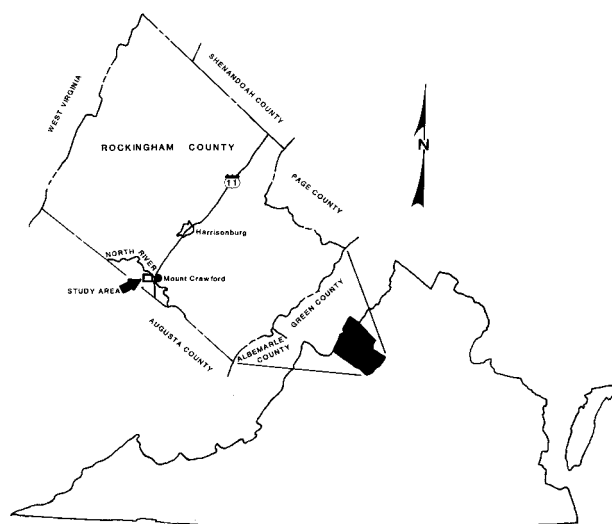


Figure 1. Location of study area in Rockingham County, Virginia.

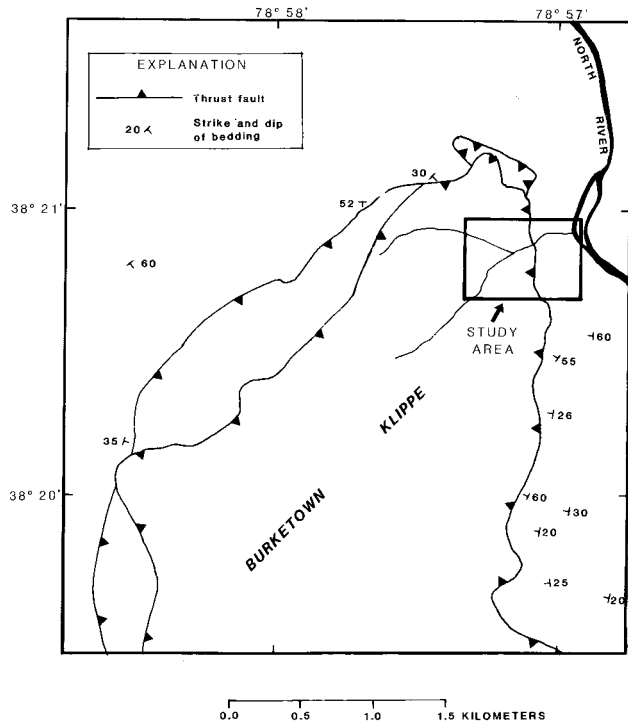


Figure 2. Geologic structure of Burketown klippe (modified from Gathright and others, 1978).

PHYSICAL SETTING

GEOLOGY

Figure 3 depicts the geology of the study area. The thrust fault bounding the Burketown klippe separates the dolomite of the Cambrian Conococheague Formation from the underlying limestone of the Ordovician Edinburg Formation and calcareous slate of the Martinsburg Formation (Gathright and others, 1978). The older dolomite of the klippe has been thrust westward over the younger limestone and slate.

The rocks adjacent to the klippe dip under it on both the east and west sides and generally strike to the northeast (Figure 2). Near the fault, bedrock exposed at the surface has well-developed slaty cleavage, numerous joints, and some slickensides. Away from the fault, cleavage is less well-developed in the shaley limestone of the Lantz Mills member of the Edinburg Formation. Cleavage is not evident in the limestone of the Liberty Hall member of the Edinburg.

MASSANETTA VARIANT SOIL SERIES

Figure 4 depicts the distribution of the Massanetta Variant Series in the study area. The Massanetta Variant Series,

a Mollisol, was classified according to the Seventh Approximation soil classification as fine-loamy, carbonatic, mesic, Fluvaquent Hapludolls (Hockman and others, 1978). Recent revisions in soil taxonomy, however, would place the Massanetta Variant Series into the family of Typic Rendolls (W. J. Edmonds, 1988, written communication). The Massanetta Variant Series typically develops on small, narrow flood plains generally below springs flowing from limestone bedrock (Hockman and others, 1978). It forms on slopes of 0 to 2°. Comparison of soil survey maps of the Massanetta Variant Series (Hockman and others, 1978) with corresponding geologic maps (Gathright and others, 1978) indicates that this soil typically develops along small streams, downstream from a fault or fault zone in carbonate rocks.

A mixture of clayey residuum and sandy gravel containing numerous sandstone cobbles was observed underlying the marl along the stream banks and in an excavated pit (Figure 4). Most of the cobbles are less than 20 cm in diameter. The sandy gravel is similar to channel deposits found in the nearby North River. It appears that this material originally was deposited in a now-abandoned channel of the North River, because the small tributary stream draining the area has no sandstone source in its basin. The clayey residuum underlying the marl in the pit is similar to residuum found over the Martinsburg slate in nearby upland areas, so it is interpreted here to be clayey residuum resulting from the weathering of calcareous slate.

PROCEDURES

FIELD

In February 1981, the bedrock geology, marl, and Massanetta Variant Series were examined in detail in the field at the Mount Crawford site. Hand augering and soil sampling were done at nine stations (Figure 4) in order to examine the soil profile and the distribution and composition of carbonate material within and beneath the Massanetta Variant Series. Augering was extended to a depth of 1.25 m, and soil samples were collected from the A, B, and C soil horizons. Two samples from a semicontinuous layer of indurated carbonate material encountered in the C horizon at station 7 and three samples from similar layers exposed in the stream bank also were collected. In October 1987, a pit was excavated (Figure 4) through the Massanetta Variant Series and marl deposit into the underlying residuum at a depth of 1.6 m. Samples of the soil, underlying residuum, and recently deposited alluvium from the flood plain of the North River were collected for comparison.

Also in February 1981, stream-water samples were collected at 10 stations (Figure 3). At each station, an unfiltered 1-L sample was collected directly from the stream, and stream-water pH was measured in the field.

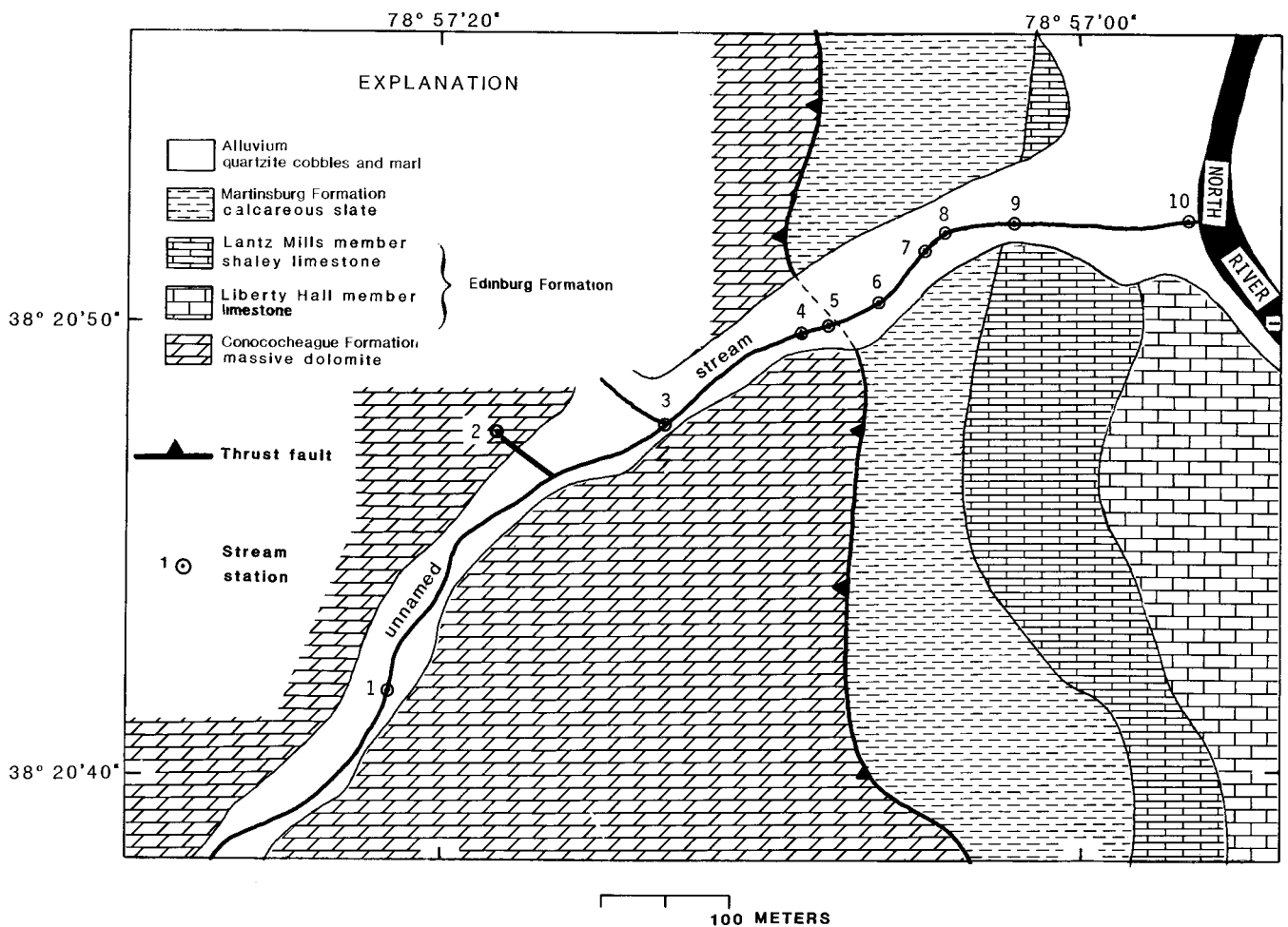


Figure 3. Geology of study area (modified from Gathright and others, 1978) and stream-sampling locations.

LABORATORY

Soil samples representative of the A, B, and C horizons encountered at each auger station were dried and split. Subsamples of 10 to 15 g were digested using a concentrated hydrochloric acid solution. The insoluble residue was dried and weighed, and the percentages of acid-insoluble and acid-soluble material were determined. The acid-soluble fraction was assumed to be composed entirely of carbonate material. Selected digestion solutions were analyzed for Ca^{2+} , Mg^{2+} , and Sr^{2+} using standard atomic-absorption techniques.

The two samples of indurated carbonate material augered from the C horizon at station 7 and three samples of carbonate material collected from the banks of the stream were analyzed by X-ray diffraction to determine the mineralogy.

Noncarbonate material was sieved from two Massanetta Variant Series samples from the pit to determine the relative amounts of silt-clay and sand. The sand fraction was examined microscopically, and grain size and morphology were noted. Identical procedures were used on the sample of residuum from below the marl in the pit and on the sample of

North River flood plain alluvium.

All stream-water samples were analyzed for Ca^{2+} , Mg^{2+} , and Sr^{2+} by atomic absorption.

DESCRIPTION OF THE MASSANETTA VARIANT SOIL SERIES

CARBONATE MATERIAL

Figure 5 shows the soil profiles and the distribution of carbonate material in the Massanetta Variant Series at stations 1 through 9. All of the samples of carbonate material that were analyzed by X-ray diffraction are composed entirely of calcite. Calcite content generally increases with depth (Figure 5). The calcite content of the A soil horizon is below 30 percent at all stations except station 8 and the pit. Calcite content of the B horizon ranges from just below 30 percent at station 6 to greater than 57.5 percent at station 8. All of the C-horizon material, with the exception of station 6, contains 57.5 to 80 percent calcite. Underlying the normal

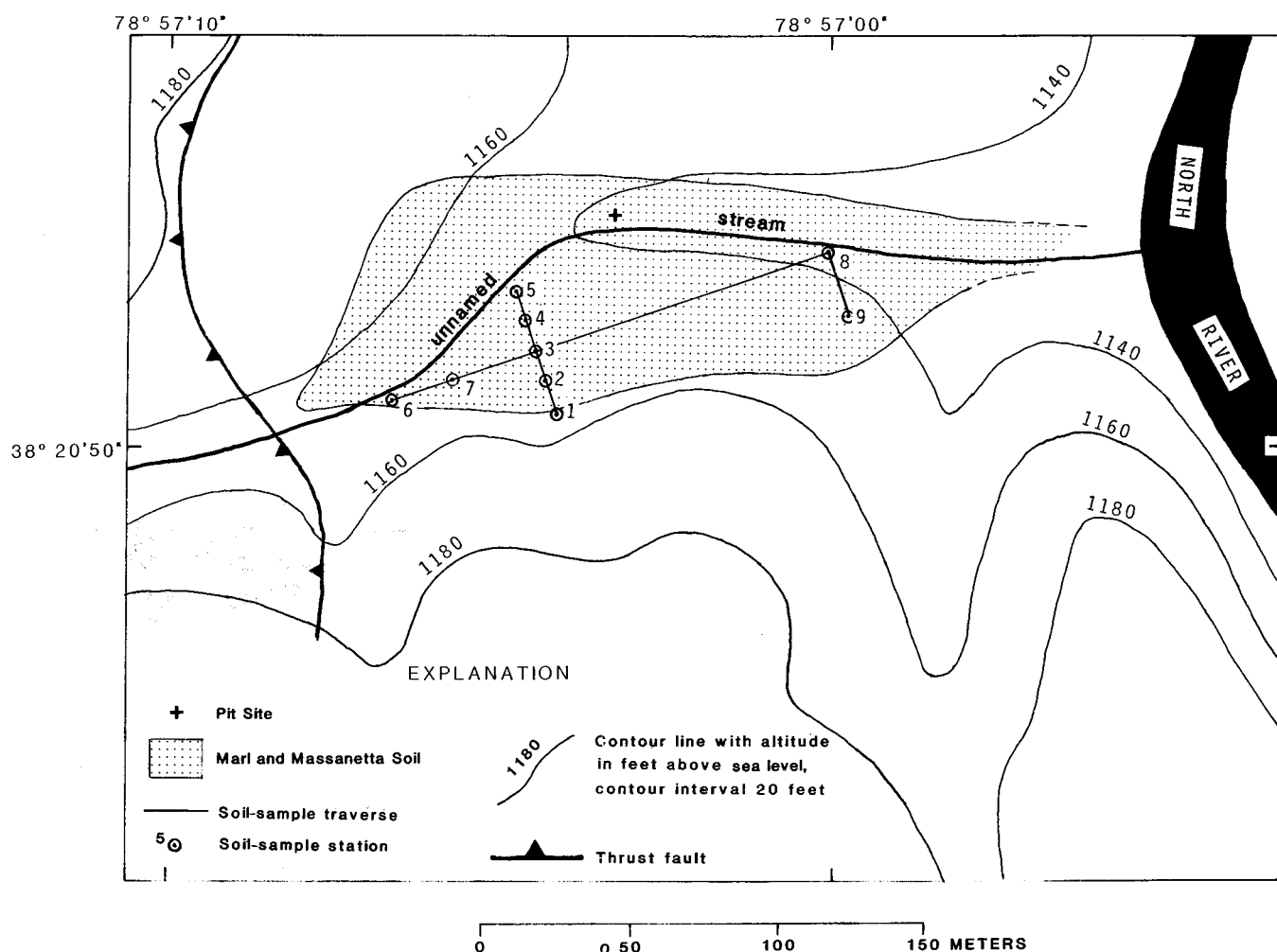


Figure 4. Topography of study area and soil-sampling locations.

C horizon at stations 2 and 4 is a layer designated C', which contains less than 57.5 percent calcite.

The increase in calcite content with depth found throughout the study area is in keeping with most soils developed over marl deposits. By definition, Rendolls exhibit a mollic epipedon and a calcium carbonate equivalent equal to or greater than 40 percent on the whole-soil basis (Soil Conservation Service, 1987).

Only scattered specks of white carbonate mineral are present in the A horizon, which consists mainly of gray to black, soft, organic-rich material. Under the microscope, most of these flakes were identified as shells or shell fragments of small snails. The shells may be composed of aragonite rather than calcite, but they were not analyzed by X-ray diffraction. As depth increases the presence of white, granular, calcite particles increases, imparting a distinctive gray color to the soil. In the C horizon, the soil has a gritty feel and light-gray color due to the abundance of calcite granules. Layers of indurated calcite are present sporadically in the C horizon.

Along the banks of the incised stream, semicontinuous

layers are exposed at distinct levels within the soil (Figure 6). The layers consist of aggregations of tubes and calcite cement (Figure 7). The underside of the layers are covered by smooth, laminated calcite and assume a mammillary configuration. The upper surfaces are rough and irregular. A similar layer was found in the C horizon at station 7.

Solutions resulting from the digestion of the soil samples from auger stations 3 and 8 were analyzed for Ca^{2+} , Mg^{2+} , and Sr^{2+} , and molar ratios for Mg/Ca and Sr/Ca were calculated (Table 1). The ratios differ between stations 3 and 8. At station 3, both ratios decrease significantly with depth, ranging from 0.0087 to 0.0017 for Mg/Ca and 0.0016 to 0.0009 for Sr/Ca . At station 8, all of the ratios approximate the lowest values found at station 3 and show little or no change with depth.

The mean value of 0.0025 for Mg/Ca found at stations 3 and 8 is relatively low compared to published data. The Mg/Ca ratio for low-magnesian calcite generally is considered to be less than 0.042, or 4 mole percent MgCO_3 . Many calcite-secreting organisms fix high-magnesian calcite, and virtually all produce calcite with magnesium levels higher than the

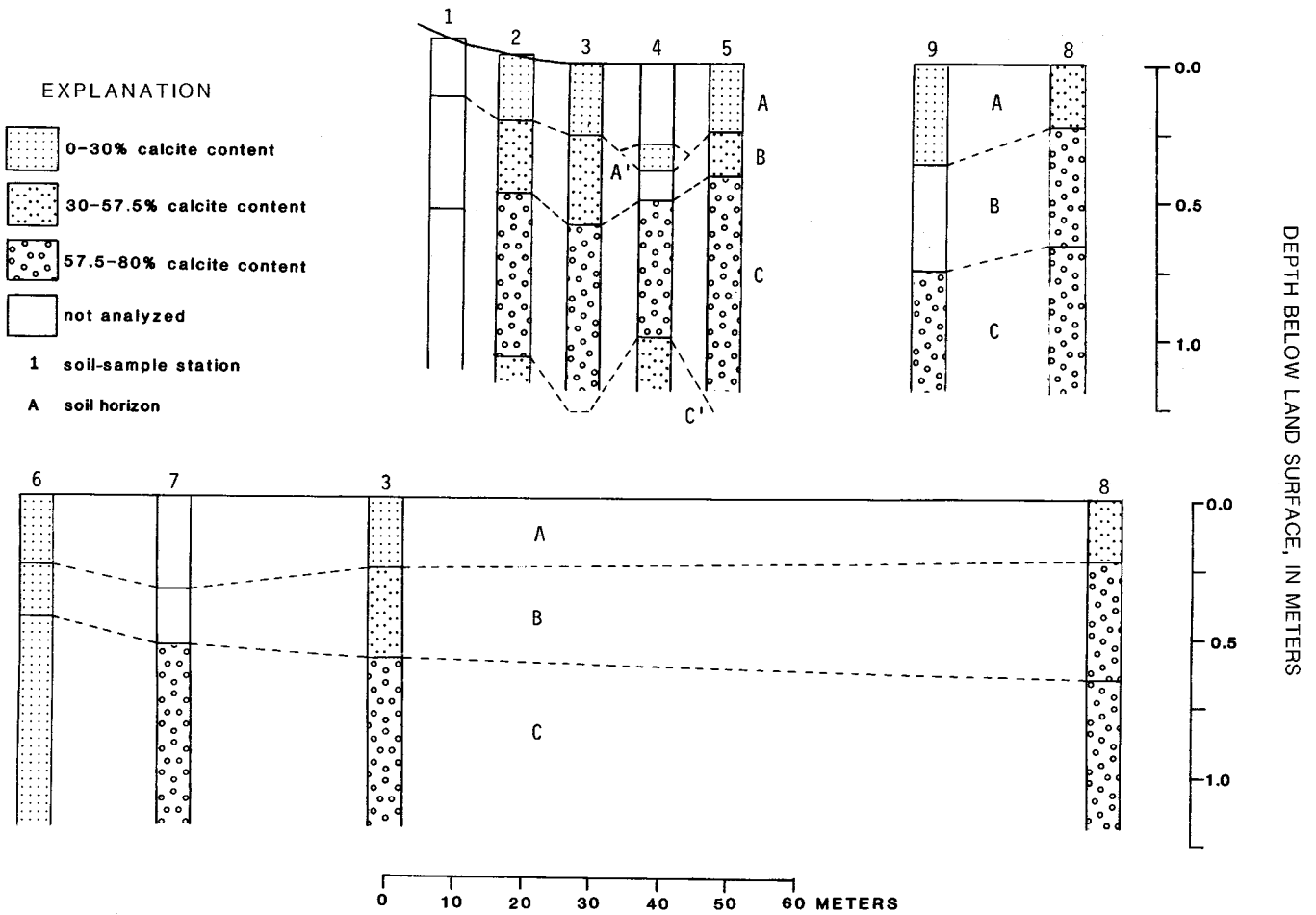


Figure 5. Cross sections showing profile development and calcite distribution in the Massanetta Variant Series at Mount Crawford.

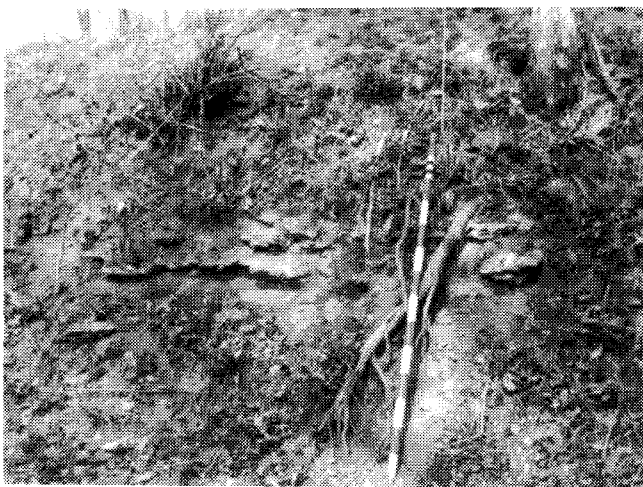


Figure 6. Photograph showing soil-calcite layers exposed in stream bank. Divisions on staff are 10 cm.

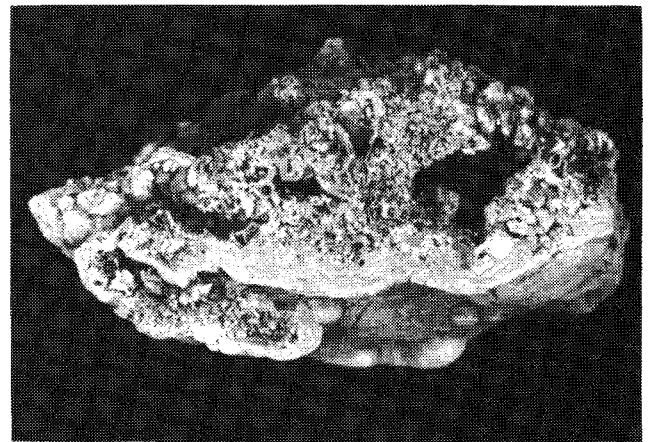


Figure 7. Photograph showing sample of soil-calcite layer. Specimen is approximately 10 cm in length.

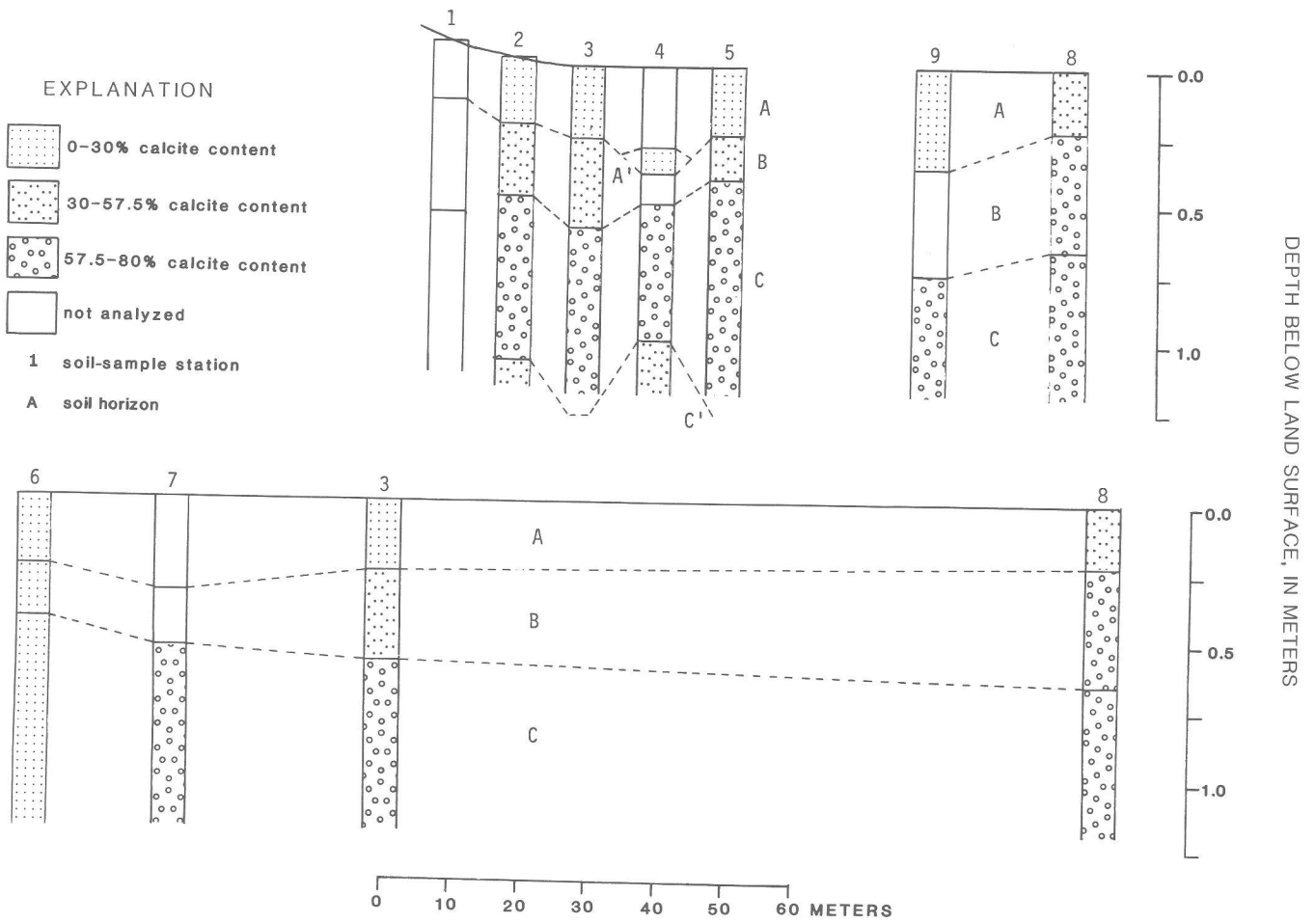


Figure 5. Cross sections showing profile development and calcite distribution in the Massanetta Variant Series at Mount Crawford.

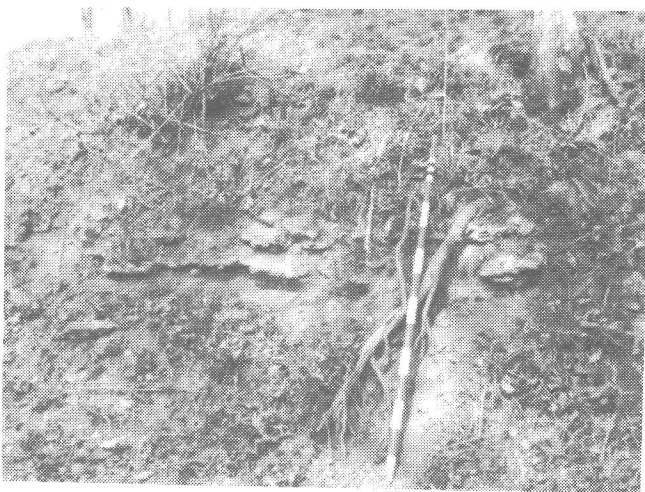


Figure 6. Photograph showing soil-calcite layers exposed in stream bank. Divisions on staff are 10 cm.

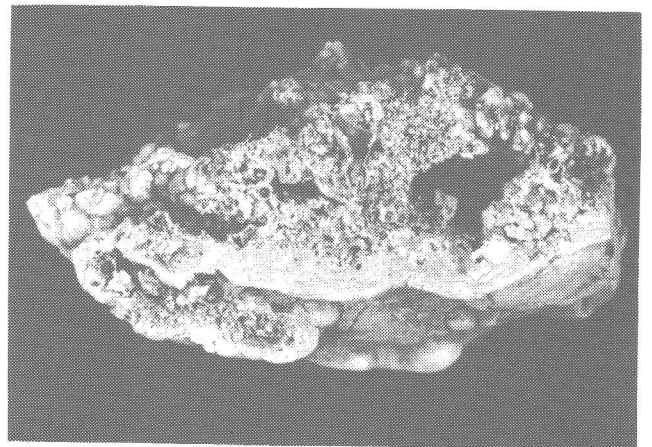


Figure 7. Photograph showing sample of soil-calcite layer. Specimen is approximately 10 cm in length.

mean ratio value of 0.0025 found here (Garrels and Mackenzie, 1971). Strong evidence has been presented (Chafetz and Folk, 1984; Love and Chafetz, this volume; Pentecost, this volume) that algae play a part in precipitating some travertine and marl. Garrels and Mackenzie (1971), however, report a range of 7 to 25 mole percent $MgCO_3$ for carbonate minerals fixed by calcareous algae; this is a much greater magnesium content than that found in the present study.

Table 1. Analysis of calcite in soil.

Hole No.	Horizon	Weight percent calcite	Molar Mg/Ca	Molar Sr/Ca
3	A	17.24	0.0087	0.00016
	B	50.04	0.0020	0.00015
	upper C	67.34	0.0020	0.00012
	lower C	66.45	0.0017	0.00009
8	A	43.13	0.0020	0.00009
	upper B	75.11	0.0017	0.00008
	lower B	73.55	0.0013	0.00009
	upper C	73.22	0.0013	0.00008
	lower C	79.30	0.0021	0.00009

The mean Mg/Ca value of 0.0025 for the soil calcite at Mount Crawford also appears to be significantly lower than that reported by other investigators in Virginia. Calculated Mg/Ca ratios from the $CaCO_3$ and $MgCO_3$ percentages reported by Shubert (circa 1921, as reported in Hubbard and others, 1985) and by Edmundson (1958) for five freshwater marls from western Virginia range from 0.0104 to 0.0505. The lowest ratio in this group is approximately four times the average value found at Mount Crawford.

A mean Sr/Ca ratio of 0.00011 indicates that a low concentration of Sr^{2+} is present in the analyzed samples. Calculation of Sr/Ca ratios from Sr^{2+} and Ca^{2+} concentration data from Turekian and Wedepohl (1961) and Conner and Shacklette (1975) resulted in a mean of 0.00091 and a range from 0.00015 to 0.00148. Holland and others (1964) found a relatively low mean molar Sr/Ca ratio in pure calcite cave deposits of 0.00019, a value very near that found in the study area.

NONCARBONATE MATERIAL

Data on the noncarbonate material in the Massanetta Variant Series and related deposits are summarized in Table 2. Samples from the Ap and B-C horizons exposed in the pit, a sample of the clayey residuum underlying the marl deposit, and a sample of recently deposited alluvium from the flood plain of the nearby North River were included in this part of the study.

Silt and clay predominate over sand in the noncarbonate

material in both the Ap and B-C horizons (Table 2). The ratios of silt-clay to sand are approximately 17 to 1 for the Ap horizon and 12 to 1 for the B-C horizons. The underlying clayey residuum has a silt-clay to sand ratio of 134 to 1. Conversely, North River alluvium is predominantly a loamy sand, with little silt and only a trace of clay.

Microscopic examination of the sand fractions of each of the four samples yielded further evidence related to the origin of the deposit. Sand grains from both Massanetta Variant Series samples and from the clayey residuum are similar and consist predominantly of fine, clear, angular quartz grains. Conversely, sand grains from the North River alluvium are coarse, well-rounded, frosted, and have ubiquitous iron stains.

The above evidence points to an origin of the noncarbonate material in the soil that essentially is unrelated to that of the North River alluvium. The high ratio of silt-clay to sand and the size and shape of the grains in the sand fraction of the soil both indicate a fine-grained clastic or carbonate-rock residuum as the logical source. The noncarbonate material in the soil probably represents a combination of sediment deposited during flood events by the small stream and colluvium from surrounding slopes. Although the area under study has the appearance of a river terrace, this evidence precludes the possibility that it is a terrace of the North River.

Table 2. Textural comparisons of the noncarbonate materials in the Ap and B-C horizons of the Massanetta Variant Series with the underlying residuum and recently deposited North River alluvium.

Sample	Noncarbonate Material (wt %)	Noncarbonate Material (wt %)	
		silt-clay	sand
Ap horizon	61.06	57.70	3.36
B-C horizon	17.92	16.50	1.42
underlying clayey residuum	100.00	99.26	0.74
recent North River alluvium	100.00	15.96	84.04

ORIGIN OF THE MASSANETTA VARIANT SOIL SERIES

RELATION OF SOIL CALCITE TO STREAM-WATER CHEMISTRY

Table 3 summarized field pH determinations and laboratory analyses for the 10 stream-water samples collected in the study area. A comparison with selected published analyses

indicates that the concentrations found here are typical of similar spring-fed streams draining faulted carbonate rock. Because the stream samples were collected during base-flow conditions and because the stream is probably fed by groundwater discharged at the fault, the concentrations of cations in shallow groundwater are likely to be similar to those in the stream.

Table 3. Stream-sample analyses. Concentrations given in mg/L; meq/L values reported in parentheses.

Station No.	pH	Ca ²⁺	Mg ²⁺	Sr ²⁺	Molar Mg/Ca	Molar Sr/Ca
1	8.9	120 (6.0)	45.8 (3.77)	0.8 (0.02)	0.63	0.0033
2	7.8	150 (7.5)	63.6 (5.23)	1.2 (0.03)	0.70	0.0040
3	8.2	170 (8.5)	56.0 (4.60)	0.8 (0.02)	0.54	0.0024
4	8.0	150 (7.5)	48.4 (3.98)	0.8 (0.02)	0.53	0.0027
5	7.9	150 (7.5)	42.8 (3.52)	0.8 (0.02)	0.47	0.0027
6	8.2	150 (7.5)	44.0 (3.62)	0.8 (0.02)	0.44	0.0027
7	8.3	150 (7.5)	44.4 (3.65)	0.8 (0.02)	0.49	0.0027
8	8.3	150 (7.5)	40.4 (3.32)	0.8 (0.02)	0.44	0.0027
9	8.4	170 (8.5)	49.4 (4.06)	0.8 (0.02)	0.48	0.0024
10	8.3	120 (6.0)	37.4 (3.08)	0.8 (0.02)	0.52	0.0033
Mean	8.2	150 (7.5)	47.2 (3.88)	0.8 (0.02)	0.53	0.0027

The mean concentration of Ca²⁺ in Table 3 of 150 mg/L is similar to Ca²⁺ concentrations found in other surface water that deposits travertine in Virginia. One analysis of Falling Spring Creek, in which extensive travertine deposits are found, yielded a Ca²⁺ concentration of 127 mg/L (U.S. Geological Survey, 1968). Other water analyses for travertine-depositing springs in Virginia (Collins and others, 1930) list Ca²⁺ on the order of 100 mg/L. The highest value for Ca²⁺ concentration found by Holland and others (1964) for Luray Caverns was 103.2 mg/L.

Because bicarbonate analyses were not performed in this study, it is not possible to make a definitive statement regarding the degree of saturation with respect to carbonate minerals represented by the Ca²⁺ concentration data. According to Hem (1985), a CO₂ partial pressure of approximately 10^{-1.0} atm would be required to attain equilibrium with calcite and water at 148 mg/L Ca²⁺ under standard conditions. Because atmospheric concentration of CO₂ is much lower, a substantial level of supersaturation with respect to calcite may exist in the stream water.

Calcite supersaturation in natural water has been reported by other investigators (Thraillkill, 1968; Jacobson and Langmuir, 1970; Jacobson and Usdowski, 1975; Dandurand and others, 1982; Chafetz and Folk, 1984; Hubbard and others, 1985; Hoffer-French and Herman, this volume; Kirby and Rimstidt, this volume; Lorah and Herman, this volume). Volatilization of dissolved carbon dioxide gas from emerging groundwater upon contact with the atmosphere may occur

more rapidly than precipitation of calcium carbonate, resulting in supersaturation with respect to CaCO₃ (Thraillkill, 1968). Hubbard and others (1985) suggested this mechanism may be a major factor in the formation of extensive travertine deposits in Virginia streams, where groundwater high in dissolved calcium carbonate has been discharged from faulted carbonate rocks. The conditions for the high Ca²⁺ concentrations found in this study appear to be similar to those described by Hubbard and his coworkers.

The mean concentration of Mg²⁺ of 47.2 mg/L (Table 3) and the mean molar Mg/Ca ratio of 0.53 are relatively high. Falling Spring Creek is reported to have 29 mg/L of Mg²⁺ and a Mg/Ca molar ratio of 0.38 (U.S. Geological Survey, 1968). Although a Mg/Ca ratio of 0.15 is reported for a spring draining limestone in the eastern United States (Hem, 1985), a higher value of 0.89 is reported for a spring draining dolomite. Additionally, Holland and others (1964) show several Mg/Ca values slightly exceeding unity for water collected in caves formed in dolomite. Analyses of groundwater from Rockingham County, Virginia (Hinkle and Sterrett, 1976), show Mg/Ca values range from about 0.08 to 0.20 for water from limestone aquifers but are about 0.70 from dolomite aquifers. The presence of dolomite in the Burketown klippe could account for the relatively high mean molar Mg/Ca of 0.53 found in this study.

The mean concentration of Sr²⁺ of 0.8 mg/L (Table 3) and the mean molar Sr/Ca ratio of 0.0027 are also relatively high. Holland and others (1964) found a range of Sr²⁺ concentrations of 0.023 to 0.182 mg/L in cave water at Luray Caverns. Although this is lower than the value at Mount Crawford, the bedrock at Luray Caverns is predominantly dolomite, with a relatively low mean Sr²⁺ content of 65 ppm. Turekian and Wedepohl (1961) found a mean of 610 ppm Sr²⁺ for carbonate rock in general, indicating that limestone has a significantly greater Sr²⁺ content than the dolomite sampled by Holland and others (1964). Because limestone is present at the Mount Crawford site, the Sr²⁺ concentration is higher in the stream water than in water samples from Luray Caverns.

Both Mg/Ca and Sr/Ca ratios are in excess of one order of magnitude greater in the stream water than in the soil calcite. The molar Mg/Ca ratio for the water is 212 times that analyzed for the soil calcite. A high degree of partitioning also is evident at Luray Caverns, where low-magnesian calcite was found to be precipitating from water in which the Mg/Ca mole ratios exceeded unity (Holland and others, 1964). Partitioning of this magnitude may be greater than that taking place at some other locations in Virginia, where Mg/Ca ratios in marls have been found to be higher than those at Mount Crawford (Shubert, circa 1921, reported in Hubbard and others, 1985; Edmundson, 1958).

The molar Sr/Ca ratio for the water is 25 times that analyzed for the soil calcite. This partitioning is about one order of magnitude less than that for the Mg/Ca ratio. Stron-

tium partitioning was described by Holland and others (1964) in the expression

$$\frac{\text{concentration Sr}^{2+}}{\text{concentration Ca}^{2+}} (\text{calcite}) = K_{\text{Sr}} \frac{\text{concentration Sr}^{2+}}{\text{concentration Ca}^{2+}} (\text{solution}) \quad (1)$$

where $K_{\text{Sr}} = 0.14 \pm 0.02$ for calcite in equilibrium with dilute solutions in the laboratory, and K_{Sr} for precipitated calcite in Luray Caverns ranged from 0.13 ± 0.06 to 0.22 ± 0.06 . The K_{Sr} calculated from the data in Table 3 is less than 0.04, indicating greater partitioning of Sr^{2+} than that found by Holland and his coworkers.

FORMATION OF THE SOIL

Two modes for the origin of calcite associated with the Massanetta Variant Series at Mount Crawford are possible. The first mode involves the gradual aggradation of marl by precipitation of calcite from the small stream now draining the deposit, followed by formation of the present Mollisol when climatic or other conditions changed. The second mode involves the formation of secondary calcite on or within the soil by the evaporation of an upward-moving concentrated solution of dissolved calcium carbonate. Prevailing evidence indicates that most of the soil calcite at the study site was deposited by primary precipitation. Secondary precipitation may take place, but apparently on a considerably smaller scale.

Perhaps the strongest line of evidence favoring the preexistence of marl at the site prior to soil formation is the very high percentages of calcite, at relatively shallow depths, found in the auger samples. Soil samples analyzed from eight of the nine auger stations showed calcite contents of between 57.5 and 80.0 percent at depths of less than 1 m. Secondary precipitation of this much calcite, within a preexisting non-carbonate or low-carbonate mineral soil, presents a formidable space problem. A mechanism would be required to remove the noncarbonate material that would have occupied this volume prior to calcite precipitation.

The possibility of secondary precipitation of calcite within a preexisting alluvial terrace of the North River was further discounted by examination of the texture of the noncarbonate material in the Massanetta Variant Series. The noncarbonate material in the soil is significantly finer-grained than flood plain alluvium from the nearby North River. Nearby residuum is clay-rich material formed from calcareous slate bedrock and closely resembles the noncarbonate material in the soil. In addition, examination of the individual sand grains found in the noncarbonate material, revealed the same fine size, clarity, and angular morphology as sand grains in nearby residuum. These sand grains are different

from the coarse, iron-stained, frosted, and well-rounded sand grains deposited by the North River. It would appear that, as the marl formed, small amounts of residual soil were moved by gravity from the surrounding hills, or carried in as sediment by the small stream, and became incorporated into the accreting marl.

A third line of evidence favoring preexistence of the marl involves recent archaeological findings. In other Virginia deposits similar to those at Mount Crawford, prehistoric archaeological artifacts have been found beneath the Mollisols and within the marl deposits (Hubbard and others, 1985; Gardner, this volume; Giannini, this volume), indicating a relatively recent origin for the deposits. This young age would virtually preclude calcite precipitation within a much older river terrace at the existing elevation above the present river channel. Although artifacts have not been reported at Mount Crawford, their existence cannot be ruled out.

Evidence favoring a secondary origin for at least some of the soil calcite centers around the morphology and distribution of semicontinuous layers of calcite found in the soil (Figures 6 and 7). Although the layers are, in some respects, similar to algal travertine deposits described by Chafetz and Folk (1984), the Mg^{2+} content of the soil calcite is much lower than that reported for algal-carbonate material (Garrels and MacKenzie, 1971).

The semicontinuous layers of calcite at Mount Crawford are composed mainly of minute tubes cemented together. Many of the tubes contain small roots and fine rootlets. As an alternative to algal precipitation, low-magnesian calcite may have precipitated inorganically to form tubes around present or pre-existing roots. The tops of the layers are rough and irregular, and the bottoms are smooth and thinly laminated. These laminated surfaces appear to have accreted after the layer had formed.

The tubes and laminations may have been formed by secondary precipitation, either during or after formation of the marl deposit. During formation of the marl, some non-accreting areas might have developed grasses or other small vegetation. Transpiration and evaporation could have resulted in precipitation of caliche-like layers, enclosing many of the plant roots at and near the surface. Subsequently, transpiration and evaporation could have resulted in a net upward movement of groundwater through the marl, and continued precipitation of laminated calcite on the underside of the tubes.

Alternatively, the tubes and laminations may have been formed in the soil after formation of the marl deposit. The Massanetta Variant Series, because of its relatively low topographic position, is frequently saturated. Clay and organic matter in the solum could increase surface tension of the interstitial water, creating an upward movement through capillary action of groundwater with a high concentration of dissolved calcium carbonate. Brown (1956) states that groundwater rising from an aquifer by capillary action to deposit calcium carbonate would do so largely in topographically

low areas and not on high areas. Transpiration and evaporation from the soil surface could then remove the water from the upper levels of the profile, resulting in a continued upward flow during periods of low rainfall. Upon evaporation, the dissolved calcium carbonate would precipitate in the soil as calcite. The possible presence of Ca^{2+} at cation-exchange sites on the surfaces of roots and transpiration by the plants may induce the calcite to precipitate on the roots rather than on some other surface. With continued upward flow and calcite precipitation, the resulting tubes would grow larger and coalesce until flow was blocked by the deposit. Precipitation would then continue on the underside of the deposit to form the smooth, laminated surface.

SUMMARY AND CONCLUSIONS

An area occupied by the Massanetta Variant Soil Series and related marl near Mount Crawford, Virginia, was chosen for study. The distribution, mineralogy, and geochemistry of the carbonate material in the soil and the texture and sand-grain morphology of the noncarbonate material in the soil were examined. Water samples from a small stream draining the deposit were analyzed for Ca^{2+} , Mg^{2+} , Sr^{2+} , and pH.

Based on these investigations, the following conclusions on the soil constituents and its origin are offered:

1. The weight percentage of carbonate material in the soil increases with depth, ranging from trace amounts at the surface to near 80 percent at depths of less than 1 m at some sampling stations.
2. All of the soil-carbonate material analyzed was calcite. The Mg^{2+} and Sr^{2+} contents of the calcite decrease with depth at one of the two stations selected for analysis but are constant with depth at the other station. Mean molar Mg/Ca and Sr/Ca ratios of 0.0025 and 0.00011 are low relative to published data for similar deposits elsewhere in Virginia.
3. Stream water draining faulted carbonate rock contains relatively high concentrations of Ca^{2+} , Mg^{2+} , and Sr^{2+} . The mean concentration of 150 mg/L Ca^{2+} in the stream is comparable to that of other springs and streams in Virginia which are actively precipitating calcium carbonate.
4. Molar ratios of Mg/Ca and Sr/Ca in stream water are 219 times and 25 times higher, respectively, than in soil calcite. Other studies indicate that this type of partitioning may be common in caves and other situations where inorganic calcite is precipitating.
5. Examination of the noncarbonate material in the Massanetta Variant Series revealed high percentages of silt and clay, with a prevalence of fine, clear, angular quartz grains in

the sand fraction. These characteristics are similar to those of local residuum but different from flood plain alluvium recently deposited by the nearby North River. This evidence precludes a river-terrace origin for the deposit.

6. Available evidence appears to favor a two-part mechanism for the origin of calcite in the Massanetta Variant Soil Series at Mount Crawford. This mechanism consists of: 1) initial formation of a marl deposit by precipitation from the stream and groundwater draining the Burkettown klippe; and 2) secondary formation of some indurated calcite at or near the marl surface during pauses in active marl formation or, subsequently, within the profile of soil developed on the marl by evaporation of shallow groundwater moving upward by capillary action.

ACKNOWLEDGMENTS

We acknowledge Dr. Lance E. Kearns and Dr. Lynn S. Fichter, James Madison University, for their aid and advice; Dr. Richard S. Mitchell, University of Virginia, for his assistance with X-ray diffraction; Mr. Randy Maupin, Soil Conservation Service, for his assistance with air-photo soil maps, and Mrs. Betty Lou Huffman for manuscript preparation and editorial help. Special thanks also are due to Mr. Cecil Myerhoffer, owner of the Myerhoffer farm in which the study area is located, for his cooperation in generously granting access to this property.

REFERENCES CITED

- Brown, C.H., 1956, Origin of caliche on the northeastern Llano Estacado: *Journal of Geology*, v. 64, p. 1-15.
- Chafetz, H.A., and Folk, R.L., 1984, Travertines: depositional morphology and the bacterially constructed constituents: *Journal of Sedimentary Petrology*, v. 54, n. 1, p. 289-316.
- Collins, W.D., Foster, M.D., Reeves, Frank, and Meachum, R.P., 1930, Springs of Virginia: Virginia Division of Water Resources and Power Bulletin 1, 55 p.
- Conner, J.J., and Shacklette, H.T., 1975, Background geochemistry of some rocks, soils, plants, and vegetables in the conterminous United States: U.S. Geological Survey Professional Paper 574-F, 168 p.
- Dandurand, J.L., Gout, R., Hoefs, J., Menschel, Günther, Schott, J., and Usdowski, Eberhard, 1982, Kinetically controlled variations of major components and carbon isotopes in a calcite-precipitating spring: *Chemical Geology*, v. 36, p. 299-315.
- Edmundson, R.S., 1958, Industrial limestones and dolomites in Virginia: James River district west of the Blue Ridge: Virginia Division of Mineral Resources Bulletin 73, 137 p.
- Garrels, R.M., and Mackenzie, F.T., 1971, Evolution of sedimentary rocks: W. Norton & Co., Inc., 397 p.

- Gathright, T.M., II, Henika, W.S., and Sullivan, J.L., III, 1978, Geology of the Mount Sidney quadrangle, Virginia: Virginia Division of Mineral Resources Publication 11, text and 1:24,000 scale map.
- Hem, J.D., 1985, Study and interpretation of the chemical characteristics of natural water: U.S. Geological Survey, Water-Supply Paper 2254, 263 p.
- Hinkle, K.R., and Sterrett, R.M., 1976, Rockingham County groundwater: Richmond, Virginia State Water Control Board, Planning Bulletin 300, 87 p.
- Hockman, J.R., McKinney, J.C., Burruss, T.R., Jones, David, Modesitt, R.E., Manhart, L.G., and Waite, W.R., 1978, Soil survey of Augusta County, Virginia: National Cooperative Soil Survey, 249 p.
- Hockman, J.R., Neal, C.F., Racey, D.L., and Wagner, D.F., 1982, Soil survey of Rockingham County, Virginia: National Cooperative Soil Survey, 233 p.
- Holland, H.D., Kirsipu, T.V., Huebner, J.S., and Oxburgh, U.M., 1964, On some aspects of the chemical evolution of cave waters: *Journal of Geology*, v. 72, p. 36-67.
- Hubbard, D.A., Jr., Giannini, W.F., and Lorah, M.M., 1985, Travertine-marl deposits of the Valley and Ridge province of Virginia - a preliminary report: Virginia Division of Mineral Resources, Virginia Minerals, v. 31, n. 1, p. 1-8.
- Jacobson, R.L., and Langmuir, Donald, 1970, The chemical history of some spring waters in carbonate rocks: *Groundwater*, v. 8, n. 3, p. 5-9.
- Jacobson, R.L., and Usdowski, Eberhard, 1975, Geochemical controls on a calcite precipitating spring: *Contributions to Mineralogy and Petrology*, v. 51, p. 65-74.
- Schubert, F.A., circa 1921, Fresh water marl in the Virginias: *Norfolk and Western Railways*, 6 p.
- Soil Conservation Service, 1987, Agricultural Handbook 436: Washington, D. C., U.S. Department of Agriculture, U.S. Government Printing Office, 489 p.
- Thraikill, J.V., 1968, Chemical and hydrologic factors in the excavation of limestone caves: *Geological Society of America Bulletin*, v. 79, p. 19-46.
- Turekian, K.K., and Wedepohl, K.H., 1961, Distribution of the elements in some major units of the earth's crust: *Geological Society of America Bulletin*, v. 72, p. 175-192.
- U.S. Geological Survey, 1968, Water resources data for Virginia: U.S. Geological Survey, Water Resources Division, 326 p.

INFLUENCE OF CaCO_3 DISSOLUTION AND DEPOSITION ON FLOOD PLAIN SOILS IN THE VALLEY AND RIDGE PROVINCE

William J. Edmonds and David C. Martens

CONTENTS

	Page
Abstract.....	164
Introduction.....	164
Literature review.....	165
Chemical properties.....	165
Soil pH.....	166
Stability of calcium carbonate in soil.....	166
Copper, iron, manganese, and zinc availabilities.....	166
Calcium, magnesium, potassium, and phosphorus availabilities.....	166
Physical properties.....	167
Materials and methods.....	167
Study area.....	167
Laboratory methods.....	167
Statistical methods.....	167
Results and discussions.....	168
Soil properties.....	168
Estimates of base saturation.....	168
Extractable micronutrients.....	169
Extractable phosphorus.....	170
Soil pH and calcium.....	171
Soil classification.....	171
Order.....	171
Suborder.....	171
Great group.....	171
Subgroup.....	172
Family.....	172
Texture.....	172
Mineralogy.....	172
Temperature.....	172
Series.....	173
Conclusions.....	173
Acknowledgments.....	173
References cited.....	173
Appendix I: Soil descriptions and data.....	175

ILLUSTRATIONS

Figure

1. Sample sites and soil map for soils derived from Holocene alluvium at the confluence of the Shenandoah River and Spout Run in Clarke County..... 165
2. Soil particles from the 0.05- to 0.50-mm fraction of the Bw horizon of Profile 2 occluded by CaCO_3 173

TABLES

Table	Page
1. Evaluation of sample distributions.....	168
2. Comparisons of laboratory methods.....	168
3. NH_4Cl bases, CEC, and BS and CaCO_3 equivalent.....	169
4. Organic matter, pH, Al^{3+} , CEC, and BS by NH_4OAc bases plus Al^{3+} and by NH_4OAc method.....	169
5. NH_4OAc bases, H^+ and CEC and BS by sum of cations.....	170
6. Selected elements extracted by the Mehlich I extractant.....	170
7. Particle-size distribution.....	172

ABSTRACT

Soils influenced by CaCO_3 dissolution and deposition have formed in Holocene alluvium deposited by streams that have carbonate rock in their drainage basins. In Virginia, soils developed on the flood plains of the Bullpasture, Calfpasture, Cowpasture, Holston, Jackson, James, Maury, New, Potomac, Roanoke, and Shenandoah rivers and their tributaries have been influenced primarily by CaCO_3 dissolution and secondarily by CaCO_3 deposition. Soils associated with the confluence of Shenandoah River and Spout Run in Clarke County were characterized and classified as being examples of the influence that CaCO_3 dissolution and deposition have on the properties and classification of soils.

Soils influenced by CaCO_3 dissolution have high pH and exchangeable Ca^{2+} levels as the result of their interaction with water high in Ca^{2+} and alkalinity. They do not effervesce with dilute HCl. Surface layers are generally thick and dark as a result of a relatively high organic matter content. Structure is moderately to strongly developed. These soils are members of the great group of Hapludolls. Soils with mollic epipedons less than 60 cm thick and irregular decreases in organic matter with depth, as the result of rapid burial of surface horizons by sediment deposition, are members of the subgroup Fluventic Hapludolls. Where the sedimentation rate is slow enough for additional sediments to be incorporated into the epipedon, mollic epipedons are greater than 60 cm thick, and the soils are members of the subgroup Cumulic Hapludolls.

Soils influenced by CaCO_3 deposition have pH levels between 7.4 and 8.7, have high Ca^{2+} levels, and effervesce with dilute HCl. Micronutrient cations of Cu, Fe, Mn, and Zn are relatively unavailable to plants because of high pH and occlusion by CaCO_3 . Phosphorus levels are generally inadequate for normal plant growth because of the formation of highly insoluble calcium phosphates. Soil particles occluded by CaCO_3 are limited in their influence on the physical and chemical behavior of soil. The laboratory method used to estimate base saturations of Mollisols and Inceptisols that contain CaCO_3 gave values greater than 100 percent because nonexchangeable Ca^{2+} was dissolved from CaCO_3 as the pH of the soil and extracting solution equilibrated. Soils with CaCO_3 equivalents greater than 40 percent located immedi-

ately below the mollic epipedon are members of the suborder Rendolls. Soils with cambic horizons are members of the subgroup Eutrochreptic Rendolls.

INTRODUCTION

Travertine-marl deposits form as carbonates precipitated from freshwater streams and springs (Hubbard and others, 1985). Concurrent with and subsequent to deposition, upper layers of these deposits are altered by organisms and climate over a period of time to form soils. Soil Survey Staff (1988) defines marl as a material that has a moist-color value (Munsell Color, 1975) of 5 or more that reacts with dilute HCl to liberate CO_2 . Marl, according to this definition, can constitute a portion of a mollic epipedon or of a cambic, argillic, or C horizon. Marl, defined as a primary, porous, carbonate deposit that contains impressions of leaves, sticks, and other objects, can be designated as a C horizon of a soil. Buried paleosols are present in most travertine-marl deposits observed by the writers (Edmonds, 1970). Therefore, the differentiation of travertine-marl in the strictest geologic sense from soil is confounded by the transitional and overlapping nature of the two concepts. In order to avoid this distinction, the influence of CaCO_3 dissolution and deposition on soil will be used in the remainder of this chapter.

Levels of dissolved Ca^{2+} and alkalinity necessary for the deposition of travertine-marl are considerably higher than levels required to influence soil chemical and physical properties and to determine classification. Travertine-marl deposition is generally confined to flood plains of streams that have a large amount of carbonate rock in their drainage basins. When compared to the extent of carbonate rock in the Valley and Ridge province, travertine-marl deposits are a secondary source of dissolved Ca^{2+} and alkalinity in stream waters. Consequently, the extent of soils influenced by carbonate rock is considerably greater than those influenced by travertine-marl. Soils on flood plains of streams with a small amount of carbonate rock in their drainage basins have been influenced by the dissolution of CaCO_3 . In Virginia, soils developed in Holocene alluvium on flood plains of the Bullpasture, Calfpasture, Cowpasture, Holston, Jackson,

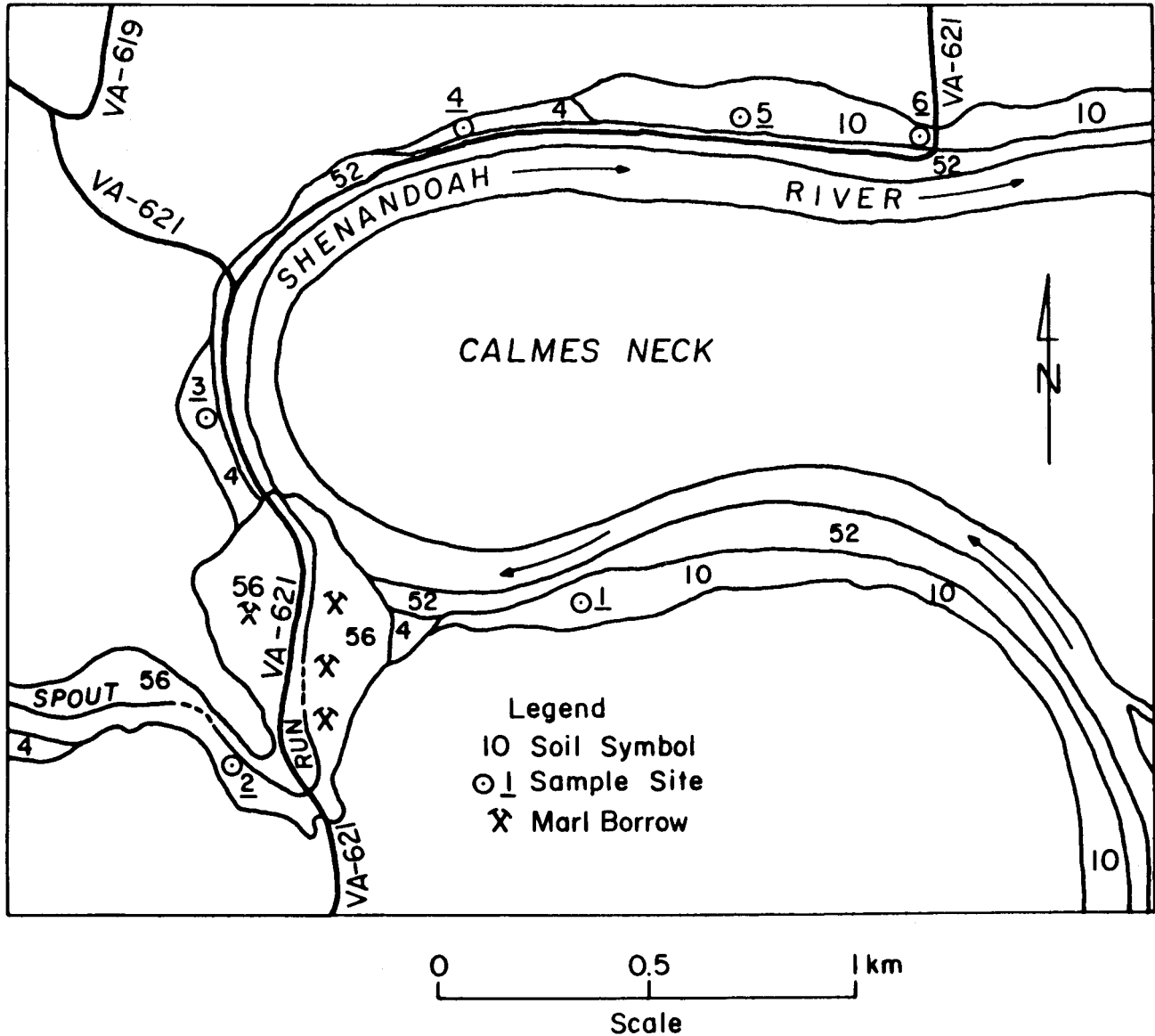


Figure 1. Sample sites and soil map for soils derived from Holocene alluvium at the confluence of the Shenandoah River and Spout Run in Clarke County. Soil symbols are those used by Edmonds and Stiegler (1982). Soil symbol: 4 = Buckton soils; 10 = Chagrins soils; 52 = Udipsamments, 0 to 8 percent slopes; and 56 = Weaver silt loam.

James, Maury, New, Potomac, Roanoke, and Shenandoah rivers and their tributaries have been influenced primarily by CaCO_3 dissolution and secondarily by travertine-marl deposition.

Soils at the confluence of the Shenandoah River and Spout Run (Figure 1) in Clarke County, Virginia, Boyce quadrangle, were characterized and classified in order to exemplify the influence that CaCO_3 dissolution and deposition have on the properties and classification of soils.

LITERATURE REVIEW

CHEMICAL PROPERTIES

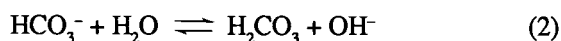
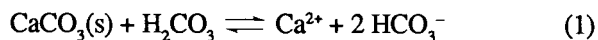
One of the earliest scientific studies of the influence of CaCO_3 on soil in the United States was conducted by Ruffin (1832). He used a procedure outlined by Sir Humphrey Davey to analyze for CaCO_3 in the upland soil on his farm near Petersburg, Virginia, and in upland soil derived from

carbonate rock in the Shenandoah Valley (Thomas, 1977). His results indicated that none of the soils contained CaCO_3 , but soil derived from limestone contained acid-soluble Ca^{2+} whereas soil on his farm did not. To remedy this problem, Ruffin applied partly decomposed oyster shells to his soil and kept careful records of the amount of shells applied and of resulting crop yields before and after "marling." Therefore, "he was the first man to lime for the right reason: To neutralize acidity" (Thomas, 1977, p. 231). Ruffin (1832) described perfectly the symptoms of Zn deficiency in corn (*Zea mays* L.) that result from overliming. Because of this work, Ruffin has been called "The father of soil chemistry in America," (Truog, 1938, p. 973). Ruffin was not the first to use lime. Lime has been used as a soil amendment to counteract acidity since ancient times (Tisdale and Nelson, 1975).

Soil pH

Soil pH is defined as the negative logarithm of the hydronium (H_3O^+) ion activity in soil solution. Well-aerated soils buffered by the $\text{CaCO}_3\text{-H}_2\text{O-CO}_2$ system with PCO_2 levels of 10^{-2} to $10^{-3.52}$ atm have pH levels between 7.4 and 8.3 (Jackson, 1979). The pH is about 7.7 for soil buffered by this system with a PCO_2 of $10^{-2.48}$ atm (Jenny, 1980) and represents the approximate boundary of CaCO_3 deposition and dissolution (Garrels and Christ, 1965).

From left to right the reactions



represent the dissolution of CaCO_3 and result in an alkaline solution. In reaction (1), the H_2CO_3 that forms as CO_2 dissolves in H_2O reacts with CaCO_3 to form dissolved Ca^{2+} and HCO_3^- . The amount of CO_2 that dissolves in H_2O and of H_2CO_3 that forms are proportional to the PCO_2 . The two reactions are coupled because the H_2CO_3 formed in reaction (2) is consumed in reaction (1).

Where the soil pH is low, growth of some plants may be restricted. The need to neutralize H_3O^+ in soil to ensure normal plant growth has been recognized for centuries (Tisdale and Nelson, 1975). When CaCO_3 is applied to soil, the pH increases as H_3O^+ is neutralized by the OH^- formed in reaction (2).

Stability of Calcium Carbonate in Soil

Calcium carbonate forms when the soil solution be-

comes supersaturated with respect to CaCO_3 . Supersaturation occurs when reaction (1) moves to the left as H_2O , CO_2 , or both are removed from the soil solution (Buol and others, 1980). Evaporation and transpiration are responsible for the removal of water. Carbon dioxide is removed as the PCO_2 of the soil atmosphere is decreased by a decrease in biological production, by an increase in diffusion from the soil atmosphere, and by movement of the soil solution to lower depths (Buol and others, 1980; Jenny, 1980).

Calcium carbonate dissolves when reaction (1) is displaced to the right. Reaction (1) moves to the right when the soil-atmospheric PCO_2 is high enough to form sufficient H_2CO_3 to react with CaCO_3 to produce Ca^{2+} and HCO_3^- ions (Buol and others, 1980). Neutralization of OH^- formed in reaction (2) by H_3O^+ in the soil solution also causes dissolution of CaCO_3 . The H_3O^+ ions that participate in the neutralization reaction dissociate into the soil solution from various soil buffer systems.

Copper, Iron, Manganese, and Zinc Availabilities

Micronutrient cations of Cu, Fe, Mn, and Zn are specifically adsorbed by carbonates, hydrous oxides, organic matter, and phyllosilicates (Udo and others, 1970; Schnitzer, 1978; Kabata-Pendias and Pendias, 1985). These cations are occluded by the precipitation of CaCO_3 or hydrous oxides of Al, Fe, or Mn. Occluded ions are no longer in contact with the soil solution and are unavailable to plants. The availability of soil Cu, Fe, Mn, and Zn to plants decreases with an increase in soil pH (Kabata-Pendias and Pendias, 1985). This decreased availability reflects specific adsorption by organic matter and by the deposition of carbonates and hydrous oxides. As observed by Ruffin (1832), deficiencies of these micronutrients may occur in soil as a result of overliming or through the influence of CaCO_3 dissolution or deposition.

Calcium, Magnesium, Potassium, and Phosphorus Availabilities

On a mass balance basis, most of the Ca, Mg, and K present in soil occupy structural positions in primary and secondary minerals and are, thus, non-exchangeable (Buol and others, 1980; Bohn and others, 1985). Potassium, unlike Ca and Mg, exists in the interlayers of clay-size micas and vermiculite and in wedge sites located in these minerals and is, thus, exchangeable (Sparks and Huang, 1985). Potassium availability to plants increases with a decrease in pH because of its displacement from wedge sites by H_3O^+ . Low Ca and Mg availabilities commonly occur when these cations are leached from soil and replaced on exchange sites by either Al^{3+} or hydroxy-Al polymers.

Plant-available P is highest in the pH range of 6.0 to 6.5. Soil P is present as insoluble calcium phosphates at pH and Ca^{2+} levels associated with the deposition of CaCO_3 . A decrease in soil pH increases P availability by dissolving calcium phosphates (Lindsay and Moreno, 1960; Marion and Babcock, 1977).

PHYSICAL PROPERTIES

Petry and Rich (1971) observed that the formation of CaCO_3 in soils alters their physical properties. They reported substantial decreases in confined swelling pressures, liquid limits, and plasticity indices as the result of treating soils with $\text{Ca}(\text{OH})_2$. They ascribed these decreases to formation of CaCO_3 intergranular bridges along pressure faces and channels and to CaCO_3 linings of interior walls of soil voids. A drastic reduction in the intensity of characteristic X-ray reflections of phyllosilicate minerals was attributed to soil particles becoming occluded as CaCO_3 formed in the soil fabric. Treatment with 1 N HCl restored characteristic X-ray reflections of the phyllosilicates to original levels. Based on these results, we assume that CaCO_3 deposition under natural conditions would produce similar reductions in confined swelling pressures, liquid limits, and plasticity indices.

MATERIALS AND METHODS

STUDY AREA

Spout Run and its tributaries, Westbrook and Roseville runs and Page Brook, drain an area underlain primarily by carbonate rock of the Rockdale Run, Stonehenge, Conococheague, and Elbrook formations and secondarily by the Lincolnshire, New Market, Oranda, Edinburg, and Rome formations (Edmundson and Nunan, 1973). High levels of dissolved Ca^{2+} in the water of numerous springs, e.g., the spring at Carter Hall, rising from the carbonate rock have resulted in the deposition of travertine-marl along Spout Run (Edmundson and Nunan, 1973). Weaver soils (soil symbol 56, Figure 1) have developed in the upper layers of these deposits (Edmonds and Stiegler, 1982).

Holocene alluvium encompassed by the area represented by the Boyce quadrangle was described by Edmundson and Nunan (1973, Plate 2) as, "Dark gray sandy clay, silt, and clay containing gravel; calcareous with massive beds of travertine along many tributary streams." Soils derived from this alluvium are described and classified by Edmonds and Stiegler (1982) using 1981 criteria (Soil Survey Staff, 1975 and 1981).

LABORATORY METHODS

Five soil profiles along the west bank of the Shenandoah River and one along Spout Run (Figure 1) were described and sampled for characterization. Exchangeable Ca^{2+} , Mg^{2+} , and K^+ were extracted with NH_4^+ from a 1 N NH_4OAc solution buffered at pH 7 and with NH_4^+ from an unbuffered 1 N NH_4Cl solution and were quantified using atomic absorption spectrophotometry (Soil Conservation Service, 1982). The CaCO_3 equivalent was estimated by the acid-neutralization method (Allison and Moodie, 1965). Exchangeable aluminum (Al^{3+}) was extracted with a 1 N KCl solution and quantified by titration (McLean, 1965). Exchange acidity (H^+) was determined by the BaCl_2 -TEA, pH 8 method (Peech, 1965). The pH of 1-to-1 soil-to-water mixtures was determined using a glass electrode. Organic-matter content was determined by the Walkley-Black method (Allison, 1965). The cation-exchange capacity (CEC) was estimated by four procedures: 1) by the sum of NH_4OAc extract bases (BASOAC) plus H^+ (CECS); 2) by BASOAC plus Al^{3+} (CECE); 3) by NH_4^+ saturation with a 1 N NH_4OAc , pH 7 solution, displacement, and distillation method (Chapman, 1965) (CECOAC); and 4) by a modification of the method given by Chapman (1965) which substituted a 1 N NH_4Cl , pH 5.4 solution as the source of NH_4^+ (CECCL). Ions of Al, Ca, Cu, Fe, K, Mg, Mn, P, and Zn were extracted with the Mehlich I solution, which consists of 0.05 N HCl and 0.025 N H_2SO_4 (Olsen and Sommer, 1982), and were quantified by inductively coupled plasma-emission spectrophotometry (Donohue and Friedericks, 1984). Subsamples for mineralogical analysis were treated with citrate-dithionite-bicarbonate to remove oxide coatings (Kunze and Dixon, 1986). The sand fraction was separated by wet sieving. Concentrations (g/kg) of minerals in the 0.05- to 0.5-mm fraction were estimated by grain counts using a Zeiss Universal M petrographic microscope. Particle-size analyses were completed by the pipette method (Day, 1965).

STATISTICAL METHODS

The Kolmogorov-Smirnov, Moses (Hollander and Wolfe, 1973), and Randles (Randles and others, 1980) procedures were used to test for normality, equal marginal dispersion, and symmetry of differences between laboratory procedures, respectively. The distribution-free Fisher sign test (Hollander and Wolfe, 1973) was used to test for significant median differences. Median differences between laboratory procedures were estimated by a method associated with the Fisher sign test (Hollander and Wolfe, 1973). Confidence limits for median differences were calculated by the distribution-free Thompson, Savur procedure (Hollander and Wolfe, 1973). Statistical calculations were performed on the Vir-

ginia Polytechnic Institute and State University's IBM 3090 mainframe computer using the Virginia Tech Nonparametric Statistics Package (Pirie, 1983).

RESULTS AND DISCUSSIONS

SOIL PROPERTIES

Estimates of Base Saturation

Nonnormal and asymmetric distributions and unequal marginal dispersions of most sample differences were indicated ($p = 0.05$) by the Kolmogorov-Smirnov, Randles, and Moses tests, respectively (Table 1). These distributions and dispersions are the result of differences between soils that contain CaCO_3 and soils that lack CaCO_3 . Consequently, parametric and nonparametric statistical procedures that assume normality, symmetry, and equal dispersion would give unreliable α -levels. Therefore, the Fisher sign test, which assumes an appropriate model, independent observations, and continuous distributions, was used to compare median differences in bases extracted and in CECs for these soils.

Median values for BASOAC and the sum of bases extracted by NH_4Cl (BASCL) were significantly different ($p = 0.05$, Table 2), the positive value for θ indicates that BASCL was greater. BASCL was considerably greater for soils that contained CaCO_3 (Tables 3 and 5). The difference between BASOAC and BASCL could result from different pH levels of the extracting solutions. The NH_4Cl solution probably dissolved more Ca^{2+} as the pH of the soils and extracting solutions equilibrated.

Table 1. Evaluation of sample distributions.

Methods Compared	$\alpha(\text{DNS})^a$	$\alpha(\text{TS})^b$	$\alpha(\text{US})^c$
BASCL-BASOAC	$0.025 > \alpha(\text{DNS}) > 0.01$	0.03394	0.00079
CECOAC-BASOAC	<0.01	0.50000	<0.00001
CECCL-BASCL	<0.01	0.07206	0.00071
CECCL-CECOAC	<0.01	0.23260	0.90837
CECS-CECOAC	<0.01	0.23220	0.00608
CECE-CECOAC	<0.01	0.35750	<0.00001
CECS-CECE	>0.15	0.03394	0.76952

^a α -levels associated with the Kolmogorov-Smirnov DNS statistic.

^b α -levels associated with the Moses TS statistic.

^c α -levels associated with the Randles US statistic.

Median values for CECOAC and CECCL were significantly lower ($p = 0.05$) than median values for BASOAC and

BASCL, respectively (Table 2). Lower values for CEC indicate a source of bases other than the exchange complex. In these soils, additional Ca^{2+} was probably dissolved from CaCO_3 as the pH of the soils and extracting solutions equilibrated. Lower values for CECs than for bases extracted result in estimates of BSCL and BSOAC greater than 100 percent (Tables 3 and 4) for soils that contain CaCO_3 . BSOAC is used to define limits of taxa in Mollisols and Inceptisols (Soil Survey Staff, 1988). Conversely, base saturation estimated by BASOAC divided by CECs times 100 (BSS, Table 5) and by BASOAC divided by CECE times 100 (BSE, Table 4) used to distinguish taxa in the Alfisol and Ultisol orders cannot be greater than 100 percent, regardless of the amount of CaCO_3 dissolved by the extracting solutions.

Table 2. Comparisons of laboratory methods.

Methods Compared	$\alpha(\text{BS})^a$	θ^b	89.99%CI for θ^c
BASCL-BASOAC	0.00004	1.00	0.40 to 1.30
CECOAC-BASOAC	0.04404	-0.50	-4.80 to 0.50
CECCL-BASCL	0.01650	-0.80	-6.20 to 0
CECCL-CECOAC	0.06681	0	-0.20 to 0
CECS-CECOAC	0.00001	3.30	2.10 to 7.50
CECE-CECOAC	0.03028	0.50	-0.50 to 4.90
CECS-CECE	0.00053	2.50	1.10 to 2.00

^a α -levels associated with Fisher sign test.

^bEstimates of the median difference. A positive value for θ indicates that the method designated by the positive sign had the greatest median value while a negative value indicated that the procedure with the negative sign had the greatest median value.

^cThompson, Savur confidence limit for θ .

Median values for CECCL and CECOAC (Table 2) were not significantly different ($p = 0.05$) which indicated a fairly constant exchange complex between pH levels of 5.4 and 7. Median values for CECS and CECOAC were significantly different. The positive value for θ indicated that CECS was greater. Differences between CECS and CECOAC were assumed to be related to pH-dependent charge. Median values between CECS and CECE were significantly different. The positive value for θ indicated that CECS was greater. Differences between CECS and CECE were also assumed to be related to pH-dependent charge. The 1 N KCl solution used to extract Al^{3+} was unbuffered while the BaCl_2 -TEA solution used to estimate H^+ was buffered at pH 8. Differences between CECS and CECE can be used to rank soils according to the magnitude of their pH-dependent charge.

Table 3. NH_4Cl bases, CEC, and BS and CaCO_3 equivalent.

Depth (cm)	Ca^{2+}	Mg^{2+} (cmol/kg soil)	K^+	CECCL	BSCL ^a (%)	CaCO_3 Eq.
Profile 1						
0-23	6.1	0.7	0.1	8.9	79	2
23-114	11.6	1.0	0.1	13.0	97	2
114-173	12.9	0.9	0.1	14.4	96	2
173-183	11.3	0.9	0.1	13.0	94	3
Profile 2						
0-30	22.6	0.4	0.1	14.0	164	60
30-56	21.2	0.2	0	3.3	654	85
56-76	19.4	0.2	0	4.5	438	88
76-127	20.0	0.2	0	4.1	496	86
127-183	18.8	0.2	0	1.1	1064	91
Profile 3						
0-38	19.6	0.5	0.1	8.5	238	4
38-79	12.4	0.4	0.1	11.4	113	3
79-107	10.0	0.4	0.1	10.1	105	3
Profile 4						
0-38	11.0	0.8	0.1	12.2	97	2
38-102	12.5	0.7	0.1	12.4	107	3
102-183	13.5	0.8	0.1	13.2	109	2
Profile 5						
0-30	13.5	0.9	0.1	8.3	176	2
30-56	10.5	0.7	0.1	11.0	102	3
56-114	11.0	0.5	0.1	11.0	105	3
114-153	11.5	0.6	0.1	11.4	106	2
Profile 6						
0-23	12.5	0.9	0.1	8.9	151	2
23-58	9.2	0.8	0.1	10.1	100	2
58-102	9.9	0.6	0.1	10.7	97	3
102-183	9.3	0.4	0.1	9.1	109	2

$$^a\text{BSCL} = ((\text{Ca}^{2+} + \text{Mg}^{2+} + \text{K}^+)/\text{CECCL}) \times 100.$$

Extractable Micronutrients

Levels of available micronutrients in soils needed for maximum biomass production are estimated by concentrations extracted by the Mehlich I solution. This solution extracts soil Al, Cu, Fe, Mn, and Zn by dissociating cation-organic matter complexes; by displacing specifically absorbed cations from carbonates, hydrous oxides, and phyllosilicate surfaces; and by releasing occluded and precipitated cations during partial acid decomposition of minerals (Rapaport and others, 1986). The acid also releases octahedrally

Table 4. Organic matter, pH, Al^{3+} , CEC and BS by NH_4OAc bases plus Al^{3+} and by NH_4OAc method.

Depth (cm)	OM (%)	pH	Al^{3+}	CECE ^{ab}	BSE ^c	CEC OAC ^{ad} (%)	BS OAC ^e (%)
Profile 1							
0-23	1.6	6.4	0.1	7.3	99	8.9	82
23-114	1.4	7.0	0.1	11.7	100	13.6	85
114-173	1.1	6.9	0.1	13.4	100	13.0	102
173-183	0.8	7.0	0.1	12.5	100	13.0	95
Profile 2							
0-30	4.1	8.3	0.1	21.1	100	16.2	129
30-56	1.8	8.5	0.1	17.4	100	3.7	472
56-76	1.8	8.7	0.1	17.0	100	4.7	360
76-127	2.0	8.6	0.1	16.7	100	4.1	406
127-183	1.1	8.7	0	15.6	100	1.9	823
Profile 3							
0-38	1.9	8.4	0.1	19.0	100	8.5	223
38-79	1.5	8.4	0.1	12.5	100	11.6	107
79-107	1.0	8.3	0.1	10.2	100	10.1	101
Profile 4							
0-38	1.7	8.0	0.1	11.8	100	10.5	112
38-102	0.9	8.3	0.1	12.3	100	11.8	103
102-183	0.8	8.1	0.1	13.8	100	13.4	102
Profile 5							
0-30	2.2	8.0	0.1	14.2	100	9.1	157
30-56	1.0	8.0	0.1	10.7	100	11.2	94
56-114	0.8	8.0	0.1	10.5	100	11.4	91
114-135	0.9	8.0	0.1	11.3	100	10.7	105
Profile 6							
0-23	2.2	7.5	0.1	12.1	100	8.9	136
23-58	1.5	7.2	0.1	9.6	100	9.3	103
58-102	1.0	7.4	0.1	9.6	100	10.7	90
102-183	0.5	7.6	0.1	9.5	100	10.1	94

^aExpressed as cmol/kg soil.

^b $\text{CECE} = \text{Ca}^{2+} + \text{Mg}^{2+} + \text{K}^+ + \text{Al}^{3+}$.

^c $\text{BSE} = ((\text{Ca}^{2+} + \text{Mg}^{2+} + \text{K}^+)/\text{CECE}) \times 100$.

^d NH_4OAc , pH 7 method.

^e $\text{NH}_4\text{OAc} = ((\text{Ca}^{2+} + \text{Mg}^{2+} + \text{K}^+)/\text{CECOAC}) \times 100$.

^f $\text{BSOAC} = ((\text{Ca}^{2+} + \text{Mg}^{2+} + \text{K}^+)/\text{CECOAC}) \times 100$.

coordinated Al, Cu, Fe, Mn, and Zn from phyllosilicates as surfaces of the minerals undergo acid decomposition. Amounts of Al, Cu, Fe, Mn, and Zn released from soil components increase with an increase in H_3O^+ activity in the soil-Mehlich I solution mixture.

Concentrations of Al, Cu, Fe, Mn, and Zn extracted by the Mehlich I solution (Table 6) were lower in Profile 2 and

Table 5. NH_4OAc base H^+ and CEC and BS by sum of cations.

Depth (cm)	Ca^{2+}	Mg^{2+}	K^+	H^+	CECS ^a	BSS ^b (%)
Profile 1						
0-23	6.5	0.7	0.1	3.3	10.5	67
23-114	10.6	0.9	0.1	4.3	16.0	73
114-173	12.3	0.9	0.1	4.3	17.6	75
173-183	11.4	0.9	0.1	2.7	15.1	82
Profile 2						
0-30	20.6	0.3	0.1	1.2	22.2	94
30-56	17.2	0.2	0	0.6	18.0	97
56-76	16.7	0.2	0	0	16.9	100
76-127	16.4	0.2	0	0	16.6	100
127-183	15.4	0.1	0	0	15.6	100
Profile 3						
0-38	18.4	0.4	0.1	0	18.9	100
38-79	12.0	0.4	0.1	1.2	13.7	91
79-107	9.6	0.4	0.1	3.7	13.8	73
Profile 4						
0-38	10.9	0.7	0.1	2.1	13.8	85
38-102	11.5	0.7	0.1	2.7	14.9	82
102-183	12.9	0.7	0.1	3.9	17.7	78
Profile 5						
0-30	13.1	0.9	0.2	2.5	16.6	85
30-56	9.9	0.6	0.1	1.7	12.3	87
56-114	9.9	0.4	0.1	3.1	13.5	77
114-135	10.6	0.5	0.1	2.7	13.9	81
Profile 6						
0-23	11.1	0.8	0.1	6.8	18.9	64
23-58	8.7	0.7	0.1	3.1	12.6	75
58-102	8.9	0.6	0.1	0	9.6	100
102-183	9.0	0.4	0.1	2.5	12.0	79

^aCECS = $\text{Ca}^{2+} + \text{Mg}^{2+} + \text{K}^+ + \text{H}^+$.

^bBSS = $((\text{Ca}^{2+} + \text{Mg}^{2+} + \text{K}^+)/\text{CECS}) \times 100$.

in the surface horizon of Profile 3 than in the other soils. The pH of soil-Mehlich I solution mixtures would be higher in these soils because of the neutralization of H_3O^+ ions by CaCO_3 shown to be present by strong to violent effervescence (Appendix A) and by high CaCO_3 equivalents (Table 3). Concentrations of Cu, Fe, Mn, and Zn observed in these soils indicate that deficiencies of these micronutrients to sensitive plants would be more likely in soils that contain CaCO_3 .

Table 6. Selected elements extracted by the Mehlich I extractant.

Depth (cm)	Al	Ca^a	Cu	Fe	K	Mg	Mn	P	Zn
Profile 1									
0-23	24.5	900	0.2	2.5	42	62	7.5	9	5.1
23-114	32.4	>1200	0.2	2.7	14	81	4.0	3	1.0
114-173	32.9	>1200	0.2	2.2	15	85	3.7	8	1.2
173-183	31.4	>1200	0.2	2.4	14	90	3.3	8	0.7
Profile 2									
0-30	0.7	>1200	0	0.1	8	42	1.2	2	0.1
30-56	0.4	>1200	0	0.1	6	33	2.2	2	0.1
56-76	0.4	>1200	0	0.1	4	30	3.2	2	0.1
76-127	0.4	>1200	0	0.1	4	30	2.4	2	0.1
127-183	0.5	>1200	0	0.2	4	31	3.7	2	0.1
Profile 3									
0-38	0.5	>1200	0	0.1	11	55	0.4	2	0.1
38-79	27.1	>1200	0.1	0.6	14	49	5.6	3	0.9
79-107	31.8	>1200	0.1	1.4	17	44	4.6	2	0.5
Profile 4									
0-38	24.9	>1200	0.1	2.8	26	89	16.1	14	6.1
38-102	31.1	>1200	0.2	1.6	14	73	4.8	4	1.4
102-183	33.5	>1200	0.2	2.0	11	75	3.3	6	0.9
Profile 5									
0-30	29.5	>1200	0.2	3.4	20	89	12.2	11	6.1
30-56	33.7	>1200	0.2	2.0	20	77	6.8	3	4.7
56-114	34.8	>1200	0.2	2.3	17	54	4.0	5	1.2
114-135	36.3	>1200	0.2	2.3	17	57	3.9	9	1.1
Profile 6									
0-23	24.8	>1200	0.2	3.5	28	81	10.5	12	6.1
23-58	29.5	>1200	0.2	2.7	15	67	6.6	10	4.0
58-102	34.8	>1200	0.2	3.0	11	62	4.3	5	1.1
102-183	39.1	>1200	0.2	4.3	14	54	4.6	23	1.1

^a1200 $\mu\text{g Ca}^{2+}/\text{kg}$ soil represents a sufficient quantity for maximum biomass production. Therefore, exact quantities above 1200 μg are not routinely determined by the Virginia Tech Soil Testing and Plant Analysis Laboratory.

Extractable Phosphorus

Concentrations of P in the soil solution needed for maximum biomass production are estimated by extraction with the Mehlich I solution. Phosphorus is extracted primarily from calcium phosphates by this solution through the action of H_3O^+ ions (Martens and others, 1969). Concentra-

tions of P extracted from Profile 2 and from the surface horizon of Profile 3 (Table 6) reflect neutralization of H_3O^+ ions by CaCO_3 and indicate an inadequate supply of P for normal growth of most agronomic crops.

Soil pH and Calcium

Distributions of soil pH (Table 4) and extractable Ca^{2+} levels (Tables 3 and 5) can be used to indicate the distribution of CaCO_3 and its influence on soils associated with the confluence of the Shenandoah River and Spout Run. Soil Profile 1 (Figure 1), upstream from the Spout Run travertine-marl deposit, has pH levels below the range reported by Jackson (1979) for well-aerated soils buffered by the CaCO_3 - H_2O - CO_2 system. An absence of CaCO_3 in this soil was indicated by observed pH levels and lack of effervescence with dilute HCl. This profile represents soils influenced by the dissolution of CaCO_3 through their interaction with flood waters that contain high levels of dissolved Ca^{2+} and alkalinity. Alluvial soils on adjacent terraces not subject to flooding and upland soils in this area have low exchangeable Ca^{2+} and pH levels. The pH levels in these terrace and upland soils are buffered by the Al system (Edmonds, 1970).

Soil Profile 2 (Figure 1), located in the Spout Run travertine-marl deposit, had pH levels above the range given by Jackson (1979) for soils buffered by the CaCO_3 - H_2O - CO_2 system which indicated a decrease in PCO_2 with depth. Based on CaCO_3 equivalents (Table 3), an average of approximately 1.14 metric tons (mt) of the Bw and C horizons of Profile 2 is equivalent to 1 mt of pure CaCO_3 . Because of high CaCO_3 equivalents and the presence of impressions of leaves, sticks, and other objects, we assume that the Bw and C horizons of this soil would qualify as primary travertine-marl in the strictest geologic sense. The concurrent and subsequent influence of organisms on this deposit to form a soil is indicated by the increase in organic matter in the surface 30 cm and the consequent formation of an A horizon. The influence of climate on this deposit is indicated by a decrease in CaCO_3 equivalent in the A horizon. The CaCO_3 has probably been dissolved from the A horizon and precipitated in lower horizons.

Soil Profiles 3 through 6 (Figure 1) were located at increasing distances along the west bank of the Shenandoah River below the Spout Run travertine-marl deposit. These soils had pH levels that decreased from Profile 2 through 6 and represented the entire range given by Jackson (1979) for well-aerated soils buffered by the CaCO_3 - H_2O - CO_2 system with PCO_2 of $10^{-2.0}$ to $10^{-3.52}$ atm. These decreasing pH and Ca^{2+} levels indicated a decreasing influence of CaCO_3 dissolution or deposition with increasing distance downstream from the Spout Run deposit.

Travertine-marl is eroded from stream beds during floods (Emig, 1917) and is deposited downstream as clastic carbon-

ate sediments. Soil pH, Ca^{2+} levels, and effervescence in Profile 3 indicated the deposition and incorporation of CaCO_3 particles in the surface layers of this soil. Soil pH, Ca^{2+} levels, and lack of effervescence in Profiles 4, 5, and 6 indicated the influence of soil water rich in Ca^{2+} and HCO_3^- ions derived from dissolution of the Spout Run deposit or from limestone that underlies the adjacent uplands.

SOIL CLASSIFICATION

Order

Soils in this study (Appendix I) have mollic epipedons and are members of the Mollisol order (Soil Survey Staff, 1988). They have BSOAC values greater than 50 percent to a depth of 1.25 m below the soil surface (Table 4), primarily as a result of their interaction with water that has high level of Ca^{2+} and pH (Edmonds, 1970). They contain less than 300 g clay per kg soil in the upper 18 cm (Table 7). Mollisols have properties that preclude serious plant toxicity from Al and Mn, and that ensure a reasonable reserve of Ca, Mg, K, and N. The structure of the mollic epipedon facilitates movement of water and air. The presence of organic matter shows that the soils receive sufficient moisture to support fair to luxuriant plant growth during most years.

Suborder

Soils represented by Profiles 1, 3, 4, 5, and 6 are members of the suborder of Udolls. They: have mean annual soil temperatures greater than or equal to 8°C (Edmonds, 1970); are well drained (Appendix I); have a horizon immediately below the mollic epipedon that has a CaCO_3 equivalent less than 40 percent (Table 3); and are not dry for as long as 90 days in most years (have a udic moisture regime).

Soils represented by Profile 2 are members of the suborder of Rendolls. They have a horizon immediately below the mollic epipedon that has a CaCO_3 equivalent greater than 40 percent (Table 3) as the result of CaCO_3 deposition.

Great Group

Soils represented by Profiles 1, 3, 4, 5, and 6 are members of the great group of Hapludolls. They have cambic horizons with less than 50 percent worm holes, worm casts, and filled animal burrows.

Table 7. Particle-size distribution.

Depth (cm)	Sand					Total	Silt	Clay
	VC	C	M	F	VF			
Profile 1								
0-23	1	10	31	40	37	119	799	82
23-114	0	2	19	137	112	270	440	290
114-173	0	2	43	144	100	290	427	284
173-183	0	3	71	160	75	310	422	269
Profile 2								
0-30	5	19	36	84	74	218	612	170
30-56	5	35	67	120	105	331	546	123
56-76	15	112	168	163	125	584	317	100
76-127	14	52	87	189	150	492	411	96
127-183	102	179	147	112	83	623	285	91
Profile 3								
0-38	8	12	21	107	198	348	506	146
38-79	2	7	18	117	200	344	458	198
79-107	0	11	37	108	142	299	459	243
Profile 4								
0-38	1	4	55	252	137	449	362	189
38-102	0	1	24	203	165	394	362	245
102-183	0	2	20	146	159	326	389	285
Profile 5								
0-30	5	22	77	209	115	428	352	220
30-56	3	10	56	233	167	469	305	226
56-114	1	10	54	215	143	424	336	240
114-135	10	15	57	190	153	425	319	256
Profile 6								
0-23	1	10	81	280	153	525	326	149
23-58	1	7	77	308	195	588	254	157
58-102	0	3	43	274	210	530	270	199
102-183	134	66	41	46	43	329	450	221

Subgroup

Soils represented by Profiles 4, 5, and 6 are members of the subgroup of Fluventic Hapludolls. They are well drained; have a mollic epipedon less than 60 cm thick (Appendix I); have a cambic (Bw) horizon that is free of CaCO₃ in the lower part (Table 3); have an irregular decrease in organic C with depth or have an organic C content greater than 0.3 percent (greater than 0.5 percent organic matter) to a depth of 1.25 m below the soil surface (Table 4); do not have a contact with bedrock within 50 cm of the soil surface; do not have cracks; do not have a coefficient of linear extensibility greater than 0.9; and do not contain more than 350 g clay per kg soil in horizons more than 50 cm thick. Mollic epipedons less than

60 cm thick and irregular decreases in organic C are the result of soil surface layers being rapidly buried by the deposition of sediment. Irregular decreases in organic matter are related to the presence of buried paleosols.

Soils represented by Profiles 1 and 3 are members of the subgroup of Cumulic Hapludolls. They have a mollic epipedon greater than 60 cm thick. Mollic epipedons greater than 60 cm thick develop where the sedimentation rate is slow enough for the added sediment to be incorporated into the epipedon.

Soils represented by Profile 2 are members to the subgroup of Eutrochreptic Rendolls. They are well drained (low chroma in the Bw horizon are assumed to result from the color of CaCO₃); do not have a contact with bedrock within 50 cm of the soil surface; do not have cracks; do not have a coefficient of linear extensibility greater than 0.9; do not contain more than 350 g clay per kg soil in horizons more than 50 cm thick; and have a cambic (Bw) horizon.

Family

Texture: Soils represented by profiles 1, 3, 4, and 5 are members of the fine-loamy textural class. They have textures finer than loamy very fine sand or very fine sand and contain between 180 and 350 g clay per kg soil between depths of 25 and 100 cm (Table 7). Soil Profiles 2 and 6 are members of the coarse-loamy textural class. They contain less than 180 g clay per kg soil.

Mineralogy: Soils represented by Profile 1 are members of the mixed (loamy) mineralogical class. The 25- to 100-cm section of profile 1 had less than 900 g quartz (855 g) per kg of the 0.05- to 0.5-mm fraction; greater than 100 g of weatherable minerals (feldspar, 143 g); and 2 g of heavy minerals (epidote, tourmaline, and zircon) between depths of 50 and 100 cm. Based on mineralogical analysis of other sites along the Shenandoah River, Profiles 1, 3, 4, 5, 6, and 7 are assumed to have similar mineral suites.

Soils represented by Profile 2 are members the carbonatic mineralogy class. The 25- to 100-cm section of Profile 2 contained about 100 percent calcite as estimated by a petrographic grain count of the 0.05- to 0.5-mm fraction. An accurate grain count was not possible, because soil particles other than calcite were occluded by calcite (Figure 2) and their optical properties could not be observed. Classification of this soil was based on the CaCO₃ equivalent. Soils represented by Profile 2 have greater than 40 percent by weight of carbonates between depths of 20 and 100 cm. Because these soils have particles occluded by calcite, we can expect them to react similarly to those observed by Pettry and Rich (1971).

Temperature: The soils in this study are members of the mesic temperature class. They are estimated to have temperatures of about 14°C at 50 cm below the soil surface (Edmonds, 1970).

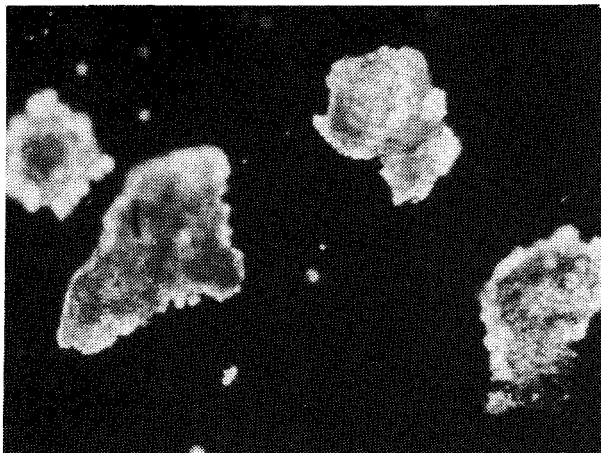


Figure 2. Soil particles from the 0.05- to 0.50-mm fraction of the Bw horizon of profile 2 occluded by CaCO_3 (crossed nicols, 80X).

Series

Identification of series in the soils developed in Holocene alluvium deposited by the Bullpasture, Calfpasture, Cowpasture, Holston, James, Jackson, Maury, New, Roanoke, and Shenandoah rivers and their tributaries has been revised in light of recent research, including an unpublished revision of soil taxonomy by the U.S. Department of Agriculture, Soil Survey Staff (1988). These soils were previously conceived to be members of the Inceptisol and Entisol orders. Detailed characterization revealed that they are members of the Mollisol order. Series names used in this study reflect the new concepts and are different from those used to correlate the Soil Survey of Clarke County (Edmonds and Stiegler, 1982). The new soil series names and their classification are given for each soil profile in Appendix I.

CONCLUSIONS

Soils influenced by the dissolution of CaCO_3 have relatively thick, dark-colored surface horizons as the result of a relatively high organic matter content, have moderately to strongly developed structure, and do not effervesce with dilute HCl. The exchange complex is saturated with Ca^{2+} . They are members of the great group of Hapludolls. Soils with mollic epipedons less than 60 cm thick are members of the subgroup of Fluventic Hapludolls because they have irregular decreases, with depth, in organic matter as the result of soil surface layers being rapidly buried by sediment deposition. Where the deposition rate is slow enough for added sediment to be incorporated into the mollic epipedon, it is

greater than 60 cm thick, and the soils are classified as members of the subgroup of Cumulic Hapludolls.

Soils influenced by CaCO_3 deposition in Holocene alluvium downstream from limestone springs have pH levels between 7.4 and 8.7 and effervesce with dilute HCl. Micro-nutrient cations of Cu, Fe, Mn, and Zn are relatively unavailable to plants because of high pH levels and occlusion by CaCO_3 . Phosphorus is generally inadequate for normal plant growth because of the formation of highly insoluble calcium phosphates. Occlusion of soil particles by CaCO_3 gave values for base saturation greater than 100 percent because nonexchangeable Ca^{2+} was dissolved from CaCO_3 as the pH of the soil and extracting solution equilibrated. Soils with CaCO_3 equivalents greater than 40 percent are members of the suborder of Rendolls. Soils with cambic horizons are members of the subgroup of Eutrochreptic Rendolls.

ACKNOWLEDGMENTS

We sincerely appreciate the help of Steve Thomas, Louis Heidel, Steve Cromer, and Bruce Legge in describing and sampling the soils. Special thanks are due Louise Price, Jim Harris, Chris Koch, and Jim Fredericks of the Virginia Tech Soils Laboratories for the chemical and physical analyses of the soils.

REFERENCES CITED

- Allison, L.E., 1965, Organic carbon, *in* Black, C.A., and others, eds., Methods of soil analysis, Part 2: Madison, Wisconsin, American Society of Agronomy, No. 9 in the Series Agronomy, p. 1367-1378.
- Allison, L.E., and Moodie, C.D., 1965, Carbonate, *in* Black, C.A., and others, eds., Methods of soil analysis, Part 2: Madison, Wisconsin, American Society of Agronomy, No. 9 in the Series Agronomy, p. 1379-1396.
- Bohn, H.L., McNeal, B.L., and O'Connor, G.A., 1985, Soil chemistry: New York, New York, John Wiley & Sons, 341 p.
- Buol, S.W., Hole, F.D., and McCracken, R.J., 1980, Soil genesis and classification: Ames, The Iowa State University Press, 406 p.
- Chapman, H.D., 1965, Cation-exchange capacity, *in* Black, C.A., and others, eds., Methods of soil analysis, Part 2: Madison, Wisconsin, American Society of Agronomy, No. 9 in the Series Agronomy, p. 891-901.
- Day, P.R., 1965, Particle fractionation and particle-size analysis, *in* Black, C.A., and others, eds., Methods of soil analysis, Part 1: Madison, Wisconsin, American Society of Agronomy, No. 9 in the Series Agronomy, p. 545-567.
- Donohue, S.J., and Friedericks, J.B., 1984, Laboratory procedures, Virginia Polytechnic Institute and State University soil testing and plant analysis laboratory: Blacksburg, Virginia Polytechnic Institute and State University Extension Publication 452-881, 30 p.
- Edmonds, W.J., 1970, Soils of Clarke County: Blacksburg, Virginia Polytechnic Institute and State University Extension Publication No. 14, 375 p.

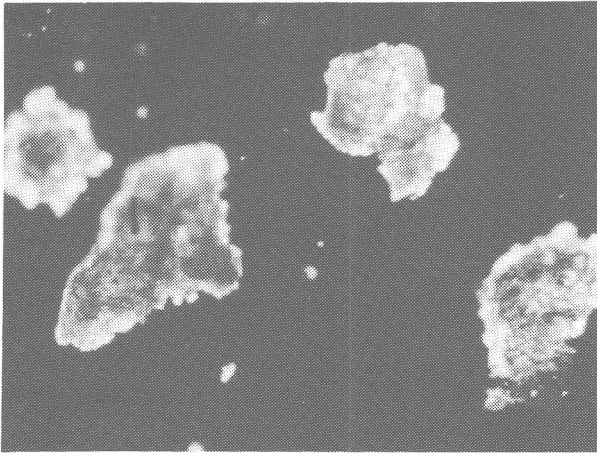


Figure 2. Soil particles from the 0.05- to 0.50-mm fraction of the Bw horizon of profile 2 occluded by CaCO_3 (crossed nicols, 80X).

Series

Identification of series in the soils developed in Holocene alluvium deposited by the Bullpasture, Calfpasture, Cowpasture, Holston, James, Jackson, Maury, New, Roanoke, and Shenandoah rivers and their tributaries has been revised in light of recent research, including an unpublished revision of soil taxonomy by the U.S. Department of Agriculture, Soil Survey Staff (1988). These soils were previously conceived to be members of the Inceptisol and Entisol orders. Detailed characterization revealed that they are members of the Mollisol order. Series names used in this study reflect the new concepts and are different from those used to correlate the Soil Survey of Clarke County (Edmonds and Stiegler, 1982). The new soil series names and their classification are given for each soil profile in Appendix I.

CONCLUSIONS

Soils influenced by the dissolution of CaCO_3 have relatively thick, dark-colored surface horizons as the result of a relatively high organic matter content, have moderately to strongly developed structure, and do not effervesce with dilute HCl. The exchange complex is saturated with Ca^{2+} . They are members of the great group of Hapludolls. Soils with mollic epipedons less than 60 cm thick are members of the subgroup of Fluventic Hapludolls because they have irregular decreases, with depth, in organic matter as the result of soil surface layers being rapidly buried by sediment deposition. Where the deposition rate is slow enough for added sediment to be incorporated into the mollic epipedon, it is

greater than 60 cm thick, and the soils are classified as members of the subgroup of Cumulic Hapludolls.

Soils influenced by CaCO_3 deposition in Holocene alluvium downstream from limestone springs have pH levels between 7.4 and 8.7 and effervesce with dilute HCl. Micro-nutrient cations of Cu, Fe, Mn, and Zn are relatively unavailable to plants because of high pH levels and occlusion by CaCO_3 . Phosphorus is generally inadequate for normal plant growth because of the formation of highly insoluble calcium phosphates. Occlusion of soil particles by CaCO_3 gave values for base saturation greater than 100 percent because nonexchangeable Ca^{2+} was dissolved from CaCO_3 as the pH of the soil and extracting solution equilibrated. Soils with CaCO_3 equivalents greater than 40 percent are members of the suborder of Rendolls. Soils with cambic horizons are members of the subgroup of Eutrochreptic Rendolls.

ACKNOWLEDGMENTS

We sincerely appreciate the help of Steve Thomas, Louis Heidel, Steve Cromer, and Bruce Legge in describing and sampling the soils. Special thanks are due Louise Price, Jim Harris, Chris Koch, and Jim Fredericks of the Virginia Tech Soils Laboratories for the chemical and physical analyses of the soils.

REFERENCES CITED

- Allison, L.E., 1965, Organic carbon, *in* Black, C.A., and others, eds., Methods of soil analysis, Part 2: Madison, Wisconsin, American Society of Agronomy, No. 9 in the Series Agronomy, p. 1367-1378.
- Allison, L.E., and Moodie, C.D., 1965, Carbonate, *in* Black, C.A., and others, eds., Methods of soil analysis, Part 2: Madison, Wisconsin, American Society of Agronomy, No. 9 in the Series Agronomy, p. 1379-1396.
- Bohn, H.L., McNeal, B.L., and O'Connor, G.A., 1985, Soil chemistry: New York, New York, John Wiley & Sons, 341 p.
- Buol, S.W., Hole, F.D., and McCracken, R.J., 1980, Soil genesis and classification: Ames, The Iowa State University Press, 406 p.
- Chapman, H.D., 1965, Cation-exchange capacity, *in* Black, C.A., and others, eds., Methods of soil analysis, Part 2: Madison, Wisconsin, American Society of Agronomy, No. 9 in the Series Agronomy, p. 891-901.
- Day, P.R., 1965, Particle fractionation and particle-size analysis, *in* Black, C.A., and others, eds., Methods of soil analysis, Part 1: Madison, Wisconsin, American Society of Agronomy, No. 9 in the Series Agronomy, p. 545-567.
- Donohue, S.J., and Friedericks, J.B., 1984, Laboratory procedures, Virginia Polytechnic Institute and State University soil testing and plant analysis laboratory: Blacksburg, Virginia Polytechnic Institute and State University Extension Publication 452-881, 30 p.
- Edmonds, W.J., 1970, Soils of Clarke County: Blacksburg, Virginia Polytechnic Institute and State University Extension Publication No. 14, 375 p.

- Edmonds, W.J., and Stiegler, James, 1982, Soil Survey of Clarke County, Virginia: Washington, D.C., U. S. Department of Agriculture, Soil Conservation Service, U. S. Government Printing Office, 211 p.
- Edmundson, R.S., and Nunan, W.E., 1973, Geology of the Berryville, Stephenson, and Boyce quadrangles, Virginia: Virginia Division of Mineral Resources Report of Investigations 34, 112 p.
- Emig, W.H., 1917, Travertine deposits of Oklahoma: Oklahoma Geological Survey Bulletin 29, 76 p.
- Garrels, R.M., and Christ, C.L., 1965, Solutions, minerals, and equilibria: San Francisco, California, Freeman, Cooper, & Company, 450 p.
- Hollander, Myles, and Wolfe, D.A., 1973, Nonparametric statistical methods: New York, New York, John Wiley & Sons, Inc., 503 p.
- Hubbard, D.A., Jr., Giannini, W.F., and Lorah, M.M., 1985, Travertine-marl deposits of the Valley and Ridge province of Virginia - a preliminary report: Virginia Division of Mineral Resources, Virginia Minerals, v.31, n.1, p. 1-12.
- Jackson, M.L., 1979, Cation exchange equilibrium of soil colloidal acids with bases, *in* Soil chemical analysis—advanced course, 2nd edition, 11th printing: Madison, Wisconsin, published by the author, p. 838-870.
- Jenny, Hans, 1980, The soil resource: New York, New York, Springer-Verlag, 377 p.
- Kabata-Pendias, Alina, and Pendias, Henryk, 1985, Trace elements in soils and plants: Boca Raton, Florida, CRC Press, Incorporated, 315 p.
- Kunze, G. W., and Dixon, J. B., 1986, Pretreatment for mineralogical analysis, *in* Klute, A., ed., Methods of Soil Analysis, Part 1: Madison, Wisconsin, American Society of Agronomy, No. 9 in the Series Agronomy, p. 91-100.
- Lindsay, W.L., and Moreno, E.C., 1960, Phosphate phase equilibria in soils: Soil Science Society of America Proceedings, v. 24, p. 177-182.
- Marion, G.M., and Babcock, K.L., 1977, The solubilities of carbonates and phosphates in calcareous soil suspensions: Soil Science Society of America Journal, v. 41, p.724-728.
- Martens, D.C., Lutz, J.A., and Jones, G.D., 1969, Form and availability of P in selected Virginia soils as related to available P tests: Agronomy Journal, v. 61, p. 616-621.
- McLean, E.O., 1965, Aluminum, *in* Black, C.A., and others, eds., Methods of soil analysis, Part 2: Madison, Wisconsin, American Society of Agronomy, No. 9 in the Series Agronomy, p. 978-998.
- Munsell Color, 1975 edition, Munsell soil color charts, Baltimore, Maryland, MacBeth Division of Kollmogen Corporation, 19 p.
- Olsen, S.R., and Sommer, L.E., 1982, Phosphorus, *in* Page, A.L., ed., Methods of soil analysis, Part 2: Madison, Wisconsin, American Society of Agronomy, No. 9 in the Series Agronomy, p. 403-430.
- Peech, Michael, 1965, Exchange acidity, *in* Black, C. A., and others, eds., Methods of soil analysis, Part 2: Madison, Wisconsin, American Society of Agronomy, No. 9 in the Series Agronomy, p. 905-913.
- Pettry, D.E., and Rich, C.I., 1971, Modification of certain soils by calcium hydroxide stabilization: Soil Science Society of America Proceedings, v. 35, p. 834-838.
- Pirie, W.H., 1983, User's guide for Virginia Tech nonparametric statistics package: Blacksburg, Virginia Polytechnic and State University, 22 p.
- Randles, R.H., Flinger, M.A. Policello, G.E., II, and Wolfe, D.A., 1980, An asymptotically distribution-free test for symmetry versus asymmetry: Journal of the American Statistical Association, v. 75, p. 168.
- Rappaport, B.D, Martens, D.C., Simpson, T.W., and Reneau, R.B., Jr., 1986, Prediction of available zinc in sewage sludge-amended soils: Journal of Environmental Quality, v. 15, p. 133-136.
- Ruffin, Edmund, 1832, An essay on calcareous manures: Petersburg, Virginia, J.W. Campbell, Reprinted by John Harvard Library, 1961, 199 p.
- Schnitzer, Morris, 1978, Humic substances: chemistry and reactions, *in* Schnitzer, M., and Khan, S.U., eds., Soil organic matter: New York, New York, Elsevier Scientific Publishing Company, p. 1-64.
- Soil Conservation Service, 1982, Procedures for collection of soil samples and methods of analysis: Washington, D.C., U. S. Department of Agriculture, Soil Survey Investigations Report No. 1, U.S. Government Printing Office, 97 p.
- Soil Survey Staff, 1975, Soil taxonomy: a basic system of soil classification for making and interpreting soil surveys: Washington, D.C., U.S. Department of Agriculture, Soil Conservation Service, U.S. Government Printing Office, Agricultural Handbook 436, 754 p.
- Soil Survey Staff, 1981, Soil series of the U.S., Puerto Rico, and the Virgin Islands: their classification: Washington, D.C., U.S. Department of Agriculture, Soil Conservation Service, U.S. Government Printing Office, 152 p.
- Soil Survey Staff, 1988, Unpublished revision of Soil taxonomy: a basic system of soil classification for making and interpreting soil surveys: Washington, D.C., U.S. Department of Agriculture, Soil Conservation Service, U.S. Government Printing Office, Agricultural Handbook 436.
- Sparks, D.L., and Huang, P.M., 1985, Physical chemistry of soil potassium, *in* Munson, R.D., ed., Potassium in agriculture: Madison, Wisconsin, American Society of Agronomy, p. 201-276.
- Thomas, G.W., 1977, Historical developments in soil chemistry: ion exchange: Soil Science Society of America Journal, v. 41, p. 230-237.
- Tisdale, S.L., and Nelson, W.L., 1975, Soil fertility and fertilizers: New York, New York, Macmillan Publishing Company, Incorporated, 694 p.
- Truog, Emil, 1938, Putting soil science to work: Journal of the American Society of Agronomy, v.30, p. 973-985.
- Udo, E.J., Bohn, H.L., and Tucker, T.C., 1970, Zinc adsorption by calcareous soils: Soil Science Society of America Proceedings, v. 34, p. 405-407.

**APPENDIX I:
SOIL DESCRIPTIONS AND DATA**

Profile 1 — Speedwell variant¹ silt loam²

Location: Above the Spout Run travertine-marl deposit about 1.6 km southeast (136°) of the junction of State Road 651 and State Road 619 and 0.6 km east-southeast (116°) of the junction of the Shenandoah River and Spout Run (Figure 1)

Elevation: 128 m

Vegetation: Hay - orchard grass

Slope: 1 percent

Classification: fine-loamy, mixed, mesic Cumulic Hapludolls

Ap — 0 to 23 cm; dark-brown (10YR 3/3) silt loam; brown (10YR 4/3) dry; moderate medium granular structure; friable, slightly sticky, slightly plastic; many fine roots; slightly acid; abrupt smooth boundary.

Bw1 — 23 to 114 cm; dark-brown (10YR 3/3) clay loam; brown (10YR 4/3) dry; moderate medium subangular blocky structure; friable, slightly sticky, slightly plastic; common fine roots; neutral; gradual smooth boundary.

Bw2 — 114 to 173 cm; very dark grayish-brown (10YR 3/2) clay loam; brown (10YR 4/3) dry; moderate medium subangular blocky structure; friable, slightly sticky, slightly plastic, few fine roots; neutral; gradual smooth boundary.

Bw3 — 173 to 183 cm; dark-brown (10YR 3/3) loam; moderate medium subangular blocky structure; friable, slightly sticky, slightly plastic; few fine roots; neutral.

Profile 2 — Massanetta variant³ silt loam

Location: In the Spout Run deposit about 1.6 km south (165°) of the junction of State Road 651 and State Road 619 and 1.1 km south (180°) of the junction of State Road 621 and State Road 651 (Figure 1)

Elevation: 134 m

Vegetation: Sycamore trees

Slope: 1 percent

Classification: coarse-loamy, carbonatic, mesic Euthrochreptic Rendolls

A — 0 to 30 cm; very dark grayish-brown (10YR 3/2) silt loam; brown (10YR 4/3) dry; moderate fine granular structure; friable, slightly sticky, slightly plastic, many fine roots; violently effervescent; moderately alkaline; clear smooth boundary.

Bw1 — 30 to 56 cm; grayish-brown (2.5Y 5/2) silt loam; light

brownish-gray (10YR 6/2) dry; moderate medium subangular blocky structure; friable, slightly sticky, slightly plastic; common fine roots; violently effervescent; strongly alkaline; gradual smooth boundary.

Bw2 — 56 to 76 cm; grayish-brown (2.5Y 5/2) sandy loam; light brownish-gray (10YR 6/2) dry; moderate medium subangular blocky structure; friable, slightly sticky, slightly plastic, few fine roots; violently effervescent; strongly alkaline; gradual smooth boundary.

Bw3 — 76 to 127 cm; grayish-brown (10YR 5/2) loam; light brownish-gray (10YR 6/2) dry; moderate medium subangular blocky structure; friable, slightly sticky, slightly plastic; violently effervescent; strongly alkaline; clear smooth boundary.

C — 127 to 183 cm; grayish-brown (10YR 5/2) sandy loam; light brownish-gray (10YR 6/2) dry; massive, friable, slightly sticky, slightly plastic; 25 percent hard marl fragments; violently effervescent; strongly alkaline.

Profile 3 — Speedwell variant⁴ silt loam

Location: Below the Spout Run deposit about 0.8 km south-southeast (154°) of the junction of State Road 619 and State Road 651 and 0.3 km south (195°) of the junction of State Road 651 and State Road 621 (Figure 1)

Elevation: 128 m

Vegetation: Hay - orchard grass, fescue

Slope: 1 percent

Classification: fine-loamy, mixed, mesic Cumulic Hapludolls

Ap — 0 to 38 cm; dark-brown (10YR 3/3) silt loam; brown (10YR 4/3) dry; moderate medium granular structure; friable, slightly sticky, slightly plastic; many fine roots; strongly effervescent; moderately alkaline; clear smooth boundary.

Bw1 — 38 to 79 cm; dark-brown (10YR 3/3) loam; brown (10YR 4/3) dry; common medium faint very dark grayish-brown (10 YR 3/2) mottled; moderate medium subangular blocky structure; friable, slightly sticky, slightly plastic; common fine roots; slightly effervescent; moderately alkaline; gradual smooth boundary.

Bw2 — 79 to 114 cm; dark-brown (7.5YR 4/4) loam; moderate medium subangular blocky structure; friable, slightly sticky, slightly plastic; few fine roots; slightly effervescent; moderately alkaline.

Profile 4 — Speedwell loam

Location: Below the Spout Run deposit about 1.0 km east (94°) of the junction of State Road 619 and State Road 651 and 0.6 km east-northeast (57°) of the junction of State Road 651 and State Road 621 (Figure 1)

Elevation: 126 m

Vegetation: Hay - orchard grass, fescue

Slope: 1 percent

Classification: fine-loamy, mixed, mesic Fluventic Hapludolls

Ap — 0 to 38 cm; dark-brown (10YR 3/3) loam; brown (10YR 4/3) dry; moderate medium granular structure; friable, slightly sticky, slightly plastic; many fine roots; moderately alkaline; abrupt smooth boundary.

Bw1 — 38 to 102 cm; dark-brown (10YR 4/3) loam; moderate fine subangular blocky structure; friable, slightly sticky, slightly plastic; common fine roots; moderately alkaline; gradual smooth boundary.

Bw2 — 102 to 183 cm; dark-brown (7.5YR 4/4) clay loam; moderate fine subangular blocky structure; friable, slightly sticky, slightly plastic; few fine roots; moderately alkaline.

Profile 5 — Speedwell loam

Location: Below the Spout Run deposit about 0.6 km east (90°) of the junction of State Road 619 and State Road 651 and 1.4 km east (73°) of the junction of State Road 651 and State Road 621 (Figure 1)

Elevation: 125 m

Vegetation: Hay - fescue and weeds

Slope: 1 percent

Classification: fine-loamy, mixed mesic Fluventic Hapludolls

Ap — 0 to 30 cm; dark-brown (10YR 3/3) loam; brown (10YR 4/3) dry; moderate medium granular structure; friable, slightly sticky, slightly plastic; many fine roots; moderately alkaline; clear smooth boundary.

Bw1 — 30 to 56 cm; dark yellowish-brown (10YR 3/4) loam; moderate medium subangular blocky structure; friable, slightly sticky, slightly plastic; common fine roots; moderately alkaline; gradual smooth boundary.

Bw2 — 56 to 114 cm; dark yellowish-brown (10YR 3/4) loam; moderate medium subangular blocky structure; friable, slightly sticky, slightly plastic; few fine roots; moderately alkaline; gradual smooth boundary.

Bw3 — 114 to 135 cm; dark-brown (10YR 3/3) loam; moderate medium subangular blocky structure; friable, slightly

sticky, slightly plastic; few fine roots; moderately alkaline.

Profile 6 — Combs fine sandy loam

Location: Below the Spout Run deposit about 2.1 km east (91°) of the junction of State Road 619 and State Road 651 and 0.6 km east (78°) of the junction of State Road 651 and State Road 621 (Figure 1)

Elevation: 123 m

Vegetation: Small grain

Slope: 1 percent

Classification: coarse-loamy, mixed, mesic Fluventic Hapludolls

Ap — 0 to 23 cm; dark-brown (10YR 3/3) fine sandy loam; brown (10YR 4/3) dry; moderate medium granular structure; friable, slightly sticky, slightly plastic; many fine roots; mildly alkaline; abrupt smooth boundary.

Bw1 — 23 to 58 cm; dark-brown (10YR 3/3) fine sandy loam; brown (10YR 4/3) dry; moderate medium subangular blocky structure; friable, slightly sticky, slightly plastic; common fine roots; neutral; gradual smooth boundary.

Bw2 — 58 to 102 cm; dark-brown (10YR 4/3) fine sandy loam; moderate medium subangular blocky structure; friable, slightly sticky, slightly plastic; few fine roots; mildly alkaline; gradual smooth boundary.

Bw3 — 102 to 183 cm; dark yellowish-brown (10YR 4/4) loam; moderate medium subangular blocky structure; friable, slightly sticky, slightly plastic; few fine roots; mildly alkaline.

¹The Speedwell series does not allow a mollic epipedon thicker than 60 cm.

²Described by S. Cromer, W. Edmonds, L. Heidel, B. Legge, and S. Thomas on May 5, 1987. Colors (Munsell Color, 1975) are for moist soil, unless stated otherwise.

³The Massanetta series is a member of coarse-loamy, carbonatic, mesic family of Fluventic Hapludolls which lack a calcareous horizon with a CaCO₃ equivalent greater than 40 percent immediately below the mollic epipedon.

⁴The Speedwell series allows neither free carbonates nor a mollic epipedon thicker than 60 cm.

SPELEOGENESIS IN A TRAVERTINE SCARP: OBSERVATIONS OF SULFIDE OXIDATION IN THE SUBSURFACE

David A. Hubbard, Jr.¹, Janet S. Herman², and Pamela E. Bell³

CONTENTS

	Page
Abstract.....	177
Introduction.....	177
Sulfuric acid reaction mechanism literature review.....	178
Site description.....	179
Methods.....	180
Results.....	181
Discussion.....	181
Conclusions.....	183
Acknowledgments.....	183
References cited.....	183

ILLUSTRATIONS

Figure	
1. Geology of the Cesspool Cave area.....	179
2. Plan view of Cesspool Cave.....	180

TABLES

1. Chemical analyses of water samples.....	182
2. Calculated partial pressure of CO ₂ and saturation indices of the water samples.....	183

ABSTRACT

The Sawmill Falls escarpment is one of four stream-deposited Quaternary travertine-marl complexes along Sweet Springs Creek in Alleghany County, Virginia. Within this escarpment, Cesspool Cave has formed by acid dissolution of the travertine. The sources of acid are H₂S hydration and oxidation and CO₂ hydration. The calcite-saturated ground-water contained as much as 7.1 mg/L H₂S and had a PCO₂ as large as 10^{-1.17} atm where it enters the cave. Along the flow path through the cave and at its resurgence, H₂S concentrations decreased by a factor of two on one sampling date and by an order of magnitude on another date. Three genera of

colorless sulfur-oxidizing bacteria, *Thiothrix*, *Beggiatoa*, and *Achromatium*, were found to be actively oxidizing sulfide along the flow path. Corrosion of the limestone walls and calcite speleothems and their gypsum encrustation indicate the importance of the sulfuric acid reaction mechanism in the development of this cave.

INTRODUCTION

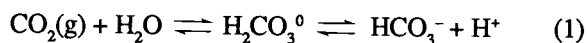
The geochemical, hydrological, and biological processes that influence cave development have been discussed at length (Jennings, 1971; Moore and Nicholas, 1964; Sweeting,

¹Virginia Division of Mineral Resources, P. O. Box 3667, Charlottesville, VA 22903

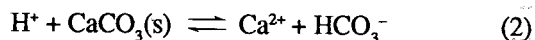
²Department of Environmental Sciences, Clark Hall, University of Virginia, Charlottesville, VA 22903

³Department of Microbiology, Jordan Hall, University of Virginia, Charlottesville, VA 22908

1972 and 1981; White, 1988). Common to the origin of all solutional cavities is the interaction of water with a soluble bedrock. Most cave development in limestone or dolomite is due to dissolution by groundwater, and the solubility of carbonate minerals is enhanced by the presence of dissolved acids. Chemical reactions that cause the formation of most caves include the hydration and dissolution of carbon dioxide gas in water to form carbonic acid which then dissociates to yield a free proton:



The proton then attacks calcite, yielding dissolved ions which are carried away by flowing groundwater



Reaction (2) is driven to the right by any source of free protons.

Sources of acid, other than carbon dioxide, exist in the geologic environment. The genesis of some caves is at least partially due to the action of such acids, most notably sulfuric acid. Sulfuric acid, a strong acid, does not exist as a molecular species in aqueous solution at pH values greater than 2.0. It completely dissociates in water to yield protons and sulfate ions. The speleological literature contains reports that sulfuric acid is generated by the oxidation of sulfide to sulfate (Howard, 1960; Jagnow, 1978). It is more accurate to describe acidity generated in this manner as the sulfuric acid reaction mechanism.

A sulfuric acid reaction mechanism is actively modifying Cesspool Cave which is developed in a stream-deposited Quaternary travertine-marl complex in Alleghany County, Virginia. This paper focuses on elucidating the speleological processes contributing to the development of Cesspool Cave.

SULFURIC ACID REACTION MECHANISM LITERATURE REVIEW

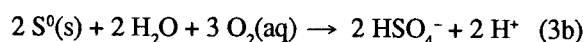
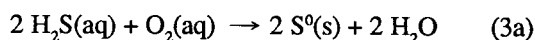
The major solution reaction ascribed to the development of the crevice caves in the dolomitic bedrock of the Iowa, Illinois, and Wisconsin lead-zinc sulfide district (Howard, 1960) and in Level Crevice Cave, Iowa (Morehouse, 1968), involves a sulfuric acid reaction mechanism. Howard (1960) hypothesized that pyrite, a common accessory mineral in the vein sulfide mineralization of the area, could be oxidized by oxygen to form ferric hydroxide ($\text{Fe}(\text{OH})_3$) or limonite ($\text{Fe}_2\text{O}_3 \cdot n\text{H}_2\text{O}$) and sulfuric acid. He suggested that sulfuric acid could dissolve the dolomite of the bedrock, leading to the formation of dissolved CO_2 , SO_4^{2-} , Ca^{2+} , and Mg^{2+} , all of which could be transported by groundwater. Howard (1960) thought carbonic acid also could be contributing to dolomite dissolution but that the sulfuric acid reaction mechanism

dominated the system in Crevice Cave. Morehouse (1968) also describes the dissolution of dolomite by acid generated by pyrite oxidation, but he added that the reaction can be catalyzed by iron-oxidizing bacteria.

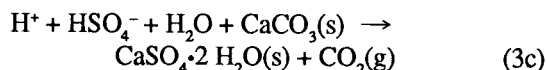
Acid generation during pyrite oxidation also was hypothesized to be the major control on the development of the caves in the Guadalupe Mountains of New Mexico (Jagnow, 1978). The disseminated pyrite, common in the formation overlying the cave-forming unit, was the probable source of the acid. The abundance of gypsum and other sulfate minerals prompted the author to speculate that, as a final step in Howard's (1960) mechanism, water high in Ca^{2+} and SO_4^{2-} precipitated gypsum.

Other mechanisms of formation have been proposed for the caves of the Guadalupe Mountains. Using geomorphic and hydrologic evidence, Davis (1979) argued that most of these caves could not have been formed by descending waters acidified by an overlying pyrite source. Rather, various solution features are indicative of development by ascending phreatic water. An alternative source of acid is the simple oxidation of the H_2S commonly associated with local oil and natural gas deposits. Acidic phreatic water, resulting from the mixing of sulfide-charged water with a deeply penetrating flow of oxygenated surface water, could form the phreatic pits and other features found in the caves of the Guadalupe Mountains.

Egemeier (1973) attributed the formation of the Kane Caves of Wyoming to the oxidation of H_2S according to



and



In his hypothesis, the ascending sulfide-rich groundwater was oxidized in the vadose zone and dissolved the limestone bedrock. Much of the hydrogen sulfide outgassed into the cave atmosphere from which it dissolved, along with oxygen, into water droplets on the cave walls and ceiling. The resulting oxidation reaction products were elemental sulfur and gypsum that replaced limestone. Large buildups of gypsum may slough off the walls and ceilings to be dissolved and removed by the cave stream. This "replacement-solution" mechanism of cave formation was also proposed for the origin of caves in the Guadalupe Mountains (Egemeier, 1973).

In detailed studies of Carlsbad Cavern and other caves in the Guadalupe Mountains, Hill (1981 and 1987) reported mineralogic and isotopic evidence of a sulfuric acid reaction

mechanism that agreed with Egemeier's (1973) and Davis's (1979) early hypotheses. The source of reduced sulfur was H_2S from the oil and gas fields in the Delaware basin located down dip. The H_2S in upwelling anoxic groundwater mixed with downward-moving oxygenated groundwater. The acid resulting from the oxidation of H_2S dissolved the limestone. Ultimately, gypsum and elemental sulfur formed as reaction products.

In studies conducted at Cesspool Cave, Virginia (Herman and others, 1986; Hubbard and others, 1986), the writers found that H_2S was present in water rising into the cave. Some of this H_2S was undergoing biologically mediated oxidation along the flow path in the cave. Three genera of colorless sulfur bacteria, *Thiothrix*, *Beggiatoa*, and *Achromatium*, occur in the cave water. Some of the H_2S outgassing from cave water into the cave atmosphere redissolved along with oxygen into water films on the cave surfaces. Acidity generated by sulfide oxidation dissolved calcite contemporaneously with gypsum precipitation, a process first proposed by Egemeier (1973). The oxidation of H_2S by biological and chemical processes generated the acid instrumental in the genesis of Cesspool Cave.

SITE DESCRIPTION

Four Quaternary travertine-marl deposits occur along Sweet Springs Creek in Alleghany County, Virginia (Figure 1). All four deposits occur at, or downstream from, two thermal carbonate-rich spring inputs, Sweet Springs and Sweet Chalybeate Springs, to the creek. Sweet Springs, West Virginia, was developed into a spa after its discovery in 1764. Early reports indicated that these springs discharged about 76 L/s of 23°C carbonate-rich water (Moorman, 1855; Walton, 1874). Approximately 1.6 km downstream from Sweet Springs, Sweet Chalybeate Springs (this spa was also known as Red Sweet Springs) reportedly discharged 16 to 51 L/s of 24 to 26°C carbonate-rich water (Moorman, 1855; Walton, 1874).

One of the travertine buildups occurs at Sweet Chalybeate Springs where Sweet Springs Creek crosses the contact between the Middle Ordovician limestone and the underlying Lower Ordovician dolomite of the Beekmantown Formation (Butts, 1933). A second travertine deposit forms Sawmill Falls. This buildup occurs 2.4 km downstream from the first deposit and is located at the contact between the Devonian Needmore Shale and Ridgely Sandstone. These rocks are part of the overturned east limb of a black-shale-cored syncline in the footwall rocks of the St. Clair fault (Butts, 1933; T.M. Gathright, II, 1985, personal communication). A third buildup, the Cascades, is located 0.6 km farther downstream, near the contact between the Devonian Brallier and Millboro shales (Butts, 1933). Beaverdam Falls, a fourth travertine

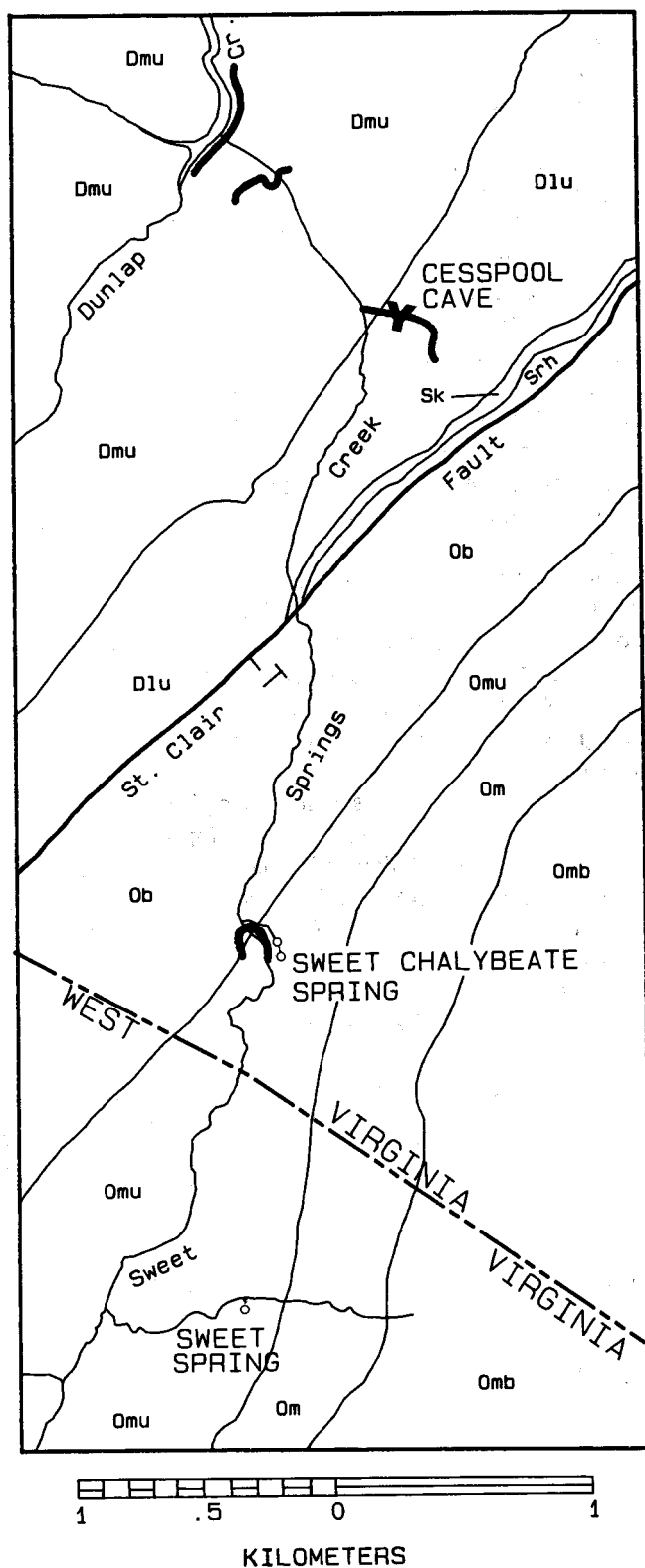


Figure 1. Geology of the Cesspool Cave area modified from Butts (1933) and Reger and Price (1925). Map symbols: **Y** cave; **T** fault, uppersheet; **○** spring, and **—** travertine buildup; **Dmu** Middle Devonian fms. undivided; **Dlu** Lower Devonian fms. undivided; **Sk** Keefer Ss.; **Srh** Rose Hill Fm.; **Omb** Martinsburg Fm.; **Om** Moccasin Fm.; **Omu** Middle Ordovician ls. undivided; **Ob** Beekmantown Fm.

deposit, is at the junction of Sweet Springs Creek and Dunlap Creek (see cover, bottom left photograph).

The travertine deposits of Sweet Springs Creek were first described in the literature by Featherstonhaugh (1835), who noted the presence of caverns, including "some spacious ones," in the travertine escarpment at Sawmill Falls. The largest of these caverns is Cesspool Cave (Figure 2). Entrance to the cave is by a stream-cut canyon-like passage approximately 3 m high. The cave is about 20 m long and consists of two rooms. The entrance room has a maximum height of 6 m and contains a pool of water that is 10 m in diameter and as much as 1 m deep. The southern end of the cave is identified as the terminal room. The two rooms are separated by a constriction in the cave passage where a gravel bar separates the pool of the entrance room from a pool in the terminal room. The gravel is composed of a mixture of carbonate and noncarbonate clastic pebbles derived as a sediment wash from the 12-m-long by 3-m-high hemi-dome of flowstone along the east wall of the cave. The terminal room pool is approximately 8 m in diameter and about 0.5 m in depth. A small stream flows from it to the entrance pool. Cesspool Spring is located at the edge of the terminal pool and the gravel bar, in the shadow of the flowstone hemi-dome (Figure 2).

Cesspool Cave is unusual for having been developed in travertine. Like many other caves developed in older limestone in Virginia's Valley and Ridge province (Holsinger, 1975), Cesspool Cave contains secondary flowstone and dripstone deposits composed of calcite. In the entrance room, both primary travertine and flowstone deposits (speleothems) are corroded, especially along the west wall. Inactive flowstone in the terminal room is encrusted with as much as 1 cm of gypsum.

The speleothems found in Cesspool Cave postdate the initial formation of the cave. The period over which this cave has been in existence is important to the study of the processes involved in its genesis. Attempts at U-Th series dating of speleothems from Cesspool Cave proved unsatisfactory. Much of the thorium was probably chelated and removed by organic acids. Significant amounts of detrital clastic materials in the speleothems contained contaminant thorium. Two samples yielded dates of "probably younger than 5000 and 10,000 years" old (Derek C. Ford, 1985, written communication).

METHODS

Four field trips were made to the Cesspool Cave sites to obtain samples for chemical and microbiological analyses in February, April, and July 1985 and April 1986. Sampling was conducted at the cave spring, the pool near the entrance, and the stream resurgence outside the cave (Figure 2). In April 1986, an additional sampling site was established at the terminal pool. Field measurements included temperature,

pH, conductivity, and alkalinity. Water samples were subsequently refrigerated and returned to the laboratory and filtered, split, and acidified. Chemical analyses were performed by atomic absorption spectroscopy for Ca^{2+} , Mg^{2+} , Na^+ , and K^+ , and by ion chromatography for SO_4^{2-} , Cl^- , NO_3^- , and PO_4^{3-} . Results of the chemical analyses were entered into a computerized equilibrium speciation model, WATEQF (Plummer and others, 1976), for calculation of the saturation state of the water samples.

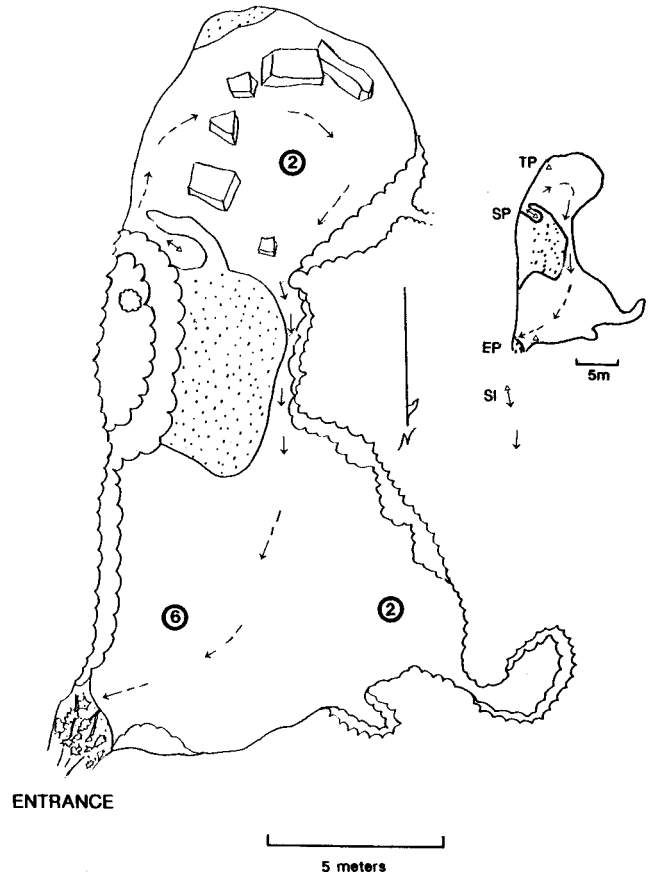


Figure 2. Plan view of Cesspool Cave. Symbols used on map include a wavy line for flowstone, dot stipple for gravel or sediment, box shapes for breakdown blocks, and solid and dashed arrows for observed or inferred water flow directions. Circled numbers indicate ceiling heights in meters. Symbols on inset diagram include small triangles at sampling locations: **SP** Cesspool Spring; **TP** terminal pool; **EP** entrance pool; **S1** surface stream.

Measurement of total aqueous sulfide (H_2S , HS^- , S^{2-}) was first conducted on the samples from July 1985. Samples were collected using glass syringes and were placed into nitrogen-evacuated serum vials fitted with crimped butyl rubber stoppers (Fulghum and Worthington, 1977). Samples were refrigerated until they were analyzed using Cline's

(1969) colorimetric method in the laboratory the following day. Concern about the stability of the aqueous sulfide constituents from the time of sampling until analysis prompted the use of a different sampling technique on the following trip. In April 1986, samples were fixed with Cline's reagent in the field and analyzed with a spectrophotometer in the laboratory that evening. We did not further evaluate whether the collection technique influenced the concentration of H_2S recovered.

Samples for microbiological analysis were collected in the cave and in the surface stream immediately below the resurgence outside the cave. Samples included coated pebbles, leaves coated with white material, filamentous strings and webs, and milky-colored water samples. Samples were placed in plastic bags or bottles and refrigerated during transport to the laboratory where they were examined using phase-contrast microscopy.

RESULTS

The chemical composition of the Cesspool Cave water is typical for groundwater in limestone terrane (Table 1). The dominant cation is Ca^{2+} (153-181 mg/L), and Mg^{2+} is an order of magnitude less concentrated (14.8-18.1 mg/L). The major anion is HCO_3^- (390-489 mg/L), and SO_4^{2-} is much less concentrated (106-127 mg/L). Concentrations of Na^+ , K^+ , Cl^- , and NO_3^- were all low (Table 1). The water temperature (10.0-13.0°C) is typical for shallow groundwater in the region and is much lower than the major spring inputs of thermal water upstream. The pH is slightly below neutral.

A significant decrease in total aqueous sulfide concentration was observed along the flow path for the two instances on which it was measured, July 1985 and April 1986 (Table 1). In July, H_2S concentration was 1.7 mg/L at the spring and 1.5 mg/L in the entrance pool. It decreased to 0.2 mg/L in the stream outside the cave. In April 1986, the H_2S concentrations were higher overall. We measured 7.1 mg/L H_2S at the spring in the cave and 5.5 and 2.4 mg/L in the terminal pool and entrance pool, respectively. In the surface stream, just outside the cave entrance, H_2S was 3.3 mg/L. Differences in SO_4^{2-} concentration along the flow path were either insignificant, as in February and July 1985 and April 1986, or showed a slight increase in concentration, as in April 1985. The concentrations of other dissolved constituents were approximately constant for each sampling trip.

Aqueous speciation calculations (Table 2) demonstrate that samples from February and April 1985 and April 1986, collected during conditions of relatively high water flows, were near equilibrium ($-0.05 < \text{SI}_c < +0.05$) or slightly undersaturated ($\text{SI}_c < -0.05$) with respect to calcite. The July samples, collected during lower flow conditions, were near equilibrium or slightly supersaturated ($\text{SI}_c > +0.05$) with respect to calcite. All samples were significantly undersatu-

rated with respect to gypsum. The calculated PCO_2 values were all significantly greater than the normal atmospheric value of $10^{-3.50}$ atm.

Three genera of colorless sulfur bacteria were identified by microscopic morphology (la Riviere and Schmidt, 1981) from water samples: *Thiothrix*, *Beggiatoa*, and *Achromatium*. All three deposit intracellular elemental sulfur granules when living in water containing dissolved sulfide and oxygen. Both *Thiothrix* and *Beggiatoa* are filamentous gliding bacteria that range from one to greater than 25 μm in width. *Thiothrix* spp. were found attached to travertine in the spring opening in the dark zone of the cave as well as in the outside stream. *Beggiatoa* spp. were found in the water column and on the surface of substrates in the cave and the outside stream. *Achromatium* spp., large ovoid cells measuring from 5 to 100 μm , were found at the bottom of the entrance pool. This organism also forms intracellular deposits of CaCO_3 .

DISCUSSION

The major-ion concentration data (Table 1) indicate that the water from Cesspool Cave and the stream it feeds is typical of water that arises from carbonate mineral dissolution by CO_2 -charged groundwater. The saturation indices (Table 2) indicate that the water is approximately saturated with respect to calcite. The PCO_2 value is above the normal atmospheric value. Therefore, this water would be expected to outgas CO_2 to the atmosphere as it enters the cave and continues along its flow path. Upon outgassing CO_2 , the stream would become supersaturated with respect to calcite, and ultimately calcite deposition would occur.

A unique component of the water in Cesspool Cave is the high total aqueous sulfide content. The range in measured values is 0.2 to 7.1 mg/L. All these concentrations are higher than are commonly encountered in natural water. Seldom does groundwater in limestone terrane have a detectable concentration of sulfide. For groundwater in the Floridan aquifer, H_2S values ranged from 0 to 3.3 mg/L (Rye and others, 1981). High sulfide values have been reported for the bad-water zone of the Edwards aquifer, with values up to 65 mg/L (Rye and others, 1981). In a very different setting noted for remarkable sulfide levels, values up to 150 mg/L have been measured at a hydrothermal vent on the Juan de Fuca Ridge in the east Pacific Ocean (U.S. Geological Survey Juan de Fuca Study Group, 1986).

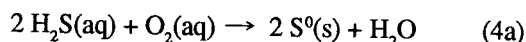
The three genera of colorless sulfur bacteria (*Thiothrix*, *Beggiatoa*, and *Achromatium*) observed in Cesspool Cave all oxidize hydrogen sulfide with molecular oxygen and deposit amorphous sulfur internally (Larkin and Strohl, 1983). Granules of S^0 were observed within the cells. Under conditions of low concentrations of H_2S , they can oxidize the stored sulfur to sulfate resulting in a two-step oxidation (Lackey and others, 1965; Strohl and Larkin, 1978):

Table 1. Chemical analyses of water samples. All concentrations are expressed in mg/L.

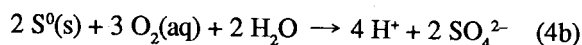
Sample ¹	T (°C)	Cond (µS/cm)	pH	Alk. ²	H ₂ S	Ca	Mg	Na	K	Cl	SO ₄	NO ₃
February 1985												
SP	12.4		6.81	464		179	15.3	5.6	5.1	11.2	123	0.12
EP	11.3		6.75	459		171	14.8	5.4	5.1	10.8	126	0.15
S1	10.9		6.78	450		181	15.0	5.2	5.0	11.0	127	0.15
April 1985												
SP	13.0	600	6.78	469		153	15.4	5.3	4.0	11.7	106	0.5
EP	11.0	640	6.84	469		155	15.9	5.4	4.0	12.1	112	0.5
S1	10.0	630	6.76	469		153	15.4	5.0	3.8	11.6	114	0.5
July 1985												
SP	12.5	600	6.96	390	1.7	166	16.6	5.4	4.6	10.3	112	0.5
EP	13.0		6.98	392	1.5	168	16.5	5.3	4.6	10.7	112	0.5
S1	13.0	550	6.97	391	0.2	166	16.6	5.7	4.4	10.5	115	0.5
April 1986												
SP	11.0	700	6.75	489	7.1	160	17.9	5.4	5.0	12.8	122	<0.10
TP					5.5							
EP	10.0	600	6.79	486	2.4	158	18.1	5.2	4.9	12.4	117	<0.10
S1	11.0	700	6.70	482	3.3	169	17.9	5.3	5.3	12.8	121	<0.10

¹Sample locations: (SP) Cesspool spring; (TP) terminal pool; (EP) entrance pool; (S1) outside stream. Samples are arranged in order along the flow path from the spring in the cave to the surface stream.

²Total alkalinity (Alk.) was determined and was taken to be entirely due to HCO₃⁻.



and



Bacterially mediated oxidation of sulfide can occur more rapidly than chemical oxidation by oxygen. *Beggiatoa* has been shown to oxidize sulfide 100 to 1000 times faster than the chemical oxidation rate (Jorgensen and Revsbech, 1983). Along the short flow path we observed in Cesspool Cave, sulfide was reduced by as much as one order of magnitude, partially as a result of bacterially mediated oxidation in the slow-moving stream and its pools. During the February and April 1985 and April 1986 visits, white filamentous networks of colorless sulfur bacteria were abundant in the milky-colored cave pools. The population of these organisms had

declined by the July 1985 visit and consisted mainly of coatings on leaves and other debris and a slight milky coloration in the pool water. The decline in populations of sulfur-oxidizing bacteria may account for the increase in sulfide in the water on that sampling trip. The reason for the large fluctuations of bacterial populations is not known, but may be related to changes in the H₂S/O₂ gradient or changes in the flow of water and therefore the energy source for the cells. Few of these bacteria have been isolated in pure culture, largely because of the technical difficulty of maintaining the appropriate H₂S/O₂ gradient, and their physiology is not well understood.

The oxidation of H₂S generates acid which increases the dissolution capacity of the cave water (Equations 3a and 3b). Because this water is in contact with calcite, no appreciable decrease in pH is actually observed. The relatively high levels of sulfide measured in the cave spring indicate a significant potential for travertine dissolution in Cesspool Cave.

Table 2. Calculated partial pressure of CO₂ and saturation indices of the water samples.

Sample	log PCO ₂	SI _C ¹	SI _G ¹
February 1985			
SP	-1.25	-0.01	-1.20
EP	-1.20	-0.11	-1.20
S1	-1.24	-0.07	-1.18
April 1985			
SP	-1.21	-0.08	-1.31
EP	-1.28	-0.05	-1.28
S1	-1.20	-0.15	-1.27
July 1985			
SP	-1.47	0.04	-1.26
EP	-1.49	0.08	-1.26
S1	-1.48	0.06	-1.25
April 1986			
SP	-1.17	-0.12	-1.24
EP	-1.22	-0.10	-1.26
S1	-1.13	-0.15	-1.23

¹SI = log [IAP(T)]/K(T), where IAP(T) and K(T) are the ion activity product and the equilibrium constant, respectively, at sample temperature. Indices are SI_C for calcite and SI_G for gypsum.

H₂S outgassing from the cave water may be responsible for the corroded flowstone in Cesspool Cave. In the terminal pool room, the extensive crusts of gypsum could have resulted from the dissolution of H₂S and O₂ into water films forming on the walls and formations during variations in temperature and humidity. The resultant sulfide oxidation produces an acidic solution that dissolves calcite. Gypsum crusts develop when the aqueous film becomes supersaturated with respect to gypsum, a result of increased Ca²⁺ concentration due to calcite dissolution and the increased SO₄²⁻ concentration due to H₂S oxidation. Alternatively, supersaturation may result from evaporation of the films of water (Hubbard and others, 1986). Similar situations of wall corrosion and formation of gypsum crusts are described by Egemeier (1973) for caves and in engineering texts (such as Clark and others, 1977, p. 461) for concrete sewer lines, whereby the acidity generated by bacterial oxidation of H₂S is quickly neutralized by calcite dissolution.

The source of the H₂S in Cesspool Cave is unknown. Sulfate concentrations are high in the spring inputs (Sweet Springs, Sweet Chalybeate Springs, and Cesspool Spring) to Sweet Springs Creek. Sulfate-reducing bacteria could be actively converting sulfate to H₂S within the subsurface supply of water to Cesspool Spring. The breakdown of

metastable iron sulfide minerals such as mackinawite (FeS) or greigite (Fe₃S₄) in the underlying black shales could produce H₂S which could then be transported in the groundwater. The degradation of organic compounds locally concentrated in the black shale units and the Helderberg Limestone is also a plausible source. Hydrocarbons in the black shales could be migrating up dip along the synclinal structure and provide an H₂S source.

CONCLUSIONS

The genesis of Cesspool Cave appears to be the combined result of CO₂ hydration (Equation 1) and H₂S hydration and oxidation (Equations 3a and 3b) causing acid dissolution of a Quaternary stream-deposited travertine buildup (Equation 2). Partial pressures of CO₂ are elevated relative to the normal atmosphere and are comparable to values in other groundwaters in limestone where carbonic acid is the primary calcite dissolution agent. High aqueous sulfide concentrations in the cave waters, decreasing sulfide concentrations along the flow path, a living population of sulfur-oxidizing bacteria, and gypsum-encrusted corroded limestone walls indicate sulfide oxidation and concomitant generation of acid. The quantitative importance of biologically mediated sulfide oxidation in the generation of acidity is not known. Because of the unusual features of limestone corrosion on the cave walls and the speleothems, we believe that the sulfuric acid reaction mechanism dominates this system. We suspect that wherever there is a source of strong acid in a groundwater, dissolution by that acid will dominate dissolution by carbonic acid.

ACKNOWLEDGMENTS

We thank Kimberly J. Hoffer for her assistance in the field and the laboratory and Terry M. Williams for helpful discussions. Thoughtful comments from Carol Hill, Carol Wicks, and Aaron Mills helped us improve this manuscript.

REFERENCES CITED

- Butts, Charles, 1933, Geologic map of the Appalachian Valley of Virginia with explanatory text: Virginia Geological Survey Bulletin 42, map.
- Clark, J.W., Viessman, Warren, Jr., and Hammer, M.J., 1977, Water Supply and Pollution Control: New York, New York, Harper & Row, Publishers, Inc., 3rd ed., 857 p.
- Cline, J.D., 1969, Spectrophotometric determination of hydrogen sulfide in natural waters: *Limnology and Oceanography*, v. 14, p. 454-458.

- Davis, D.G., 1979, Geology and speleogenesis of Ogle Cave: discussion: National Speleological Society Bulletin, v. 41, p. 21-22.
- Egemeier, S.J., 1973, Cavern development by thermal waters with a possible bearing on ore deposition [Ph.D. dissert.]: Palo Alto, California, Stanford University, 88 p.
- Featherstonhaugh, G.W., 1835, Account of the travertin [sic] deposited by the waters of the Sweet Springs, in Alleghany County in the State of Virginia, and of an ancient travertine [sic] discovered in the adjacent hills: Geological Society of Pennsylvania, Transactions, v. 1, p. 328-334.
- Fulghum, R.S., and Worthington, J.M., 1977, Butyl rubber stoppers increase the shelf life of prerduced, anaerobically sterilized media: Applied and Environmental Microbiology, v. 33, p. 1220-1221.
- Herman, J.S., Bell, P.E., and Hubbard, D.A., Jr., 1986, Cesspool Cave: a natural analog for sulfide contamination in carbonate aquifers [abs.]: American Association for the Advancement of Science, 152nd National Meeting, p. 28.
- Hill, C.A., 1981, Speleogenesis of Carlsbad Cavern and other caves of the Guadalupe Mountains, in Beck, B. F., ed., Proceedings of the Eighth International Congress of Speleology: Huntsville, Alabama, National Speleological Society, v. 1, p. 143-144.
- Hill, C.A., 1987, Speleogenesis of Carlsbad Cavern and other caves in the Guadalupe Mountains: New Mexico Bureau of Mines and Mineral Resources Bulletin 117, 150 p.
- Holsinger, J.R., 1975, Descriptions of Virginia Caves: Virginia Division of Mineral Resources Bulletin 85, 450 p.
- Howard, A.D., 1960, Geology and origin of the crevice caves of the Iowa, Illinois, and Wisconsin lead-zinc district: New Haven, Connecticut, Journal of the Yale Speleological Society, v. 2, n. 4, pt. 1, p. 61-95.
- Hubbard, D.A., Jr., Herman, J.S., and Bell, P.E., 1986, The role of sulfide oxidation in the genesis of Cesspool Cave, Virginia, U.S.A.: Barcelona, Spain, 9th International Congress of Speleology, Communications, v. 1, p. 255-257.
- Jagnow, D.H., 1978, Geology and speleogenesis of Ogle Cave: National Speleological Society Bulletin 40, p. 7-18.
- Jennings, J.N., 1971, Karst: Cambridge, Massachusetts, MIT Press, 252 p.
- Jorgensen, B.B., and Revsbech, N.P., 1983, Colorless sulfur bacteria, *Beggiatoa* spp., and *Thiovulum* spp., in O₂ and H₂S microgradients: Applied and Environmental Microbiology, v. 45, p. 1261-1270.
- Lackey, J.B., Lackey, E.W., and Morgoon, G.B., 1965, Taxonomy and ecology of the sulfur bacteria: Gainesville, University of Florida, College of Engineering Bulletin Series No. 19, p. 1-23.
- la Riviere, J.W.M., and Schmidt, K., 1981, Morphologically conspicuous sulfur-oxidizing eubacteria, in Starr, M.P., Stolp, H., Truper, H.G., Balows, A., and Schlegel, H.G., eds., The prokaryotes: Springer-Verlag, p. 1035-1048.
- Larkin, J.M., and Strohl, W.R., 1983, *Beggiatoa*, *Thiothrix* and *Thioplaca*: Annual Reviews in Microbiology, v. 37, p. 341-367.
- Moore, G.W., and Nicholas, G., 1964, Speleology, the study of caves: Boston, Massachusetts, D.C. Heath, 120 p.
- Mooman, J.J., 1855, The Virginia springs: comprising an account of all the principal mineral springs of Virginia, with remarks on the nature and medical applicability of each: Richmond, Virginia, J. W. Randolph, 319 p.
- Morehouse, D.F., 1968, Cave development via the sulfuric acid reaction: National Speleological Society Bulletin 30, p. 1-10.
- Plummer, L.N., Jones, B.F., and Truesdell, A.H., 1976, WATEQF-A FORTRAN IV version of WATEQ, a computer program for calculating chemical equilibria of natural waters: U.S. Geological Survey Water Resources Investigation 76-13, 63 p.
- Reger, D.B., and Price, P.W., 1925, Map IV, Monroe County showing general geology and economic geology, in Reger, D.B., 1926, Mercer, Monroe, and Summers counties: West Virginia Geological Survey County Report, 936 p.
- Rye, R.O., Back, William, Hanshaw, B.B., and Pearson, F.J., Jr., 1981, The origin and isotopic composition of dissolved sulfide in groundwater from carbonate aquifers in Florida and Texas: Geochimica et Cosmochimica Acta, v. 45, p. 1941-1950.
- Strohl, W.R., and Larkin, J.M., 1978, Enumeration, isolation, and characterization of *Beggiatoa* from freshwater sediments: Applied and Environmental Microbiology, v. 36, p. 755-757.
- Sweeting, M.M., 1972, Karst landforms: London, England, Macmillan, 362 p.
- Sweeting, M.M., ed., 1981, Karst geomorphology: Benchmark Papers in Geology 59, Stroudsburg, Pennsylvania, Hutchinson Ross, 427 p.
- U.S. Geological Survey Juan de Fuca Study Group, 1986, Submarine fissure eruptions and hydrothermal vents on the southern Juan de Fuca Ridge: Preliminary observations from the submersible Alvin: Geology, v. 14, p. 823-827.
- Walton, G.E., 1874, The mineral springs of the United States and Canada, with analyses and notes on the prominent spas of Europe, and a list of seaside resorts: New York, New York, D. Appleton and Company, 414 p.
- White, W.B., 1988, Geomorphology and hydrology of karst terrains: New York, Oxford University Press, 464 p.